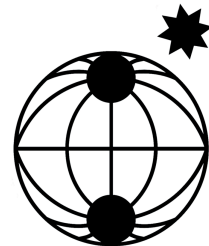


# Berichte

zur Polar-  
und Meeresforschung

584  
2008

**Reports  
on Polar and Marine Research**



**Russian-German Cooperation SYSTEM LAPTEV SEA:**  
The Expedition Lena - New Siberian Islands 2007  
during the International Polar Year 2007/2008

---

Edited by  
**Julia Boike, Dmitry Yu. Bolshiyarov,  
Lutz Schirrmeister, Sebastian Wetterich**



HELMHOLTZ  
| GEMEINSCHAFT

ALFRED-WEGENER-INSTITUT FÜR  
POLAR- UND MEERESFORSCHUNG  
In der Helmholtz-Gemeinschaft  
D-27570 BREMERHAVEN  
Bundesrepublik Deutschland

ISSN 1866-3192

# Hinweis

Die Berichte zur Polar- und Meeresforschung werden vom Alfred-Wegener-Institut für Polar- und Meeresforschung in Bremerhaven\* in unregelmäßiger Abfolge herausgegeben.

Sie enthalten Beschreibungen und Ergebnisse der vom Institut (AWI) oder mit seiner Unterstützung durchgeführten Forschungsarbeiten in den Polargebieten und in den Meeren.

Es werden veröffentlicht:

- Expeditionsberichte (inkl. Stationslisten und Routenkarten)
- Expeditionsergebnisse (inkl. Dissertationen)
- wissenschaftliche Ergebnisse der Antarktis-Stationen und anderer Forschungs-Stationen des AWI
- Berichte wissenschaftlicher Tagungen

Die Beiträge geben nicht notwendigerweise die Auffassung des Instituts wieder.

# Notice

The Reports on Polar and Marine Research are issued by the Alfred Wegener Institute for Polar and Marine Research in Bremerhaven\*, Federal Republic of Germany. They appear in irregular intervals.

They contain descriptions and results of investigations in polar regions and in the seas either conducted by the Institute (AWI) or with its support.

The following items are published:

- expedition reports (incl. station lists and route maps)
- expedition results (incl. Ph.D. theses)
- scientific results of the Antarctic stations and of other AWI research stations
- reports on scientific meetings

The papers contained in the Reports do not necessarily reflect the opinion of the Institute.

The „Berichte zur Polar- und Meeresforschung“  
continue the former „Berichte zur Polarforschung“

## \* Anschrift / Address

Alfred-Wegener-Institut  
Für Polar- und Meeresforschung  
D-27570 Bremerhaven  
Germany  
[www.awi.de](http://www.awi.de)

Editor in charge:  
Dr. Horst Bornemann

Assistant editor:  
Birgit Chiaventone

Die "Berichte zur Polar- und Meeresforschung" (ISSN 1866-3192) werden ab 2008 ausschließlich als Open-Access-Publikation herausgegeben (URL: <http://epic.awi.de>).

Since 2008 the "Reports on Polar and Marine Research" (ISSN 1866-3192) are only available as web based open-access-publications (URL: <http://epic.awi.de>)

**Russian-German Cooperation SYSTEM LAPTEV SEA:**  
The Expedition Lena - New Siberian Islands 2007  
during the International Polar Year 2007/2008

---

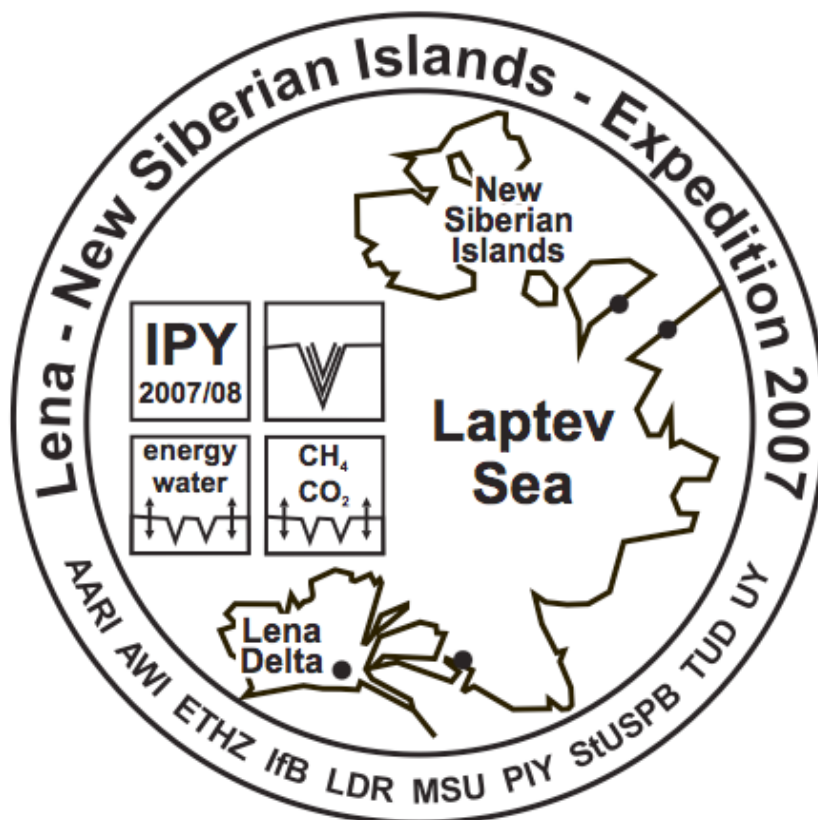
**Edited by**  
**Julia Boike, Dmitry Yu. Bolshiyarov,**  
**Lutz Schirrmeister, Sebastian Wetterich**

**Please cite or link this item using the identifier**  
**hdl: 10013/epic.31638 or <http://hdl.handle.net/10013/epic.31638>**  
**ISSN 1866-3192**

**Russian-German Cooperation SYSTEM LAPTEV SEA:  
The Expedition Lena - New Siberian Islands 2007**

during the International Polar Year 2007/2008

*edited by Julia Boike, Dmitry Yu. Bolshiyarov,  
Lutz Schirrmeister and Sebastian Wetterich*



# Contents

## The Expedition Lena - New Siberian Islands 2007

<b>1.</b>	<b>Introduction</b> .....	1
<b>2.</b>	<b>Expedition itinerary and general logistics</b> .....	2
<b>3.</b>	<b>Studies in the Lena River Delta</b> .....	5
3.1	High resolution digital elevation model of polygonal patterned ground on Samoylov Island, Siberia, using small-format photography.....	5
3.2	Sensitivity of the permafrost system's – water and energy balance under changing climate: A multi-scale perspective .....	8
3.3	Microbial studies on nitrification from permafrost environments.....	12
3.4	Morphology and properties of recent gelisols and palaeosols of the southern Lena Delta, Siberia, Russia.....	16
3.5	Long-term studies on methane fluxes from permafrost ecosystems	19
3.6	A high resolution orthorectified picture of Samoylov.....	22
3.7	Hydrobiological investigations in the Lena River Delta.....	23
3.8	Hydrological and geomorphological investigations studies in the Lena Delta.....	28
3.9	Studies of coastal dynamics and subsea permafrost.....	30
3.10	References .....	33
<b>4.</b>	<b>Permafrost and environmental dynamics during Quaternary climate variations – Studies along the Dmitrii Laptev Strait</b> .....	35
4.1	Scientific background and objectives.....	35
4.2	Geological and geographical characteristics.....	37
4.3	Field methods and exposure description.....	39
4.4	Stratigraphical and geomorphological studies along the south coast of Bol'shoy Lyakhovsky Island and along the Oyogos Yar coast...	41
4.4.1	Preliminary stratigraphic scheme.....	41
4.4.2	The coast west of the Zimov'e River.....	45
4.4.3	The coast between Zimov'e and Vankina River.....	45
4.4.4	The coast east of the Vankina River.....	47
4.4.5	The coast of Oyogos Yar.....	48
4.5	Palaeoenvironmental studies on Bol'shoy Lyakhovsky Island.....	51
4.5.1	Studies of Tertiary to Holocene permafrost sections west of the Zimov'e River mouth.....	52
4.5.1.1	Exposure L7-17, Tertiary (?) deposits.....	52
4.5.1.2	Exposure L7-01, Yukagirsky to Kuchchugui Suite.....	53
4.5.1.3	Exposure L7-02, Yukagirsky ice wedge.....	57
4.5.1.4	Exposure L7-03, Yukagirsky Suite.....	58
4.5.1.5	Exposure L7-05, Yukagirsky to Kuchchugui Suite.....	59
4.5.1.6	Exposure L7-06, Krest Yuryakh Suite.....	60
4.5.1.7	Exposure L7-18, Yedoma Suite.....	61
4.5.1.8	Exposure L7-07.....	62
4.5.1.9	Exposure L7-08, Alas Complex.....	64

4.5.2	Studies of Middle to Late Pleistocene permafrost sections near the Vankina River mouth.....	69
4.5.2.1	Exposure L7-12, Kuchchugui Suite.....	69
4.5.2.2	Exposure L7-14, Kuchchugui to Krest Yuryakh Suite.....	70
4.5.2.3	Exposure L7-15, Bychchagy Suite.....	75
4.5.3	Studies of permafrost sections east of the Zimov'e River mouth..	79
4.5.3.1	Exposure L7-11, Krest Yuryakh Suite.....	79
4.5.3.2	Exposure L7-16, Taberal Bychchagy (?) Suite to Krest Yuryakh Suite.....	80
4.5.4	Stratigraphic conclusion from the studied sequences.....	82
4.6	Palaeoenvironmental studies on the Oyogos Yar coast.....	85
4.6.1	Geographical characteristics and introduction.....	85
4.6.2	Studies of Eemian (Krest Yuryakh Suite) and pre Eemian (Kuchchugui, Bychchagy Suite) sections.....	88
4.6.2.1	Exposure Oy7-01, Krest Yuryakh Suite.....	88
4.6.2.2	Exposure Oy7-03, Kuchchugui to Bychchagy Suite.....	91
4.6.2.3	Exposure Oy7-09, Kuchchugui to Krest Yuryakh Suite.....	93
4.6.2.4	Exposure Oy7-07, Kuchchugui to Krest Yuryakh Suite.....	95
4.6.2.5	Exposure Oy7-10, Bychchagy Suite (14.08.).....	98
4.6.3	Studies of a sequences from the Eemian Krest Yuryakh Suite to the Yedoma Suite (Exposure Oy7-08).....	101
4.6.3.1	The Krest Yuryakh segment between 2 and 6 m a.sl. ....	101
4.6.3.2	The Ice Complex sequence between 9 and 28 m a.s.l. ....	104
4.6.3.3	Summarizing stratigraphic interpretation of Oy7-08 sequence.....	108
4.6.4	Sediment sequences below the alas bottom.....	109
4.6.4.1	Exposure Oy7-04, Krest Yuryakh Suite to Holocene.....	109
4.6.4.2	Exposure Oy7-11, taberal Yedoma Suite to Holocene.....	111
4.6.5	Ground ice studies.....	115
4.6.5.1	Introduction and Methods.....	115
4.6.5.2	Studies of ground ice in Pre-Yedoma deposits.....	117
4.6.5.3	Studies of Yedoma ground ice.....	121
4.6.5.4	Studies of Holocene and recent ground ice.....	130
4.6.6	Fossils of the mammoth fauna.....	139
4.6.7	Sedimentological studies of selected profiles.....	141
4.6.7.1	Study site and objectives.....	141
4.6.7.2	Profile I.....	142
4.6.7.3	Profile II.....	145
4.6.7.4	Additional outcrops.....	147
4.7.	References.....	151
<b>5.</b>	<b>Modern environmental dynamics – Studies along the Dmitrii Laptev Strait.....</b>	<b>155</b>
5.1	Scientific background and objectives .....	155
5.2	Limnological studies in the Dmitrii Laptev Strait region.....	155
5.3	Modern vegetation in the coastal lowlands of Oyogos Yar.....	165
5.4	References.....	173

<b>6.</b>	<b>Appendices to the chapters 4 and 5.....</b>	<b>175</b>
6.1	List of sediment samples - sedimentological and cryolithological sample characteristics.....	175
6.2	List of ground ice, water and precipitation samples.....	195
6.3	List of bone samples from the Oyogos Yar 2007.....	215
6.4	Features of the studied waters.....	249
6.4.1	Geographical features of the studied waters.....	249
6.4.2	Morphological and sedimentological features of the studied waters.....	250
6.4.3	Physico-chemical features of the studied waters.....	251
6.5	List of vegetation records from Oyogos Yar 2007.....	253



## 1. Introduction

*Lutz Schirrmeister and Julia Boike*

This report summarizes activities and field work results of the joint Russian-German expedition “Lena – New Siberian Islands 2007” during the International Polar Year 2007/2008. The tenth expedition to the Lena River Delta and the Laptev Sea region is part of the Russian-German science cooperation “System Laptev Sea” and continues the long-term investigations of permafrost and periglacial environments in Arctic Siberia. The expedition focused on five research topics:

- Sensitivity of the permafrost system – water and energy budget during climate changes
- Carbon dynamics and microbial processes in periglacial areas
- Carbon and nitrogen fluxes in permafrost soils and the consequences of climate change
- Hydrological conditions of the Lena River Delta
- Coastal dynamics and subsea permafrost
- Permafrost and environmental dynamics during Quaternary climate variations
- Modern environmental dynamics of aquatic ecosystems and vegetation

The expedition was coordinated by Prof. H.-W. Hubberten (AWI, Potsdam), Prof. D.Yu. Bolshiyarov (AARI, St. Petersburg) and Dr. M.N. Grigoriev (PIY, Yakutsk).

The various research activities in the summer of 2007 were contributions to different national and international projects, research groups, observation programs and network activities

- HGF- young research group SPARC
- IPY-Project “Past Permafrost” (ID 15); INTAS Project “permafrost dating by cosmogenic  $^{36}\text{Cl}$  and  $^{10}\text{Be}$ ” (8133); DFG project “Late Quaternary warm stages in the Arctic” (SCHI 975/1-2)

The report is structured in three parts concerning various studies of periglacial conditions in the Lena Delta region in broader sense (chapter 3), palaeo-environmental studies along the Dmitrii Laptev Strait (chapter 4), and studies of the modern environment in areas of the Laptev Strait coast region (chapter 5).

The authors of the separate chapters are responsible for content and correctness.

## 2. Expedition itinerary and general logistics

The expedition was realized in two periods between July 1<sup>st</sup> and September 3<sup>rd</sup> 2007. In total, 29 participants (Table 2-1) from 8 institutions (Table 2-2) took part in nine weeks of field work.

The studies were carried out in three different regions (Figure 2-1). The first study area comprises the Lena River Delta, especially Kurungnakh Island and Samoylov Island in the central delta. The joint Russian-German research station is located on Samoylov Island.

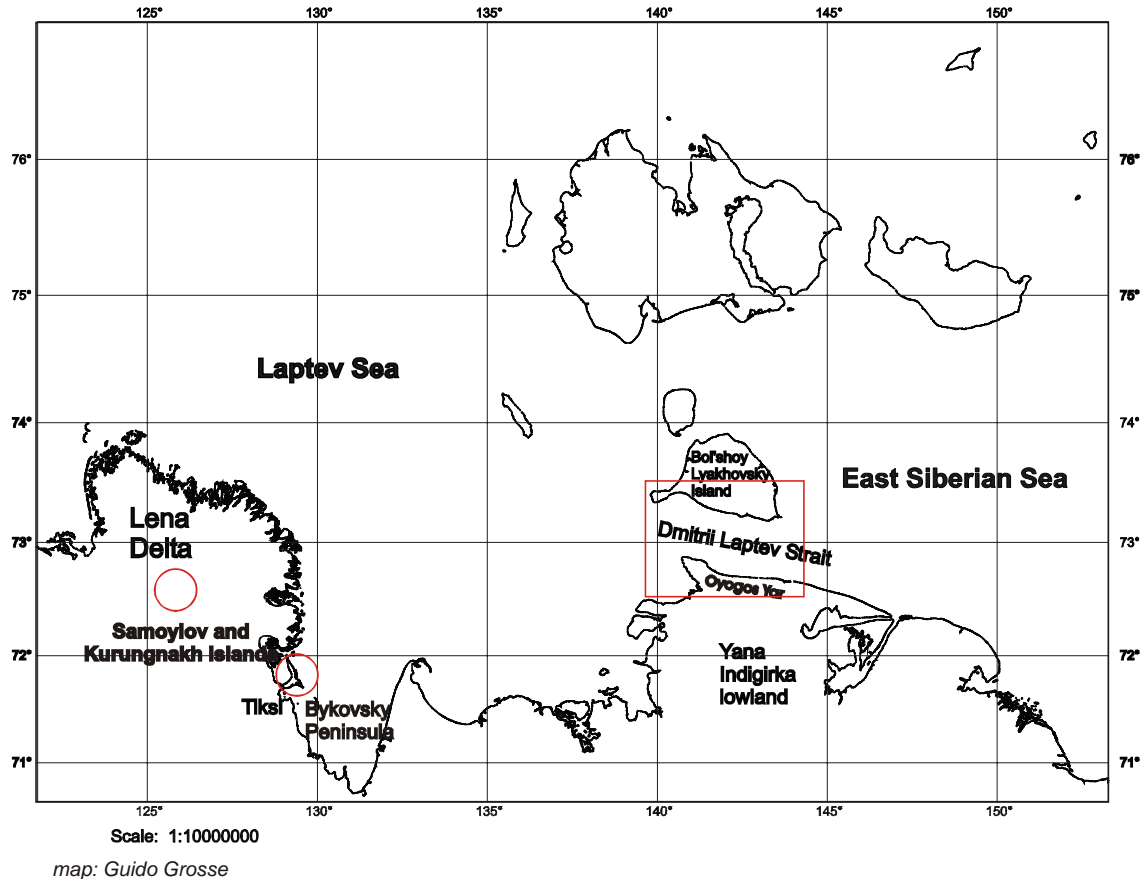


**Figure 2-1:** Study areas of the expedition “Lena – New Siberian Islands 2007”

The second and the third study area are located along the Dmitrii Laptev Strait at the south coast of Bol'shoy Lyakhovskiy Island and at the north coast of the Yana-Indigirka lowland.

**Table 2-1:** List of participants

<b>Name</b>	<b>Email</b>	<b>Institute</b>	<b>Time</b>
Boike, Julia	Julia.Boike@awi.de	AWI	01.07-30.07
Bolshiyarov, Dmitry	bolshiyarov@aari.nw.ru	ARRI	30.07-13.08
Germogenova, Anastasia	nastjonysh@hotmail.com	MSU	01.07-03.09
Grigoriev, Mikhail	grigoriev@mpi.ysn.ru	PIY	02.07-30.07
Joseph, Jürgen	juejo1@web.de	AWI	01.07-03.09
Landolt, Maryvonne	zeyer@env.ethz.ch	ETH	01.07-30.07
Langer, Moritz	Moritz.Langer@awi.de	AWI	01.07-03.09
Makarov, Alexander	makarov@aari.nw.ru	AARI	01.07-03.09
Pfeiffer, Eva-Maria	E.M.Pfeiffer@ifb.uni-hamburg.de	UH	30.07- 03.09
Piel, Konstanze	Konstanze.Piel@awi.de	AWI	01.07-03.09
Sanders, Tina	T.Sanders@ifb.uni-hamburg.de	UH	01.07-30.07
Scheritz, Marita	scheritz@ipg.geo.tu-dresden.de	TUD	01.07-30.07
Schneider, Waldemar	Waldemar.Schneider@awi.de	AWI	01.07-03.09
Stoof, Günther	Guenther.Stoof@awi.de	AWI	01.07-03.09
Terekhova, Raisa	terekhova@aari.nw.ru	AARI	30.07- 03.09
Wischnyakova, Irina	irivishnya@gmail.com	LDR	01.07-03.09
Zeyer Joseph	zeyer@env.ethz.ch	ETH	01.07-30.07
Zubrzycki, Sebastian	sebastian@zubrzycki.de	UH	01.07-03.09
Dereviagin, Alexander	dereviag@online.ru	MSU	30.07- 03.09
Dobrynin, Dmitry	ddobrynin@yandex.ru	MSU	01.07-03.09
Gordinsky, Alexander	shureetz@bk.ru	AARI	30.07- 03.09
Kienast, Frank	fkienast@senckenberg.de>	AWI/Senckenberg	30.07- 03.09
Kudrevataya, Lyubov	Lubasha.79@mail.ru	LDR	30.07- 03.09
Kunitsky, Viktor	kunitsky@mpi.ysn.ru	PIY	30.07- 03.09
Kuznetsova, Tatyana	tatkuz@orc.ru	MSU	30.07- 03.09
Opel, Thomas	Thomas.Opel@awi.de	AWI	30.07- 03.09
Schirrmeister, Lutz	Lutz.Schirrmeister@awi.de	AWI	01.07-03.09
Tumskoy, Vladimir	tumskoy@orc.ru	MSU	01.07-03.09
Wetterich, Sebastian	Sebastian.Wetterich@awi.de	AWI	01.07-03.09

**Table 2-2:** Institutions of the participants

---

ARRI:	Arctic and Antarctic Research Institute, Bering St. 38, 199397 St. Petersburg, Russia
AWI:	Alfred Wegener Institute for Polar and Marine Research, Section Periglacial Research; Telegrafenberg A43, D-14473 Potsdam, Germany
ETH:	Institute for Biogeochemistry and Pollutant Dynamics (IBP), Federal Institute of Technology, ETH-Zentrum CHN G47, Universitaetstrasse 16. CH-8092 Zürich, Switzerland
LDR:	Lena Delta Reserve, 28 Academician Fyodorov St., Tiksi 678400, Yakutia, Russia
MSU:	Moscow State University Vorob'evy Gory, Department of Geocryology, Departement of Palaeontology, Geological Faculty, Moscow, 119992, Faculty of Soil Science, Moscow, 11989, Russia
PIY:	Melnikov Permafrost Institute, Russian Academy of Science, Merslotnaya 35, 677010 Yakutsk, Russia
TUD	Technical University Dresden, Institute of Planetary Geodaesy, Helmholtzstraße 10, D-01062 Dresden, Germany
UH	University Hamburg, Institute of Soil Science, Allende-Platz 2, D-20146 Hamburg, Germany

---

### *Acknowledgements*

*The success of the expedition "Lena–New Siberian Islands 2007" would not have been possible without the support by several Russian, Yakutian, and German institutions and authorities.*

*In particular, we would like to express our appreciation to the Tiksi Hydrobase and the Lena Delta Reserve, especially to D. Melnichenko, A. Gukov and F.V. Selyakhov. The members of the expedition wish to thank the captains and crewmembers of the vessel "Puteyski 405" and the staff of the Lena Delta Reserve station on Samoylov Island.*

### 3. Studies in the Lena River Delta

#### 3.1 High resolution digital elevation model of polygonal patterned ground on Samoylov Island, Siberia, using small-format photography

*Marita Scheritz, Waldemar Schneider and Julia Boike*

##### Objectives

Accurate land cover, such as high-resolution digital elevation models (DEM) are needed to obtain reliable inputs for modeling the hydrology and the exchange between surface and atmosphere. The landscape of Samoylov Island in the Lena Delta, Northern Siberia (72.2°N/126.3°E), is shaped by the micro topography of the wet polygonal tundra. This micro relief is not represented with sufficient resolution in satellite images with resolutions between 15 and 30 m. So the main objective of the geodetic work on Samoylov Island was the generation of a high-resolution DEM with an accuracy of the coordinates of each point in the DEM better than 1 m and with a resolution better than 10 m.

##### Methods and equipment

The basic idea was to map the patterned ground on Samoylov Island with photogrammetric methods (stereoscopy) using aerial images with overlapping areas. Therefore we used small-format aerial photography with help of balloons and a helicopter. The equipment for the aerial photography consists of a Nikon D200 camera with a 14 mm lens (Figure 3.1-1 A) and 26 ground control points (Figure 3.1-1 A-C). The Nikon D200 is a digital mirror reflex camera with a CCD sensor of 10.2 megapixel. With the calculated flight height of 800 m one pixel maps an area of ~0.35 m<sup>2</sup> on the ground. In dependency on the flight height and the 14 mm lens and under the condition that each ground control point represents an area of not less than 6 x 6 Pixel in the digital pictures the diameter has to be greater than 2.0 m. The whole network of all ground control points is shown in Figure 3.1-1 C. All ground control points were measured with a tachymeter ELTA C30.

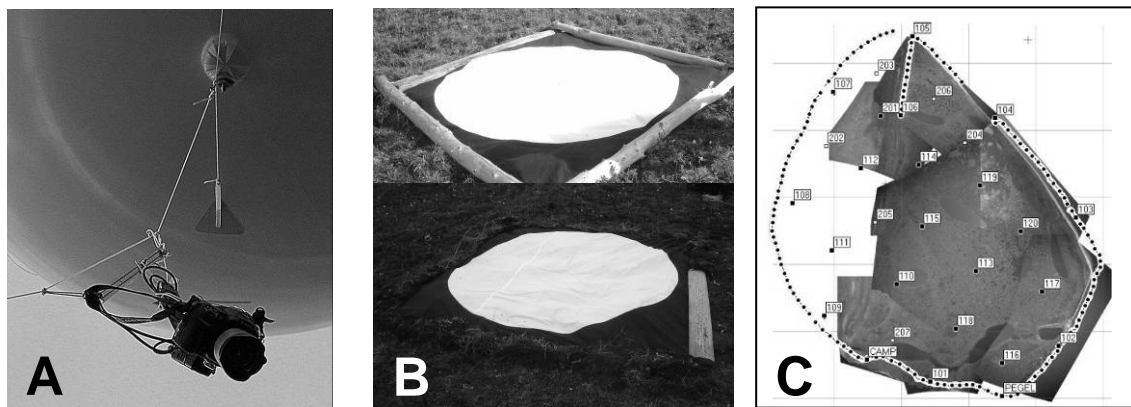


**Figure 3.1-1:** A: Nikon D200, 14 mm lens; B: ground control points; C: Network of 26 control points

## Fieldwork

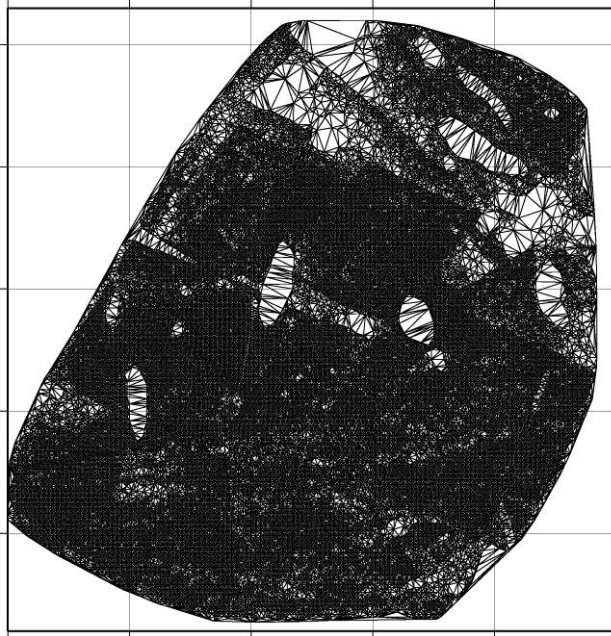
The fieldwork was divided into two parts. First, ground control points were laid out and their coordinates were measured. Second, aerial photographs were taken with the help of a balloon and a helicopter. The registration of all ground control points took place in a local coordinate system. Therefore 4 datum points were set up, each marked with an 1 m iron pipe in the permafrost. The distances between these points reached from 800 m to 1200 m. The accuracy of the distances between the datum points and to the ground control points is better than 1 cm. The accuracy of the coordinates of the datum points is less than  $\pm 2$  cm. The coordinates of all ground control points have an absolute accuracy of better than  $\pm 5$  cm. For mapping the patterned ground on Samoylov Island we first took pictures with help of a balloon (Figure 3.1-1 A). The pre-conditions for taking photos with the camera, hanging at the balloon, are a calm day and good illumination conditions. With the balloon we could cover one third of the entire Island (western part, flood plain, Figure 3.1-1 C) from a height of nearly 800 m. Additionally, images were captured from a helicopter from altitudes between 600 m and 900 m. With the helicopter we could cover the middle part of the Island with a flight height of  $\sim 600$  m. The East part of the Island could be covered with flight heights of nearly 800-900 m.

## Data Analysis

The first step of data analysis was a data check. Second, we had to calculate the calibration parameters of the camera system (parameter of inner orientation). The calculations of the coordinates of the points of the DEM are based on the Colinearity equations, which correlate the picture coordinates (x,y) and the object coordinates (X,Y,Z) for each point. First we calculated a backward intersection for each picture to determine the outer orientation (perspective center and rotation). Second a regular point raster was calculated in dependency of the local coordinate system and the coordinates of the ground control points. So we estimated approximated coordinates for each point of the DEM on the Island. With the known orientation of the pictures a backward intersection was calculated for each point of the DEM so approximately positions for the point could be found in the images. After detecting the correct position of the point in all possible pictures a forward intersection was implemented as a least square adjustment to get 3D-coordinates for each point of the DEM. The output dataset consists of all calculated coordinates, the standard deviation with a confidence of 68% and the correlation factor for the matching of one point between different pictures. The elimination criteria were the correlation factor which had to be better than 0.7 and also the standard deviations of the coordinates which had to be less than 1.0 m.

## Results

Figure 3.1-2 shows the triangulated DEM with an accuracy of the coordinates of each point better than 1.0 m and with a confidence interval of 68%. Polygonal lakes are easy to distinguish, because the algorithm was not able to match over the uniform water surface. Also areas with bad data coverage are recognizable, for example in the upper part of Figure 3.1-2. The main reason for this was the



helicopter height which changed very fast during the registration of the subsequent pictures. So the scaling factor between these pictures is also changing and the matching gave depressed correlation factors. Other reasons are bad illumination conditions and not enough contours for degraded correlation. So the correlation factors were mostly lower than 0.5. Only a few points are found and calculated with a correlation factor better than 0.7.

**Figure 3.1-2:** Triangulated DEM of Samoylov Island

The center of the island and the lower part of the picture in Figure 3.1-2 have the best coverage of points. The helicopter was flying over the center of the island in a nearly constant height of 600 m. Also the height of the balloon over the flood plain of the island (lower part in Figure 3.1-2) was nearly constant so that the calculations were really successful. The estimated points from both datasets could be matched with correlation factors up to 0.99.

Nevertheless there are possibilities to improve the results, such as the use of more and smaller ground control points concomitant with a lower flight height and thus a higher resolution and accuracy. Furthermore the standard deviation of the coordinates improves, if the points can be found in more than 2 pictures. Therefore a sufficient coverage with aerial images of the whole island is desirable.

### **3.2 Sensitivity of the permafrost system's water and energy balance under changing climate: A multi-scale perspective**

*Julia Boike, Konstanze Piel, Marita Scheritz and Moritz Langer*

#### **Objectives**

Main objective are the energy exchange processes in the complex Arctic landscape at different scales, from meters to kilometers. This includes processes of heat transfer as well as the water cycle. The improved spatial understanding of these processes will allow us to close the gap between small scale field measurements and larger scales which are accessible to satellite remote sensing. Thus the focus of the research group rests upon: (i) establishing spatial and temporal linkages between water and energy fluxes at the plot and landscape scales of different permafrost affected ecosystems; (ii) developing a process-oriented model for typical Arctic permafrost systems to predict subsurface processes (soil water and heat).

#### **Methods**

Field work (July to September)

- The already established instrumentation on soil thermal and hydrologic dynamic and micrometeorology was controlled and data retrieved. Defect sensors were replaced and some sites were supplemented by new probes.
- The new Eddy Covariance System which has been established during the expedition in April was shifted to a new location. This modification was done due to possible interferences from of the microclimate tower and the wind generator. The Licor-System, for measuring H<sub>2</sub>O and CO<sub>2</sub> fluxes, was mounted during the expedition time.
- Balloon based aerial pictures were made due to photogrammetric mapping of the island. Therefore a local coordinate system was established and ground control points were installed all over the island. Furthermore all measurement sites were mapped by terrestrial leveling.
- Water table measurements of polygonal lakes were continued and expanded.
- Soil water flow experiments were made by pump trials.
- Long and short wave radiation scanner system was installed for measuring small scale variations of surface temperature and reflectance.
- Continual measurement sites of soil surface temperature and moisture were established along the scanner track.
- Surface elements of the polygonal tundra were mapped based on vegetation units and spectral characteristics (spectrometer measurements).

- Heat and water diffusion experiments were done on different soil samples; density and porosity were determined by simple field methods.
- Soil samples were taken for further more accurate laboratory experiments.



**Figure 3.2-1:** Radiation Scanner System for measuring differences in the outgoing short and long wave radiation. The scanner track is 10 meters long and crosses two adjacent polygons. Soil temperature and soil moisture probes underneath the scanner track observe differences in ground heat fluxes.



**Figure 3.2-2:** Metreological station for the observation of standard climate parameters like air temperature, humidity, soil surface temperature, wind speed and direction, precipitation and snow height.

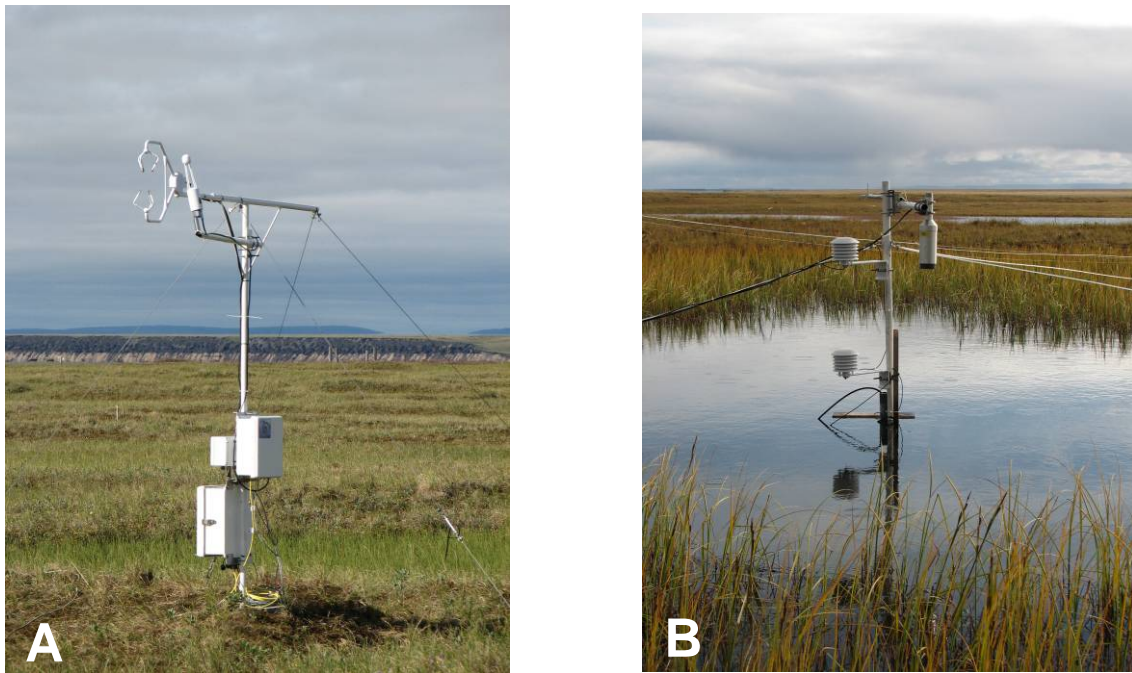


**Figure 3.2-3:** A: Eddy covariance system for observing sensible and latent heat fluxes. The system is equipped with a three dimensional sonic anemometer and an open path gas analyser unit which is capable for measuring  $H_2O$  and  $CO_2$ .

B: Metrological lake station for the observation of energy balance components of polygonal lakes. The Station detects air and water temperatures at different heights and water depth respectively. Radiation balance of the lake is observed at different positions with net radiometers. Lake level and snow height are measured with a sonic ranging sensor.

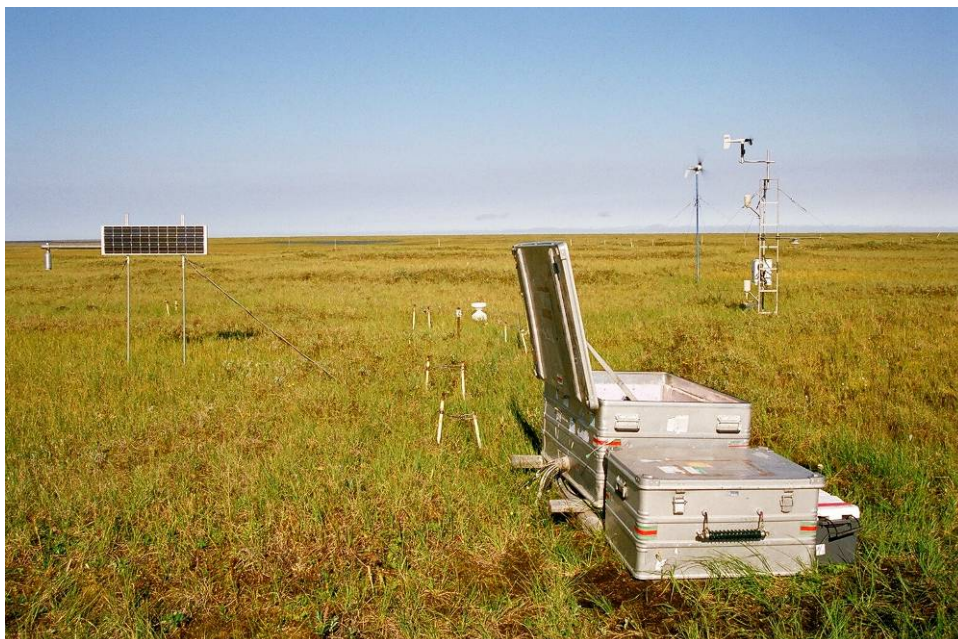


**Figure 3.2-4:** The soil station consists of 32 temperature sensors and 20 soil moisture probes. The station provides data of the ground thermal regime since 2002.

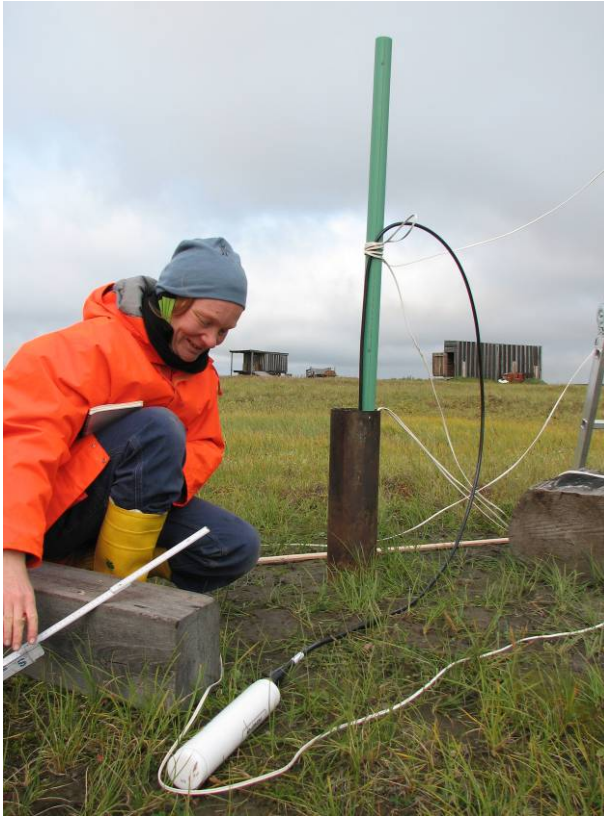


**Figure 3.2-5:** Soil temperatures are measured by 24 sensors up to a depth of 26.8 m with the borehole temperature chain.

### 3.3 Microbial studies on nitrification from permafrost environments

*Tina Sanders, Claudia Fiencke and Eva-Maria Pfeiffer*

#### Introduction

Nitrogen as well as carbon cycling in arctic ecosystems is dominated by physical and biogeochemical controls which are unique to the generally cold-dominated environment. Drastic seasonal fluctuations in temperature, a short growing season, cold soil temperature and the occurrence of permafrost are some of the obvious physical controls on nitrogen cycling and biological activity. Most of the nitrogen accumulates in the organic substance in response to low soil temperatures, excessive soil moisture and low soil oxygen concentration (Gersper et al., 1980, Marion and Black, 1987; Nadelhoffer et al., 1991, Schimel et al., 1996). Standing crop in tundra vegetation store about 2 times more nitrogen than temperate grasslands (Van Cleve and Alexander, 1981) but through the low N-mineralisation rates and lack of N-input by N-fixation and N-pollution the soils are nitrogen deficient and rely to a large extent on internal recycling (McCown, 1978).

N-cycling in the soil is crucial for growth of plants and microorganisms. Imbalances in N-cycling due to nitrate leaching, nitrogen oxide release and increase the methane emission (Adamsen and King, 1993; Carini et al., 2003). Most of the N-transformations were catalyzed by microorganisms.

Nitrification, the microbiological oxidation of ammonia to nitrate via nitrite, occupies a central position within the terrestrial nitrogen cycle. Aerobic chemolithoautotrophic ammonia and nitrite oxidizing bacteria (AOB and NOB) represent the most important group of nitrifying bacteria (Fiencke et al., 2005). As a result of nitrate and acid formation, the nitrification process has various direct and indirect implications for soil systems. It increases the loss of soil nitrogen due to leaching of nitrate and volatilization of nitrogen gases directly or by denitrification. As a result the nitrogen supply to plants is influenced.

Recently, it has been detected that beside bacteria (AOB) also archaea (AOA) participate in the process of ammonia oxidation as they have been found in different soils and habitats (Nicol and Schleper, 2006; Leininger et al., 2006). One representative specimen of the AOA was cultivated in enrichment culture (Könneke et al., 2005). In some habitats more archaea than bacteria genes were detected (Leininger et al., 2006). At this moment it is not definitely clear which group of microorganisms take the decisive role in the N-cycle.

Generally, nitrifying bacteria are found in the upper layer of soils, especially the rhizosphere where organic matter is mineralized, and ammonia and oxygen are present. But the slow growth rates and difficulties in recovering pure cultures have hampered cultivation-dependent approaches to investigate the number, community composition and dynamics of nitrifiers in soil. The number and turn-

over rate is therefore determined by traditionally methods like most-probable-number (MPN) technique and activity tests.

### Material and Methods

Field investigations on nitrification were carried out on Samoylov in July and August 2007. Soil samples were taken from two polygons, at the polygon rim and polygon center, at 3 depths (0-5, 5-15, 15-25 cm) (Figure 3.3-1 A and B). From the fresh samples potential ammonia oxidizing activities were measured at about 4 to 6°C for 32 days by ISO DIN 15685. This ISO standard is normally used for activated sludge and soils in moderate climates. So a modified method was developed which takes the conditions in permafrost soils under consideration. For the ISO-method 25 g of fresh soil sample in 100 ml medium with 0,75 mM ammonia sulfate as substrate is used. In the adapted method less soil sample (5 g) is used and both ammonia and nitrite as substrate are applied. Therefore in the modified activity tests beside the potential ammonia oxidation, the second step of nitrification, the nitrite oxidation was measured.



**Figure 3.3-1:** A: Soil sample polygon rim; B: Soil sample polygon center

The microbial DNA of the fresh polygon samples was isolated by PowerSoil DNA Isolation kit and was transported to University of Hamburg. The DNA isolated in Siberia will be compared to the DNA isolated after transportation. In this DNA mixture screens for bacteria, archaea and ammonia oxidizing organisms will be carried out. The screening will be performed by fingerprint analysis denaturing gradient gel electrophoresis (DGGE) with probes against their key enzymes and 16S rRNA. Furthermore it is planned to adapt the method of real time PCR to quantify the gene copies of ammonia oxidizing bacteria and archaea.

After transportation of frozen and unfrozen soil samples, measurement of cell numbers of nitrifiers by the most probably number test (MPN) and further activity tests at different temperatures are planned. Enrichment and isolation of the ammonia oxidizing bacteria and archaea will be carried out under low temperatures and by use of small concentrations of substrate. To enrich archaea, growth of bacteria will be inhibited by addition of the antibiotic streptomycin.

The main aim is to understand how nitrification takes place in Permafrost soils of the arctic tundra and to clarify if ammonia oxidizers of the domain Bacteria or Archaea dominate.

### Preliminary results

In fresh soil samples of the polygonal tundra, potential ammonia oxidation was measured by ISO DIN 15685-test. During the test period (32 days) ammonia oxidation could only be detected in soil samples from the polygon rim (5-15 cm) (Figure 3.3-2). The other soil samples still offered no or very little activities.

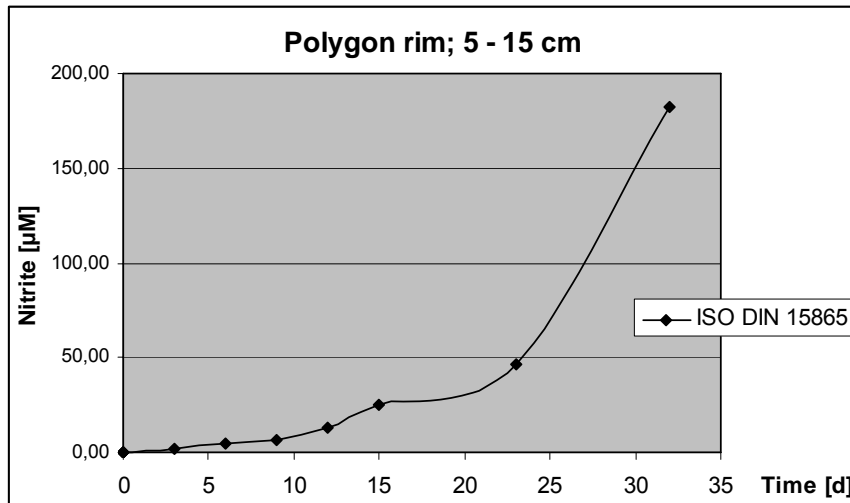


**Figure 3.3-2:** Potential ammonia oxidation activity in soil samples of the polygon rim at 5 – 15 cm measured by test ISO DIN test. This means an activity of 50.1 ng N-nitrite/g dw\*h.

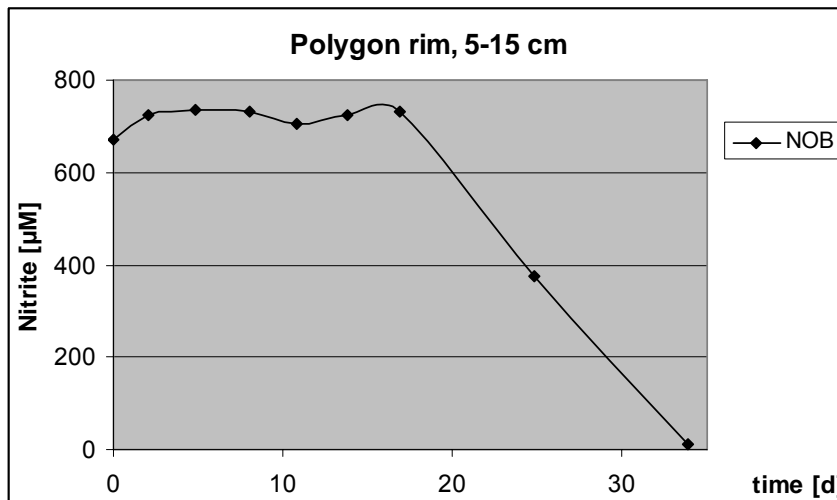


**Figure 3.3-3:** Potential nitrite oxidation activity in soil samples of the polygon rim at 5 – 15 cm measured by the modified method. This means an activity of 147.9 ng N-nitrite/g dw\*h.

In the modified approaches no ammonia oxidation but nitrite oxidation activities were detected. In the samples of the polygon rim (0–5 cm and 5–15 cm) and polygon center (0–5 cm) a decrease of nitrite was measured. The complete

consumption of nitrite can be shown in the sample polygon rim (5 – 15 cm) (Figure 3.3-3).

The activity tests will be repeated with transported soil samples, the method modified once more and the test adapted as far as possible to situ conditions.

In previous tests on samples from the Lena Expedition 2005 potential ammonia oxidizing activity was shown in all depths of polygon rim and center (Sanders, 2006).

### **3.4 Morphology and properties of recent gelisols and palaeosols of the southern Lena Delta, Siberia, Russia**

*Sebastian Zubrzycki, Anastasia Germogenova and Eva-Maria Pfeiffer*

#### **Introduction**

Permafrost-affected soils (Gelisols or Cryosols), which cover nearly one fourth of the terrestrial surfaces in the northern hemisphere play a major role in the global carbon cycle. About 14 % of the global organic carbon is stored in permafrost soils and sediments. Spatial distribution and genesis of soil types in the southern Lena Delta provide a basis for evaluation of the impact of environmental and climate change on permafrost landscapes. Based on an existing soil map of Island Samoylov of the year 2005 additional soils studies have been carried out during the expedition Lena 2007.

#### **Investigation area**

The investigation sites are located on Island Samoylov and Island Kurungnakh. The islands are situated at one of the main Lena River channels, the Olenyokskaya Channel in the southern part of Lena Delta. The Lena Delta is at the north coast of Siberia, where the Lena cuts through the Verkhoyansk Mountains Ridge and discharges into the Laptev Sea, which is part of the Arctic Ocean.

The Island Samoylov can be divided into two major geomorphological units. There is a relative young floodplain in the western part that is annually flooded in spring and a higher-elevated river terrace of Late Holocene age, the 'first' terrace in the eastern part. The first terrace is flooded only during extreme high water events (Kutzbach, 2006).

The Island Kurungnakh belongs to the third river terrace complex of the Lena Delta. The third terrace is the oldest in the delta. It was formed in Middle and Late Pleistocene (Kuzmina et al., 2003; Wagner et al., 2003). This terrace forms autonomous islands along the Olenyokskaya and Bykovskaya Channels. The Island Kurungnakh is located at the southeastern end of Olenyokskaya Channel (Schwamborn et al., 2002).

The climate in the Lena Delta is true-arctic, continental and characterized by low temperatures and low precipitation. The mean annual air temperature, measured by the meteorological station in Tiksi located about 110 km to the south-east directly at the coast of the Laptev Sea, was -13.6°C (7.5°F) during the 30-year period 1961...1990; the mean annual precipitation in the same period was 319 mm. The average temperatures of the warmest month August and the coldest month January were 7.1°C (44.8°F) and -32.4°C (-26.3°F), respectively (Roshydromet, 2007), demonstrating the extreme climatic contrasts between the polar day and polar night for continental Polar Regions.

## Objectives

The goal of this study is to compare recent cryosols with palaeosols of deeper sediment layers of the Islands Samoylov and Kurungnakh.

Morphological and analytical data are taken into account to understand the properties and genesis of the buried soils of the ice rich permafrost sediments and recent soils in the southern Lena Delta.

A special consideration is put on different pedogenic formed iron-oxides. Research of different iron-oxides helps to estimate the conditions during which active pedogenesis took place. Palaeosols are often characterized by their iron-oxides fractions and data facilitates an estimate of the relative age of a given soil-sequence.

## Material and Methods

The main soil unit of the first terrace above the floodplains of Island Samoylov is covered mainly by the soil-plant-complex Glacic Aquiturbels/ Typic Historthels. The Typic Historthels are Gelisols that have in 30 % or more of the pedon more than 40 %, by volume, organic materials from the surface to a depth of 50 cm (Soil Survey Staff, 2006). They are situated in the depressed centers of low-centred ice-wedge polygons characterized by a water level directly at the soil surface and predominant anaerobic accumulation of organic matter. The Glacic Aquiturbels are situated at the elevated borders of the polygons and are characterized by a distinctly deeper water level, lower accumulation of organic matter, and pronounced cryoturbation properties. So Glacic Aquiturbels are Gelisols that have one or more horizons showing cryoturbation in the form of irregular, broken, or distorted horizon boundaries, involutions, the accumulation of organic matter on top of the permafrost, ice or sand wedges, and oriented rock fragments. They have within 50 cm of the mineral soil surface, redox depletions with chroma of 2 or less and also aquic conditions during normal years and a glacic layer with its upper boundary within 100 cm of the mineral soil surface (Soil Survey Staff, 2006).

Close to the erosion cliffs various dryer and sandy soil complexes such as Psammorthels and Psammoturbels are typical. That means soils that have less than 35 %, by volume, rock fragments and a texture of loamy fine sand or coarser in all layers within the particle-size control section (Soil Survey Staff, 2006). Thermal erosion leads in that erosion cliff area to formation of high-centred polygons which are often covered by aeolian sands.

On Kurungnakh similar Glacic Aquiturbels and Aquic Histurbels as on Samoylov are typical. These recent soils are compared with paleosols such as Histels of different decomposition, iron-rich Aquorthels and Aquiturbels of exposures on both islands. For investigations of soils two exposures of 7.10 and 5.40 m thickness were selected on Island Samoylov (Figure 3.4-1) and as well as two on Kurungnakh.

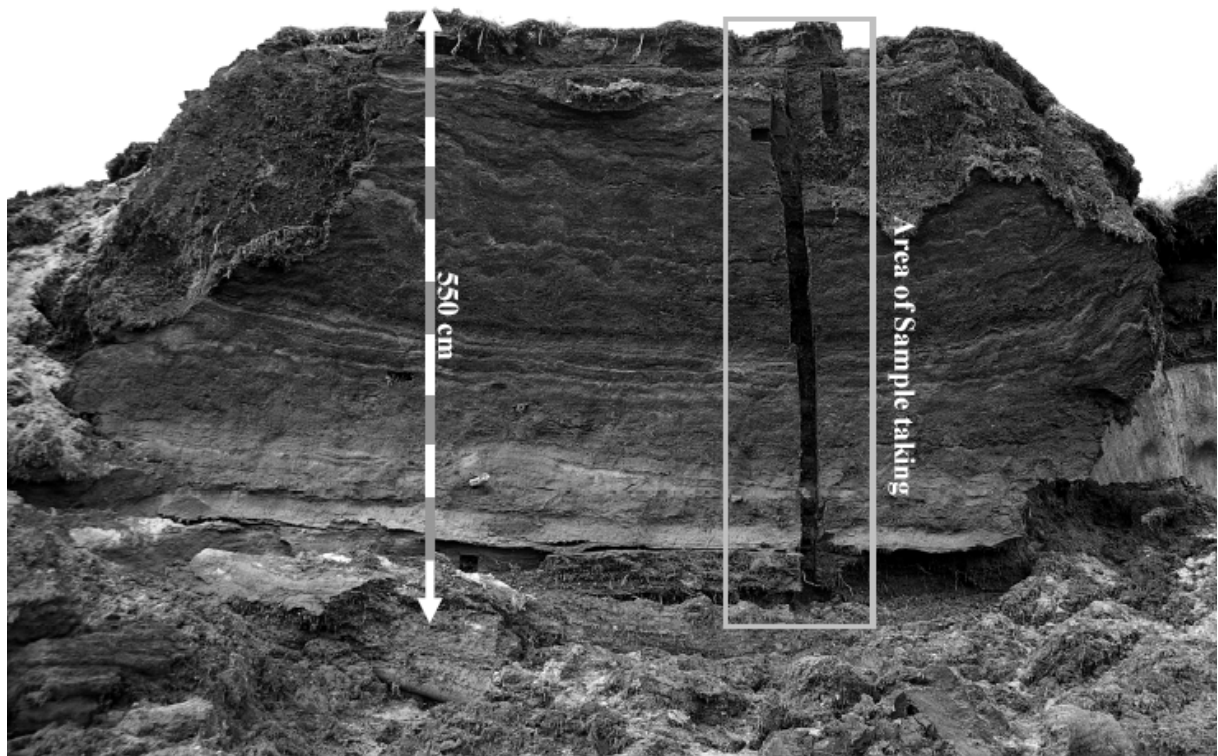


**Figure 3.4-1:** Exposure on Island Samoylov.

On Kurungnakh it was possible to collect samples of different age of genesis; from 2.500 to 40.000 years BP; of exposures of 12 and 30 m thickness. Samples of recent soils have been taken from the active layer as well as of palaeosols from above mentioned exposures. Additional, on Island Samoylov two soil-cross-sections of a high-centered and a low-centered polygon were investigated and compared with the recent soils of Island Kurungnakh.

Samples were collected from single layers of individual exposures. First pedological descriptions of Munsel-Color, hydromorphic features, bulk density, organic substance, roots,  $\text{CaCO}_3$  and fresh weight were done in field.

The oxalate-extractable iron ( $\text{Fe}_o$ ) will be determined by the method of Schwertmann (1964) at room temperature, darkness with acid ammonium oxalate at pH 3.25. The dithionite-extractable iron ( $\text{Fe}_d$ ) will be determined by the DCB method of Mehra & Jackson (1960) with dithionite-citrate buffered by bicarbonate at pH 7.3. Iron in all extracts will be determined by ICP-Emissions-Spectrometer. To make an estimate of the relative age of a soil-horizon using analysis of different forms of Fe, the following fractions will be used:  $\text{Fe}_o$  as “active” Fe-oxides, probably ferrihydrit,  $\text{Fe}_d$  minus  $\text{Fe}_o$  as Fe in less “active” well crystallised form, probably goethite and the ratio  $\text{Fe}_o/\text{Fe}_d$  as a degree of activity and pedogenesis.

### 3.5 Long-term studies on methane fluxes from permafrost ecosystems

*Dirk Wagner, Jürgen Joseph, Anastasia Germogenova, Maryvone Landolt and Joseph Zeyer*

#### Introduction

The Arctic plays a key role in the Earth's climate system for two reasons. On one hand, global warming is predicted to be most pronounced at high latitudes, and observational evidence over the past 25 years suggests that this warming is already under way (Serreze et al., 2000; Richter-Menge et al., 2006). On the other hand, one third of the global carbon pool is stored in ecosystems of the northern latitudes (Post et al., 1982; Gorham, 1991). Thus there is considerable socio-economic interest in predicting how the carbon balance of the northern ecosystems will respond to ongoing climate warming.

Global warming will have important implications for the functional diversity of microbial communities in these systems. It is likely that temperature increase in high latitudes may stimulate microbial activity and carbon decomposition in Arctic environments and are accelerating climate change through the increase of trace gas (CH<sub>4</sub>, CO<sub>2</sub>) release (Melillo et al., 2002; Zimov et al., 2006).

The microorganisms, which are the drivers of methane production and oxidation in Arctic wetlands, have remained obscure. Their function, population structure and reaction to environmental change, which are important parts of the process knowledge on methane fluxes in permafrost ecosystems, are largely unknown (Wagner, 2008). This hampers prediction of the effects of climate warming on arctic methane fluxes, in particular when these predictions are based on models that do not take into account the specific nature of microbial populations in permafrost soils and sediments. Understanding these microbial populations is therefore highly important for understanding the global climatic effects of a warming Arctic.

Under the umbrella of the Russian-German Cooperation SYSTEM LAPTEV SEA a multidisciplinary research concept was developed and since 1998 applied on the Arctic methane cycle that connects methane flux measurements with studies on microbial processes and communities (cp. Wagner, 2007). During the expedition LENA 2007 methane fluxes were measured, microbial methane oxidation under in situ conditions were studied, and samples from different permafrost ecosystems were taken for further molecular ecological analyses. In particular, the objectives of the field campaign were:

- To measure methane fluxes from polygonal tundra on Samoylov and Kurungnakh islands.
- To characterize soil ecological parameters determining microbial processes in permafrost ecosystems.
- To gain more insights into the control functions of methane oxidation as the major sink for methane.

## Field Work

Daily measurements of methane emission, thaw depth and soil temperature were determined from July 6 to August 25, 2007 at the long-term study site on Samoylov Island. Additional measurements of methane fluxes from wet polygon tundra were carried out on Kurungnakh Island (N 72°19; E 126°13). The used method and the main investigation sites were described previously (Wagner et al., 2003).

In addition to the close chamber measurements of methane fluxes a new system for passive soil air sampling called GASSYS (KaiserGEOconsult GmbH, 2005) was installed in the active layer (horizontally) and the perennially frozen ground (vertically) for the determination of in situ methane concentrations in the different horizons of permafrost (Figure 3.5-1). The main feature of this system is a membrane only permeable for gas diffusion, which is mechanically protected by an EVA-tube. When a steady state was reached between the gas phases in the column and the free gases in the soil, samples could be taken by a syringe from the different permafrost depth (chambers depending on column length). The horizontal system consisted of only one chamber containing tube and was implemented 25 cm below the surface. The vertical system was installed in a borehole down to 5.60 meter permafrost depth. After reaching a plateau in the chamber pressure curve samples were frequently taken. To learn more about the minimal possible measuring intervals in permafrost soils, pressure gradient decrease experiments were executed. First sample measurements in the vertical system showed high methane (> 20%) concentrations.



**Figure 3.5-1:** Methane gradient analysis in the perennially frozen ground: A: study site on Samoylov Island, Lena Delta; B: tube of the installed GASSYS system for gas sampling and C: pressure measurements.

To gain more information about the activity of methane producing and methane oxidizing microorganism, vertical methane profiles were measured and dissolved organic carbon (DOC) were analyzed for the polygonal centre and rim. Soil methane gradients were measured using brass probes attached to a Luer-

lock three-way stop cock. Every 5 cm a probe was set until the permafrost table was reached. Gas samples were taken by a syringe and directly analyzed by gas chromatography in the field lab. Further details of the gas analyses were described previously (Wagner et al., 2003). DOC was extracted from soil samples of two vertical profiles. Each 5 cm fresh soil material (9 g) was taken to a depth of 30 cm for the polygon centre and to a depth of 40 cm for the polygon border. The samples from each layer were weight into glass flasks (50 ml) and mixed with 45 ml distilled water. The flasks were closed and shaken for 2 h in darkness. Afterwards the suspension was filtered (mesh 0.45  $\mu\text{m}$ , Gelman Science) and the clear solution was inactivated by the addition of sodium acid. Samples where taken with a syringe and stored in salt tubes with a defined  $\text{N}_2$  volume for later analyses in the home lab.

### 3.6. A high resolution orthorectified picture of Samoylov

*SPARC group (Julia Boike, Bob Bolton, Maren Grüber, Moritz Langer, Sina Muster, Konstanze Piel, Torsten Sachs, Günter Stoof, Sebastian Westermann) and Marita Scheritz*

A high-resolution picture of the island Samoylov was needed for the classification of vegetation and surface characteristics and hydrologic modeling. This image was created using aerial pictures with a resolution of 0.5 m/pixel and standard photogrammetry software.

The field work for obtaining the aerial pictures from balloons or helicopter flights is described in Chapter 3.1. Furthermore, Scheritz et al. (2008) describe in detail the method for creating the digital elevation model, including camera calibration, ground survey and photogrammetric analysis.

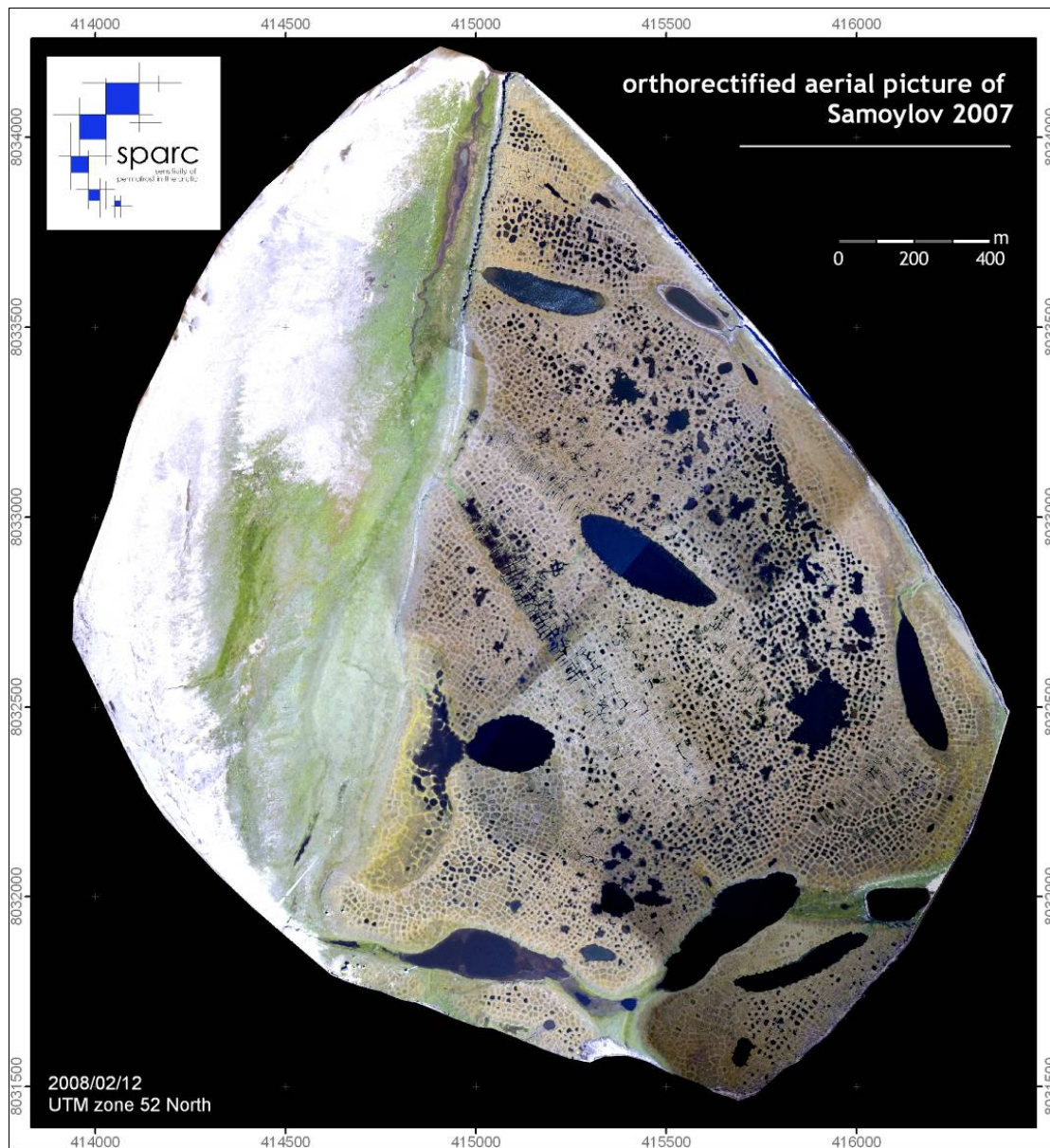


**Figure 3.6-1:** Orthorectified aerial picture of Samoylov Island 2007.

### 3.7. Hydrobiological investigations in the Lena River Delta

*Irina Vishnyakova and Ekaterina Abramova*

#### Introduction

Low species composition and short food chains are typical for polygonal lakes as well as for most arctic ecosystems. Caused by freezing to the bottom in winter the distinguishing feature of polygonal lakes is the absence of fishes as characteristic predators for most other types of water pools. The benthic organisms are not abundant, among them the amphibiotic insect larvae, nematodes and ostracods are dominant. Predatory planktonic crustaceans and water birds are terminal links in food chains. The low predator press and good adaptation of zooplankton organisms to the evident variations of abiotic conditions cause active zooplankton development, which plays a significant role in organic, mineral and energy fluxes in polygonal lakes and in the whole Lena Delta ecosystem. Given that these polygonal lakes are not exposed to direct anthropogenic pollutions, investigations on them could also be used as model objects of natural water ecosystems. This hydrobiological investigations in polygonal lakes are part of a monitoring in the southern part of the Lena Delta River within the expedition "Lena - New Siberian Islands 2007" and are carried out for obtaining detailed data about different aspects of zooplankton existence: species composition, seasonal and inter annual dynamic of quantitative characteristic, ecology and dominant species life circles.

#### Materials and methods

190 qualitative and quantitative zooplankton samples were gathered from the beginning of July to the end of August in summer 2007. For these monitoring hydrobiological investigation we divided all polygons into water of two types: shallow (0,2-0,6 m depths, partly or completely vegetated by *Carex sp.* and *Arc-tophilla sp.*) and deep polygonal lakes (1-1,5 m, without vegetation). The investigations had been carried out in 6 polygonal lakes (3 deep and 3 shallow ones – the same as last year) on Samoylov Island (Figure 3.7-1) and episodically in 11 polygonal lakes on other islands of southern parts of the Delta. The lake water of both types was transparent, the reaction of water was neutral (pH = 6,5-7). Temperature stratification was almost absent, average monthly temperature varied from 12,2 to 12,7°C in July and from 10,4 to 11°C in August.

Zooplankton samples were collected with a periodicity of 5-7 days. Sampling was performed by filtering 50-100 liters of water through an 80-µm mesh size net from the shore of the polygons. A rubber boat was used for sampling from the centre of the lakes. There, a 100-µm mesh size small hand net was extended from the bottom to the surface. Samples were fixed with 70% alcohol or 4% borax-buffered formalin. For statistic calculations, 3 samples from each polygon were collected concurrently. At the same time, the water temperature was measured at the bottom and in surface layers. Also, data on the pH of water, depth and size of each polygon were obtained.

Zooplankton samples were analyzed in a Bogorov chamber under the binocular microscope MBS-10. Species, sex and moulting stages of each zooplankton organism were determined, abundance of organisms was calculated. For calculation of individual wet weights of organisms the formula  $W = ql^b$  was used ( $W$  = body weight,  $l$  = body length in mm,  $q$  = weight at 1 mm body length,  $b$  = index). Data were recalculated to 1 m<sup>3</sup> of water.

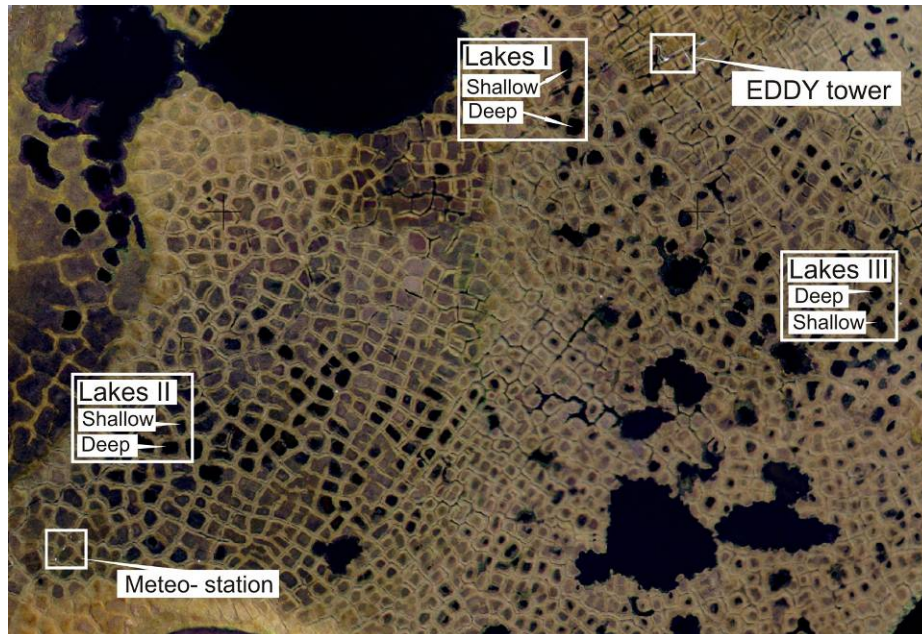


**Figure 3.7-1:** Polygonal lakes of Samoylov Island are objects of monitoring hydrobiological investigations.

### Preliminary results

Same as in our previous investigations qualitative and quantitative characteristics of the zooplankton were similar in all studied polygonal lakes. The seasonal dynamic of abundance and biomass recurs from year to year with small variations in period. Usually three to five maximums of abundance and biomass were noticed for polygonal lakes. The development of zooplankton populations begins directly after ice melting, which occurred in 2007 in the middle of May.

One well pronounced peak of total abundance and biomass was fixed over the period of investigations (July-August) in polygonal lakes of both types. A correlation between quantitative characteristics and water temperature wasn't noticed.

In the following we review in details the structures and dynamics of zooplankton populations of the two polygonal lake types (shallow and deep), where we carry out investigations for more than 5 years.

The zooplankton communities consisted of Cyclopoida and Calanoida populations. The *Leptodiatomus angustilobus* dominated during the whole period of investigations. The crustaceans of this species composed about 90 % from the total zooplankton abundance in some samples. The young copepodite stages

(CI-III) of *Diaptomus sp.* and Cyclopoida families (*Cyclops sp.*, *Eucyclops sp.* and *Acantocyclops sp.*) were abundant at the beginning of studies (early in July). Individuals of Cyclopoida species matured to copepodite stages IV-V by beginning of August (Figure 3.7-2 A).

The populations of Cyclopoida were represented by numerous CIV-V stages by the middle of August and during the rest of observation in all studied lakes. The Copepodits of IV-V stages were dominant in Calanoida populations in the beginning of August. Calanoida populations were consisted entirely of adult males and reproducing females with eggs by the middle of august (Figure 3.7-2 B).

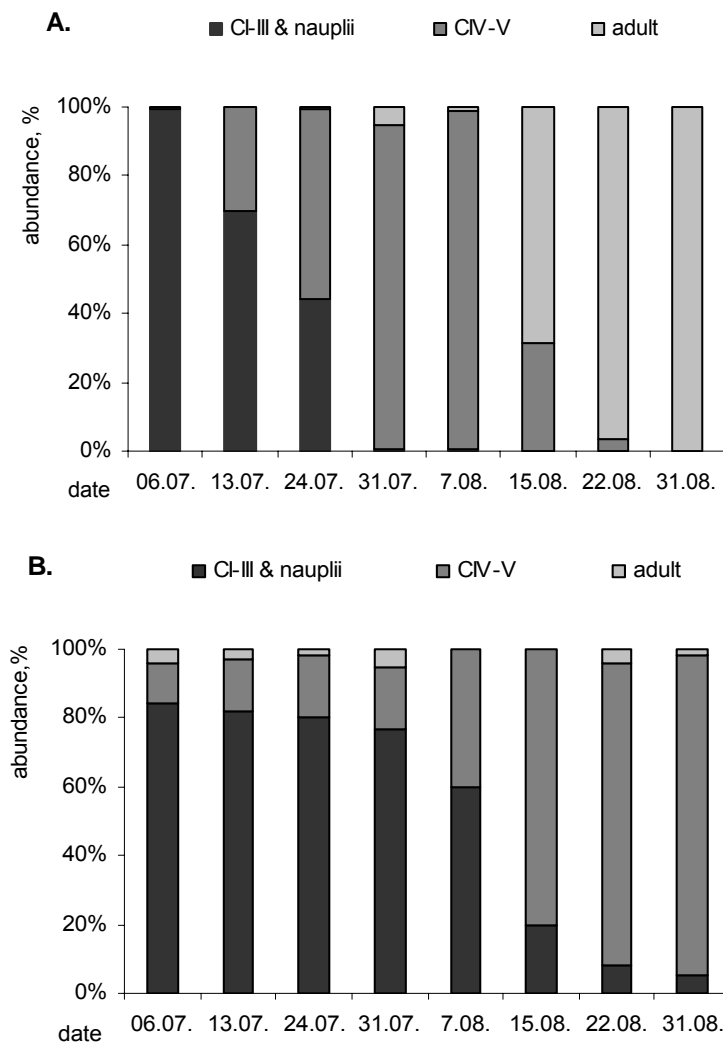


**Figure 3.7-2:** The population's age-structure of *Leptodiaptomus angustilobus* (A.) and Cyclopoida (B.) in the deep polygonal lake I, summer 2007.

The abundance of *Daphnia pulex* was low during the whole summer period. It should be mentioned that the adult females of *Daphnia* with efiplas were already noted early in July. Efiplia is the diapausal stage of *Daphnia*, which they form before the beginning of unfavorable conditions.

In the deep polygon the maximum of abundance and biomass (38 222 ind./m<sup>3</sup> and 2,8 g/m<sup>3</sup> respectively) was recorded in the beginning of August at the temperature of 9,1°C. *L. angustilobus* was the most represented species during that period; the main part of this population was composed of CIV-V stages of males and females. The average abundance was the 17825 ind./m<sup>3</sup> and biomass - 1,4 g/m<sup>3</sup> for two months of observations (Figure 3.7-3 A).

In the shallow polygon maximum of quantitative characteristics (abundance - 22111 ind./m<sup>3</sup>, biomass - 1,8 g/m<sup>3</sup>) was marked in the end of July at 16,3°C and was concerned with reproduction of different *Diaptomus sp.* The young copepodite stages of *L. angustilobus*, *Arctodiaptomus angustilobus* and *Mixodiaptomus theeli* (CI-III) composed the main mass of zooplankton community. The average zooplankton abundance for shallow polygon was 118999 ind./m<sup>3</sup>, biomass – 0,9 g/m<sup>3</sup> (Figure 3.7-3 B).

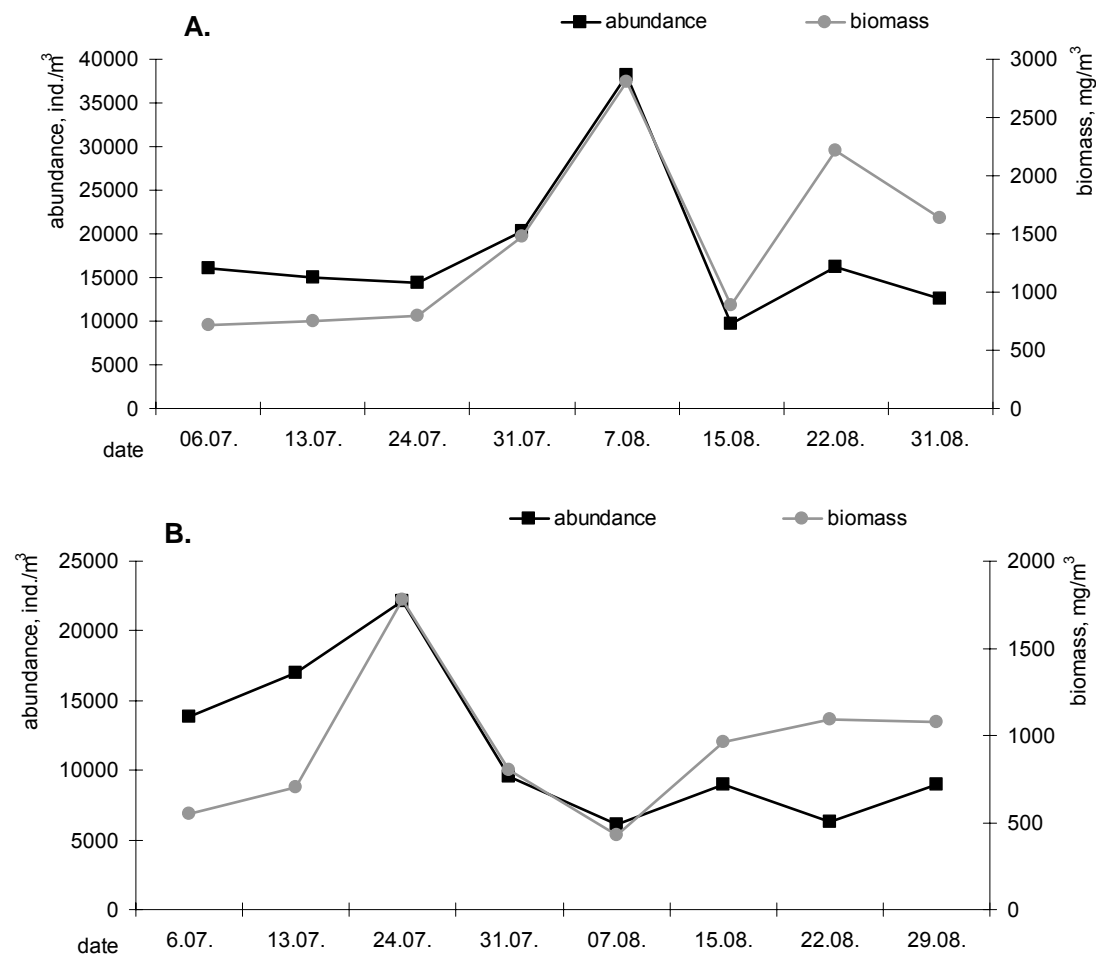


**Figure 3.7-3:** Seasonal dynamic of total zooplankton abundance and biomass in the deep (A) and shallow (B) polygonal lakes I, summer 2007.

## Conclusion

The data about zooplankton species composition, structure and quantitative characteristic' rate of polygonal lakes of the southern part of Lena Delta River obtained in summer 2007 are very similar to our data obtained during previous years (2002-2006). Replacement of periods of dominant species reproduction in time concerned with early ice-melting in lakes and consequently earlier beginning of favorable conditions for zooplankton communities is a distinguishing feature of abundance and biomass dynamic course of zooplankton. Therefore we recorded only one maximum of total zooplankton abundance and biomass (dominant species - *L. angustilobus*) during July-August. Probably 1-2 maximums of qualitative zooplankton characteristics concerned with other dominant species development (*Cyclopoida sp.*, *Heterocope borealis*, *Diaptomus sp.*, *D. pulex*) from the end of May to middle of June – a period that is not included in the investigations.

### 3.8 Hydrological and geomorphological investigations

*Dmitry Bolshiyarov, Alexander Makarov and Raisa Terekhova*

Hydrometrical measurements in the Lena Delta channels are providing new data of water discharge, sediment load and redistribution of flow between the main branches of the delta (Figure 3.8-1, Table 3.8-1). Investigations of this year concentrated in the central part of the delta. The boat "Kazanka 5M" with Johnson 30 engine was used for hydrological measurements and for geomorphological routes. The small ship "Orlan" which is belonging to "Lena Delta Reserve" was used for hydrometric measurements in main channels (Main Stream, Bykovskaya Channel, Trofimovskaya Channel). The point of water level measurements has been founded on Samoylov Island.

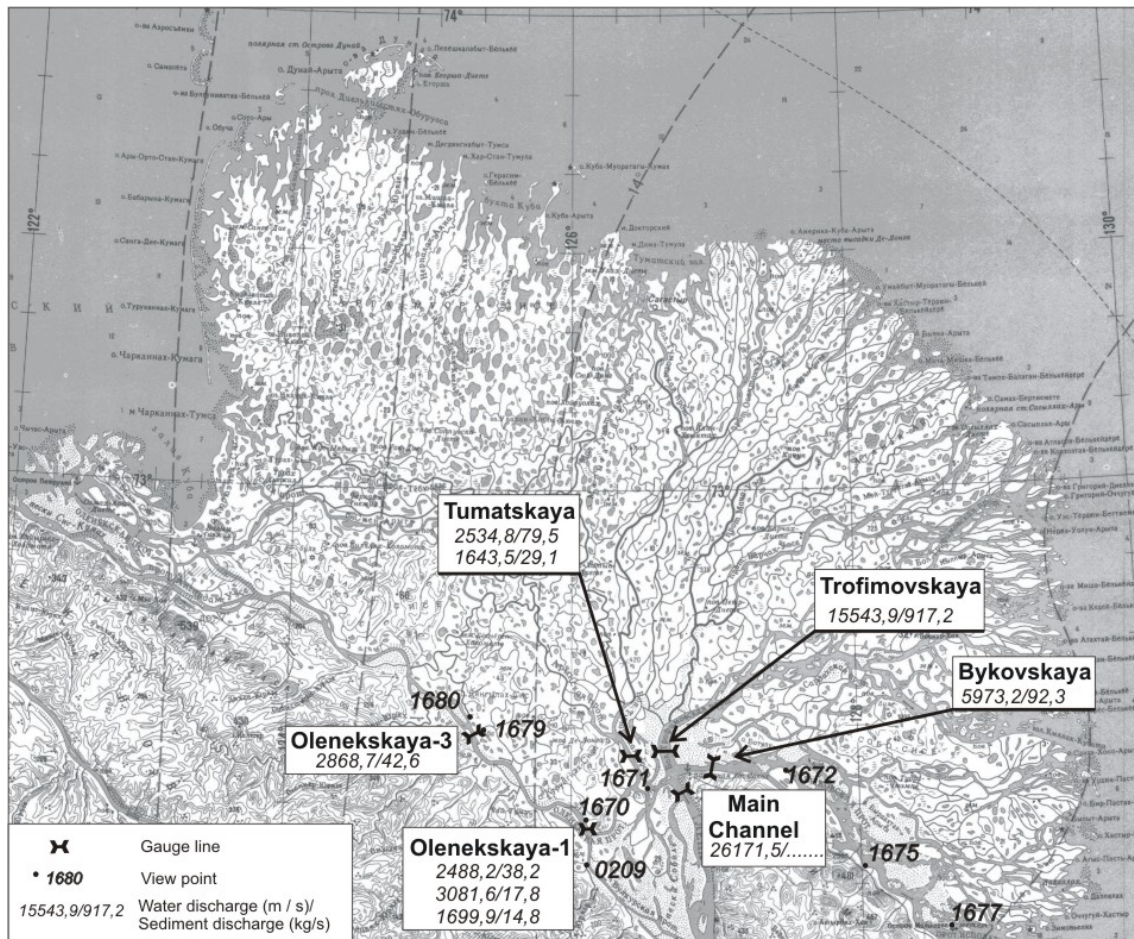


**Figure 3.8-1.** Investigation area

The additional work has been made in Bulkurskaya Channel. The leveling of water table showed a negative inclination of it in the middle of August. It means that water flow is going from Olenekskaya Channel to Bulkurskaya Channel during the low water period.

**Table 3.8-1:** Water discharge and sediment load measured in 2007

Gauge line	Date	Measured water discharge, m <sup>3</sup> /s	Calculated water discharge, m <sup>3</sup> /s	Measured sediment load, kg/s	Mean turbidity, g/l	Water discharge distribution %
Bykovskaya	23.08.2007	5973,2		92,3	0.015	23,5
Main channel	23.08.2007		26171,5			100
Trofimovskaya	23.08.2007	15543,9		917,2	0.078	56,6
Tumatskaya	02.08.2007	2534,8		79,5	0.034	9,7
Tumatskaya	17.08.2007	1643,5		29,1	0.046	6,5
Olenekskaya-3	08.08.2007	2868,7		42,6	0.08	11,8
Olenekskaya-1	02.08.2007	2488,2		38,2	0.069	9,5
Olenekskaya-1	08.08.2007	3081,6		17,8	0.053	11,0
Olenekskaya-1	19.08.2007	1699,9		14,8	0.082	6,5

The aim of geomorphological and geological investigations was to find key sections of the first terrace and take samples for <sup>14</sup>C dating from sediments. One such key cross section is represented on Figure 3.8-2. This cross section illustrates that fact that almost all islands in the Delta consist of different parts, which have different age of formation in spite of height of terraces. These features are very important for the understanding of the Delta formation.

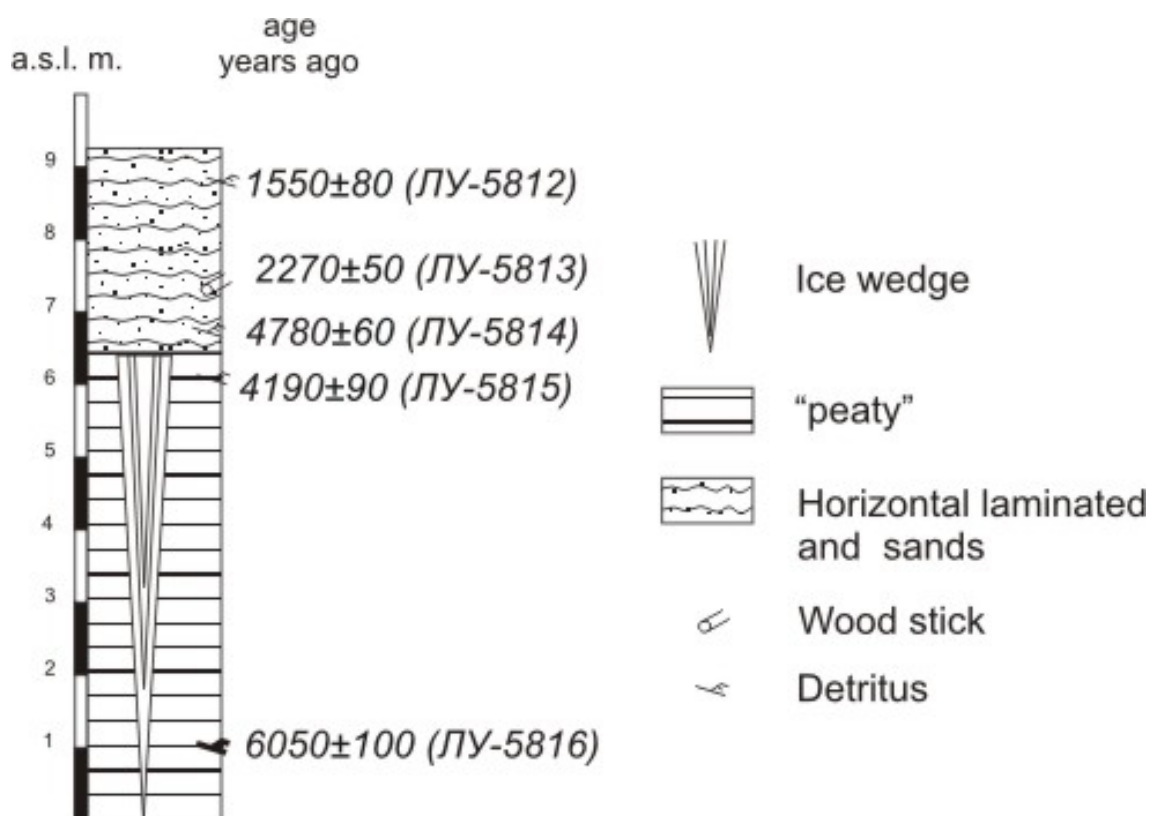


**Figure 3.8-2:** Gusinka outcrop (point 1680. see Figure 3.8-1) is situated: 72°19'27.5" N, 126°16'45.9" E

### 3.9. Studies of coastal dynamics and subsea permafrost

*Paul Overduin, Waldemar Schneider and Mikhael Grigoriev*

#### Introduction and Goals

Following sea level rise during the global Holocene optimum, terrestrial permafrost on the broad coastal plains of Siberia was inundated. Most of the current shelf area is affected by and underlain by relict permafrost. Ice melting, permafrost degradation and coastal erosion continue to affect large regions of the Laptev Sea shelf. The low subsurface temperatures and the low diffusivity of the permafrost have the potential to hold and confine gas and gas hydrates beneath and within the permafrost, as has been observed on the Yamal Peninsula and in the MacKenzie Delta.

Drilling and geophysical sounding of the shallow near-shore sediments of the Laptev and East Siberian Seas show great spatial variability in the depth to the upper bound of ice-bound permafrost and in changes in sediment temperature profile with distance from the shore. The influence of near-shore processes (especially the formation of bottom fast ice and brines, wave action and sediment transport, and thermoerosion) on permafrost and permafrost stability beneath the sea bed require study. To determine the net effect of these processes on the boundary conditions at the seabed for subsea permafrost, the field work undertaken in the nearshore zone of the Bykovsky Peninsula includes:

1. repeated annual surveying of the position of the coastal bluff (shoreline) along the eastern coast of the Bykovsky Peninsula and around the northern end and along the eastern coast of Muostakh Island
2. improving nearshore bathymetry in an area affected by thermokarst processes prior to inundation
3. the deployment of data-loggers to measure temperature, salinity and pressure in the nearshore zone over an annual cycle

#### Data logger deployment

Data loggers were deployed from the "Puteyski 405", a vessel operated by the Yakutian River-going Shipping Office, on August 6, 2007. Loggers were bolted to ca. 50 cm x 50 cm square anchoring plates which had been fitted with anchoring rings, to which 50 m lengths of nylon rope were attached (Figure 3.9-1). Metal anchors were attached to the ends of these ropes. The ship was used to deploy the anchors and logger-plates roughly parallel to the peninsula shoreline west of the data-logger location (roughly NW to SE, Table 3.9-1). To minimize the chances of ice disturbing the data loggers, they were placed in local depressions in water depth, ranging between 4.2 and 7.5 m. Figure 3.9-2 shows the location of the data logger deployments, superimposed on a map of borehole locations, most from 1983. Previous attempts to deploy data loggers on the sea and river bed in the Lena Delta resulted in the loss of all loggers (From Appendix 4.6, Table A4-1, Rachold, 1999)



**Figure 3.9-1:** A data logger, attached to a steel plate fitted with attachment rings for the ropes in the background, on board the “Puteyski 405” in preparation for deployment.

**Table 3.9-1:** Data logger positions, deployed on August 6, 2007

Device	Water depth [m]	Latitude	Longitude
CTD datalogger 1	4.2	N 71° 47' 19.0"	E 129° 25' 46.7"
CTD data logger 2	6.3	N 71° 47' 58.7"	E 129° 32' 56.7"
CTD data logger 3	6.2	N 71° 48' 35.0"	E 129° 38' 30.2"
CTD data logger 4	7.5	N 71° 49' 33.9"	E 129° 46' 26.6"
Water depth logger	10	N 71° 31' 52.3"	E 129° 33' 32.8"

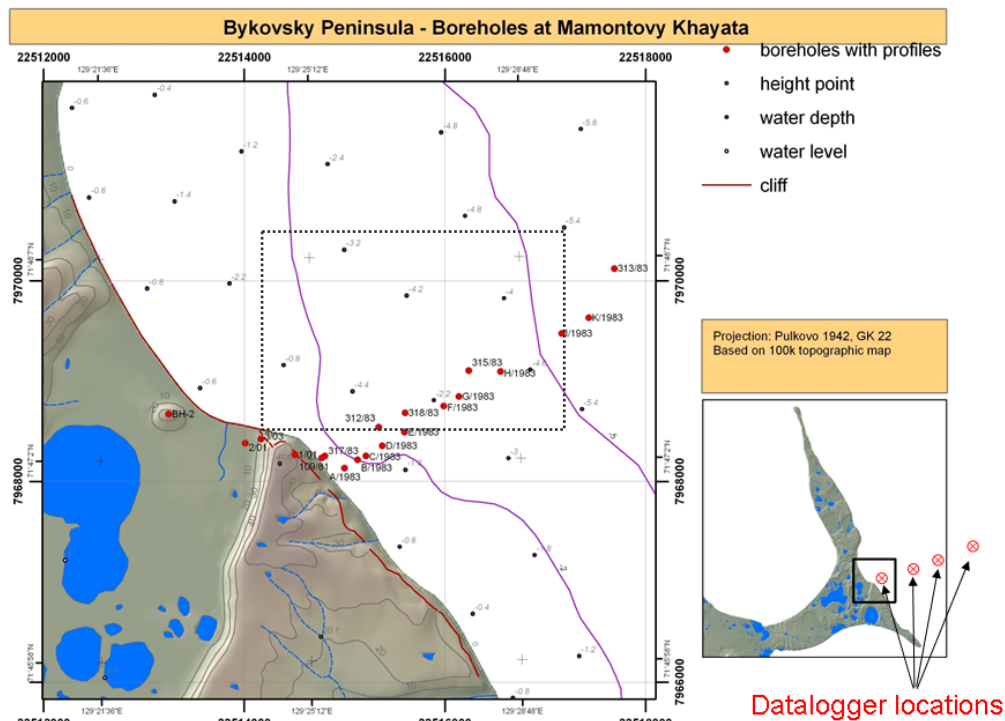


**Figure 3.9-2:** Red circles in the larger map indicate availability of historical data from boreholes. Bathymetry was measured within the area marked by the dashed rectangle. The inset map shows the Bykovsky Peninsula. The black square indicates the outline of the larger map and the red symbols show the locations of the data loggers deployed in 2007. Background map created by Guido Grosse.

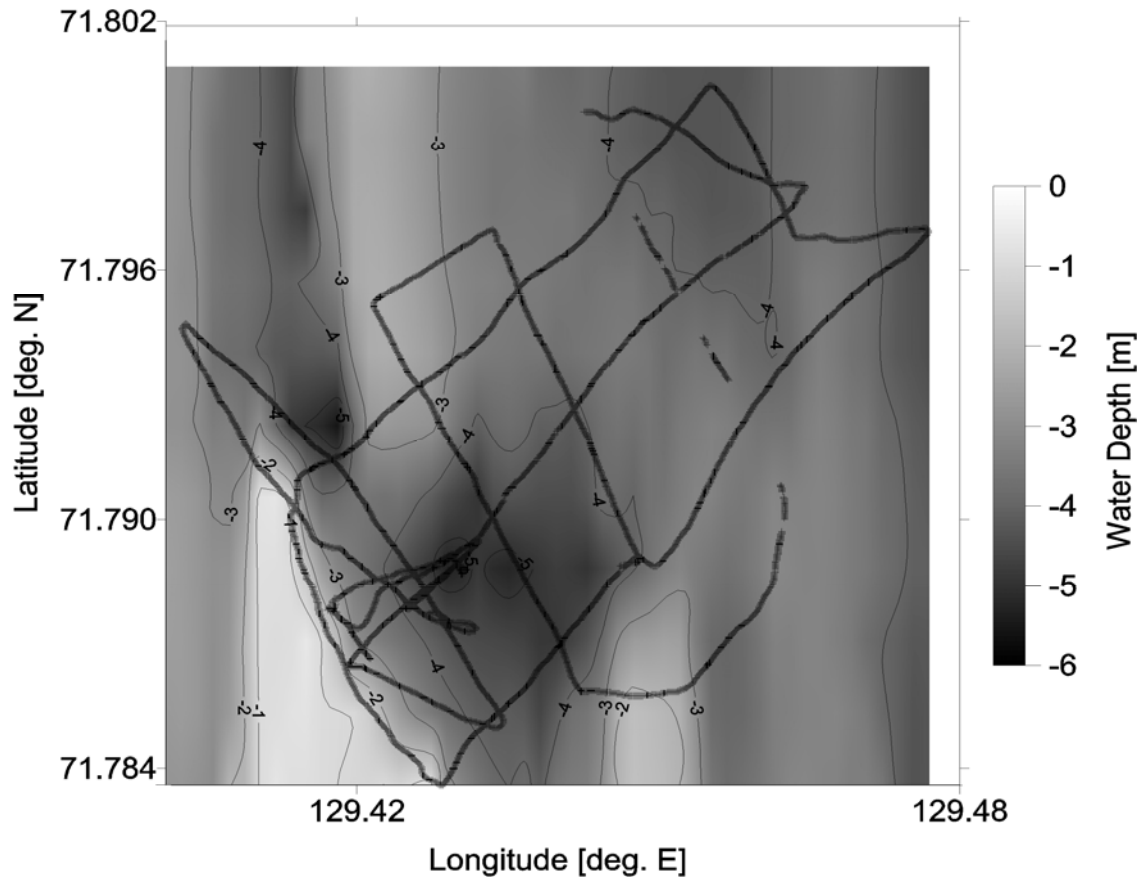


**Figure 3.9-3:** Bathymetry measured in the near-shore zone east of the Bykovsky Peninsula during cruising and logger deployment. A total of 10828 depth values are interpolated. As shown here, the bathymetry is not tide or sea-surface height corrected, and was collected on August 6th and 7th, 2007.

### 3.10 References

- Adamsen, A.P.S. and King, G.M. (1993). Methane consumption in temperate and subarctic forest soils: rates, vertical zonation, and responses to water and nitrogen. *Appl. Env. Microbiol.* 59: 485-490.
- Carini, S.A.; Orcutt, B.N. and Joye, S.B. (2003). Interactions between methane oxidation and nitrification in coastal sediments 20: 355-374.
- Fiencke, C., Spieck, E. and Bock, E. (2005). Nitrifying bacteria. In D. Werner, and W. E. Newton (eds.), *Nitrogen Fixation in Agriculture, Forestry, Ecology, and the Environment*. Springer, The Netherlands, Dordrecht. 12: 255-276.
- Gersper, P.L., Alexander, V. and Barkley, S.A. (1980). The soils and their nutrients. In: Brown, J., P.C. Miller, L.L. Tieszen, F.L. Bunnell (eds.). *An Arctic Ecosystem. The coastal Tundra at Barrow, Alaska*. Stoudsburg: Dowden, Hutchinson & Ross, 219-254.
- Gorham, E. (1991). Northern peatlands role in the carbon cycle and probable responses to climatic warming. *Ecological Applications* 1: 182-195.
- Könneke, M., Bernhard, A. E., de la Torre, J. R., Walker, C. B., Waterburs, J. B. and Stahl, D. A. (2005). Isolation of an autotrophic ammonia-oxidizing marine archaeon. *Nature* 437: 543.
- Kutzbach, L. (2006). The Exchange of Energy, Water and Carbon Dioxide between Wet Arctic Tundra and the Atmosphere at the Lena River Delta, Northern Siberia. *Berichte zur Polar- und Meeresforschung* 541: 1-141.
- Kuzmina, S., Wetterich, S. and Meyer, H. (2003). Paleoecological and sedimentological studies of Permafrost deposits in the Central Lena Delta (Kurungnakh and Samoylov Islands). *Berichte zur Polar- und Meeresforschung* 466: 71-81.
- Leiniger, S., Urich, T., Schloter, M., Schwark, L., Qi, J., Nicol, G.W., Prosser, J.I., Schuster, S.C. and Schleper, C. (2006). Archaea predominate among ammonia-oxidizing prokaryotes in soils. *Nature Letters*: 442.
- Scheritz, M., Dietrich R., Scheller S., Schneider W. and Boike, J. (2008). Digital Elevation Model of Polygonal Patterned Ground on Samoylov Island, Siberia, Using Small Format Aerial Photography. *Proceedings of the Ninth International Conference on Permafrost, Fairbanks, Alaska*.
- Marion, G.M., and Black, C.H. (1987). The effect of time and temperature on nitrogen mineralization in Arctic tundra soils. *Soil Science Society of America Journal* 51:1501-1508.
- McCown, B.H. (1978). The interactions of organic nutrients, soil nitrogen and soil temperature and plant growth and survival in the arctic. In: Tieszen, L.L. (ed.). *Vegetation and production ecology of an Alaskan arctic tundra*. New York: Springer, 435-456.
- Mehra, O.P. and Jackson, M.L. (1960). Iron oxide removal from soils and clays by dithionite-citrate systems buffered with sodium bicarbonate. *7th National Conference on Clays and Clay Minerals*, 317-327.
- Melillo, J.M., Steudler, P.A., Aber, J.D., Newkirk, K., Lux, H., Bowles, F.P., Catricala, C., Magill, A., Ahrens, T. and Morrisseau, S. (2002). Soil warming and carbon-cycle feedbacks to the climate system. *Science* 298: 2173-2176.
- Nadelhoffer, K.J., Giblin, A.E., Shaver, G.R., and Laudre, G.R. (1991). Effects of temperature and substrate quality on element mineralization in six arctic soils. *Ecology* 72: 242-253.
- Nicol, G. W. and Schleper, C. (2006). Ammonia-oxidizing Crenarchaeota: important players in the nitrogen cycle? *Trends in Microbiology* 14: 207-212.
- Post, W.M., Emanuel, W.R., Zinke, P.J., and Stangenberger, A.G. (1982). Soil carbon pools and world life zones. *Nature* 298: 156-159
- Rachold, V. (ed.), (1999). *Russian-German Cooperation SYSTEM LAPTEV SEA 2000: The Lena Delta 1998 Expedition*. *Berichte zur Polarforschung*, Vol. 315.
- Richter-Menge, J., Overland, J., Proshutinsky, A. et al. (2006). *State of the Arctic Report*. NOAA OAR Special Report, NOAA/OAR/PMEL, Seattle, WA, 36 pp.

- Roshydromet. (2007). Russian Federal Service for Hydrometeorology and Environmental Monitoring. Weather Information for Tiksi. <http://www.worldweather.org/107/c01040.htm>.
- Sanders, T. (2006). Vergleichende Untersuchungen kälteliebender nitrifizierender Bakterien aus Permafrostböden im Lena Delta, Sibirien. Diplomarbeit, Universität Hamburg.
- Schimel, J.P., Kielland, K. and Chapin III, F.S. (1996). Nutrient availability and uptake by tundra plants. In: Reynolds, J.F., Tenhunen, J.D. (eds.). Landscape function and disturbance in arctic tundra. Ecological Studies 120. Berlin: Springer, 203-221.
- Schwamborn, G., Rachold, V. and Grigoriev, M.N. (2002). Late quaternary sedimentation history of the Lena Delta. Quaternary International 89: 119-134.
- Schwertmann, U. (1964). Differenzierung der Eisenoxide des Bodens durch photochemische Extraktion mit saurer Ammoniumoxalat-Lösung. Zeitschrift für Pflanzenernährung, Düngung und Bodenkunde 105: 194-202.
- Serreze, M.C., Walsh, J.E., Chapin III, F.S., Osterkamp, F.S., Dyrgerov, T., Romanovsky, M., Oechel, V., Morison, W.C., Zhang, J., T. and Barry, R.G. (2000). Observational evidence of recent change in the northern high-latitude environment. Climatic Change 46: 159-206.
- Soil Survey Staff. (2006). Keys to Soil Taxonomy. Washington, D.C.: United States Department of Agriculture & Natural Resources Conservation Service, 332 pp.
- Van Cleve, K., and Alexander, V. (1981). Nitrogen cycling in tundra and boreal ecosystems. In: Clark, E.E. and Rosswall, T. (eds.). Terrestrial nitrogen cycles. Ecol. Bull. Stockholm. 33: 375-404.
- Wagner, D. (2007). Microbial perspectives of the methane cycle in permafrost ecosystems in the eastern Siberian Arctic. Habilitation thesis, University of Potsdam [<http://nbn-resolving.de/urn:nbn:de:kobv:517-opus-15434>].
- Wagner, D. (2008). Microbial communities and processes in Arctic permafrost environments. In: Dion, P. and C.S. Nautiyal (eds.), Microbiology of Extreme Soils, Soil Biology 13, Springer, Berlin, pp. 133-154.
- Wagner, D., Kobabe, S., Pfeiffer, E.M. and Hubberten, H.W. (2003). Microbial controls on methane fluxes from a polygonal tundra of the Lena Delta, Siberia. Permafrost Periglacial Processes 14: 173-185.
- Wagner, D., Kurchatova, A., Schneider, W., Stoof, G. and Grigoriev, M.N. (2003). Permafrost drilling on Kurunghakh Island. Berichte zur Polar- und Meeresforschung 466: 70.
- Zimov, S.A., Schuur, E.A.G and Chapin III, F.S. (2006). Permafrost and the global carbon budget. Science 312: 1612-1613.

#### 4. Permafrost and environmental dynamics during Quaternary climate variations – Studies along the Dmitrii Laptev Strait

##### 4.1 Scientific background and objectives

*Lutz Schirrmeister*

Within the framework of the IPY project “Past Permafrost” (ID 15), the INTAS project “Permafrost Dating” (INTAS 8133), the DFG project “Late Quaternary warm stages in the Arctic” (SCHI 975/1-1), and the RFFI project № 06-05-64197 fieldwork was performed in the East Siberian Sea region along the Dmitrii Laptev Strait on the south coast of Bol’shoy Lyakhovsky Island (July 2007) and on the mainland coast of Oyogos Yar (August 2007). The main goal of the joint Russian-German expedition was a multidisciplinary study of middle and late Quaternary permafrost sequences exposed on both coasts. These sequences are the largest and most extended Arctic permafrost archive containing traces of two to three glacial-interglacial-cycles. Large coastal sections were studied in order to generate a comprehensive picture of the Quaternary landscape dynamics and to understand the complex local stratigraphy. The work is based on previous studies in 1999 and 2004 on Bol’shoy Lyakhovsky Island and Cape Svyatoy Nos as well as in 2002 on Oyogos Yar by teams from AWI Potsdam and MSU. In addition, the modern environment was studied as reference to palaeo records.

Several topics were investigated during two months of fieldwork:

- Stratigraphic composition of permafrost sequences exposed along the sea coasts
- Cryolithological and sedimentological characteristics of selected sections
- Sampling of frozen sediment profiles for sedimentological (e.g. grain-size, biogeochemistry, mineralogy), palaeoecological (e.g. pollen, plant macrofossils, ostracods) and geochronological (radiocarbon, luminescence, U/Th) studies
- Sampling of ground ice (ice wedges, segregation ice), surface water and precipitation for stable isotope analyses, hydrochemistry analyses, and geochronological studies ( $^{36}\text{Cl}/^{10}\text{Be}$ )
- Collection of mammal bones *in-situ*, in thermo-erosional cirques and on the sea beach
- Detailed surveys of plant associations for understanding of the indications of modern vegetation for changing permafrost landscapes
- Sampling of modern ostracods and their host waters in polygonal ponds and thermokarst lakes including hydrochemical field analyses as well as description and measuring of additional host water characteristics

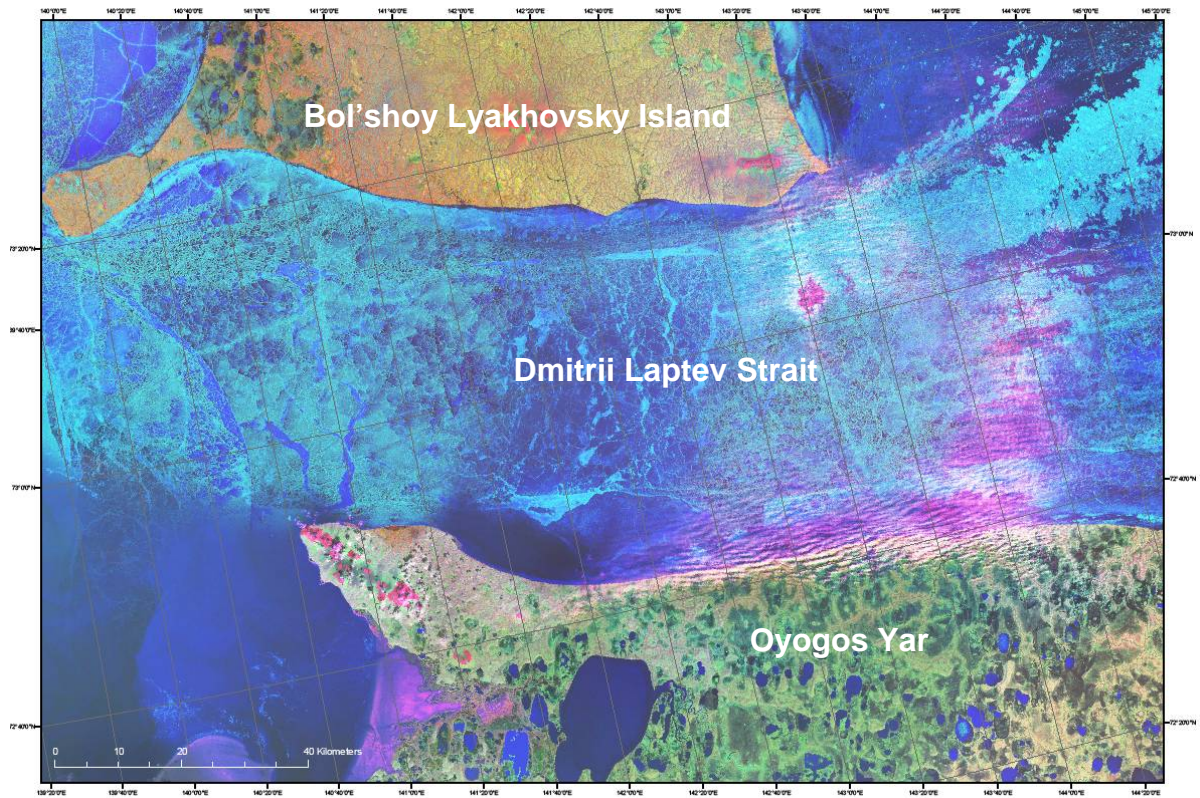


**Figure 4.1-1:** The coasts of the Dmitrii Laptev Strait with both study areas in July (south coast of Bol'shoy Lyakhovsky Island) and August 2008 (Oyogos Yar coast). Map compiled by H. Lantuit, AWI Potsdam using satellite images: (a) LANDSAT 7 ETM+ 29.06.2001.

## 4.2 Geological and geographical characteristics

*Lutz Schirrmeister, Viktor Kunitsky and Alexander Derevyagin*

Long ago, the coasts of the Dmitrii Laptev Strait are of geographical and geological interest. Since its discovery in the 18<sup>th</sup> century, Bol'shoy Lyakhovsky Island is known for the occurrence of fossil mammal bones. Almost 2000 bones have been collected during the New Siberian Islands Expedition of 1886 (Bunge, 1887; von Toll, 1897). Many species of fossil mammals such as Saiga antelope, large lion-like panther, woolly rhinoceros, and others previously not known in the Arctic, were discovered on the island (Chersky, 1891; Kuznetsova et al., 2004), which subsequently became one of the most important Pleistocene mammal sites in Siberia. The deposits of the south coast of Bol'shoy Lyakhovsky Island were first studied in the 19th century (Bunge, 1887; von Toll, 1897). However, detailed geocryological and palaeoenvironmental studies started much later (Romanovsky, 1958a-c; Pirumova, 1968; Igarashi et al., 1995; Nagaoka et al., 1995; Arkhangelov et al., 1996; Kunitsky, 1996, 1998; Kunitsky & Grigoriev, 2000).

Quaternary deposits of the south coast of Bol'shoy Lyakhovsky Island were first described in detail by Romanovsky (1958a-c). According to these studies the Quaternary consists of flood plain deposits in different terrace levels and ages with thermokarst lakes and fluvial deposits. Whereas Kunitsky (1998) explains the Quaternary deposits of the south coast as formations connected with Pleistocene perennial snow patches (snezhniki) on cryoplanation terraces, Japanese scientists consider especially the Ice Complex deposits as formations of a big swampy marshland on the Pleistocene Laptev Sea shelf (Nagaoka, 1994; Nagaoka et al., 1995).

The fieldwork in 2007 is the continuation of the Russian-German expedition in 1999 studying the island's palaeo-environmental permafrost archives around the Zimov'e River mouth (Schirrmeister et al., 2000, 2002; Tumskoy et al., 2000; Meyer et al., 2002a; Gavrilov et al., 2003; Andreev et al., 2004; Ilyashuk et al., 2006; Kienast et al., 2007). Additional studies were carried out by a team from the MSU Department of Geocryology (V. Tumskoy, A. Basylyan) on Bol'shoy Lyakhovsky Island in 2004.

The coast of Oyogos Yar was already the study object of some Russian expeditions during the last decades. Two main units characterize the coastal section. The stratigraphical classification of the lower unit is still under discussion. The interpretation ranges from middle Pleistocene to upper Pleistocene ages of the exposed sediments (Kayalaynen & Kulakov, 1966; Ivanov, 1972; Vereshagin, 1982). The dark bluish-grey, bedded deposit with shells is clearly a subaquatic formation and was named Khomsky-Suite (Vereshagin, 1982). The Khomsky-Suite is exposed in the Yana-Indigirka lowland up to 100 m a.s.l. and more (Kayalaynen & Kulakov, 1966) and contains freshwater diatoms as well as saltwater forms. Therefore, it could be deposited in a lagoon or bay environment.

The upper unit with large ice wedges is named Oyogossky Suite and presents the Ice Complex in this region. Ice Complex deposits cover the less inclined step-like surface of the Yana-Indigirka lowland and were formerly interpreted as sequences of interlocked lake terraces (Kayalaynen & Kulakov, 1966). The step-like distribution of this horizon is supposed to be connected with steps of cryoplanation terraces there (Kunitsky, 1996). Gravis (1978) as well as Konishchev & Kolesnikov (1981) supposed that the Oyogossky-Suite was formed within a thermokarst depression (alas). But Tomirdiaro (1970, 1980) assumed an aeolian origin of these deposits. In general, the situation is comparable to that of the south coast of Bol'shoy Lyakhovsky Island.

According to former studies of Russian scientists (e.g. Romanovsky, 1958a-c; Romanovsky et al., 2000; Arkhangelov et al., 1996; Kunitsky, 1998) and results of joint Russian-German projects (Schirrmeister et al., 2000, 2002; Andreev et al., 2004, 2008) different stratigraphic units of middle and late Quaternary age were described and partly dated. Tertiary deposits and weathering crusts were found as well as Middle Pleistocene ice-rich deposits, represented as fine-grained and well-sorted loess-like sequences. Eemian horizons of lacustrine deposits containing ice wedge casts and late Pleistocene ice-rich deposits of the Yedoma Suite as well as Holocene thermokarst deposits are exposed in the study region. All these units and some recently separated horizons of rather unclear stratigraphic position (Tumskoy et al., 2006) compose the permafrost coast along both sides of the Dimitrii Laptev Strait (Table 4.2-1).

**Table 4.2-1:** Synopsis of the stratigraphic units exposed on the Dimitrii Laptev Strait. The stratigraphical position of the Bychchagy Suite (grey highlighted) is still unclear

№	Name / period	Description	References
8	Holocene Alas complex	Lake and bog deposits	Andreev et al. 2008
7	Yedoma Suite	Very ice-rich deposits of the Late Pleistocene Ice Complex	Nagaoka et al. 1995 Nikolsky & Basilyan 2004 Andreev et al. 2004, 2008
6	Krest Yuryakh Suite	Eemian lake deposits with freshwater mussels	Nikolsky & Basilyan 2004 Andreev et al. 2004 Ilyashuk et al. 2006 Kienast et al. 2007
5	Bychchagy Suite	Ice-rich deposits of controversial stratigraphic position (pre or post Eemian)	Tumskoy & Basilyan 2006
4	Kuchchugui Suite	Well sorted flood plain deposits,	Andreev et al. 2004
3	Zimov'e Strata	Palaeo active layer	Tumskoy & Basilyan 2006
2	Yukagirsky Suite	Ice-rich sequence ("old Ice Complex"), Middle Pleistocene, 200 to 160 ka	Arkhangelov et al. Schirrmeister et al. 2002, Andreev et al. 2004, Tumskoy & Basilyan 2006
1	Cryogenic eluvium	Periglacial reworked Tertiary (?) weathering crust	

### 4.3 Field methods and exposure description

*Lutz Schirrmeister*

The main objectives of our studies are the completion of knowledge of the Quaternary stratigraphy and continuation of former research along the Dimitrii Laptev Strait. The field records presented here are mostly ordered according to their stratigraphic position. Therefore they are not in a chronological order as studied during the expedition.

After first reconnaissance, sites mostly situated along the sea coasts were selected for detailed studies. Profiles were dug by spades, partly exposed by water with a motor pump, and cleaned with hacks. The exposed sequences were surveyed, described, photographed, and sketched according to sediment structures and cryostructures. Afterwards, the mostly frozen deposits were sampled for further multidisciplinary studies (sedimentology, palaeo-ecology, geochronology) using hammers and small axes. Sediment samples were packed in plastic bags. In addition, samples were taken in closed aluminium boxes in order to determine the gravimetric ice content (grav. ice content) already in the field. Ice wedges were sampled in horizontal transects using a chain saw for high-resolution studies and for taking larger ice blocks. Numerous ice samples were taken with ice screws. The handling with ice and water samples will be explained more detailed in chapter 4.6.5 (Ground ice studies).

Specific samples were taken for various geochronological analyses. Larger blocks of still frozen peat were cut and densely packed for U/Th dating. Sediment samples for luminescence dating were horizontally drilled with an electric drill (Hilti). These samples were protected from daylight during sampling and after. Larger ice wedge samples of 1.5 to 2 litres were taken for  $^{36}\text{Cl}/^{10}\text{Be}$  dating of ground ice (Gilichinsky et al., 2007).

The code for each sediment and ice sample is composed of:

- study area and year: L7 – Lyakhovsky 2007, Oy7 – Oyogos Yar 2007
- a number for each study site: e.g. L7-14
- the sample number: e.g. L7-14-01 for sediment, L7-14-100 for ice samples
- if profiles were sampled by different persons, a letter was added for the name: L7-14-01-T (Tumskoy), -S (Schirrmeister), -TO (Thomas Opel).

The following detailed descriptions of the sampled sites are accompanied by photographs and profile schemes. The legend for these figures is given in Figure 4.3-1.

## Legend of the profil schemes

	Active layer boundary		Peaty layer, light-brown, grass roots, moss, lens-like cryostructure
	Vegetation cover of arctic tundra		Grey loam (alevrite), brownish-grey, peat inclusion (Holocene alas deposits)
	Segregation ice, lense-like cryotexture		Well-bedded fine-grained sand, alternated bedded with plant detritus layers, lattice-like cryostructure (Holocene lake deposits.)
	Segregation ice, reticulated cryotexture		Grey loam (alevrite); vertical in situ grass roots; lens-like (reticulated) cryostructure, concave bended ice belts (Yedomia S.)
	Segregation ice, ice belts		Grey loam (alevrite); spotty, no plant remains, lens-like cryostructure (taberal Yedomia S.)
	Ice wedge grey, compact		Peaty soil, dark brown/grey, ice-rich, peat inclusions
	Sand-Ice wedge (polosatic), close alternation (mm to cm) of sand and ice veins, 2-3 m wide		Dark grey loam; vertical in situ grass roots; lens-like, reticulated cryostructure, concave bended ice belts (Ice Complex / Bychchagy S.)
	White ice wedge; less compact; with small silty parts,		greyish silty sand, tabaeral deposits of the Bychchagy Suite
	Sample position for luminescence dating		Well-bedded fine-grained sand, alternated bedded with plant detritus layers, in ice wedge casts (Krest Yuryakh S.)
	Sample position for U/Th dating of peat		Well-laminated lacustrine silty sand with shells (Krest Yuryakh S.)
	Sample position for $^{36}\text{Cl}/^{10}\text{Be}$ dating of ice wedge		Silty, loess-like sand with black spots, weakly bedded, dark grey, (taberal Kuchchugui S.)
	Sample position for stable isotope and hydrochemistry studies of ice wedge		Silty, loess-like sand with vertical grass roots, weakly bedded, yellowish grey, ice cement (Kuchchugui S.)
	Sediment sample position and sample number		Pebble horizon of the palaeo active layer
	Middle-grained sand, grey (Tertiary ?)		Coarse-grained sand, gravels, single pebbles., strong cryoturbated, brownish grey, ice cement (palaeo active layer)
	Fine-grained sand, pebbles, dark-brown, organic-rich, wood fragments (Tertiary ?)		Loamy silty sand (alevrite), single pebbles, peat inclusions, vertical grass roots, bedded, dark grey to brownish grey, ice belts, lens-like reticulated cryotexture (Yukagirsky S.)
	Coarse-grained sand, gravely, pebbles, yellowish-brown (Tertiary ?)		Autochthonous brownish peat, grass and moss remains, in places with roots and twigs of various diameters and several lenses
	Fine-grained sand, coaly, petrified wood fragments, grey (Tertiary ?)		Yellowish loamy gravel with large pebbles (5-20 cm), residue of a Tertiary (?) weathering crust
	Coal, black, frozen (Tertiary ?)		
	Debris		
	Active layer zone		

Figure 4.3-1: Legend of the signatures used in the following profile schemes

## 4.4 Stratigraphical and geomorphological studies along the south coast of Bol'shoy Lyakhovsky Island and along the Oyogos Yar coast

*Vladimir Tumskoy and Dimitry Dobrynin*

### 4.4.1 Preliminary stratigraphic scheme

The preliminary stratigraphic scheme is based on studies of coastal sections on the southern coast of Bol'shoy Lyakhovsky Island in 1999, 2004, and 2007.

A weathering crust of < 1 m thickness was found on the beach level ca 2 km west of the Zimov'e River mouth. It consists of rock debris in a greyish, bluish, and yellowish clay matrix. There are single epigenetic ice wedges of 0.2-0.3 m width.

Deposits of the Yukagirsky Suite were firstly described by Arkhangelov et al. (1996) and established as a separate suite by Nikolsky and Basilyan (1999). At the south coast of Bol'shoy Lyakhovsky Island these sediments were found 0.7 to 2.4 km west of the Zimov'e River mouth. These up to 5 m thick sediments cover the weathering crust. The Yukagirsky Suite consists of ice-rich sediments with syngenetic ice wedges, which are similar to the widely distributed Late Pleistocene Ice Complex deposits. Generally, sediments of the Yukagirsky Suite are composed of silty fine-grained sand, which contains large amounts of rock debris with various stages of rounding (mostly gravel, debris, small stones) and peat inclusions. The content of rock debris that comes from the underlying basement rocks and from the weathering crust decreases upwards. While the amount of peat inclusions increases. Peat lenses exist in the upper part of the Yukagirsky Suite. Ice wedges of the main generation are up to 2-2.5 m wide forming a polygonal net with sediment blocks of about 15 m in diameter. Between 0.7 and 1 km west of the Zimov'e River mouth the horizon of the Yukagirsky Suite contains autochthonous, up to 1.2 m thick intra-polygonal peat lenses, separated by special ice wedge generations of 0.2-0.5 m (max 1 m) width. Different independent U/Th dating of these peat lenses show ages between 160-200 ka.

Deposits of the Yukagirsky Suite are covered by a characteristic indicator horizon of 0.5-0.6 m thickness, which was firstly described as Zimov'e Strata by Tumskoy and Basilyan (2006). This horizon is continuously connected with the Yukagirsky Suite and occurs only on the top of it. The Zimov'e Strata consists of material from the Yukagirsky Suite and the overlying sediments – reddish, brownish or yellowish-grey loams with rock debris or brown silts. The layer is characterized by subvertical wedge-like, tongue-like structures and concentrations of rock debris in the upper part parallel to the upper boundary of the layer. The subvertical structures are assumed to be tracks of cryoturbation processes and the concentration of rock debris in the upper part seems to be the result of frost sorting processes. Thus, we can assume that the Zimov'e

Strata is a buried cover layer of a fossil active layer on top of the Yukagirsky Suite.

The sediments above were described as Kuchchugui Suite by O.A. Ivanov (1970, 1972), but previously described as Khromsky Suite by Kayalainen and Kulakov (1965). They are presented by two types of deposits. The first one is a brownish-grey silty fine-grained sand with low ice content and massive or micro-schlieren cryostructures. They contain numerous tiny roots of grass vegetation, which partly form denser concentrations (like turf). There are also non-regular wavy and horizontal laminations and initial small-size ground wedges. Smaller syngenetic ice wedges are characteristic for the lower deposits of this type of the Kuchchugui Suite, while the bigger ones are characteristic for the upper part. There are single narrow epigenetic ice wedges up to 0.2 m wide, almost penetrating the Kuchchugui Suite horizon. The second type of deposits of the Kuchchugui Suite consists of dark grey and bluish-grey silty fine-grained sand and loam with a massive cryostructure. Spotty black concretions of up to 1-1.5 cm in diameter are very common, which are sometimes concentrated in several horizons. These two types of the deposits laterally alternate each other almost everywhere. Deposits of the first type of the Kuchchugui Suite with a maximal thickness of up to 14-15 m were found in the study area 1 to 1.5 km to the west from Zimov'e River. The bottom of deposits of the second deposit type are located almost everywhere under the sea level but the top is mostly disturbed by series of large notches resulting in strong thickness variations between 1-2 to 5-8 m.

Based on field studies in 2004 Tumskey and Basilyan (2006) described the so-called Bychchagy Suite above the Kuchchugui Suite. It consists of grey and brownish-grey ice-rich silty fine-grained sand or loam of up to 6-8 m thickness. The deposits contain 3-4 m wide ice wedges, which penetrate the underlying sediments. Distances between ice wedges are 10-12 m. Two horizons of intrapolygonal autochthonous peaty layers (up to 1 m thick) are characteristic for the Bychchagy Suite. The upper peat layer is generally thicker and more uniform. The vertical distance between the two layers within a sediment block amounts to 2 m. This interlayer of mineral deposits often contains ice wedges of the second generation, which separate the sediment blocks in two parts. According to their cryolithological features deposits of the Bychchagy Suite sediments could be considered as similar to the Late Pleistocene Ice Complex.

Larger parts of the costal section consist of special structures named by N.N. Romanovskii (1958a-c) as "strukturny oblikaniya" (subaquatic ice wedge cast structures) filled by sediments, which were described by O.A. Ivanov (1970, 1972) as Krest Yuryakh Suite. According to Romanovskii (1958a-c) these structures were ice wedge casts formed under subaquatic (limnic) conditions. We believe that these ice wedge casts were formed from ice-rich sediments of the Bychchagy Suite below thermokarst lakes at the beginning of Late Pleistocene. The ice wedge casts are up to 3-4 m high and 5-8 m wide and reached some hundred of meters along the coast. The casts are filled by well-laminated bluish-grey, silty fine-grained sand with low ice content and have a

massive cryostructure. They contain a lot of plant detritus and fragments of shrub vegetation, which underline the lamination. On ice wedge cast edges as well as inside are large numbers of small faults, disturbing the lacustrine lamination. Practically everywhere between ice wedge casts there are two lenses of compressed peat, which lay one on another and stretch horizontally. We believe that thermokarst lake processes in the ice-rich Ice Complex deposits of the Bychchagy Suite finally lead to melting of ice wedges, which initially penetrated the upper horizons of the Kuchchugui Suite. This process resulted in the formation of large ice wedge casts of wavy structure. Taberal deposits of the Bychchagy Suite are preserved between ice wedge casts and are characterised by dense peat lenses. The deposits of the Kuchchugui Suite reworked under lake talik conditions during the Krest Yuryakh interval were transformed in taberites and present now the second type of Kuchchugui Suite deposits. Another variant of the transformation of the first deposit type into the second deposit type of the Kuchchugui Suite will be discussed later. This scheme explains well the spatial limitation of this sediment type, which was mostly found below the Krest Yuryakh Suite.

Deposits of the Krest Yuryakh Suite and preserved deposits of the Bychchagy Suite are covered by ice-rich deposits of the Late Pleistocene Ice Complex (Yedomia Suite). The thickness of this Ice Complex amounts to 40 m and more on Bol'shoy Lyakhovskiy Island. The Ice Complex surface is relief-forming. Its base is situated below sea level as well as up to 15 m a.s.l.. Large syngenetic ice wedges composing significant parts of the Ice Complex have various widths between 2 and 8 m. Distances between ice wedges vary from 5 to 18 m depending on the place and the height. The Late Pleistocene Ice Complex is composed of disperse deposits from silty loam to silty sand with high content of organic matter including intrapolygonal autochthonous peat inclusions and peaty lenses. Bended cryostructures are characteristic for these deposits. A detailed study shows that the Ice Complex was not continuously formed but contains evidences of local gaps, erosional cuts filled by similar sediments, cryogenic transformations etc. The Ice Complex sequence at the south coast of Bol'shoy Lyakhovskiy Island could be probably separate in series of erosional cuts filled by similar Ice Complex deposits, which are however different by their composition and cryogenic structure in comparison to surrounding older sediments. Such erosional cuts are up to 100-300 m wide and 15-30 m deep. They often reach the underlying sediments of the Krest Yuryakh and the Kuchchugui Suites. Sediments filling the cuts are predominantly light-brown and greyish-brown fine-grained sands often with thin slanting and horizontal bedding marked by large amount of reworked, allochthonous organics. Deposits filling the erosional cuts include syngenetic ice wedges of often irregular forms and variable width (0.5 to 3-4 m) with numerous shoulders and alternations.

Ice Complex sediments of the Yedomia Suite are separated by numerous thermokarst depressions (alases), river valleys, and thermoerosional valleys (logs). The complex of alas deposits consists of taberal, lacustrine and alas deposits as such (i.e. polygonal peat deposits). Their total thickness reaches 5-

15 m. It is usually difficult to separate taberal and lacustrine sediments. Taberal deposits are not laminated and contain no shells of freshwater molluscs and large plant remains. Lacustrine bluish-grey silty fine-grained sands show layered epigenetic cryostructures and contain sometimes traces of subaquatic slumping. The facies of polygonal peat contains large syngenetic ice wedges up to 4.5 m width. Sediments are characterised by bended cryostructure. Taliks, which existed below Holocene thermokarst lakes were several tens of meters deep and influenced the underlying sediments of the Kuchchugui and the Bychchagai Suites. Ice wedges of the Bychchagy Suite thawed under Holocene taliks and on top of the Kuchchugui Suite, which was transformed in taberal deposits. Newly formed ice wedge casts are similar to those formed under thermokarst lakes of the Krest Yuryakh period. In some cases, if below Holocene thermokarst lakes Krest Yuryakh sediments are underlain by Kuchchugui Suite sediments of the second type, such sediments were influenced a second time by thermokarst processes. Then, ice wedge casts were formed on top of the Krest Yuryakh Suite, which follow the ice wedges structures of Ice Complex. In such cases the exposures contain two horizons of ice wedge casts: the lower horizon is presented by wavy structures of the Krest Yuryakh Suite and the upper one contains taberal deposits of the Yedoma Suite and Holocene lacustrine sediments. The later ones usually have wedge-like forms or rounded triangular shapes in contrast to the bowl-shapes ice wedge casts of the lower horizon.

Holocene thermo-erosional valleys are often presented in outcrops by slightly concave cuts (logs) filled by ice-rich deposits. The thickness of such sediments reaches usually a few meters, sometimes (in large thermo-erosional valleys with several stages of activation) it reaches 10 m. The width of such valleys is about several ten meters. Normally, they are filled by reworked material of Ice Complex sequences: silty fine-grained sand and loam, which contain large amounts of organic matter. The lamination is often visible, which is also marked by parallel-layered cryostructures. Large single ice wedges of up to 2-3 m width, which penetrates into the underlying frozen deposits, are also characteristic for sediments in thermo-erosional valleys.

The above-described units can be absent on some parts of the section because of erosion processes or lacking of favourable accumulation conditions. Generally, thermokarst and thermo-erosional processes played an active role in cryogenic reworking of ice-rich deposits resulting in changes of the section stratigraphy. Such processes could follow each other and/or act together. However, studies of structure in horizontal orientation and lateral (permafrost-facies) contacts help to decode the complex history of sedimentation and cryogenesis of Quaternary deposits.

#### 4.4.2 The coast west of the Zimov'e River

One part of the southern coast of Bol'shoy Lyakhovsky Island 0.7 to 2.4 km west of the Zimov'e River mouth is very special because only there deposits of the Yukagirsky Suite (preserved remnants of the Middle Pleistocene Ice Complex) are exposed, which are overlain by the weathering crust. The studied coast segment belongs to the northern part of the Chokhchuro-Chokurdakh uplift stretching northward from the Svyatoy Nos Peninsula to the other side of the Dimitrii Laptev Strait. Since the Middle Pleistocene this area was relatively high and thermokarst lakes did not form here during the Krest Yuryakh (Eemian) period and the Holocene, resulting in the absence of the Krest Yuryakh and Bychchagy Suite. Sediments of the first type the Kuchchugui Suite are present in exposures. There are syngenetic and epigenetic ice wedges of the different types, single composite ice-ground wedges, and initial ground wedges. According to the vertical amount of the tiny roots as well as the distribution and structure of ice wedges it is possible to distinguish three horizons (low, middle, and upper) of the Kuchchugui Suite.

Further west from this relatively high-elevated site towards the Kigilyakh Peninsula the roof of the basement is gradual decreasing. Already 2.5 km west of the Zimov'e River mouth deposits of the Krest Yuryakh Suite are exposed, which continued for several km westwards. The number of the Holocene alases is also increasing in the western direction marking the approach to the Bel'kovsky-Svyatoy Nos suture zone. This zone is especially notable in the relief of the western part of Bol'shoy Lyakhovsky Island, where alases are combined to a so-called alas plain, pointing to an area of permanent subsidence. Taberite sediments of the Kuchchugui and the Krest Yuryakh Suites in the lower part of the outcrops continue up to the Yipsa River mouth. Here, in the area of developed Holocene alases, two ice wedge cast horizons are exposed – a Krest Yuryakh and a Holocene horizon. Westwards from the Yipsa River mouth the base of the Yedoma Suite Ice Complex is preserved between alases as separate remnants, which continue below sea level. Even the base of Holocene alases is located below sea level.

#### 4.4.3 The coast between Zimov'e and Vankina Rivers

The 16 km long coast between the mouths of the Zimov'e and the Van'kina Rivers has the most complicated structure of Quaternary permafrost deposits in the area. The exposure basis consists of undisturbed or taberal deposits of the Kuchchugui Suite. Deposits of the Yukagirsky Suite are present in single sites under the undisturbed sediments of the Kuchchugui Suite, but they do not outcrop at the surface. Their presence is indirectly assumed due to the rare finds of the Zimov'e Strata that exist only on the top of the Yukagirsky Suite in beach level.

Bychchagy Suite sediments on this coast segment are well distinguishable in the exposure by two indicator horizons of autochthon peat. The entire sequence is up to 8 m thick. The exposed lateral contacts between the Krest Yuryakh and the Bychchagy Suite show that the first deposits were formed due to thermokarst thawing of the second deposits. Therefore deposits of the Krest Yuryakh Suite occurred only locally as horizontal lenses covered by Ice Complex deposit of the Yedoma Suite. In addition, sites of Krest Yuryakh inter-alas areas, consisting of preserved ice-rich deposits of the Bychchagy Suite are also covered by Ice Complex deposit of the Yedoma Suite, which are similar to Bychchagy Suite sediments by their structure and composition. However, on the transition zone there are well-visible cryogenic changes in ice wedges and texture ice of sediment blocks, which were formed simultaneously to the period of Krest Yuryakh Suite accumulation.

In this coastal segment it was possible to observe the complex structure consisting of several steps of margin parts of Holocene alases. The total thickness of alas deposits reaches 15-20 m because of intensive material transport on slopes of Yedoma remnants. Periodical activation of these processes resulted in several covers of slope deposits containing their own ice wedges. The sedimentation gaps are highlighted by changes in the cryogenic structure. High organic contents in the sediments allow us to reconstruct the sedimentation chronology for every case in detail.

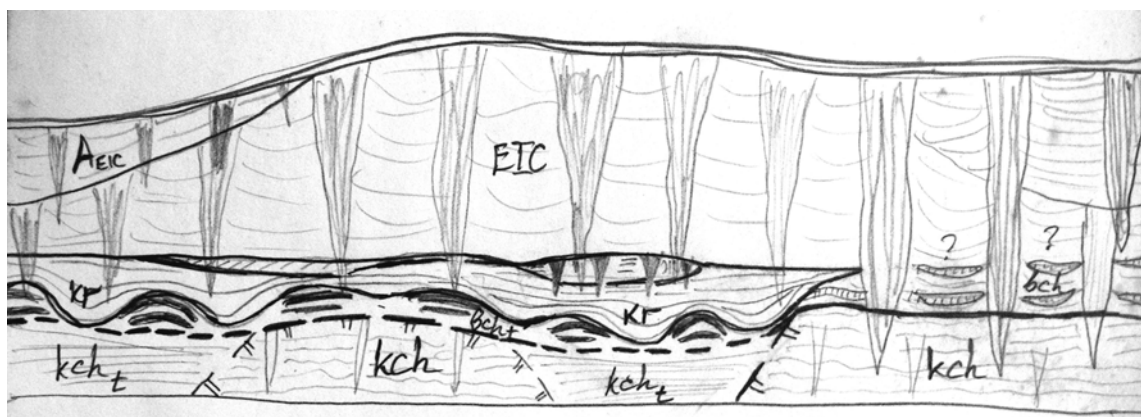


**Figure 4.4-1:** Principal stratigraphic scheme of the Quaternary deposits between mouths Zimov'e and Vankina rivers (according to V.Tumskoy, 18.07.2007).

EIC – Yedoma Ice-Complex; A<sub>EIC</sub> – Holocene alas deposits formed on EIC; kr – Krest Yurakh Suite; bch – Bychchagy Suite; bch<sub>t</sub> – thawed Bychchagy Suite deposits; kch – initial Kuchchugui Suite deposits; kch<sub>t</sub> – thawed Kuchchugui Suite deposits.

#### 4.4.4 The coast east of the Vankina River

The structure of Quaternary deposits east of the Van'kina River was studied until the Bychchagy River mouth situated about 7.5 km further southeast. In general, it is similar to those between the mouths of Zimov'e and Van'kina Rivers. The outcrop basis exposes undisturbed or one or two times taberated deposits of the Kuchchugui Suite. Their lower part continues below sea level. Ice Complex deposits of the Bychchagy and the Yedoma Suites cover the upper part. In-filled Late Pleistocene erosional cuts were observed within these sequences. Deposits of Holocene alas depressions and of thermo-erosional valleys (logs) are also widely distributed at this coast segment.

Quaternary deposits of similar structure are also known eastwards of the Bychchagy River mouth until Cape Burus Tas, which consists of basement rocks (upper Jurassic to lower Cretaceous sandstones of the Burustasskoy Suite) in the lower part covered by Ice Complex deposits of the Yedoma Suite. Further east to Cape Shalauraova only basement rocks exist. Therefore there are no natural exposures in this coastal segment.

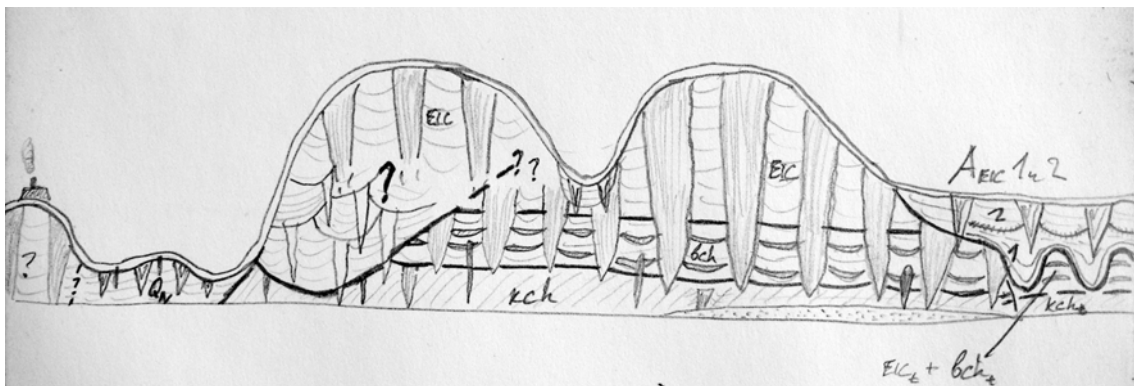


**Figure 4.4.-2:** Principal stratigraphic scheme of the Quaternary deposits east of the Vankina River mouth from Povarnya up to 2 km (according to V.Tumskoy, 18.07.2007).

EIC – Ice Complex deposits of the Yedoma Suite; A<sub>EIC</sub> – Holocene alas deposits formed on EIC; bch – Bychchagy Suite; bch<sub>t</sub> – taberal deposits Bychchagy Suite; kch – initial deposits of the Kuchchugui Suite; kch<sub>t</sub> – taberal deposits of the Kuchchugui Suite; EIC<sub>t</sub> – taberal Ice Complex deposits of the Yedoma Suite; Q<sub>IV</sub> – Holocene alas deposits.

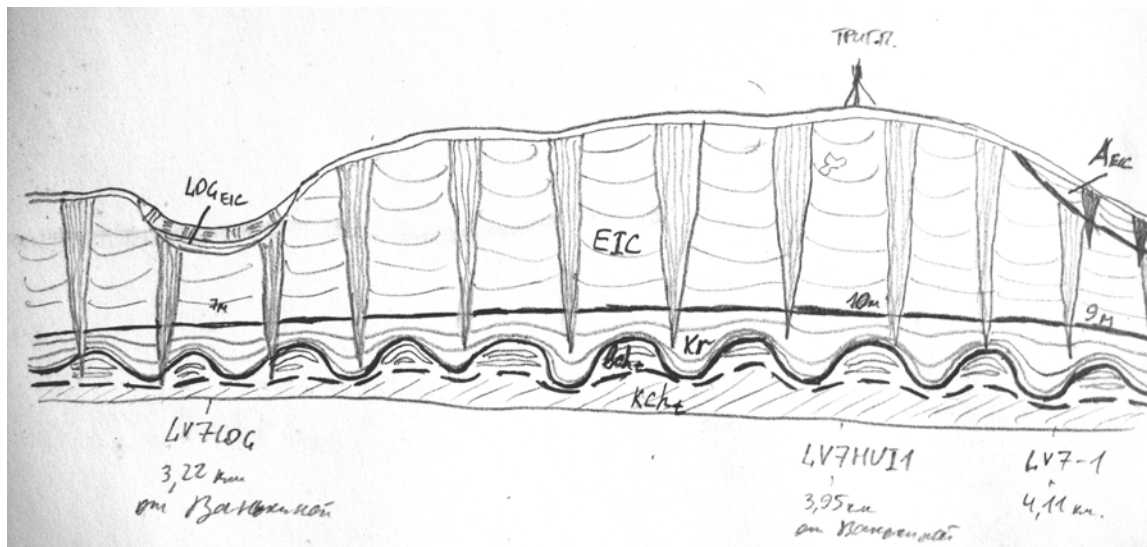


**Figure 4.4-3:** Principal stratigraphic scheme of the Quaternary deposits east of the Vankina River between 3.2 and 4.1 km from its mouth (according to V. Tumskoy, 18.07.2007).

EIC – Ice Complex deposits of the Yedoma Suite; A<sub>EIC</sub> – Holocene alas deposits formed on EIC; kr – Deposits of the Krest Yurakh Suite; bch<sub>t</sub> – taberal deposits of the Bychchagy Suite; kch<sub>t</sub> – taberal deposits of the Kuchchugui Suite; LOG<sub>EIC</sub> – Holocene deposits formed in the frames of small thermo-erosional valleys (“log”) on the EIC deposits.

#### 4.4.5 The coast of Oyogos Yar

Stratigraphic and geological-geomorphological studies of the northern margin of the Yana-Indigirka lowland were carried out along the south coast of the Dmitrii Laptev Strait named Oyogos Yar in August 2007. The main camp site of the field team was located at the margin of an alas depression 19.4 km east of the mouth of the Rebro River (see Figure 4.6.1-1). Detailed studies were realized 5.5 km east of the camp site, where one of the rare remnants of the Late Pleistocene Ice Complex deposits from the Oyogos Yar coast are preserved. In addition, mapping survey was carried out along the entire about 125 km long Oyogos Yar coast from the Cape Svyatoy Nos (west) to the mouth of the Konechnoy River (east). Objectives and methods of these studies were similar to those along the coast of Bol'shoy Lyakhovskiy Island. Besides of stratigraphical, palaeogeographical, micropalaeontological, and stable isotope studies additional tasks were the stratigraphical correlation and comparison of Quaternary sequences of the northern and the southern coast of the Dmitrii Laptev Strait.

Stratigraphical studies of Quaternary deposits from the Oyogos Yar coast started in the middle of the 50ies of the last century (see chapter 4.4.1). Actually an official local stratigraphical scheme for the area of the Dmitrii Laptev Strait does not exist. The decision of the stratigraphical commission in 1982 (Decision, 1982) did not recommend to use parts of the former orders of Ivanov (1970, 1972) (e.g. Kuchchugui Suite) although there was no new proposal for

this area. Because of the missing scheme we use the nonofficial proposal of O.A. Ivanov, which is well applicable in the exposures and for comparison.

The mapping survey along the entire coast of Oyogos Yar allows to characterize the general features of their structure.

The elevated segments of the coast that belong to the western part of Oyogos Yar and the border of the western area of the mainland coast, the Syatoy Nos Peninsula, the rock massive of Svyatoy Nos are located in the axis of the submerdial Chokhchuro-Chokhurdakhsky uplift that continues further north to the side of the Kigilyakh Peninsula in the western part of Bol'shoy Lyakhovsky Island. The top of Svyatoy Nos is characterized by 300-400 m height and by outcrops of basement rocks (granites) in most of the coastal exposures. Further southwest of Cape Svyatoy Nos marine near shore deposits of the Serkinskoy Suite were described by Ivanov (1970). At the north coast of Svyatoy Nos Peninsula above the basement rocks gravely debris deposits of 6 m visible thickness crop out (Nikolsky et al., 1999), which are however not easy comparable with deposits of the Serkinskoy Suite. Further upwards they are covered by ice-rich deposits with syngenetic ice wedges, which belong to the Yukagirsky Suite. The thickness is limited to < 3 m. According to all peculiarities including the 0.5 m cover layer on top of the Yukagirsky Suite these sediments are similar of those studied west of the Zimov'e River mouth on the Bol'shoy Lyakhovsky Island (see chapter 4.4.2).

Deposits of the Yukagirsky Suite on Svyatoy Nos are covered by characteristic brownish silty fine-sand of low ice content determined as Kuchchugui Suite. Their stratotype is located a little bit to the east, in the western part of Oyogos Yar in the area of the Kuchchugui Creek. Further east of Cape Svyatoy Nos the base of Quaternary deposits continues below sea level and already in western part of the Oyogos Yar coast the Yukagirsky Suite does not outcrop. Loams with intrapolygonal peat lenses are exposed at the western flank of the Syatoy Nos Peninsula in the area of the Ulakhan Tala Creek below the base of the Kuchchugui Suite, which is situated here not higher than 6 m a.s.l. (Konishev and Koselnikov 1981). These are deposits, which were initially ice-rich due to simultaneous accumulation and freezing but later they thawed and were strongly compressed. Probably it was happen before the accumulation of the Kuchchugui Suite because these sediments were not transformed. They are similar to first type sediments of the Kuchchugui Suite already described on Bol'shoy Lyakhovsky Island (chapter 4.4.2). Maybe they are taberites of Ice Complex deposits of the Yukagirsky Suite or of still older formations.

East of the Ulakhan Tala Creek ice wedge casts were found on top of Kuchchugui Suite deposits that belong to the Krest Yuryakh Suite. They are covered by Late Pleistocene Ice Complex deposits of the Yedoma Suite, which were already found on Svyatoy Nos Peninsula, where they were deposited directly on the Kuchchugui Suite. Preserved fragments of the Bychchagy Suite were not found on the western part of the Oyogos Yar coast; most likely because of limited studies in this area. The stratigraphical highest deposits are

the widely distributed Holocene alas complexes and alluvial deposits of small streams and terraces of larger rivers

In eastern direction the base of the Kuchchugui Suite descends and in the area of the Rebrov and Kondrat'ev River mouths such sediments were exposed only fragmentarily up to 3-4 m a.s.l.. In the valley of the Kondrat'ev River the base of the Yedoma Suite is also situated below sea level. However, further to the west the upper part of Krest-Yuryakh Suite is exposed at the base of the outcrops covered by Ice Complex remains or by deposits of the Holocene alas complex. Westwards of the Kondrat'ev River, in the central part of the preserved large Ice Complex massive we found a small fragments of non-taberated loamy deposits with ice wedges, which were situated above the Kuchchugui Suite. The presence of two horizons of characteristic intrapolygonal peat layers in a vertical distance of 2-3 m suggested that these could be preserved fragments of the Bychchagy Suite as described on Bol'shoy Lyakhovsky Island (chapter 4.4.3).

Further to the east the outcrop base gradually descends and in the area of the Konechnaya River at the easternmost end of the Oyogos Yar coast of the upper part of the Krest Yuryakh Suite is exposed at the beach level covered by Ice Complex deposits of the Yedoma Suite, which were strongly intersected by alas deposits. The height of the Yedoma remains and of alas level decrease in the same direction.

Thus we can preliminarily conclude that all stratigraphic units found on the southern coast of Bol'shoy Lyakhovsky Island are present also along the Oyogos Yar coast and at Svyatoy Nos Peninsula. Similar stratigraphy and types of lateral contacts show that during the Middle and Late Pleistocene period the area of the Dmitrii Laptev Strait developed as one region

### 4.5 Palaeoenvironmental studies on Bol'shoy Lyakhovsky Island

*Lutz Schirrmeyer, Sebastian Wetterich, Vladimir Tumskoy and Dimitry Dobrynin*

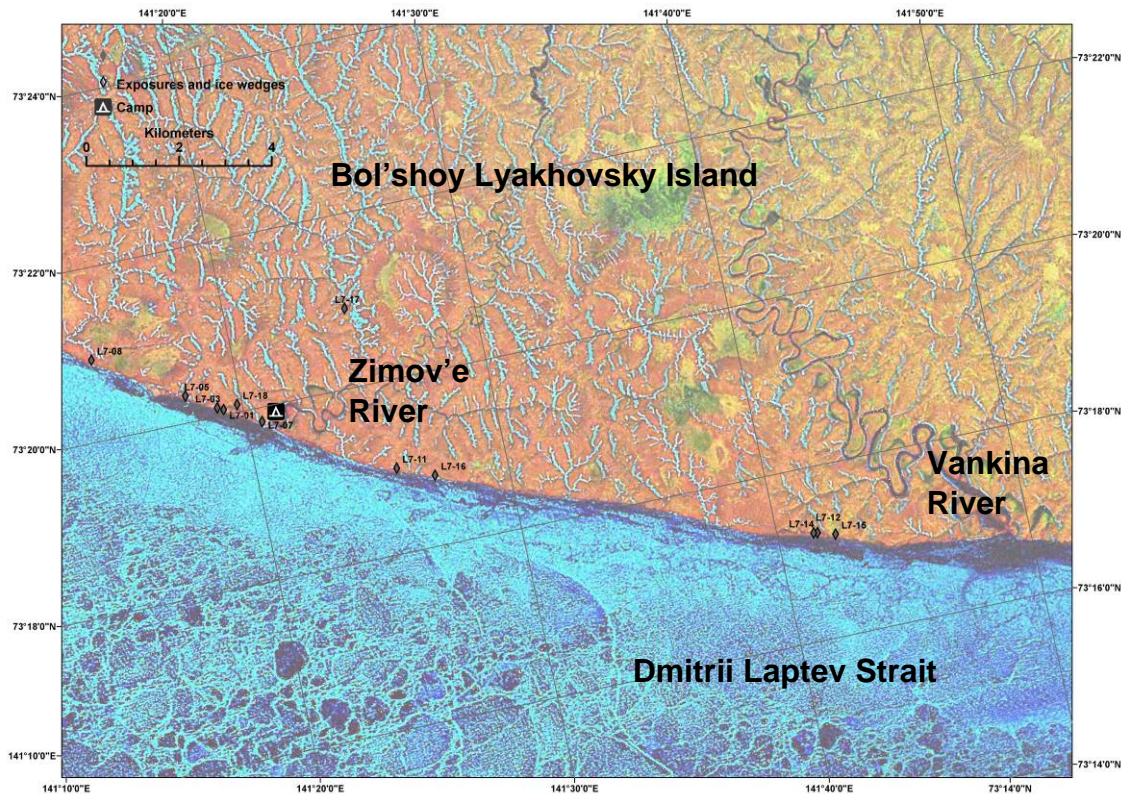


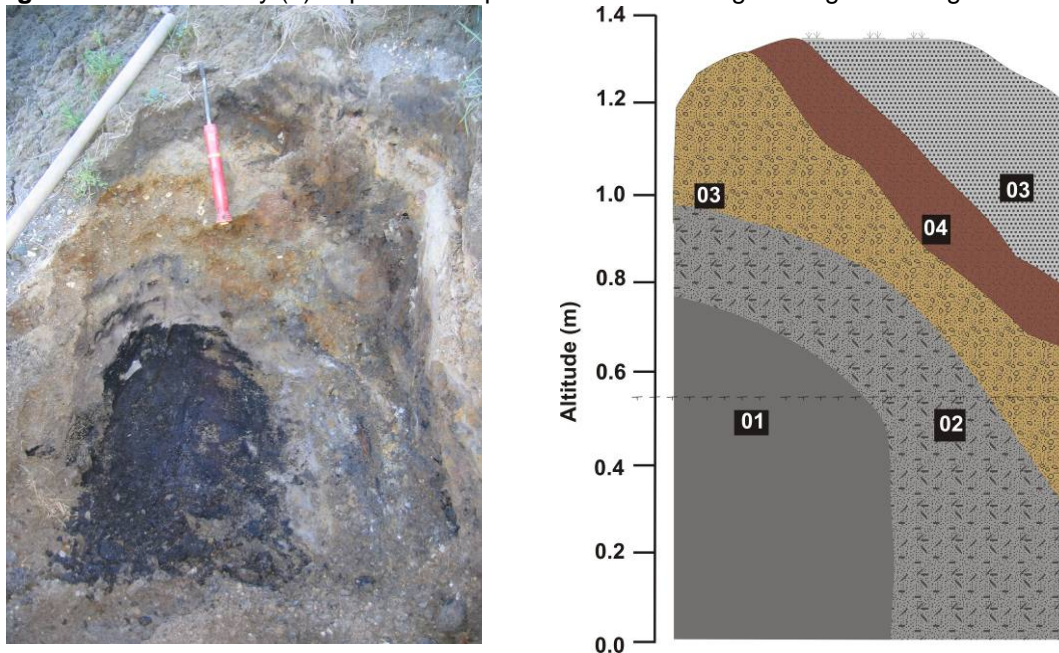
**Figure 4.5-1:** Distribution of the studied exposures presented in the following chapters along a 15 km coastal segment of Bol'shoy Lyakhovsky Island Map compiled by H. Lantuit, AWI Potsdam using satellite images: (a) LANDSAT 7 ETM+ 29.06.2001.

#### 4.5.1 Studies of Tertiary to Holocene permafrost sections west of the Zimov'e River mouth

##### 4.5.1.1 Exposure L7-17, Tertiary (?) deposits (29.07.2007)

The outcrop was located inland about 3 km north of the coast at the right branch of the Vetvistyi River, a small tributary of the Zimov'e River. It probably contained Tertiary deposits. The exposure situated 0.5 m above the river level was about 1 m high and 0.7 m wide (Figure 4.5.1-1). The layers were diagonal erected. The lower part was frozen and consisted of black coal material (116 wt% ice content) with large (5-10 cm) wood fragments on the left and of silty fine sand (0.2 m thick, ice content 36 wt%) with smaller coal inclusions and petrified (iron oxide soaked) wood fragments on the right. Both layers continued in the unfrozen part of the section. A layer of yellowish-brown gravelly coarse sand with pebbles (diameter 2-10 cm) covered the previous layer. It was covered by organic-rich dark-brown pebble-bearing fine sand containing again numerous petrified wood fragments. The last exposed layer consisted of homogenous light-grey fine sand. Each layer was sampled (L7-17-01 to L7-17-05). In addition, coaly wood fragments (L7-17-06) and petrified wood fragments (L7-17-07) were collected.

**Figure 4.5.1-1:** Tertiary (?) deposits of exposure L7-17. The legend is given in Figure 4.3-1.



## 4.5.1.2 Exposure L7-01, Yukagirsky to Kuchchugui Suite (10./12.07.2007)

About 1.1 km west of the Zimov'e River mouth an about 300 m long section of large ice wedges, big peat lenses and ice-rich deposits covered (Yukagirsky Suite) by a brownish coloured cryoturbated layer (Zimov'e Strata, palaeo active layer) and relative homogenous fine-grained deposits (Kuchchugui Suite) were exposed from the beach level up to 5 m a.s.l.. This section (Figure 4.5.1-2/3) showed a buried ice wedge polygon system of complex composition that was studied in several subprofiles and smaller exposures (L7-17-A to E), which are described in more detail below.

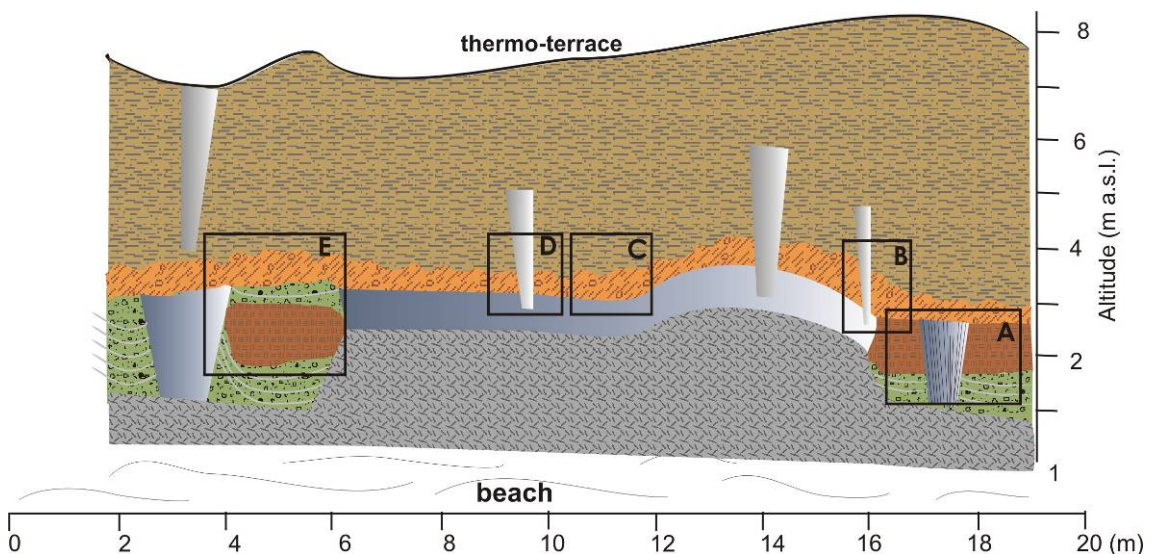


**Figure 4.5.1-2:** Overview schema of the exposure L7-01 with positions of the sampling sites. Subprofiles A to E are shown in Figures 4.5.1-3 to 4.5.1-9. The legend is given in Figure 4.3-1.



**Figure 4.5.1-3:** Peat lenses and ice wedges of the Yukagirsky Suite covered by deposits of the Kuchchugui Suite, overview photograph of exposure L7-01.

*Subprofile L7-01-A* exposed a grey ice-rich sediment (grav. ice content 170 wt%) of dominantly silty sand with small peat inclusions (2-5 cm) that formed the layers below large peat lenses. Ice bands of 1.5 to 2 cm thickness alternated with sediment layers of fine-lens-like texture (samples L7-01-01, 02). Ice wedges of several meters width were observed between sediment columns. They were studied in the exposures L7-02 and L7-03 (see chapter 4.5.1.3 and 4.5.1.4). The peat lenses were 1 to 1.5 m thick and consisted of weakly decomposed light to dark-brown moss peat. The gravimetric ice content was very high (590 wt%). Samples were taken from two peat lenses for standard sedimentological analyses (samples L7-01-03 to 05), for U/Th-dating (samples L7-01-10 to 12; L7-01-16 to 18) as well as for botanical analyses. The studied peat lens was dissected by a vertically laminated composite ground-ice wedge of 1.2 m width (Figure 4.5.1-4). Single stripes of ice and ground were 0.5 to 1 cm broad. A sample transect was taken by ice screw in about 10 cm distance (samples L7-01-101 to 107). In addition, a large sample (L7-01-108) of 1.5 l was collected by axe for  $^{36}\text{Cl}/^{10}\text{Be}$ -dating.

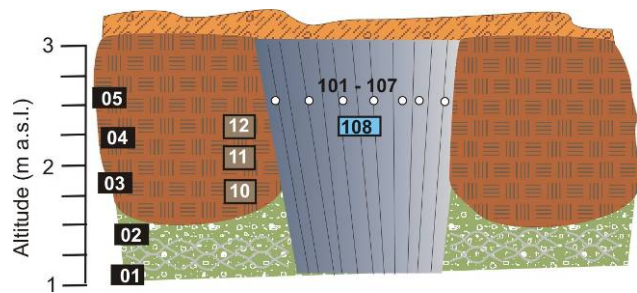


**Figure 4.5.1-4:** Peat lenses dissected by ground ice wedges, Yukargirsky Suite (subprofile L7-01-A). The legend is given in Figure 4.3-1.

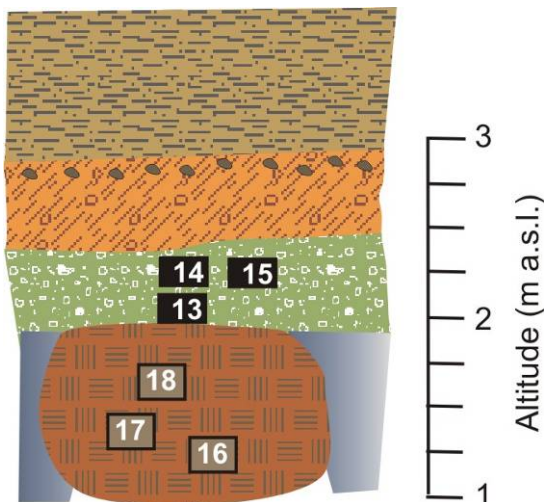


**Figure 4.5.1-5:** Second studied peat lens of the Yukargirsky Suite covered by coarse grained ice-rich deposits (subprofile L7-01-E). The legend is given in Figure 4.3-1.

The peat lenses were covered again by ice-rich deposits (ice content 187 wt%) studied in *subprofile L7-01-E* (Figure 4.5.1-5), which are composed of coarser sand, gravels and single pebbles and contain additional peat inclusions and separate plant fragments. The cryostructure was banded and lens-like reticulated (samples L7-01-13 to 15).

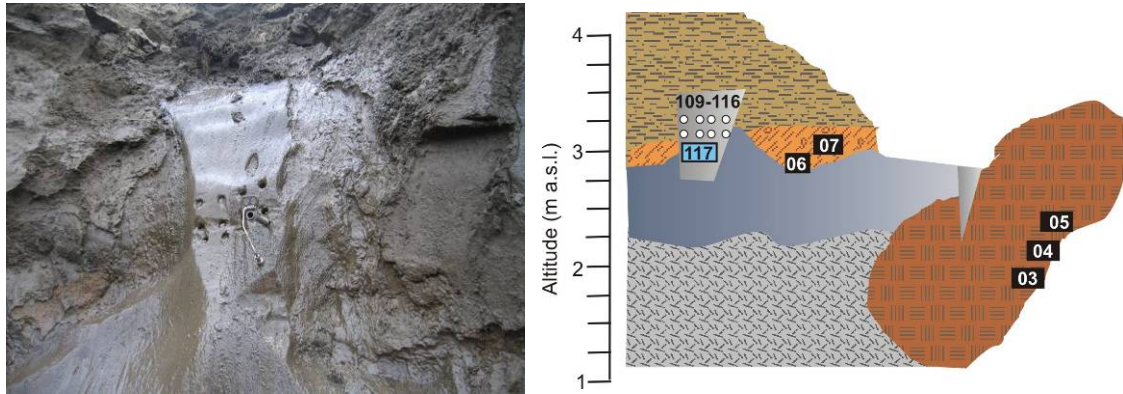


**Figure 4.5.1-6:** Ice wedge of the Kuchchugui Suite penetrates into a large ice wedge of the Yukagirsky Suite (subprofile L7-01-B). The legend is given in Figure 4.3-1.

In *subprofile L7-01-B* (Figure 4.5.1-6) a very remarkable about 0.5 m thick layer was studied, which was interpreted as palaeo active layer covering the entire sequence of the Yukagirsky Suite. This layer was strongly cryoturbated and contained brownish lenses of gravels and 5-10 cm large yellowish pebbles, which were strongly weathered. In addition, a grey-brown bedded fine-grained matrix was visible between the coarse-grained components. Beside of colour, sediment composition, and structure, the layer was characterized by a small subhorizon of gravel and pebbles enrichment (samples L7-01-06/07), which could be interpreted as a pebble layer formed by periglacial frost heave. The cryostructure was massive, no segregation ice was visible. The gravimetric ice content was low (24 to 27 wt%). This layer was preliminary related to the Zimov'e Strata.

Above the cryoturbated horizon rather homogenous-grained deposits composed the so-called Kuchchugui Suite, which was studied in the *subprofile L7-01-C* (Figure 4.5.1-7). This brownish sediment was fine, but non-regularly bedded and contains numerous vertical thin filamentary grass roots (samples L7-01-08/09). Two additional samples (L7-01-19/20) were drilled in the Kuchchugui Suite for luminescence dating. The cryostructure was massive and the gravimetric ice content was low (32 to 36 wt%). Specific small ice wedges of 0.2 to 0.4 m width attributed to the Kuchchugui Suite penetrated into the large underlain ice wedge of the Yukagirsky Suite (Figure 4.5.1-8).

Two small ice wedges of the Kuchchugui Suite were sampled in *subprofile L7-01-D* (Figure 4.5.1-8) in 3.0 to 3.2 m a.s.l. height for stable isotope studies (samples L7-01-109 to 116; L7-01-118/119 for AWI-Potsdam; L7-01-120/121 for MSU). From the first ice wedge a large sample was additionally taken for  $^{36}\text{Cl}/^{10}\text{Be}$  dating (samples L7-01-117).

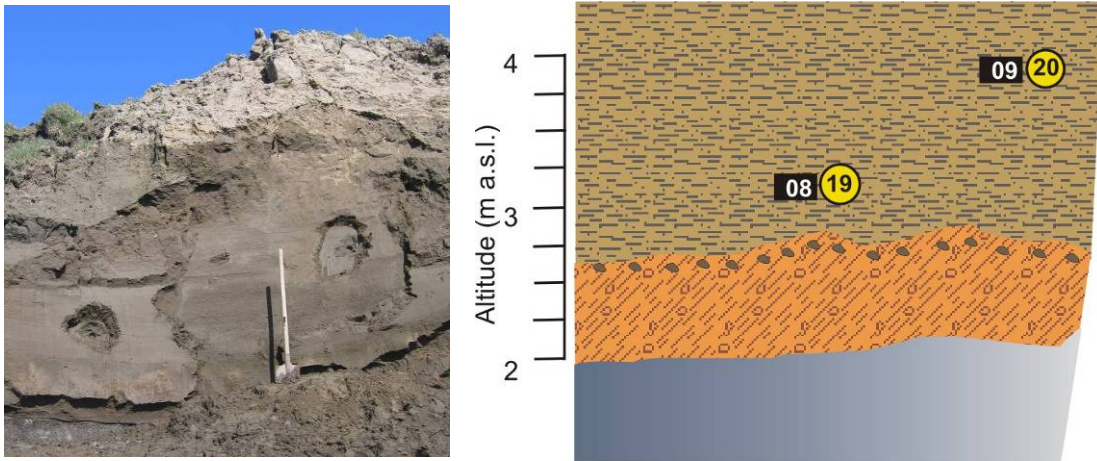


**Figure 4.5.1-7:** OSL sampling site within the Kuchchugui Suite (subprofile L7-01-C). The legend is given in Figure 4.3-1.

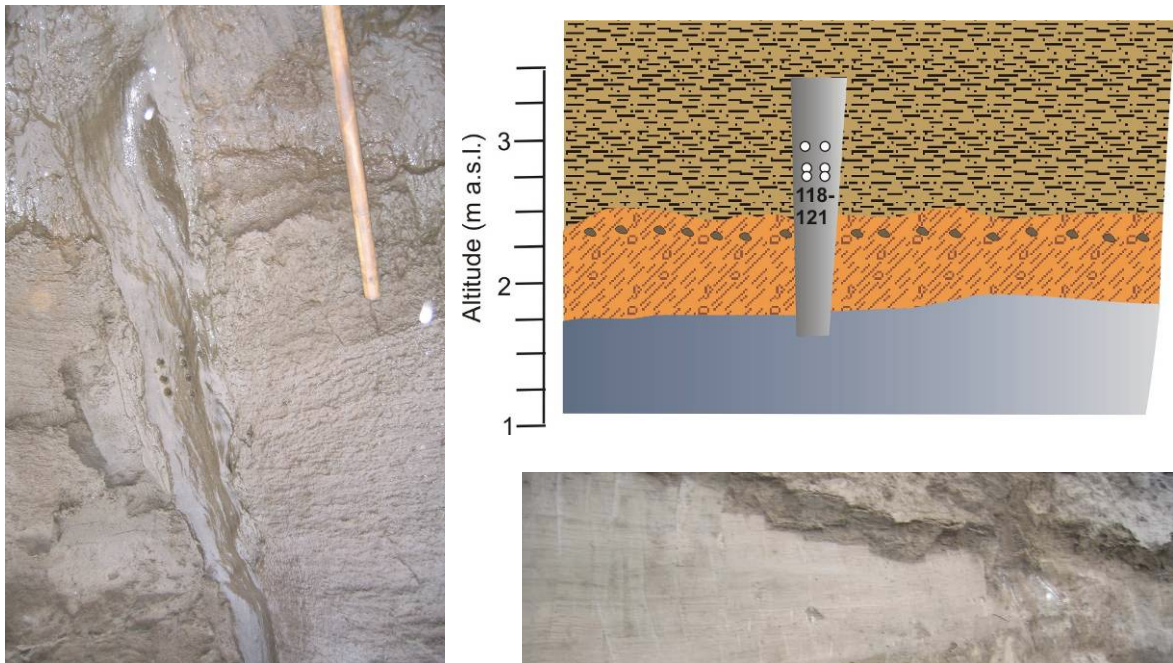


**Figure 4.5.1-8:** The cryoturbated palaeo active layer (Zimov'e Strata) covering the Yukargirsky Suite and an ice wedge of the Kuchchugui Suite above (subprofile L7-01-D). The legend is given in Figure 4.3-1.



#### 4.5.1.3 Exposure L7-02, Yukagirsky ice wedge (12.07.2007)

An about 2 m wide ice wedge of the Yukagirsky Suite was sampled 25 m east of the exposure L7-01 in 10 to 15 cm distance using an ice screw (L7-02-102 to 113 for MSU, L7-02-114 to 116 for AWI Potsdam) and a chain saw (L7-02-101,  $^{36}\text{Cl}/^{10}\text{Be}$  dating). The about 3 m wide ice wedge consisted of non-regular ice veins containing numerous air bubbles and about 1 mm wide sediment laminas. The entire ice wedge was covered by the 0.5 m thick palaeo active layer of the Zimov'e strata (Figure 4.5.2-9).

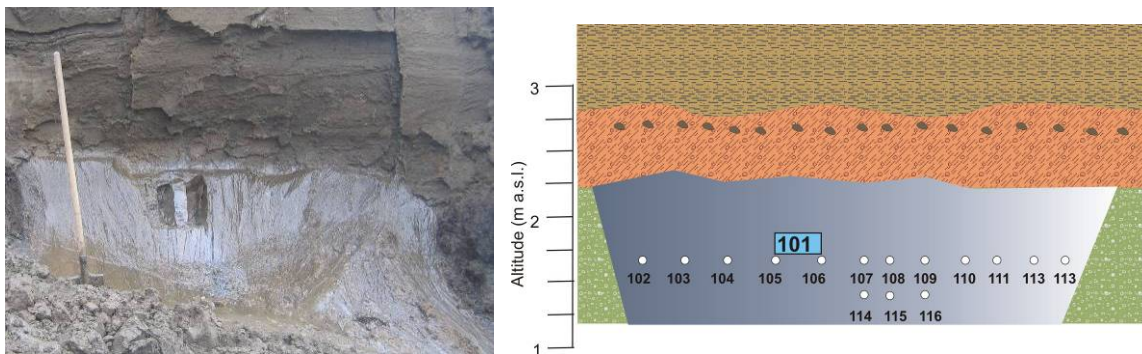


**Figure 4.5.1-9:** Ice wedge of the Yukagirsky Suite covered by palaeo active layer and deposits of the Kuchchugui Suite (subprofile L7-02). The legend is given in Figure 4.3-1.

## 4.5.1.4 Exposure L7-03, Yukagirsky Suite (12.07.2007)

This profile (Figure 4.5.2-10) is characteristic for ice-rich deposits of the Yukagirsky Suite (samples L7-03-01 to 07). Sandy to silty layers alternated with coarse-grained sand to gravel bearing layers. In addition, greyish-brown iron-impregnation zones and peat inclusions were observed there. Ice bands, upwards bended to an ice wedge, and lattice-like cryostructures were typical for this horizon. The gravimetric ice content varied between 50 to 200 wt%. An about 2.5 m wide ice was sampled for stable isotope analyses (L7-03-102 to 109 and for  $^{36}\text{Cl}/^{10}\text{Be}$  dating (L7-03-101). Again, the 0.5 m thick palaeo active layer, described above, covered the entire sequence of ice-rich sediment and of the ice wedge.

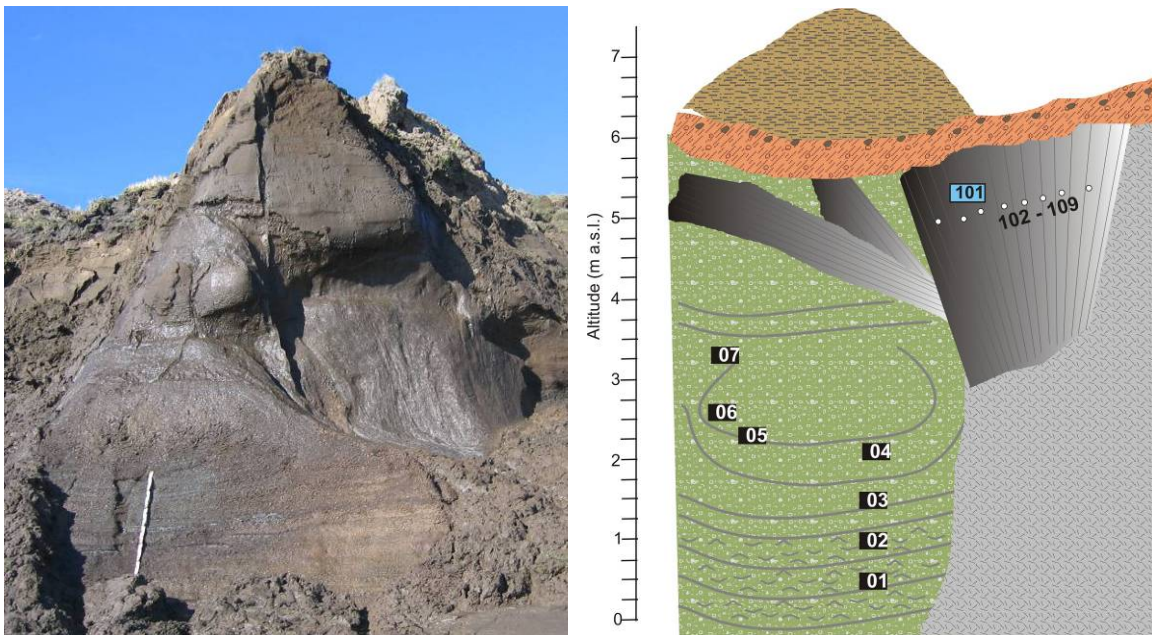


**Figure 4.5.1-10:** Ice-rich deposits and ice wedge of the Yukagirsky Suite (exposure L7-03). The legend is given in Figure 4.3-1.

#### 4.5.1.5 Exposure L7-05, Yukagirsky to Kuchchugui Suite (14.07.2007)

In order to describe more detailed the transition between the Yukagirsky and Kuchchuguy Suites such a sequence was studied in a thermo-erosional ravine about 2 km west of the Zimov'e River mouth. Several large rocks of quartzitic sandstone bedrock were observed at the beach near this site.

In general, the exposure L7-05 (Figure 4.5.1-11) is similar to the previously described exposure L7-01. The deposits of the Yukagirsky Suite consisted of greyish-brown silty sand with gravels (L7-05-01). The cryostructure was coarse lens-like reticulated (grav. ice content 200 wt%). The covering cryoturbated palaeo active layer contained brownish peat lenses and gravels (samples L7-05-03 and 05) as well as large pebbles coated by a crust of white soft clayish material (sample L7-05-04). A layer of linear ordered gravels was observed on top of this horizon. The cryostructure is diagonal lens-like or dotted (grav. ice content 117 to 31 wt%). In addition, a small (5 to 20 cm thick) belt of yellowish, clayish to gravelly sand bent upward between a large peat lens an ice wedge was sampled (sample L7-05-06) 1.5 m a.s.l.. This sediment is considered to be a reworked residue of an old Tertiary weathering crust.

The following samples are characteristic for the Kuchchugui Suite. This greyish-brown sediment was non-regular laminated and contained single gravels and numerous vertical oriented (*in-situ*) thin grass roots (L7-05-07 to 15). The cryostructure is dominantly massive (grav. ice content 34 to 40 wt%). Only several separate ice veins traversed the sediment.

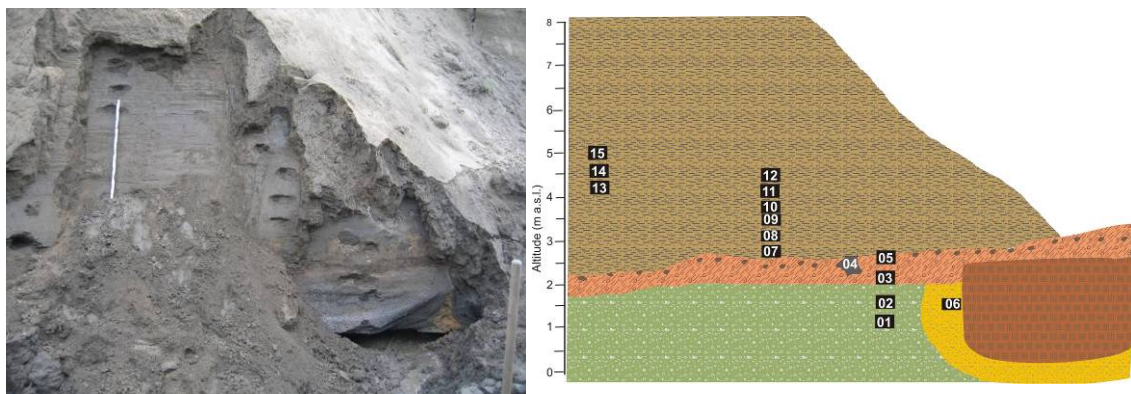


**Figure 4.5.1-11:** Fine-grained deposits of the Kuchchugui Suite cover the palaeo active layer (subprofile L7-05). The legend is given in Figure 4.3-1.

#### 4.5.1.6 Exposure L7-06, Krest Yuryakh Suite

Near the location “Mys Kameny” (Cape of Rocks) well laminated sandy and peat alternate bedding was exposed between about 3 and 5 m a.s.l.. These lake deposits were covered after a small thermo-terrace by ice-rich deposits, containing large ice wedges.



**Figure 4.5.1-12:** Well laminated lake deposits of the Krest Yuryakh Suite (Eemian) exposed at 3 m a.s.l. (exposure L7-06).

#### 4.5.1.7 Exposure L7-18, Yedoma Suite (30.07.2007)

The study of a complete sequence of the ice-rich Yedoma Suite was one of the most important tasks of the field work in 2007. Therefore, using alpinist equipment, a steep wall (Figure 4.5.1-13) of the first thermocirque was selected for more detailed cryolithological and sedimentological observations and sampling in a distance of 0.5 to 1 m. Hopefully, these studies will close the still existing information gap about the upper part of the Yedoma Suite at Bol'shoy Lyakhovsky Island, especially the supposed lack of late Pleistocene Sartan deposits.

During fieldwork, the sequence was classified into several layers, which vary clearly in color, cryostructures and sediment composition (layer 1 to 10). In addition, according to cryolithological features the sequence was separated into eight cryogenic cycles. These are units with rather similar cryostructures. We suppose that such cycles were formed repeatedly under similar surface and subsurface conditions.

The upper part of the section (0 to 0.35 m below surface, m b.s.) included the silty to fine-sand brownish grey active layer. The main part of the section (0.35 to 4.2 m b.s.) was composed of brown to brownish-grey loam (alevrite, silty fine-sand) and often contained peat inclusions of various diameters (5 to 40 cm). The cryostructures was dominantly banded, with thicknesses of separate ice bands of 1 to 5 cm and distances between them of 5-15 cm.

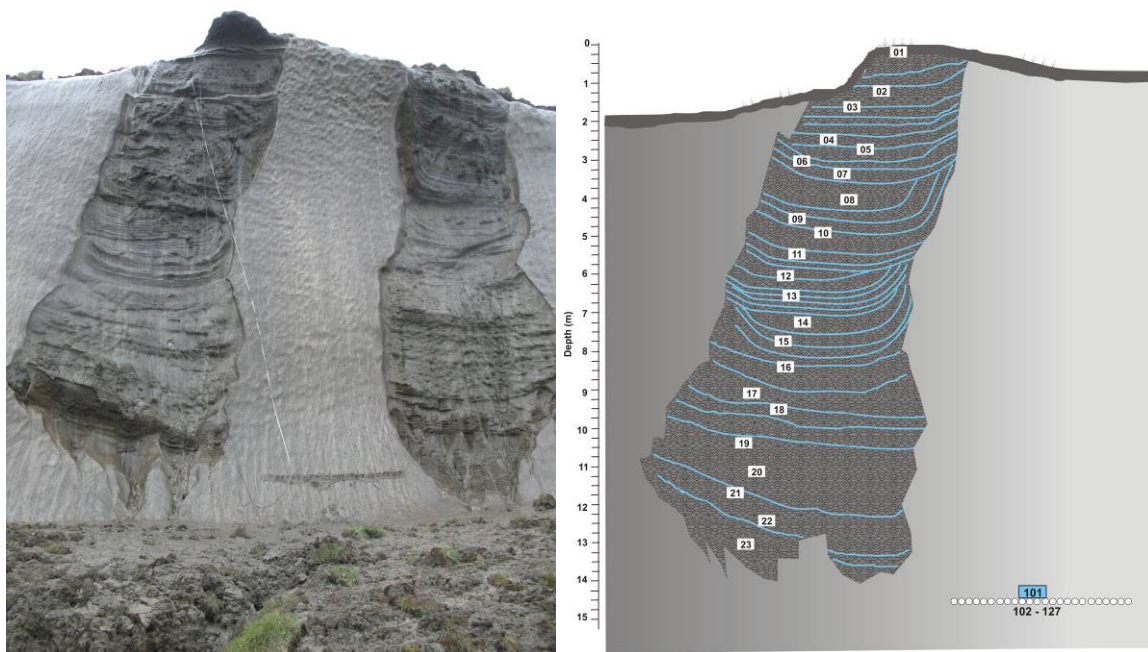


**Figure 4.5.1-13:** Ice Complex deposits of the Yedoma Suite (exposure L7-18). The legend is given in Figure 4.3-1.

## 4.5.1.8 Exposure L7-07 (26.07.2008)

The exposure L7-07 presents another kind of ice-rich deposits of still unclear origin. We supposed that this sequence was formed already in the valley of the Zimov'e River. According to the assumption of V. Tumskey, Sartanian (Late Weichselian) Ice Complex deposits were accumulated only in valley positions (see chapter 4.4). Therefore, sediments and ice wedges were studied and sampled in two subprofiles (L7-07-A and B) and two transects in order to get a comprehensive characteristic of these sequences.

The exposure was located at the western edge of the Zimov'e River mouth directly at the sea beach (Figure 4.5.1-14). The exposure wall was about 10 m high. The lower part was covered by muddy debris up to 2 m a.s.l.. The uppermost part was not accessible because of the very steep wall. Therefore, only the section between 2 and 7 m a.s.l. could have been studied in more detail.



**Figure 4.5.1-14:** Position of the ice-rich sequence of exposure L7-07 at the edge of the Zimov'e River mouth

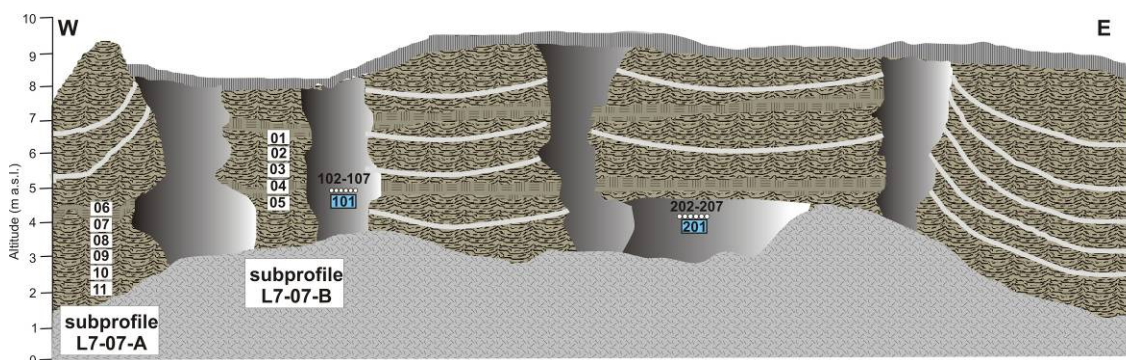


**Figure 4.5.15:** Scheme of the exposure L7-07 with sampling positions. The legend is given in Figure 4.3-1.

In *subprofile L7-07-B* the lowermost layer (2.0 to 2.8 m a.s.l.) consisted of light-brown to grey silty sand containing roots and plant detritus (samples L7-07-10 and 11). The cryostructure was banded with diagonal lenses between ice bands (grav. ice content 35 wt%). Further up in this subprofile (3 m a.s.l.) the sediment color changed to dark-grey (sample L7-07-09) and the cryostructure was coarse lens-like reticulated (grav. ice content 117 wt%). At about 3.5 m a.s.l. a sediment boundary was exposed. The next part between 3.5 m and 5 m a.s.l.

consisted of irregularly bedded light-brown to grey sand/silt alternations (samples L7-07-08 to 06). The cryostructure was fine-lens-like (grav. ice content 87 wt%). Numerous plant remains and peat inclusions were observed there. A peat layer, which continued horizontally through the entire exposure, was sampled in 4.5 m a.s.l. (sample L7-07-06). In the same level, an ice wedge was studied 15 m eastwards for  $^{36}\text{Cl}/^{10}\text{Be}$  dating (sample L7-07-201) and for stable isotope ground ice analyses (samples L7-07-202 to 209).

*Subprofile L7-07-A* started in the same peat horizon at 4.5 m a.s.l. (sample L7-07-05). This sequence was characterized by clear sandy bedding. Fine-grained plant detritus marked the ripple bedding (L7-07-04 to 01). The cryostructure was ice-banded with fine lens-like between ice bands (grav. ice content 56 wt%). The interlayers are also characterized lattice-like cryostructure of thin vertical and diagonal ice veins. In order to compare ice wedges of different generations a younger ice wedge was studied further up at 5 m a.s.l. and samples were taken again for  $^{36}\text{Cl}/^{10}\text{Be}$  dating (sample L7-07-101) and for stable isotope ground ice analyses (samples L7-07-102 to 107). This ice wedge was 1.8 m wide at the sampling position and was exposed about 3 m below the surface level (right ice wedge in Figure 4.5.1-15).

Some additional bones as well as skin remains were found *in-situ* in 2.5 m (position of sample L7-07-01) and 3.5 m a.s.l. (bone samples L707-O3 to O11, see chapter 6.3



**Figure 4.5.1-16:** Upper part of the exposure L7-07, position of subprofile L7-07-A and the upper ice wedge transect for stable isotope ground ice analyses

## 4.5.1.9 Exposure L7-08, Alas Complex (15./25.07.2007)

The last exposure in the stratigraphical sequence of Bol'shoy Lyakhovsky Island covers the sequence of thermokarst deposits within an alas depression, cut by the coastal cliff, which were very well exposed about 4.1 km west of the Zimov'e River mouth. The main objectives of the studies there are the reconstruction of the Late Pleistocene to Holocene transition as well as higher-resolution study of Holocene environmental variations. The general profile of exposure consists of tabular (thawed and refrozen) Ice Complex deposits covered by lake sediments and subaerial boggy deposits. Because of the steep walls and the difficult accessibility this exposure had to be studied again in several subprofiles at different positions (Figure 4.5.1-17) covering the entire sediment sequence.

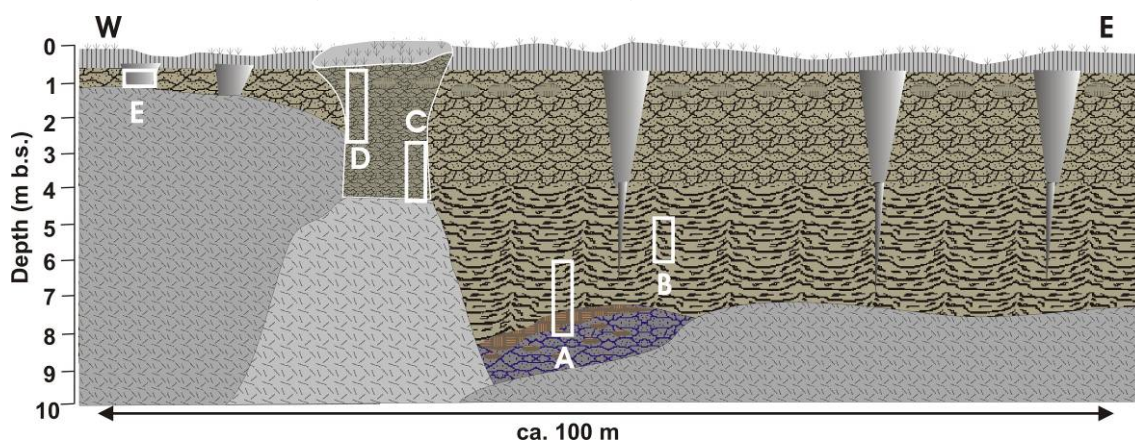


**Figure 4.5.1-17:** General scheme of the alas exposure L7-08 with position of the separate subprofiles. The legend is given in Figure 4.3-1.



**Figure 4.5.1-18:** Exposure situation of the coastal cliff along the thermokarst depression (the photo site is not the exact position of the exposure L7-08)



**Figure 4-5-1-19:** Taberale Ice Complex deposits covered by lake sediments and boggy deposits of a thermokarst depression (left: subprofile L7-08-A, right: subprofile L7-08-B)

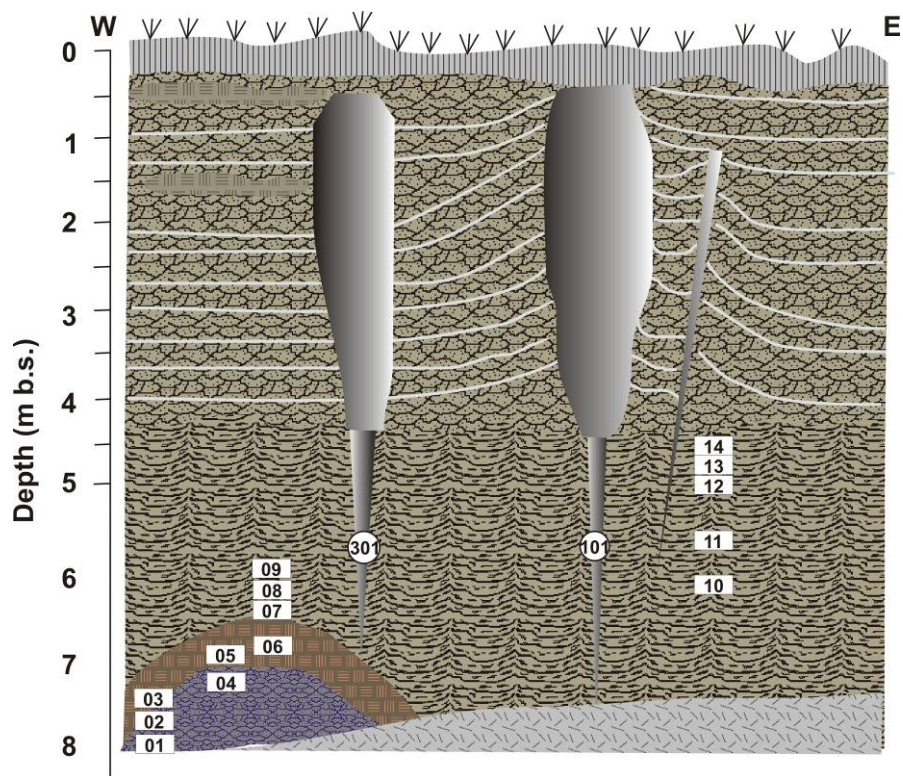


**Figure 4.5.1-20:** Schematic sequence of sediments filling the thermokarst depression underlain by taberale Ice Complex deposits (left: subprofile L7-08-A, right: subprofile L7-08-B). The legend is given in Figure 4.3-1.

The lowermost part of the *subprofile L7-08-A* (Figure 4.5.1.-19/20) consisted of greenish grey silty sand that was interpreted to be thawed and refrozen remains of Ice Complex deposits of the Yedoma Suite containing peat lenses of 5-10 cm length (sample L7-08-01). The cryostructure was coarse-lens-like reticulated. The gravimetric ice content was relatively low (26 wt%). Above this horizon a peaty palaeosol of fresh, less decomposed, light-brown moss peat and a dark-brown peat layer with wood fragments and a silty sandy matrix was exposed (samples L7-08-02 to 07). The cryostructure was net-like to lens-like (ice lenses 4-5 cm long, grav. ice content 38 to 46 wt%). *Subprofile L7-08-A* was covered by dark-grey clayish silt with 2 cm thick dark-grey layer of plant detritus (samples L7-08-08 and 09). The cryostructure was lattice like (distance between ice veins 5-10 cm, grav. ice content 30 wt%). The entire *subprofile L7-08-A* was exposed between 8 m and 6 m below surface.

The *subprofile L7-08-B* continues the sequence about 7 m to the right (east) between 6 m and 4.5 m b.s. (Figs. 4.5.1-19/20). Similar dark-grey clayish-silty probably lake sediment with lattice-like to net-like cryostructure (grav. ice content 42 wt%) composed this part, which was additionally marked by 2 to 3 cm broad brownish zone of iron oxide impregnations along cracks. Small segments of two syngenetic ice wedges were sampled there (samples L7-08-101 and 301).

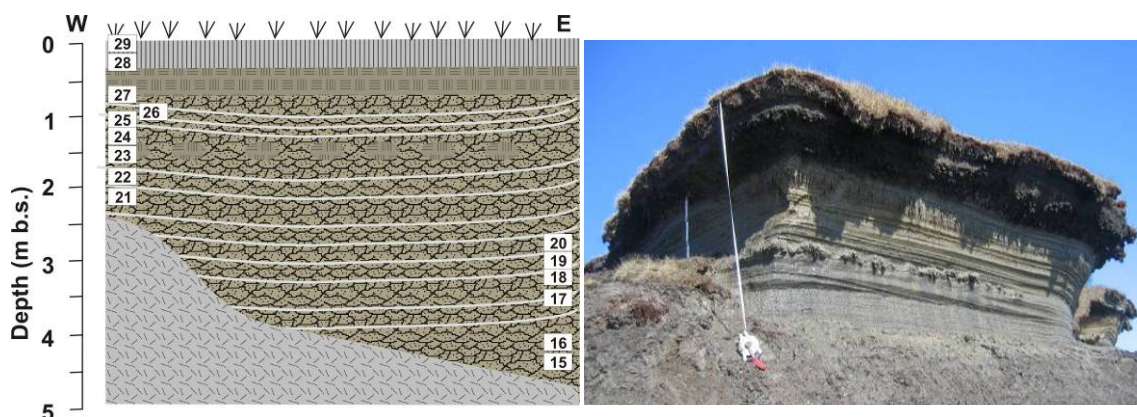


**Figure 4.5.1-21:** Subaerial alas deposits 0 to 4.5 m below surface (right. subprofile C; left: subprofile D). The legend is given in Figure 4.3-1.

The continuation of the alas sequence by the *subprofiles L7-08-C and D* was studied at an exposure opposite of the described subprofiles A and B where the upper segments were accessible between 4.4m b.s. and the surface (Figure 4.5.1-21). The lower part (subprofile L7-08-C, samples L7-08-16 to 20) still consisted of similar grey, clayish silty sediment with iron oxide impregnations along cracks and ice veins. The lattice-like cryostructure consisted of thin ice veins (grav. ice content 45 wt%).

The uppermost segment of the alas complex sequence was characterized by light-brown peat inclusions (10 to 15 cm long) in light grey silty sandy matrix (samples L7-08-22 to 24) reflecting more subaerial accumulation conditions. The cryostructure was banded and lens-like between ice bands (grav. ice content 37 to 74 wt%). Near the surface (1.1 to 0.3 m b.s.) grass roots and peat

layers occurred (samples L7-08-25 to 28) and the cryostructure consisted of diagonal ordered, partly broken ice veins and lenses or of lattice like structures. The uppermost sample was taken from the unfrozen vegetation cover (L7-08.29).

In order to study an typical ice wedge formed in deposits of a thermokarst depression an transect was sampled 1.2 m b.s. by ice screw for isotope studies (L7-08-201 to 212) in *subprofile L7-08-E* (Figure 4.5.1-22). The ice wedge was 2.8 m broad at the transect site. The studied ice wedge consisted of parallel striated, milky-white, bubble-rich ice. Some diagonal ice-filled cracks crossing the ice body were additionally observed. This ice wedge was also sampled for  $^{36}\text{Cl}/^{10}\text{Be}$  dating (sample L7-08-201).

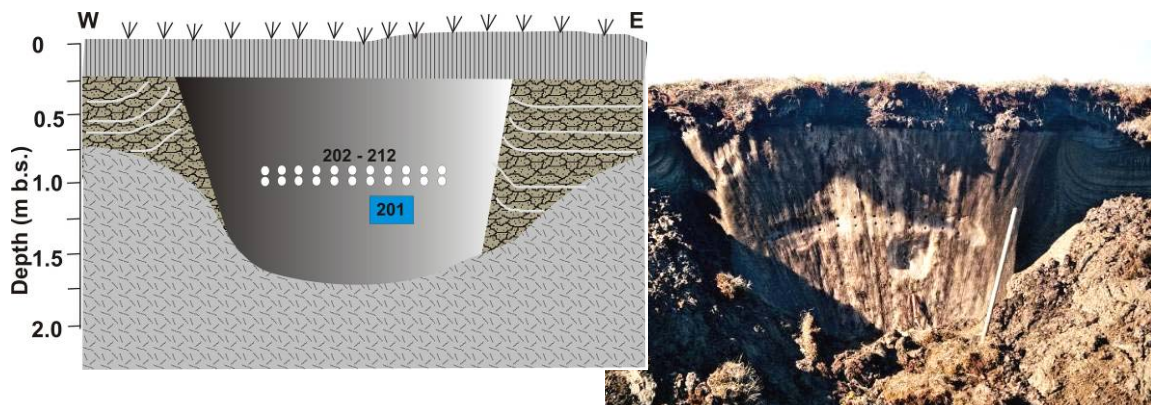


**Figure 4.5.1-22:** Sample position of an alas ice wedge transect (subprofile L7-08-E). The legend is given in Figure 4.3-1.



## 4.5.2 Studies of Middle to Late Pleistocene permafrost sections near the Vankina River mouth

### 4.5.2.1 Exposure L7-12, Kuchchugui Suite (18.07.2007)

The studied sequence was located about 12 km west of the Vankina River mouth directly above the beach level (Figure 4.5.2-1). Typical deposits of the Kuchchugui Suite were exposed there (samples L7-12-01 to 06). The non-regularly bedded, greyish-brown sediments contained small separate ice lenses and numerous thin grass roots. An inclusion of organic-rich material perhaps of a fossil lemming nest was found within these rather uniform deposits. In the upper part of the studied section dark-grey to black spots were observed, which were interpreted as manganese oxide aggregates formed by decomposition of plant residues. Two samples were drilled in 2.0 m (L7-12-07) and 2.9 m (L7-12-08) a.s.l. for luminescence dating. In addition, a narrow ice wedge of 20 to 30 cm width was sampled for stable isotope studies (L7-12-102 to 105) and for  $^{10}\text{Be}/^{36}\text{Cl}$  dating (L7-12-101). Beside some small ice lenses the cryostructure was dominantly massive (grav. ice content 42 to 44 wt%).

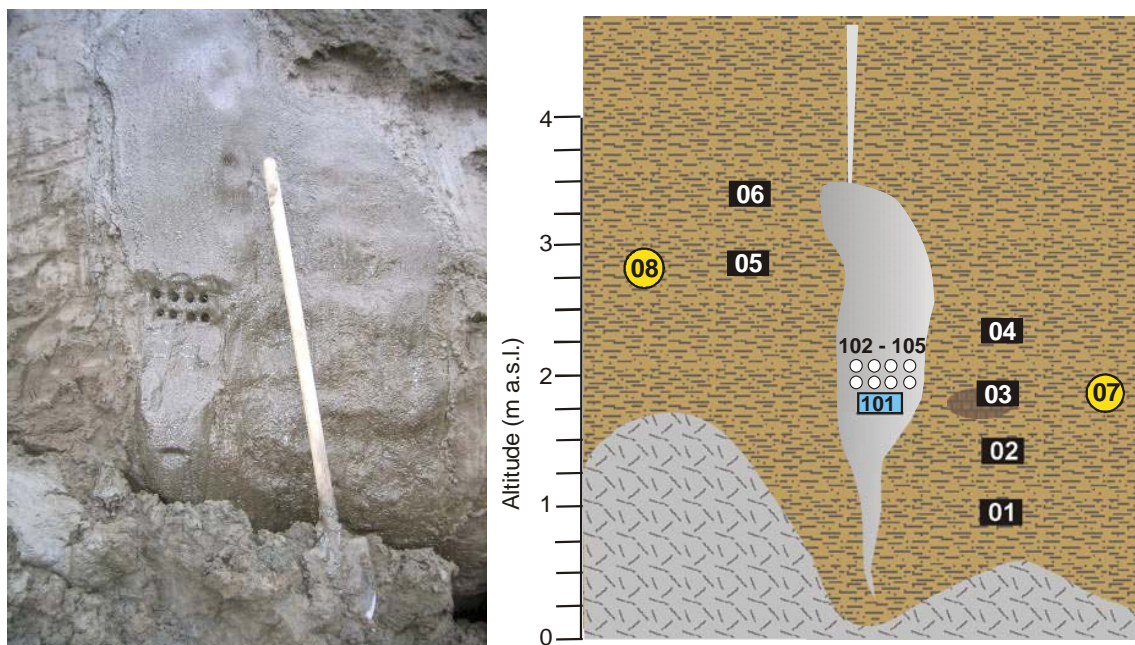


**Figure 4.5.2-1:** Sediment sequence and ice wedge of the Kuchchugui Suite. The legend is given in Figure 4.3-1.

## 4.5.2.2 Exposure L7-14, Kuchchugui to Krest Yuryakh Suite (19./21.07.2007)

Only some hundred meters further west an about 10 m long sequence presented the stratigraphical continuation of the exposure L7-12 that included deposits of the Kuchchugui Suite, the Krest Yuryakh Suite (Eemian), and an ice-rich peat packet of still unclear stratigraphic order. Seven subprofiles (L7-14-A to G) were studied in order to cover the entire sequence in different levels (Figure 4.5.2-2).

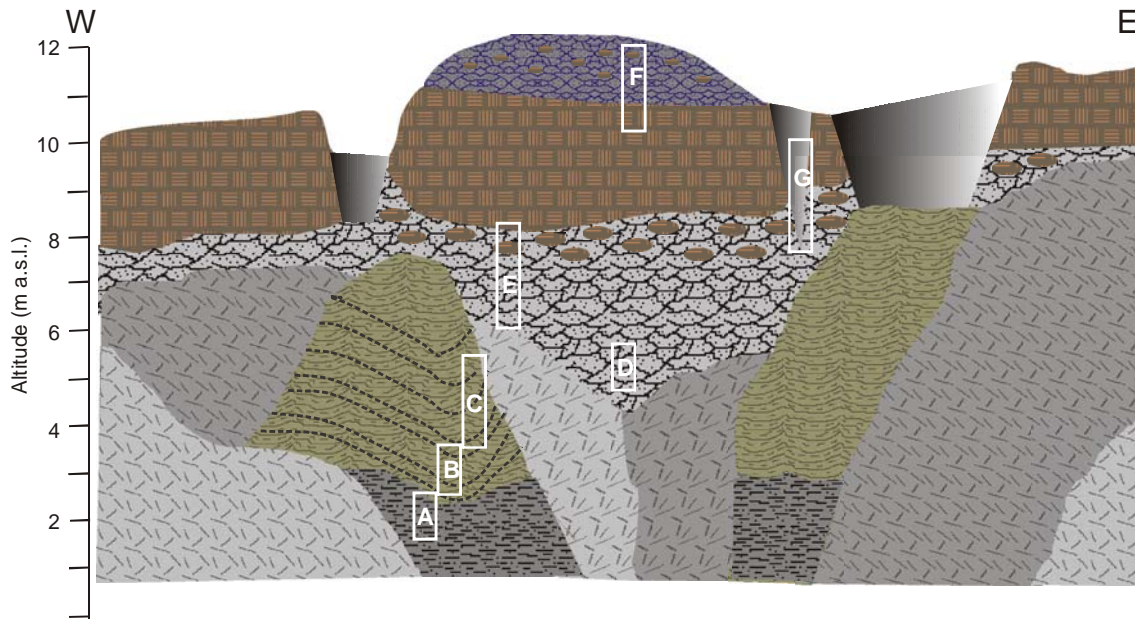


**Figure 4.5.2-2:** Overview scheme of the exposure L7-14 with positions of the sampling sites (details to subprofile L7-14-A to G are shown in Figures 4.5.2-3 to 4.5.2-9). The legend is given in Figure 4.3-1.



**Figure 4.5.2-3:** Overview photograph of exposure L7-14.

The lowermost *subprofile L7-14-A* between 1.5 and 2.5 m a.s.l. (samples L7-14-01 to 03) consisted of grey, irregularly fine-laminated sediment with single white laminas (< 1 mm thick). No plant remains were observed, but numerous small, dark-grey circular spots were visible. The cryostructure was massive (grav. ice content 34 wt %). This subprofile presents thawed and refrozen (taberal) deposits of the Kuchchugui Suite.

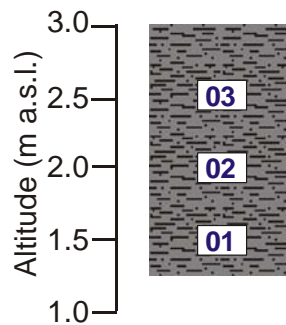


**Figure 4.5.2-4:** Taberale Kuchchugui Suite (subprofile L7-14-A) with sample positions.

A section within an ice wedge cast filled with alternate bedding of peaty brownish plant detritus layers and grey clayish silt layers was exposed between 2.6 and 5.2 m a.s.l. by the next both *subprofiles L7-14-B and C* (samples L7-14-04 to 15). Ripple bedding (ripple 1-2 cm high, 2-5 cm distance), fine laminated layers (each lamina 5-10 mm thick), small-scale synsedimentary slumping structures were very common there. Several layers contained 5-10 mm large mussel shells. Larger twig fragments and peat inclusions of 2-3 cm were also observed. This sequence is considered to represent deposits of the interglacial Krest Yuryakh Suite (Eemian). The cryostructure was dominantly massive. Only single thin ice veins (<1mm thick) were visible parallel to the bedding (grav. ice content 37-44 wt%). Additional OSL-samples were taken in 3 m (L7-14-27) and 5.2 m (L7-14-28) height.

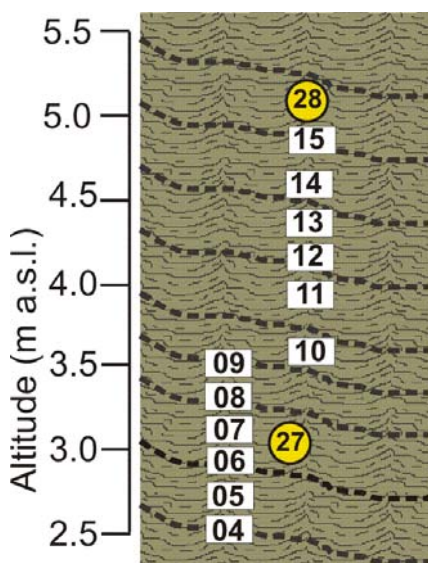


**Figure 4.5.2-5:** Sample positions of the subprofiles L7-14-B and C (Krest Yuryakh Suite).



**Figure 4.5.2-6:** Alternate bedding of peaty plant detritus and silty-sand layers of the subprofile L7-14 B (left) and subprofile L7-14-C (right): lake deposits within an ice wedge cast (Krest Yuryakh Suite, Eemian).

The peaty alternate bedding structures of the ice wedge casts were discordantly covered by more ice-rich deposits, which we could not reach in this position. Similar deposits were exposed by *subprofile L7-14-D* three meters to the right between 4.8 m and 5.5 m a.s.l. (samples L7-14-15 to 19). This sequence presented the transition between laminated lake deposits and weakly bedded ice-rich sediments (grav. ice content 42 to 116 wt%). The latter were characterized by lens-like cryostructure, ice bands, and the occurrence of single twig fragments.

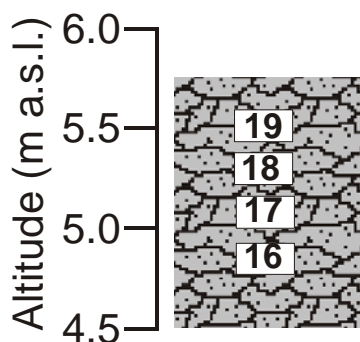


**Figure 4.5.2-7:** Small sequence of ice-rich deposits of subprofile L7-14-D.

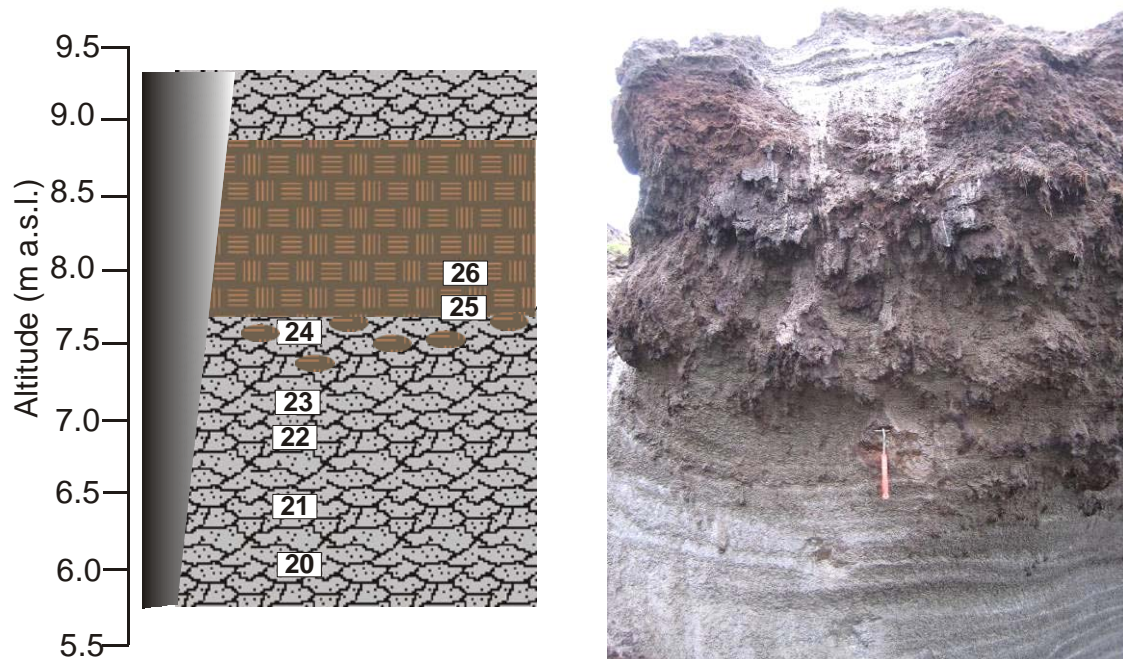


**Figure 4.5.2-8:** Ice rich deposits and frozen peat layer of subprofile L7-14-E. The legend is given in Figure 4.3-1.

The ice-rich sequence of silty sand deposits continued in *subprofile L7-14-E* between 6.2 and 8 m height (samples L7-12-20 to 26) and transformed gradually into a thick peat horizon (Figure 4.5.2-7). The transition horizon contained several large peat inclusions of about 30 cm in diameter. One of these inclusions was additionally sampled for U/Th dating of peat (sample L7-14-24a to 24c, 7.6 m height). The cryostructure was coarse lens-like (grav. ice content 220 wt%). The entire sequence was framed by about 1 m wide ice wedges to the left and to the right, and is therefore considered to be polygon filling. The peat horizon, which appeared homogenous, in fact consisted of numerous large peat lenses embedded in greyish silty sand. Similar thick peaty horizons were also observed several times to the right and to the left at the coast. Therefore it can be concluded that the sequence of interglacial fine laminated lake deposits covered by ice-rich silty sands and a peat layer is of stratigraphic importance. The peat was covered again by ice-rich silty sands that were studied and sampled in another position in subprofile L7-14-F.

Because of the steep exposure wall *subprofile L7-14-F* was sampled only from 12.1 to 10 m a.s.l. above the peat horizon (samples L7-14-29 to 35). This layer of greyish-brown silty sand contained irregular peat inclusions of 10-20 cm in diameter. The cryostructure was banded (2-5 cm thick bands) and coarse lens-like reticulated, reflecting ice supersaturated conditions (grav. ice content 110-185 wt%). The lowest sample of this subprofile (L7-14-35, 9.9 m height) was again taken from the peaty horizon described above. Several vertical veins (1-to 1.5 cm broad, 20 cm long) were observed in 20 cm distance in the upper part of the peat horizon. Two ice veins were sampled for stable isotope studies (L7-14-101 and 102).

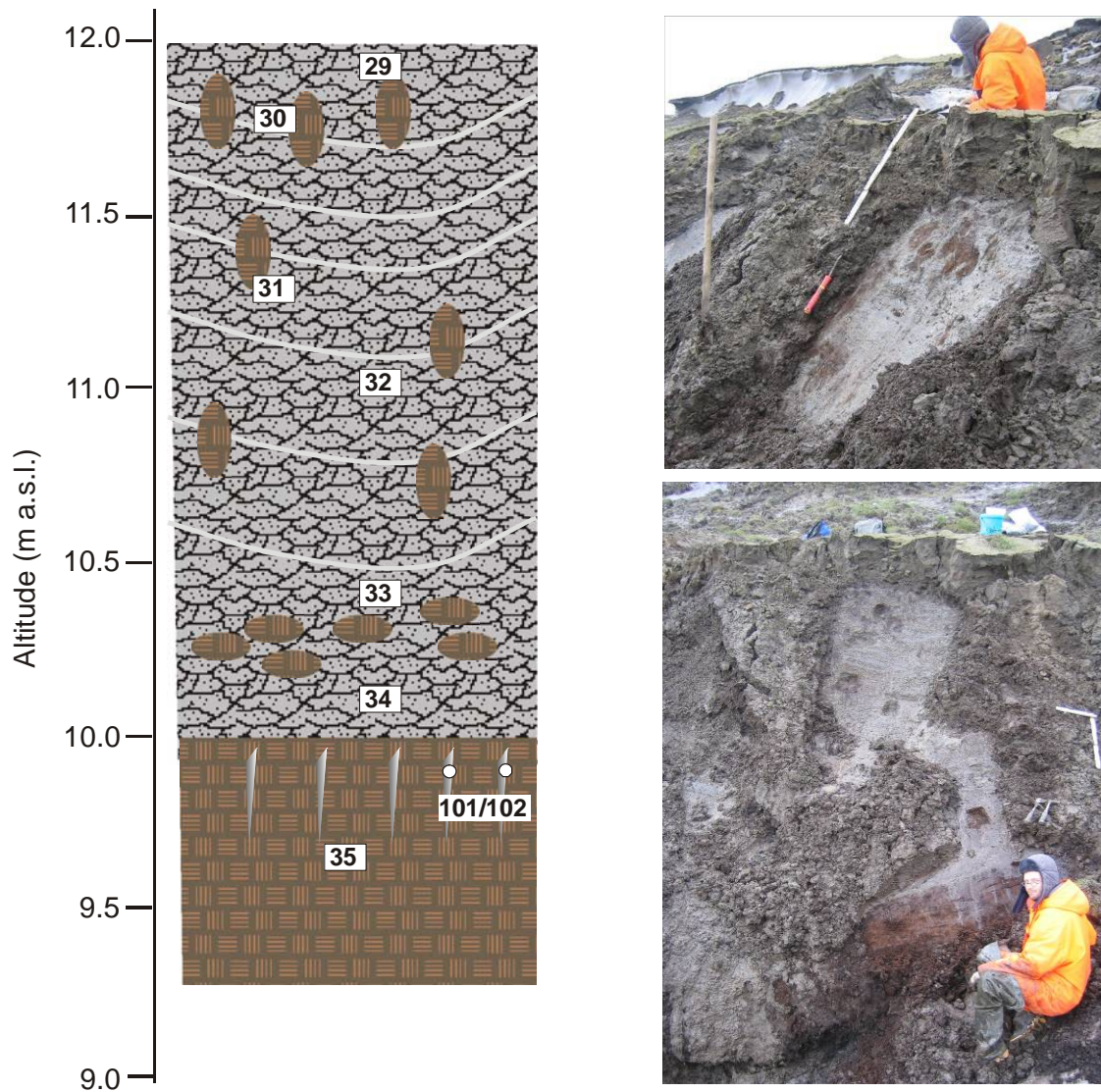


**Figure 4.5.2-9:** The uppermost subprofile L7-14-F was sampled from the thermo terrace below Ice Complex deposits. The legend is given in Figure 4.3-1.

Finally, one of the ice wedges crossing the peat horizon and the ice-rich deposit below was sampled in *subprofile* L7-14-G for  $^{36}\text{Cl}$ -dating (L7-14-201, 8.1 m height) and for stable isotope analyses (L7-14-202 to 204, 8.5 m height). The sampled ice was coarse grained and relatively soft.

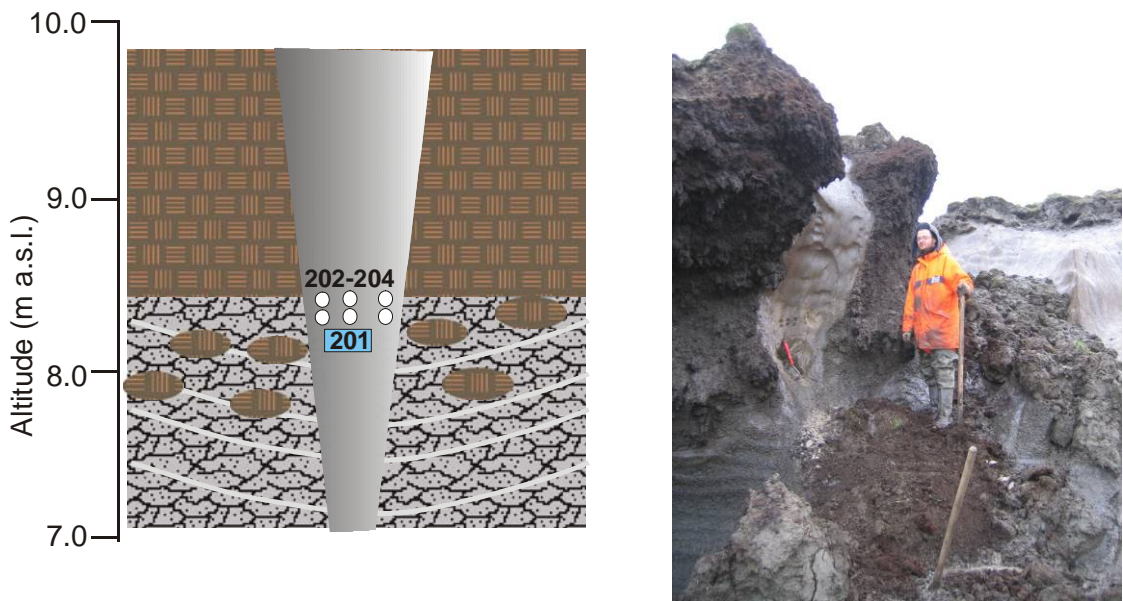


**Figure 4.5.2-9:** Ice wedge crossing the peat horizon (subprofile L7-14-G). The legend is given in Figure 4.3-1.

4.5.2.3 Exposure L7-15, Bychchagy Suite (22.07.2007)

This section was located some hundred meters east of the exposure L7-14. The focus at this site was concentrated on studies of the so-called Bychchagy Suite, an ice-rich sequence, which is characterised by two large peat horizons. Such edges were often observed along the coast between the Vankina and the Zimov'e River mouth (Figure 4.5.2-10).



**Figure 4.5.2-10:** Coast section west of the Vankina River mouth characterised by two edges of peat horizon. The legend is given in Figure 4.3-1..

The exposure L7-15 was studied in two subprofiles and one ice wedge sequence. *Subprofile L7-15-A* covers large parts of this steep cliff from about 12m to 3 m a.s.l.. Most of the samples there were collected from top to bottom by V. Tumskoy using climber equipment. Both peat horizons were sampled for U/Th dating (Figure 4.5.2-11).

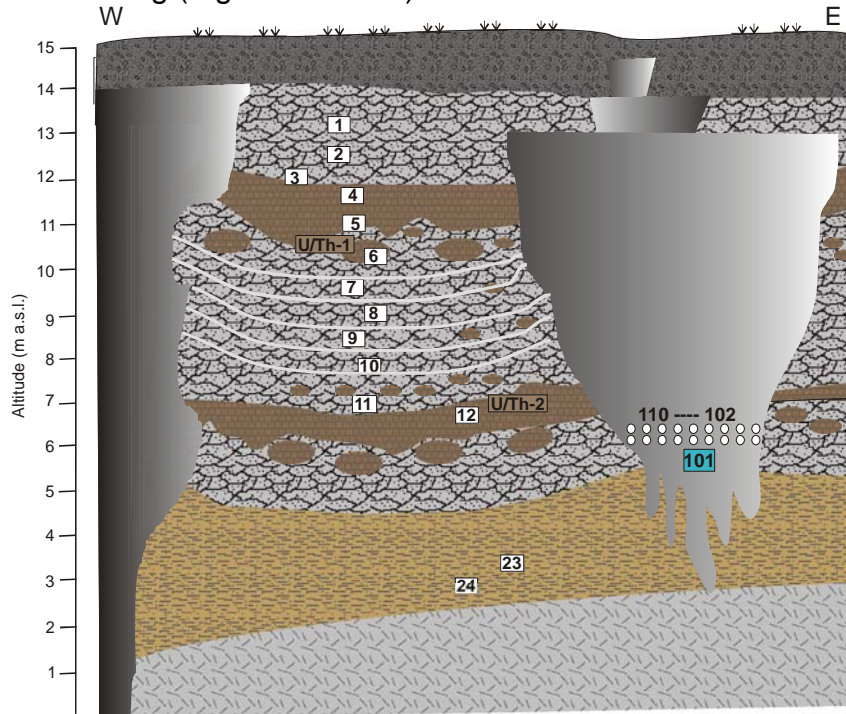


**Figure 4.5.2-11:** Scheme of the subprofile L7-15-A with sampling sites. The legend is given in Figure 4.3-1.



**Figure 4.5.2-12:** Deposits of the Kuchchugui and Bychchagy Suites exposed in subprofile L7-15-A. The legend is given in Figure 4.3-1.

The lower part of the profile exposed between 2 m and 3.5 m a.s.l. was composed of light-grey to brownish irregular laminated fine-grained sand containing numerous grass roots (samples L7-15-24 and -23). Several separate thin peat inclusions (7 x 2 cm) were observed similar to L7-01, which seem to be typical for the Kuchchugui Suite. The cryostructure was massive (grav. ice content 100 wt%).

The Kuchchugui deposits were covered with a sharp contact by an about 1.5 m thick, dark-brown, strongly decomposed dense peat horizon (samples L7-14-12, L7-15-U/Th-2). The peat horizon was composed of large peat inclusions and a greyish silty sand matrix. The cryostructure was dominated by 3-4 cm thick ice bands.

An ice-rich horizon of about 3 m thickness above consisted of non-laminated greyish silty sand. Several peat small lenses existed in the upper zone at about 11 m a.s.l.. The cryostructure was irregular reticulated (sample L7-15-11 to 7). Single ice veins were 1 to 1.5 mm thick and occurred in a distance of 5 to 10 mm. In addition, ice bands of 1 to 3 cm thickness were typical (grav. ice content 70 – 106 wt%).

A second peat horizon exposed between 10 and 11.5 m a.s.l. consisted of numerous dark-brown peat lenses in a matrix of greyish silty sand (samples L7-15-6 to 4, L7-15-U/Th-1). The cryostructure was also banded (1.5 – 2 cm thick, 5-10 cm distance, grav. ice content 54-84 wt%).

Above the second peat horizon silty sand was exposed between 11.5 and 13.5 m a.s.l. that shows a weakly bedding structure and contained rare peat fragments (2-3 mm in diameter) and numerous black spots. These deposits resemble the lower Kuchchugui sediments. The cryostructure was layered and micro lens-like (grav. ice content 38 wt%). The small lenses (2 mm thick, 5-15 mm long) were often arranged in stripes.

The sequence is finished by loamy deposits of a thermoerosional valley, which could not be sampled because of the very steep wall.

One of the two large ice wedges framing the exposure was sampled for stable isotope studies (samples L7-15-102 to 110) as well as for <sup>36</sup>Cl dating (sample L7-15-101).

In order to study the transition from the Kuchchugui Suite to the first peat horizon of the Bychchagy Suite (Figure 4.5.2-13), which was inaccessible in the first subprofile we found a second *subprofile* L7-15-B only some hundred meters east of L7-15-A between 7 to 5 m a.s.l.. Light-brown fine-grained sand with grass roots and massive cryostructure (grav ice content 48 wt%) composed the lower (Kuchchugui) part of this subprofile at about 5 m a.s.l. (samples L7-15-22 and 21). Upwards the ice content was rising (grav. ice content 60-110 wt%). The cryostructure was fine lens-like. The sediment consisted of light-brown greyish silty sand without bedding and grass roots (samples L7-15-20 to 18). Lenses of fresh (light-brown) peat (10 x 15 cm) surrounded by greyish silty sand belonged to the upper peat horizon (samples

L7-15-17 to 15). The cryostructure was coarse lens-like reticulated and banded (grav. ice content 146 and 225 wt%).

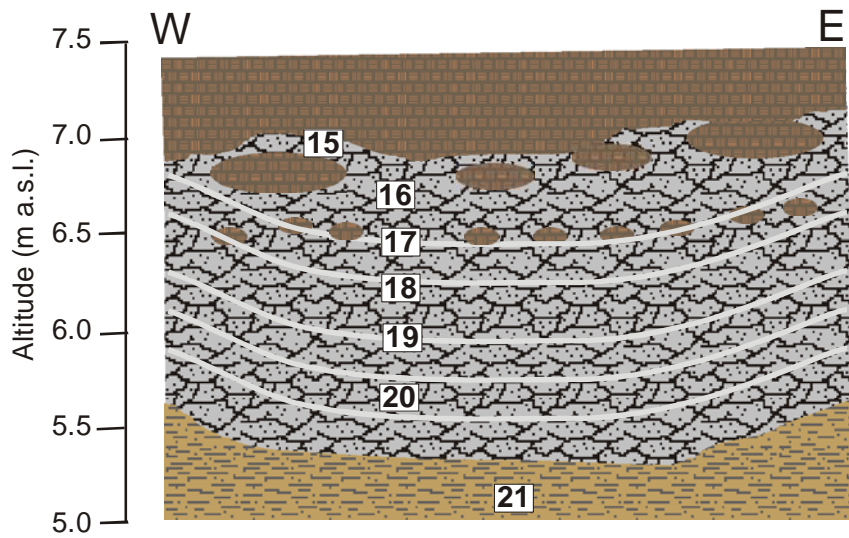


**Figure 4.5.2-13:** Sequence from the Kuchchugui Suite to the first peat horizon of the Bychchagy Suite (subprofile L7-15-B). The legend is given in Figure 4.3-1.

### 4.5.3 Studies of permafrost sections east of the Zimov'e River mouth

#### 4.5.3.1 Exposure L7-11, Krest Yuryakh Suite (27.07.2007)

A well-exposed ice wedge cast of probably Eemian origin could be studied in two subprofiles in a kind of thermo-well, an about 6 m deep hole surrounded by steep walls (Figure 4.5.3-1). The *subprofile L7-11-A*, between 3 m and 5 m a.s.l., consisted of greyish-brown, fine-laminated probably lacustrine deposits (samples L7-11-01 to 05) that contained plant remains and shells. The cryostructure was dominantly massive (grav. ice content 27 wt%), but several thin ice veins were observed. In contact to the ice wedge cast the cryostructure changed to lattice-like diagonal ice veins.

*Subprofile L7-11-B* between 3.7 and 5.4 m a.s.l. was taken vertically through the ice-wedge cast (samples L7-11-06 to 12). The entire sequence consisted of alternate bedding of plant detritus layers partly with wood fragments and fine-laminated silty sand layers with ripples. The cryostructure was lens-like to layered (grav. ice content 30-39 wt%). Ice veins were > 2 mm thick and several cm long.

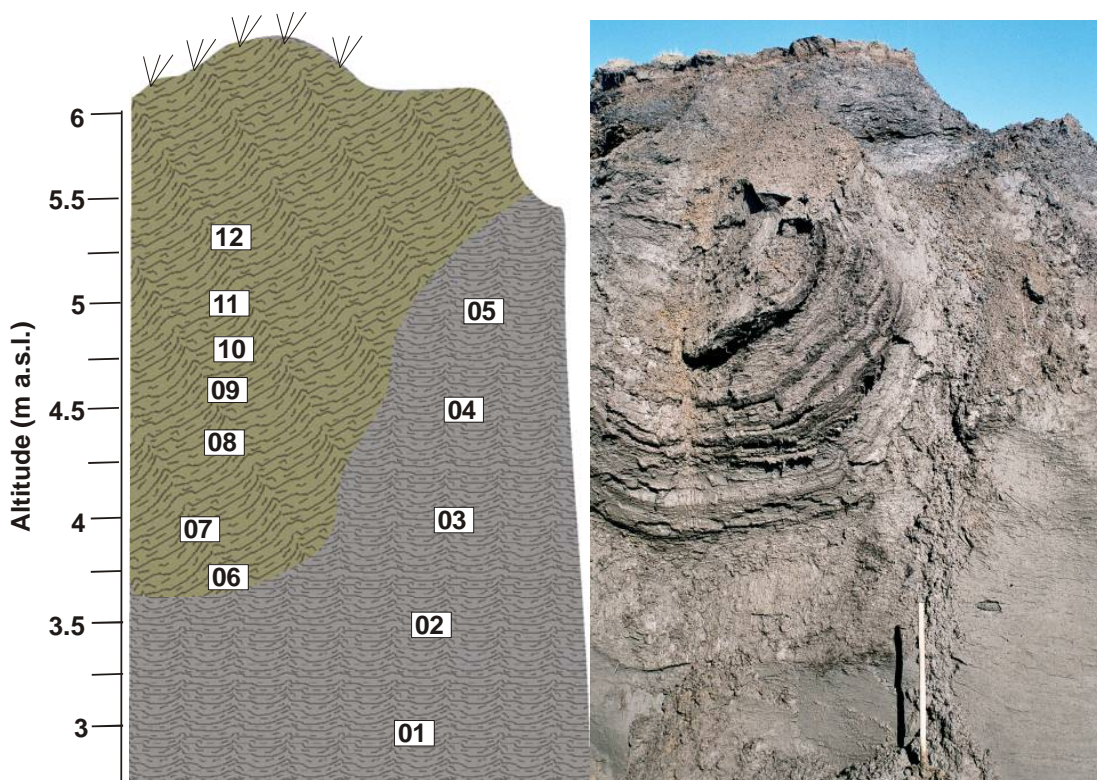


**Figure 4.5.3-1:** Ice wedge cast in lacustrine deposits of the Krest Yuryakh Suite. The legend is given in Figure 4.3-1.

#### 4.5.3.2 Exposure L7-16, taberal Bychchagy (?) Suite to Krest Yuryakh Suite (27./28.07.2007)

The main focus of studying this exposure were deposits, which underlain an ice wedge cast of the Krest Yuryakh Suite. That was interpreted by V. Tumskey as "doubled-taberated" Bychchagy Suite (see chapter 4.4). Especially a horizon of two peaty layers outcropping at the cliff wall could be characteristic for this sequence. The general stratigraphic situation was comparable with the exposure L7-14 (chapter 4.5.2.2). The samples were taken from above to below, but the description here is in stratigraphic order.

The lowermost *subprofile* L7-16-C between 5 to 6 m a.s.l. was composed of dark-grey silty sand with peat inclusions and plant remains (samples L7-16-14 and 13), followed by a yellowish-brown weakly bedded sand (L7-16-12) and a peaty horizon with light-grey silty sand matrix. The cryostructure changed between lens-like layered and massive (grav. ice content 30 to 38 wt%). Peat inclusions of this horizon were 10-20 x 5-10 cm large (sample L7-16-09). Two unfrozen samples were collected for botanical analyses (L7-16-10 and 11).

*Subprofile* L7-16-B covered the section directly below the ice wedge casts. The sediments consisted of grey to dark-grey silty sand partly coloured by light-brown iron oxide impregnations and contained plant detritus (sample L7-16-04). The cryostructure was diagonal, lattice-like and broken (grav. ice content 27 wt%). From the peaty layer below a frozen sample (L7-16-05) and an unfrozen sample (L7-16-06) were taken. This layer consisted of light-brown inclusions of moss peat (10-20 x 5-10 cm) in a non-bedded greyish silty sand matrix. The cryostructure was coarse lattice-like with 1-2 mm thick ice veins in a distance of 3-4 cm. This subprofile ended in the bottom part of the ice wedge cast (sample L7-16-08) were grey, fine-laminated silty sand alternates with brownish plant detritus layers. This part was also impregnated by iron oxide and showed a coarse lattice-like cryostructure (grav. ice content 27 wt%).

The uppermost *subprofile* L7-16-A was taken from a side part of the ice wedge cast, which was composed of alternate bedded fine-laminated silty sand layers and plant detritus layers (samples L7-16-01 and 02) and underlain by a layer of peat inclusions (sample L7-16-06). The ice wedge cast contained numerous relatively large (2-4 cm in diameter) wood fragments, which were collected in an additional sample (L7-16-Holz). Ice veins were observed surrounding wood fragments (grav. ice content 36 wt%).

The studied sequence was finally covered by alas deposits, which were only observed from afar but not sampled because of the steep wall there. This section was characterised by thick peaty horizons, ice-rich layers and separate ice wedges (Figure 4.5.3-2). A fragment of a mammoth bone was found within the debris left of the study site (sample L7-16-O12)

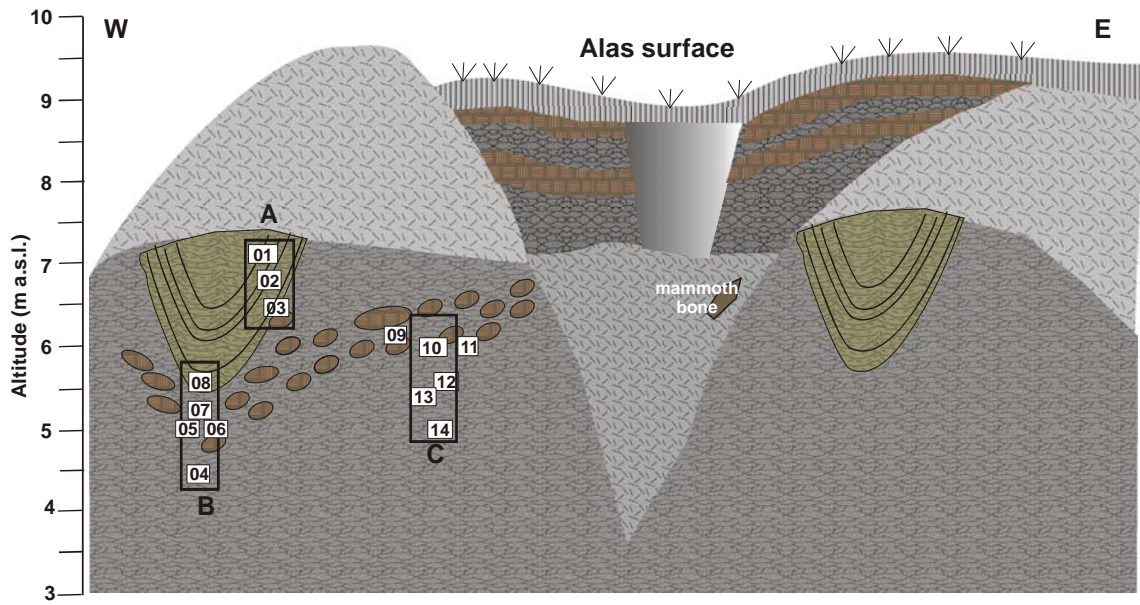


**Figure 4.5.3-2:** Ice wedge casts of the Krest Yuryakh Suite underlain by tabular deposits of the Bychchagy Suite. The legend is given in Figure 4.3-1.



**Figure 4.5.3-3:** Exposure situation of L7-16 with outcropping peaty layers

#### 4.5.4. Stratigraphic conclusion from the studied sequences

Finally, we try to combine the observation of all sequences to a preliminary stratigraphic scheme, which also include the still unclear stratigraphic positions of several units. The stratigraphic terms were used corresponding to Tumskoy & Basilyan (2006), where a new stratigraphic order for the exposed Quaternary profile of Bol'shoy Lyakhovsky Island is presented.

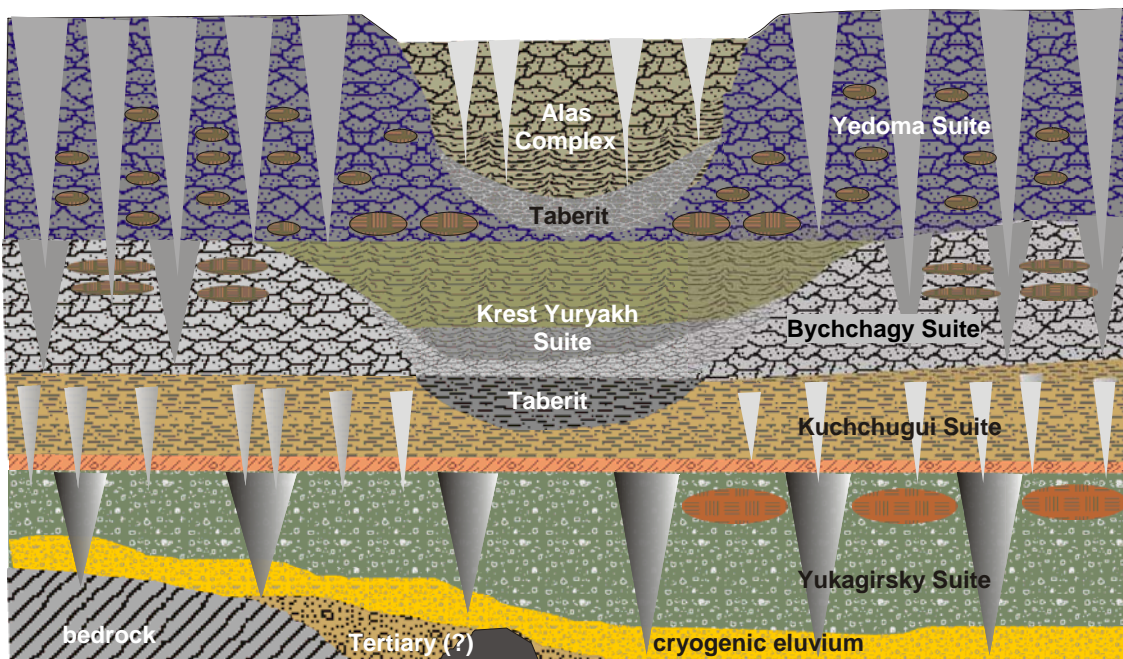


**Figure 4.5.4-1:** General stratigraphic scheme concluded from the studied exposures on Bol'shoy Lyakhovsky Island. The legend is given in Figure 4.3-1.

The observed section starts with massive quartzitic sandstones that outcrop only at the beach 3 km west of the Zimov'e River mouth (Kamennyi Mys). Fragments of similar rocks were observed within the ice-rich deposits of the Yukagirsky Suite. Remains of a Tertiary clayish weathering crust probably periglacially reworked (cryogenic eluvium) were repeatedly exposed as upward banded layers at the contact to large ice wedges of the Yukagirsky Suite (L7-15). In addition, coaly and sandy fluvial deposits of probably Tertiary age were exposed further inland (L7-17).

The ice-rich sequence of the Yukagirsky Suite is characterized by segments with large peat lenses and wide ice wedges, ice-banded and lens-like reticulated cryostructures reflecting syncryogenic formation of ice wedges and deposits, and a cover horizon of a palaeo active layer, which sharply cut both ice wedges and sediment sequences. This layer, named Zimov'e strata is a good indicator of the lower stratigraphic unit because it is widespread on top of the Yukagirsky Ice Complex (L7-01, L7-02, L7-03). The main characteristics of the Zimov'e strata are the brownish-yellowish colour, frequently observed cryoturbation structures and especially a layer of gravels and larger rock fragments in the upper part of this layer.

Totally different in sediment and cryostructure are the deposits of the Kuchchugui Suite. They are characterised by rather low ice contents, massive cryostructures, a non-regular lamination, and numerous vertical *in-situ* grass roots. Small ice wedges occur in the lower part of the Kuchchugui sequence, which penetrate into the underlain large ice wedges of the Yukagirsky Suite (L7-01, L7-05)

A further ice-rich (Ice Complex) unit named Bychchagy Suite is marked by two peat horizons, which outcrop hundreds of meters along the coast, and by large ice wedges. These deposits were underlain by sediments of the Kuchchugui Suite (L7-15).

Indicators of permafrost degradation were observed within the Krest Yuryakh Suite due to the occurrence of lake sediments with mollusc shells and cross- and fine-laminated structures as well as numerous ice wedge casts. The latter are composed of alternately bedded silty sand and plant detritus layers (L7-14, L7-11). The Krest Yuryakh Suite is considered to be a formation of the Eemian interglacial. As a result of permafrost degradation taberal deposits, which were derived from the Kuchchugui Suite or perhaps from the Bychchagy Suite existed below the Krest Yuryakh Suite. Such taberites are characterised by low ice contents and dense sediments, and frequent black spots originated from decomposed plant remains (L7-14, L7-16).

The large sections of the described sequence were often covered by ice-rich (Ice Complex) deposits of the Yedomia Suite. This upper part of the Quaternary sequence is well-exposed in numerous thermo-erosional cirques or thaw slumps. Steep and high walls, long ice wedges, ice banded and lens-like reticulated cryostructure of ice-supersaturated deposits are the most important features of the Yedomia Suite (L7-18). This unit often starts with peat-rich layers, which are exposed in thermokarst mounds (baydzherakhs) at the thermo-terrace below the ice wall.

The stratigraphic composition and relations between the Krest Yuryakh Suite and the surrounding units are complicated. Probably not all of the units were accumulated at all places. Maybe in some places the Kuchchugui Suite is only covered by the Bychchagy Suite (L7-15). The Ice Complex of the Bychchagy Suite could also pass into the Ice Complex of the Yedomia Suite without clear visible differences and boundaries. In other places the existence of Eemian lake deposits resulted in transformations of the underlain deposits to taberites. In such cases non-transformed deposits of the same unit could also surround the Krest Yuryakh Suite in higher positions.

Lake deposits and boggy formations of the Alas Complex close the stratigraphic succession. The Alas Complex is underlain by taberal deposits of the Yedomia Suite. Lake deposits consist of more clayish sediments, contain again some mollusc shells and show a lattice-like cryostructure. Only thin ice wedges of probably epigenetic origin penetrate the lake deposits. The ice wedges change to a broader appearance and a syngenetic character in the covering boggy sediments. These youngest deposits were formed in an ice wedge polygon

system at the bottom of alas depressions and contain numerous peat inclusions and peat layers.

## 4.6 Palaeoenvironmental studies on the Oyogos Yar coast

*Lutz Schirrmeister, Sebastian Wetterich, Viktor Kunitsky, Vladimir Tumskoy, Dimitry Dobrynin, Alexander Derevyagin, Thomas Opel, Frank Kienast, Tatyana Kuznetsova and Alexander Gorodinski*

### 4.6.1 Geographical characteristics and introduction

*Alexander Derevyagin*

The coast named “Oyogos Yar” is located in the northern part of the wide Yana-Indigirka lowland and extends from the Cape Svyatoy Nos to the mouth of Kondrat’eva River along the south side of the Dmtrii Laptev Strait (boundary zone of Laptev Sea and East-Siberian Sea). “Oyogos” is Yakutian name for foal edge. Most of the investigations were concentrated in the eastern part of Oyogos Yar close to the Kondrat’eva River (Figure 4.6.1-1).

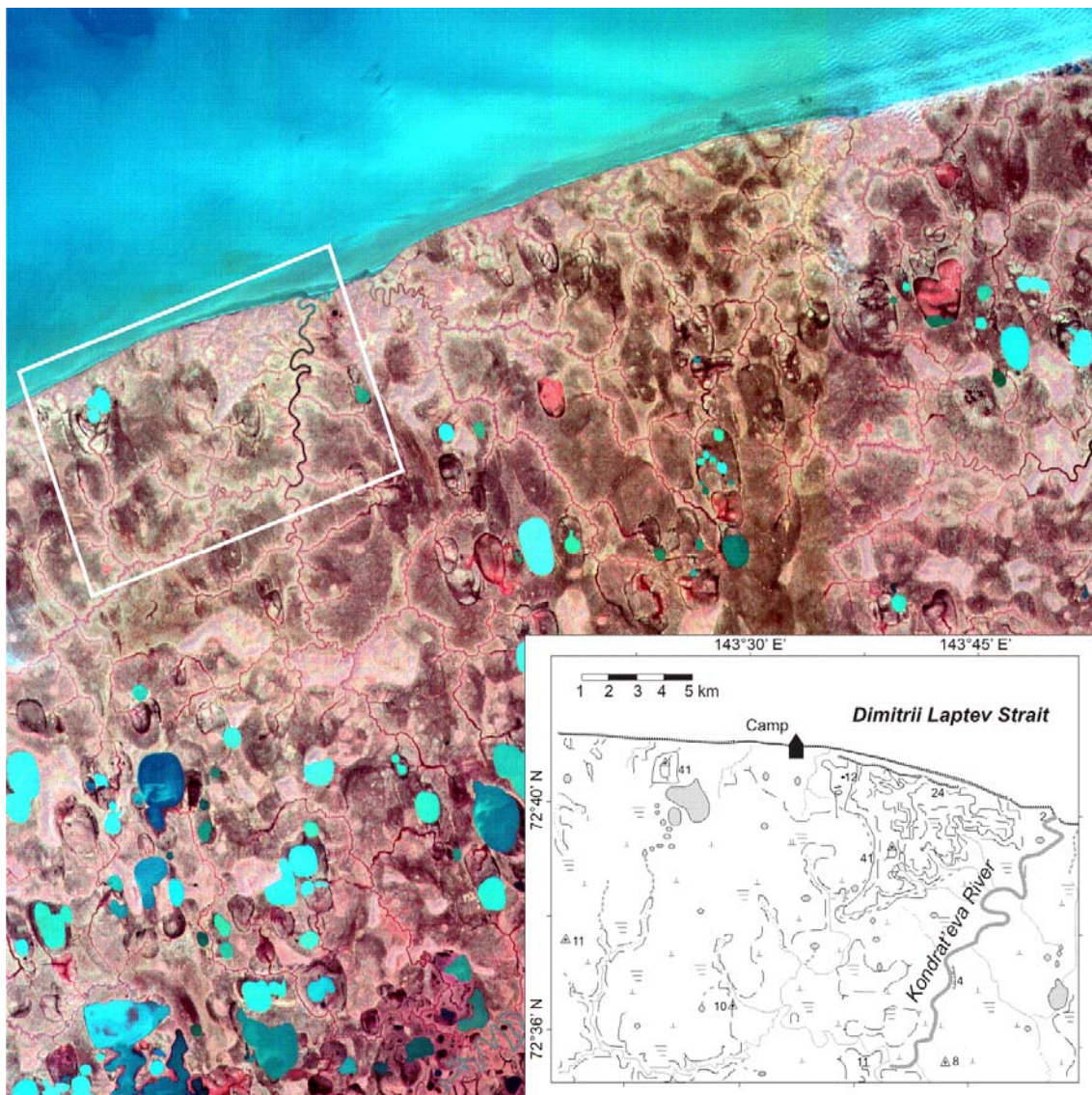


**Figure 4.6.1-1:** Study area west of the Kondrateva River. (satellite image, SPOT 24.07.2007)

The climate of the region is characterized by long severe winters and short rainy and cold summers. The nearest meteorological stations are located at Cape Shalaurova, Cape Kigilyakh (Bol'shoy Lyakhovsky Island) and Cape Svyatoy Nos. The available meteorological data covers the period from 1929 to 1986 (with some gaps). The mean annual air temperature in the region is about -15.0 to -15.5°C. The mean winter air temperature is close to -21.6°C and the mean summer air temperature is about 1.6°C. The warm period (with daily air temperature > 0°C starts in the first decade of June and finishes in the second or third decade of September. There are about of 150-200 mm of annual precipitation, more than 60% is precipitated in summer. Snow begins to accumulate in September-October and reaches a maximum depth in spring. The mean thickness of snow cover is not more than 20-25 cm. Snow patches in August were observed only in deep cracks along the coastal cliff.

There is specific tide regime due to wind direction and speed observed in the region. Strong eastern winds during summer usually initiated wide ebb tides. Sometimes the regression of sea reaches ca. 1 km to the north. In contrast western winds lead to sea level rising. During this period deep wave cut niches (ca. 5-10m) in the bottom part of coastal cliff can form.

The region belongs to the zone of continuous permafrost with the thickness about of 400-600 m. The mean annual ground temperature is about -12 to -14°C (Yershov, 1989). Mean thickness of active layer is about 30-40 cm.

The modern relief is characterized by alternation of wide thermokarst depressions (alases) and hills of Ice Complex remains – so called “Yedoma”. The alas depressions reach about 5-10 km in diameter and have a flat surface with numerous ponds, small valleys (creeks, brooks, ovrags) and nets of polygon systems (size ca. 10-20 m). The height of alas bottoms along the coast is about 8-12 m a.s.l.. The maximum height of Ice Complex hills is about 37 m a.s.l.. The remains of Ice Complex have flat slopes where solifluction occurred as well as steep ice walls (height ca. 15-20 m) where huge ice wedges and frozen ground columns are exposed along the coast.

Because of the larger group in August the research tasks were more separated to smaller subgroups. The mapping of larger coastal sections was realized using a rubber boat by V. Tumskoy and D. Dobrynin, sometimes during trips of several days. The entire mapped section of about 100 km length reach from the Kondrateva River mouth east of the main study area to Cape Syatoy Nos to the west (see chapter 4.4.5).

In order to summarize our actual stage of knowledge with all the partly different opinions and observations during field work we present the various stratigraphic interpretations and some additional general schemes of several sections. If there are various stratigraphic interpretations this will be underlined in the corresponding figure captions.

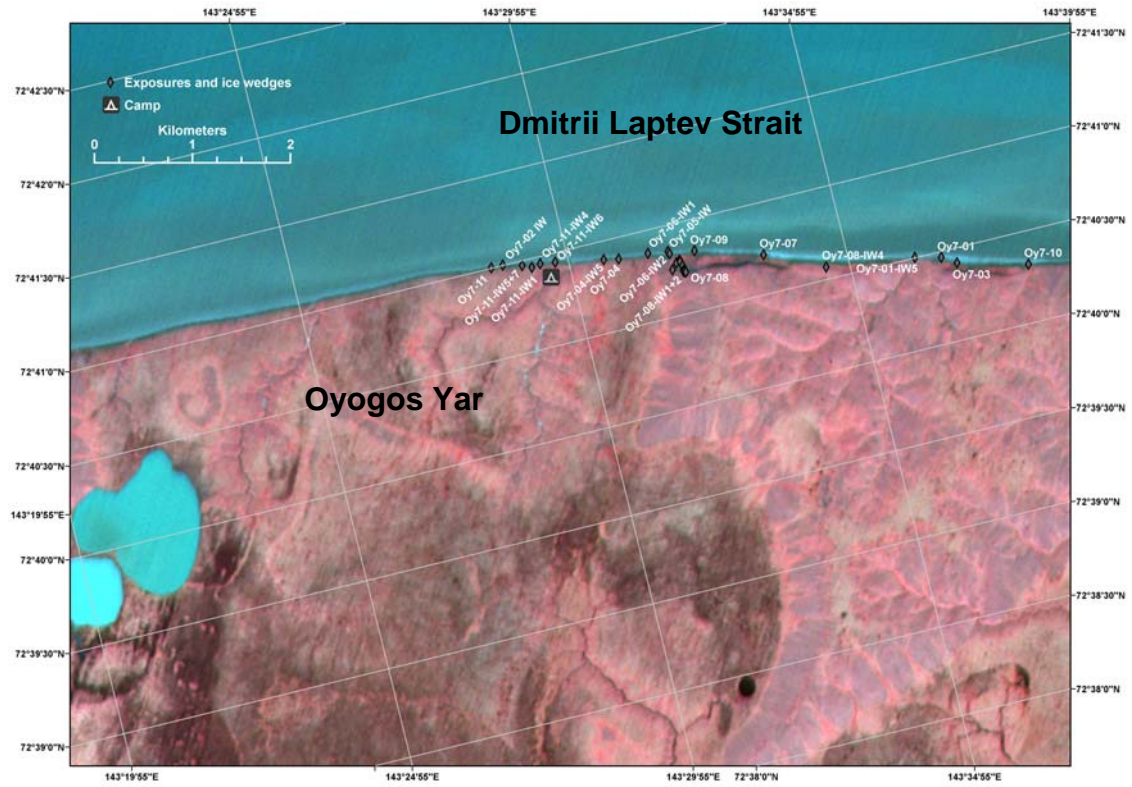


**Figure 4.6.1-2:** Distribution of the studied exposures presented in the following chapters along a 5 km coastal segment of Oyogos Yar. (satellite image, SPOT 24.07.2007)

#### 4.6.2 Studies of Eemian (Krest Yuryakh Suite) and pre Eemian (Kuchchugui, Bychchagy Suite) sections

*Lutz Schirrmeister, Sebastian Wetterich, Viktor Kunitsky and Alexander Derevyagin*

##### 4.6.2.1 Exposure Oy7-01, Krest Yuryakh to Bychchagy Suite (06./09.08.2007)

Three lower subprofiles probably exposed a sequence of Eemian lake deposits, which were covered by ice-rich deposits.

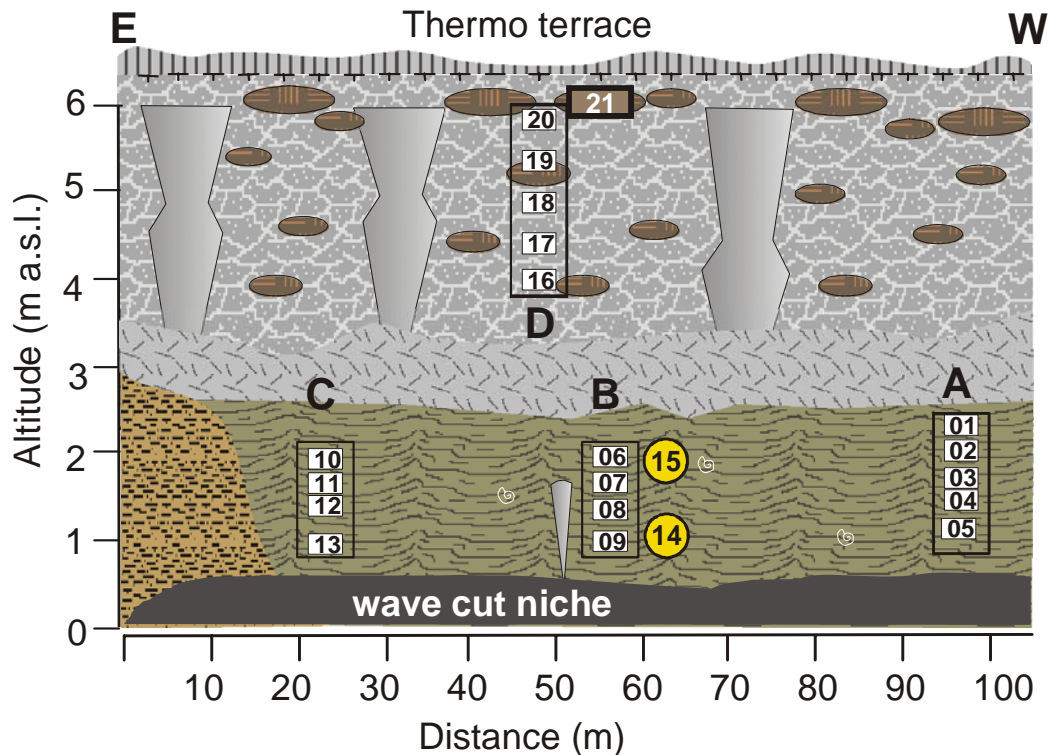


**Figure 4.6.2-1:** Lacustrine deposits of the Krest Yuryakh Suite covered by ice-rich deposits (exposure Oy7-01). The legend is given in Figure 4.3-1.



**Figure 4.6.2-2:** Exposure situation of Oy7-01; The lacustrine sequence is covered by ice-rich deposits

*Subprofile Oy7-01-A* consisted of dark-grey silt with mussel shells. No bedding was visible. The cryostructure was coarse lens-like reticulated in the lower part and fine lens-like reticulated in the upper part (grav. ice content 23 to 34 wt%). In the lowermost sample (*Oy7-01-05*) light-brownish iron oxide coats were observed on cracks.

About 40 m further east *subprofile Oy7-01-B* exposed dark-grey silt that alternated with light-brown plant detritus layers. These deposits also contained mollusk shells. The cryostructure was again fine lens-like reticulated in the upper part and coarse-lens-like reticulated in the lower part (grav ice content 23 to 36 wt%). Two samples for luminescence dating (*Oy7-01-14* and *15*) were drilled at 1.2 m and 1.9 m a.s.l.

The *subprofile Oy7-01-C* consisted of alternated bedded grey-brown silty clay and plant detritus layers or inclusions (1 x 0.5 cm) and contained wood fragments. A lot of plant detritus was also fine-distributes in silty layers. Mollusk shells were not observed there. The cryostructure varied from ice lenses parallel to the bedding, small diagonal ice lenses and coarse lens like reticulated (grav. ice content 34 to 43 wt%). The about 100 m long section is interpreted to be a succession of a fossil lake margin.



**Figure 4.6.2-3:** The subprofile *Oy7-01-A* (right), *Oy7-01-B* (middle), and *Oy7-01-C* (left)

The covering ice-rich deposits were studied in *subprofile Oy7-01-D*, which was exposed between 4 to 6 m a.s.l. The greyish-brown silty sand contained ice bands of up to 5 cm thickness that changed with sediment interlayers of coarse lens-like cryostructure. The gravimetric ice content varied between 97 and 113 wt%. In the uppermost part at about 6 m a.s.l. a peat soil covered the ice-rich sequence. From this horizon an additional sample (*Oy7-01-21*) was taken for U/Th dating. This sampled peat lens of 0.3 m thickness and 1 m length was subdivided into three subsamples (A, B, C).



**Figure 4.6.2-4:** The covering ice-rich sequence of subprofile Oy7-01-D (left) and the site of the uppermost sample Oy7-01-21 (peat lens for U/Th dating)

The studied exposure was stratigraphically interpreted in two different versions by V.V. Kunitsky (Figure 4.6.2-5). In version A and B deposits of the Kuchchugui Suite were affected by aquatic conditions of the Krest Yuryakh period forming taberites and ice wedge casts. In version A this part is covered a small horizon of ice-rich deposits of the Bychchagy Suite. In version B the covering horizon consists of peat and other subaerial aerial deposits that were formed during the silting up of the Krest Yuryakh (Eemian) lake. In both cases this section was covered by Ice Complex deposits.

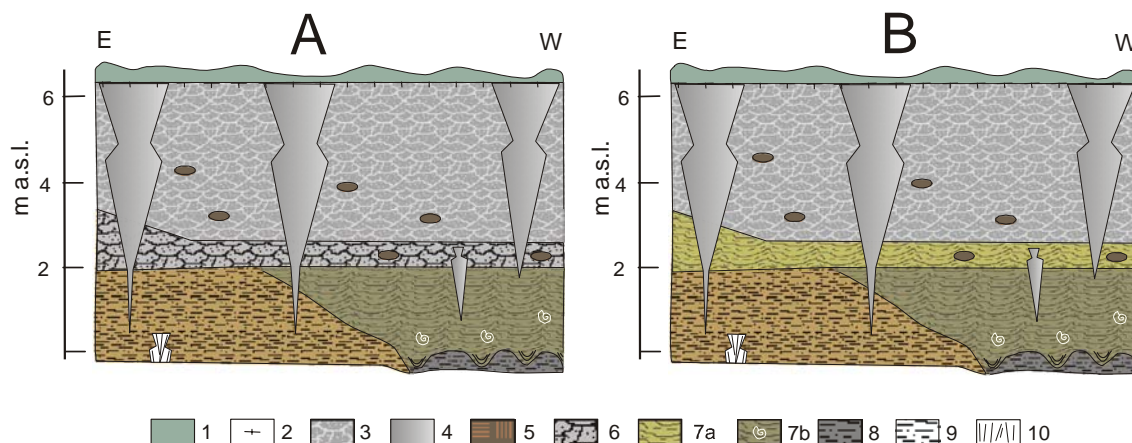


**Figure 4.6.2-5:** Two various stratigraphical interpretations of the above-presented exposure (according to V.V. Kunitsky)

1- active layer (loam with grass roots), 2- lower boundary of the active layer, Ice Complex deposits: 3- grey loam, in situ grass roots, ice bands, 4- dirty (grey) ice wedge, 5- inclusions of autochthonous peat; deposits of the Bychchagy Suite: 6- dark-grey loam, hydrophyte remains, shrub twigs, lens-like reticulated cryostructure, ice bands; deposits of the presumed Krest Yuryakh Suite: 7a- dark-grey loam, hydrophyte remains, shrub twigs, lens-like reticulated cryostructure, ice bands (bog and subaerial facies); deposits of the Krest Yuryakh Suite: 7b- bluish-grey loam with fragments and complete shells fill ice wedge casts (aquatic facies), massive cryostructure (ice cement); deposits of the Kuchchugui Suite: 8- bluish-grey loam, the cover is affected by the formation of the ice wedge casts (taberit transformation in talik deposit), 9- yellowish grey sandy loam, in situ grass roots, ice cement, 10- composite ice-ground wedge (polosatic)

## 4.6.2.2 Exposure Oy7-03, Kuchchugui to Bychchagy Suite (08.08.2007)

The probably oldest deposits of the Oyogos Yar section were studied at the exposure Oy7-03 about 300 m east of Krest Yuryakh outcrop Oy7-01. The first *subprofile* Oy7-03-A (Figure 4.6.2-6 and Figure 4.6.2-7 left) exposed at 0.5 to 1.0 m a.s.l. light-brown, fine-grained sand that contains several flat peat inclusions as well as numerous thin grass roots. No bedding was visible. The cryostructure was massive (grav. ice content 43 to 53 wt%). These features are typical for deposits of the Kuchchugui Suite as described on Bol'shoy Lyakhovsky Island. For this reason an additional sample (Oy7-03-07) was drilled for luminescence dating there. The lower horizon was covered by more ice-rich silty sand (grav. ice content 140 wt%) with ice bands of 1 to 2 cm thickness in 10 to 15 cm distance and higher in 5-10 cm distance. The cryostructure was coarse lens-like reticulated with broken ice lenses of about 1 mm thickness. At about 2.0 m a.s.l. this subprofile was characterized by a peat soil horizon. Brown peat inclusions (5 to 30 cm in diameter) of weakly decomposed moss peat were surrounded by a grey silty sand matrix. The cryostructure was coarse lens-like (grav. ice content 219 wt%). Ice bands of 1-2 cm thickness in 5 cm distance penetrated the peat inclusions.

The second *subprofile* Oy7-03-B (Figure 4.6.2-6 and Figure 4.6.2-7 right) was studied between 7 and 9 m a.s.l. at a thermokarst mound above. This exposure reflects a typical Ice Complex sequence with a peaty soil horizon of grey silty sand with light-brown less decomposed peat inclusions (5-10 in diameter) and larger dark-brown stronger decomposed peat inclusions of 10-30 cm in diameter in a greyish plant detritus bearing matrix. The cryostructure was fine lens-like (grav. ice content 230 wt%) with several ice bands of 1 cm thickness. The later did not penetrate the peat inclusions.

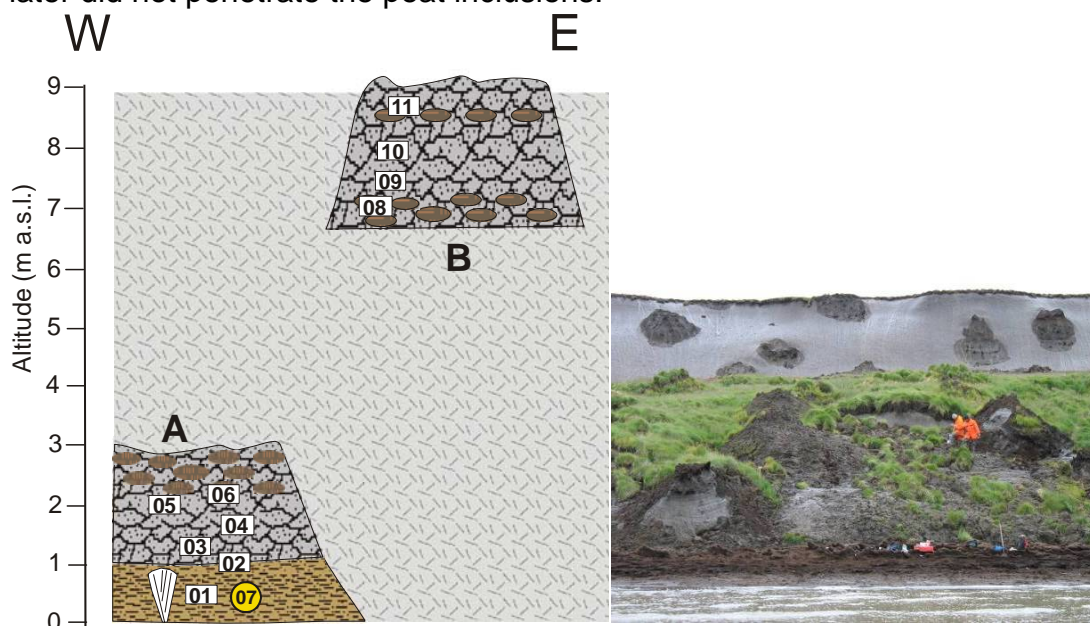


**Figure 4.6.2-6:** Exposure situation and stratigraphic scheme of the exposure Oy7-03. The legend is given in Figure 4.3-1.



**Figure 4.6.2-7:** The subprofile Oy7-03-A (left) with a composite ice-ground wedge in Kuchchugui deposits and subprofile Oy7-03-B (right) with a thick peat horizon

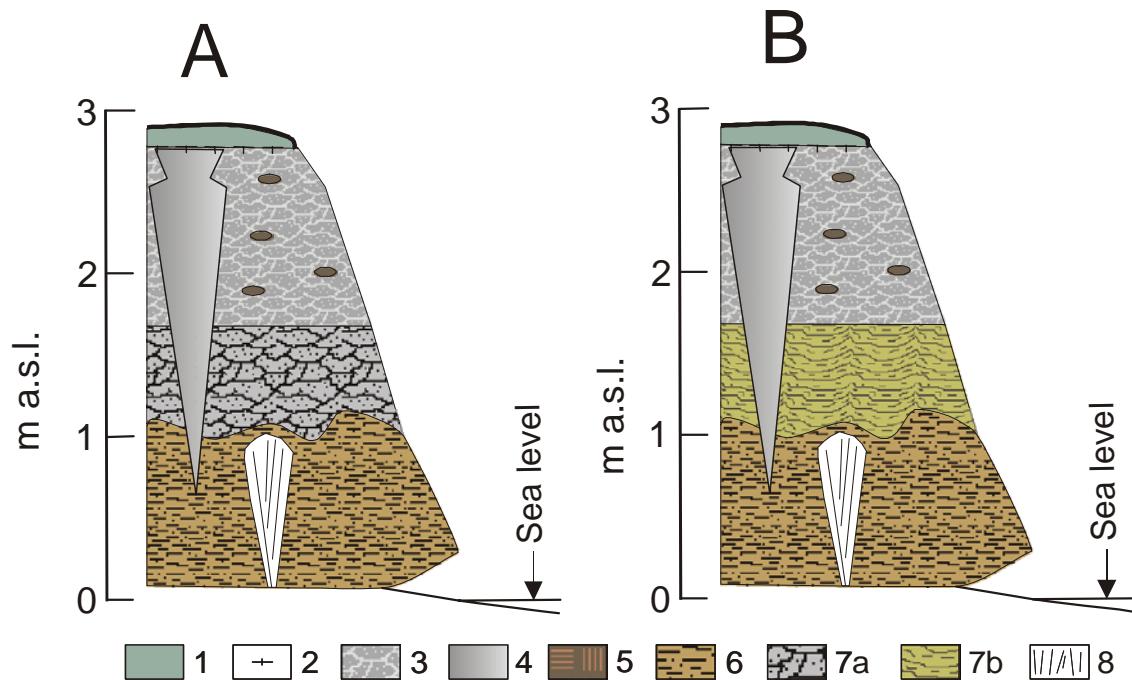


**Figure 4.6.2-8:** Two various stratigraphical interpretations of the above-presented exposure (according to V.V. Kunitsky)

1- active layer (loam with grass roots), 2- lower boundary of the active layer, Ice Complex deposits: 3- grey loam, in situ grass roots, ice bands, 4- dirty (grey) ice wedge, 5- inclusions of autochthonous peat; deposits of the Kuchchugui Suite: 6 brown loam, in situ grass roots, ice cement; deposits of the presumed Bychchagy Suite: 7a- dark-grey loam, ice bands; deposits of the presumed Krest Yuryakh Suite: 7b- grey loam, ice bands; 8- composite ice-ground wedge (polosatic)

The studied sequence is assumed to be representative for the pre Eemian to Eemian transition. According to the stratigraphic interpretation of V.V. Kunitsky (Figure 4.6.2-8) there are two ideas that differ in the stratigraphic position of the horizon covering the Kuchchugui Suite deposits. In version A this horizon was

interpreted as deposits of the Bychchagy Suite and in version B as the lowermost part of the Krest Yuryakh Suite.

4.6.2.3 Exposure Oy7-09, Kuchchugui to Krest Yuryakh Suite (09.08.2007)

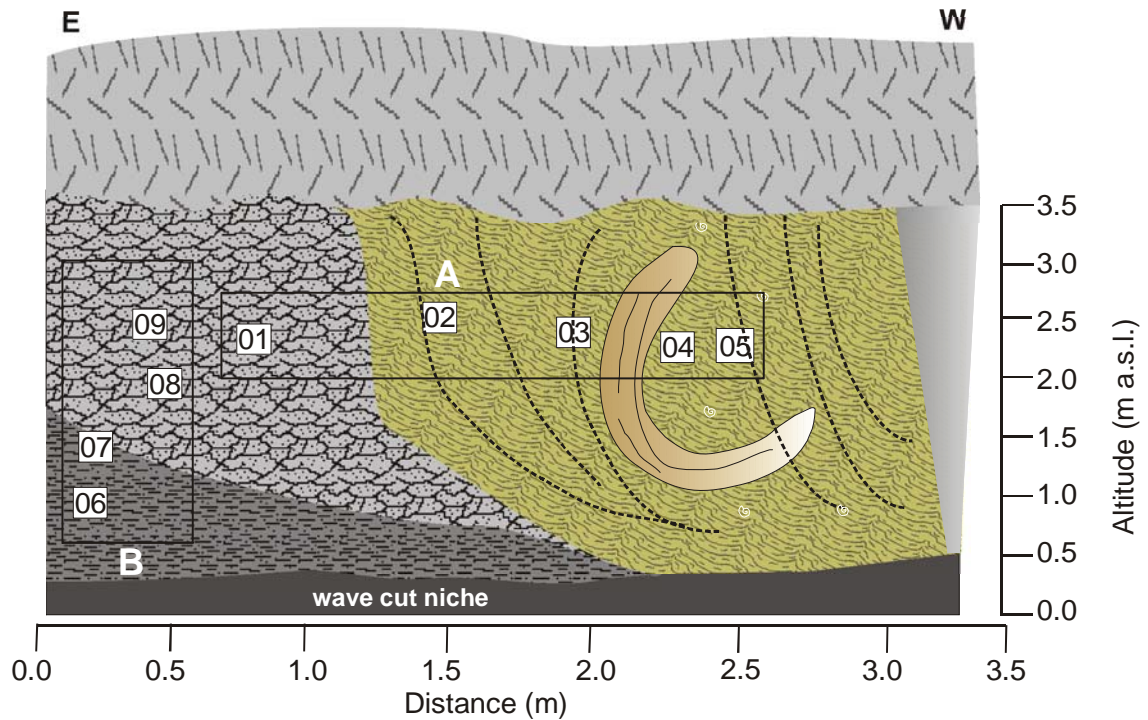


**Figure 4.6.2-9:** Schematic profile of the exposure Oy7-09, ice wedge cast surrounded by tabular deposits. The legend is given in Figure 4.3-1.



**Figure 4.6.2-10:** Mammoth tusk frozen in an Eemian ice wedge cast, exposure Oy7-09

A special exposure was studied about 1500 m east of the camp site direct above the beach level. First a mammoth tusk (bone sample number Oyg-07-O303, see appendix 6.3) frozen in the wall was found (Figure 4.6.2-10). After cleaning the wall it was visible that this tusk is incorporated within an ice wedge cast (Figure 4.6.2-9). Two subprofiles were sampled in order to cover the entire section.

*Subprofile Oy7-09-A* was horizontally collected crossing the ice wedge cast (Figure 4.6.2-9). The sample most to the left (Oy7-09-01) was still located within the surrounding taberal deposits. It consists of non-bedded grayish-brown silty sand, which contains dispersed plant detritus, wood fragments and small peat inclusions (2-3 cm). The cryostructure was coarse lens-like. 1-2 mm thick lenses occurred in 5-15 cm distance (grav. ice content 37 wt%). An inclusion of dark-brown strongly decomposed peat with woody fragments of twigs and roots were sampled at the left rim of the ice wedge cast (Oy7-09-02). The ice wedge cast was filled by alternate bedding of grey fine laminated silty sand layers and dark-grey to brown plant detritus layers. Some parts show ripple bedding and convolute bedding. Thin ice veins of about 1 mm thickness in 5 to 10 cm distance are vertically orientated to the bedding reflecting epigenetic origin (grav. ice content 33 to 56 wt%).

*Subprofile Oy7-09-B* vertically covered the surrounding taberal deposits. The lower part (samples Oy7-09-06/07) consisted of weakly bedded and disturbed dark-grey silty sand with numerous black spots. The sediment contained plant detritus and several small peat inclusions. The cryostructure (grav. ice content 28 wt%) was lens-like to coarse lens-like (1mm thick ice lenses) and layered (5 cm distance of ice veins). This lower part is considered as taberal sediment of the Kuchchugui Suite. In the upper part brownish-grey non-bedded silty sand again with black spots contained disperse plant detritus and single small twigs. Ice lenses of 1 mm thickness were parallel (layered) orientated in 5 cm distance (grav. ice content (31 to 38 wt%). The upper part is preliminarily interpreted as taberal deposits of the Bychchagy Suite.

4.6.2.4 Exposure Oy7-07 Kuchchugui to Krest Yuryakh Suite (14.08. 2007)

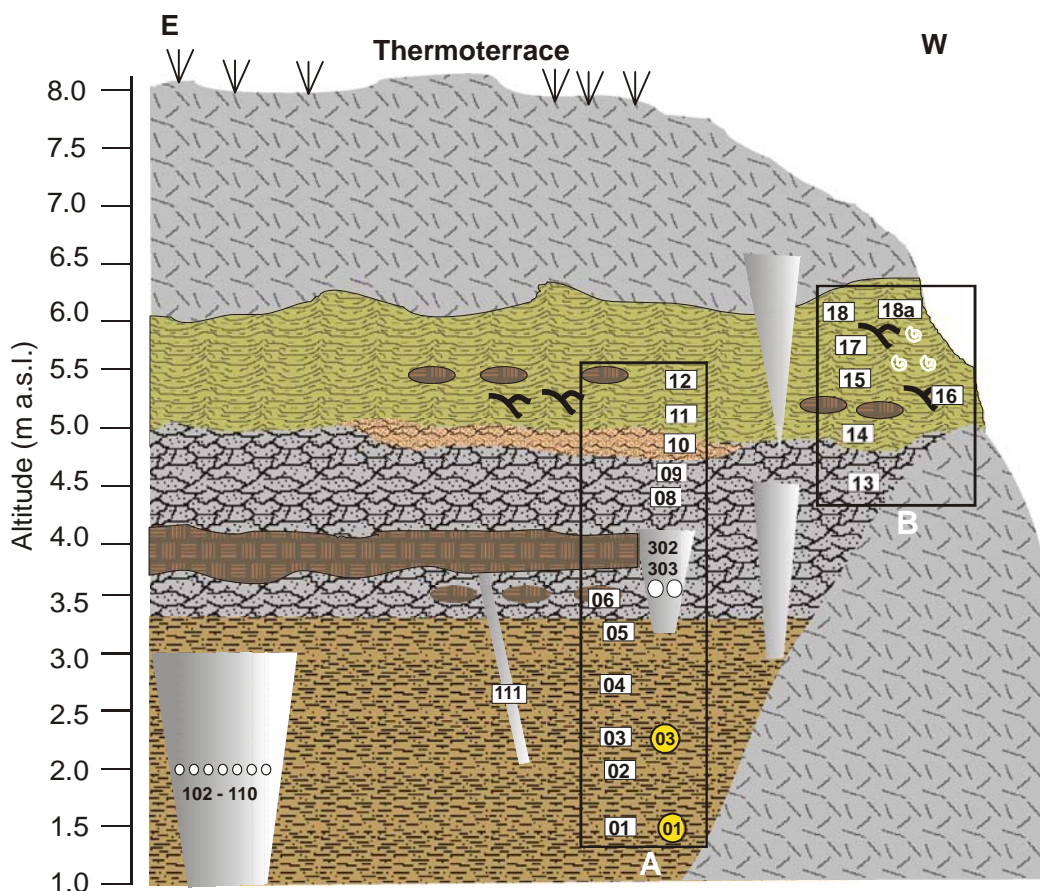


**Figure 4.6.2-11:** The sequence of Kuchchugui to Krest Yuryakh Suite deposits of the exposure Oy7-07. The legend is given in Figure 4.3-1.



**Figure 4.6.2-12:** Exposure situation of Oy7-07; Kuchchugui Suite covered by peaty Krest Yuryakh Suite



**Figure 4.6.2-13:** The upper part of the exposure Oy7-07 with the Krest Yurakh (Eemian) deposits top left

The exposure Oy7-07 presents a transition from the Kuchchugui Suite to the Krest Yuryakh Suite. Two overlapping subprofiles were studied.

*Subprofile Oy7-07-A* started 1 m a.s.l. with grey-brown moderate laminated silty sand sediments containing numerous thin *in situ* grass roots of the Kuchchugui Suite (samples Oy7-07-01 to 03). The cryostructure was massive (grav. ice content 31 wt%). In the uppermost part the ice content was rising (48 wt%). This material showed a broken, lens-like lattice cryostructure with ice lenses of < 1mm thickness in 0.5 to 2 cm distance. Two samples for luminescence dating were additionally drilled at the sample sites of Oy7-07-01 and Oy7-07-03. Further upwards (between 3.5 and 4.5 m a.s.l.), a cryoturbated peat soil horizon occurred which was also sampled for U/Th dating (sample Oy7-07-07-A to C). Light-brown moss peat inclusions (10-15 cm) are surrounded by a grey sandy silt matrix. The cryostructure was again broken and lens-like and lattice-like (grav. ice content 108 wt% matrix, 424 wt% peat). Ice bands crossed the peat inclusions. The peat soil was covered by grey-brown silty sand that contains numerous black spots. The cryostructure changed from massive to broken lens-like and lattice-like (grav. ice content 54 to 64 wt%). According to V. Tumskoy this middle horizon is considered as deposits of the Bychchagy Suite (samples Oy7-07-06 to 09). A small yellowish sand layer with bedding structures was visible at about 4.8 to 5 m a.s.l.. The cryostructure there was massive. This layer was finally covered by grey silty sand with peat inclusions (2-5 x 5-10 cm). This sediment contains black spots and thin whitish non-regular lines that probably are formed due to thawing. Ice veins of 1 mm thickness and 5 cm length are rare (grav. ice content 37 wt%).

The *subprofile Oy7-07-B* mainly covered deposits, which were preliminary classified as Krest Yuryakh Suite. Alternate bedded fine-laminated silty sand and plant detritus layers contain additionally numerous twig fragments and peat inclusions between 5.0 and 6.0 m a.s.l.. Ripple bedding was visible as well as mussel shells. (samples Oy7-07-14 to 18). The cryostructure is lens-like layered (grav. ice content 25 to 31 wt%).

Two versions of the general stratigraphic sequence around the exposure Oy7-07 according to observations of V.V. Kunitsky are presented in Figure 4.6.2-14. In version A the ice-rich deposits of the Buchchagy Suite are shown as an own stratigraphic unit whereas in version B the deposits above the Kuchchugui Suite are considered as basic segment of the Krest Yuryakh Suite. Finally the entire pre Eemian to Eemian sequence is covered by Ice Complex deposits.

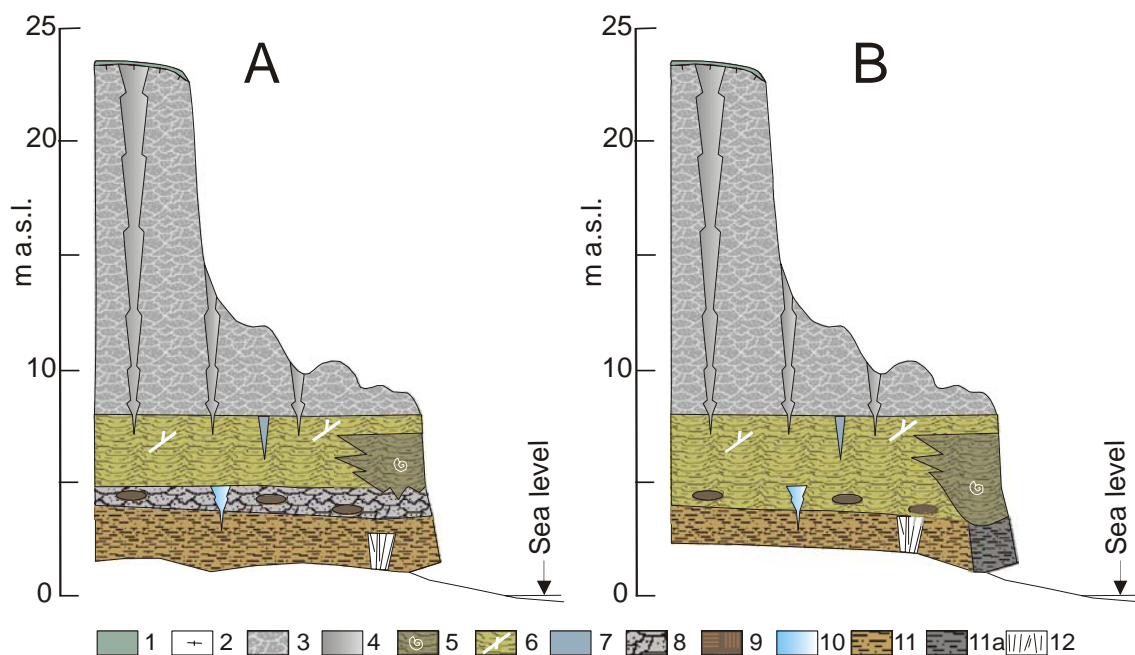


**Figure 4.6.2-14:** Two various interpretations of the stratigraphic situation below the Yedoma Suite according to observations of V.V. Kunitsky around the above presented exposure Oy7-07  
 1- active layer (loam with grass roots), 2- lower boundary of the active layer,  
Ice Complex deposits: 3- grey loam, in situ grass roots, ice bands, 4- syngenetic ice wedge,  
deposits of the Krest Yuryakh Suite: 5- Bluish-grey loam with mussel shells; 6- grey loam interbeds of plant detritus, with wood fragments (shrub twigs and roots); 7- brownish coloured ice wedge; deposits of the Bychchagy Suite: 8- brownish-grey loam with peat inclusions and ice bands; 9- brown autochthon lenses of moss peat; 10- syngenetic grey ice wedge; deposits of the Kuchchugui Suite: 11- brown loam, in situ grass roots, ice cement; 11a- bluish-grey and grey loam, cover which surrounded ice wedge casts formations, taberite; 12- composite ice-ground wedge (polosatic)

## 4.6.2.5 Exposure Oy7-10, Bychchagy Suite (14.08. 2007)

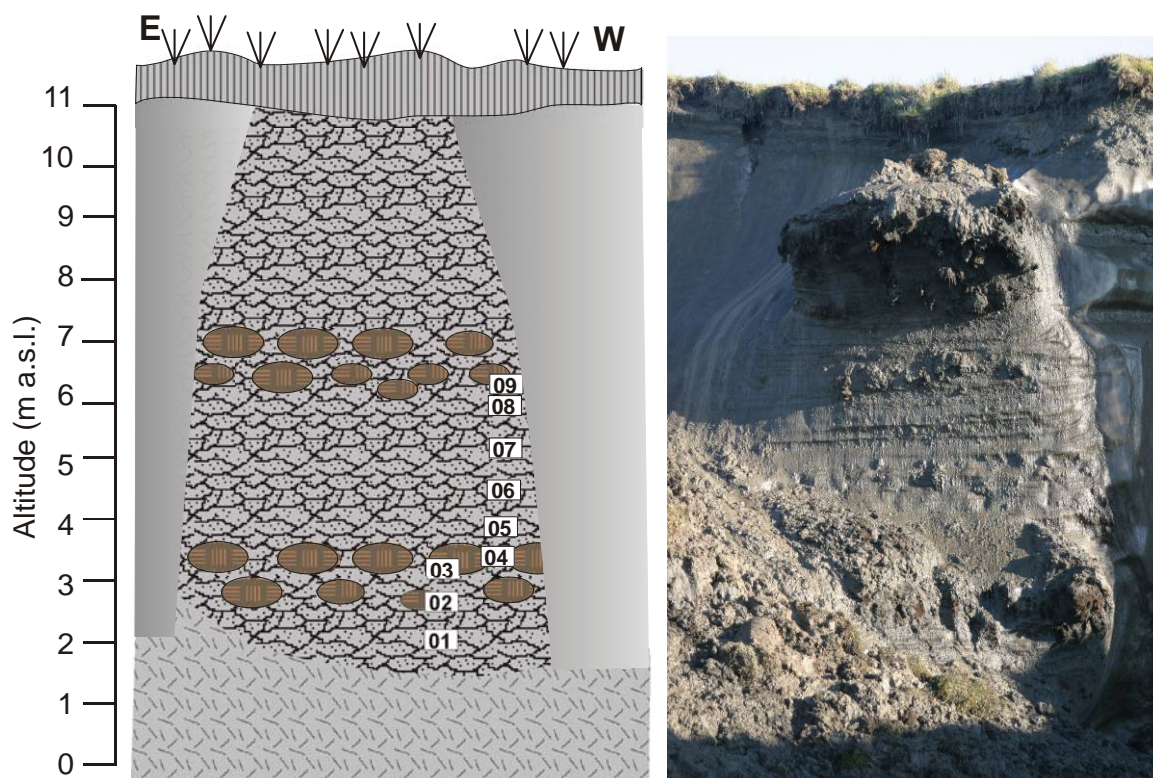


**Figure 4.6.2-15:** Peaty soil horizons within the ice-rich sequence of the exposure Oy7-10. The legend is given in Figure 4.3-1.

The eastern most section which was studied for palaeo-environmental reconstruction was situated about 5 km east of the camp site left of a 10 m high waterfall. The exposure had a steep wall (Figure 4.6.2-15) that could be sampled only between 2 and 6.2 m a.s.l. the studied section was framed by two large ice wedges of several meters width.

The lowermost exposed horizon consisted of brown silty sand with ice bands (4-10 mm thick, 40-60 mm distance) and lens-like layered cryostructure (sample Oy7-10-01/2, grav. ice content 38 wt%). Further upward peat inclusions up to 0.3 m in diameter occurred and the colour changed to brownish blue-grey. The ice content increased to 97 wt%. The cryostructure was dominated banded (3 cm thick ice bands) and coarse lens-like layered (1-2 mm thick lenses in 1-1.5 cm distance). Peat inclusions were ice supersaturated with grav. ice content between 100 and 800 wt%. The lower peaty horizon is covered by brown-grey silty sand that contains fewer peaty remains and some twigs. This horizon shows ice bands (5-20 mm thick, 5-10 cm distance) and alternate cryostructure of diagonal lens-like and lens-like layered parts (gravimetric ice content (61 to 112 wt%). At about 5.8 m a.s.l. a second peaty horizon occurred, which is about 1 m thick (Figure 4.6.2-15).

According to V. Tumskey this exposure belongs to the Bychchagy Suite, which is evident by the existence of two thick peat horizons within ice-rich deposits

that contain large ice wedges comparable with similar situation at Bol'shoy Lyakhovsky Island (see exposure L7-15, chapter 4.5.2.3).

A interpretation of the general stratigraphic situation between the exposures Oy7-10 (east) and Oy7-01 (west) according to observations of V.V. Kunitzky is given in Figure 4.6.2-16. Lake and boggy deposits of the Krest Yuryakh Suite are underlain by Kuchchugui Suite sediments, which are transformed to taberal deposits below the former lake due to permafrost thawing. The entire lower sequence is covered by Ice Complex deposits. The later are cut by a thermo-erosional valley filled with boggy Holocene deposits.

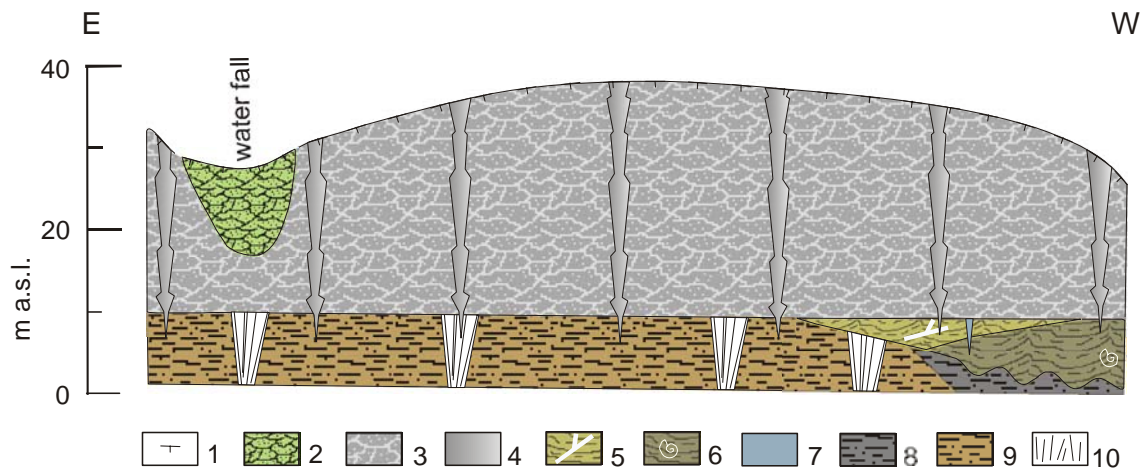


**Figure 4.6.2-16:** General scheme of the stratigraphic sequence in the easternmost part of the studied section

1- lower boundary of the active layer; Holocene deposits in a thermo-erosional valley: 2- brownish-grey loam with interbeds of autochthonous grass-moos peat, layered cryostructure, thin ice wedges; Ice Complex deposits: 3- grey loam, in situ grass roots, ice bands, 4- syngenetic grey ice wedge, deposits of the Krest Yuryakh Suite: 5- grey loam with inclusions of wood fragments (shrub twigs and roots); 6- bluish-grey loam with mussel shells 7- brownish coloured ice wedge; deposits of the Kuchchugui Suite: 8- bluish-grey and grey loam, cover which surrounded ice wedge casts formations, taberite; 9- brown loam, in situ grass roots, ice cement; 10- composite ice-ground wedge (polosatic)



#### 4.6.3 Studies of a sequences from the Eemian Krest Yuryakh Suite to the Yedoma Suite (Oy7-08)

*Lutz Schirrmeister, Sebastian Wetterich, Viktor Kunitsky and Alexander Derevyagin*

An about 28 m long profile was collected from the beach level up to the top of the Yedoma elevation at about 1.5 km east of the camp site. In order to present the field studies clearly we subdivided this sequence into eight subprofiles Oy7-08-A to H.

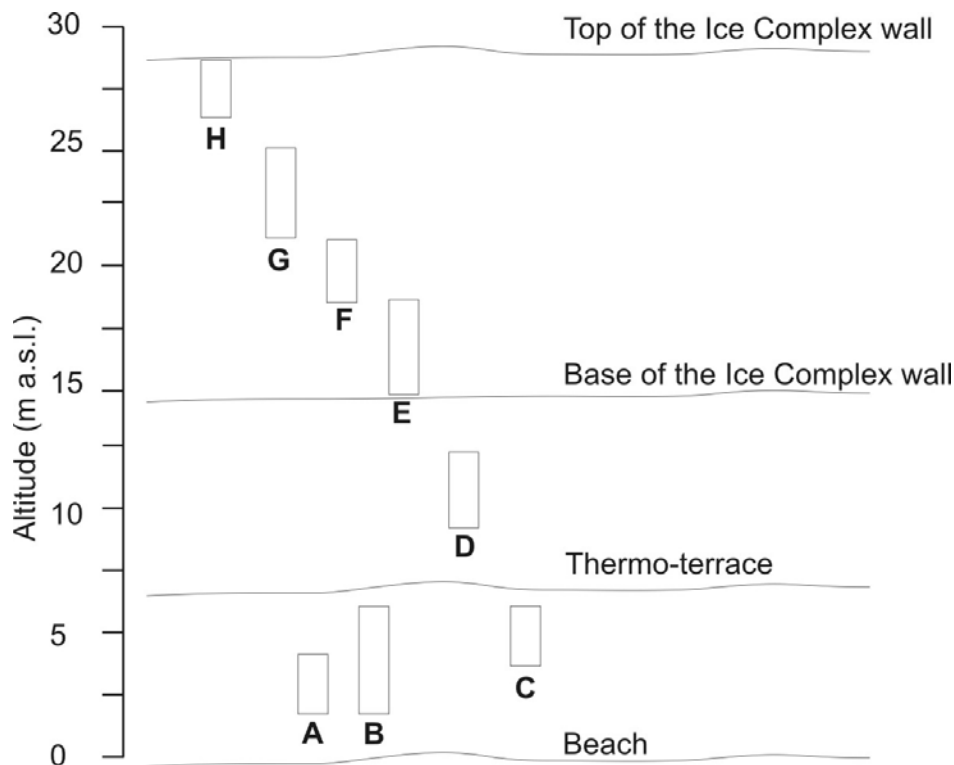


**Figure 4.6.3-1:** Positions of the subprofiles composing the exposure Oy7-08

##### 4.6.3.2 The Krest Yuryakh segment between 2 and 6 m a.sl. (16./17.08. 2007)

The lower section of the subprofiles Oy7-08-A to C was exposed at the cliff wall of the thermo-terrace to the sea and in a small thermoerosional gully cutting the surface of the thermo-terrace (Figure 4.6.3-2).

*Subprofile Oy7-08-A* contained still tabular deposits of the Kuchchugui Suite (sample Oy7-08-01). Grey silty sand with black spots and several plant remains characterized this horizon. The cryostructure was massive (grav. ice content 25 wt%). These deposits were covered by light-brown peat lenses (5x2 to 10x15 cm) in grey sandy silt matrix (samples Oy7-08-02 to 03) with lens-like reticulated cryostructure (grav. ice content 36 to 51 wt%) In addition single ice lenses of 5 mm size were visible. Disturbed layering and whitish lines of thaw structures in between were observed. The subprofile was completed by the lowest parts of an ice wedge cast that consisted of fine-laminated alternations of

brownish plant detritus layers (1-2 to 5-10 mm thick) and grey silty sand layers. Two peat bands were sampled (Oy7-08-05 and 06). The cryostructure was fine lens-like reticulated (grav. ice content 36 wt%).

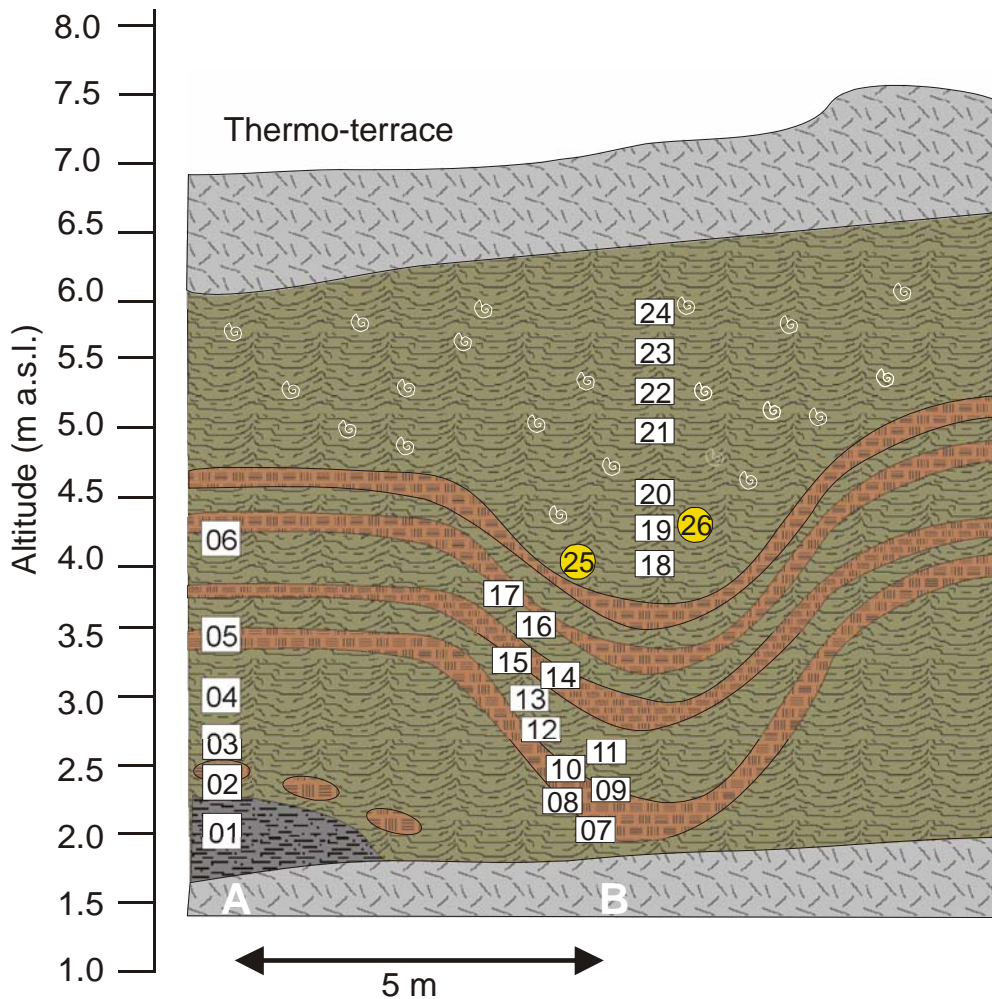


**Figure 4.6.3-2:** Ice wedge cast underlain by tabular Kuchchugui deposits and covered by lake deposits with mollusc shells. The legend is given in Figure 4.3-1.



**Figure 4.6.3-3:** Exposure situation of the subprofiles Oy7-08-A and-B (left) and the interbedded layering of the ice wedge cast (right)

*Subprofile Oy7-08-B* continues the Krest Yuryakh sequence in the centre of the ice wedge cast (Figure 4.6.3-3). This segment was composed of numerous alternations of 5-10 cm thick plant detritus layers and sandy silt layers (samples Oy7-08-07 to 18). Ripple bedding, synsedimentary slumping structures and separate peat lenses were observable in some layers. The cryostructure was lens-like layered. Ice lenses were oriented parallel to the bedding (grav. ice content 36 to 66 wt%). Two samples (Oy7-08-25 and 26) were drilled in 4 m a.s.l. and 4.3 m a.s.l. for luminescence dating. Further upwards the bedding was disturbed and the content of plant detritus decreased (samples Oy7-08-19 to 24). Grey sandy silt dominated this horizon, which contained numerous fragments and complete mollusc shells. The cryostructure changed upward from lens-like layered to lens-like reticulated (grav. ice content 22 to 40 wt%).

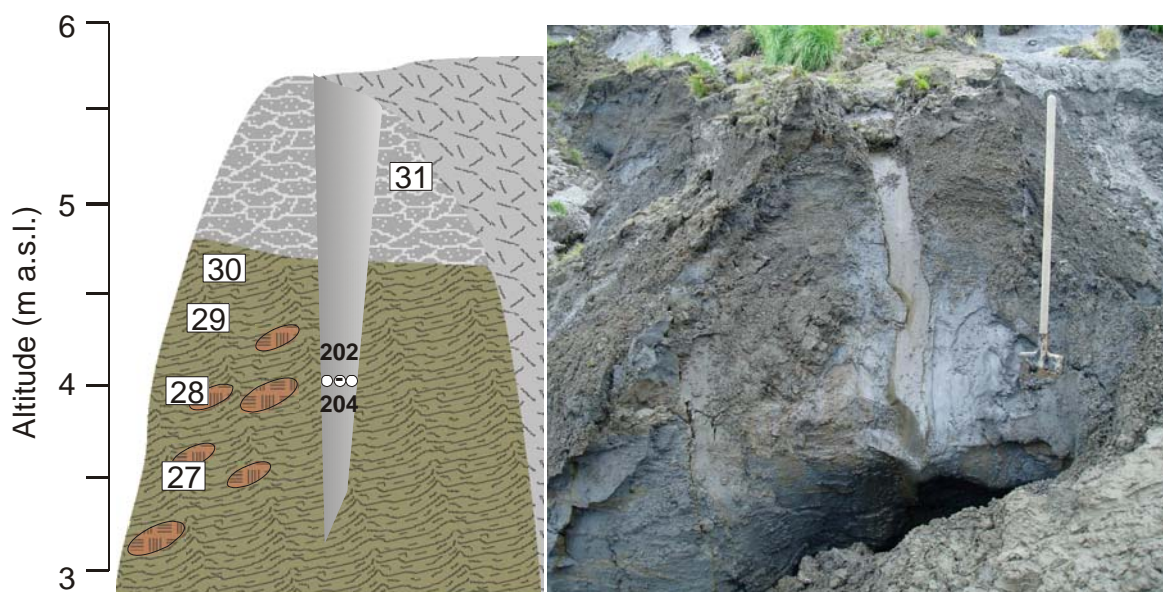


**Figure 4.6.3-4:** Uppermost exposed part of the Krest Yuryakh Suite; may be the boundary to the covering Ice Complex of the Yedoma Suite, subprofile Oy7-08-C. The legend is given in Figure 4.3-1.

In a distance of about 20 m from the last subprofile B in the gully cutting the thermo-terrace the *subprofile Oy7-08-C* was studied (Figure 4.6.3-4). The lower part of this profile consisted of grey clayish to silt or silty sand, which contained peat inclusions (2-5 cm in diameter) and several wood fragments. The sediment was partly in patches coloured by light-brown iron oxide impregnations. The cryostructure was lens-like layered (grav. ice content 31 to 39 wt%). In the upper part, dark-grey silty sand was exposed containing plant detritus and mollusc shells. The cryostructure of these deposits was coarse lens-like reticulated (grav. ice content 59 wt%). In addition the section contained a small epigenetic ice wedge of 0.2 to 0.3 m width. The ice wedge was composed of thin (1-2 mm) ice veins and contained numerous small air bubbles. Three samples were taken for stable isotope studies (Oy7-08-201 to 203).

#### 4.6.3.2 The Ice Complex sequence between 9 and 28 m a.s.l. (17./19./20. 08. 2007)

Starting from the thermo-terrace beneath the ice wall five subprofiles in thermokarst mounds (Oy7-08-D to H, Figure 4.6.1-1) were studied which cover almost the entire exposed sequence of the Yedoma Suite (Figure 4.6.3-5). The composition and cryostructures of this sequence were rather similar.



**Figure 4.6.3-5:** Thermokarst mounds (baydzherakhs) in the area of exposure Oy7-08

*Subprofile Oy7-08-D* (9-12 m a.s.l.) consisted of grey-brown silty sand with peat inclusions (1-3 to 2-3 cm) and separate plant inclusions. Ice bands in changing distances (3-5 to 5-10 cm) occurred. Samples (Oy7-08-32 to 37) were collected in 0.5 m distance (Figure 4.6.3-6). The cryostructure between ice bands were coarse lens-like reticulated. Lenses are 2-3 cm thick, 10-30 mm long and had distances to one another of 10 mm (grav. ice content 69 to 167 wt%).

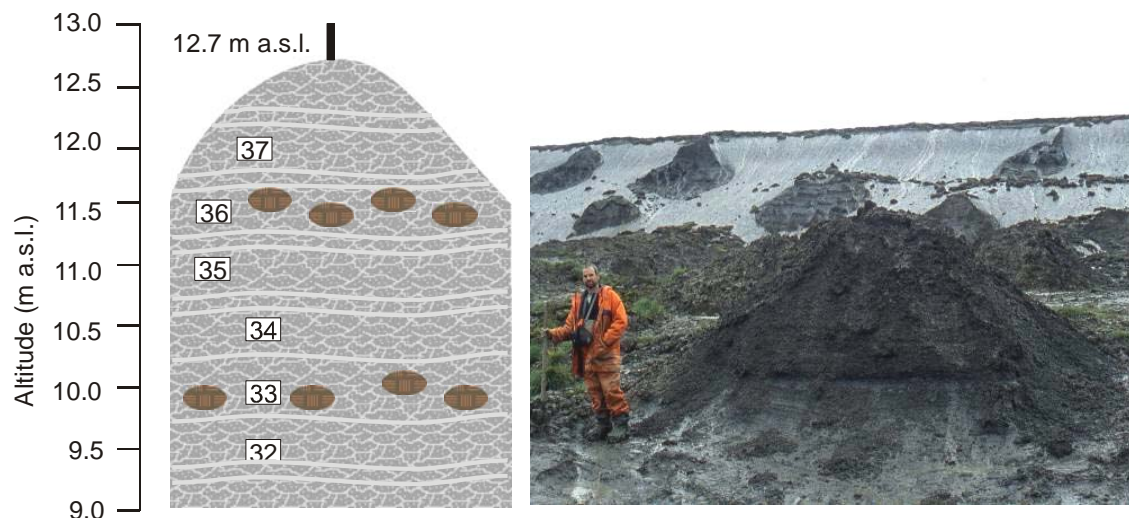


**Figure 4.6.3-6:** Sample positions and exposure situation of the lowermost subprofile Oy7-08-D of the Yedoma Suite located at the thermo-terrace. The legend is given in Figure 4.3-1.

Further upwards *subprofile Oy7-08-E* is located directly below the ice wall between 15 and 19 m a.s.l.. Grey to patchy light-brown sandy silt composed these deposits (samples Oy7-08-38 to 45). They repeatedly contained numerous small and large brown peat inclusions (2x2 to 20x40 cm large) forming peat palaeo-sols. In addition separate plant remains and numerous thin grass roots occurred. Samples were collected first from a small thermokarst mound and from a larger one behind (Figure 4.6.3-7). Besides ice bands in 5 to 10 cm distance the cryostructure changed between fine and coarse lens-like reticulated (grav. ice content 82 to 212 wt%).

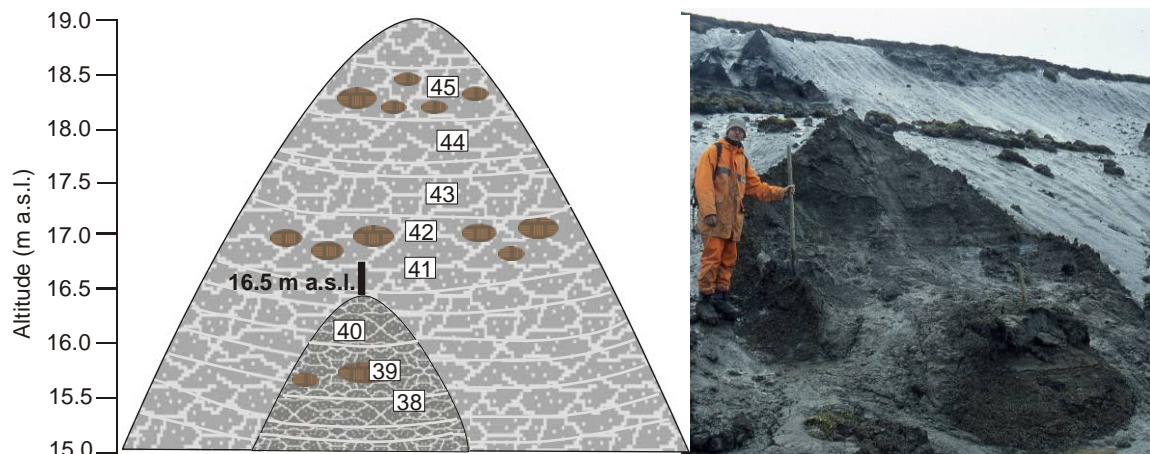


**Figure 4.6.3-7:** Studied thermokarst mounds of subprofile Oy7-08-E. The legend is given in Figure 4.3-1.

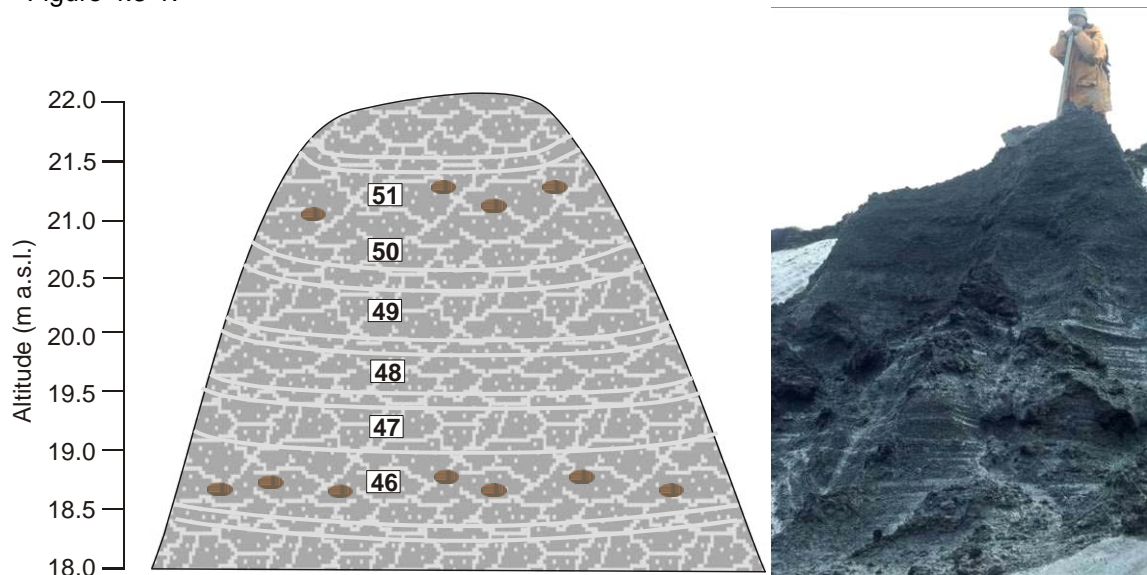


**Figure 4.6.3-8:** The segment of the subprofile Oy7-08-F (left) and the complete exposed thermokarst mound. The legend is given in Figure 4.3-1.

The studied Ice Complex sequence was continued by subprofile *Oy7-08-F* between 18 to 22 m a.s.l. at the ice wall (Figure 4.6.3-8). Grey sandy silt with brown patches, single grass roots and fine distributed plant detritus and several small wood fragments characterised this sediment (samples Oy7-08-46 to 51). The cryostructure was banded with 1-2 mm thick ice bands in 5 to 10 cm

distance. Between ice bands the cryostructure was fine lens-like to coarse lens-like reticulated (grav. ice content 71-81 wt%).

*Subprofile Oy7-08-G* was studied between 21 and 26 m at the ice wall only 20 m east of the previous subprofile F (Figure 4.6.3-9). The composition of both sequences was rather similar (samples Oy7-08-52 to 61): greyish-brown silty sand; peat inclusions of 2x3 to 5x10 cm size; several additional plant remains of grass roots, leaves, and wood fragments. The content of plant remains increased in peat palaeo-sol horizons. The cryostructure was banded and lens-like reticulated (grav. ice content 69-122 wt%). In the lower part of this subprofile the ice bands were upwards bended and covered by horizontal oriented ice bands. Such changes of the orientation of ice bands were interpreted as different cryo-cycles (see chapter 4.5.1.7).

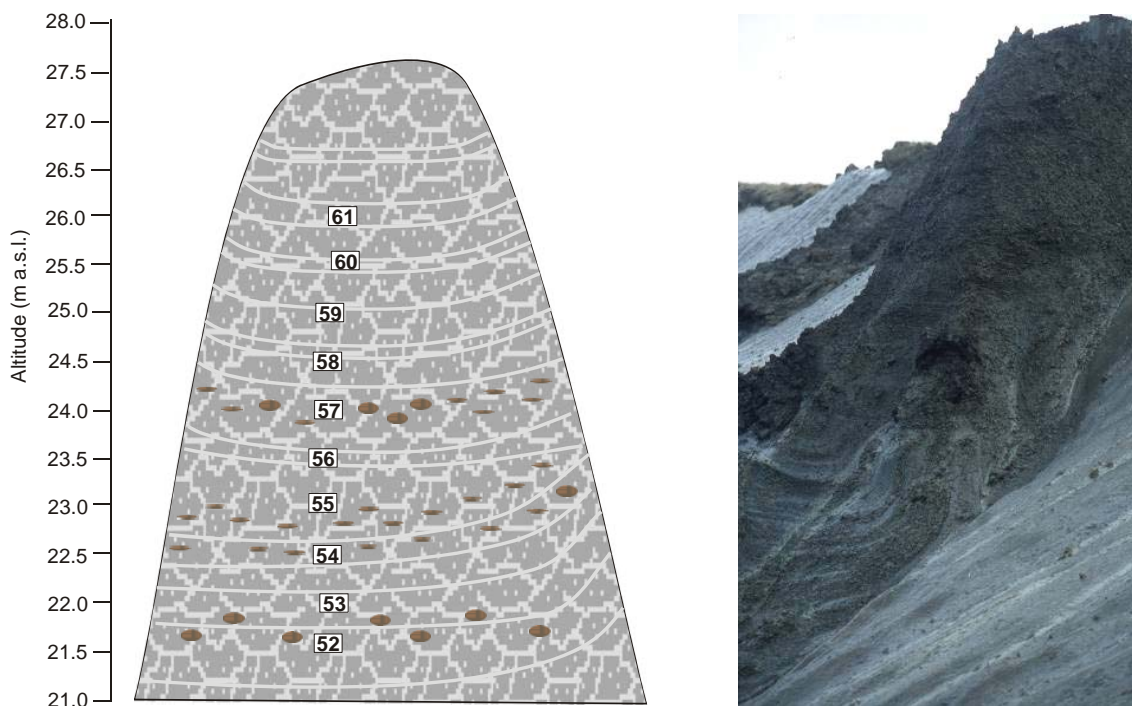


**Figure 4.6.3-9:** Schematic profile and exposure situation of subprofile Oy7-08-G. The legend is given in Figure 4.3-1.

The last *subprofile Oy7-08-H* of the combined exposure Oy7-08 was situated between 26 and 28 m a.s.l. directly below the top of the Ice Complex. In the lower part, the greyish-brown silty sand was partly reddish-brown coloured (samples Oy7-08-62 to 64) and contained fine distributed plant detritus and grass roots. The cryostructure in the lower section was banded and lens-like reticulated (grav. ice content 223 to 242 wt%). The orientation of the ice bands was first upward bent covered by horizontal oriented ice bands (Figure 4.6.3-10). The active layer horizon was formed as dark-brown peat soil. The transition zone (samples Oy7-08-65) contained 2-3 mm thick ice band composed of vertical ice needles. The uppermost sample Oy7-08-66 consisted of unfrozen, greyish-brown silty sand with numerous grass roots.

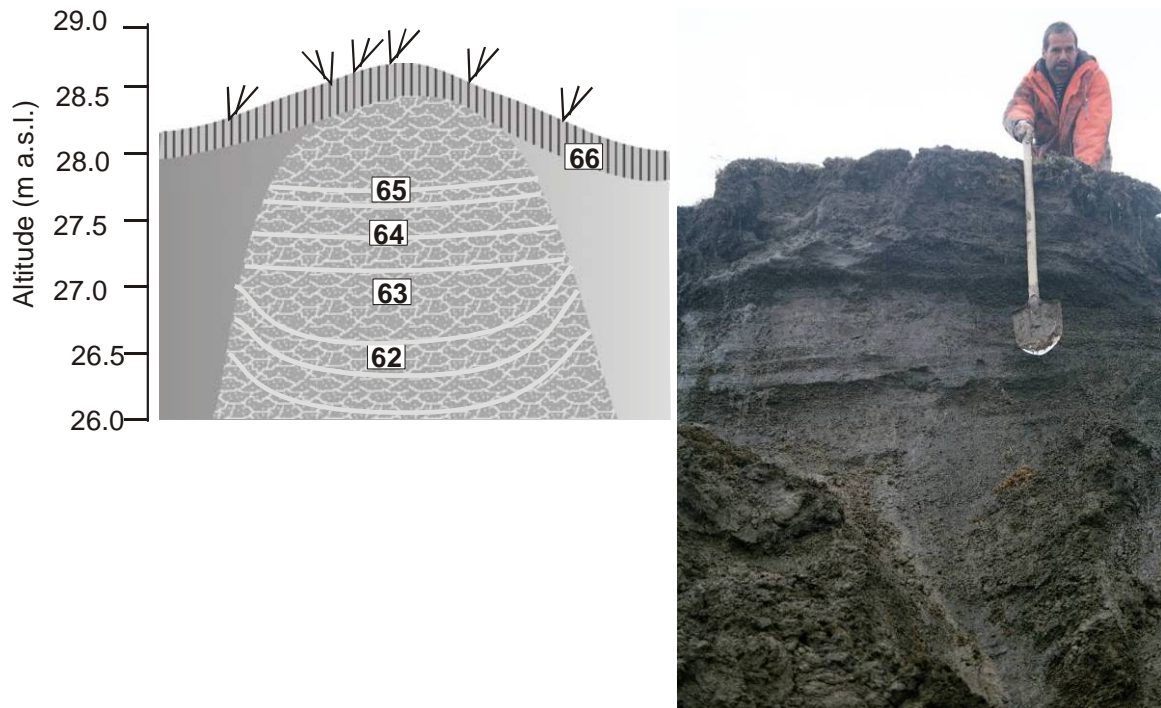


**Figure 4.6.3-10:** The final subprofile Oy7-08-H on top of the Ice Complex sequence, The legend is given in Figure 4.3-1.

## 4.6.3.3 Summarizing stratigraphic interpretation of Oy7-08 sequence

According to the observations of V.V. Kunitsky the lowermost segment of the studied complete sequence belongs to the Eemian Krest Yuryakh Suite. This part was covered by more than 15 m of Ice Complex deposits with large syngenetic ice wedges (Figure 4.6.3-11). The sequence was finished with Holocene slope deposits that contain separate ice wedges.

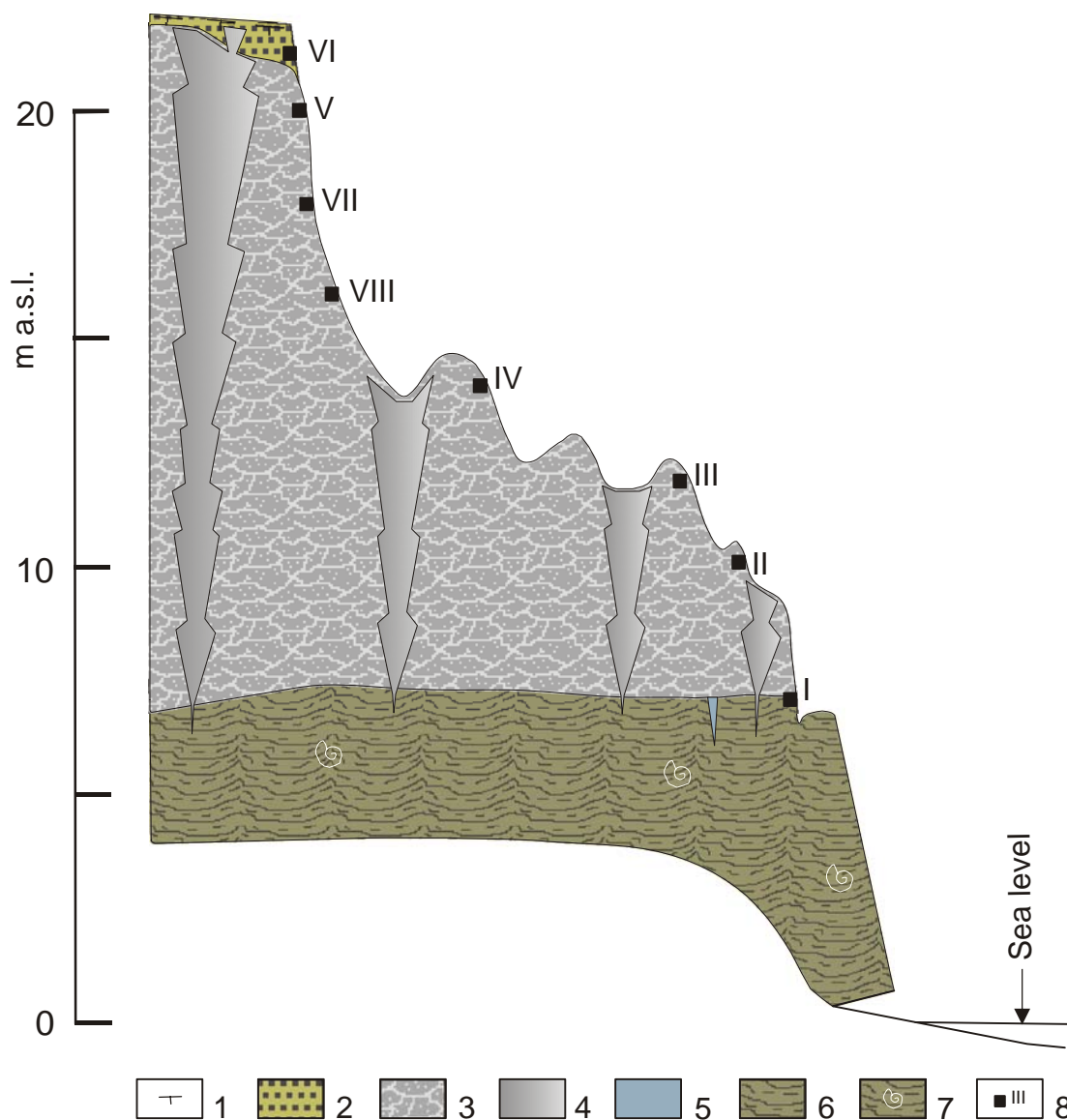


**Figure 4.6.3-11:** General stratigraphic scheme of the area of exposure Oy7-08 according to observations of V.V. Kunitsky

1- lower boundary of the active layer; Holocene slope deposits: 2- brownish-grey loam with interbeds of autochthonous grass-moos, in places with shrub roots and twigs, lens-like cryostructure; Ice Complex deposits: 3- grey loam with peat inclusions, in situ grass roots, ice bands, 4- syngenetic grey ice wedge, deposits of the assumed Krest Yuryakh Suite; 5- brownish coloured ice wedge, 6- bluish-grey loam with interbeds of plant detritus, wood fragments (shrub twigs and roots); 7- bluish-grey loam with fragments and complete mussel shells and rare gastropod shells 8- sample sites of V.V. Kunitsky.

### 4.6.4 Sediment sequences below the alas bottom

*Lutz Schirrmeister, Sebastian Wetterich and Viktor Kunitsky*

#### 4.6.4.1 Exposure Oy7-04, Krest Yuryakh Suite to Holocene(?) (11./12.08.2007)

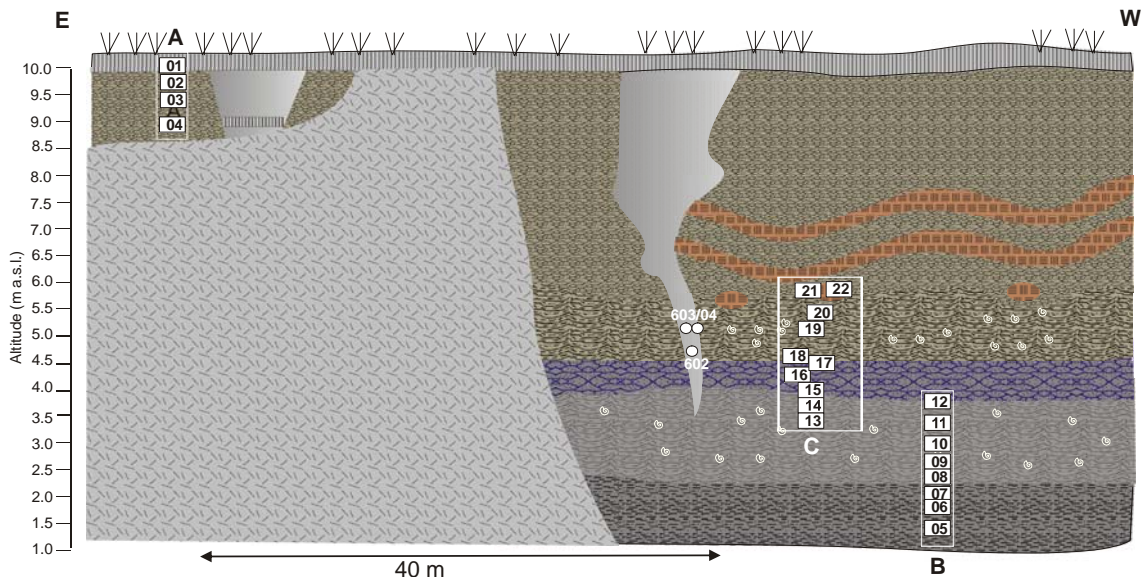


**Figure 4.6.4-1:** Stratigraphic scheme and sample positions of the exposure Oy7-04. The legend is given in Figure 4.3-1.



**Figure 4.6.4-2:** Exposure situation of Oy7-04, Holocene lake and alas deposits cover assumed Krest Yuryakh (Eemian) deposits: an Holocene ice wedge penetrates almost the entire exposed sequence

Exposure Oy7-04 was studied near the eastern rim of the thermokarst depression, where the coast cuts the various stratigraphic units below the alas bottom. Three subprofiles were studied (Figure 4.6.4-1), which will be presented in their stratigraphic order.

*Subprofile Oy7-04-B* exposed the lower part. The lowermost sample Oy7-04-05 consists of greyish-brown silty sand with small (1cm in diameter) peat inclusions and wood fragment. The cryostructure was coarse lens-like reticulated (grav. ice content 72 wt%). This could be taberal deposits of the Kuchchugui Suite or only beach deposits accumulated in the wave cut niche. The next segment of this subprofile between 1.9 and 2.3 m a.s.l. consisted of well-bedded alternations of grey silt layers and brown plant detritus layers. Ripples structure were visible as well as synsedimentary convolute bedding structures (samples Oy7-04-06/08). The cryostructure was massive (grav. ice content 40 wt%). In addition a clear ice band of 1 cm thickness without gas bubbles was sampled for stable isotope analyses (sample Oy7-04-07). At 2.6 m a.s.l. mollusc shells occurred in grey silty sand with plant fragments and many fine distributed plant detritus. The bedding changed between synsedimentary or syncryogene disturbed layers and well-laminated layers again with ripple marks. (samples Oy7-04-09 to 12). The cryostructure was dominantly massive but also characterised by several diagonal and horizontal oriented ice lenses (<1 mm thick, 3 mm long; grav. ice content 32 wt%).

Only a few metres to east the *subprofile Oy7-04-C* was studied between 3.5 and 6 m a.s.l., which cover presumably horizons of Eemian and Holocene deposits. Synsedimentary disturbed or cryoturbated alternations of grey silty sand and brown detritus layers (samples Oy7-04-13/14) are similar to the uppermost samples of the previous subprofile. Thin whitish lines tracing the cryoturbated bedding structures were interpreted as thawing structures. The cryostructure was massive (grav. ice content 46 wt%). Further upward (samples Oy7-04-15 to 18) the lamination was more regular and the cryostructure was lens-like layered (grav. ice content 33-40 wt%). The silty sand there contained again mollusc shells. The upper boundary of Krest Yuryakh deposits was assumed between 5.0 to 5.5 m a.s.l. because of changes in sediment structure, colour and cryostructures. Small and larger peat inclusions occurred (samples Oy7-04-19-21). The cryostructure was coarse lens-like. Two peaty layers containing larger twig fragments were visible (Figure 4.6.4-2) that could not be studied in detail because of the height of the exposure wall. Only several wood fragment were collected (sample Oy7-04-21). The ice wedge, which penetrated the entire sequence had the characteristic form of alas ice wedge already described for Bol'shoy Lyakhovsy Island (see chapter 4.5.1.9). The lower thin part (10 to 30 cm) penetrated epigenetically into former lake deposits. The upper about 1 m wide part was syngenetic formed under subaerial condition at the bottom of the thermokarst depression.

The uppermost *subprofile Oy7-04-A* was studied parallel to the high-resolution sampling of an Holocene ice wedge (see chapter 4.6.5). The frozen sediments below the surface consisted of grey silty sand partly with peat inclusions in the

transition zone to the active layer (samples Oy7-04-04 to 02) The cryostructure was banded and coarse lens-like reticulated (grav. ice content 100 to 137 wt%). The uppermost unfrozen sample Oy7-04-01 (peat, grass, moss) was taken from the active layer.

#### 4.6.4.2 Exposure Oy7-11, taberal Yedoma Suite to Holocene (23.08.2007)

This exposure consists of two subprofiles that were studied at the coast about 0.6 km west of the camp site on both sides of an erosional crack. The sediment sequence was exposed at a about 10 m height wall, where the lower subprofile Oy7-11-A was studied and at a fallen block opposite to the wall, where the upper subprofile Oy7-11-B was available (Figure 4.6.4-3).



**Figure 4.6.4-3:** The exposure situation of Oy7-11 below the alas bottom

*Subprofile Oy7-11-A* (Figure 4.6.4-4) exposed in the lower part taberal deposits of the Yedoma Suite (samples Oy7-11-01 to 03). The light-grey silty sand contained no or only a little visible plant detritus. The cryostructure was lens-like layered. Ice lenses of 1 mm thickness and 5-15 cm length occurred in 1-2 cm distance (grav. ice content 42 wt%). In addition non-regular white line were observed, which were interpreted as thaw structures. Such whitish structures increasingly occurred at the boundary to the overlaying peaty soil (sample Oy7-11-04). This layer also contained twigs and peat inclusions. Above this boundary zone alternate bedding of silty fine-sand and plant detritus layers composed lacustrine deposits. Ripple marks, small faults, wood fragments and mussel shells were observed. The cryostructure was lens-like layered (grav. ice content 52-71 wt%). An additional unfrozen sample (Oy7-11-frank spezial) was taken for plant macro fossil analyses from the nearby ice wedge cast, composed of similar lacustrine sediment. The small epigenetic "roots" of an

broad alas ice wedge were samples for future stable isotope analyses (Oy7-11-302 to 304).

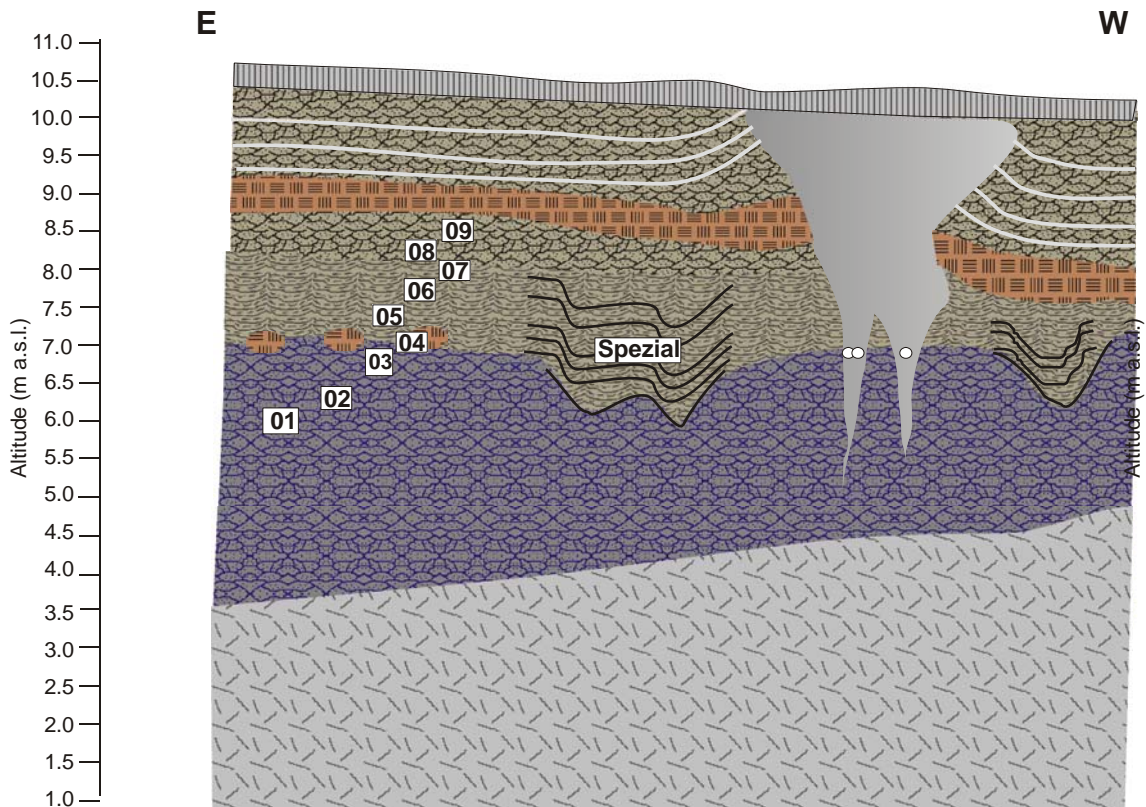


**Figure 4.6.4-4:** Sediment sequence below the alas bottom; subprofile Oy7-11-A, tabular deposits of the Yedoma Suite are covered by Holocene lake sediments with ice wedge casts and alas deposits with ice wedges. The legend is given in Figure 4.3-1.



**Figure 4.6.4-5:** Overview Picture of the alas sequence of subprofile Oy7-11-A with ice wedge casts (left) and a typical wide alas ice wedge with thin epigenetic "roots"

Because of the bad accessibility (steep wall) of the upper part of the alas sequence we studied the second *subprofile* Oy7-11-B at the fallen erosional block direct in front of the wall (Figure 4.6.4-6). This profile started with a 20 to 30 cm thick dense and platy peat (sample Oy7-11-10). This horizon contained also wood fragments (2-3 cm in diameter) and 1-2 mm thick silt layers. An additional sample Oy7-11-10a was collected for plant macrofossil analyses. Further upward greyish silty sand and light-brown peat lenses were found (samples Oy7-11-11 to 15). The cryostructure was banded and coarse lens-like reticulated. Ice lenses up to 1 cm thickness were composed of vertical ice needles (grav. ice content 131 to 183 wt%). The latest sample Oy7-11-16 of this subprofile was taken from the unfrozen surface material of grass, roots and moss.

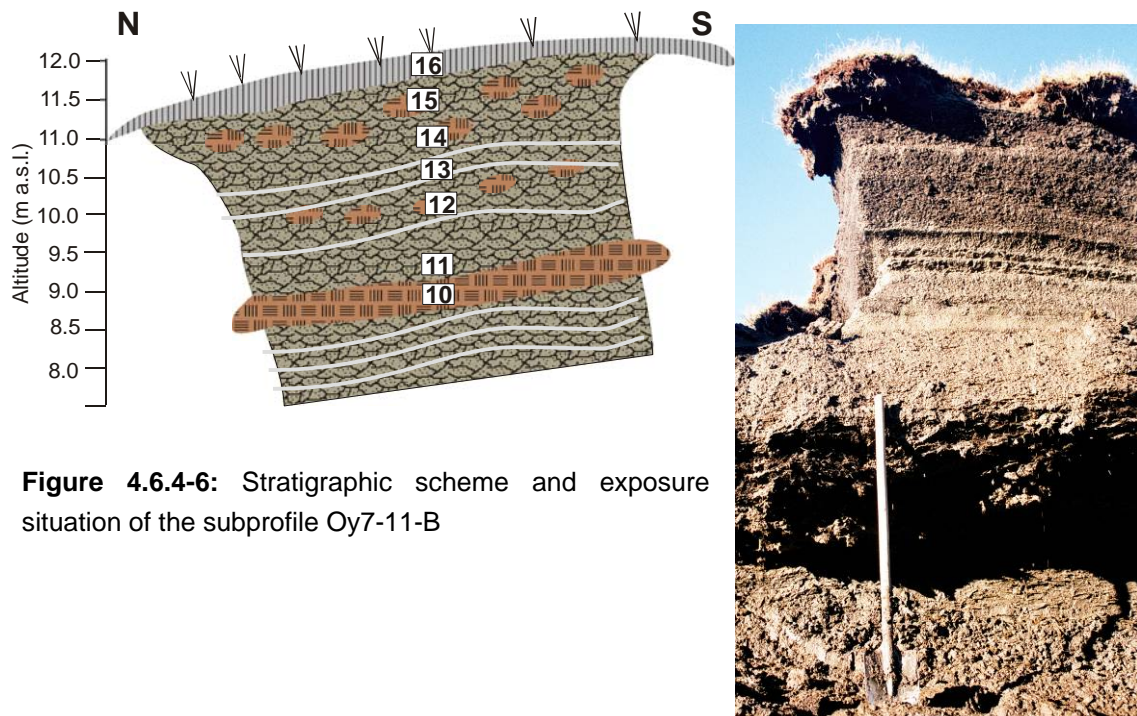


**Figure 4.6.4-6:** Stratigraphic scheme and exposure situation of the subprofile Oy7-11-B

The general stratigraphic order in the area of the thermokarst depression and the flanking Yedoma hill is summarised in two schemes of V.V. Kunitsky (Figures 4.6.4-7/8). The lowermost part consisted of tabular deposits of the Kuchchugui Suite, covered by a horizon of ice wedge casts, which contained lacustrine deposits of the Eemian Krest Yuryakh Suite. The Krest Yuryakh Suite continued further upwards and was covered by Holocene alas deposits in the area of the thermokarst depression and by Ice Complex deposits in the area of the Yedoma hill. In addition slope deposits covered the Yedoma Suite sequence.

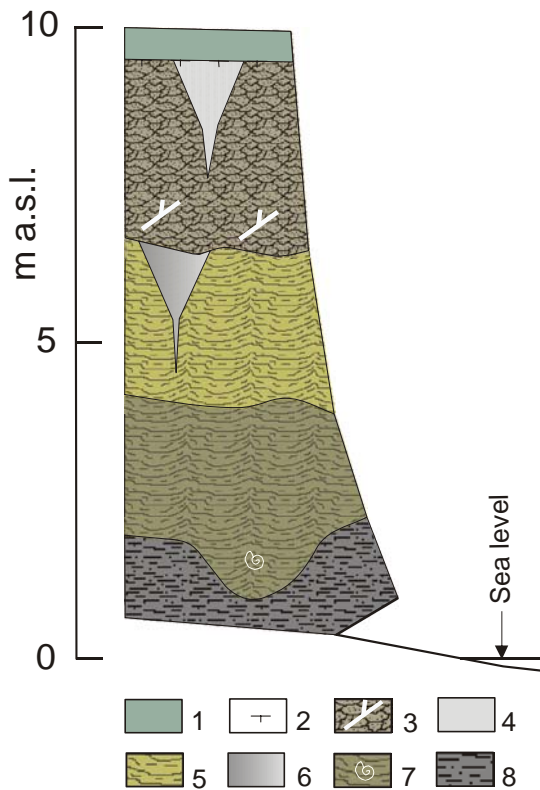


**Figure 4.6.4-7:** Profile of the eastern part of the Alas basement

1- active layer; 2- lower boundary of the active layer; Holocene alas deposits: 3- brownish-grey loam with shrub roots and twigs, lens-like cryostructure; 4- syngenetic white ice wedge; deposits of the Krest Yuryakh Suite: 5- grey loam interbeds of plant detritus, with wood fragments (shrub twigs and roots), 6- syngenetic grey ice wedge, 7- bluish-grey loam with fragments and complete mussel shells and rare gastropod shells; taberal deposits of the Kuchchugui Suite: 8- bluish-grey and bluish loam, ice wedge casts and ground wedges penetrate into this deposits

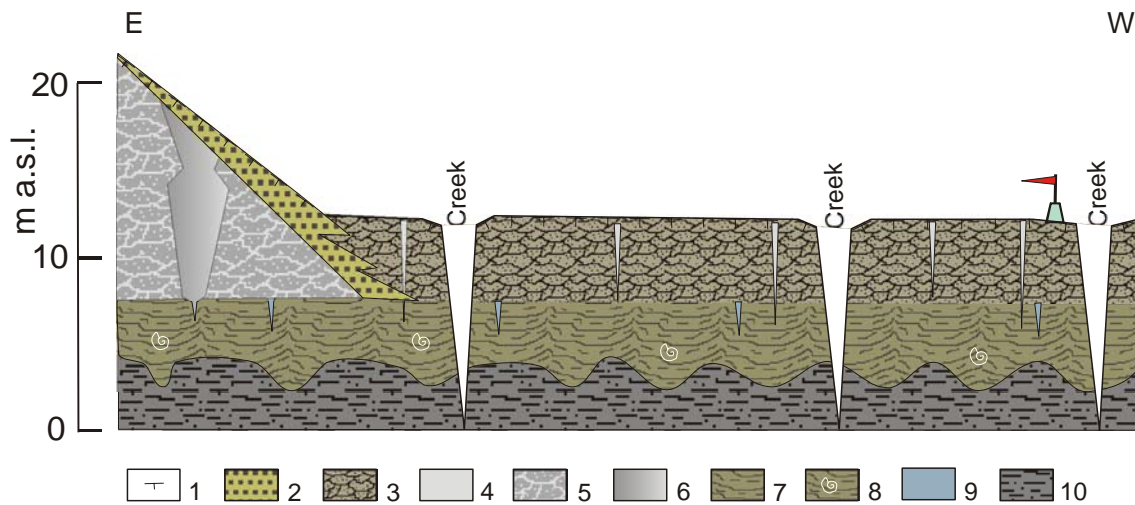


**Figure 4.6.4-8:** General stratigraphic scheme below the bottom of the alas depression and below the alas border

1- lower boundary of the active layer; Holocene slope deposits: 2- brown loam with interbeds of autochthonous grass-moss-peat, partly with shrub roots and twigs and in situ shrubs; Holocene alas deposits: 3- grey loam and hydrophyte remains (lake deposits), with a cover of brownish-grey loam, containing lenses and interbeds of autochthonous grass-moss-peat (boggy and fluvial deposits); 4- syngenetic white ice wedge; Ice Complex deposits: 5- grey loam, in situ grass roots, ice bands, 6- syngenetic grey ice wedge; deposits of the Krest Yuryakh Suite: 7- grey loam interbeds of plant detritus, with wood fragments (shrub twigs and roots), deposits of the aquatic and subaerial facies (not subdivided); 8- bluish-grey loam with fragments and complete mussel shells and rare gastropod shells, in ice wedge casts (aquatic facies); 9- brownish coloured ice wedge; taberal deposits of the Kuchchugui Suite: 9- bluish-grey and bluish loam, ice wedge casts penetrate into this deposits

#### 4.6.5 Ground ice studies

*Alexander Derevyagin and Thomas Opel*

##### 4.6.5.1 Introduction and Methods

Both ice wedges and texture (segregated) ice of Late Pleistocene, Holocene and recent sequences were studied at the site Oyogos Yar. Studies of ground ice focus on investigations of cryogenic structure features of sediments and isotopic ( $\delta^{18}\text{O}$ ,  $\delta\text{D}$ ,  $^3\text{H}$ ) as well as hydrochemical (major ions) composition of ice. For an understanding of the recent isotopic background we also sampled precipitation (rain) and snow patches as well as surface and ground waters during the field season.

Nowadays it is known that the ground ice contains information of past atmospheric precipitation, which left isotopic signals, stored in the permafrost. Former field investigations and studies of isotopic composition of modern ice wedges in different regions of Arctic support that the formation of ice wedges occurs mostly due to freezing of snowmelt water of winter precipitation in frost cracks. In winter time frost cracks are open in the frozen ground. In spring, snowmelt water trickles down into the cracks where it freezes forming a vertical (sometimes subvertical) wedge-shaped elementary ice vein. Ice wedge growth takes place due to the almost annual repeat of such processes. Therefore, the isotopic composition of ice wedges can be related to winter precipitation and reflect mean winter temperatures of the ice wedge formation time (Meyer et al., 2002b).

Texture ice may be assumed as a mixture of summer and winter precipitation accumulated in the active layer during a long time (ca. 300-500 years). To interpret isotope variations within sediment columns in terms of temperature is more difficult due to possible repetitive processes of isotopic fractionation in the active layer which can change the isotopic signal. At this moment the interpretation of texture (segregated) ice isotopic composition is in development.

Ice wedge ice is the most abundant type of ground ice in this Northeast Siberian region. Its formation took place over a long period during the Pleistocene, the Holocene and at the present time. In the accordance with stratigraphical units at the Oyogos Yar site we studied ice wedges formed from the Pre-Eemian to the Holocene. Nets of ice wedges form a very specific type of surface relief – polygonal relief. The size of the Holocene (alas) polygons is about 10-12 m, whereas the size of Late Pleistocene polygons (at the surface of Ice Complex) can reach 15-20 m.

One of the main geological and cryolithological features of the study area is the occurrence of the Ice Complex: very ice rich Late Pleistocene sediments with huge polygonal syngenetic ice wedges (thickness up to about 30 m and width from 3-3.5 m to 10-11 m). These ice rich sediments form remains of vast accumulation plains with the heights of about 35-40 m a.s.l. The formation of the Late Pleistocene Ice Complex in the region is associated with the Zyriansky,

Karginsky and Sartansky periods of the Russian Late Pleistocene stratigraphy, which are corresponding to the MIS 4, MIS 3 and MIS 2 of the global classification.

In general, the ice wedges were sampled using a special ice screw (diameter 15 mm), a chain saw and an axe depending on ice wedge size and sampling strategy.

The huge Ice Complex ice wedges were sampled by ice screw in horizontal profiles located on the different levels above sea level with resolution steps from 0.15 m to 0.35 m. Such a sampling strategy of Ice Complex can span the main time period of Yedoma Suite formation (Dereviagin et al., 1997, Meyer et. al., 2000). The sampled Yedoma Suite profiles are presented in Table 4.6.5-1.

**Table 4.6.5-1:** Sampling profiles of Ice Complex.

No	No of IW	No of samples	Height m a.s.l.	Width of IW (m)	Width of ice veins (mm)	Characteristics of sediments	Remarks
1	Oy7-01 IW 4	5	1.5	0.5	1-3	Grey silty sand	Tail of IC IW (?)
2	Oy7-05 IW 1	2	2.0	0.3-0.4	1	Grey silty sand	Tail of IC IW (?)
3	Oy7-06 IW 1	35	9-10	3.5	1-5	Grey loam, peat inclusions	
4	Oy7-06 IW 2	22	20-21	2.0	1-5	Grey loam	very ice rich sediments
5	Oy7-08 IW 1	36	25-26	5.7	1-5	Grey loam, peat inclusions	
6	OY7-08 IW 3	32	30	5.0	2-10	Grey loam	with Holocene (?) ice veins
7	Oy7-08 IW 4	28	35-36	10.2	no clear size	Grey loam, peat inclusions	very ice rich sediments

Smaller ice wedges located in Pre-Yedoma deposits were sampled by ice screw and axe.

The Holocene ice wedges were sampled using both ice screw and chain saw. Three high-resolution profiles were sampled by chain saw. In the first two cases thin (about 2-3 cm) ice pieces were cut. In the third case ice blocks (length ca. 25 cm) were cut from the Holocene alas ice wedge by chain saw. These blocks were transported frozen to the cold laboratory of AWI. Particular emphasis has been given to organic remains in the ice wedges which can give us the possibility to determine  $^{14}\text{C}$  ages.

The texture ice was sampled in the vertical sediment profiles with steps of about 0.5 m in accordance to the cryogenic structure. Organic remains in the texture ice enclosing sediments were also sampled for radiocarbon age determination.

The most recent parts of ice wedges were sampled by axe. Usually, recent ice veins ("modern growth" of ice wedges) can be clearly observed in the upper part of Holocene ice wedges. The recent ice veins penetrate into the so-called "head" of an older ice wedge down to the depth of modern frost cracks (ca. 0.6-1.2 m). According to the field observations the width of modern elementary ice veins varies from 1 to 5 mm, and the width of "modern growth" reach from 2 to 8 cm.

Ground ice samples were melted in the field laboratory (excluding ice blocks sampled for investigations in detail in Germany). The melted samples were filled in 30 ml narrow-mouth PE bottles for measurements of the isotopic composition. Additionally, parts of selected samples were filtered (cellulose-acetate filtration set, pore size 0.45 µm) and bottled in wide-mouth HDPE bottles (8 and 15 ml) for hydrochemical measurements.

#### 4.6.5.2 Studies of ground ice in Pre-Yedoma deposits

##### *Ice wedges Oy7-01 IW 1, IW 2, IW 3, IW 5, IW 6, IW 7*

Six similar small epigenetic ice wedges IW 1, IW 2, IW 3, IW 5, IW 6 and IW 7 were sampled in Krest Yuryakh deposits. These ice wedges were located at the coastal cliff of a thermo-terrace of about 2-2.5 m height with distances of 5 to 50 m from each to other. The enclosing deposits were presented by grey, blue-grey (dark blue) clay loam. This clay loam had a characteristic nut-like structure with brown iron oxide films and included shells (molluscs) and detritus. The cryostructure of clay loam was bended and reticulate (net-like) with an ice schlieren thickness of about 1-1.5 cm. The ice wedges width was from 5-10 cm to 30-40 cm. The visible thickness was about 0.7-0.9 m. The bottom parts of the ice wedges were cut by wave-cut notch. The ice wedge ice was yellowish grey, brownish grey and showed clearly observed vertical oriented ice veins (widths about 2-3 mm). There was brown iron oxide film in the contact of ice wedges and sediments.

Each ice wedge was sampled by axe in the height from 0.8 to 1.2 m a.s.l. Sample points of the ice wedges IW 1, IW 2, IW 3 and IW 5 are displayed in Figure 4.6.5-1. IW 3 was also sampled for  $^{36}\text{Cl}$  and  $^{10}\text{Be}$  dating (sample Oy7-01-301).

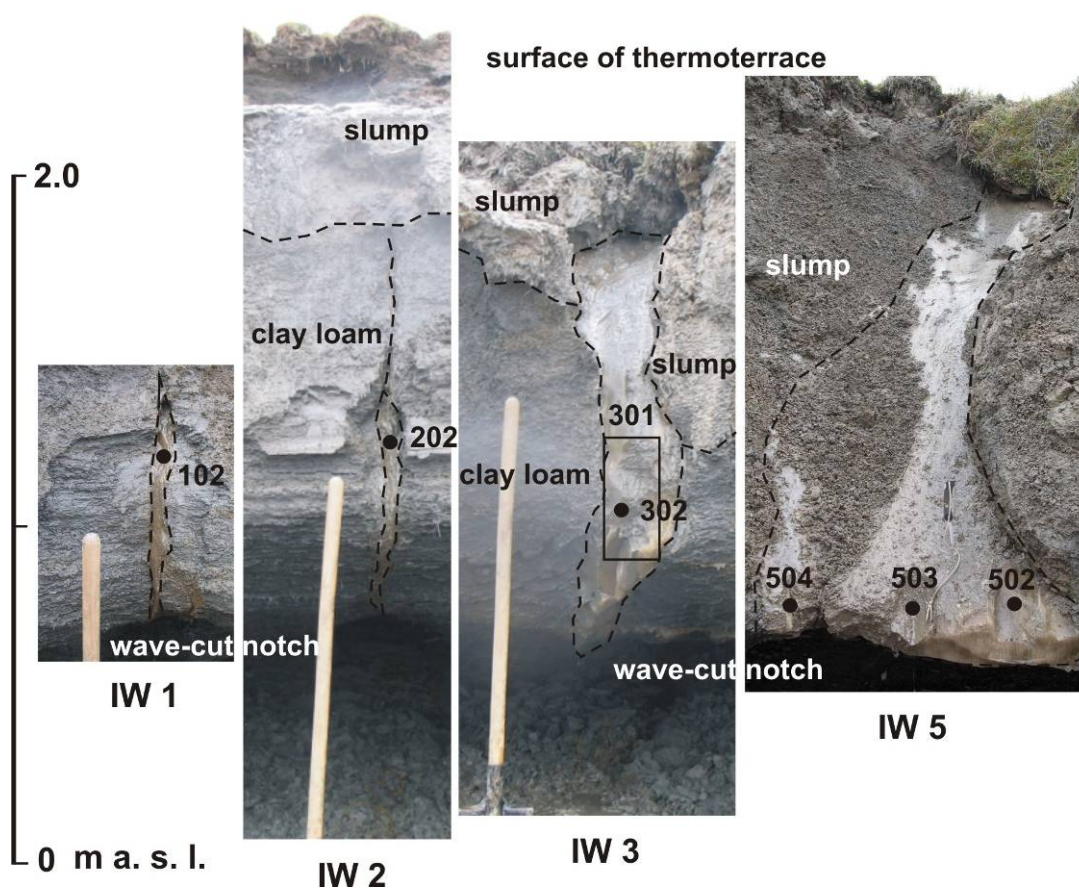


Figure 4.6.5-1: The similar ice wedges IW 1, IW 2, IW 3 and IW 5 in the section Oy7-01.

#### *Ice wedges Oy7-03 IW 1, IW 2, IW 3, IW 5*

The ice wedges IW 1, IW 2, IW 3 and IW 5 were studied in the section Oy7-03, which exposes Pre-Krest Yuryakh deposits. The ice wedges were located at the coastal cliff in a height of about 5 m. The enclosing deposits consisted of brownish-grey silty fine (laminated) sand. In the upper part sand sediments were covered by red-brown, dark-brown peat and peaty silt layers.

The section had a very complicated cryogenic construction, which is still subject of discussion (Figure 4.6.5-2). In the bottom part (about 1-2 m a.s.l.) composite sand ice wedges (IW 1 and IW 5) were located. The composite sand ice wedges were comparable to Oy7-03 IW 4 attributing to the oldest stratigraphical unit Kuchchugui Suite. The width of the composite wedges was about 0.3-0.4 m. The visible thickness was about 0.5-0.7 m. The Composite sand ice wedges passed into an ice wedge (IW 1) in the middle part of the section (about 2.0-2.4 m a.s.l.).

Ice wedge IW 1 crossed ice wedge IW 2. Apparently, we observed the corner of a polygon relic. Ice wedges IW 1 and IW 2 can be considered as syngenetic ice wedges because of their characteristic cryogenic construction. The enclosing sediments were characterized by a belt like cryostructure. The width of ice belts was about 2-3 cm. The distance between ice belts was about 10-12 cm. The width of ice wedges was about 0.4-1 m. The ice wedge ice was clean and

transparent and had big crystals (size ca. 0.3-0.5 mm). The ice was characterized by a lot of air bubbles (1-5 mm in diameter) which showed a vertical orientation. The width of the well pronounced elementary ice veins was about 3-6 mm.

A small epigenetic ice wedge (IW 3) penetrated from peat layers into silty sand in the upper part of the section (ca. 3.5-4.5 m a.s.l.). The width of the ice wedge was about 5-8 cm. The ice was clean, transparent and had no visible air bubbles. The width of elementary ice veins was about 2-8 mm.

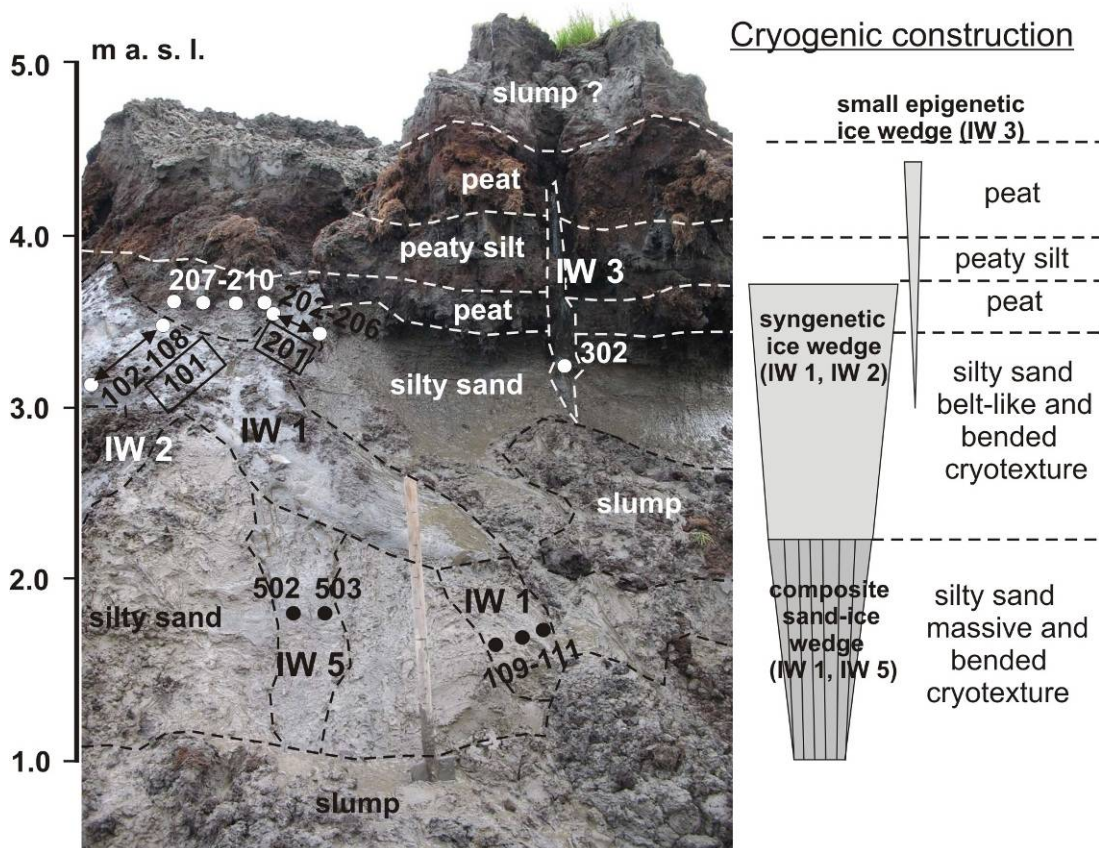
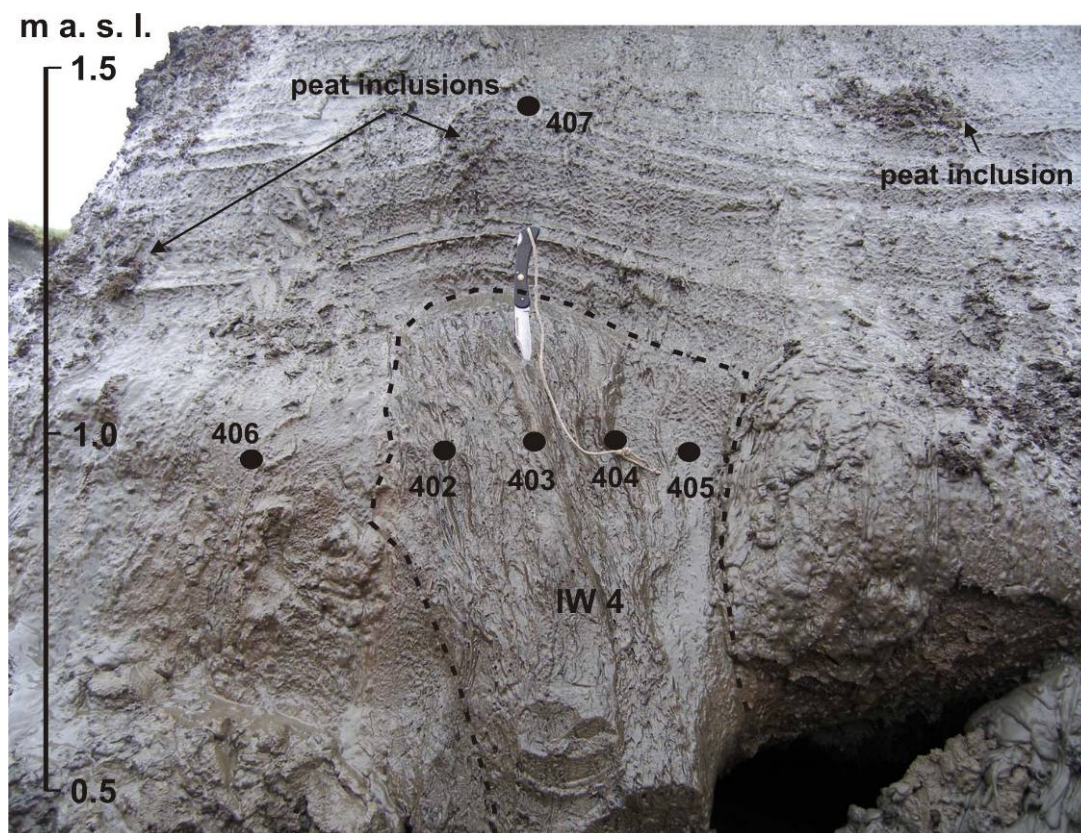


Figure 4.6.5-2: Section Oy7-03 ice wedges IW 1, IW 2, IW 3 and IW 5.

#### *Ice wedge Oy7-03 IW 4*

The ice wedge IW 4 (composite sand-ice wedge, sand-ice wedge) in the section Oy7-03 can be attributed to the oldest stratigraphical unit Kuchchugui Suite. This IW was located in the 2 m high cliff of the coastal outcrop. The surrounding sediments consisted of brownish-grey covered by yellowish-grey silty fine laminated sand. In the upper part sand sediments included vertically oriented grass roots in situ and peat inclusions. This section was covered by a dark-brown peat layer. The cryogenic structure of the silty sand was belt-like near the ice wedge, and massive and bended (with a thickness of the ice layers of about 1 cm) in the covered yellowish-grey silty fine laminated sand.

The composite sand-ice wedge consisted of vertically and sub-vertically oriented ice layers and sediment (sand) rich layers. The thickness of ice and ice-sand veins varied from 1-2 to 8-10 mm. The width of the composite sand-ice wedge was about 0.4 m, the visible height about 0.8 m. The composite sand-ice wedge had a rounded thawed head and was buried under the yellowish-grey silty sand with a well pronounced bended cryostructure. Clear detectable was the rounded character of the bended cryogenic structure above the ice wedge head. Four samples of the sand-ice wedge and two samples of texture ice near and above composite sand-ice wedge were taken (Figure 4.6.5-3). A similar ice wedge from the oldest unit was described and sampled in 2002 (Schirrmeister et al., 2003).



**Figure 4.6.5-3:** The composite sand-ice wedge Oy7-03 IW 4 in sediments of the Kuchchugui Suite.

#### *Ice wedge Oy7-07 IW 1*

The ice wedge IW 1 in the section Oy7-07 (Figure 4.6.5-4) was located in a 6 m high cliff of the coastal outcrop. The section exposed Eemian and Pre-Eemian deposits. The geological profile consisted of yellowish-grey silty fine laminated sand with vertically oriented grass roots (this horizon can be associated with the Kuchchugui Suite). The silty sand was characterized by a massive cryostructure and was covered by well-bedded grey loam with peat lenses and showed bended and belt-like cryostructures. The thickness of ice lenses was about 1-3

cm. In the upper part of geological profile there was dark grey loam with peat inclusions and lenses and plant remains (this horizon can be associated with the Krest Yuryakh Suite). The cryogenic structure of this horizon was massive and basal. The width of the ice wedge was about 1.7 m and the visible height was about 2 m. The ice wedge had a thawed head and was buried under the dark grey loam with peat inclusions.

The colour of ice wedge IW 1 was dirty yellowish-grey with numerous mineral patterns and air bubbles (size ca. 1-5 mm in diameter). The width of vertical oriented elementary ice veins was about 3-5 mm. Seven samples were taken.

Small epigenetic ice wedges (vertical oriented cracks) penetrated from covering dark grey loam with peat inclusions (ca. 4-5 m a.s.l.) into silty sand in the upper part of the section. The width of these ice wedges was about 3-8 cm. The ice was clean, transparent and had no visible air bubbles. Sample numbers Oy7-07-111, -302 and -303 were taken from these small epigenetic ice wedges (not shown here).

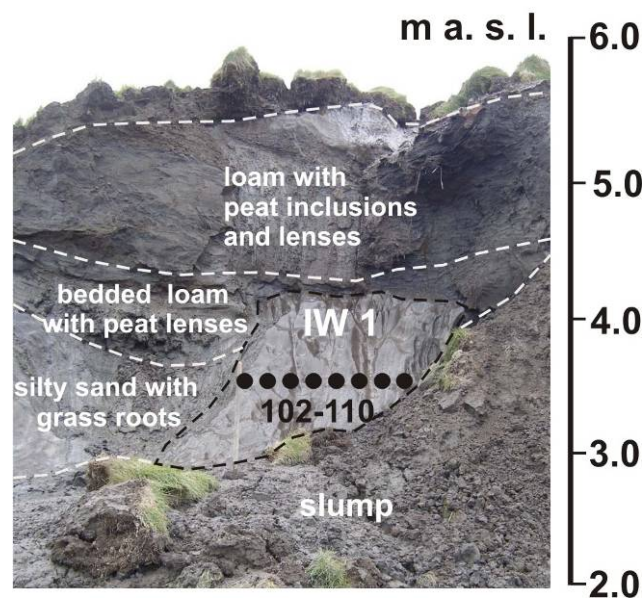


**Figure 4.6.5-4:** Outcrop Oy7-07 exposed the ice wedge IW 1 with a thawed head.

#### 4.6.5.3 Studies of Yedoma ground ice

##### *Ice wedge Oy7-01 IW 4*

The ice wedge Oy7-01 IW 4 was located at the coastal cliff of the about 2.5 m high thermo-terrace with a distance of ca. 60 m from Oy7-01 IW 1. The ice wedge enclosing deposits are the same as for IW 1, IW 2, and IW 3 and consist

of blue-grey (dark blue) clay loam. The cryostructure was bended and net-like with an ice schlieren thickness of about 1-1.5 cm.

Preliminary, the ice wedge Oy7-01 IW 4 can be considered as remain of an Ice Complex ice wedge tail, penetrated from the covering Ice Complex into Krest Yuryakh deposits. The ice wedge had characteristic grey-dirty colour (typical for Ice Complex ice wedges) with numerous mineral patterns. The thickness of vertical oriented elementary ice veins was about 1-3 mm. In contrast to IW 1, IW 2, and IW 3 no brown iron oxide film in the contact of the ice wedge and sediments have been observed. Five samples (402-406) were taken by ice screw (Figure 4.6.5-5).

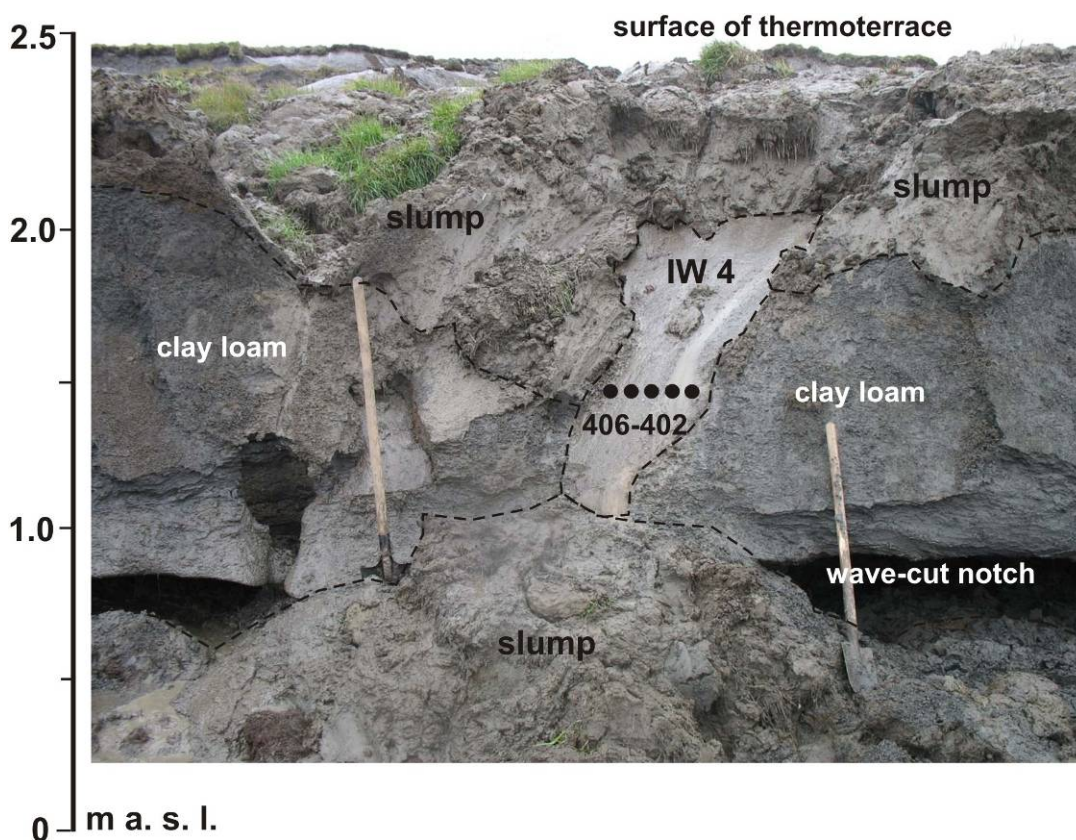


**Figure 4.6.5-5:** Ice wedge Oy7-01 IW 4, probably a tail of an Ice Complex ice wedge in Krest Yuryakh deposits.

#### *Ice wedge Oy7-05 IW 1*

The ice wedge IW 1 of the section Oy7-05 was located at the coastal cliff of an alas (height of about 7-8 m). The ice wedge enclosing deposits were associated with the Krest Yuryakh Suite. They consisted of grey, blue-grey well bedded fine grained sand (silty sand), alternating with plant detritus layers in ice wedge casts, including grass roots and shells. The thickness of the Krest Yuryakh taberal deposits was about 3-3.5 m. The deposits were characterized by bended, lens-like and massive cryostructure. In the upper part of the section, Krest Yuryakh deposits were covered by Holocene alas deposits consisting of

grey, brownish-grey loam with peat inclusions and plant remains. Here occurred Holocene ice wedges (thickness about 4-5 m) in alas deposits.

Preliminary, ice wedges observed in Krest Yuryakh taberal deposits can be considered as the remains of Ice Complex ice wedge tails which penetrated into deposits of the Krest Yuryakh Suite (see also Oy7-01 IW 4). The width of the ice wedge tail was about 0.3-0.4 m, and the thickness was about 1.5-1.8 m. The ice wedge ice was dirty (grey-brownish), alternating with clear ice veins and showed a well pronounced vertically oriented structure. The width of elementary ice veins was about 1 mm. Two samples of the ice wedge were taken (Figure 4.6.5-6).

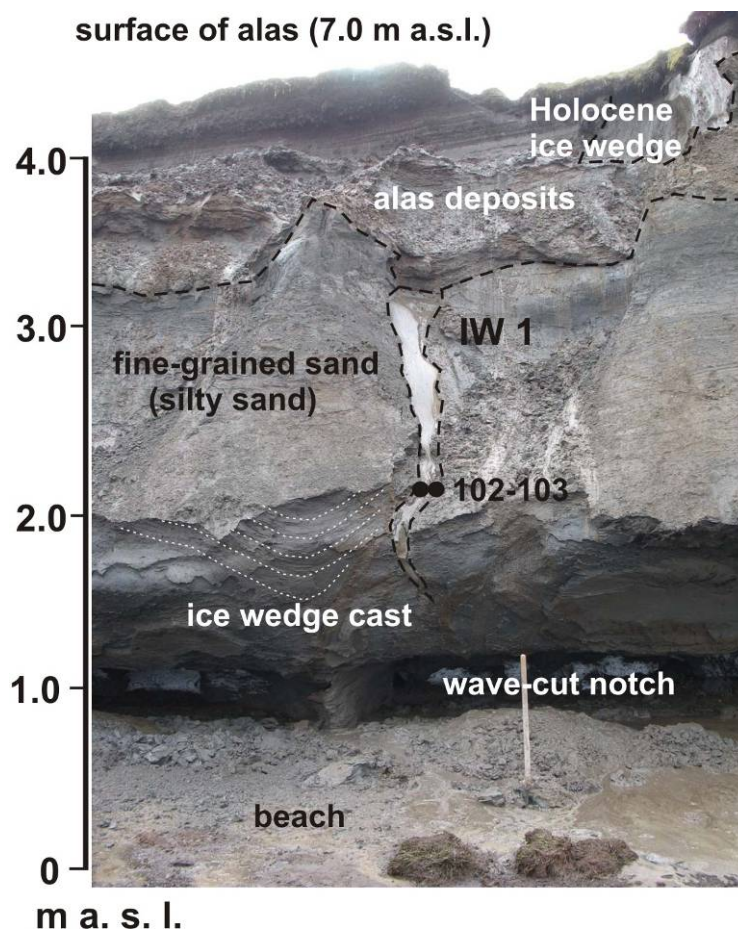


**Figure 4.6.5-6:** Ice wedge Oy7-05 IW 1 – tail of an Ice Complex ice wedge, penetrated into deposits of the Krest Yuryakh Suite.

#### *Ice wedge Oy7-06 IW 1*

An ice wedge from the lowermost visible part of the Ice Complex was sampled in the section Oy7-06 (IW 1). This ice wedge was located at the thermo-terrace in a height of about 7-8 m a.s.l. and had a visible thickness of about 4 m and a width of about 3.5 m. The bottom part of the ice wedge (tail) was buried under the surface of the thermo-terrace. Thermodenudation cut the upper part of the ice wedge. A thin (0.5 m) layer of brown loam and soil horizon with an active

layer depth of about 0.4 m covered the ice wedge. The enclosing sediments consisted of grey loam with vertical in-situ grass roots and peat inclusions (nests, lenses) and were characterized by a typical banded (belt-like) cryostructure. The distances between the 4-5 cm thick ice belts were about 7-10 cm. The ice wedge ice was dirty, grey and transparent with numerous air bubbles. Vertically oriented ice veins showed widths of about 1-5 mm. The height of the sampled profile was about of 9 m a.s.l. Sample points (in both ice wedges and ice belts) are displayed in Figure 4.6.5-7.

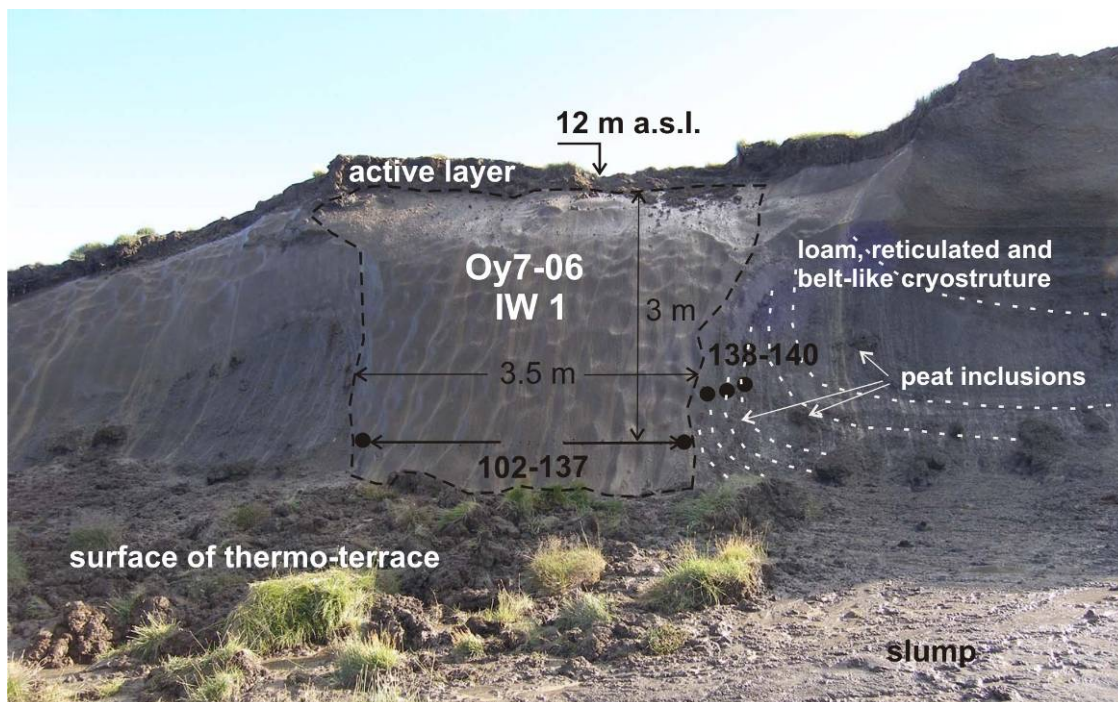


**Figure 4.6.5-7:** Lowermost part of the Ice Complex with the ice wedge Oy7-06 IW 1.

#### *Ice wedge Oy7-06 IW 2*

The next level of Ice Complex ice wedges was sampled in the section Oy7-06 IW 2. The altitude of the sampled profile was about of 20-21 m a.s.l. This ice wedge was located at the slope of thermocirque close to gauge mark Rp-3 (22.4 m a.s.l.). The visible thickness of the ice wedge was about 4-5 m, whereas the bottom part was buried below the surface of the wide thermo-terrace. The about 2 m wide ice wedge was covered by a thin (0.5 m) layer of brown loam and soil horizon. The active layer thickness was about 0.3-0.4 m. The enclosing sediments consisted of grey loam. They were very ice-rich and characterized by a belt-like cryostructure. The thickness of the ice belts was about 2-3 cm. The distance between the belts was about 7-10 cm. The colour of the ice wedge ice was grey (due to mineral patterns) and transparent with numerous air bubbles (size ca. 1-2 mm). The width of vertical oriented ice veins was about 1-5 mm. In Figure 4.6.5-8 the sample points of both the ice wedges and the ice belts are shown. The sample resolution was about 10 cm.

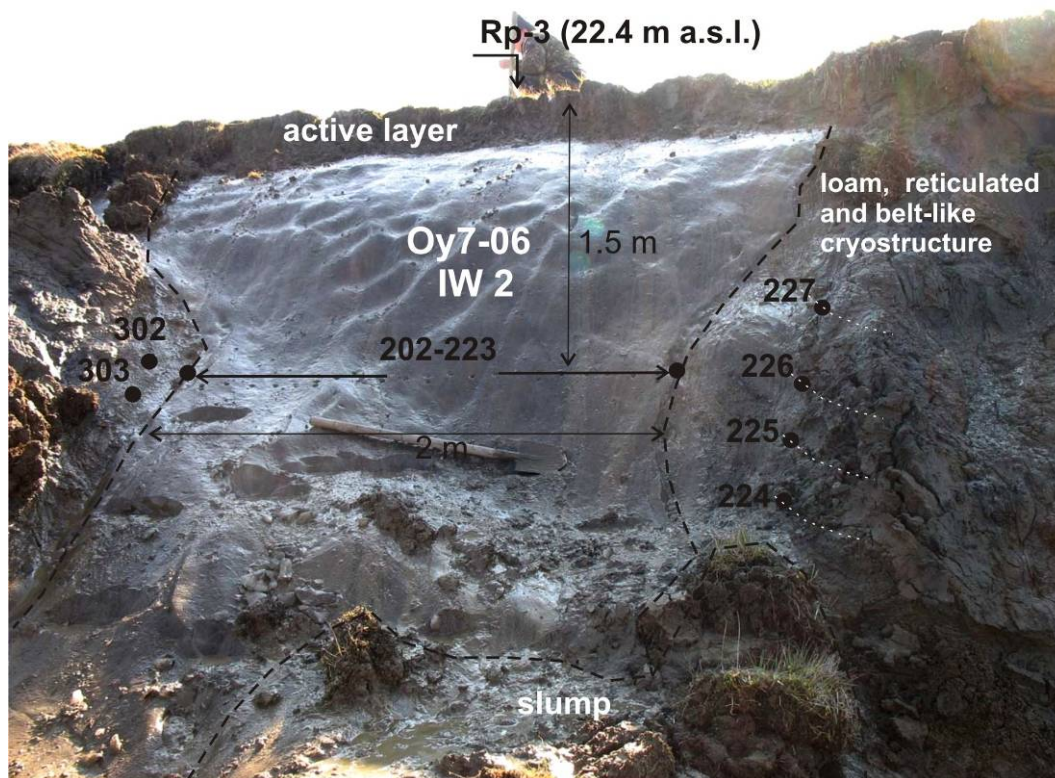


**Figure 4.6.5-8:** Ice Complex ice wedge Oy7-06 IW 2.

#### *Ice wedge OY7-08 IW 1*

The next level of Ice Complex ice wedges was sampled in the section Oy7-08 IW 1. The altitude of the sampled profile was about 25-26 m a.s.l. This ice wedge was located at the slope of the thermocirque close to gauge mark Rp-2 (29.4 m a.s.l.). The width of the ice wedge was about 5.7 m and the visible thickness was about 8-9 m. The bottom part was buried under the surface of the wide thermo-terrace. The ice wedge was covered by a thin (0.5 m) layer of brown loam and soil horizon with an active layer thickness of about 0.3-0.4 m. The enclosing sediments consisted of grey loam with peat inclusions (nests, lenses). The sediments were characterized by a belt-like, reticular and massive cryostructure. The ice wedge ice was dirty (grey and transparent) with numerous mineral patterns. There were a lot of vertically oriented oval air bubbles (size ca. 1 x 5 mm). The widths of the vertically oriented ice veins ranged from 1 to 10 mm. The sample points are displayed in Figure 4.6.5-9. The sample resolution was about 15 cm. Ice was also sampled for  $^{36}\text{Cl}$  measurements (Oy7-08-101).

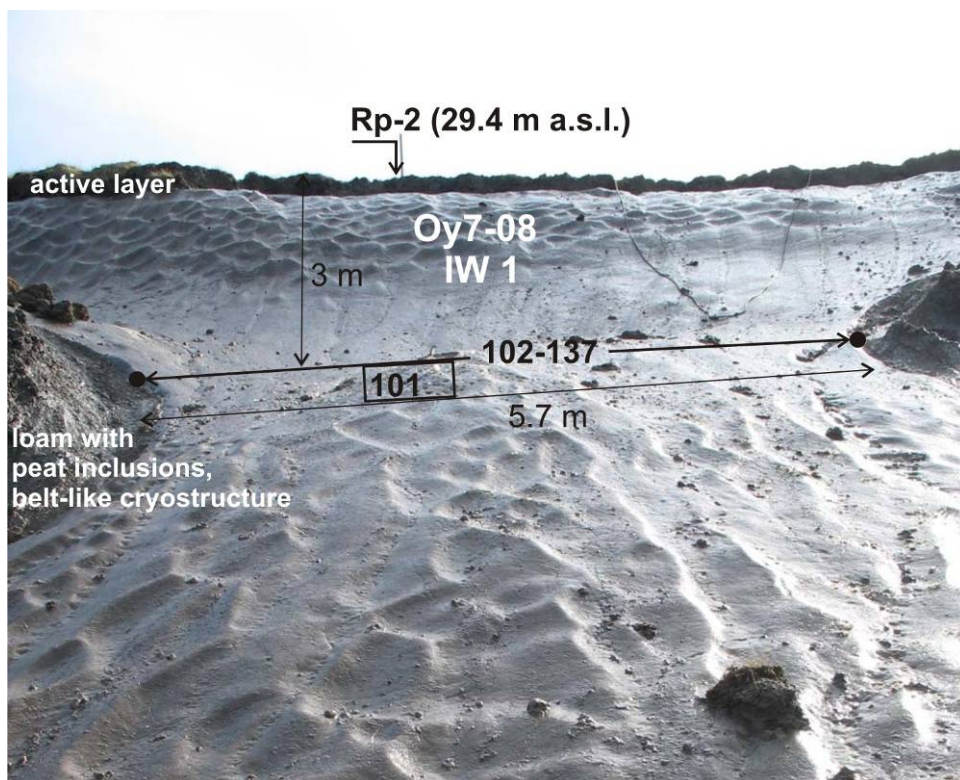
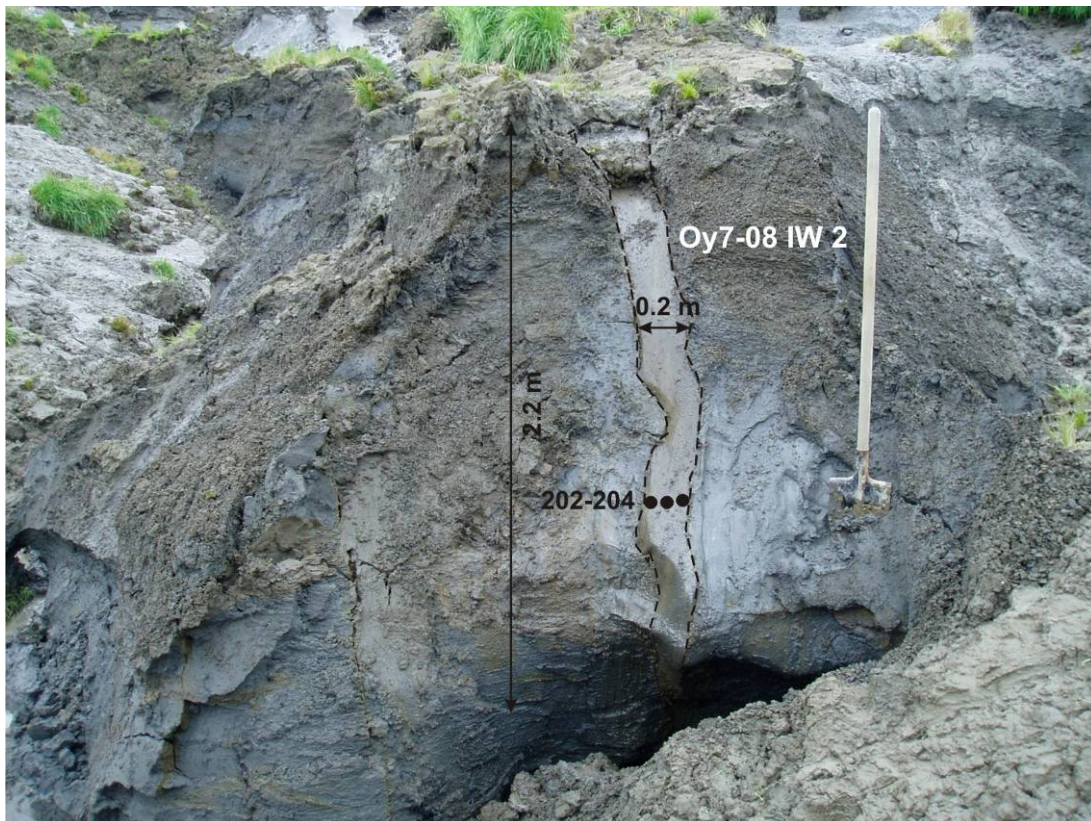


Figure 4.6.5-9: Upper part of the Ice Complex with the ice wedge Oy7-08 IW 1.

#### *Ice wedge Oy7-08 IW 2*

In the bottom part of the Ice Complex (5.5 m a.s.l.) a small ice wedge (Oy7-08 IW 2) was sampled (Figure 4.6.5-10). This ice wedge was located at the probable boundary of Krest Yuryakh and Ice Complex deposits. It was exposed in a baydzherakh (thermokarst mound) close to gauge mark Rp-4 (12.7 m a.s.l.) and can be considered as an epigenetic ice wedge. The surrounding sediments were characterized by peaty silt. The ice wedge width was about 0.2 m and the visible thickness was about 2.15 m. It was characterized by thin ice veins (1-2 mm) and numerous small air bubbles. Three samples (Oy7-08-202-204) were taken in a height of 4.4 m a.s.l.



**Figure 4.6.5-10:** A small epigenetic ice wedge (Oy7-08 IW 2) at the border of Krest Yuryakh to Ice Complex deposits

### *Ice wedge Oy7-08 IW 3*

The section Oy7-08 IW 3 presents an Ice Complex ice wedge at the altitude of about 30 m a.s.l. This ice wedge was located in the upper part of the thermocirque close to Oy7-08 IW 1. The width of the ice wedge was about 5 m and the visible thickness was about 9 m. The bottom part was buried under the surface of wide thermo-terrace. The ice wedge was covered by a thin (0.4 m) layer of brown loam and soil horizon with an active layer thickness of about 0.3-0.4 m. The lowermost 2-3 cm were characterized by a dark grey clayish layer. The ice wedge enclosing sediments consisted of grey (brownish-grey) loam, which showed a belt-like cryostructure. The ice belts were 2-3 cm thick with distances of about 5-8 cm between the single ice belts. The ice wedge was milky white (with a lot of both vertically oriented and non-oriented oval air bubbles) and dirty transparent (with mineral patterns). The vertically oriented ice veins were not well pronounced and exhibited widths of 2 to 10 mm. In the ice wedge profile were numerous cross oriented smaller ice veins. These well pronounced transparent (without air bubbles and mineral patterns) ice veins crossed the system of vertically oriented ice veins. The widths of these transparent ice veins were about 1-3 cm. The crossing ice veins were also sampled. Sample points (both the ice wedges and the ice belts) are presented in Figure 4.6.5-11. The sampling resolution was about 15-18 cm.

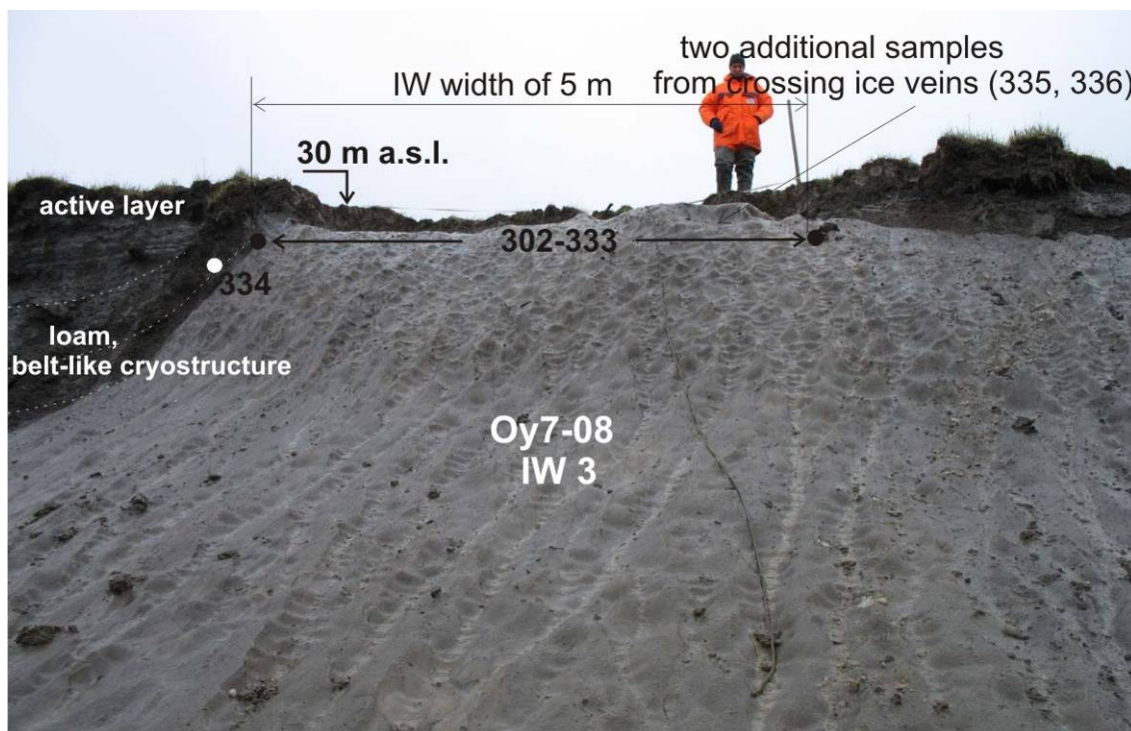
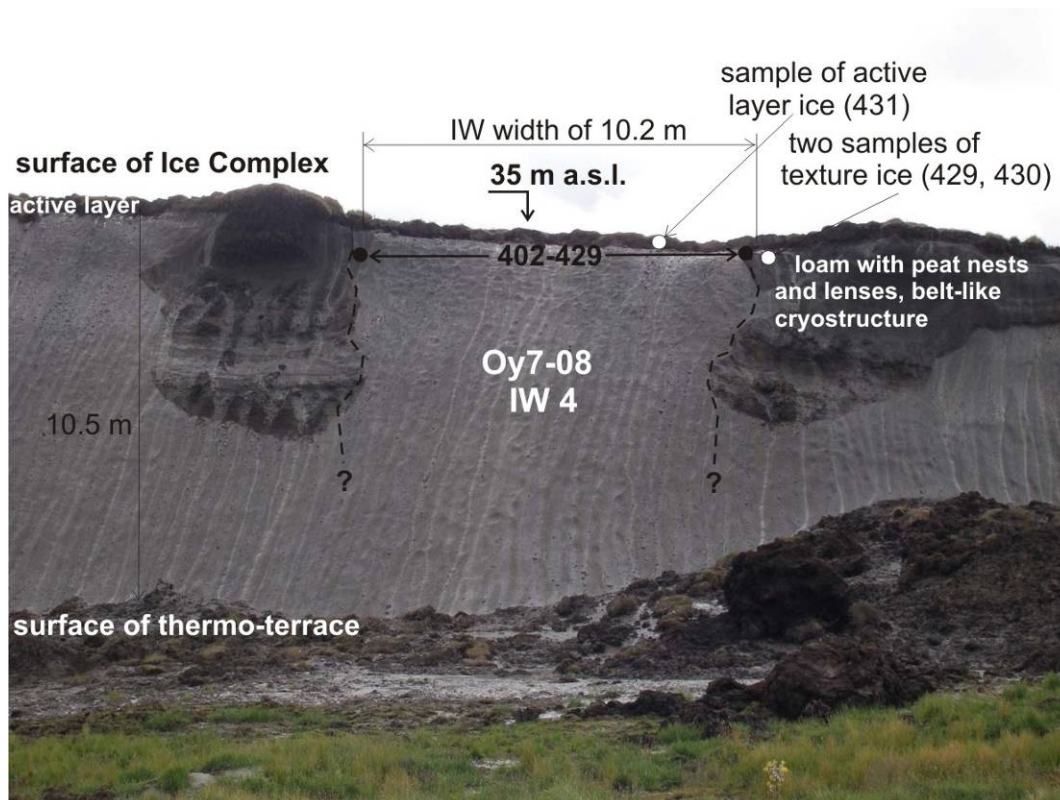


Figure 4.6.5-11: Upper part of the Ice Complex with the ice wedge Oy7-08 IW 3.

#### *Ice wedge Oy7-08 IW 4*

The ice wedge Oy7-08 IW-4 was located close to the top of the Ice Complex in a height of about 35-36 m a.s.l. The ice wedges in the top of the Ice Complex were characterized by extremely high widths of ca. 10 m (measurements of the ice wedges widths at the top of Ice Complex were carried out by A. Derevyagin and V. Kunitsky). The visible thickness of the ice wall was about 10-11 m, whereas the bottom part of the ice wedge was buried under the surface of a wide thermo-terrace. The ice wedge was covered by a thin (0.5 m) layer of brown loam and soil horizon. The thickness of the active layer was about 0.3-0.4 m. In the bottom part of the active layer a 2-3 cm thick layer of dark grey clay with a non-regular cryostructure and grass roots was found (sample 431). The surrounding sediments consisted of grey (blue-grey) loam with peat inclusions. They were very ice-rich and were characterized by belt-like and reticulated cryostructures. The ice belts thickness was about 4-5 cm and the distances between the single belts were about 5-10 cm. The colour and structure of the ice wedge ice is similar to that of Oy7-08 IW 3. Sample points (both ice wedges and ice belts) are displayed in Figure 4.6.5-12. The sampling resolution was about 35 cm.



**Figure 4.6.5-12:** Upper part of the Ice Complex, ice wedge Oy7-08 IW 4.

#### *Ice wedge Oy7-08 IW 5*

The ice wedge Oy7-08 IW 5 was a small one, located close to the top of the Ice Complex at the level of about 36 m a.s.l. This ice wedge could possibly be interpreted as a Holocene ice wedge. There were lenses of Holocene (?) sediments in the top of the Ice Complex associated with small initial thermokarst depressions (bylar). These sediments were characterized by grey, brownish-grey loam with numerous peat inclusions (lenses, nests) and by a bended cryostructure. These sediment lenses in the top of Ice Complex were about 1.2-1.7 m thick and extended about 20-25 m in length. The width of the ice wedge was about 0.5-0.6 m. The ice wedge penetrated into a huge Ice Complex ice wedge. The height of the ice wall in this site was about 18 m. Two samples of ice were taken (502 and 503).

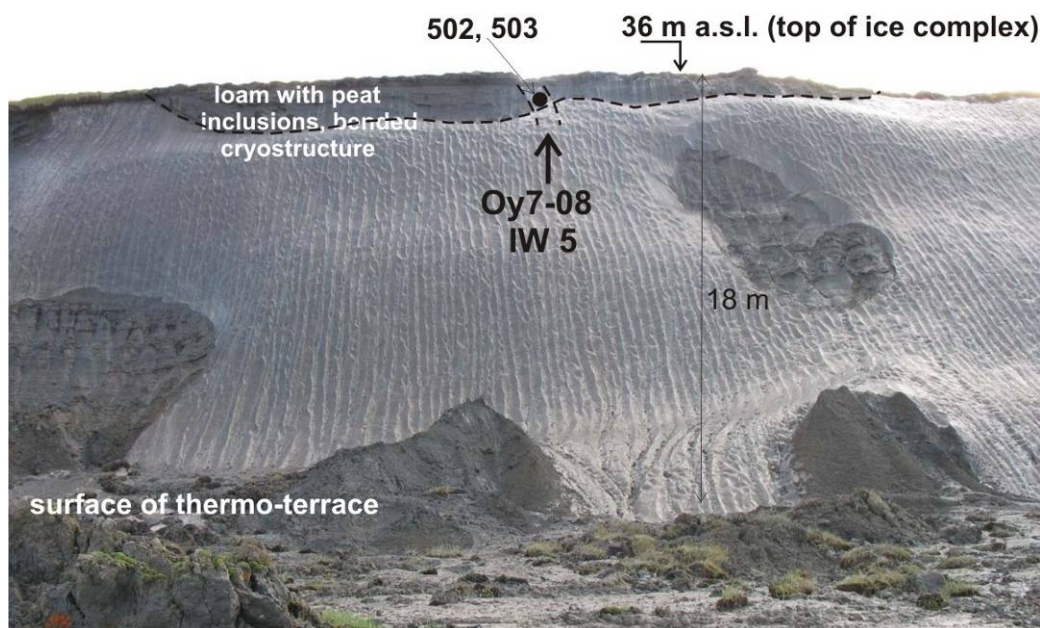


**Figure 4.6.5-13:** Ice Complex, ice wedge Oy7-08 IW 5 within a Holocene (?) lens.

#### 4.6.5.4 Studies of Holocene and recent ground ice

##### *Ice wedges Oy7-02 IW 1, IW 2, IW 3*

The studied outcrop Oy7-02 with the ice wedges IW 1, IW 2, IW 3 was located at the coastal cliff in the central Alas area in a height of about 10 m a.s.l..

The enclosing sediments were characterised by grey-to-brownish silty clays with thin films of iron oxide and a belt-like reticular cryostructure. The bottom part of the section consisted of layers of grey-yellowish clay and layers of peat with numerous inclusions of grass roots and twigs. Thick ice belts (about 10 cm) with typical vertical and subvertical curves located close to the ice wedge (Figure 4.6.5-14 left) were observed in the upper part of the profile, indicating a syngenetic type of ice wedge formation.

The 4 m high IW 1 had a complicated construction and consisted of two parts, which enclose a sediment section with peat inclusions (Figure 4.6.5-14 right). This could indicate the coalescence of two former independent ice wedges. Most likely we observed the corner of a polygon. The width of IW 1 was about 3 m in its thickest upper part. Its lowest visible part penetrated an about 40 cm thick peat layer. IW 1 consisted of a clear, white-to-milky ice. The thickness of single ice veins varied from 1-2 to 10 mm. A lot of vertically oriented air bubbles up to 5 mm were detectable. From the western shoulder a small up to 10 cm wide ice wedge tie penetrated 0.5 m into the surrounding sediments (IW 2). At the eastern edge of IW 1, divided by about 20 to 30 cm of sediments and peat, an up to 20 cm wide small ice wedge with a thickness of about 2 m was detected (IW 3). We sampled all 3 ice wedges at about 3 m below surface, the

sample resolution of the profile of IW 1 was 10 cm. In addition, we took a sample (Oy7-02-101) for age determination ( $^{36}\text{Cl}$ ).

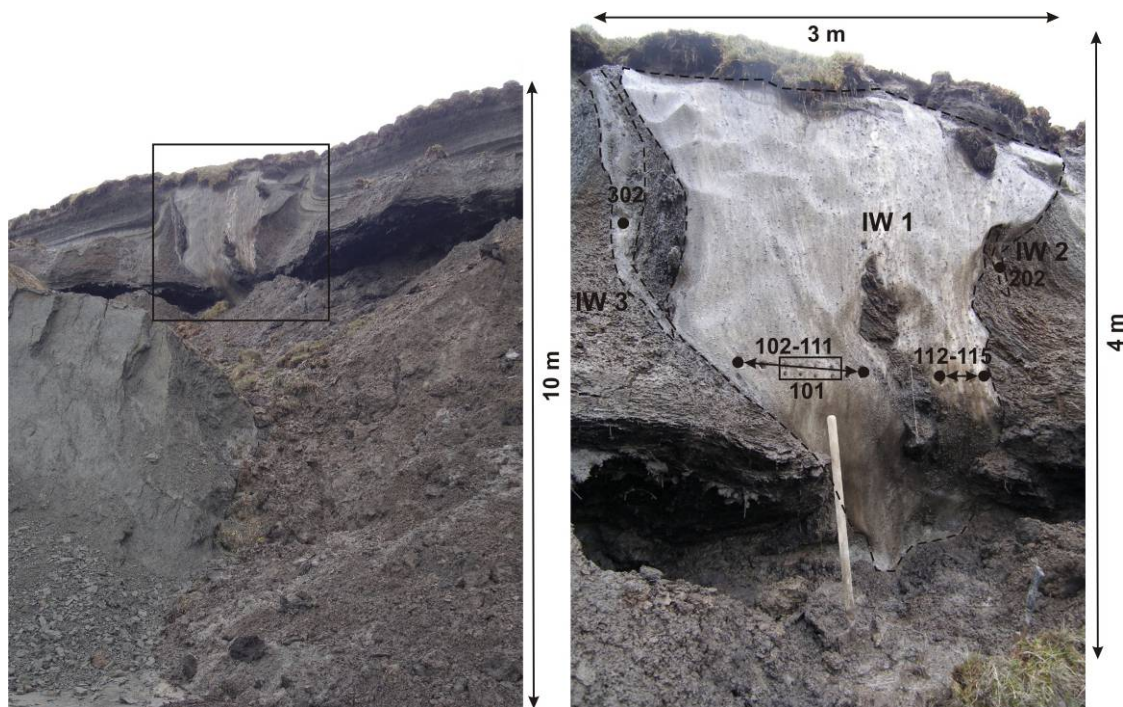


**Figure 4.6.5-14:** Outcrop Oy7-02 with the studied Holocene ice wedges IW 1, IW 2 and IW 3.

#### *Ice wedges Oy7-04 IW 1, IW 2, IW 4, IW 5, IW 6*

In the section Oy7-04 at the slope from the Yedoma hill to the Alas depression we studied five ice wedges. The outcrops were located close to each other at the coastal cliff in a height of about 10 m a.s.l., except IW 6 with a height of 4.5 to 5 m a.s.l.

The ice wedges IW 1, IW 2, IW 4 and IW 5 were sampled 0.5 to 2 m below the recent alas surface. The surrounding sediments were typical for alas deposits: mainly grey, silty clays with a net-like cryostructure. At the contact zone to the ice wedge, the sediments are more brownish. The ice wedges are covered by a 50 to 70 cm grey-brownish loam horizon with grass roots and peat inclusions with a net-like texture (regular reticulate). The active layer thickness was between 20 and 40 cm.

The focus of the study of ice wedges IW 1, IW 4 and IW 5 was the recent growth and development of ice wedges. Therefore, we sampled only the most recent parts for stable water isotope and  $^3\text{H}$  measurements (Figure 4.6.5-15). These heads of ice wedges topped the ice wedge surface by about 20 cm with a width of about 2 to 8 cm. They consisted of a very milky, white and also clear ice, with very small air bubbles and mineral inclusions. The thickness of single ice veins was 1-3 mm.

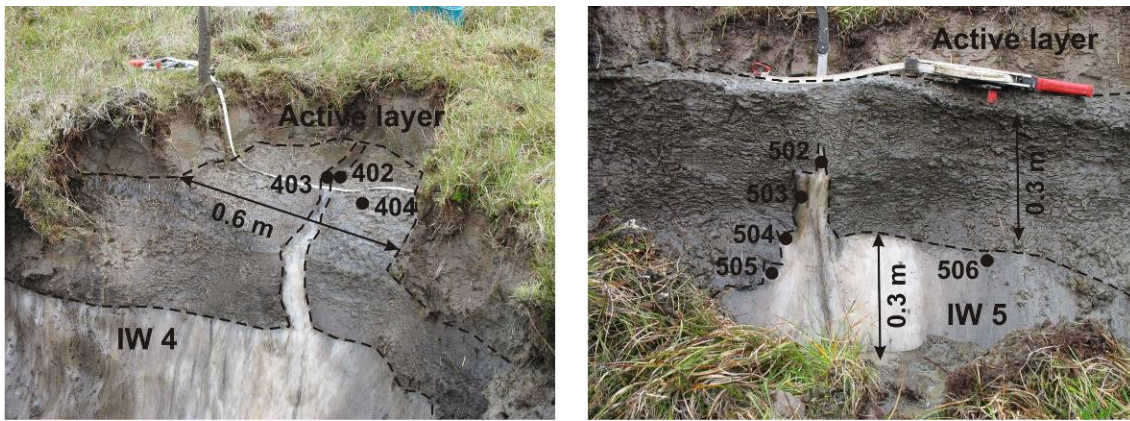


**Figure 4.6.5-15:** Examples of the studied recent ice wedge parts in the outcrop Oy7-04. Left: IW 4. Right: IW 5

Additionally, we took a high resolution sampling profile from the symmetrically structured Holocene ice wedge IW 2. The enclosing sediments were characterised by bended ice belts (thickness about 2 cm, difference between belts about 10 cm), indicating a syngenetic ice wedge formation. The width of this ice wedge was about 3.20 m, the visible thickness 1.50 m. The bottom part of the ice wedge was buried. The ice wedge consisted of white to transparent ice with a lot of vertically oriented air bubbles up to 1 cm. Also some mineral inclusions and organic matter were found in the general clean ice. Elementary ice veins had a thickness of 1 to 3 mm. In total, we took 107 samples in a resolution of about 2.5 cm by chainsaw (Figure 4.6.5-16 top). Additional samples for  $^{36}\text{Cl}$  dating (Oy7-04-201) as well as for measurements of stable water isotope and  $^3\text{H}$  content were taken directly below the recent ice wedge head. Between the ice wedge and the sediment profile Oy7-04-A (see chapter 4.6.4) texture ice samples (Oy7-04-313 to 322) from the surrounding ice belts were taken (Figure 4.6.5-16 bottom).

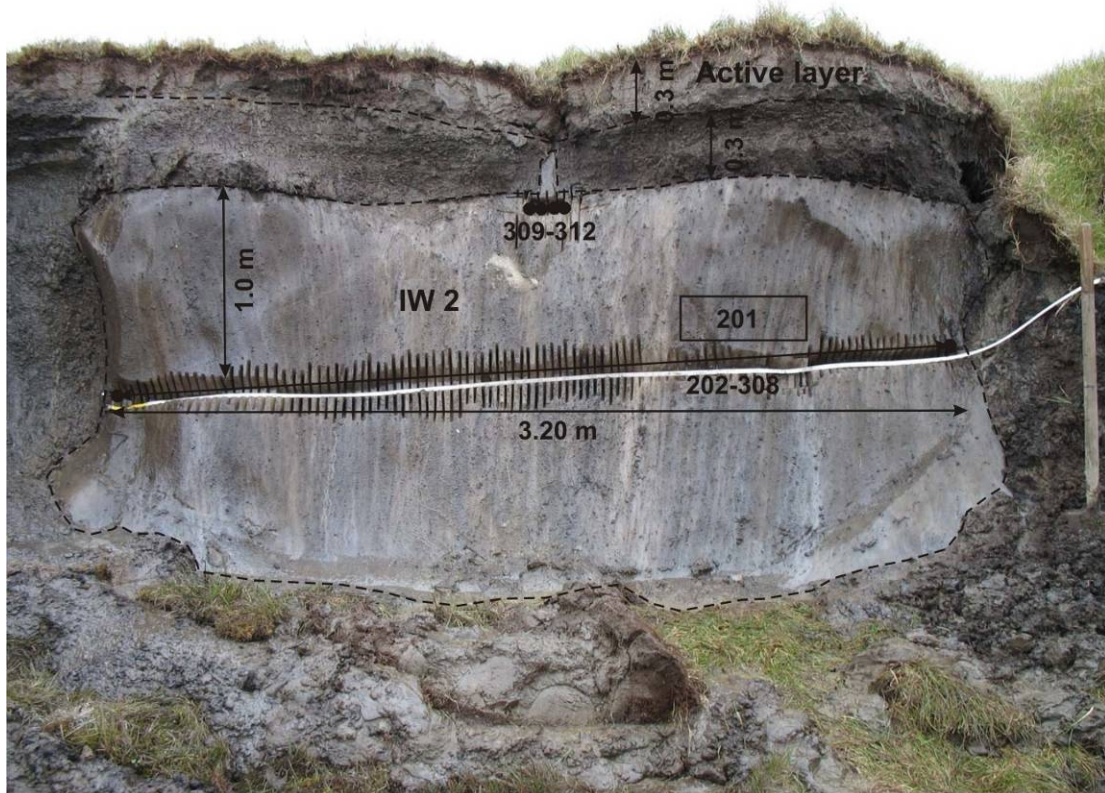


**Figure 4.6.5-16:** Top: High resolution profile of the Holocene ice wedge Oy7-04 IW 2. Bottom: Sample points of ice belts and the sediment profile Oy7-04-A.

Ice wedge IW 6 represents the tail of an epigenetic Holocene ice wedge, which penetrated into tabular deposits of the former Ice Complex. They were characterised by grey sandy silts with a layered fine lens-like cryostructure. Most likely this is the oldest part of alas (Holocene) ice wedge like Oy7-11 IW 3. We took three samples from this small ice wedge tail with a width of about 10 to 20 cm (Figure 4.6.5-17).



**Figure 4.6.5-17:** Epigenetic Holocene ice wedge Oy7-04 IW 6, penetrating in former Ice Complex deposits.

#### *Ice wedge Oy7-05 IW 2*

In this outcrop at the slope of the Ice Complex (transition Yedoma-Alas) we sampled the recent part of a Holocene ice wedge. This outcrop was located at the coastal cliff in a height of about 10 m a.s.l..

We excavated the ice wedge surface below the active frost crack of a polygon with a diameter of about 10 m, which was cut by the coastal cliff. The outcrop was about 90 cm x 90 cm in area (Figure 4.6.5-18).

The active layer had a thickness of about 35 to 40 cm and consisted of brownish grey clayish loam with grass roots and peat lenses. The frozen deposits between active layer and ice wedge were of the same composition and exhibit a net-like cryostructure. We sampled both the recent ice wedge head and the texture ice of the frozen sediments.

The recent ice wedge part consisted of a milky, white ice, characterised by a lot of very small, not oriented air bubbles. In the ice wedge head with a width of about 3 to 4 cm no single ice veins were detectable. We took samples from the ice wedge surface as well as from the recent ice wedge head for measurements of both the stable water isotopes and  $^3\text{H}$ .

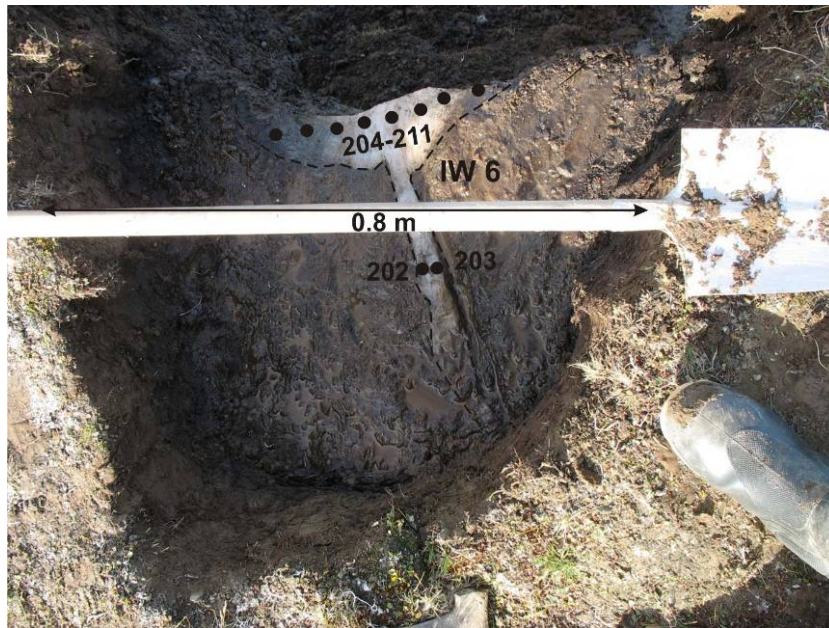


**Figure 4.6.5-18:** The recent part of the ice wedge Oy7-05 IW 2 viewed from top.

#### *Ice wedges Oy7-11 IW 1, IW 3, IW 4, IW 5, IW 6*

The section Oy7-11 was located at the coastal cliff in the central part of at the Alas area in an altitude of about 10 m a.s.l. We studied five ice wedges in this section.

Ice wedge IW 1 was an about 3.50 m wide ice wedge with clearly detectable bended ice layers at its western border. This indicates a syngenetic formation of this Holocene ice wedge. Since the bottom part was buried under debris, the visible thickness was about 2 m. The enclosing sediments are grey silts with some brownish layers and an non-regular cryostructure. The ice wedge was covered by 40 to 50 cm sediments with an active layer thickness of about 20 to 25 cm. The recent ice wedge head was not located in the central part of the ice wedge, but 70 to 80 cm away from the western edge. The ice wedge consisted of dirty ice and was rich of organic and mineral patterns as well as of small vertically oriented air bubbles. The high resolution sampling profile was located about 1.5 m below the surface. In total, we took 123 samples in a resolution of 1.5 to 3 cm as well as samples from the recent ice wedge head and from the bended ice layers (Figure 4.6.5-19).

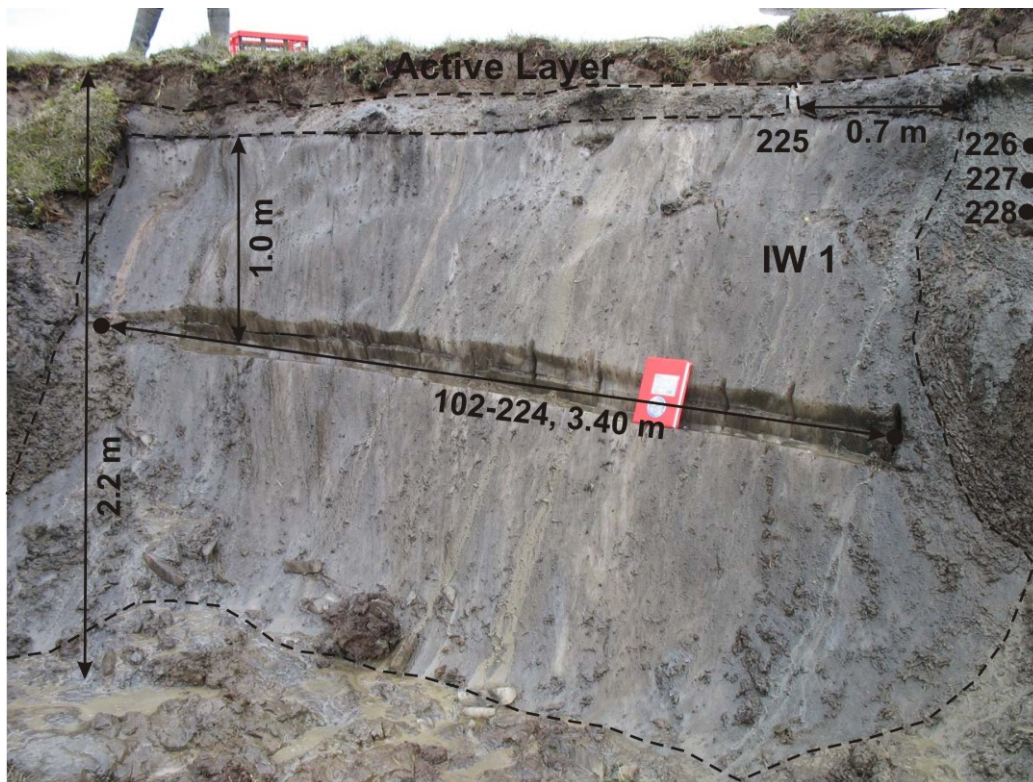


**Figure 4.6.5-19:** The high-resolution sampled profile of the Holocene ice wedge Oy7-11 IW1.

Ice wedge IW 3 represents the lowest and oldest part of an alas (Holocene) ice wedge, whose tails penetrated as epigenetic ice wedges into tabular alas deposits. These are most likely former Ice Complex deposits (grey, sandy, silty, lens-like layered). Both tails (15 and 5 cm width) were sampled 7 m a.s.l (Figure 4.6.5-20).

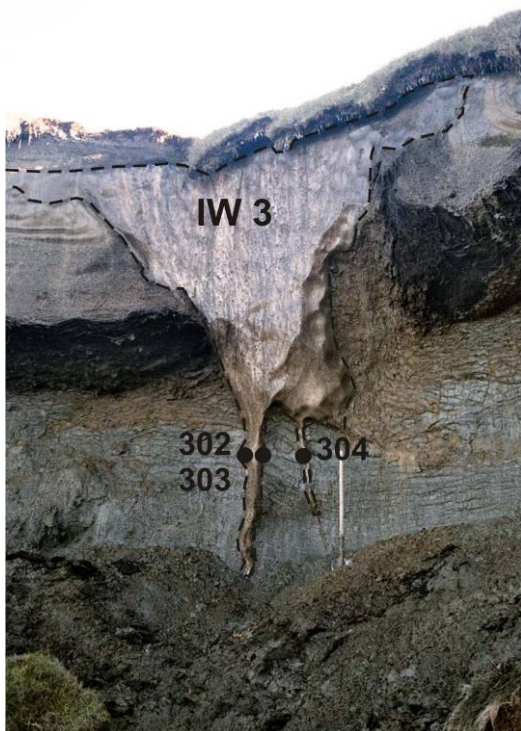


**Figure 4.6.5-20:** The tails of the Holocene ice wedge Oy7-11 IW 3 penetrated in tabular aluvial deposits.

The ice wedges IW 4 and IW 6 were studied in order to characterise the recent ice wedge growth. Therefore, we excavated the ice wedge surface below the active frost cracks of polygons, which were cut by the coastal cliff. The active layer had a thickness of about 20 to 25 cm and consisted of brownish-grey clayish loam with grass roots and peat lenses. The frozen deposits between active layer and ice wedge (1 to 3 cm) were of the same composition and exhibited a net-like cryostructure. We sampled both the recent ice wedge head and the texture ice of the frozen sediments. The recent ice wedge part consisted of a relatively clear, white ice, characterised by a lot of air bubbles. The ice wedge heads had widths of about 3-4 and 5-6 cm and contained 6 to 8 and 10 to 15 single ice veins. We took samples from the recent ice wedge head as well as from the texture ice for measurements of both the stable water isotopes and  $^3\text{H}$  (Figure 4.6.5-21).

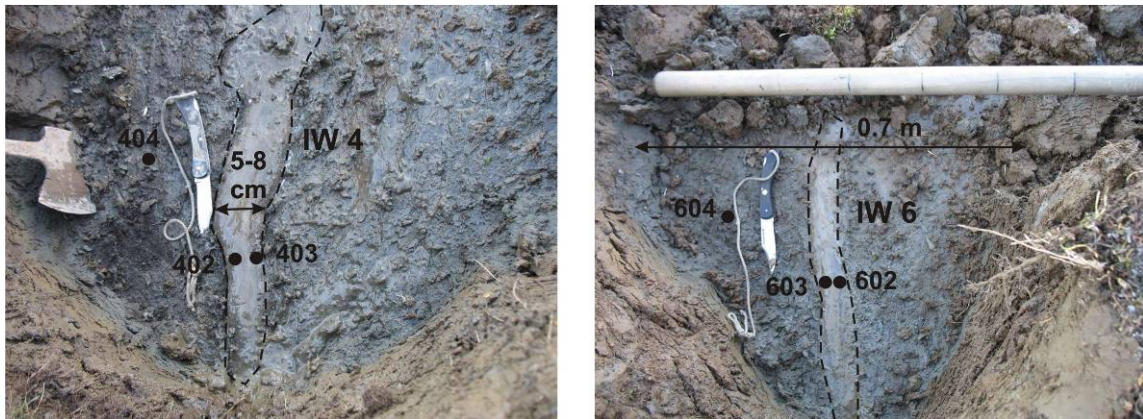


**Figure 4.6.5-21:** Recent ice wedge heads of the ice wedges Oy7-11 IW 4 (left) and IW 6 (right) viewed from the top.

The ice wedge IW 5 was a symmetrically structured syngenetic Holocene ice wedge with pronounced bended ice belts. It was surrounded by grey, silty sediments. The active layer accounted for 25 cm and the frozen sediments directly above the ice wedge for about 10 cm. The ice wedge had a width of about 2.50 m and a visible thickness of 1.20 m with a buried bottom part. It exhibited a very good pronounced recent ice wedge head of about 3 cm width, which consisted of about five elementary ice veins. The ice wedge head and the most recent part of the ice wedge were more milky-white due to more air bubbles than the other parts. Single ice veins showed a width of up to 1 cm. We sampled the recent ice wedge head as well as a horizontal transect in the most recent part 20 cm below the top of the ice wedge (Figure 4.6.5-22 left). Additionally, we sampled a horizontal profile 50 cm below the top of the ice wedge and took 12 compact blocks (4.6.5-22 right). These blocks were transported to Potsdam in frozen state and were sampled later under cold laboratory conditions (sample numbers Oy7-11-702 to Oy7-11-913).



**Figure 4.6.5-22:** The sampled Holocene ice wedge Oy7-11 IW 5. Left: Detail of the most recent IW part. Right: The whole profile.

#### 4.6.6 Fossils of the mammoth fauna

*Tatayana V. Kuznetsova*

During our fieldwork mammal bones and their fragments were collected. Afterwards, these fossil remains of the Mammoth fauna were identified. The bones were obtained (a) *in-situ*, i.e. within the frozen sediment, (b) in thermo-erosional cirques, where the original position within the sediments can be determined, (c) within the thawed debris of the outcrop, and (d) on the beach, and (e) at the tundra surface.

Samples belonging to (a) and (b) have direct importance for the geological interpretation of the deposits since the altitude is known for *in-situ* findings (a) or the minimum altitude of the original position can be estimated and the approximate altitude from which these bones come, can be defined (b).

The mammal bone collection consists of 1582 bones sampled by all members of the Oyogos Yar team in August 2007 (Chapter 6.3, Figure 4.6.6-1). The most common bones belong to mammoths, bisons, horses and reindeers. Interesting are the rare remains of saiga antelopes, mosses and Pleistocene lions.

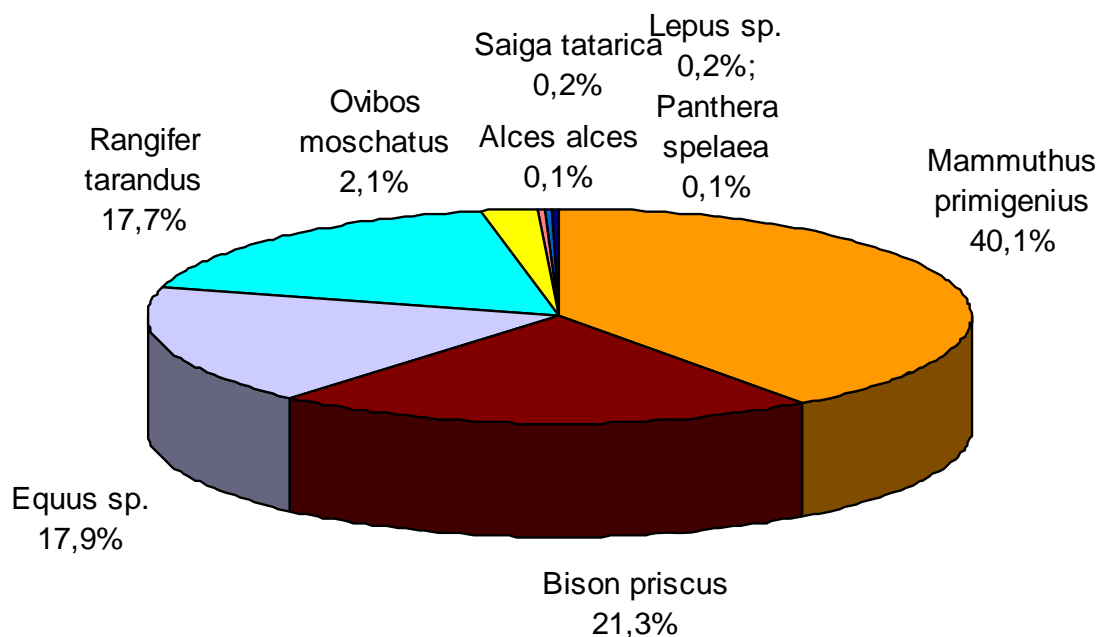


**Figure 4.6.6-1:** Composition of mammal bones collection from Oyogos Yar, 2007 (total number of samples: 1582)

The composition of the studied bone collection is typical for the late Pleistocene “mammoth fauna” of the Siberian Arctic. Fossil remains of listed below are found (Table 4.6.6-1).

**Table 4.6.6-1:** List of mammalian taxa identified in the Oyogos Yar collection in 2007 (for the complete list see chapter 6.3).

Taxa	Common name
Class Mammalia	
Order Proboscidea	
<i>Mammuthus primigenius</i> (BLUMENBACH 1799)	Woolly mammoth
Order Artiodactyla	
Family Bovidae	
<i>Bison priscus</i> (BOJANUS 1827)	Bison
<i>Ovibos moschatus</i> (ZIMMERMANN 1780)	Muskox
<i>Saiga tatarica</i> LINNAEUS 1758	Saiga antelope
Family Cervidae	
<i>Rangifer tarandus</i> LINNAEUS 1758	Reindeer
<i>Alces alces</i> (LINNAEUS 1758)	Moose
Order Perissodactyla	
Family Equidae	
<i>Equus caballus</i> LINNAEUS 1758	Horse
Order Carnivora	
Family Felidae	
<i>Panthera spelaea</i> (GOLDFUSS 1810)	Pleistocene lion
Family Canidae	
<i>Alopex lagopus</i> (LINNAEUS 1758)	Polar fox
<i>Canis</i> sp.	Wolf
Order Lagomorpha	
<i>Lepus</i> sp.	Hare
Order Rodentia	
Family Myomorpha	
<i>Dicrostonyx</i> sp.	Collared lemming
<i>Lemmus</i> sp.	Lemmings

#### 4.6.7 Sedimentological studies of selected profiles

*Alexander Gorodinskiy*

##### 4.6.7.1 Study site and objectives

All work has been carried out at different outcrops of Oyogos Yar permafrost sequences. The position of studied Ice Complex section was around 1 to 2 km eastward from camp which had approximate coordinates (72.68131°N, 143.49247°E).



**Figure 4.6.7-1:** Principal scheme of the investigated Oyogos Yar permafrost sequences. Red spots mark all described and sampled outcrops. Outcrops VI-A'; VI-A''; VI-A'''; VIII and IV-A correspond to outcrops described by the AWI team. Samples from there are listed below.

Major aim is studying the variations of the palaeoenvironmental conditions, in particular sea level changes during the Pleistocene period based on micro palaeontological methods. In order to reach this goal 80 samples have been taken from thirteen outcrops of permafrost sequences for forameniferal, diatom and grain-size analysis. Some of the outcrop descriptions are combined to distinguish possibly full profiles for Kuchchugui – Krest Yurakh – Yedoma Suites of permafrost sequences. Finally, we completed the description of two major profiles which probably cover upper Pleistocene deposits.

##### Legend

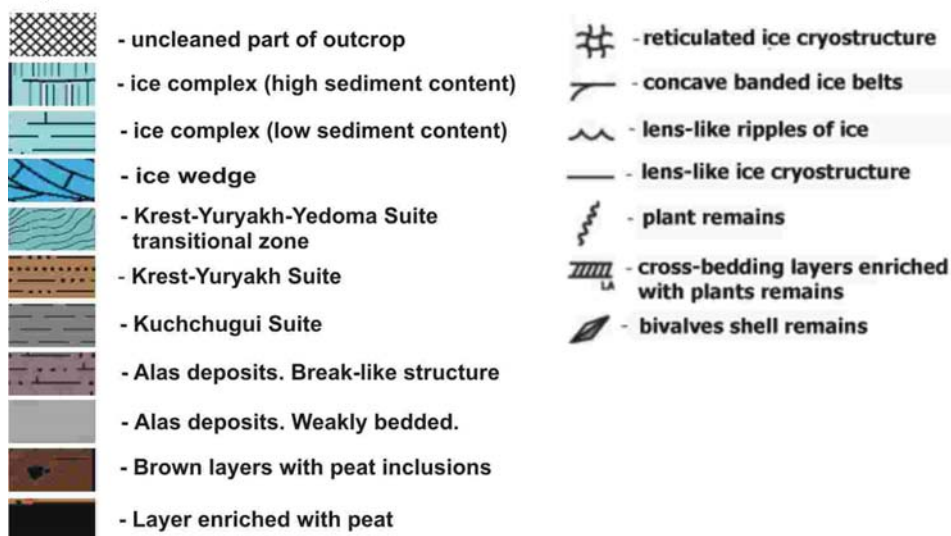


**Figure 4.6.7-2:** Legend of symbols used to separate different permafrost sequences and patterns.

## 4.6.7.2 Profile I

1. Outcrop VI-A: Position - Yedoma section\*, pedestal of the thermo-terrace near the sea shore (~ 1.5 km eastward from camp). Five samples have been taken near a thermoerosional gully. The outcrop height is about 3 m. The description of the exposed part starts with 1 m height (from bottom = sea level) and reaches 0.3 m below surface. For certain depths of each sample see figure 4.6.7-3.

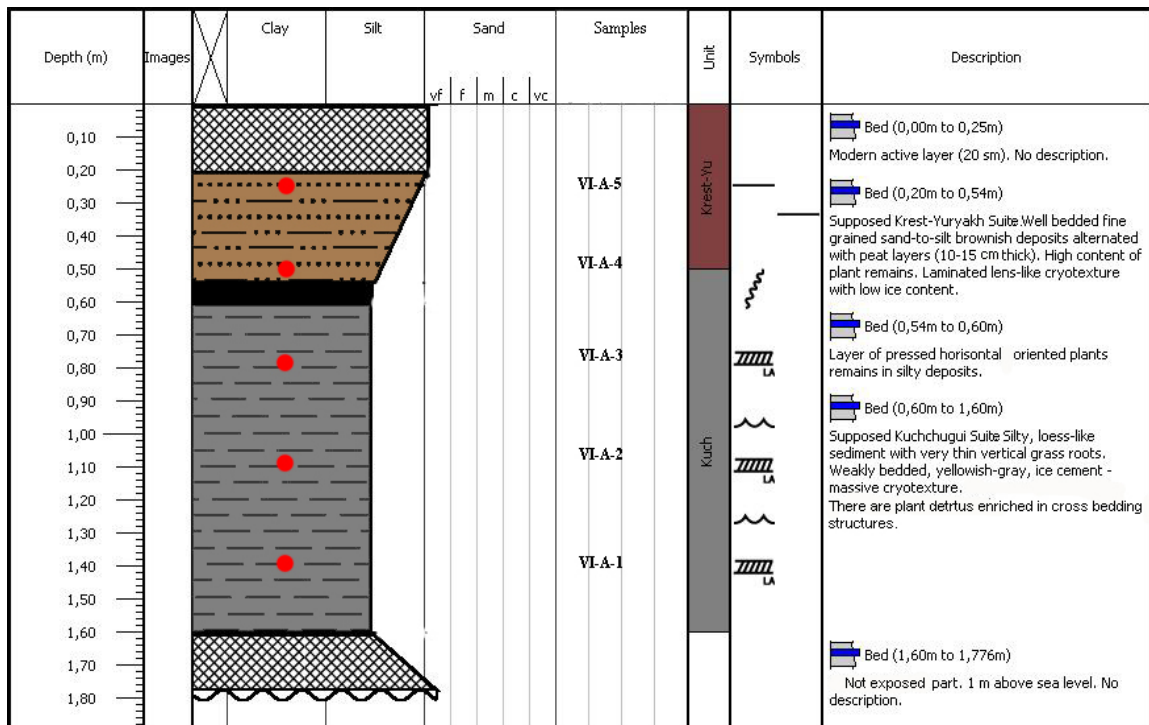


**Figure 4.6.7-3.** First (lower) part of the outcrop VI-A. The cleaned and described area is shown in colours. Five samples have been taken at different depths. The position of the outcrop is shown Figure 4.6.7-1.

\* Here we use two notations of working places: 1 – Yedoma section (implying any place at Yedoma elevation); 2 – Alas section (any place at Alas area)

2. Outcrop IX-A: Position - Yedoma section, pediment of the thermo-terrace in the thermoerosional gully 30 m from sea shore and Outcrop VI-A (~1.5 km eastward from camp). The outcrop height is about 6 m. The exposed part is described from 0.25 m (below surface) to 2.20 m depth. Six samples have been taken.

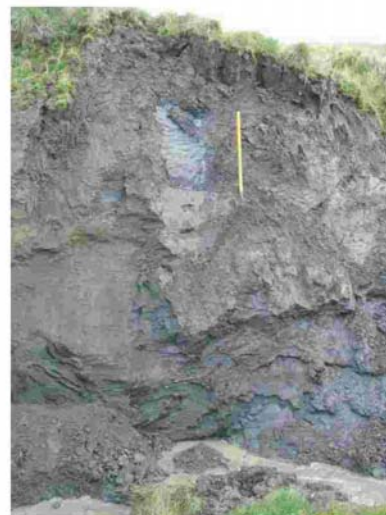
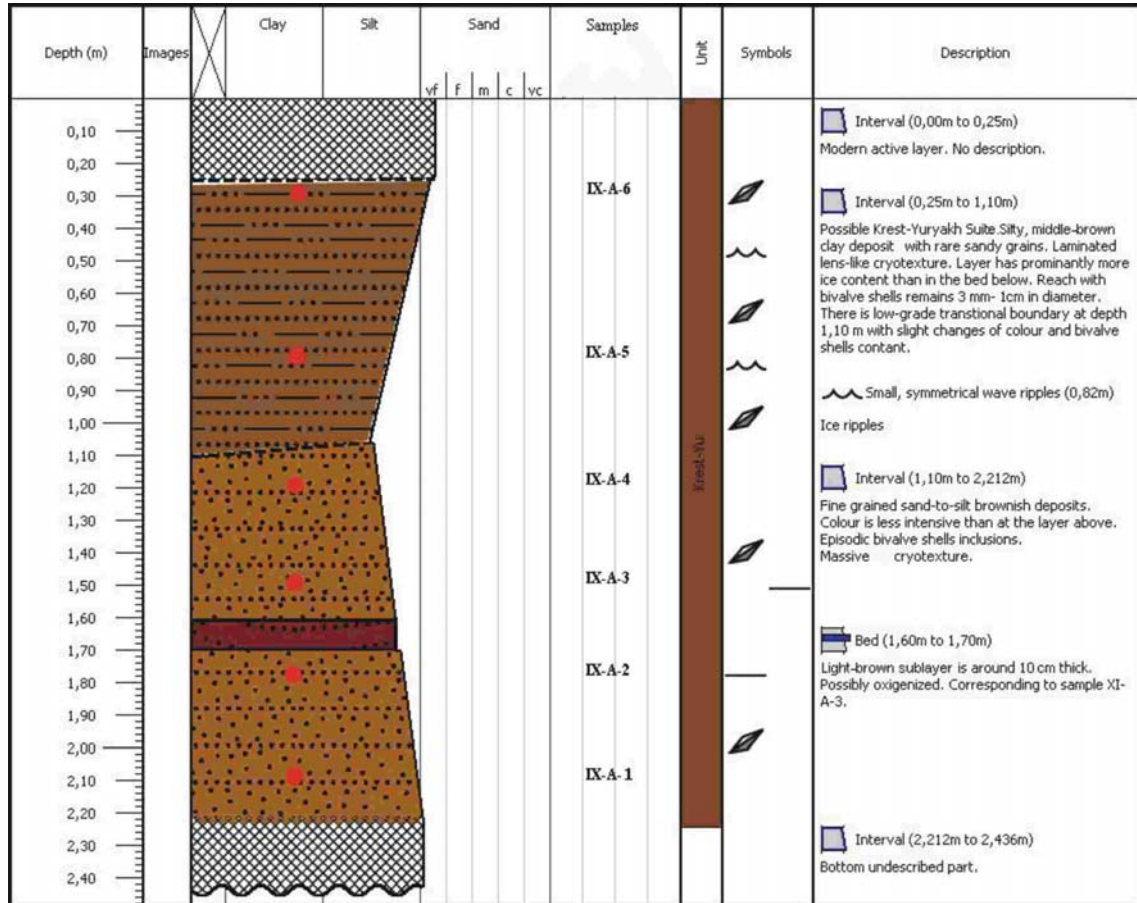


**Figure 4.6.7-4:** Description of the outcrop IX-A including a field picture. Six samples have been taken at different depths. The position of the outcrop is shown in Figure 4.6.7-1

3. Outcrop X-A: Position - Yedoma section, Baydzherakh (thermokarst mound) at the thermocirque slope, ca. 25 m a.s.l. and 1.5 m below modern surface (~1.5 km eastward from camp). Six samples have been taken.

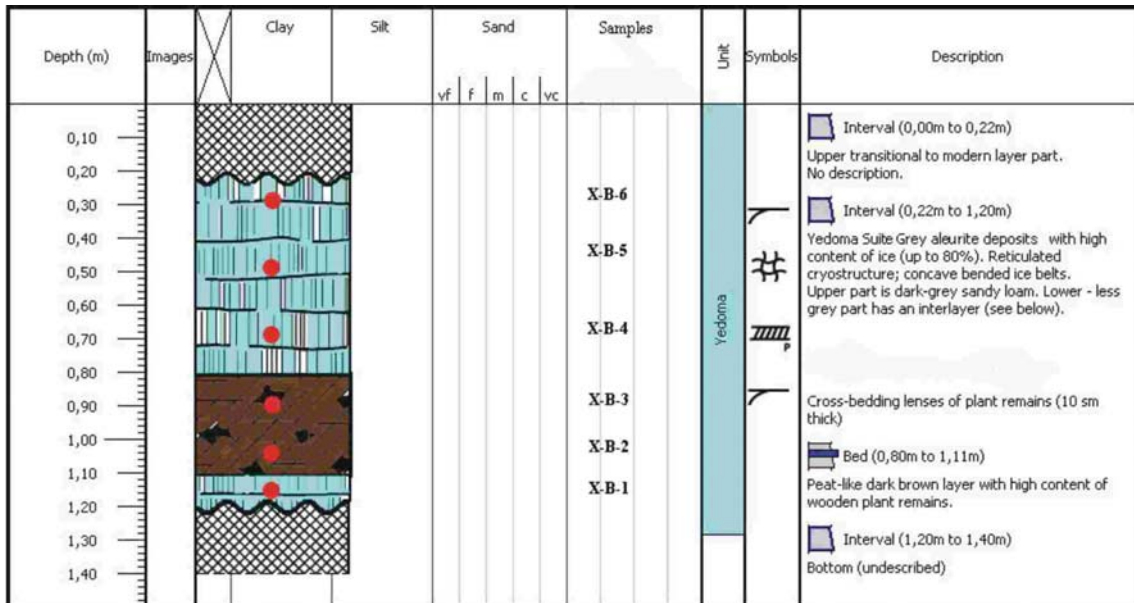


**Figure 4.6.7-5:** Description and field picture of the outcrop X-A. Six samples have been taken at different depths. The position of the outcrop is shown in Figure 4.6.7-1.

4.6.7.3 Profile II

1. Outcrop VII-A: Position - Yedoma section, pedestal of thermo-terrace near the sea shore (~2 km eastward from camp). The outcrop height is about 7 m. The sampling of the outcrop started 1.5 m a.s.l.. Nine samples have been taken. Unfortunately, there is no supporting field picture for this outcrop.

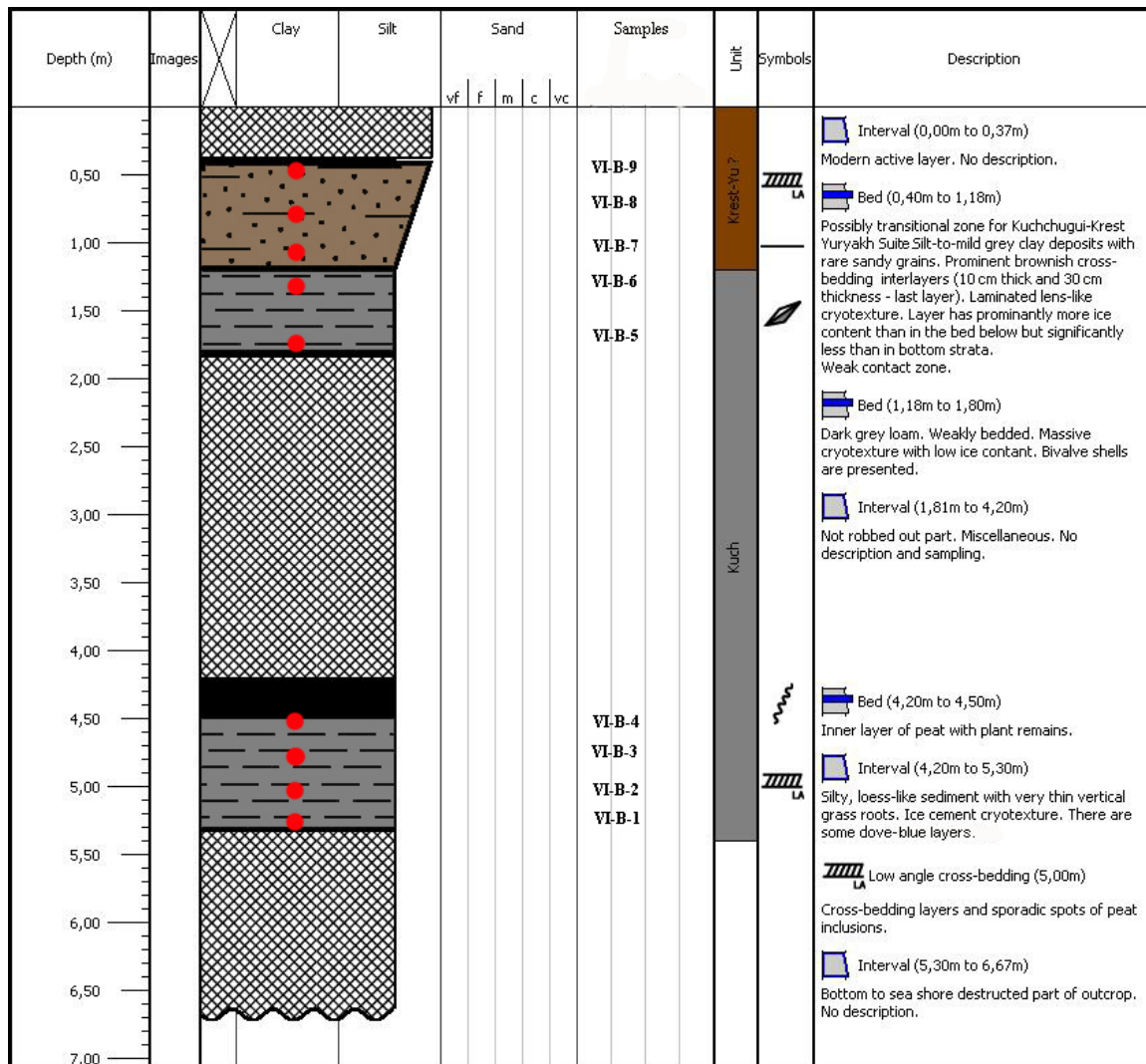


Figure 4.6.7-6: Description of the outcrop VII-A. Nine samples have been taken at different depths. The position of the outcrop is shown in Figure 4.6.7-1.

2. Outcrop XI-B: Position - Yedoma section, Ice Complex remnant on the thermo-terrace edge above outcrop VII-A. The height is about 3 m and the altitude is 12 m a.s.l.. Four samples have been taken from ice cemented ground between two ice wedges.

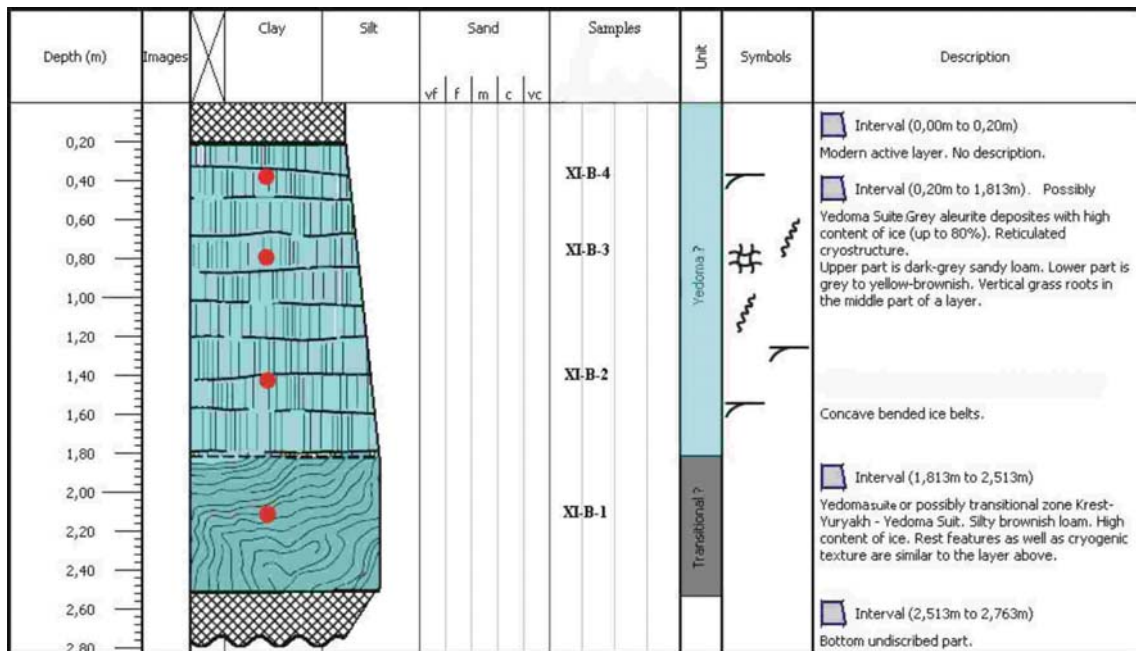


Figure 4.6-5-7: Description and field picture of outcrop XII-B. Four samples have been taken at different depths. The position of the outcrop is shown in Figure 4.6.7-1

3. Outcrop XI-B': Position - Yedoma section, melting Baydzherakh (thermokarst mound) at the pedestal of Yedoma Ice Complex, about 30 m from outcrop XI-B upslope to thermocirque. Three samples have been taken 13-15 m a.sl..

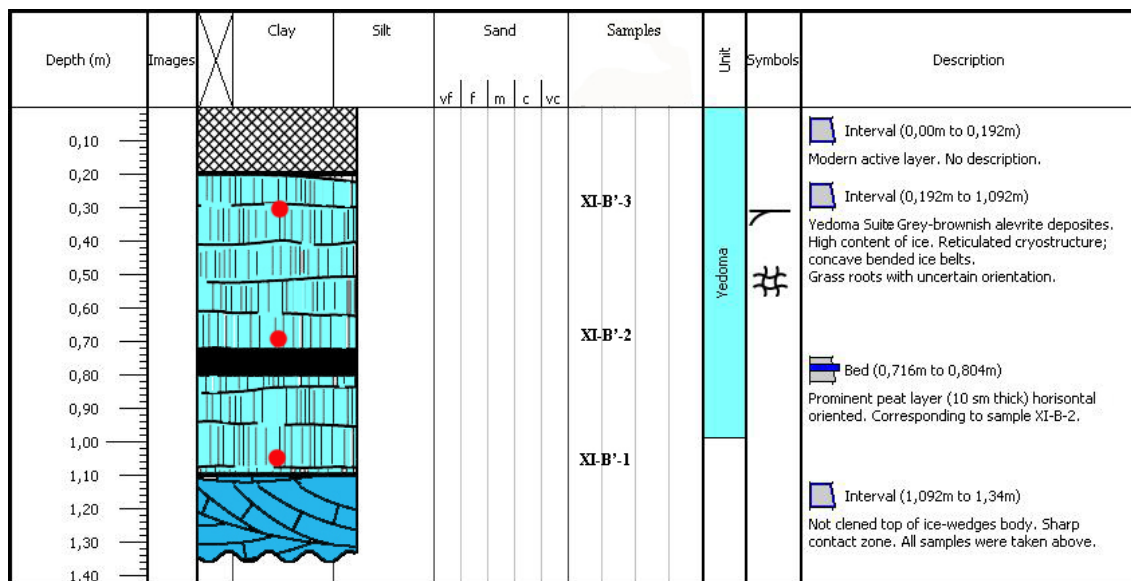


Figure 4.6.7-8: Description of the outcrop XII-B'. Three samples have been taken at different depths. The position of the outcrop is shown Figure 4.6.7-1

4.6.7.4 Additional outcrops

Further we present outcrops that were not included in the profiling described above. These outcrops represent different parts of Oyogos Yar.

1. Outcrop III-A: Position - Transitional zone between Yedoma complex and Alas at sea shore. Three samples have been taken from the ground block, which total height is 3.5 m.

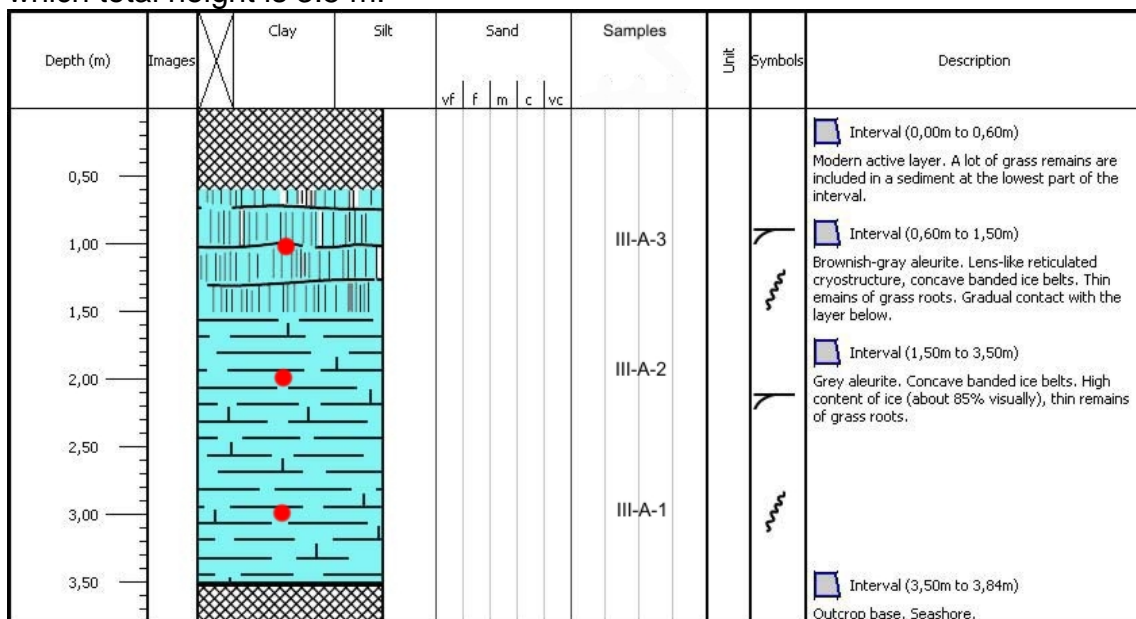
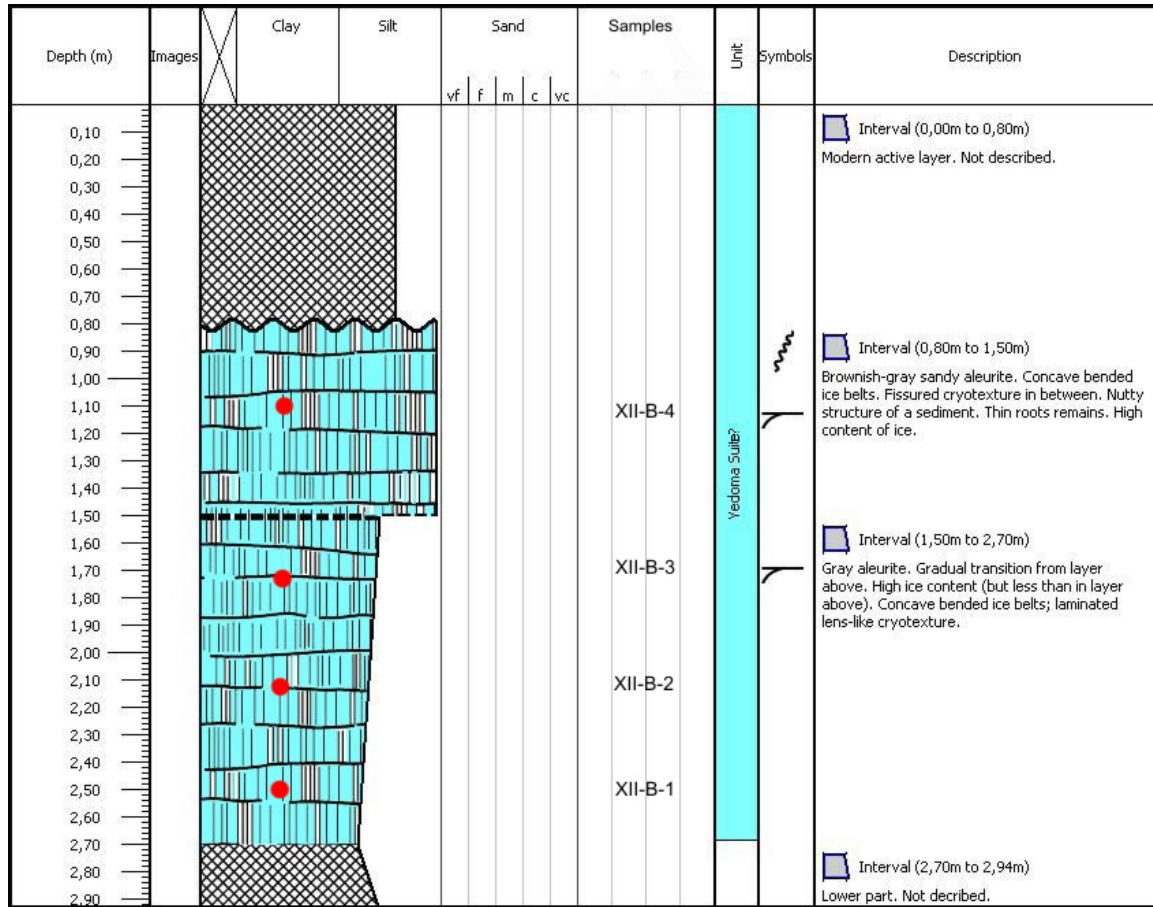


Figure 4.6.7-9: Description of the outcrop III-A. Three samples have been taken at different depths. The position of the outcrop does not match to major scheme and is situated eastwards.

2. Outcrop XII-B: Position - Yedoma section, thermo-terrace edge, 12 m a.s.l. (~1.5 km eastward from the camp). The height of the outcrop is 4 m. It represents possibly the bottom part of Yedoma Suite.



**Figure 4.6.7-10:** Description of the outcrop XII-B'. Four samples have been taken at different depths. The position of the outcrop is shown in Figure 4.6.7-1.

3. Outcrop V-B: Position - in the thermoerosional gully of Alas 30 m from sea shore, ~150 m from Yedoma elevation (~ 800 m from camp)

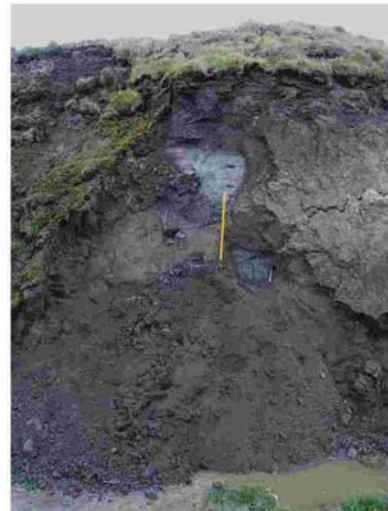
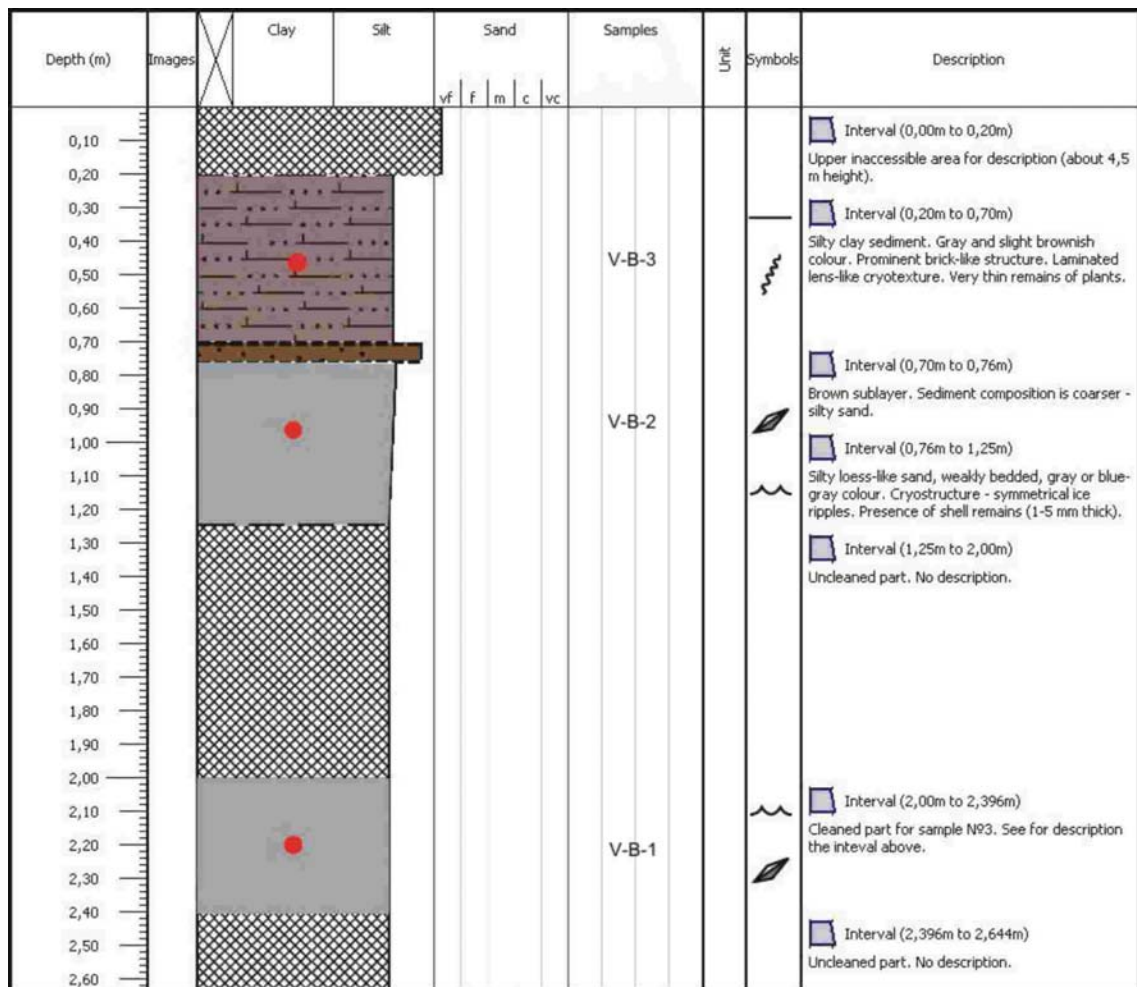


Figure 4.6.7-11: Description of the outcrop V-B. Three samples have been taken at different depths. The position of the outcrop is shown in Figure 4.6.7-1.

Further we list outcrops that correspond to those described by other colleagues in these report (chapters 4.6.2.1. and 4.6.2.3).

Outcrop I-A' (corresponds to Oy7-01-C): Pedestal of thermo-terrace at Yedoma elevation near sea shore (~2 km eastward from camp). Five samples were taken about 30 cm from each other.

Outcrop I-A'' (corresponds to Oy7-01-B): Pedestal of thermo-terrace at Yedoma elevation near sea shore (~2 km eastward from camp). Position is 30-50 m from outcrop I-A'. Four samples were taken about 30 cm from each other.

Outcrop I-A''' (corresponds to Oy7-01-A): Pedestal of thermo-terrace at Yedoma elevation near sea shore (~2 km eastward from camp). The position is 30-50 m from outcrop I-A''. Four samples were taken about 30 cm from each other.

Outcrop IV-A (corresponds to Oy7-09): Pedestal of thermo-terrace at Yedoma elevation near sea shore (1 km eastward from camp). Three samples have been taken about 30 cm from each other.

## 4.7 References

- Alekseev, M. N. (1989). Stratigraphy of the Quaternary deposits of the Novosibirskie Islands. In: Alekseev, M. N. and Nikiforova, K. V. (eds.): *Chetvertichnyy period. Stratigrafiya*. Nauka, Moscow, pp. 159-167 (in Russian).
- Alekseev, M. N. (1997). Palaeogeography and geochronology in the Russian Eastern Arctic during the second half of the Quaternary. *Quaternary International* 41/42: 11-15.
- Andreev, A. A., Grosse, G., Schirrmeister, L., Kuzmina, S. A., Novenko, E. Yu., Bobrov, A. A., Tarasov, P. E., Kuznetsova, T. V., Krbetschek, M., Meyer, H. and Kunitsky, V. V. (2004). Late Saalian and Eemian palaeoenvironmental history of the Bol'shoy Lyakhovsky Island (Laptev Sea region, Arctic Siberia), *Boreas* 33(4): 319-348.
- Andreev, A., Grosse, G., Schirrmeister, L., Kuznetsova, T. V., Kuzmina, S. A., Bobrov, A. A., Tarasov, P. E., Novenko, E. Yu., Meyer, H., Derevyagin, A. Yu., Kienast, F., Bryantseva, A., & Kunitsky, V. V. (2008). Weichselian and Holocene palaeoenvironmental history of the Bol'shoy Lyakhovsky Island, New Siberian Archipelago, Arctic Siberia. *Boreas* (submitted).
- Arkhangelov, A. A., Mikhalev, D. V. and Nikolaev, V. I. (1996). About early epochs of permafrost formation in northern Yakutia and age of ancient relicts of underground glaciation. In: Velichko, A. A., Arkhangelov, A. A., Borisova, O. K., Gribchenko, Yu. N., Drenova, A. N., Zelikson, E. M., Kurenkova, E. N., Mikhalev, D. V., Nikolaev, V. I., Novenko, E. Yu. and Timireva, S. A. (eds.): *Razvitie oblasti mnogoletnei merzloty i periglyatsial'noi zony Severnoi Evrazii i usloviya rasseleniya drevnego cheloveka*. RAS Institute of Geography, Moscow, pp. 102-109 (in Russian).
- Bunge, A. A. (1887). Bericht ueber den ferneren Gang der Expedition. Reise nach den Neusibirischen Inseln. Aufenthalt auf der Grossen Ljachof-Insel. In: Schrenk, L. V. & Maximovicz, C. J. (eds.): *Expedition zu den Neusibirischen Inseln und dem Jana-Lande (1885), Beitrage zur Kenntnis des russischen Reiches und der angrenzenden Laender* Vol. III, pp. 231-284.
- Chersky, I.D. (1891). The description of the collection of post-Tertiary mammals, collected by New Siberian expedition of 1885-86, *Zapiski Imper. Akademii Nauk (Prilozhenie k LXV tomu)* 65/1, 707 pp. (In Russian).
- Decisions of Interdepartmental Stratigraphic Conference on the Quaternary of the Eastern USSR. Magadan, 1982. USSR Academy of Sciences, Far-Eastern Branch, North-Eastern Complex Research Institute, Magadan, USSR, 29-69 (in Russian).
- Dereviagin, A., Siegert, C., Troshin, E. and Simonov, E. (1997). Permafrost Landscapes and Geocryology of Cape Sabler. *Reports on Polar Research* 237: 89-97.
- Gavrilov, A.V., Romanovsky, N.N., Romanovsky, V.E., Hubberten, H.-W. and Tumskey, V.E. (2003). Reconstruction of Ice Complex remnants on the Eastern Siberian Arctic shelf. *Permafrost and Periglacial Processes* 14: 187-198.
- Gravis, G.F. (1978). Cyclicity of thermokarst at the coastal lowlands during the late Pleistocene and Holocene. In: *Publications of the 3rd International Permafrost Conference, July 10-13 1978, Edmonton, Alberta, Canada Volume 1*, pp. 283-287.
- Gilichinsky, D. A., Nolte, E., Basilyan, A.E., Beer, J., Blinov, A., Lazarev, V., Kholodov, A., Meyer, H., Nikolsky, P.A., Schirrmeister, L. and Tumskey, V. (2007). Dating of syngenetic ice wedges in permafrost with  $^{36}\text{Cl}$  and  $^{10}\text{Be}$ , *Quaternary Science Reviews* 26: 1547-1556.
- Igarashi, Y., Fukuda, M., Nagaoka, D. and Saljo, K. (1995). Vegetation and climate during accumulating period of yedoma, inferred from pollen records. In: Takahashi, K., Osawa, A. & Kanazawa, Y. (eds.): *Proceedings of the third symposium on the joint Siberian permafrost studies between Japan and Russia in 1994*. Hokkaido University, Tsukuba, pp. 139-146.
- Ilyashuk, B.P. Andreev, A.A. Bobrov, A.A. Tumskey V.E. and E.A. Ilyashuk, 2006. Interglacial history of a palaeo-lake deposit and regional environment: a multi-proxy study of a permafrost deposit from Bol'shoy Lyakhovsky Island, Arctic Siberia. *Journal of Paleolimnology*, 35 (4): 855-872

- Ivanenko, G.V. (1998). State geological map of Russian Federation, New Siberian Islands, 1:100.000 Map of Quaternary formations. Ministry of Natural Resources of the Russian Federation
- Ivanov O.A. (1970). The main stages of North-East coastal lowlands development in the Cenozoic. In: Severnyi Ledovityi okean I ego poberezhya v kaynozoe, Gidrometeoizdat, Leningrad, pp. 474-479 (in Russian).
- Ivanov, O.A. (1972). Stratigraphy and correlation of Neogene and Quaternary deposits of subarctic plains in Eastern Yakutia. In: Problems of the study of Quaternary Period. Nauka, Moscow, pp. 202-211 (in Russian).
- Kayalainen, V.I. and Kulakov, Yu.N. (1966). To the questions of Paleogeography of the Yana-Indigirka coastal lowland during the Neogene-Quaternary period. In: Quaternary Period in Siberia. Nauka, Moscow, pp. 274-283 (in Russian).
- Kienast, F., Tarasov, P., Schirrmeyer, L., Grosse, G. and Andreev, A.A. (2007). Continental climate in the East Siberian Arctic during the last interglacial: implications from palaeobotanical records, *Global and Planetary Change* 60(3/4): 535-562
- Konishchev, V.N. and Kolesnikov, S.F. (1981). Specifics of structure and composition of late Cenozoic deposits in the section of Oyogossky Yar. In: Problems of Cryolithology, Vol. IX. Moscow State University Publishing, pp. 107-117 (in Russian).
- Kos'ko, M.K., Lopatin, B.G. and Gamelin, V. G. (1990). Major geological features of the islands of the East Siberian and the Chukchi Seas and the northern coast of Chukotka. *Mar. Geol.* 93, 349-367.
- Krasny, L. I. (ed.)(1981). *Geology of Yakutian ASSR*. Nedra, Moscow, 300 pp. (in Russian).
- Kunitsky, V.V. (1996). Chemical content of ice wedges of the Ice complex. In: Development of the Cryolithozone of Eurasia during the upper Cenozoic. RAS, Permafrost Institute Yakutsk, pp. 93-117 (in Russian).
- Kunitsky, V.V. (1998). Ice Complex and cryoplanation terraces of Bol'shoy Lyakhovsky Island. In: Kamensky, R.M., Kunitsky, V.V., Olovin, B.A. and Shepelev, V.V. (eds.): Problems of Geocryology. Collected papers. RAS, Permafrost Institute Yakutsk, pp. 210.
- Kunitsky, V.V. and Grigoriev, M.N. (2000). Boulders and cobble roundstones near the Svyatoy Nose Cape and on Big Lyakhovsky Island. In: Fourth QUEEN Workshop, Lund, Sweden, 7-10 April 2000. Abstracts, pp. 62.
- Kuznetsova, T., Schirrmeyer, L. and Noskova, N. G. (2004). "Mammoth Fauna" collections of the Laptev Sea Region in museums and institutes of the Russian Academy of Science. In: Kalabin G.V. et al. (eds.): Problems of regional geology: a museum perspective. Proceedings of the scientific-practical conference devoted to 150th anniversary of Academician M.V. Pavlov (1854-1938). Moskva, Akropol 1030, pp. 155-160 (in Russian).
- Lopatin, V.G. (ed.) (1998). State geological map of Russian Federation, New Siberian Islands, 1:100.000 Map of Pre-Quaternary formations. Ministry of Natural Resources of Russian Federation.
- Moriizumi, J., Lida, T. and M. Fukuda (1995). Radiocarbon dating of methane obtained from air in the ice complex (Edoma), in Arctic coast area of east Siberia. In: Proceedings of the Third symposium on the joint Siberian permafrost studies between Japan and Russia in 1994. Sapporo, Hokkaido Univ. Press, pp. 14-21.
- Meyer, H., Dereviagin, A. Yu., Siegert, C., Schirrmeyer, L. and Hubberten, H.-W. (2002a). Paleoclimate reconstruction on Big Lyakhovsky Island, North Siberia - Hydrogen and oxygen isotopes in ice wedges, *Permafrost and periglacial processes* 13: 91-105.
- Meyer, H., Dereviagin, A., Siegert, Ch. and Hubberten, H.-W. (2002b). Paleoclimate studies on Bykovsky Peninsula, North Siberia - hydrogen and oxygen isotopes in ground ice. *Polarforschung* 70: 37-51.
- Meyer, H., Dereviagin, A. and Syromyatnikov, I. (2000). Ground ice studies. *Reports on Polar Research* 315: 155-163.
- Nagaoka, D. (1994). Properties of Ice Complex deposits in eastern Siberia. In Inoue, G. (ed.): Proceedings of the Second Symposium on the Joint Siberian Permafrost Studies between Japan and Russia in 1993: 14-18. Hokkaido University, Isebu.

- Nagaoka, D., Saijo, K. & M.Fukuda (1995). Sedimental environment of the Edoma in high Arctic eastern Siberia. In: Proceedings of the Third symposium on the joint Siberian permafrost studies between Japan and Russia in 1994. Sapporo, Hokkaido Univ. Press, pp. 8-13.
- Nikolsky, P.A., Basilyan, A. E. & Simakova, A.N. (1999). New stratigraphical data of upper Cenozoic deposits in the area of Cape Svyatoy Nos (coast of the Laptev Sea). In: Landscape-climate change, fauna and man during Late Pleistocene and Holocene. Moscow, IGRAN, pp. 51-60 (in Russian).
- Nikolsky, P.A. & Basilyan, A. E. (2004). The main Quaternary cross section of the Yana-Indigirka lowland. Late Pleistocene and Holocene of Siberian Arctic: Paleogeography, Geology and Archeology. GEOS, Moscow, pp. 27-34, (in Russian).
- Pirumova, L.G. (1968). Diatoms in Quaternary Sediments of Northern Yana-Indigirka Lowland and Bol'shoy Lyakhovsky Island. In: Fossil diatoms of the USSR. Nauka, Moscow, pp. 80-83 (in Russian).
- Romanovsky, N. N. (1958a). New data about Quaternary deposits structure on the Bol'shoy Lyakhovsky Island (Novosibirskie Islands). Nauchnye doklady vysshei shkoly. Seriya geologogeograficheskaya 2: 243-248 (in Russian).
- Romanovsky, N. N. (1958b). Paleogeographical conditions of formation of the Quaternary deposits on Bol'shoy Lyakhovsky Island (Novosibirskie Islands). In: Bogorov, V. G. (ed.): Voprosy fizicheskoi geografii polyarnykh stran Vol. I, pp. 80-88. Moscow State University, Moscow (in Russian).
- Romanovsky, N. N. (1958c). Permafrost structures in Quaternary deposits. Nauchnye doklady vysshei shkoly. Seriya geologogeograficheskaya 3: 185-189 (in Russian).
- Romanovsky, N.N. (1961a). Erosional-thermokarst kettles in the north of the coastal lowland of Yakutia and Novosibirsky Islands. Permafrost studies 1: 124-144 (in Russian).
- Romanovsky, N.N. (1961b). About the construction of Yana-Indigirka Coastal Lowland and its forming conditions. Permafrost studies 2: 129-139 (in Russian).
- Romanovskii, N.N., Gavrilov, A.V., Tumskoy, V.E., Kholodov, A.L., Siegert, C., Hubberten, H.-W., and Sher, A.V.(2000). Environmental evolution in the Laptev Sea region during Late Pleistocene and Holocene., *Polarforschung*, 68 (Jahrgang 1998), 237-245.
- Schirrmeister, L., Grosse, G., Kunitsky, V., Meyer, H., Deriviyagin, A. and Kusnetzova, T. (2003). Permafrost, periglacial and paleo-environmental studies on New Siberian Islands. *Reports on Polar and Marine Research* 466: 195-341.
- Schirrmeister L., Kunitsky V., Grosse V., Meyer H., Kuznetsova T., Kuzmina S., Tumskoy V., Derevyagin A., Akhmadeeva I. and Syromyatnikov I. (2000). Quaternary deposits of Bol'shoy Lyakhovsky Island. *Reports on Polar Research Bremerhaven* 354: 113-168.
- Schirrmeister, L., Oezen, D. and Geyh, M. A. (2002). <sup>230</sup>Th/U dating of frozen peat, Bol'shoy Lyakhovsky Island (North Siberia). *Quaternary Research* 57: 253-258.
- Toll von, E. V. (1897). Fossil glaciers of New Siberian Islands and their relation to mammoth corpses and Glaciation Period. *Zapiski Imperatorskogo Russkogo Geograficheskogo obshestva po obshei geografii* 32: 1-137 (in Russian).
- Tormirdiario, S.V. (1970). Eolian-cryogene origin of Yedoma-Complex deposits of North-east USSR. In: Abstracts of the allunion permafrost conference; Moscow State University, Moscow, pp. 106-107 (in Russian).
- Tomirdiario, S.V. (1980). Loess-ice formation of east Siberia during Late Pleistocene and Holocene. Nauka, Moscow, 184 pp. (in Russian).
- Tumskoy, V.E., Nikolsky, P.A., Basilyan, A.E., Kuznetsova, T.V. and Gavrilov A.V. (2000). Evolution of perennially frozen deposits on the coast of the Dimitrii Laptev strait in the late Cenozoic. In: Rhythms of natural processes in the Earth Cryosphere: Abstracts. Pushchino, pp. 272-273.
- Tumskoy, V.E. and Basilyan, A.E. (2006). Key section of Quaternary deposits on Bol'shoy Lyakhovsky Island. In: Correlation of Pleistocene Events in the Russian North (COPERN): Abstracts, December 4-6 2006, St. Petersburg, pp. 106-107 (in Russian).
- Basilyan, A.E., Nikolsky, P.A., Tumskoy, V.E. and Anisimov, M.A. (2006). Stratigraphy of Quaternary deposits on the New Siberian Islands and in the northern Yana-Indigirka lowland. In: Correlation of Pleistocene Events in the Russian North (COPERN): Abstracts, December 4-6 2006, St. Petersburg, pp. 16-17 (in Russian).

Vereshagin, V.N. (ed.) (1982): Stratigraphical dictionary USSR. Palaeogene, Neogene, Quaternary system.- Moscow, Nauka, 128 p. (in Russian).

Yershov, Y.D. (ed.) (1989). Krilotologiya SSSR – Vostochnaya Sibir' I Dal'nii Vostok (Cryolithology of the USSR – eastern Siberia and Far East) M. Nedra, Moscow : pp. 515 (in Russian).

## **5. Modern environmental dynamics – Studies along the Dmitrii Laptev Strait**

### **5.1 Scientific background and objectives**

*Sebastian Wetterich and Frank Kienast*

The studies and investigations presented in chapter 5 deal with the state and biological inventory of modern tundra landscapes along the Dmitrii Laptev Strait. The aim of this work is to estimate the interactions between single components (relief, permafrost, polygon ponds, vegetation) in order to understand landscape variability and dynamics under modern climate conditions.

The second topic of the fieldwork on present-day environments was to obtain modern analogue data and reference material of several bioindicators such as plants, pollen, diatoms, chironomids, rhizopods and ostracods, which were already and are planned to be used in palaeo-environmental applications based on the study of Quaternary permafrost deposits (see chapter 4).

Our intended study of recent environmental conditions in Arctic polygon wetlands aims at collecting modern reference data necessary for understanding polygon dynamics and their climate-driven changes in the Quaternary past as well as in the future.

### **5.2 Limnological studies in the Dmitrii Laptev Strait region**

*Sebastian Wetterich and Lutz Schirrmeister*

#### **Introduction**

Polygonal tundra landscapes are characteristic features of the Northeast Siberian permafrost zone. Their formation is caused by ice wedge growth and lead to typical polygonal pattern (Figure 5.2-1). Depending on their position in the relief and the stage of development, polygons are often occupied by shallow waters, so-called polygon ponds. Frozen sediments of polygons are already used in late Quaternary palaeoenvironmental reconstructions (e.g. Schirrmeister et al., 2002a, b, 2003; Wetterich et al., 2005, 2008), but modern reference data on polygon development, pond hydrology and flora and fauna are still rare.

The main idea of our limnological fieldwork in summer 2007 in the Dmitrii Laptev Strait region was the record and monitoring of abiotic parameters such as climate conditions, temperature fluctuations, vegetation, ionic and stable isotope composition in the ponds in relation to bioindicators such as pollen, diatoms, chironomids, rhizopods and ostracods. The investigation of the modern conditions in the ponds allows the quantification of influencing parameters, which control the modern occurrence of these indicator organisms. In future, results of the study can be useful for interpretations of fossil data from sediment cores and outcrops and also for quantitative palaeoenvironmental reconstructions of the region using several palaeo-bioindicators.



**Figure 5.2-1:** Polygonal patterned tundra landscape in the East Siberian lowlands with ponds and initial thermokarst lakes (Photograph during helicopter flight by Frank Kienast, Senckenberg Weimar)

### **Pond types and study sites**

The relief in the study region is characterised enormous thermokarst depressions (alases) which are bordered by Yedoma hills (up to 40 m a.s.l.). These hills represent unthawed remains of Late Pleistocene Ice Complex deposits. Other common geomorphological features are thermoerosional valleys (logs) and distinct river valleys.

To infer the influence of polygon development on the life conditions of indicator organisms, we sampled ponds according to different stages in several geomorphological units.

In July 2007, limnological investigations were performed in the southern part of Bol'shoy Lyakhovsky Island (73°N, 141°E) in 15 waters (Figure 5.2-2a).

The studied ponds are situated on the floodplain of the Zimov'e and Vankina Rivers, in alas bottom, on different slope levels connecting alases and Yedoma hills and on the tops of Yedoma hills. Ponds on river floodplains are of intrapolygonal genesis i.e. the waters occur in the low-centred polygons between the rim-covered ice wedges (Figure 5-3a). In alases and on the top and on the slope of Yedoma hills, the ponds are located interpolygonal, i.e. between high-centred polygons in small scale depressions over the thawed ice wedges (Figure 5.2-3b, c).

The second study area was located at the coast south of the Dmitrii-Laptev-Strait at the location Oyogos Yar (72°N, 143°E) (Figure 5.2-2b). In August 2007, 16 lakes were investigated in this region which is also mainly structured by the above described geomorphological combination of alas depression and Yedoma hills. The sampled ponds in the alas depression and on Yedoma slopes and tops belong to the above described interpolygonal type. (Figure 5.2-3d-f). Additionally, we sampled the margin of one thermokarst lake and one thermoerosion valley (log) with slowly floating water.

In September two ponds and one lake at the bottom of a mountainous valley near Tiksi were sampled.

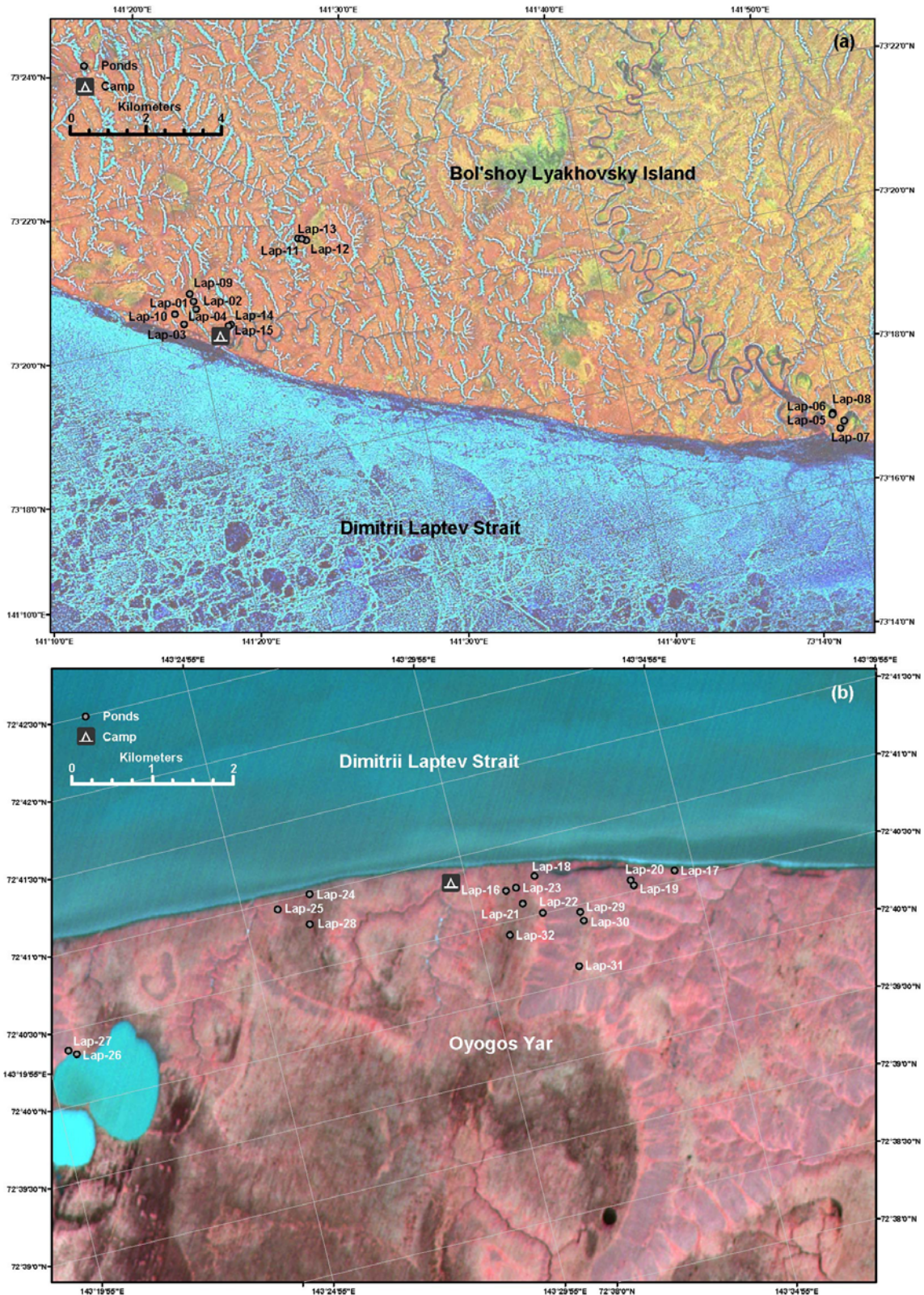


**Figure 5.2-2:** Location of the sampled polygon ponds (a) on Bol'shoy Lyakhovsky Island and (b) on Oyogos Yar. Map compiled by H. Lantuit, AWI Potsdam using satellite images: (a) LANDSAT 7 ETM+ 29.06.2001 and (b) SPOT 24.07.2007.



**Figure 5.2-3a-f:** Different types of polygon ponds on Bol'shoy Lyakhovsky Island and on Oyogos Yar.

### Material and methods

Investigations on properties of water chemistry and physics in the waters were undertaken in order to describe the recent life conditions for organisms. Our investigations included the estimation of water and size. We quantified pH, electrical conductivity (EC) and temperature using a WTW pocket meter. Still in the field, the determination of oxygen concentrations, total hardness, alkalinity and acidity was performed on means of titrimetric test kits (Viscolor).

For hydrochemical analyses in lab the pond water was sampled above the sediment surface from each site. Samples for cation analyses (15 ml) were acidified with 200  $\mu$ l  $\text{HNO}_3$ , whereas samples for anion analysis and residue samples were cool stored. Before conservation, samples for cation and anion analyses were filtered by a cellulose-acetate filtration set (pore size 0.45  $\mu$ m). Additionally, precipitation and pond water samples for  $\delta^{18}\text{O}$  and  $\delta\text{D}$  isotope analyses (30 ml) were preserved without any conservation.

Surface sediments of the ponds were sampled for sedimentological and botanical, zoological and paleontological analyses at the centre of the ponds. For these purposes studies on pollen, diatoms, chironomids, rhizopods and ostracods are planned. Live ostracods were caught in surface sediment samples

from different pond zones using an exhaustor system (Viehberg, 2002) and preserved in 70 % alcohol. Further taxonomical work using soft body characteristics will provide the first description of modern ostracod assemblages from the study area.

In July, one pond (Lap-01) on Bol'shoy Lyakhovsky Island on the Yedomas top, and in August one pond (Lap-16) on Oyogos Yar in an alas depression were selected as monitoring sites. Here, we performed continuous temperature measurements at three levels using temperature logger (MinidanTemp 0.1, ESYS). The loggers were placed in the centre of the pond at the pond bottom, below the water surface and in the air (Figure 5.2-4).

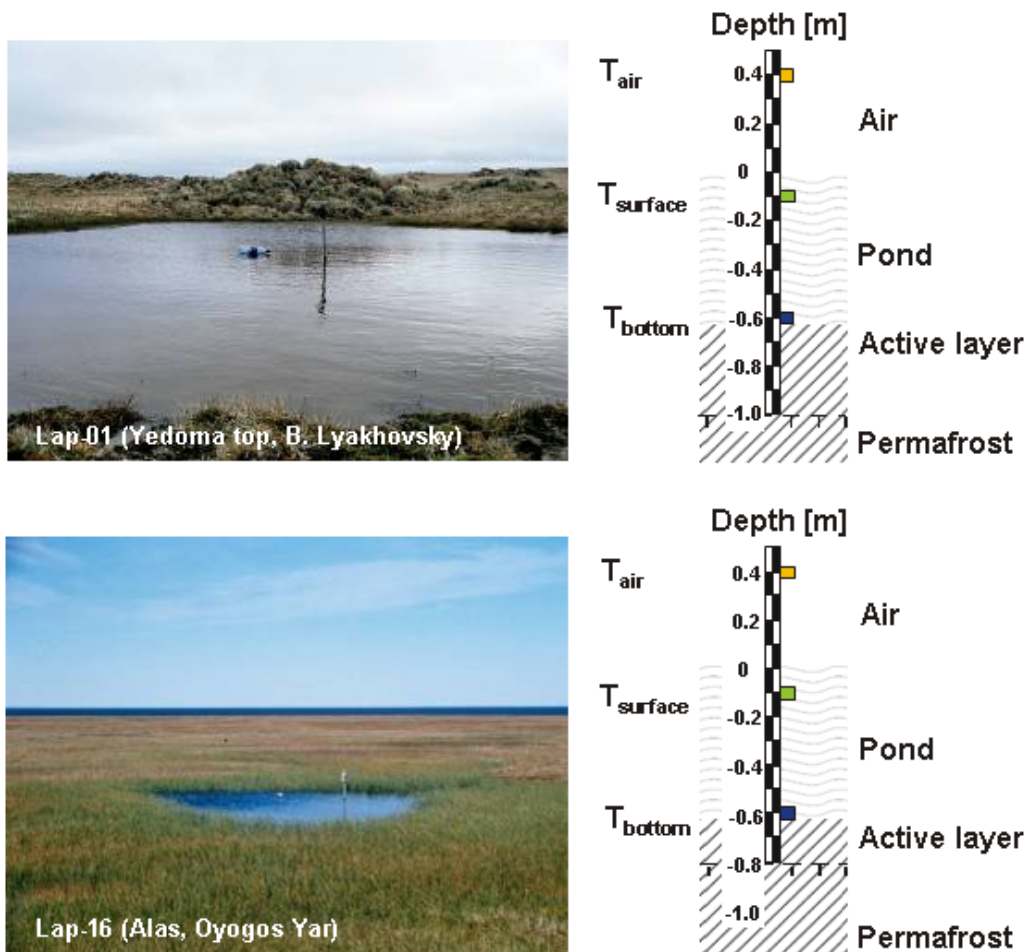


**Figure 5.2-4:** Temperature monitoring in two ponds; in July on Bol'shoy Lyakhovsky Island (Lap-01) and in August on Oyogos Yar (Lap-16). Three levels (above the pond sediments: in blue; below the water surface: in green; above the water surface: in yellow) were instrumented with temperature loggers in order to obtain daily and seasonal temperature amplitudes during the summer.

Additionally, every four/eight days repeated hydrochemical measurements and sampling of water, sediments and ostracods were performed in order to obtain seasonal dynamics of the studied parameters and proxy as well as their relationships among each other.

## Results

The studied polygon ponds in both study regions belong to the interpolygonal type according to their location in alas depressions, and Yedoma slopes and tops (Chapter 6.4-1, 6.4-2). The size of the polygon ponds reaches from 2 x 5 m up to 20 x 100 m whereas the shape often delineates the position of the thawing underlying ice wedge system (Figure 5.2-3). The observed intrapolygon ponds on floodplains extend from 5 x 7 m to 19 x 19 m and represent water filled low centre polygons (Figure 5.2-3). The water depth in such waters is low and do not exceed 0.7 m.

The pond substrate is mostly represented by silty or sandy material and rich in more or less decomposed plant detritus. The composition of mineral and organic components results in a general muddy substrate. Freshly flooded parts are underlain by tundra soil. The studied ponds are mostly covered by submerge mosses and/or marsh plants. Genuine water plants are generally lacking. Most abundant vegetation is composed of *Arctophila*, *Eriophorum* and *Arctagrostis* species at the pond margins on Yedoma sites, and *Carex* sedges, *Eriophorum* species and *Sphagnum* moss at ponds in alas depressions (for details see Chapter 5.3).

Results of the finger-print hydrochemistry during the fieldwork are presented in Figure 5.2-5 and in Chapter 6.4-3. In general, ponds studied on B. Lyakhovsky Island are characterised by neutral to slightly alkaline pH (pH 6.5 to 8.7;  $\text{pH}_{\text{mean}} = 7.7$ ) and higher EC (48 to 245  $\mu\text{S}/\text{cm}$ ;  $\text{EC}_{\text{mean}} = 148 \mu\text{S}/\text{cm}$ ) as compared to ponds on Oyogos Yar, where neutral to slightly acidic (pH 6 to 7;  $\text{pH}_{\text{mean}} = 6.5$ ) waters with very low EC (17 to 175  $\mu\text{S}/\text{cm}$ ;  $\text{EC}_{\text{mean}} = 72 \mu\text{S}/\text{cm}$ ) occur (Figure 5.2-5a, b). Except of two outlier, the acidity (Figure 5.2-5c) of the waters varies mostly between 0.2 and 0.6 mmol/l in both regions and amounts to a mean value of  $\text{Aci}_{\text{mean}} = 0.4 \text{ mmol/l}$ . The alkalinity (Figure 5.2-5d) in ponds on Bol'shoy Lyakhovsky Island ranges from 0.4 to 2.3 mmol/l and shows general higher values ( $\text{Alk}_{\text{mean}} = 1.3 \text{ mmol/l}$ ) as compared to ponds on Oyogos Yar which ranges from 0.2 to 1.4 mmol/l ( $\text{Alk}_{\text{mean}} = 0.8 \text{ mmol/l}$ ).

Trends over the monitored period in July on Bol'shoy Lyakhovsky Island (Lap-01) and in August on Oyogos Yar (Lap-16) are obvious by increasing EC and alkalinity in Lap-01 (Figure 5.2-5b, d). These parameters remained unchanged in Lap-16. Acidity and pH do not show distinct gradients over the monitored periods in both regions. The observed increases in July are most likely caused by high evaporation during sunny days and no precipitation, which results in low P/E ratio. In contrast, the August was rainy that leads to higher P/E ratio and unchanged ionic concentrations in the ponds.

The temperature monitoring was performed in July on Bol'shoy Lyakhovsky Island in a 0.6 m deep interpolygon pond with a 0.4 m deep thawed zone below on Yedoma top (Lap-01) and in August on Oyogos Yar in a 0.65 m deep interpolygon pond with a 0.2 m deep thawed zone below in an alas depression. The data reflect the dependence of pond water temperatures from two main influences: air temperature and active layer depth below the ponds (Figure 5.2-6).

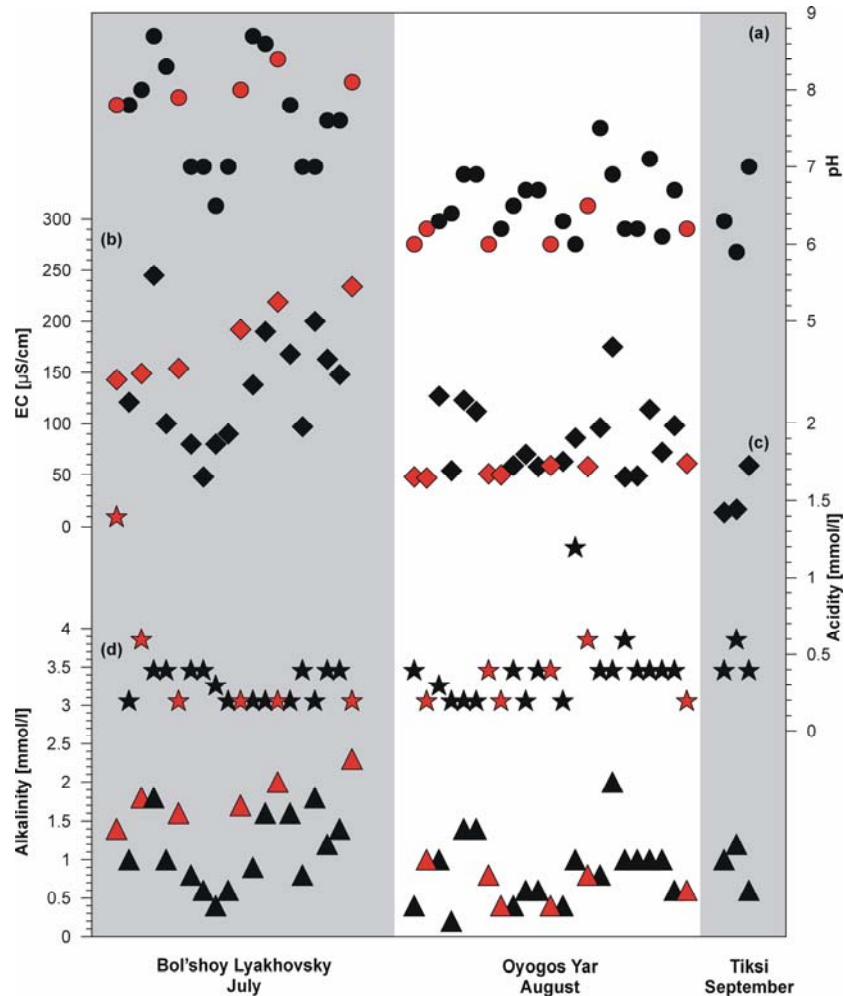


**Figure 5.2-5:** Ranges of hydrochemical parameters measured during the summer 2008 on Bol'shoy Lyakhovsky Island (July), on Oyogos Yar (August) and near Tiksi (September): (a) pH as dots; (b) electrical conductivity (EC) as diamonds; (c) acidity as stars and (d) alkalinity as triangles. The repeated measured monitoring ponds Lap-01 on Bol'shoy Lyakhovsky Island and Lap-16 on Oyogos Yar are marked by red symbols. One-time measured ponds are marked by black symbols.

Pond Lap-01 bottom ( $T_{\text{bottom}}$ ) and surface ( $T_{\text{surface}}$ ) water temperatures are co-varying in lower amplitude with air temperature variations and shows the same variations. Daily  $T_{\text{air}}$  amplitudes reach up to about 20 °C at the end of July with absolute  $T_{\text{air}}$  maxima of about 25 °C and  $T_{\text{air}}$  minima of about -1 °C at the beginning of July. The highest daily amplitude in  $T_{\text{surface}}$  and  $T_{\text{bottom}}$  amounts to about 9 °C in the beginning of July, whereas absolute maxima of about 17 °C occur at the end of July and minima of about 3 °C at the beginning (Figure 5.2-6).

The Lap-01 temperature record and its daily variations are mainly controlled by air temperature. The underlying permafrost table is here of minor importance due to its relatively high thickness.

In pond Lap-16 only  $T_{\text{surface}}$  co-varies with  $T_{\text{air}}$  and follows its daily variations, whereas  $T_{\text{bottom}}$  remains stable at about 3.6 °C, what is most likely controlled by an active layer depth of 0.2 m. Obviously, the close permafrost table affect  $T_{\text{bot-}}$

tom by cooling more than the warming influence of  $T_{\text{bottom}}$ . Daily  $T_{\text{air}}$  amplitudes reach up to about 23 °C at the middle of August with absolute  $T_{\text{air}}$  maxima of about 28 °C and  $T_{\text{air}}$  minima of about -1 °C at the end of August. The highest daily amplitude in  $T_{\text{surface}}$  amounts to about 17 °C in the end of August with absolute maxima of about 17 °C and minima of about 0 °C (Figure 5.2-6).

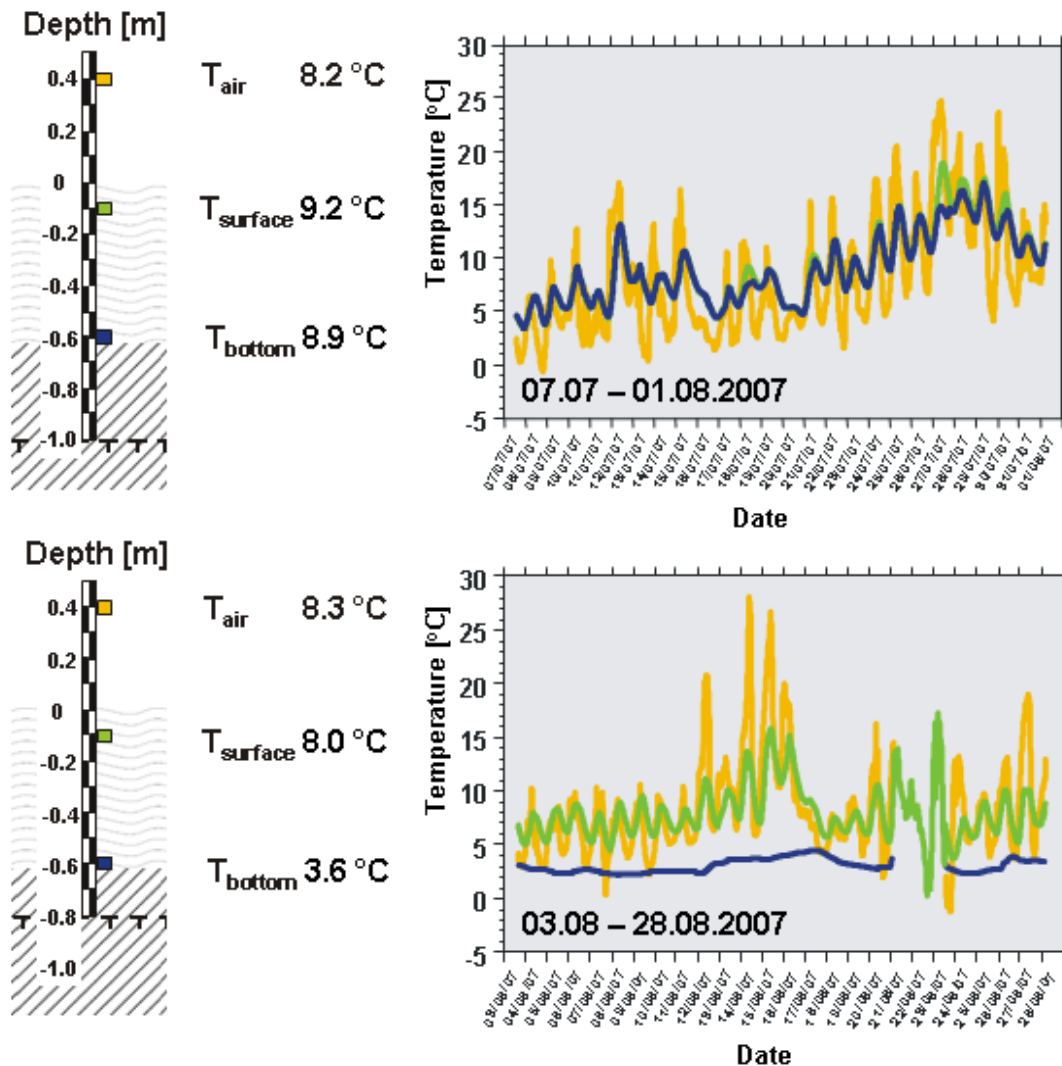


**Figure 5.2-6:** Daily temperature variations and means in two ponds; in July on B. Lyakhovsky Island (Lap-01) and in August on Oyogos Yar (Lap-16). Three levels are figured out ( $T_{\text{bottom}}$  above the pond sediments: in blue;  $T_{\text{surface}}$  below the water surface: in green;  $T_{\text{air}}$  above the water surface: in yellow).

## Outlook

Pollen, diatoms, chironomids, rhizopods and ostracods will be investigated to illuminate their relationship to environmental factors such as temperature, pH and conductivity. This information will later be applied to fossil assemblages, obtained from sediment cores and permafrost deposits, in order to infer quantitative environmental changes via organism-environment transfer-functions.

In laboratory, water samples will be analysed for element content by means of an ICP-OES and anion content by Ion Chromatography. Furthermore, analyses

of  $\delta^{18}\text{O}$  and  $\delta\text{D}$  isotopes on water and precipitation samples will be performed in order to compare these data with isotope values in calcareous ostracod valves. The understanding of the recent relationship between isotope ratios in waters and in ostracod valves will lead to an interpretation tool for palaeoenvironmental information preserved in fossil ostracods. For the same purpose trace element analyses (e.g. Ca, Mg, Sr) in waters and ostracod valves will be undertaken.

On surface sediment samples analyses of nitrogen, organic and total carbon contents by CN-Analyzer as well as grain-size distribution by laser granulometry will be carried out in order to characterize the sedimentological setting of the investigated ponds.



### 5.3 Modern vegetation in the coastal lowlands of Oyogos Yar

*Frank Kienast*

#### Introduction

The present is the key to the past – this is the basic principle in Quaternary palaeo-ecology. For the interpretation of fossil plant species spectra expected to be obtained from sampled Quaternary permafrost sequences along both sides of the Dmitrii Laptev Strait (see chapter 4), it is therefore necessary to record the modern vegetation of the study area in correlation to its environment.

The modern arctic tundra vegetation is suggested to be without analogue during the Quaternary in the ice-free regions of NE-Siberia and Alaska (Beringia). The main reason for that non-analogue situation is regarded the sustained paludification of the Siberian coastal lowlands occurring in the course of the Holocene as result of extensive thermal degradation of the ice rich permafrost and due to increasing oceanic climate influence after the marine transgression (Kienast et al., 2008, Romanovskii et al., 2000). Owing to the impermeability of permafrost and due to a lacking drainage system in the coastal lowlands, the paludification is additionally strengthened resulting in the formation of extensive wetlands in the Far North.

Aim of the conducted vegetation studies was it to detect the vegetational differentiation under the influence of gradient moisture in the high Arctic of Oyogos Yar. For this purpose, we recorded a vegetational profile along a 10 km transect from the top of a Yedoma ridge down to the adjacent Alas depression between 40 m to 10 m a.s.l. in August 2007 (Figure 5.3-1). In comparison with the results of vegetation studies at disjunctive relict occurrences of Pleistocene steppe vegetation in Central and Northeast Yakutia (Kienast & Gogoleva, 2007) and with subarctic vegetation in the Lena River Delta (Kienast & Tsherkasova, 2001), the results shall reveal the influence of oceanicity or, respectively, continentality on arctic vegetation. Collecting reference material for the Herbarium and the carpological collection was the other main focus of the field work during that expedition.

#### Study area

Oyogos Yar is the name of the mainland coast of the Dmitrii Laptev Strait between the mouth of the Kondrat'eva River in the east and Cape Svyatoy Nos in the west (Figure 4.1-1). This landscape is part of the Yana-Indigirka Lowland in Northeastern Siberia. Up to 500 m thick continuous permafrost and wide spread thermokarst characterize the coastal lowland. Oyogos Yar's topography is dominated by extremely flat plains covered by mires and shallow lakes.

There are two main topographic elements: low elevations, so-called Yedoma ridges, which represent the Pleistocene ground level and thermokarst depressions (alases), which formed as result of thermal degradation of the ice-rich permafrost that constitutes the Yedoma.



**Figure 5.3-1:** The transect - view from the alas bottom to the Yedoma hill

The study area is located about 8 km west of the Kondrat'eva River mouth (Figure 5.3-2 opposite to Cape Shalaurova, the eastern edge of Bol'shoy Lyakhovskiy Island. Its climate is characterized by cold winters, cool summers and low precipitation. Climate data from the weather station Cape Shalaurova, about 80 km north of the study site, reflect a mean July air temperature of 2.8 °C, a mean January air temperature of -32.2 °C and an annual precipitation of 253 mm (Rivas-Martínez, 1996-2004).

The study region is, according to the Circumpolar Arctic vegetation map (CAVM-Team, 2003), covered with sedge/grass, moss wetland (W1) mainly composed of *Carex aquatilis*, *Arctophila fulva*, *Dupontia* sp., and *Eriophorum* spp.. According to Aleksandrova (1980), Oyogos Yar belongs to the Sellyakh Inlet – Indigirka Delta district of the East Siberian province of the southern arctic tundra characterized by the dominance of *Alopecurus alpinus* and *Salix polaris*, the presence of *Carex ensifolia* ssp. *arctisibirica* and the absence of subarctic elements like *Betula nana* s.l.

The studied transect extends across the bottom of a large alas depression of about 10 km in diameter (5 to 10 m a.s.l.) and the adjacent slope and top areas of a Yedoma hill of up to 40 m height (Figures 5.3-1 and 5.3-2). The alas bottom dominantly consists of polygonal wetland tundra with a 0.5 to 1.0 m thick peat cover. The thermokarst depression is cut by the coast of the Dimitrii Laptev Strait in the north and additionally intersected by several thermo-erosional valleys that drain to the coast.

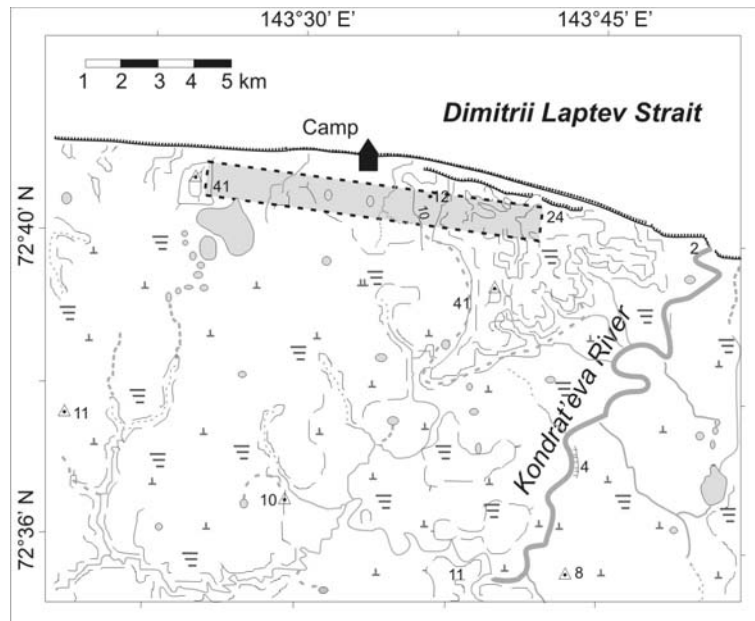


**Figure 5.3-2:** The study transect in the west of the Kondrat'eva River mouth

### Material and Methods

Resembling Kienast & Gogoleva (2007), the inventory of plant species at the investigated sites was recorded each on a minimal area of the respective community that contains the complete combination of characteristic species existing there and that is homogenous in environmental conditions and in combination and structure of plant spectra. Following variables were recorded:

- Time of the record
- Location
- Site description including substrate, moisture, exposition, aspect, declination, disturbances
- All plant species including phenology and cardinality (Artmaechtigkeit: semiquantitative, combined estimation of relative abundance and coverage of plant species occurring in a given area) according to Braun-Blanquet (1928)

Herbarium material was taken always in the case when an exact identification was not possible in the field. The herbarium specimens were then used for subsequent identification. Photos were taken from every record and sometimes additionally from characteristic plants.

If available, fruits and seeds were collected from all plant species. They were packed in small folded paper-bags, where they could respire and, if necessary, dry. All taken plant material was labelled and documented.

### Preliminary results

Within the recorded transect, six main landscape units can be distinguished with respect to their floristic composition: Yedoma with thermokarst mounds; mud boil; Yedoma slopes; small thermokarst ponds; thermo-erosional valleys; bottom of thermokarst depressions.

### *Thermokarst mounds on the Yedoma*

Thermokarst mounds are the best drained habitats in the study area (Figure 5.3-3). Their plant cover is mainly composed of *Salix polaris*, *Dryas punctata*, and *Alopecurus alpinus*. Other grasses such as *Festuca brachyphylla* and *Deschampsia borealis* and dicots like *Potentilla hyparctica*, *Oxyria digyna*, *Papaver polare* and *Valeriana subcapitata* also occur.



**Figure 5.3-3:** Thermokarst mounds on the Yedoma at Oyogos Yar

### *Mud boils*

Mud boils are the result of cryoturbation caused by frost pressing. In consequence, muddy soil flooded the ground.



**Figure 5.3-4:** Mud boil at the top of the Yedoma

The substrate is silty and well drained. Mud boils occur at places most exposed and windswept on the Yedoma. Plants occur here only between such mud spots; the coverage is consequently very low with 20 to 40 % (Figure 5.3-4). *Potentilla hyparctica*, *Salix polaris* and low growing grasses and rushes like *Festuca brachyphylla*, *Deschampsia borealis* and *Luzula confusa* are the main constituents of such habitats. In addition, herbs such as *Lloydia serotina*, *Cardamine bellidifolia*, *Androsace triflora*, and *Tephroseris atropurpurea* occur in lower abundances. This vegetation is similar in composition to cryptogam, herb barren (B1) or to the gramioid tundra (G1), described in the Circumpolar Arctic vegetation map (CAVM-Team 2003).

#### *Yedoma slopes*

At Yedoma slopes, the coverage is in general > 80%. In the upper parts of slopes in SW exposition, *Dryas punctata* is one of the main constituents.



**Figure 5.3-5:** Lower part of a Yedoma slope with dominating *Arctagrostis latifolia*. In the background, a thermo-erosional valley with reddish spectral signature (here: dark) is visible

*Salix polaris* and several grass species (*Alopecurus alpinus*, *Deschampsia borealis*, *Festuca brachyphylla*) and *Luzula confusa* are characteristic of Yedoma slopes. In lower parts of the slopes, where it is less drained and consequently moister, *Arctagrostis latifolia*, *Petasites frigidus*, several saxifrages (*S. nelsoniana*, *S. cernua*, *S. hieracifolia*) and other herbs (*Gastrolychnis apetala*, *Tephroseris atropurpurea*, *Ranunculus* spp.) are typical (Figure 5.3-5).

#### *Small thermokarst ponds*

In small depressions on the Yedoma, ponds with *Pleuropogon sabinei* and on the shore, *Arctophila fulva*, *Arctagrostis latifolia*, *Dupontia fischeri*, *Eriophorum polystachion* and *E. scheuchzeri* occur (Figures 5.3-6 and 5.3-7). Interestingly, genuine aquatics were widely lacking. Only *Hippuris vulgaris* was solitarily

found in a sterile form. *Caltha palustris* and the white-flowered *Ranunculus pallasii* grew emerged in some ponds of the Alas depressions.



**Figure 5.3-6:** Thermokarst pond on the degrading Yedoma



**Figure 5.3-7:** *Pleuropogon sabinei* growing emerged in the thermokarst ponds

#### *Thermo-erosional valleys*

Thermo-erosional valleys are permanently supplied by running water. They are characteristically coloured and recognizable from far distant (Figure 5.3-4). Dark green and reddish signatures are mainly caused by different *Eriophorum* species: green with diffuse white spots – *E. scheuchzeri*, reddish – *E. polystachion* (Figures 5.3-5 and 5.3-8). Other plants of thermo-erosional valleys are *Petasites frigidus* and several crowfoot and grass species (*Dupontia fischeri*, *Calmagrostis holmii*).



**Figure 5.3-8:** Thermo-erosional valley intersecting the Yedoma of Oyogos Yar. Main constituent is here *Eriophorum scheuchzeri* causing a spotty green – white spectral signature.

#### *Bottom of thermokarst depressions*

The bottom of thermokarst depressions is, in contrast to thermo-erosional valleys, characterized by stagnant water. Alases are covered mainly with sedges (*Carex ensifolia* ssp. *arctisibirica*) and cotton grass (*Eriophorum polystachion*).



**Figure 5.3-9:** Bottom of a thermokarst depression with a water table above the ground. The polygonal surface patterns are visually strengthened by vegetational differentiation (compare Figure 5.3-10).

The vascular plant diversity is here the lowest in the study area. *Sphagnum* moss is widely present, causing irregular pale green spots in polygonal wetlands where the surface of water is above the ground (Figure 5.3-9).

At sites outside water bodies, rushes (*Luzula nivalis*, *L. confusa*) cover large areas together with several grasses (*Dupontia fischeri*, *Calamagrostis holmii*, *Poa alpigena* and *Arctophila fulva*). The wettest places are almost exclusively occupied by *Eriophorum polystachion*, which produces reddish patterns on the ground indicating the water trenches between polygons (Figures 5.3-9 and 5.3-10).



**Figure 5.3-10:** The wettest places in high center polygonal wetland tundra are the inter-polygonal trenches. Here, *Eriophorum polystachion* is the main constituent, causing a reddish (here dark) pattern.

### Acknowledgements

I would like to thank Lutz Schirrmeister for his dedication and patience in preparing and conducting the expedition. Thanks to Alexander Derevyagin (“the Great Sasha”) and Viktor Kunitsky for their help in building up the camp and for drying and warming plant material, equipment and field workers in their tent. Many thanks to all participants, who accounted for a warm-hearted atmosphere under arctic conditions.

## 5.4 References

- Aleksandrova, V.D. (1980). *The Arctic and Antarctic: their division into geobotanical areas*. Cambridge University Press, Cambridge.
- Braun-Blanquet, J. (1928). *Pflanzensoziologie*, Springer, Berlin.
- CAVM-Team (2003). *Circumpolar Arctic vegetation map. Conservation of Arctic Flora and Fauna (CAFF) Map no. 1*. U.S. Fish and Wildlife Service, Anchorage, Alaska.
- Kienast, F., Tsherkasova, J. (2001). Comparative botanical recent-studies in the Lena River Delta, *Berichte zur Polarforschung* 388: 24-44.
- Kienast, F., Gogoleva, P. A. (2007). Vegetation studies in extremely continental regions of Yakutia, *Berichte zur Polarforschung* 550: 275-289.
- Kienast, F., Tarasov, P., Schirrmeyer, L., Grosse, G., and Andreev, A. (2008). Continental climate in the East Siberian Arctic during the last interglacial: implications from palaeobotanical records, *Global and Planetary Change* 60 (3/4): 535-562.
- Rivas-Martínez, S. (1996-2004). *Climate diagrams, worldwide bioclimatic classification system*. Phytosociological Research Center, Spain. Online database, <http://www.globalbioclimatics.org/plot/rumys-s.htm>.
- Romanovskii, N.N., Hubberten, H.W., Gavrilov, A.V., Tumskey, V.E., Tipenko, G.S., Grigoriev, M.N. and Siegert, C. (2000). Thermokarst and land-ocean interactions, Laptev sea region, Russia. *Permafrost and Periglacial Processes* 11 (2): 137-152.
- Schirrmeyer, L., Kunitsky, V. V., Grosse, G., Schwamborn, G., Andreev, A. A., Meyer, H., Kuznetsova, T., Bobrov, A., and Oezen, D. (2003). Late Quaternary history of the accumulation plain north of the Chekanovsky Ridge (Lena Delta, Russia) - a multidisciplinary approach, *Polar Geography*, 27(4): 277-319.
- Schirrmeyer, L., Siegert, C., Kuznetsova, T., Kuzmina, S., Andreev, A.A., Kienast, F., Meyer, H. and Bobrov, A.A. (2002b). Paleoenvironmental and paleoclimatic records from permafrost deposits in the Arctic region of Northern Siberia, *Quaternary International*: 89: 97-118.
- Schirrmeyer, L., Siegert, C., Kunitsky, V.V., Grootes, P.M. and Erlenkeuser, H. (2002a). Late Quaternary ice-rich permafrost sequences as an paleoenvironmental archive for the Laptev Sea Region in northern Siberia, *International Journal of Earth Sciences*: 91, 154-167.
- Viehberg, F.A. (2002). A new and simple method for qualitative sampling of meiobenthos-communities. *Limnologia* 32: 350-351.
- Wetterich, S., Schirrmeyer and L., Pietrzyński, E. (2005). Freshwater ostracodes in Quaternary permafrost deposits from the Siberian Arctic, *Journal of Paleolimnology* 34: 363-376.
- Wetterich S., Kuzmina, S., Andreev, A., Kienast, F., Meyer, H., Schirrmeyer, L., Kuznetsova and T., Sierralta, M. (2008). Palaeoenvironmental dynamics inferred from late Quaternary permafrost deposits on Kurungnakh Island (Lena Delta, Northeast Siberia, Russia). *Quaternary Science Reviews* (DOI:10.1016/j.quascirev.2008.04.007).



## 6. Appendices to the chapters 4 and 5

### 6.1 List of sediment samples - sedimentological and cryolithological sample characteristics

a.s.l. – above sea level; b.s. – below surface; Ice abs. – absolute ice content; ice grav. – gravimetric ice content; TI – texture ice samples (see chapter 6.2); green: samples for U/Th dating, yellow: samples for OSL dating

sample	sedimentology	cryolithology (cryostructure)	m a.s.l.	m b.s.	Ice, abs. [wt%]	Ice grav. [wt %]	remarks	TI
<b>L7-01; 73.33464° N; 141.32043°E (10.07.2007)</b>								
L7-01-01-S	grey-brown silty sand; alternating ice bands	ice band 1.5-2 cm thick; lens-like reticulated	1				lowest exposed horizon below Yukagirsky peat	X
L7-01-02-S	grey-brown silty sand; peat inclusions 2-2.5 cm	fine lens-like	1.4		62.8	168.9	10 cm below the peat base	X
L7-01-03-S	brown peat, weakly decomposed	ice rich	1.8				<i>Eriophorum, hypnum mosses, no sphagnum</i>	X
L7-01-04-S	brown peat weakly decomposed	ice rich	2.2		85.5	590.3		X
L7-01-05-S	brown peat weakly decomposed	ice rich	2.6					
L7-01-06-S	palaeo active layer (0.4-0.5 m thick); gravels 2-10 mm, light brown grey, cryoturbated	massive, single ice lenses < 1cm	2.8		19.3	23.9	sample from 20 cm above the Yukagirsky S. ice wedge	
L7-01-07-S	palaeo active layer; single gravels linear ordered, greyish brown, silty sand	massive	3		21.1	26.7	upper part of the active layer with enrichments of gravels	X
L7-01-08-S	Kuchchugui S., brown, fine non regularly layered, grass roots	massive, low ice content	3.1					
L7-01-09-S	Kuchchugui S., greyish brown, fine non regularly layered, grass roots	massive, low ice content	3.7		24.4	32.3	convolute bedding	
L7-01-10-S			1.7					
L7-01-11-S	brown peat weakly decomposed		2				U/Th dating	
L7-01-12-S			2.2					
L7-01-13-S	Yukagirsky S., peat inclusions, silty sandy, dark-brown grey, single gravels (5-10 mm); single plant remains;	ice bands; lens-like reticulated	2.1				profile below a peat lens; transition to the palaeo active	X
L7-01-14-S	Yukagirsky S.; peat inclusions, silty sandy, dark-brown grey, single gravels (5-10 mm); one large stone (7 x 5 cm); single plant remains	ice bands; lens-like reticulated	2.2					X
L7-01-15-S	Yukagirsky S., sandy, light-brown grey, weathered single gravels (5-10 mm)	ice bands (5-10 cm); lens-like reticulated	2.4		65.1	186.7		X
L7-01-16-S		ice rich	1.5					
L7-01-17-S	Moss peat, light brown, weakly decomposed	ice rich	1.7				U/Th dating	
L7-01-18-S		ice rich	1.8					
L7-01-19-S	Kuchchugui S., brown, fine non regularly layered, grass roots	massive, low ice content	3.1		24.9	33.1	OSL; $\gamma$ -Spectrometry	
L7-01-20-S			3.9		26.6	36.2		

sample	sedimentology	cryolithology (cryostructure)	m a.s.l.	m b.s.	Ice, abs. [wt%]	Ice grav. [wt %]	remarks	TI
<b>L7-03, 73.33525°N; 141.31648°E (12.07.2007)</b>								
L7-03-01-S	Yukagirsky Suite, grey brown, gravel	ice bands (1-2 cm), lens-like, transparent ice	0.5		36.2	56.7	Yukagirsky Suite without peat below Kuchchugui S.	X
L7-03-02-S	Yukagirsky S., brown patches sandy silty, no gravel,	fine lens-like	1					X
L7-03-03-S	Yukagirsky S., grey, no gravel, sandy silty	ice bands; lattice-like	1.4		51.1	104.7		X
L7-03-04-S	Yukagirsky S., sandy silty; brown	ice bands; lattice-like	2					X
L7-03-05-S	Yukagirsky S, sandy peat lenses; ; iron oxide impregnation	line lens-like reticulated	2.3		33.4	50.0		X
L7-03-06-S	Yukagirsky S., brown grey, sandy silty; iron oxide impregnation	fine lens-like; single ice lenses	3					X
L7-03-07-S	Yukagirsky S., grey brown; sandy silt; peat inclusions; single gravel and coarse sand	ice bands (0,5-1 cm); fine lens-like	3.4		45.8	84.6		X
<b>L7-05, 73.33874°N; 141.29704°E (14.07.2007)</b>								
L7-05-01-S	Yukagirsky Suite, gravels, grey-brown	coarse, lens-like reticulated	1.5		67.0	203.2		X
L7-05-02-S	greyish-brown, transition palaeo-active layer	Yukagirsky IC to Palaeo-active layer	1					X
L7-05-03-S	palaeo-active layer, brown, peat inclusion, gravels	lens-like, diagonal	2.1		54.0	117.2	lower part of the active layer	X
L7-05-04-S	autigenic clay, weathering crust, white, soft, 0.5 mm thick		2.5				Crust on a larger stone, small whirlpack bag	
L7-05-05-S	palaeo-active layer, cryoturbated, brown, single gravels (3-5 cm), sand	dotted	2.5		23.7	31.0	upper part of the active layer, flame structures	X
L7-05-06-S	yellowish, gravely, clayish	ice rich	1.5				Remnants of a weathering crust, up bent along the ice wedge contact	X
L7-05-07-S	Kuchchugui Suite, greyish-brown, non-regular fine layered, single gravels, vertical grass roots	massive	2.7					
L7-05-08-S		massive	3		25.6	34.3		
L7-05-09-S		single vertical ice veins	3.3					
L7-05-10-S		massive	3.5					X
L7-05-11-S		massive	3.8					
L7-05-12-S		massive	4		28.6	40.1		
L7-05-13-S		massive	4.2					
L7-05-14-S		massive	4.5					
L7-05-15-S		massive	4.8		25.8	34.8		

sample	sedimentology	cryolithology (cryostructure)	m a.s.l.	m b.s.	Ice, abs. [wt%]	Ice grav. [wt %]	remarks	TI
<b>L7-07; 73,33086°N; 141,34423°E (25/26.07.2007)</b>								
L7-07-01-S	grey-brown, many plant detritus, interbedded	fine lens bedded, single diagonal ice veins	2.5				in situ bone fragment, in horizontal position	X
L7-07-02-S	greyish-brown, plant detritus	Ice bands, fine lens	6				Subprofile L7-07-A	X
L7-07-03-S	sandy, light brown, grey, ripples, plant detritus	Ice bands, fine lens	5.4		36.0	56.3		X
L7-07-04-S	sandy, light brown, grey, ripples, plant detritus, small peat inclusion	fine lens	5					
L7-07-05-S	grey-brown, many plant detritus, interbedded	fine lens-like layered, single diagonal ice veins	4.7		53.0	113.0		
L7-07-06-S			4.5					X
L7-07-07-S	light brown, dry, sandy silt, non regular bedded, peat inclusions, plant remains		4		46.6	87.1		
L7-07-08-S	grey, silty sand, black spots, many plant detritus	fine lens	3.7					
L7-07-09-S	dark grey, silty sand, single plant remains	coarse lens like reticulated	3.3		53.8	116.7	Subprofile L7-07-B	X
L7-07-10-S	light brown, grey, sandy silt, plant detritus, vertical roots	diagonal and vertical ice lens	2.6					
L7-07-11-S			2		25.9	34.9		
<b>L7-08; 73,3492°N; 141,24007°E (15./25.07.2007)</b>								
L7-08-01-S	greenish, silty sand, taberal Yedoma Suite, peat lenses (5-10 cm) and peat layers	coarse net-like	4	8	20.9	26.4	Subprofile L7-08-A	X
L7-08-02-S	peat layer, moss peat, light brown, weakly decomposed	net-like	4.2	7.8			Subprofile L7-08-A, peat layer	
L7-08-03-S	peat inclusion, palaeo-sol	coarse, lens-like (1x5 cm)	4.5	7.5	31.7	46.4	Subprofile L7-08-A	
L7-08-04-S	silty sandy, taberal Yedoma S.	net-like, lens-like	4.8	7.2			Subprofile L7-08-A, directly below the peat horizon	X
L7-08-05-S	peat, light brown, peat stripes		5	7			Subprofile L7-08-A. transition to the basic peat	
L7-08-06-S	basic peat, dark brown peat inclusions in dark grey silty sand, wood fragments,	lens-like	5.2	6.8			Subprofile L7-08-A	
L7-08-07-S	dark grey, peaty, silty	fine lens-like reticulated	5.5	6.5	27.5	38.0	Subprofile L7-08-A, transition to lake deposits	
L7-08-08-S	clayish silt, grey, homogeneous	lattice-like, fine lenses	5.7	6.3			Subprofile L7-08-A	
L7-08-09-S	clayish silt, grey, homogeneous, single plant detritus layers light brown, up to 2 mm thick, 5-10 cm between single layers	lattice-like, fine lenses	5.9	6.1	22.6	29.2	Subprofile L7-08-A	

sample	sedimentology	cryolithology (cryostructure)	m a.s.l.	m b.s.	Ice, abs. [wt%]	Ice grav. [wt %]	remarks	TI
L7-08-10-S	clayish silt, dark-grey, homogeneous	lattice-like, fine lenses	6	6			Subprofile L7-08-B	
L7-08-11-S			6.4	5.6	29.6	42,1		
L7-08-12-S	clayish silt, dark-grey, homogeneous, brownish iron oxide impregnations 2-3 cm thick		6.8	5.2				
L7-08-13-S	clayish silt, dark-grey, homogeneous		7.2	4.8				
L7-08-14-S	clayish silt, dark grey, homogeneous, brownish iron oxide impregnations in cracks		7.5	4.5				
L7-08-15-S	clayish silt, grey, homogeneous, iron oxide impregnations as concentric circles	lattice-like, fine lenses	7.6	4.4	31.2	45,3	Subprofile L7-08-C	
L7-08-16-S	clayish silt, grey, homogeneous	lattice-like, fine lenses	7.9	4.1				
L7-08-17-S	clayish silt, brownish, homogeneous, iron oxide impregnation along ice lenses en	lattice-like, fine lenses	8.4	3.6				
L7-08-18-S	oxide impregnation along ice lenses en	lattice-like, fine lenses	8.7	3.3				X
L7-08-19-S	clayish silt, brown-grey, homogeneous, iron oxide impregnations in cracks	lattice-like, fine lenses, layered ice bands 1 cm thick	9.0	3	30.7	44,2		
L7-08-20-S	clayish silt, brown-grey, homogeneous	fine lenses	9.2	2.8				X
L7-08-21-S	sandy silt, light-grey	lens-like	9.6	2.2			Subprofile L7-08-D	X
L7-08-22-S	sandy silt, light-grey	ice bands, thin horizontal ice veins	10.0	1.8	27.2	37,4		
L7-08-23-S	peat lens, light brown, surrounded by grey sandy silt	lens-like	10.3	1.5				X
L7-08-24-S	sandy silt, grey	ice banded, diagonal lens	10.5	1.3	42.5	73,9		X
L7-08-25-S	sandy silt, grey	ice bands 0.5 cm thick, broken cryostructure	10.7	1.1				X
L7-08-26-S	grass roots horizon, grey, iron oxide impregnations in cracks	ice banded, diagonal lens	10.9	0.9				X
L7-08-27-S	peat lenses in a layer 5- 10 cm in diameter each, surrounded by grey sandy silt	ice bands, lens- like	11.1	0.7				X
L7-08-28-S	brown, humous, frozen lower part of the active layer	lattice like	11.5	0.3				X
L7-08-29-S	unfrozen active layer, brown, humus, living Eriophorum on the top, rooted		11.7	0.1				
L7-09-01-S	Peat inclusion in yellowish sandy silt							300 m west of the Zimov'e R. mouth

sample	sedimentology	cryolithology (cryostructure)	m a.s.l.	m b.s.	Ice, abs. [wt%]	Ice grav. [wt %]	remarks	TI
<b>L7-11; 73.31672°N; 141.42628°E (27.07.2007)</b>								
L7-11-01-S	grey-brown, sandy silt, thin light bands, fine bedded, single plant remains, black spots, shells	massive	3				Subprofile L7-11-A	
L7-11-02-S		massive	3.5		21.2	26.9		
L7-11-03-S		massive	4					
L7-11-04-S		layered, thin ice veins	4.5		21.8	27.9		
L7-11-05-S		lattice like, diagonal ice veins	5				Subprofile L7-11- A, contact to the ice wedge cast	
L7-11-06-S		layered, thin ice veins	3.7					
L7-11-07-S	plant detritus layer, bedded, sandy silty, small wood fragments, light brown, light grey	lens-like layered	4				Subprofile L7-11-B, ice wedge cast	
L7-11-08-S	sandy silt grey, peat inclusions wood fragments	lens-like layered	4.3		23.1	30.1		
L7-11-09-S	sandy silt grey, plant detritus fine bedded	lens-like layered, ice veins < 1mm thick, 5-7 cm long	4.6					
L7-11-10-S	interbedding, ripples, silty sand grey and plant detritus light brown	ice bands > 1mm and several cm long	4.8					
L7-11-11-S			5		28.0	38.9		
L7-11-12-S	interbedding, ripples, silty sand grey and plant detritus light brown, wood fragments	ice bands > 1mm and several cm long, fine diagonal ice veins	5.4					
<b>L7-12; 73.2876°N; 141.69351°E (18.07.2007)</b>								
L7-12-01-S	Kuchchugui S., greyish- brown, non-regular fine layered, many in situ (vertical) grass roots	single elongated ice lenses (<1mm thick, 2-5 cm long)	1					
L7-12-02-S			1.5		29.9	42.6		
L7-12-03-S			peat inclusion in Kuchchugui S.	1.9				Lemming nest or peat lens (?)
L7-12-04-S	Kuchchugui S., greyish- brown, non-regular fine layered, many in situ (vertical) grass roots, dark-grey black spots 2-5 mm in diameter	massive	2.4					
L7-12-05-S			2.9		30.7	44.4		
L7-12-06-S			3.4					
L7-12-07-S	Kuchchugui S., greyish- brown, non-regular fine layered, many in situ (vertical) grass roots, dark-grey black spots 2-5 mm in diameter	massive	2		29.7	42.3	OSL dating; γ- Spectrometry	
L7-12-08-S			2.9				OSL dating; γ- Spectrometry	
<b>L7-14, 73.2877°N; 141.69097°E (19.07.2007)</b>								
L7-14-01-S	taberal Kuchchugui S., grey, non-regular fine layered, single light stripes < 1mm, no plant roots, dark-grey spots 5 mm in diameter	massive	1.5				Subprofile L7-14-A	
L7-14-02-S			2		25.4	34.0		
L7-14-03-S			2.5					

sample	sedimentology	cryolithology (cryostructure)	m a.s.l.	m b.s.	Ice, abs. [wt%]	Ice grav. [wt %]	remarks	TI
L7-14-04-S	fine layered alternated bedding of brown plant detritus and grey silt, 10 cm peaty layer with wood fragments	massive	2.6				Subprofile L7-14-B	
L7-14-05-S	clayish silt, grey, peat inclusion, wood fragments	separate fine ice veins < 1mm thick	2.7		27.3	37.6		
L7-14-06-S	six layered alternated bedding of brown plant detritus and grey silt, every 5-10 mm thick	massive	2.9					
L7-14-07-S	fine layered clayish silt, with spotty peat inclusions and wood fragments	massive	3.1					
L7-14-08-S	layered alternated bedding brown plant detritus and grey silt, ripples, spotty peat inclusions 2-3 cm	massive	3.3					
L7-14-09-S	layered alternated bedding brown plant detritus and grey silt, ripples	massive	3.5		27.5	37.9		
L7-14-10-S	layered alternated bedding brown plant detritus and grey silt, ripples (1 cm in height, 2 cm between two ripples)	massive, ice in cracks may be recent formations caused by thermokarst mound destruction	3.7					
L7-14-11-S	layered alternated bedding brown plant detritus and grey silt, ripples (2-3 cm in height, 5 cm between two ripples)	massive	3.9					
L7-14-12-S	Strong disturbed lamination, fine-folded syndimentary slumping structures, shells, wood fragments	rare fine ice veins < 1mm thick	4.2		30.4	43.6		Subprofile L7-14-C
L7-14-13-S	alternated bedding of brown plant detritus and grey silt, internal folded		4.4					
L7-14-14-S	layered alternated bedding brown plant detritus and grey silt, laminated ripples, spotty peat inclusions, molluscs shells	separate fine ice veins < 1mm thick, parallel to the lamination	4.6					
L7-14-15-S	alternated bedding brown plant detritus and grey silt, laminated, ripples, single wood fragments;		4.9		30.8	44.5	Subprofile L7-14-C transition to ice-rich deposits	
L7-14-16-S	layered alternated bedding brown plant detritus and grey silt, laminated ripples, single wood fragments	massive	4.8				Subprofile L7-14-D; transition to ice-rich deposits	

sample	sedimentology	cryolithology (cryostructure)	m a.s.l.	m b.s.	Ice, abs. [wt%]	Ice grav. [wt %]	remarks	TI
L7-14-17-S	layered alternated bedding brown plant detritus and grey silt, non-regularly bedding	separate fine ice veins, ice rich	5		29.8	42.4	Subprofile L7-14-D	
L7-14-18-S	grey-brown. weakly bedded, silty sand, single wood fragments	ice rich, lens-like, fine	5.3					
L7-14-19-S	layered alternated bedding brown plant detritus and grey silt, non-regularly bedding	separate fine ice veins, ice rich	5.5		53.7	116.1		X
L7-14-20-S	grey silty sand .single plant remains	coarse lens-like reticulated, ice bands	6.2		68.8	220.4	Subprofile L7-14-E	X
L7-14-21-S			6.5					X
L7-14-22-S			6.8					X
L7-14-23-S	peat lens, light-brown, 7 cm, in grey silty sand matrix	peat lens: massive, sediment matrix: coarse lens-like reticulated	7.1				Subprofile L7-14-E	X
L7-14-24-S	peat lens 30 cm in diameter, light-brown, with grey silty sand inclusions	peat lens: massive, sediment matrix: coarse lens-like reticulated	7.6		53.8	116.3	Subprofile L7-14-E; base of the covering peat horizon	X
L7-14-24a-S	peat lens 30 cm in diameter, light-brown, with grey silty sand inclusions,	peat lens: massive, sediment matrix: coarse lens-like reticulated	7.6		53.8	116.3	Subprofile L7-14-E; U/Th dating	
L7-14-24b-S								
L7-14-24c-S								
L7-14-25-S	grey silty sand matrix	ice rich, ice bands	7.7				Subprofile L7-14-E;	X
L7-14-26	peat lens 30 cm in diameter, light-brown, with grey silty sandy inclusions, surrounded by grey silty sandy matrix	peat inclusion, massive; matrix coarse lens-like reticulated	8				Subprofile L7-14-E;	
L7-14-27	layered alternated bedding brown plant detritus and grey silt, ripples, peat inclusions 5-7 cm	massive	3		28.0	38.9	Subprofile L7-14-B: OSL dating	
L7-14-28	layered alternated bedding brown plant detritus and grey silt, ripples,	single ice veins (<1 mm)	5.2		32.6	48.3		
L7-14-29-S	peat inclusion, light-brown, matrix: grey-brown, silty sand	ice bands (2-5 cm thick)	12				Subprofile L7-14-F	
L7-14-30-S	grey, silty-sandy	ice bands (1-2 cm thick), coarse lens-like reticulated	11.2		64.8	184.2		X
L7-14-31-S	peat inclusion, light-brown, matrix: grey-brown, silty sand	vertical and horizontal ice veins	11.3		52.2	109.3		
L7-14-32-S	grey, silty sand, peat inclusion (5 cm in diameter)		11					X
L7-14-33-S	grey sandy silt, plant remains, non-bedded, yellowish spots	ice bands (white, 1 cm thick), coarse ice lenses (transparent)	10.6					X
L7-14-34-S	peat inclusion, light-brown, matrix: grey-brown, silty sand		10.2		63.6	174.9		X
L7-14-35-S	peat, dense, brown, wood remains, alternated bedding, fine-detritus, stronger decomposed		9.9		75.1	302.4		

sample	sedimentology	cryolithology (cryostructure)	m a.s.l.	m b.s.	Ice, abs. [wt%]	Ice grav. [wt %]	remarks	TI	
<b>L7-15, 73.28661°N; 141.7052°E (22.07.2007)</b>									
L7-15-01-T	brown, fine sandy silt, rare peat fragments (2-3 mm), black spot (1-2 mm), weakly bedded	horizontal, micro lens-like (to 2mm thick, 5-15 mm long, distance 5-10 cm)		2			Subprofile L7-15-A, looks like Kuchchugui S.	X	
L7-15-02-T				2.5	27.5	37.8		X	
L7-15-03-T				3.2					
L7-15-04-T	peat inclusions, brown, matrix: grey, silty sand	ice bands (1,5-2 cm thick, 5-10 cm distance)		3.7	34.9	53.7	Subprofile L7-15-A, upper "Bychchagy peat"	X	
L7-15-05-T				4					
L7-15-U/Th-1-T				4.5					
L7-15-06-T				5	45.8	84.4			
L7-15-07-T	grey, silty sand, non-bedded, single peat inclusions	ice bands (1,5-2 cm thick, 3-5 cm distance), lens-like, non-regular reticulated (lenses 1-2 mm thick, 5-10 cm distance)		5.1	40.8	69.0	Subprofile L7-15-A	X	
L7-15-08-T	grey, silty sand, non-bedded			5.8	51.4	105.8		X	
L7-15-09-T	brown, fine sand	ice bands (1-1,5 cm thick, 3-5 cm distance), micro-lens-like texture		6.5				X	
L7-15-10-T				7.1	41.9	72.1		X	
L7-15-11-T				7.9	40.7	68.6		X	
L7-15-12-T	peat inclusion, dark-brown, denser, stronger decomposed	ice bands (3-4 cm thick)		8.2				Subprofile L7-15-A, "lower Bychchagy peat"	X
L7-15-U/Th-2-T				8.5					
L7-15-15-S	peat lens, light-brown, 10x15 cm, medium decomposed	fine ice veins	7				Subprofile L7-15-B		
L7-15-16-S	grey sandy silt,	coarse lens-like reticulated, ice bands (2-3 cm thick)	6.7		69.3	225.7			
L7-15-17-S	peat lens, light-brown, 10x15 cm, medium decomposed	fine ice veins (< 1mm)	6.4		59.3	145.7			
L7-15-18-S	sandy silt, light brown, grey, without peat, without grass roots, non bedded	ice bands fine lens-like	6.2					X	
L7-15-19-S			5.9		52.0	108.3		X	
L7-15-20-S	sandy silt, light brown, no bedding	fine lens-like, no ice bands	5.6		37.0	58.7		X	
L7-15-21-S	light-brown, plant detritus, sandy silt, Kuchchugui Suite (?)	massive	5.3		32.3	47.7		X	
L7-15-22-S		massive	5					X	
L7-15-23-S	flat peat inclusion (kotletki), matrix: light-grey brown, sandy grass roots non-regular bedded	massive	3.3		49.7	98.8		Subprofile L7-15-C, below subprofile L7-15-A	
L7-15-24-S			3						
<b>L7-16; 73,31385°N; 141,4505°E (27.07.2007)</b>									
L7-16-01-S	ice wedge cast, grey-brown, sandy silt, plant remains, wood fragments	ice lenses surrounding plant remains	7				Subprofile L7-16-A		
L7-16-02-S	ice wedge cast, grey-brown, sandy-silty, plant remains, wood fragments, interbedding of sandy silt and plant detritus	massive	6.8		26.6	36.3			
L7-16-03-S	peat lenses in the lower part of the ice wedge cast, dark brown 15 cm in diameter, within the interbedding	lens-like	6.5						

sample	sedimentology	cryolithology (cryostructure)	m a.s.l.	m b.s.	Ice, abs. [wt%]	Ice grav. [wt %]	remarks	TI
L7-16-04-S	below ice wedge cast (taberal Bychchagy S. ?), grey, dark-grey, light brown Fe-Oxide spots, plant detritus, silty sand	lattice-like broken texture (1-2 cm), diagonal	4.5		21.3	27.1	Subprofile L7-16-B	
L7-16-05-S	lower Bychchagy peat (?) peat inclusion (moss?), 5-10 x 10-20 cm, surrounded by grey silty sand	massive	5					
L7-16-06-S	same like L7-16-05-S unfrozen	unfrozen	5					
L7-16-07-S	grey sandy silt, plant remains, non-bedded, yellowish spots	lattice-like, lenses 1-2 mm, distance 3-4 cm	5.3					
L7-16-08-S	inside of the ice wedge cast, interbedding of grey sandy silt and light brown plant detritus, yellowish spots	coarse lattice-like	5.7		21.4	27.3		
L7-16-09-S	upper Bychchagy peat (?), peat inclusion 5-10 x 10-20 cm, light brown, wood fragments, surrounded by sandy silt light grey	small ice lenses	6				Subprofile L7-16-C	
L7-16-10-S	same like L7-16-09-S unfrozen	unfrozen	6					
L7-16-11-S	unfrozen		6					
L7-16-12-S	yellowish brown, sandy silt, weakly bedded	single coarse ice lenses	5.7		22.9	29.8		
L7-16-13-S	dark grey sandy silt, non bedded, plant remains, peat lenses 2-4 cm in diameter	massive	5.4					
L7-16-14-S	light grey sandy silt, no plant remains,	layered, horizontal ice veins	5		27.6	38.2		
L7-16-Holz	Wood fragments	unfrozen					3 m east of L7-16-A	
<b>L17; 73.34897°N; 141,41412°E (29.07.2007)</b>								
L7-17-01-S	black-brown, coal with wood fragments	frozen, massive	0.5		53.8	116.5	Exposure at the Vetvistyi River, tributary of the Zimov'e R. Tertiary (?)	
L7-17-02-S	grey, with coal inclusions, fine sand-silt, wood fragments partly fossilised		0.5		26.4	35.9		
L7-17-03-S	yellowish brown, gravely, coarse sand, pebbles (2-10 cm)	unfrozen	1					
L7-17-04-S	dark brown, fine sand, single pebbles, wood fragments partly fossilised		0.9					
L7-17-05-S	light grey, middle sand		1					
L7-17-06-S	wood fragments		0.5-1					
L7-17-07-S	fossilised wood fragments		0.5-1					

sample	sedimentology	cryolithology (cryostructure)	m a.s.l.	m b.s.	Ice, abs. [wt%]	Ice grav. [wt %]	remarks	TI
L18; 73,33512°N; 141,3300°E (30.07.2007)								
L7-18-01-T	silty fine-sand (loam), greyish-brown, active layer	frozen, massive		0.25	36.4	57.1	active layer, layer 1 (0-0,35 m)	X
L7-18-02-T	silty fine-sand (loam), brown, peat inclusion (2-3 cm in diameter), roots	ice bands (5-10 mm thick, 5-8 cm distance), lens-like reticulated (lenses 1-2 mm long, 5-10 mm distance)		1.2			1. cryogene cycle, layer 2 (0,35-0,95 m)	X
L7-18-03-T	silty fine-sand (loam), brown, peat inclusion (2-3 cm in diameter), roots	ice bands (1-2 cm thick, 5-8 cm distance), lens-like reticulated (lenses 3 x 8 to 5 x 10 mm), many subvertical veins		1.7	63.4	173.3	2. cryogene cycle, layer 3 (0,95-2,8 m)	X
L7-18-04-T				2.5	51.4	105.8		X
L7-18-05-T		ice band (10 cm )		2.75				X
L7-18-06-T	silty fine-sand (loam), grey to grey-brown, peat inclusion (15x20 cm in diameter)	ice bands (to 2 cm thick, 10-15 cm distance), horizontal between ice bands, rare lenses (0,5-1 mm thick)		3	44.1	78.8	3. cryogene cycle, layer 4 (2,8-4,2 m)	X
L7-18-07-T				3.3				X
L7-18-08-T				4.1	37.8	60.7		X
L7-18-09-T	silty fine-sand (loam), brown-grey, peat inclusion (< 5 cm in diameter)	ice bands (1-1,5 cm thick, 1-5 cm distance, massive and lens-like (1-1,5 mm) between ice bands)		4.6	40.3	67.6	4. cryogene cycle, layer 5 (4,2-4,8 m)	
L7-18-10-T				4.85				
L7-18-11-T	silty fine-sand (loam), grey-brown, peat inclusion (<5 cm in diameter)	ice bands (1-3 cm thick, 1-5 cm distance, massive and lens-like (1-1,5 mm) in peat inclusions)		5.4	40.4	67.8	5. cryogene cycle, layer 6 (4,8-5,8 m)	X
L7-18-12-T				6				
L7-18-13-T	silty fine-sand (loam), grey-brown	ice bands (1-3 cm thick, 1-5 cm distance, massive and lens-like (1-1,5 mm) in peat inclusions)		6.6			6. cryogene cycle, layer 7 (5,8-7 m)	X
L7-18-14-T	silty fine-sand (loam), grey-brown, peat inclusion (<5 cm in diameter), two large peat inclusion (40 cm in diameter)	ice bands (1-2 cm thick, 5-10 cm distance), horizontal reticulated (lenses 2 mm thick, distance 5x20 mm)		7.2				
L7-18-15-T	silty fine-sand (loam), olive-brown, small peat inclusion	ice bands (1-2 cm thick, 5-10 cm distance), horizontal reticulated (lenses 2 mm thick, distance 5x20 mm)		7.7			7. cryogene cycle, layer 8 (7-7,8)	X
L7-18-16-T	silty fine-sand (loam), grey-brown, plant detritus, without peat inclusions	ice bands (3-4 cm thick, 5-10 cm distance)		8.4	58.3	139.9		X

sample	sedimentology	cryolithology (cryostructure)	m a.s.l.	m b.s.	Ice, abs. [wt%]	Ice grav. [wt %]	remarks	TI
L7-18-17-T	silty fine-sand (loam), grey-brown, plant detritus, without peat inclusions	ice bands (3-4 cm thick, 5-10 cm distance)		9.1			8. cryogene cycle, layer 9 (7,8-9,2 m)	X
L7-18-18-T				9.65	54.3	118.7		X
L7-18-19-T	silty fine-sand (loam), grey-brown, rare plant detritus, without peat inclusions	porphyric texture, micro-lens-like		10.4			layer 10 (9,2-13,3 m)	X
L7-18-20-T				11.1	36.1	56.4		X
L7-18-21-T				11.7				
L7-18-22-T				12.5	30.0	42.9		X
L7-18-23-T				13.2				

Oy7-01; 72,67454°N; 143,60981°E (06./09.08.2007)								
Oy7-01-01-S	dark grey, silty, shells, no visible bedding,	fine lens-like reticulated, > 1 mm thick, 1-5 mm long	2.5		18.9	23.3	Subprofile Oy7-01-A, lake sediments	
Oy7-01-02-S			2.2					
Oy7-01-03-S		fine lens-like coarse reticulated (> 1 mm)	1.9					
Oy7-01-04-S		coarse lens-like reticulated	1.6		25.1	33.6		
Oy7-01-05-S	dark grey, silty, shells, no visible bedding, Fe-oxide in cracks	coarse lens-like reticulated	1.3					
Oy7-01-06-S	dark grey, silty, shells, plant detritus, fine interbedding	fine lens-like coarse reticulated (> 1 mm)	2		18.5	22.7	Subprofile Oy7-01-B, transition zone, 40 m east ob subprofile A	
Oy7-01-07-S			1.7					
Oy7-01-08-S			1.4					
Oy7-01-09-S			1.1		26.5	36.0		
Oy7-01-10-S		layered	1.8		30.2	43.2		
Oy7-01-11-S	grey brown, silty sandy, non bedded, coarse plant fragments, detritus lenses 1 x 0,5 cm	fine lens-like, diagonal ice lenses	1.6				Subprofile Oy7-01-C, lake shore, 85 m east of Subprofile A	
Oy7-01-12-S		coarse lens-like reticulated	1.4					
Oy7-01-13-S	grey brown, silty sandy, non bedded, many detritus lenses	lens-like reticulated	1.2		25.3	33.9		
Oy7-01-14-S	dark grey, silty, shells, plant detritus, fine interbedding	fine lens-like coarse reticulated (> 1 mm)	1.2		23.3	30.4	OSL dating; $\gamma$ -Spectrometry, Subprofile Oy7-01-B, transition zone	
Oy7-01-15-S			1.9		27.4	37.7		
Oy7-01-16-S	grey brown, silty sandy	coarse lens-like reticulated	4		49.3	97.3	Subprofile Oy7-01-D,	X
Oy7-01-17-S		Ice bands 5 cm thick, 20 cm between ice bands, coarse lens-like reticulated	4.4		51.0	104.3		X
Oy7-01-18-S			4.8					X
Oy7-01-19-S			5.3					X
Oy7-01-20-S	dark brown peat schlieren, decomposed in grey brown silty sandy, peat soil 20-25 cm thick	fine lens-like	5.8		53.1	113.2		X
Oy7-01-21a-S	dark brown peat schlieren, decomposed in grey brown silty	coarse lens-like	6				U/Th dating, Subprofile Oy7-01-D,	
Oy7-01-21b-S	sand, peat soil horizon	coarse lens-like	6					
Oy7-01-21c-S	30 cm thick, 1 m long	coarse lens-like	6					

sample	sedimentology	cryolithology (cryostructure)	m a.s.l.	m b.s.	Ice, abs. [wt%]	Ice grav. [wt %]	remarks	TI
<b>Oy7-03; 72,67368°N; 143,61408°E (08.08.2007)</b>								
Oy7-03-01-S	light brown, silty sand, non bedded, peat (kotletki), single roots, fine distributed plant detritus	massive	0.5		34.5	52.8	Contact Kuchchugui- Bychchagy S. (?) Subprofile Oy7-03-A	X
Oy7-03-02-S	light brown, silty sand, non bedded	Ice bands 1-2 cm thick, 10-15 cm distance, lens-like reticulated, vertical ice vein	0.9		33.8	51.1		X
Oy7-03-03-S		Ice bands 1-2 cm thick, 5-10 cm distance, coarse lens-like	1.3		58.8	142.5		X
Oy7-03-04-S	grey, silty sand, Fe-oxide spots	reticulated, broken ice lenses	1.6					X
Oy7-03-05-S	peat inclusions 5 - 30 cm in diameter (Drepanucladus and Eriophorum) moss peat, weakly decomposed, brown, surrounding sediment grey silty sand	Ice bands 1-2 cm thick, 5 cm between ice bands, there coarse lens-like	1.9					
Oy7-03-06-S			2.1		68.6	218.0		X
Oy7-03-07-S	light brown, silty sand, non bedded, flat peat inclusions (kotletki), single roots, fine distributed plant detritus	massive	0.5		29.9	42.7	OSL dating, $\gamma$ -Spectrometry, Subprofile Oy7-03-A	
Oy7-03-08-S	grey, silty sand, light brown peat inclusions 5-10 cm in diameter	ice bands	7		69.8	230.8	Contact Kuchchugui- Bychchagy S. (?) Subprofile Oy7-03-B	X
Oy7-03-09-S	dark brown moss peat inclusions 10-30 cm, stronger decomposed, surrounded by grey silty sand with plant detritus	fine lens-like	7.5					
Oy7-03-10-S	grey silty sand	ice bands 1 cm thick, between	8					X
Oy7-03-11-S	peat inclusions 5 - 7 cm in diameter, matrix grey silty sand	coarse lens-like reticulated	8.5		59.3	145.6		X
<b>Oy7-04; 72,68146°N; 143,51376°E (11.08.2007)</b>								
Oy7-04-01-S	active layer, brown grey strongly rooted, grass and moss	unfrozen	10	0.2			Subprofile Oy7-04-A	
Oy7-04-02-S	light-brown grey silty sand, cryoturbated peat soil horizon, peat lenses 5 cm in diameter	lens-like reticulated	9.7	0.3	50.0	100.0		X
Oy7-04-03-S	grey brown, silty sand	ice bands, coarse lens-like	9.3	0.7	57.8	137.1		X
Oy7-04-04-S			8.8	1.2	52.6	110.9		X
Oy7-04-05-S	grey brown, silty sand, small plant detritus inclusions 1 cm in diameter, wood fragments	coarse lens-like reticulated	1.5		41.9	72.2	Subprofile Oy7-04-B, beach deposits(?)	X
Oy7-04-06-S	brown, bedded, plant detritus, silty sand, convolute bedding	massive	1.9					

sample	sedimentology	cryolithology (cryostructure)	m a.s.l.	m b.s.	Ice, abs. [wt%]	Ice grav. [wt %]	remarks	TI
Oy7-04-07-S		ice band 1 cm thick, clear ice without bubbles	2.1					X
Oy7-04-08-S	brown grey interbedding of plant detritus and silt, ripples, convolute bedding, wood fragments	massive	2.3		28.7	40.3		
Oy7-04-09-S	grey, silty, shells, plant fragments, fine distributed plant detritus, disturbed bedding	fine lens-like, diagonal ice lenses < 1 mm	2.6				Subprofile Oy7-04-B	
Oy7-04-10-S	grey, silty, shells, plant fragments, fine distributed plant detritus, fine detritus layers		3		24.3	32.1		
Oy7-04-11-S	grey sandy silt - brown plant detritus interbedding, ripples	layered lens-like 1 mm thick, 1-2 cm long	3.4					
Oy7-04-12-S	grey sandy silt, disturbed bedding, fine distributed plant detritus, black spots	massive	3.9					
Oy7-04-13-S	grey sandy silt - brown plant detritus interbedding, cryoturbated, wood fragments, white lines (thaw structures?)	massive	3.5		31.3	45.5		Subprofile Oy7-04-C, similar to Oy7-04-11-S
Oy7-04-14-S	grey sandy silt - brown plant detritus interbedding, cryoturbated, wood fragments	single lenses	3.8				Subprofile Oy7-04-C	
Oy7-04-15-S	grey sandy silt, fine bedded	layered fine lens-like	4.1		24.7	32.7		
Oy7-04-16-S	grey sandy silt - brown plant detritus interbedding, ripples	layered lens-like	4.3					
Oy7-04-17-S	grey sandy silt, shells	layered fine lens-like	4.6					
Oy7-04-18-S	grey silty sand, no plant detritus, weakly bedded, disturbed, shells, brown iron oxide impregnations on ice lenses	fine lens-like	4.7		28.8	40.5	Subprofile Oy7-04-C, boundary between lake and alas deposits	
Oy7-04-19-S	grey sandy silt, single brown plant detritus inclusions 0.5-2 cm in diameter	layered lens-like	5.2		22.7	29.4	Subprofile Oy7-04-C	
Oy7-04-20-S	grey sandy silt - brown plant detritus interbedding, peat lenses	coarse lens-like	5.7					
Oy7-04-21-S	peat lens, brown, stronger decomposed 30 cm in diameter,	horizontal ice lenses	5.8					
Oy7-04-22-S	twigs from the same horizon	unfrozen	5.8					

sample	sedimentology	cryolithology (cryostructure)	m a.s.l.	m b.s.	Ice, abs. [wt%]	Ice grav. [wt %]	remarks	TI
Oy7-07; 72,67865°N, 143,55718°E (14.08.2007)								
Oy7-07-01-S	Grey-brown, silty sand, in situ grass roots, non regularly weakly bedded (taberal Kuchchugui ?)	massive	1.5		23.6	30.9	OSL dating, $\gamma$ -Spectrometry, Subprofile Oy7-07-A	
Oy7-07-02-S		massive	1.8				Subprofile Oy7-07-A	
Oy7-07-03-S	grey-brown, silty sand, in situ grass roots, non regularly weakly bedded (taberal Kuchchugui ?), black spots	massive	2.3		23.7	31.0	OSL dating, $\gamma$ -Spectrometry, Subprofile Oy7-07-A	
Oy7-07-04-S	grey brown silty sand, plant roots, black spots	lens-like < 1 mm thick, 0.5 - 2 cm between lenses, broken reticulated	2.7		32.5	48.1	Subprofile Oy7-07-A	
Oy7-07-05-S	grey brown silty sand	ice bands 2 mm thick, 3-5 cm between them, lens-like broken reticulated	3.2		52.0	108.5	Subprofile Oy7-07-A	X
Oy7-07-06-S	grey brown silty sand, light brown peat inclusions (brown moos peat) 10-15 cm in diameter	ice bands 2 mm thick, 3-5 cm between them, lens-like broken reticulated	3.5				Subprofile Oy7-07-A (lower non thawed Bychchagy peat in sensu V. Tumskey)	
Oy7-07-07-S	grey brown silty sand, light brown moos peat inclusions, 15-20 cm thick and up to 0,5 m long, single twigs, cryoturbated in the upper part	single lenses	3.9		80.9	423.9		
Oy7-07-07a-S	peat from one lens of Oy7-07-07-S		3.9				U/Th dating, Subprofile Oy7-07-A	
Oy7-07-07b-S	peat from one lens of Oy7-07-07-S		3.9					
Oy7-07-07c-S	peat from one lens of Oy7-07-07-S		3.9					
Oy7-07-08-S	grey brown silty sand, black spots	massive	4.3		35.1	54.0		
Oy7-07-09-S	grey silty sand	lens-like, broken reticulated, lenses < 1 mm, ice bands 1-2 mm thick every 5 cm	4.6		38.8	63.5		X
Oy7-07-10-S	yellowish light brown silty sand, 10 cm thick horizon, weakly bedded,	massive	4.8				Subprofile Oy7-07-A	X
Oy7-07-11-S	grey silty sand, black spots, white lines (thaw structures), peat lenses 5-10 x 2-5 cm, twigs	rare single small lenses 1 mm thick 5 cm long	5.1		27.2	37.4		
Oy7-07-12-S			5.5					
Oy7-07-13-S	grey silty sand, black spots, twigs	layered coarse lens-like 1-2 mm thick lenses	4.5		20.4	25.6		
Oy7-07-14-S	grey sandy silt, fine bedded detritus layers, peat inclusions 2 cm in diameter, twig-peat inclusion 20 x 50 cm, yellowish to light brown silt (Krest Yuryakh?)	single horizontal lenses < 1 mm thick, ice lenses below wood fragments	5				Subprofile Oy7-07-B "1st twig-horizon"	

sample	sedimentology	cryolithology (cryostructure)	m a.s.l.	m b.s.	Ice, abs. [wt%]	Ice grav. [wt %]	remarks	TI
Oy7-07-15-S	grey sandy silt - brown plant detritus interbedding, ripples	single horizontal lenses < 1 mm thick	5.4		23.6	30.9	Subprofile Oy7-07-B	
Oy7-07-16-S	in situ twigs	unfrozen	5.5				Subprofile Oy7-07-B	
Oy7-07-17-S	grey sandy silt - brown plant detritus interbedding, wood fragments, shells	single horizontal lenses < 1 mm thick	5.7				Subprofile Oy7-07-B	X
Oy7-07-18-S	grey sandy silt - brown plant detritus interbedding, wood fragments, convolute bedding	lens-like layered	6				Subprofile Oy7-07-B "2nd twig-horizon",	
Oy7-07-18a-S		unfrozen	5.9					
<b>Oy7-08-A/B, 72,68002°N; 143,53181°E (16.08.2007)</b>								
Oy7-08-01-S	grey sandy silt, black spots, single plant remains (taberal Kuchchugui S. ?)	massive	2		19.8	24.7	Subprofile Oy7-08-A	
Oy7-08-02-S	allochthonous peat lenses 10 x 5 cm in diameter with wood fragments, grey sandy silt matrix	fine lens-like reticulated	2.4		34.0	51.5		
Oy7-08-03-S	grey fine sandy silt, peat inclusions 2x5 to 5x10 cm white lines (thaw structures ?), small plant detritus inclusions	lens-like reticulated, single bigger ice inclusions 0.5 cm	2.7					
Oy7-08-04-S		single thin lenses	3.2		26.5	36.1		
Oy7-08-05-S	interbedding of grey sandy silt (0.5-3 cm thick) and brown plant detritus (0.5-1 cm) wood fragments, peat lenses	single thin lenses	3.5		26.4	35.8		
Oy7-08-06-S	interbedding of yellowish sandy silt and brown plant detritus (1-2 mm)	fine lens-like reticulated	4.2					
Oy7-08-07-S	corresponding to Oy7-08-05-S, 15 cm interbedding of grey sandy silt- brown plant detritus (0.5-1 cm), 26 layers	massive	2		39.9	66.4	Subprofile Oy7-08-B in ice wedge cast	
Oy7-08-08-S	interbedding, of grey sandy silt- brown plant detritus silt dominated, ripples, convolute bedding	fine lenses, not parallel to bedding	2.2				Subprofile Oy7-08-B	
Oy7-08-09-S	5 cm interbedding of grey sandy silt and brown plant detritus (1-2 mm thick) non disturbed, peat lens	massive	2.3					
Oy7-08-10-S	interbedding of grey sandy silt and brown plant detritus, silt dominated, ripples, convolute bedding	fine lenses, not parallel to bedding	2.6		26.4	35.8		
Oy7-08-11-S	corresponding to Oy7-08-06-S, grey sandy silt- brown plant detritus interbedding, many small wood fragments, ripples, detritus dominated	massive	2.7					

sample	sedimentology	cryolithology (cryostructure)	m a.s.l.	m b.s.	Ice, abs. [wt%]	Ice grav. [wt %]	remarks	TI	
Oy7-08-12-S	disturbed grey sandy silt- brown plant detritus interbedding,	fine lens-like	2.9				Subprofile Oy7-08-B		
Oy7-08-13-S	10 cm interbedding of grey sandy silt and brown plant detritus, silt dominated	fine lens-like, parallel to bedding	3.1		32.8	48.9			
Oy7-08-14-S	15 cm interbedding of grey sandy silt and brown plant detritus (up to 1 cm thick), detritus dominated, 11 detritus layers	fine lens-like, parallel to bedding	3.2						
Oy7-08-15-S	10 cm interbedding of grey sandy silt and brown plant detritus (2-4 mm thick), detritus dominated, 23 layers	single fine lenses	3.3						
Oy7-08-16-S	interbedding, of grey sandy silt and brown plant detritus (2-3 mm) silt dominated, convolute bedding	single fine lenses horizontal	3.5		27.0	36.9			
Oy7-08-17-S	disturbed grey sandy silt- brown plant detritus (4 mm thick) interbedding, wood remains (as subsample)		4		21.2	26.8			
Oy7-08-18-S	grey sandy silty, fine distributed plant detritus, weakly bedded	layered, lens-like	4.3						
Oy7-08-20-S	grey sandy silty, shells, yellowish to light brown next to ice lenses, single detritus layers	reticulated, lens-like	4.7		18.2	22.2			
Oy7-08-21-S	grey sandy silt, shells, yellowish light brown next to ice lenses, non bedded		5		28.1	39.2			
Oy7-08-22-S	grey sandy silty, shells, disturbed bedding		5.3						
Oy7-08-23-S			5.6		28.7	40.3			
Oy7-08-24-S		5.9							
Oy7-08-25-S	disturbed grey sandy silt- brown plant detritus (4 mm thick) interbedding, wood remains	layered, lens-like	4		23.9	31.4		OSL dating, $\gamma$ -Spectrometry, Subprofile Oy7-08-B	
Oy7-08-26-S	grey sandy silty, fine distributed plant detritus, weakly bedded	layered, lens-like	4.3		13.0	15.0			

sample	sedimentology	cryolithology (cryostructure)	m a.s.l.	m b.s.	Ice, abs. [wt%]	Ice grav. [wt %]	remarks	TI
<b>Oy7-08-C; 72,67989°N; 143,53184°E (17.08.2007)</b>								
Oy7-08-27-S	grey clayish silt, peat inclusions 2-3 cm in diameter, strongly disturbed bedding	layered, lens-like (1 mm thick 2-4 cm long)	3.5		25.4	34.1	Subprofile Oy7-08-C	
Oy7-08-28-S	grey sandy silt, light brown spotty, peat inclusions 3-5 cm in diameter, wood fragments, non bedded	layered, lens-like	4		28.0	39.0		
Oy7-08-29-S	brown sandy silt, grey spotty, peat inclusions 2-3 cm in diameter,	layered, lens-like (< 1 mm, 3-5 mm distance between single lenses)	4.4		25.5	34.2		
Oy7-08-30-S	light brown sandy silt grey spotty		4.7		23.8	31.3		
Oy7-08-31-S	dark grey brown silty sand, plant remains, shells,	coarse lens-like	5.2		37.1	59.1		X
<b>Oy7-08-D; 72,67945°N; 143,53227°E (17.07.2007)</b>								
Oy7-08-32-S	grey brown sandy silt,	ice bands (3-5 cm distance), coarse lens-like reticulated	9.5		40.9	69.2	Subprofile Oy7-08-D	X
Oy7-08-33-S	grey brown sandy silt, peat inclusions 1-2 cm in diameter		10		42.2	73.0		
Oy7-08-34-S	grey brown sandy silt, peat inclusions 1-2 cm in diameter, single plant remains		10.5		52.2	109.3		X
Oy7-08-35-S			11					X
Oy7-08-36-S		ice bands 5-10 cm thick , coarse lens-like reticulated 2-3 mm thick 1-3 cm long 1 cm distance between lenses	11.5					X
Oy7-08-37-S	ice bands (3-5 cm distance), coarse lens-like reticulated	12		62.5	167.0	X		
<b>Oy7-08-E; 72,679°N; 143,53218°E (19.08.2007)</b>								
Oy7-08-38-S	light brown sandy silt, small peat inclusions, plant remains, grass roots	ice bands (10 cm distance), coarse lens-like reticulated	15.5		67.9	211.9	Subprofile Oy7-08-E, Reper 5 (16,5 m a.s.l.)	X
Oy7-08-38a-S		unfrozen					For macrofossil analyses	
Oy7-08-39-S	peat inclusion dark brown (20 x 40 cm) in light brown sandy silt matrix, many peat lenses (2 x 2 cm)	ice bands (10 cm distance), coarse lens-like reticulated	15.8		45.2	82.5	Subprofile Oy7-08-E, Reper 5 (16.5 m a.s.l.)	
Oy7-08-40-S	grey sandy silt, reddish-brown coloured, small peat lenses (2-3 cm), <i>in-situ</i> grass roots	ice bands (5 cm distance), lens-like reticulated	16.2					X
Oy7-08-41-S	grey sandy silt with light brown spots, plant remains	ice bands, lens-like reticulated	16.7		54.4	119.4		X
Oy7-08-42-S			17.1					X
Oy7-08-43-S	grey brown sandy silt with light brown spots, peat inclusion (2-3 x 4-5 cm)	ice bands, lens-like to fine lens-like reticulated	17.4		56.1	127.9		X
Oy7-08-44-S			17.9		51.1	104.7		
Oy7-08-45-S	dark grey peat lenses (5-10 cm in diameter) in grey sandy silt matrix with reddish-brown coloured spots	changing coarse to fine lens-like reticulated	18.4				X	

sample	sedimentology	cryolithology (cryostructure)	m a.s.l.	m b.s.	Ice, abs. [wt%]	Ice grav. [wt %]	remarks	TI
<b>Oy7-08-F; 72,67892°N; 143,53237°E (19.07.2007)</b>								
Oy7-08-46-S	grey sandy silt with brown coloured spots, peat lenses	ice bands, lens-like reticulated	18.7		41.4	70.7	Subprofile Oy7-08-F	X
Oy7-08-47-S	grey brown sandy silt, fine distributed plant detritus, grass roots	ice bands (5-10 cm distance), lens-like to fine lens-like reticulated	19.2					X
Oy7-08-48-S			19.7		19.8	24.6		X
Oy7-08-49-S	grey brown sandy silt, fine distributed plant detritus, grass roots	ice bands 1-2 mm thick (10 cm distance), fine lens-like reticulated	20.2					X
Oy7-08-50-S	grey brown sandy silt, fine distributed plant detritus, small wood fragments	ice bands, lens-like to fine lens-like reticulated	20.7		44.8	81.2		X
Oy7-08-51-S	grey brown sandy silt, peat inclusions 1 cm in diameter, plant roots	ice bands, lens-like to fine lens-like reticulated	21.2					X
<b>Oy7-08-G; 72,67882°N; 143,53285°E (19.07.2007)</b>								
Oy7-08-52-S	grey brown sandy silt	ice bands (10 cm distance), coarse lens-like	21.5		40.7	68.7	Subprofile Oy7-08-G	X
Oy7-08-53-S	dark brown peat inclusion (5-10 cm in diameter) in grey brown sandy silt matrix	ice bands (10 cm distance), coarse lens-like	22					X
Oy7-08-54-S	peat soil horizon, peat lenses (2 x 3 to 5 x 10 cm) grass roots, leaf fragments, fine distributed plant detritus	ice bands (10 cm distance), lens-like reticulated	22.5		46.3	86.2		X
Oy7-08-55-S			23					X
Oy7-08-56-S	grey brown sandy silt	coarse lens-like reticulated	23.6		47.2	89.5		X
Oy7-08-57-S	peat soil horizon 40 cm thick, wood fragments, single plant residues, peat inclusions (10 cm) grey brown sandy silt matrix	ice bands, lens-like to fine lens-like reticulated	24					X
Oy7-08-58-S	grey brown sandy silt, plant residues partly green	ice bands, lens-like reticulated	24.5		46.7	87.6		X
Oy7-08-59-S			25				X	
Oy7-08-60-S			25.6		54.9	121.7	X	
Oy7-08-61-S			26				X	
<b>Oy7-08-H; 62.67873°N; 143.5341°E (10.07.2007)</b>								
Oy7-08-62-S	grey brown sandy silt, fine distributed plant detritus, grass roots	coarse lens-like	26.5		70.7	241.7	Subprofile Oy7-08-H	X
Oy7-08-63-S	grey brown sandy silt, reddish-brown coloured spots, fine distributed plant detritus, grass roots	lens-like reticulated	27					X
Oy7-08-64-S	sandy silt, plant remains	ice bands (5 cm distance), lens-like reticulated	27.4		69.1	223.1		X
Oy7-08-65-S	peat soil horizon below the active layer, transition zone, dark brown	ice bands (2-3 cm distance), vertical ice needles, coarse lens-like reticulated	27.8					X
Oy7-08-66-S	active layer, grey brown sandy silt, strongly rooted, grass and moss	unfrozen	28					X

sample	sedimentology	cryolithology (cryostructure)	m a.s.l.	m b.s.	Ice, abs. [wt%]	Ice grav. [wt %]	remarks	TI
<b>Oy7-09; 72,68054°N; 143,53695°E (09.08.2007)</b>								
Oy7-09-01-S	grey-brown, silty sand, non bedded, plant detritus, wood fragments, peat inclusions 2-3 cm in diameter	coarse lens-like 1-2 mm thick 5-15 cm distance between single lenses	2.5		27.1	37.3	Subprofile Oy7-09-A (horizontal in ice wedge cast) taberal Bychchagy S. (?)	
Oy7-09-02-S	peat lens 30 cm in diameter dark brown strongly decomposed, large wood fragments	lens-like < 1 mm thick	2.5				Subprofile Oy7-09-A (horizontal in ice wedge cast) 0,5 m west of Oy7-09-01-S	
Oy7-09-03-S	interbedding of sandy silt grey and brown plant detritus, ripples, vertical part of an ice wedge cast, wood fragments,	lens-like > 1 mm thick, perpendicular to sediment structures	2.5		24.8	33.0	Subprofile Oy7-09-A (horizontal in ice wedge cast) 1 m west of Oy7-09-01-S	
Oy7-09-04-S	well bedded, grey, fine distributed plant detritus, wood fragments,	lens-like, perpendicular to sediment structures	2.5				Subprofile Oy7-09-A (horizontal in ice wedge cast) 1,4 m west of Oy7-09-01-S	
Oy7-09-05-S	interbedding of grey sandy silt and plant detritus, ripples, , wood fragments, vertical part of the ice wedge cast	lens-like, perpendicular to sediment structures	2.5		35.8	55.8	Subprofile Oy7-09-A (horizontal in ice wedge cast) 1,6 m west of Oy7-09-01-S	
Oy7-09-06-S	grey, silty sand, weakly bedded, black spots,	lens-like	1		21.7	27.7	Subprofile Oy7-09-B (vertical left of the ice wedge cast), taberal Kuchchugui S. (?)	
Oy7-09-07-S	single plant detritus inclusions, small roots,	coarse lens-like layered	1.4					
Oy7-09-08-S	grey-brown, silty sand black spots, single twigs, fine distributed	lens-like layered, lenses 1 mm thick 5 mm between single lenses	2				Subprofile Oy7-09-B (vertical left of the ice wedge cast)	
Oy7-09-09-S	plant detritus non bedded		2.5		23.6	30.8		
<b>Oy7-10; 72.672°N; 143.63514°E (14.08.2007)</b>								
Oy7-10-01-S	brown, silty sand, no visible plant remains,	ice bands, 5-10 mm thick, 4-6 cm distance between, layered lens-like in between	2		27.6	38.1	Bychchagy Suite (?)	
Oy7-10-02-S	brown, silty sand, autochthonous peat inclusions 5-10 cm in diameter	ice bands, 5-10 mm thick, 4-6 cm distance between, layered lens-like in between	2.7					X
Oy7-10-03-S	grey brown silty sandy,	ice bands, up to 30 mm thick, 1-1,5 cm distance between, layered coarse lens-like in between lenses 1-2 mm thick 8-10 cm long	3.1		49.2	96.7		X
Oy7-10-04-S	peat inclusion light brown, weakly decomposed 30 cm in diameter	ice bands, coarse lens-like reticulated	3.3		88.8	793.8	lower, non thawed Bychchagy peat in sensu V. Tumskoy	
Oy7-10-05-S	grey brown silty sand with peat inclusions	ice bands, coarse lens-like reticulated	3.7		52.0	108.5		X
Oy7-10-06-S	grey brown silty sand weakly peaty, single twigs	ice bands, up to 5-20 mm thick, 6-10 cm distance, lens-like reticulated, ataxitic	4.4		38.0	61.4		X

sample	sedimentology	cryolithology (cryostructure)	m a.s.l.	m b.s.	Ice, abs. [wt%]	Ice grav. [wt %]	remarks	TI
Oy7-10-07-S	brown fine sandy silt grass roots, autochthonous peat inclusions (10-20 cm in diameter)	ice bands, coarse lens-like	5.3		52.9	112.2	upper non thawed Bychchagy peat in sensu V. Tumskoy	X
Oy7-10-08-S	grey sandy silt	ice bands, coarse lens-like	5.9		42.1	72.8		X
Oy7-10-09-S	peat inclusion, Drepanocladus	ice bands, coarse lens-like	6.2		53.1	113.3		
<b>Oy7-11, 72.68347°N; 143.47526°E (22.08.2007)</b>								
Oy7-11-01-S	taberal Yedoma Suite, light grey sandy silt, white lines (thaw structures), no visible plant remains	lens-like, layered, 1 mm thick, 5-15 cm long, 1-2 cm distance between	6		29.7	42.3	Subprofile Oy7-11-A	
Oy7-11-02-S			6.4		29.5	41.9		
Oy7-11-03-S	taberal Yedoma Suite, light grey sandy silt, white lines (thaw structures), fine distributed plant detritus		6.8					
Oy7-11-04-S	Grey, clayish silt, peat inclusions, 0.5-1 cm in diameter, wood fragments		7.1		27.9	38.6		
Oy7-11-04a-S	twigs from the same horizon	unfrozen	7.1					
Oy7-11-05-S	interbedding of grey sandy silt and brown plant detritus silt dominated, ripples, wood fragments, small synsedimentary faults	horizontal ice veins	7.4					
Oy7-11-frank spezial	peat layer in ice wedge cast	unfrozen	7.5				for plant macrofossil analyses	
Oy7-11-06-S	interbedding of grey sandy silt and brown plant detritus, detritus dominated	horizontal ice veins	7.7		41.4	70.8		
Oy7-11-07-S	interbedding of grey sandy silt and brown plant detritus, detritus dominated, shells???	horizontal ice veins	8					
Oy7-11-08-S			8.3					
Oy7-11-09-S	grey sandy silt, not bedded, single wood fragments,	lens-like	8.6		34.4	52.4		
Oy7-11-10-S	peat horizon 20-30 cm thick, dense and platy, wood fragments 2-3 cm in diameter, 1-2 mm thick silt layers	lens-like layered 1 mm thick, 2-3 cm long	8.8				Subprofile Oy7-11-B	
Oy7-11-10a-S	peat and twigs (frank spezial)	unfrozen	8.8				For macrofossil analyses	
Oy7-11-11-S	grey brown sandy silt, iron oxide on ice lenses	coarse lens-like reticulated 1 cm thick lenses, vertical ice crystals	9.1		56.7	131.1	Subprofile Oy7-11-B	X
Oy7-11-12-S			10.1					X
Oy7-11-13-S	grey sandy silty, plant remains	ice bands, coarse lens-like reticulated	10.6		64.7	183.3		X
Oy7-11-14-S	light brown peat lenses (peat soil horizon) in grey brown sandy silt matrix, grass roots	coarse lens-like reticulated	11.1					X
Oy7-11-15-S			11.6					X
Oy7-11-16-S	active layer grey brown, grass moss und roots	unfrozen	11.9					

## 6.2 List of ground ice, water and precipitation samples

Chain saw+ – Chain saw and band saw (in the cold lab), corresponding sediment samples – see Chapter 6.1

Sample number	Sample type	Sampled By	Date	Sampled for measurement of				Corresponding sediment sample
				$\delta^{18}\text{O}/\delta\text{D}$	$^3\text{H}$	Anions/Cations	$^{36}\text{Cl}$	
L7-01; 73.33464°N; 141.32043°E								
L7-01-101-S	IW	Ice screw	10.07.2007	X				
L7-01-102-S	IW	Ice screw	10.07.2007	X				
L7-01-103-S	IW	Ice screw	10.07.2007	X				
L7-01-104-S	IW	Ice screw	10.07.2007	X				
L7-01-105-S	IW	Ice screw	10.07.2007	X				
L7-01-106-S	IW	Ice screw	10.07.2007	X				
L7-01-107-S	IW	Ice screw	10.07.2007	X				
L7-01-108-S	IW	Axe	10.07.2007				X	
L7-01-109-S	IW	Ice screw	10.07.2007	X				
L7-01-110-S	IW	Ice screw	10.07.2007	X				
L7-01-111-S	IW	Ice screw	10.07.2007	X				
L7-01-112-S	IW	Ice screw	10.07.2007	X				
L7-01-113-S	IW	Ice screw	10.07.2007	X				
L7-01-114-S	IW	Ice screw	10.07.2007	X				
L7-01-115-S	IW	Ice screw	10.07.2007	X				
L7-01-116-S	IW	Ice screw	10.07.2007	X				
L7-01-117-S	IW	Axe	10.07.2007				X	
L7-01-118-S	IW	Ice screw	10.07.2007	X				
L7-01-119-S	IW	Ice screw	10.07.2007	X				
L7-01-120-S	IW	Ice screw	10.07.2007	X				
L7-01-121-S	IW	Ice screw	10.07.2007	X				
L7-01-01-S	TI		11.07.2007	X				X
L7-01-02-S	TI		12.07.2007	X				X
L7-01-03-S	TI		13.07.2007	X				X
L7-01-04-S	TI		14.07.2007	X				X
L7-01-07-S	TI		15.07.2007	X				X
L7-01-13-S	TI		16.07.2007	X				X
L7-01-14-S	TI		17.07.2007	X				X
L7-01-15-S	TI		18.07.2007	X				X
L7-02; 73.33439°N; 141.32164°E								
L7-02-101-S	IW	Chain saw	10.07.2007				X	
L7-02-102-S	IW	Ice screw	12.07.2007	X				
L7-02-103-S	IW	Ice screw	12.07.2007	X				
L7-02-104-S	IW	Ice screw	12.07.2007	X				
L7-02-105-S	IW	Ice screw	12.07.2007	X				
L7-02-106-S	IW	Ice screw	12.07.2007	X				
L7-02-107-S	IW	Ice screw	12.07.2007	X				
L7-02-108-S	IW	Ice screw	12.07.2007	X				
L7-02-109-S	IW	Ice screw	12.07.2007	X				
L7-02-110-S	IW	Ice screw	12.07.2007	X				
L7-02-111-S	IW	Ice screw	12.07.2007	X				
L7-02-112-S	IW	Ice screw	12.07.2007	X				
L7-02-113-S	IW	Ice screw	12.07.2007	X				
L7-02-114-S	IW	Ice screw	12.07.2007	X				
L7-02-115-S	IW	Ice screw	12.07.2007	X				
L7-02-116-S	IW	Ice screw	12.07.2007	X				
L7-03; 73.33525°N; 141.31648°E								
L7-03-101-S	IW	Axe	12.07.2007				X	
L7-03-102-S	IW	Ice screw	12.07.2007	X				
L7-03-103-S	IW	Ice screw	12.07.2007	X				
L7-03-104-S	IW	Ice screw	12.07.2007	X				
L7-03-105-S	IW	Ice screw	12.07.2007	X				
L7-03-106-S	IW	Ice screw	12.07.2007	X				
L7-03-107-S	IW	Ice screw	12.07.2007	X				
L7-03-108-S	IW	Ice screw	12.07.2007	X				
L7-03-109-S	IW	Ice screw	12.07.2007	X				
L7-03-01-S	TI		12.07.2007	X				X
L7-03-02-S	TI		12.07.2007	X				X
L7-03-03-S	TI		12.07.2007	X				X
L7-03-04-S	TI		12.07.2007	X				X
L7-03-05-S	TI		12.07.2007	X				X
L7-03-06-S	TI		12.07.2007	X				X
L7-03-07-S	TI		12.07.2007	X				X

Sample number	Sample type	Sampled By	Date	Sampled for measurement of				Corresponding sediment sample
				$\delta^{18}\text{O}/\delta\text{D}$	$^3\text{H}$	Anions/Cations	$^{36}\text{Cl}$	
L7-05; 73.33874°N; 141.29704°E								
L7-05-01-S	TI		14.07.2007	X			X	
L7-05-02-S	TI		14.07.2007	X			X	
L7-05-03-S	TI		14.07.2007	X			X	
L7-05-05-S	TI		14.07.2007	X			X	
L7-05-06-S	TI		14.07.2007	X			X	
L7-05-10-S	TI		14.07.2007	X			X	
L7-07; 73.33086°N; 141.34423°E								
L7-07-101-S	IW	Axe	26.07.2007				X	
L7-07-102-S	IW	Ice screw	26.07.2007	X				
L7-07-103-S	IW	Ice screw	26.07.2007	X				
L7-07-104-S	IW	Ice screw	26.07.2007	X				
L7-07-105-S	IW	Ice screw	26.07.2007	X				
L7-07-106-S	IW	Ice screw	26.07.2007	X				
L7-07-107-S	IW	Ice screw	26.07.2007	X				
L7-07-201-S	IW	Axe	26.07.2007				X	
L7-07-202-S	IW	Ice screw	26.07.2007	X				
L7-07-203-S	IW	Ice screw	26.07.2007	X				
L7-07-204-S	IW	Ice screw	26.07.2007	X				
L7-07-205-S	IW	Ice screw	26.07.2007	X				
L7-07-206-S	IW	Ice screw	26.07.2007	X				
L7-07-207-S	IW	Ice screw	26.07.2007	X				
L7-07-208-S	IW	Ice screw	26.07.2007	X				
L7-07-209-S	IW	Ice screw	26.07.2007	X				
L7-07-01-S	TI		25.07.2007	X			X	
L7-07-02-S	TI		26.07.2007	X			X	
L7-07-03-S	TI		27.07.2007	X			X	
L7-07-06-S	TI		28.07.2007	X			X	
L7-07-09-S	TI		28.07.2007	X			X	
L7-08; 73.3492°N; 141.24007°E								
L7-08-101-S	IW	Axe	15.07.2007	X				
L7-08-201-S	IW	Axe	25.07.2007				X	
L7-08-202-S	IW	Ice screw	25.07.2007	X				
L7-08-203-S	IW	Ice screw	25.07.2007	X				
L7-08-204-S	IW	Ice screw	25.07.2007	X				
L7-08-205-S	IW	Ice screw	25.07.2007	X				
L7-08-206-S	IW	Ice screw	25.07.2007	X				
L7-08-207-S	IW	Ice screw	25.07.2007	X				
L7-08-208-S	IW	Ice screw	25.07.2007	X				
L7-08-209-S	IW	Ice screw	25.07.2007	X				
L7-08-210-S	IW	Ice screw	25.07.2007	X				
L7-08-211-S	IW	Ice screw	25.07.2007	X				
L7-08-212-S	IW	Ice screw	25.07.2007	X				
L7-08-301-S	IW	Axe	25.07.2007	X				
L7-08-01-S	TI		15.07.2007	X			X	
L7-08-04-S	TI		15.07.2007	X			X	
L7-08-18-S	TI		15.07.2007	X			X	
L7-08-20-S	TI		15.07.2007	X			X	
L7-08-21-S	TI		25.07.2007	X			X	
L7-08-23-S	TI		25.07.2007	X			X	
L7-08-24-S	TI		25.07.2007	X			X	
L7-08-25-S	TI		25.07.2007	X			X	
L7-08-26-S	TI		25.07.2007	X			X	
L7-08-27-S	TI		25.07.2007	X			X	
L7-08-28-S	TI		25.07.2007	X			X	
L7-12; 73.2876°N; 141.69351°E								
L7-12-101-S	IW	Axe	18.07.2007				X	
L7-12-102-S	IW	Ice screw	18.07.2007	X				
L7-12-103-S	IW	Ice screw	18.07.2007	X				
L7-12-104-S	IW	Ice screw	18.07.2007	X				
L7-12-105-S	IW	Ice screw	18.07.2007	X				
L7-14; 73.2877°N; 141.69097°E								
L7-14-101-S	IW	Axe	18.07.2007	X				
L7-14-102-S	IW	Axe	19.07.2007	X				
L7-14-201-S	IW	Axe	20.07.2007				X	
L7-14-202-S	IW	Ice screw	21.07.2007	X				
L7-14-203-S	IW	Ice screw	21.07.2007	X				

Sample number	Sample type	Sampled By	Date	Sampled for measurement of				Corresponding sediment sample
				$\delta^{18}\text{O}/\delta\text{D}$	$^3\text{H}$	Anions/Cations	$^{36}\text{Cl}$	
L7-14-204-S	IW	Ice screw	21.07.2007	X				
L7-14-205-S	IW	Ice screw	21.07.2007	X				
L7-14-19-S	TI		19.07.2007	X				X
L7-14-20-S	TI		19.07.2007	X				X
L7-14-21-S	TI		19.07.2007	X				X
L7-14-22-S	TI		19.07.2007	X				X
L7-14-23-S	TI		19.07.2007	X				X
L7-14-24-S	TI		19.07.2007	X				X
L7-14-25-S	TI		19.07.2007	X				X
L7-14-30-S	TI		21.07.2007	X				X
L7-14-32-S	TI		21.07.2007	X				X
L7-14-33-S	TI		21.07.2007	X				X
L7-14-34-S	TI		21.07.2007	X				X
L7-15; 73.28661°N; 141.7052°E								
L7-15-101-S	IW	Axe	22.07.2007				X	
L7-15-102-S	IW	Ice screw	22.07.2007	X				
L7-15-103-S	IW	Ice screw	22.07.2007	X				
L7-15-104-S	IW	Ice screw	22.07.2007	X				
L7-15-105-S	IW	Ice screw	22.07.2007	X				
L7-15-106-S	IW	Ice screw	22.07.2007	X				
L7-15-107-S	IW	Ice screw	22.07.2007	X				
L7-15-108-S	IW	Ice screw	22.07.2007	X				
L7-15-109-S	IW	Ice screw	22.07.2007	X				
L7-15-110-S	IW	Ice screw	22.07.2007	X				
L7-15-01-T	TI		22.07.2007	X				X
L7-15-02-T	TI		22.07.2007	X				X
L7-15-04-T	TI		22.07.2007	X				X
L7-15-07-T	TI		22.07.2007	X				X
L7-15-08-T	TI		22.07.2007	X				X
L7-15-09-T	TI		22.07.2007	X				X
L7-15-10-T	TI		22.07.2007	X				X
L7-15-11-T	TI		22.07.2007	X				X
L7-15-12-T	TI		22.07.2007	X				X
L7-15-18-S	TI		22.07.2007	X				X
L7-15-19-S	TI		22.07.2007	X				X
L7-15-20-S	TI		22.07.2007	X				X
L7-15-21-S	TI		22.07.2007	X				X
L7-15-22-S	TI		22.07.2007	X				X
L18; 73.33512°N; 141.3300°E								
L7-18-101-S	IW	Axe	30.07.2007				X	
L7-18-102-S	IW	Ice screw	30.07.2007	X				
L7-18-103-S	IW	Ice screw	30.07.2007	X				
L7-18-104-S	IW	Ice screw	30.07.2007	X				
L7-18-105-S	IW	Ice screw	30.07.2007	X				
L7-18-106-S	IW	Ice screw	30.07.2007	X				
L7-18-107-S	IW	Ice screw	30.07.2007	X				
L7-18-108-S	IW	Ice screw	30.07.2007	X				
L7-18-109-S	IW	Ice screw	30.07.2007	X				
L7-18-110-S	IW	Ice screw	30.07.2007	X				
L7-18-111-S	IW	Ice screw	30.07.2007	X				
L7-18-112-S	IW	Ice screw	30.07.2007	X				
L7-18-113-S	IW	Ice screw	30.07.2007	X				
L7-18-114-S	IW	Ice screw	30.07.2007	X				
L7-18-115-S	IW	Ice screw	30.07.2007	X				
L7-18-116-S	IW	Ice screw	30.07.2007	X				
L7-18-117-S	IW	Ice screw	30.07.2007	X				
L7-18-118-S	IW	Ice screw	30.07.2007	X				
L7-18-119-S	IW	Ice screw	30.07.2007	X				
L7-18-120-S	IW	Ice screw	30.07.2007	X				
L7-18-121-S	IW	Ice screw	30.07.2007	X				
L7-18-122-S	IW	Ice screw	30.07.2007	X				
L7-18-123-S	IW	Ice screw	30.07.2007	X				
L7-18-124-S	IW	Ice screw	30.07.2007	X				
L7-18-125-S	IW	Ice screw	30.07.2007	X				
L7-18-126-S	IW	Ice screw	30.07.2007	X				
L7-18-01-T	TI		30.07.2007	X				X

Sample number	Sample type	Sampled By	Date	Sampled for measurement of				Corresponding sediment sample
				$\delta^{18}\text{O}/\delta\text{D}$	$^3\text{H}$	Anions/Cations	$^{36}\text{Cl}$	
L7-18-02-T	TI		30.07.2007	X				X
L7-18-03-T	TI		30.07.2007	X				X
L7-18-04-T	TI		30.07.2007	X				X
L7-18-05-T	TI		30.07.2007	X				X
L7-18-06-T	TI		30.07.2007	X				X
L7-18-07-T	TI		30.07.2007	X				X
L7-18-08-T	TI		30.07.2007	X				X
L7-18-11-T	TI		30.07.2007	X				X
L7-18-13-T	TI		30.07.2007	X				X
L7-18-15-T	TI		30.07.2007	X				X
L7-18-16-T	TI		30.07.2007	X				X
L7-18-17-T	TI		30.07.2007	X				X
L7-18-18-T	TI		30.07.2007	X				X
L7-18-19-T	TI		30.07.2007	X				X
L7-18-20-T	TI		30.07.2007	X				X
L7-18-22-T	TI		30.07.2007	X				X

Oy7-01 IW 1, IW 2, IW 3, IW 4, IW 5, IW 6; 72.67509°N; 143.60195°E								
Oy7-01-102-TO	IW	Axe	06.08.2007	X				
Oy7-01-202-TO	IW	Axe	06.08.2007	X				
Oy7-01-301-TO	IW	Axe	06.08.2007				X	
Oy7-01-302-TO	IW	Axe	06.08.2007	X				
Oy7-01-402-TO	IW	Ice screw	06.08.2007	X				
Oy7-01-403-TO	IW	Ice screw	06.08.2007	X				
Oy7-01-404-TO	IW	Ice screw	06.08.2007	X				
Oy7-01-405-TO	IW	Ice screw	06.08.2007	X				
Oy7-01-406-TO	IW	Ice screw	06.08.2007	X				
Oy7-01-502-TO	IW	Axe	05.08.2007	X				
Oy7-01-503-TO	IW	Axe	05.08.2007	X		X		
Oy7-01-504-TO	IW	Axe	05.08.2007	X				
Oy7-01-602-TO	IW	Axe	05.08.2007	X				
Oy7-01 IW 7 and texture ice samples; 72.67454°N; 143.60981°E								
Oy7-01-702-TO	IW	Ice screw	09.08.2007	X				
Oy7-01-703-TO	IW	Ice screw	09.08.2007	X				
Oy7-01-16-S	TI		10.08.2007	X				X
Oy7-01-17-S	TI		11.08.2007	X				X
Oy7-01-18-S	TI		12.08.2007	X				X
Oy7-01-19-S	TI		13.08.2007	X				X
Oy7-01-20-S	TI		14.08.2007	X				X
Oy7-02; 72.68345°N; 143.47892°E								
Oy7-02-101-TO	IW	Axe	07.08.2007				X	
Oy7-02-102-TO	IW	Ice screw	07.08.2007	X				
Oy7-02-103-TO	IW	Ice screw	07.08.2007	X		X		
Oy7-02-104-TO	IW	Ice screw	07.08.2007	X				
Oy7-02-105-TO	IW	Ice screw	07.08.2007	X				
Oy7-02-106-TO	IW	Ice screw	07.08.2007	X				
Oy7-02-107-TO	IW	Ice screw	07.08.2007	X				
Oy7-02-108-TO	IW	Ice screw	07.08.2007	X				
Oy7-02-109-TO	IW	Ice screw	07.08.2007	X		X		
Oy7-02-110-TO	IW	Ice screw	07.08.2007	X				
Oy7-02-111-TO	IW	Ice screw	07.08.2007	X				
Oy7-02-112-TO	IW	Ice screw	07.08.2007	X				
Oy7-02-113-TO	IW	Ice screw	07.08.2007	X				
Oy7-02-114-TO	IW	Ice screw	07.08.2007	X		X		
Oy7-02-115-TO	IW	Ice screw	07.08.2007	X				
Oy7-02-202-TO	IW	Ice screw	07.08.2007	X				
Oy7-02-302-TO	IW	Ice screw	07.08.2007	X				
Oy7-03; 72.67368°N; 143.61408°E								
Oy7-03-101-TO	IW	Axe	08.08.2007				X	
Oy7-03-102-TO	IW	Ice screw	08.08.2007	X		X		
Oy7-03-103-TO	IW	Ice screw	08.08.2007	X				
Oy7-03-104-TO	IW	Ice screw	08.08.2007	X				
Oy7-03-105-TO	IW	Ice screw	08.08.2007	X		X		
Oy7-03-106-TO	IW	Ice screw	08.08.2007	X				
Oy7-03-107-TO	IW	Ice screw	08.08.2007	X				

Sample number	Sample type	Sampled By	Date	Sampled for measurement of				Corresponding sediment sample
				$\delta^{18}\text{O}/\delta\text{D}$	$^3\text{H}$	Anions/Cations	$^{36}\text{Cl}$	
Oy7-03-108-TO	IW	Ice screw	08.08.2007	X		X		
Oy7-03-109-TO	IW	Ice screw	08.08.2007	X				
Oy7-03-110-TO	IW	Ice screw	08.08.2007	X		X		
Oy7-03-111-TO	IW	Ice screw	08.08.2007	X				
Oy7-03-201-TO	IW	Axe	08.08.2007				X	
Oy7-03-202-TO	IW	Ice screw	08.08.2007	X				
Oy7-03-203-TO	IW	Ice screw	08.08.2007	X				
Oy7-03-204-TO	IW	Ice screw	08.08.2007	X		X		
Oy7-03-205-TO	IW	Ice screw	08.08.2007	X				
Oy7-03-206-TO	IW	Ice screw	08.08.2007	X				
Oy7-03-207-TO	TI	Axe	08.08.2007	X				
Oy7-03-208-TO	TI	Axe	08.08.2007	X				
Oy7-03-209-TO	TI	Axe	08.08.2007	X				
Oy7-03-210-TO	TI	Axe	08.08.2007	X				
Oy7-03-302-TO	IW	Axe	08.08.2007	X				
Oy7-03-402-TO	IW	Axe	08.08.2007	X				
Oy7-03-403-TO	IW	Axe	08.08.2007	X				
Oy7-03-404-TO	IW	Axe	08.08.2007	X				
Oy7-03-405-TO	IW	Axe	08.08.2007	X				
Oy7-03-406-TO	TI	Axe	08.08.2007	X				
Oy7-03-407-TO	TI	Axe	08.08.2007	X				
Oy7-03-502-TO	IW	Axe	08.08.2007	X				
Oy7-03-503-TO	IW	Axe	08.08.2007	X				
Oy7-03-01-S	TI		09.08.2007	X				X
Oy7-03-02-S	TI		10.08.2007	X				X
Oy7-03-03-S	TI		11.08.2007	X				X
Oy7-03-04-S	TI		12.08.2007	X				X
Oy7-03-06-S	TI		13.08.2007	X				X
Oy7-03-08-S	TI		14.08.2007	X				X
Oy7-03-10-S	TI		15.08.2007	X				X
Oy7-03-11-S	TI		16.08.2007	X				X
Oy7-04 IW 1, IW 2, IW 4; 72.68146°N; 143.51376°E								
Oy7-04-102-TO	TI	Axe	09.08.2007	X				
Oy7-04-103-TO	IW	Ice screw	09.08.2007	X	X			
Oy7-04-104-TO	IW	Ice screw	09.08.2007	X	X			
Oy7-04-105-TO	IW	Ice screw	09.08.2007	X	X			
Oy7-04-106-TO	IW	Ice screw	09.08.2007	X	X			
Oy7-04-107-TO	IW	Axe	09.08.2007	X		X		
Oy7-04-108-TO	IW	Axe	09.08.2007	X		X		
Oy7-04-109-TO	IW	Ice screw	09.08.2007	X		X		
Oy7-04-201-TO	IW	Axe	11.08.2007				X	
Oy7-04-202-TO	IW	Chain saw	10.08.2007	X				
Oy7-04-203-TO	IW	Chain saw	10.08.2007	X		X		
Oy7-04-204-TO	IW	Chain saw	10.08.2007	X				
Oy7-04-205-TO	IW	Chain saw	10.08.2007	X				
Oy7-04-206-TO	IW	Chain saw	10.08.2007	X				
Oy7-04-207-TO	IW	Chain saw	10.08.2007	X				
Oy7-04-208-TO	IW	Chain saw	10.08.2007	X				
Oy7-04-209-TO	IW	Chain saw	10.08.2007	X				
Oy7-04-210-TO	IW	Chain saw	10.08.2007	X				
Oy7-04-211-TO	IW	Chain saw	10.08.2007	X				
Oy7-04-212-TO	IW	Chain saw	10.08.2007	X				
Oy7-04-213-TO	IW	Chain saw	10.08.2007	X				
Oy7-04-214-TO	IW	Chain saw	10.08.2007	X				
Oy7-04-215-TO	IW	Chain saw	10.08.2007	X				
Oy7-04-216-TO	IW	Chain saw	10.08.2007	X				
Oy7-04-217-TO	IW	Chain saw	10.08.2007	X				
Oy7-04-218-TO	IW	Chain saw	10.08.2007	X				
Oy7-04-219-TO	IW	Chain saw	10.08.2007	X				
Oy7-04-220-TO	IW	Chain saw	10.08.2007	X				
Oy7-04-221-TO	IW	Chain saw	10.08.2007	X				
Oy7-04-222-TO	IW	Chain saw	10.08.2007	X				
Oy7-04-223-TO	IW	Chain saw	10.08.2007	X				
Oy7-04-224-TO	IW	Chain saw	10.08.2007	X				
Oy7-04-225-TO	IW	Chain saw	10.08.2007	X				
Oy7-04-226-TO	IW	Chain saw	10.08.2007	X				

Sample number	Sample type	Sampled By	Date	Sampled for measurement of				Corresponding sediment sample
				$\delta^{18}\text{O}/\delta\text{D}$	$^3\text{H}$	Anions/Cations	$^{36}\text{Cl}$	
Oy7-04-227-TO	IW	Chain saw	10.08.2007	X				
Oy7-04-228-TO	IW	Chain saw	10.08.2007	X				
Oy7-04-229-TO	IW	Chain saw	10.08.2007	X				
Oy7-04-230-TO	IW	Chain saw	10.08.2007	X				
Oy7-04-231-TO	IW	Chain saw	10.08.2007	X				
Oy7-04-232-TO	IW	Chain saw	10.08.2007	X				
Oy7-04-233-TO	IW	Chain saw	10.08.2007	X				
Oy7-04-234-TO	IW	Chain saw	10.08.2007	X				
Oy7-04-235-TO	IW	Chain saw	10.08.2007	X				
Oy7-04-236-TO	IW	Chain saw	10.08.2007	X		X		
Oy7-04-237-TO	IW	Chain saw	10.08.2007	X				
Oy7-04-238-TO	IW	Chain saw	10.08.2007	X				
Oy7-04-239-TO	IW	Chain saw	10.08.2007	X				
Oy7-04-240-TO	IW	Chain saw	10.08.2007	X				
Oy7-04-241-TO	IW	Chain saw	10.08.2007	X		X		
Oy7-04-242-TO	IW	Chain saw	10.08.2007	X				
Oy7-04-243-TO	IW	Chain saw	10.08.2007	X				
Oy7-04-244-TO	IW	Chain saw	10.08.2007	X				
Oy7-04-245-TO	IW	Chain saw	10.08.2007	X				
Oy7-04-246-TO	IW	Chain saw	10.08.2007	X				
Oy7-04-247-TO	IW	Chain saw	10.08.2007	X				
Oy7-04-248-TO	IW	Chain saw	10.08.2007	X		X		
Oy7-04-249-TO	IW	Chain saw	10.08.2007	X				
Oy7-04-250-TO	IW	Chain saw	10.08.2007	X				
Oy7-04-251-TO	IW	Chain saw	10.08.2007	X				
Oy7-04-252-TO	IW	Chain saw	10.08.2007	X				
Oy7-04-253-TO	IW	Chain saw	10.08.2007	X				
Oy7-04-254-TO	IW	Chain saw	10.08.2007	X				
Oy7-04-255-TO	IW	Chain saw	10.08.2007	X				
Oy7-04-256-TO	IW	Chain saw	10.08.2007	X				
Oy7-04-257-TO	IW	Chain saw	10.08.2007	X				
Oy7-04-258-TO	IW	Chain saw	10.08.2007	X				
Oy7-04-259-TO	IW	Chain saw	10.08.2007	X				
Oy7-04-260-TO	IW	Chain saw	10.08.2007	X				
Oy7-04-261-TO	IW	Chain saw	10.08.2007	X				
Oy7-04-262-TO	IW	Chain saw	10.08.2007	X				
Oy7-04-263-TO	IW	Chain saw	10.08.2007	X				
Oy7-04-264-TO	IW	Chain saw	10.08.2007	X				
Oy7-04-265-TO	IW	Chain saw	10.08.2007	X				
Oy7-04-266-TO	IW	Chain saw	10.08.2007	X				
Oy7-04-267-TO	IW	Chain saw	10.08.2007	X				
Oy7-04-268-TO	IW	Chain saw	10.08.2007	X				
Oy7-04-269-TO	IW	Chain saw	10.08.2007	X				
Oy7-04-270-TO	IW	Chain saw	10.08.2007	X				
Oy7-04-271-TO	IW	Chain saw	10.08.2007	X				
Oy7-04-272-TO	IW	Chain saw	10.08.2007	X				
Oy7-04-273-TO	IW	Chain saw	10.08.2007	X				
Oy7-04-274-TO	IW	Chain saw	10.08.2007	X				
Oy7-04-275-TO	IW	Chain saw	10.08.2007	X				
Oy7-04-276-TO	IW	Chain saw	10.08.2007	X				
Oy7-04-277-TO	IW	Chain saw	10.08.2007	X				
Oy7-04-278-TO	IW	Chain saw	10.08.2007	X				
Oy7-04-279-TO	IW	Chain saw	10.08.2007	X				
Oy7-04-280-TO	IW	Chain saw	10.08.2007	X				
Oy7-04-281-TO	IW	Chain saw	10.08.2007	X				
Oy7-04-282-TO	IW	Chain saw	10.08.2007	X				
Oy7-04-283-TO	IW	Chain saw	10.08.2007	X				
Oy7-04-284-TO	IW	Chain saw	10.08.2007	X		X		
Oy7-04-285-TO	IW	Chain saw	10.08.2007	X				
Oy7-04-286-TO	IW	Chain saw	10.08.2007	X				
Oy7-04-287-TO	IW	Chain saw	10.08.2007	X				
Oy7-04-288-TO	IW	Chain saw	10.08.2007	X				
Oy7-04-289-TO	IW	Chain saw	10.08.2007	X		X		
Oy7-04-290-TO	IW	Chain saw	10.08.2007	X				
Oy7-04-291-TO	IW	Chain saw	10.08.2007	X				
Oy7-04-292-TO	IW	Chain saw	10.08.2007	X				

Sample number	Sample type	Sampled By	Date	Sampled for measurement of				Corresponding sediment sample
				$\delta^{18}\text{O}/\delta\text{D}$	$^3\text{H}$	Anions/Cations	$^{36}\text{Cl}$	
Oy7-04-293-TO	IW	Chain saw	10.08.2007	X				
Oy7-04-294-TO	IW	Chain saw	10.08.2007	X				
Oy7-04-295-TO	IW	Chain saw	10.08.2007	X		X		
Oy7-04-296-TO	IW	Chain saw	10.08.2007	X				
Oy7-04-297-TO	IW	Chain saw	10.08.2007	X				
Oy7-04-298-TO	IW	Chain saw	10.08.2007	X				
Oy7-04-299-TO	IW	Chain saw	10.08.2007	X				
Oy7-04-300-TO	IW	Chain saw	10.08.2007	X				
Oy7-04-301-TO	IW	Chain saw	10.08.2007	X				
Oy7-04-302-TO	IW	Chain saw	10.08.2007	X				
Oy7-04-303-TO	IW	Chain saw	10.08.2007	X				
Oy7-04-304-TO	IW	Chain saw	10.08.2007	X				
Oy7-04-305-TO	IW	Chain saw	10.08.2007	X				
Oy7-04-306-TO	IW	Chain saw	10.08.2007	X				
Oy7-04-307-TO	IW	Chain saw	10.08.2007	X				
Oy7-04-308-TO	IW	Chain saw	10.08.2007	X				
Oy7-04-309-TO	IW	Chain saw	10.08.2007	X	X	X		
Oy7-04-310-TO	IW	Chain saw	10.08.2007	X	X	X		
Oy7-04-311-TO	IW	Chain saw	10.08.2007	X	X	X		
Oy7-04-312-TO	IW	Chain saw	10.08.2007	X	X	X		
Oy7-04-313-TO	TI	Axe	11.08.2007	X				
Oy7-04-314-TO	TI	Axe	11.08.2007	X				
Oy7-04-315-TO	TI	Axe	11.08.2007	X				
Oy7-04-316-TO	TI	Axe	11.08.2007	X				
Oy7-04-317-TO	TI	Axe	11.08.2007	X				
Oy7-04-318-TO	TI	Axe	11.08.2007	X				
Oy7-04-319-TO	TI	Axe	11.08.2007	X				
Oy7-04-320-TO	TI	Axe	11.08.2007	X				
Oy7-04-321-TO	TI	Axe	11.08.2007	X				
Oy7-04-322-TO	TI	Axe	11.08.2007	X				
Oy7-04-402-TO	IW	Axe	11.08.2007	X	X			
Oy7-04-403-TO	IW	Axe	11.08.2007	X	X			
Oy7-04-404-TO	TI	Axe	11.08.2007	X				
Oy7-04 IW 5; 72.68172°N; 143.50931°E								
Oy7-04-502-TO	IW	Ice screw	11.08.2007	X	X			
Oy7-04-503-TO	IW	Ice screw	11.08.2007	X				
Oy7-04-504-TO	IW	Ice screw	11.08.2007	X				
Oy7-04-505-TO	IW	Ice screw	11.08.2007	X				
Oy7-04-506-TO	IW	Ice screw	11.08.2007	X	X			
Oy7-04 IW 6 and texture ice samples; 72.68146°N; 143.51376°E								
Oy7-04-602-TO	IW	Axe	12.08.2007	X				
Oy7-04-603-TO	IW	Axe	12.08.2007	X				
Oy7-04-604-TO	IW	Axe	12.08.2007	X				
Oy7-04-02-S	TI		11.08.2007	X				X
Oy7-04-03-S	TI		11.08.2007	X				X
Oy7-04-04-S	TI		11.08.2007	X				X
Oy7-04-05-S	TI		12.08.2007	X				X
Oy7-04-07-S	TI		12.08.2007	X				X
Oy7-05; 72.68104°N; 143.529°E								
Oy7-05-102-TO	IW	Axe	12.08.2007	X				
Oy7-05-103-TO	IW	Axe	12.08.2007	X				
Oy7-05-202-TO	IW	Axe	15.08.2007	X	X			
Oy7-05-203-TO	IW	Axe	15.08.2007	X	X			
Oy7-05-204-TO	IW	Ice screw	15.08.2007	X				
Oy7-05-205-TO	IW	Ice screw	15.08.2007	X				
Oy7-05-206-TO	IW	Ice screw	15.08.2007	X				
Oy7-05-207-TO	IW	Ice screw	15.08.2007	X				
Oy7-05-208-TO	IW	Ice screw	15.08.2007	X				
Oy7-05-209-TO	IW	Ice screw	15.08.2007	X				
Oy7-05-210-TO	IW	Ice screw	15.08.2007	X				
Oy7-05-211-TO	IW	Ice screw	15.08.2007	X				
Oy7-06 IW 1; 72.68131°N; 143.52295°E								
Oy7-06-102-TO	IW	Ice screw	12.08.2007	X		X		
Oy7-06-103-TO	IW	Ice screw	12.08.2007	X				
Oy7-06-104-TO	IW	Ice screw	12.08.2007	X				
Oy7-06-105-TO	IW	Ice screw	12.08.2007	X				

Sample number	Sample type	Sampled By	Date	Sampled for measurement of				Corresponding sediment sample
				$\delta^{18}\text{O}/\delta\text{D}$	$^3\text{H}$	Anions/Cations	$^{36}\text{Cl}$	
Oy7-06-106-TO	IW	Ice screw	12.08.2007	X				
Oy7-06-107-TO	IW	Ice screw	12.08.2007	X		X		
Oy7-06-108-TO	IW	Ice screw	12.08.2007	X				
Oy7-06-109-TO	IW	Ice screw	12.08.2007	X				
Oy7-06-110-TO	IW	Ice screw	12.08.2007	X				
Oy7-06-111-TO	IW	Ice screw	12.08.2007	X				
Oy7-06-112-TO	IW	Ice screw	12.08.2007	X		X		
Oy7-06-113-TO	IW	Ice screw	12.08.2007	X				
Oy7-06-114-TO	IW	Ice screw	12.08.2007	X				
Oy7-06-115-TO	IW	Ice screw	12.08.2007	X				
Oy7-06-116-TO	IW	Ice screw	12.08.2007	X				
Oy7-06-117-TO	IW	Ice screw	12.08.2007	X		X		
Oy7-06-118-TO	IW	Ice screw	12.08.2007	X				
Oy7-06-119-TO	IW	Ice screw	12.08.2007	X				
Oy7-06-120-TO	IW	Ice screw	12.08.2007	X				
Oy7-06-121-TO	IW	Ice screw	12.08.2007	X				
Oy7-06-122-TO	IW	Ice screw	12.08.2007	X		X		
Oy7-06-123-TO	IW	Ice screw	12.08.2007	X				
Oy7-06-124-TO	IW	Ice screw	12.08.2007	X				
Oy7-06-125-TO	IW	Ice screw	12.08.2007	X				
Oy7-06-126-TO	IW	Ice screw	12.08.2007	X				
Oy7-06-127-TO	IW	Ice screw	12.08.2007	X		X		
Oy7-06-128-TO	IW	Ice screw	12.08.2007	X				
Oy7-06-129-TO	IW	Ice screw	12.08.2007	X				
Oy7-06-130-TO	IW	Ice screw	12.08.2007	X				
Oy7-06-131-TO	IW	Ice screw	12.08.2007	X				
Oy7-06-132-TO	IW	Ice screw	12.08.2007	X		X		
Oy7-06-133-TO	IW	Ice screw	12.08.2007	X				
Oy7-06-134-TO	IW	Ice screw	12.08.2007	X				
Oy7-06-135-TO	IW	Ice screw	12.08.2007	X				
Oy7-06-136-TO	IW	Ice screw	12.08.2007	X				
Oy7-06-137-TO	IW	Ice screw	12.08.2007	X		X		
Oy7-06-138-TO	TI	Axe	12.08.2007	X				
Oy7-06-139-TO	TI	Axe	12.08.2007	X				
Oy7-06-140-TO	TI	Axe	12.08.2007	X				
Oy7-06 IW 2; 72.67932°N; 143.52902°E								
Oy7-06-202-TO	IW	Ice screw	14.08.2007	X				
Oy7-06-203-TO	IW	Ice screw	14.08.2007	X		X		
Oy7-06-204-TO	IW	Ice screw	14.08.2007	X				
Oy7-06-205-TO	IW	Ice screw	14.08.2007	X				
Oy7-06-206-TO	IW	Ice screw	14.08.2007	X				
Oy7-06-207-TO	IW	Ice screw	14.08.2007	X				
Oy7-06-208-TO	IW	Ice screw	14.08.2007	X		X		
Oy7-06-209-TO	IW	Ice screw	14.08.2007	X				
Oy7-06-210-TO	IW	Ice screw	14.08.2007	X				
Oy7-06-211-TO	IW	Ice screw	14.08.2007	X				
Oy7-06-212-TO	IW	Ice screw	14.08.2007	X				
Oy7-06-213-TO	IW	Ice screw	14.08.2007	X		X		
Oy7-06-214-TO	IW	Ice screw	14.08.2007	X				
Oy7-06-215-TO	IW	Ice screw	14.08.2007	X				
Oy7-06-216-TO	IW	Ice screw	14.08.2007	X				
Oy7-06-217-TO	IW	Ice screw	14.08.2007	X				
Oy7-06-218-TO	IW	Ice screw	14.08.2007	X		X		
Oy7-06-219-TO	IW	Ice screw	14.08.2007	X				
Oy7-06-220-TO	IW	Ice screw	14.08.2007	X				
Oy7-06-221-TO	IW	Ice screw	14.08.2007	X				
Oy7-06-222-TO	IW	Ice screw	14.08.2007	X				
Oy7-06-223-TO	IW	Ice screw	14.08.2007	X		X		
Oy7-06-224-TO	TI	Axe	14.08.2007	X				
Oy7-06-225-TO	TI	Axe	14.08.2007	X				
Oy7-06-226-TO	TI	Axe	14.08.2007	X				
Oy7-06-227-TO	TI	Axe	14.08.2007	X				
Oy7-06-302-TO	IW?	Ice screw	14.08.2007	X		X		
Oy7-06-303-TO	IW?	Ice screw	14.08.2007	X				
Oy7-07; 72.67865°N; 143.55718°E								
Oy7-07-102-TO	IW	Ice screw	13.08.2007	X				

Sample number	Sample type	Sampled By	Date	Sampled for measurement of				Corresponding sediment sample
				$\delta^{18}\text{O}/\delta\text{D}$	$^3\text{H}$	Anions/Cations	$^{36}\text{Cl}$	
Oy7-07-103-TO	IW	Ice screw	13.08.2007	X				
Oy7-07-104-TO	IW	Ice screw	13.08.2007	X				
Oy7-07-105-TO	IW	Ice screw	13.08.2007	X				
Oy7-07-106-TO	IW	Ice screw	13.08.2007	X				
Oy7-07-108-TO	IW	Ice screw	13.08.2007	X				
Oy7-07-110-TO	IW	Ice screw	13.08.2007	X				
Oy7-07-111-TO	IW	Ice screw	13.08.2007	X				
Oy7-07-302-TO	IW	Axe	14.08.2007	X				
Oy7-07-303-TO	IW	Axe	14.08.2007	X				
Oy7-07-05-S	TI		14.08.2007	X				X
Oy7-07-09-S	TI		14.08.2007	X				X
Oy7-07-10-S	TI		14.08.2007	X				X
Oy7-07-17-S	TI		14.08.2007	X				X
Oy7-08 IW 1; 72.67984°N; 143.53071°E								
Oy7-08-101-TO	IW	Axe	16.08.2007				X	
Oy7-08-102-TO	IW	Ice screw	16.08.2007	X				
Oy7-08-103-TO	IW	Ice screw	16.08.2007	X		X		
Oy7-08-104-TO	IW	Ice screw	16.08.2007	X				
Oy7-08-105-TO	IW	Ice screw	16.08.2007	X				
Oy7-08-106-TO	IW	Ice screw	16.08.2007	X				
Oy7-08-107-TO	IW	Ice screw	16.08.2007	X				
Oy7-08-108-TO	IW	Ice screw	16.08.2007	X		X		
Oy7-08-109-TO	IW	Ice screw	16.08.2007	X				
Oy7-08-110-TO	IW	Ice screw	16.08.2007	X				
Oy7-08-111-TO	IW	Ice screw	16.08.2007	X				
Oy7-08-112-TO	IW	Ice screw	16.08.2007	X				
Oy7-08-113-TO	IW	Ice screw	16.08.2007	X		X		
Oy7-08-114-TO	IW	Ice screw	16.08.2007	X				
Oy7-08-115-TO	IW	Ice screw	16.08.2007	X				
Oy7-08-116-TO	IW	Ice screw	16.08.2007	X				
Oy7-08-117-TO	IW	Ice screw	16.08.2007	X				
Oy7-08-118-TO	IW	Ice screw	16.08.2007	X		X		
Oy7-08-119-TO	IW	Ice screw	16.08.2007	X				
Oy7-08-120-TO	IW	Ice screw	16.08.2007	X				
Oy7-08-121-TO	IW	Ice screw	16.08.2007	X				
Oy7-08-122-TO	IW	Ice screw	16.08.2007	X				
Oy7-08-123-TO	IW	Ice screw	16.08.2007	X		X		
Oy7-08-124-TO	IW	Ice screw	16.08.2007	X				
Oy7-08-125-TO	IW	Ice screw	16.08.2007	X				
Oy7-08-126-TO	IW	Ice screw	16.08.2007	X				
Oy7-08-127-TO	IW	Ice screw	16.08.2007	X				
Oy7-08-128-TO	IW	Ice screw	16.08.2007	X		X		
Oy7-08-129-TO	IW	Ice screw	16.08.2007	X				
Oy7-08-130-TO	IW	Ice screw	16.08.2007	X				
Oy7-08-131-TO	IW	Ice screw	16.08.2007	X				
Oy7-08-132-TO	IW	Ice screw	16.08.2007	X				
Oy7-08-133-TO	IW	Ice screw	16.08.2007	X		X		
Oy7-08-134-TO	IW	Ice screw	16.08.2007	X				
Oy7-08-135-TO	IW	Ice screw	16.08.2007	X				
Oy7-08-136-TO	IW	Ice screw	16.08.2007	X				
Oy7-08-137-TO	IW	Ice screw	16.08.2007	X				
Oy7-08 IW 2; 72.68002°N; 143.53181°E								
Oy7-08-202-TO	IW	Ice screw	17.08.2007	X				
Oy7-08-203-TO	IW	Ice screw	17.08.2007	X				
Oy7-08-204-TO	IW	Ice screw	17.08.2007	X				
Oy7-08 IW 3; 72.67984°N; 143.53071°E								
Oy7-08-302-TO	IW	Ice screw	18.08.2007	X				
Oy7-08-303-TO	IW	Ice screw	18.08.2007	X		X		
Oy7-08-304-TO	IW	Ice screw	18.08.2007	X				
Oy7-08-305-TO	IW	Ice screw	18.08.2007	X				
Oy7-08-306-TO	IW	Ice screw	18.08.2007	X				
Oy7-08-307-TO	IW	Ice screw	18.08.2007	X				
Oy7-08-308-TO	IW	Ice screw	18.08.2007	X		X		
Oy7-08-309-TO	IW	Ice screw	18.08.2007	X				
Oy7-08-310-TO	IW	Ice screw	18.08.2007	X				
Oy7-08-311-TO	IW	Ice screw	18.08.2007	X				

Sample Number	Sample type	Sampled By	Date	Sampled for measurement of				Corresponding sediment sample
				$\delta^{18}\text{O}/\delta\text{D}$	$^3\text{H}$	Anions/Cations	$^{36}\text{Cl}$	
Oy7-08-312-TO	IW	Ice screw	18.08.2007	X				
Oy7-08-313-TO	IW	Ice screw	18.08.2007	X		X		
Oy7-08-314-TO	IW	Ice screw	18.08.2007	X				
Oy7-08-315-TO	IW	Ice screw	18.08.2007	X				
Oy7-08-316-TO	IW	Ice screw	18.08.2007	X				
Oy7-08-317-TO	IW	Ice screw	18.08.2007	X				
Oy7-08-318-TO	IW	Ice screw	18.08.2007	X		X		
Oy7-08-319-TO	IW	Ice screw	18.08.2007	X				
Oy7-08-320-TO	IW	Ice screw	18.08.2007	X				
Oy7-08-321-TO	IW	Ice screw	18.08.2007	X				
Oy7-08-322-TO	IW	Ice screw	18.08.2007	X				
Oy7-08-323-TO	IW	Ice screw	18.08.2007	X		X		
Oy7-08-324-TO	IW	Ice screw	18.08.2007	X				
Oy7-08-325-TO	IW	Ice screw	18.08.2007	X				
Oy7-08-326-TO	IW	Ice screw	18.08.2007	X				
Oy7-08-327-TO	IW	Ice screw	18.08.2007	X				
Oy7-08-328-TO	IW	Ice screw	18.08.2007	X		X		
Oy7-08-329-TO	IW	Ice screw	18.08.2007	X				
Oy7-08-330-TO	IW	Ice screw	18.08.2007	X				
Oy7-08-331-TO	IW	Ice screw	18.08.2007	X				
Oy7-08-332-TO	IW	Ice screw	18.08.2007	X				
Oy7-08-333-TO	IW	Ice screw	18.08.2007	X		X		
Oy7-08-334-TO	TI	Axe	18.08.2007	X				
Oy7-08-335-TO	IW	Ice screw	18.08.2007	X				
Oy7-08-336-TO	IW	Ice screw	18.08.2007	X				
Oy7-08 IW 4; 72.67618°N; 143.57487°E								
Oy7-08-402-TO	IW	Ice screw	19.08.2007	X				
Oy7-08-403-TO	IW	Ice screw	19.08.2007	X		X		
Oy7-08-404-TO	IW	Ice screw	19.08.2007	X				
Oy7-08-405-TO	IW	Ice screw	19.08.2007	X				
Oy7-08-406-TO	IW	Ice screw	19.08.2007	X				
Oy7-08-407-TO	IW	Ice screw	19.08.2007	X				
Oy7-08-408-TO	IW	Ice screw	19.08.2007	X		X		
Oy7-08-409-TO	IW	Ice screw	19.08.2007	X				
Oy7-08-410-TO	IW	Ice screw	19.08.2007	X				
Oy7-08-411-TO	IW	Ice screw	19.08.2007	X				
Oy7-08-412-TO	IW	Ice screw	19.08.2007	X				
Oy7-08-413-TO	IW	Ice screw	19.08.2007	X		X		
Oy7-08-414-TO	IW	Ice screw	19.08.2007	X				
Oy7-08-415-TO	IW	Ice screw	19.08.2007	X				
Oy7-08-416-TO	IW	Ice screw	19.08.2007	X				
Oy7-08-417-TO	IW	Ice screw	19.08.2007	X				
Oy7-08-418-TO	IW	Ice screw	19.08.2007	X		X		
Oy7-08-419-TO	IW	Ice screw	19.08.2007	X				
Oy7-08-420-TO	IW	Ice screw	19.08.2007	X				
Oy7-08-421-TO	IW	Ice screw	19.08.2007	X				
Oy7-08-422-TO	IW	Ice screw	19.08.2007	X				
Oy7-08-423-TO	IW	Ice screw	19.08.2007	X		X		
Oy7-08-424-TO	IW	Ice screw	19.08.2007	X				
Oy7-08-425-TO	IW	Ice screw	19.08.2007	X				
Oy7-08-426-TO	IW	Ice screw	19.08.2007	X				
Oy7-08-427-TO	IW	Ice screw	19.08.2007	X				
Oy7-08-428-TO	IW	Ice screw	19.08.2007	X		X		
Oy7-08-429-TO	IW	Ice screw	19.08.2007	X				
Oy7-08-430-TO	TI	axe	19.08.2007	X				
Oy7-08-431-TO	TI	axe	19.08.2007	X				
Oy7-08 IW 5; 72,6808167 N; 143,5293500 E								
Oy7-08-502-TO	IW	Axe	26.08.2007	X				
Oy7-08-503-TO	IW	Axe	26.08.2007	X				
Oy7-08 texture ice samples; different coordinates, see chapter 6.1 (list of sediment samples)								
Oy7-08-31-S	TI		17.08.2007	X				X
Oy7-08-32-S	TI		17.08.2007	X				X
Oy7-08-34-S	TI		17.08.2007	X				X
Oy7-08-35-S	TI		17.08.2007	X				X
Oy7-08-36-S	TI		17.08.2007	X				X
Oy7-08-37-S	TI		17.08.2007	X				X

Sample Number	Sample type	Sampled By	Date	Sampled for measurement of				Corresponding sediment sample
				$\delta^{18}\text{O}/\delta\text{D}$	$^3\text{H}$	Anions/Cations	$^{36}\text{Cl}$	
Oy7-08-38-S	TI		17.08.2007	X				X
Oy7-08-40-S	TI		17.08.2007	X				X
Oy7-08-41-S	TI		17.08.2007	X				X
Oy7-08-42-S	TI		17.08.2007	X				X
Oy7-08-43-S	TI		17.08.2007	X				X
Oy7-08-45-S	TI		17.08.2007	X				X
Oy7-08-46-S	TI		17.08.2007	X				X
Oy7-08-47-S	TI		17.08.2007	X				X
Oy7-08-48-S	TI		17.08.2007	X				X
Oy7-08-49-S	TI		17.08.2007	X				X
Oy7-08-50-S	TI		17.08.2007	X				X
Oy7-08-51-S	TI		17.08.2007	X				X
Oy7-08-52-S	TI		17.08.2007	X				X
Oy7-08-53-S	TI		17.08.2007	X				X
Oy7-08-54-S	TI		17.08.2007	X				X
Oy7-08-55-S	TI		17.08.2007	X				X
Oy7-08-56-S	TI		17.08.2007	X				X
Oy7-08-57-S	TI		17.08.2007	X				X
Oy7-08-58-S	TI		17.08.2007	X				X
Oy7-08-59-S	TI		17.08.2007	X				X
Oy7-08-60-S	TI		17.08.2007	X				X
Oy7-08-61-S	TI		17.08.2007	X				X
Oy7-08-62-S	TI		17.08.2007	X				X
Oy7-08-63-S	TI		17.08.2007	X				X
Oy7-08-64-S	TI		17.08.2007	X				X
Oy7-08-65-S	TI		17.08.2007	X				X
Oy7-10; 72.672°N; 143.63514°E								
Oy7-10-02-S	TI		14.08.2007	X				X
Oy7-10-03-S	TI		14.08.2007	X				X
Oy7-10-05-S	TI		14.08.2007	X				X
Oy7-10-06-S	TI		14.08.2007	X				X
Oy7-10-07-S	TI		14.08.2007	X				X
Oy7-10-08-S	TI		14.08.2007	X				X
Oy7-11 IW 1; 72.68262°N; 143.48736°E								
Oy7-11-102-TO	IW	Chain saw	21.08.2007	X				
Oy7-11-103-TO	IW	Chain saw	21.08.2007	X		X		
Oy7-11-104-TO	IW	Chain saw	21.08.2007	X				
Oy7-11-105-TO	IW	Chain saw	21.08.2007	X				
Oy7-11-106-TO	IW	Chain saw	21.08.2007	X				
Oy7-11-107-TO	IW	Chain saw	21.08.2007	X				
Oy7-11-108-TO	IW	Chain saw	21.08.2007	X				
Oy7-11-109-TO	IW	Chain saw	21.08.2007	X				
Oy7-11-110-TO	IW	Chain saw	21.08.2007	X				
Oy7-11-111-TO	IW	Chain saw	21.08.2007	X				
Oy7-11-112-TO	IW	Chain saw	21.08.2007	X				
Oy7-11-113-TO	IW	Chain saw	21.08.2007	X		X		
Oy7-11-114-TO	IW	Chain saw	21.08.2007	X				
Oy7-11-115-TO	IW	Chain saw	21.08.2007	X				
Oy7-11-116-TO	IW	Chain saw	21.08.2007	X				
Oy7-11-117-TO	IW	Chain saw	21.08.2007	X				
Oy7-11-118-TO	IW	Chain saw	21.08.2007	X				
Oy7-11-119-TO	IW	Chain saw	21.08.2007	X				
Oy7-11-120-TO	IW	Chain saw	21.08.2007	X				
Oy7-11-121-TO	IW	Chain saw	21.08.2007	X				
Oy7-11-122-TO	IW	Chain saw	21.08.2007	X				
Oy7-11-123-TO	IW	Chain saw	21.08.2007	X		X		
Oy7-11-124-TO	IW	Chain saw	21.08.2007	X				
Oy7-11-125-TO	IW	Chain saw	21.08.2007	X				
Oy7-11-126-TO	IW	Chain saw	21.08.2007	X				
Oy7-11-127-TO	IW	Chain saw	21.08.2007	X				
Oy7-11-128-TO	IW	Chain saw	21.08.2007	X				
Oy7-11-129-TO	IW	Chain saw	21.08.2007	X				
Oy7-11-130-TO	IW	Chain saw	21.08.2007	X				
Oy7-11-131-TO	IW	Chain saw	21.08.2007	X				
Oy7-11-132-TO	IW	Chain saw	21.08.2007	X				
Oy7-11-133-TO	IW	Chain saw	21.08.2007	X		X		

Sample number	Sample type	Sampled By	Date	Sampled for measurement of				Corresponding sediment sample
				$\delta^{18}\text{O}/\delta\text{D}$	$^3\text{H}$	Anions/Cations	$^{36}\text{Cl}$	
Oy7-11-134-TO	IW	Chain saw	21.08.2007	X				
Oy7-11-135-TO	IW	Chain saw	21.08.2007	X				
Oy7-11-136-TO	IW	Chain saw	21.08.2007	X				
Oy7-11-137-TO	IW	Chain saw	21.08.2007	X				
Oy7-11-138-TO	IW	Chain saw	21.08.2007	X				
Oy7-11-139-TO	IW	Chain saw	21.08.2007	X				
Oy7-11-140-TO	IW	Chain saw	21.08.2007	X				
Oy7-11-141-TO	IW	Chain saw	21.08.2007	X				
Oy7-11-142-TO	IW	Chain saw	21.08.2007	X				
Oy7-11-143-TO	IW	Chain saw	21.08.2007	X		X		
Oy7-11-144-TO	IW	Chain saw	21.08.2007	X				
Oy7-11-145-TO	IW	Chain saw	21.08.2007	X				
Oy7-11-146-TO	IW	Chain saw	21.08.2007	X				
Oy7-11-147-TO	IW	Chain saw	21.08.2007	X				
Oy7-11-148-TO	IW	Chain saw	21.08.2007	X				
Oy7-11-149-TO	IW	Chain saw	21.08.2007	X				
Oy7-11-150-TO	IW	Chain saw	21.08.2007	X				
Oy7-11-151-TO	IW	Chain saw	21.08.2007	X				
Oy7-11-152-TO	IW	Chain saw	21.08.2007	X				
Oy7-11-153-TO	IW	Chain saw	21.08.2007	X		X		
Oy7-11-154-TO	IW	Chain saw	21.08.2007	X				
Oy7-11-155-TO	IW	Chain saw	21.08.2007	X				
Oy7-11-156-TO	IW	Chain saw	21.08.2007	X				
Oy7-11-157-TO	IW	Chain saw	21.08.2007	X				
Oy7-11-158-TO	IW	Chain saw	21.08.2007	X				
Oy7-11-159-TO	IW	Chain saw	21.08.2007	X				
Oy7-11-160-TO	IW	Chain saw	21.08.2007	X				
Oy7-11-161-TO	IW	Chain saw	21.08.2007	X				
Oy7-11-162-TO	IW	Chain saw	21.08.2007	X				
Oy7-11-163-TO	IW	Chain saw	21.08.2007	X		X		
Oy7-11-164-TO	IW	Chain saw	21.08.2007	X				
Oy7-11-165-TO	IW	Chain saw	21.08.2007	X				
Oy7-11-166-TO	IW	Chain saw	21.08.2007	X				
Oy7-11-167-TO	IW	Chain saw	21.08.2007	X				
Oy7-11-168-TO	IW	Chain saw	21.08.2007	X				
Oy7-11-169-TO	IW	Chain saw	21.08.2007	X				
Oy7-11-170-TO	IW	Chain saw	21.08.2007	X				
Oy7-11-171-TO	IW	Chain saw	21.08.2007	X				
Oy7-11-172-TO	IW	Chain saw	21.08.2007	X				
Oy7-11-173-TO	IW	Chain saw	21.08.2007	X		X		
Oy7-11-174-TO	IW	Chain saw	21.08.2007	X				
Oy7-11-175-TO	IW	Chain saw	21.08.2007	X				
Oy7-11-176-TO	IW	Chain saw	21.08.2007	X				
Oy7-11-177-TO	IW	Chain saw	21.08.2007	X				
Oy7-11-178-TO	IW	Chain saw	21.08.2007	X				
Oy7-11-179-TO	IW	Chain saw	21.08.2007	X				
Oy7-11-180-TO	IW	Chain saw	21.08.2007	X				
Oy7-11-181-TO	IW	Chain saw	21.08.2007	X				
Oy7-11-182-TO	IW	Chain saw	21.08.2007	X				
Oy7-11-183-TO	IW	Chain saw	21.08.2007	X		X		
Oy7-11-184-TO	IW	Chain saw	21.08.2007	X				
Oy7-11-185-TO	IW	Chain saw	21.08.2007	X				
Oy7-11-186-TO	IW	Chain saw	21.08.2007	X				
Oy7-11-187-TO	IW	Chain saw	21.08.2007	X				
Oy7-11-188-TO	IW	Chain saw	21.08.2007	X				
Oy7-11-189-TO	IW	Chain saw	21.08.2007	X				
Oy7-11-190-TO	IW	Chain saw	21.08.2007	X				
Oy7-11-191-TO	IW	Chain saw	21.08.2007	X				
Oy7-11-192-TO	IW	Chain saw	21.08.2007	X				
Oy7-11-193-TO	IW	Chain saw	21.08.2007	X		X		
Oy7-11-194-TO	IW	Chain saw	21.08.2007	X				
Oy7-11-195-TO	IW	Chain saw	21.08.2007	X				
Oy7-11-196-TO	IW	Chain saw	21.08.2007	X				
Oy7-11-197-TO	IW	Chain saw	21.08.2007	X				
Oy7-11-198-TO	IW	Chain saw	21.08.2007	X				
Oy7-11-199-TO	IW	Chain saw	21.08.2007	X				

Sample number	Sample type	Sampled By	Date	Sampled for measurement of				Corresponding sediment sample
				$\delta^{18}\text{O}/\delta\text{D}$	$^3\text{H}$	Anions/Cations	$^{36}\text{Cl}$	
Oy7-11-200-TO	IW	Chain saw	21.08.2007	X				
Oy7-11-201-TO	IW	Chain saw	21.08.2007	X				
Oy7-11-202-TO	IW	Chain saw	21.08.2007	X				
Oy7-11-203-TO	IW	Chain saw	21.08.2007	X				
Oy7-11-204-TO	IW	Chain saw	21.08.2007	X				
Oy7-11-205-TO	IW	Chain saw	21.08.2007	X				
Oy7-11-206-TO	IW	Chain saw	21.08.2007	X				
Oy7-11-207-TO	IW	Chain saw	21.08.2007	X				
Oy7-11-208-TO	IW	Chain saw	21.08.2007	X				
Oy7-11-209-TO	IW	Chain saw	21.08.2007	X				
Oy7-11-210-TO	IW	Chain saw	21.08.2007	X				
Oy7-11-211-TO	IW	Chain saw	21.08.2007	X				
Oy7-11-212-TO	IW	Chain saw	21.08.2007	X				
Oy7-11-213-TO	IW	Chain saw	21.08.2007	X				
Oy7-11-214-TO	IW	Chain saw	21.08.2007	X				
Oy7-11-215-TO	IW	Chain saw	21.08.2007	X		X		
Oy7-11-216-TO	IW	Chain saw	21.08.2007	X				
Oy7-11-217-TO	IW	Chain saw	21.08.2007	X				
Oy7-11-218-TO	IW	Chain saw	21.08.2007	X				
Oy7-11-219-TO	IW	Chain saw	21.08.2007	X				
Oy7-11-220-TO	IW	Chain saw	21.08.2007	X				
Oy7-11-221-TO	IW	Chain saw	21.08.2007	X				
Oy7-11-222-TO	IW	Chain saw	21.08.2007	X				
Oy7-11-223-TO	IW	Chain saw	21.08.2007	X				
Oy7-11-224-TO	IW	Chain saw	21.08.2007	X				
Oy7-11-225-TO	IW	Axe	21.08.2007	X	X			
Oy7-11-226-TO	TI	Axe	21.08.2007	X				
Oy7-11-227-TO	TI	Axe	21.08.2007	X				
Oy7-11-228-TO	TI	Axe	21.08.2007	X				
Oy7-11 IW 3; 72.68347°N; 143.47526°E								
Oy7-11-302-TO	IW	Axe	23.08.2007	X				
Oy7-11-303-TO	IW	Axe	23.08.2007	X				
Oy7-11-304-TO	IW	Axe	23.08.2007	X				
Oy7-11 IW 4; 72.68274°N; 143.49014°E								
Oy7-11-402-TO	IW	Axe	27.08.2007	X	X			
Oy7-11-403-TO	IW	Axe	27.08.2007	X	X			
Oy7-11-404-TO	TI	Axe	27.08.2007	X				
Oy7-11 IW 5; 72.68298°N; 143.48462°E								
Oy7-11-502-TO	IW	Ice screw	27.08.2007	X				
Oy7-11-503-TO	IW	Ice screw	27.08.2007	X				
Oy7-11-504-TO	IW	Ice screw	27.08.2007	X				
Oy7-11-505-TO	IW	Ice screw	27.08.2007	X				
Oy7-11-506-TO	IW	Ice screw	27.08.2007	X				
Oy7-11-507-TO	IW	Ice screw	27.08.2007	X				
Oy7-11-508-TO	IW	Axe	27.08.2007	X	X			
Oy7-11-702-TO	TI	Chain saw+	29.08.2007	X				
Oy7-11-703-TO	TI	Chain saw+	29.08.2007	X				
Oy7-11-704-TO	TI	Chain saw+	29.08.2007	X				
Oy7-11-705-TO	TI	Chain saw+	29.08.2007	X				
Oy7-11-706-TO	TI	Chain saw+	29.08.2007	X				
Oy7-11-707-TO	IW	Chain saw+	29.08.2007	X				
Oy7-11-708-TO	IW	Chain saw+	29.08.2007	X				
Oy7-11-709-TO	IW	Chain saw+	29.08.2007	X				
Oy7-11-710-TO	IW	Chain saw+	29.08.2007	X				
Oy7-11-711-TO	IW	Chain saw+	29.08.2007	X				
Oy7-11-712-TO	IW	Chain saw+	29.08.2007	X				
Oy7-11-713-TO	IW	Chain saw+	29.08.2007	X				
Oy7-11-714-TO	IW	Chain saw+	29.08.2007	X				
Oy7-11-715-TO	IW	Chain saw+	29.08.2007	X				
Oy7-11-716-TO	IW	Chain saw+	29.08.2007	X				
Oy7-11-717-TO	IW	Chain saw+	29.08.2007	X				
Oy7-11-718-TO	IW	Chain saw+	29.08.2007	X				
Oy7-11-719-TO	IW	Chain saw+	29.08.2007	X				
Oy7-11-720-TO	IW	Chain saw+	29.08.2007	X				
Oy7-11-721-TO	IW	Chain saw+	29.08.2007	X				
Oy7-11-722-TO	IW	Chain saw+	29.08.2007	X				

Sample number	Sample type	Sampled By	Date	Sampled for measurement of				Corresponding sediment sample
				$\delta^{18}\text{O}/\delta\text{D}$	$^3\text{H}$	Anions/Cations	$^{36}\text{Cl}$	
Oy7-11-723-TO	IW	Chain saw+	29.08.2007	X				
Oy7-11-724-TO	IW	Chain saw+	29.08.2007	X				
Oy7-11-725-TO	IW	Chain saw+	29.08.2007	X				
Oy7-11-726-TO	IW	Chain saw+	29.08.2007	X				
Oy7-11-727-TO	IW	Chain saw+	29.08.2007	X				
Oy7-11-728-TO	IW	Chain saw+	29.08.2007	X				
Oy7-11-729-TO	IW	Chain saw+	29.08.2007	X				
Oy7-11-730-TO	IW	Chain saw+	29.08.2007	X				
Oy7-11-731-TO	IW	Chain saw+	29.08.2007	X				
Oy7-11-732-TO	IW	Chain saw+	29.08.2007	X				
Oy7-11-733-TO	IW	Chain saw+	29.08.2007	X				
Oy7-11-734-TO	IW	Chain saw+	29.08.2007	X				
Oy7-11-735-TO	IW	Chain saw+	29.08.2007	X				
Oy7-11-736-TO	IW	Chain saw+	29.08.2007	X				
Oy7-11-737-TO	IW	Chain saw+	29.08.2007	X				
Oy7-11-738-TO	IW	Chain saw+	29.08.2007	X				
Oy7-11-739-TO	IW	Chain saw+	29.08.2007	X				
Oy7-11-740-TO	IW	Chain saw+	29.08.2007	X				
Oy7-11-741-TO	IW	Chain saw+	29.08.2007	X				
Oy7-11-742-TO	IW	Chain saw+	29.08.2007	X				
Oy7-11-743-TO	IW	Chain saw+	29.08.2007	X				
Oy7-11-744-TO	IW	Chain saw+	29.08.2007	X				
Oy7-11-745-TO	IW	Chain saw+	29.08.2007	X				
Oy7-11-746-TO	IW	Chain saw+	29.08.2007	X				
Oy7-11-747-TO	IW	Chain saw+	29.08.2007	X				
Oy7-11-748-TO	IW	Chain saw+	29.08.2007	X				
Oy7-11-749-TO	IW	Chain saw+	29.08.2007	X				
Oy7-11-750-TO	IW	Chain saw+	29.08.2007	X				
Oy7-11-751-TO	IW	Chain saw+	29.08.2007	X				
Oy7-11-752-TO	IW	Chain saw+	29.08.2007	X				
Oy7-11-753-TO	IW	Chain saw+	29.08.2007	X				
Oy7-11-754-TO	IW	Chain saw+	29.08.2007	X				
Oy7-11-755-TO	IW	Chain saw+	29.08.2007	X				
Oy7-11-756-TO	IW	Chain saw+	29.08.2007	X				
Oy7-11-757-TO	IW	Chain saw+	29.08.2007	X				
Oy7-11-758-TO	IW	Chain saw+	29.08.2007	X				
Oy7-11-759-TO	IW	Chain saw+	29.08.2007	X				
Oy7-11-760-TO	IW	Chain saw+	29.08.2007	X				
Oy7-11-761-TO	IW	Chain saw+	29.08.2007	X				
Oy7-11-762-TO	IW	Chain saw+	29.08.2007	X				
Oy7-11-763-TO	IW	Chain saw+	29.08.2007	X				
Oy7-11-764-TO	IW	Chain saw+	29.08.2007	X				
Oy7-11-765-TO	IW	Chain saw+	29.08.2007	X				
Oy7-11-766-TO	IW	Chain saw+	29.08.2007	X				
Oy7-11-767-TO	IW	Chain saw+	29.08.2007	X				
Oy7-11-768-TO	IW	Chain saw+	29.08.2007	X				
Oy7-11-769-TO	IW	Chain saw+	29.08.2007	X				
Oy7-11-770-TO	IW	Chain saw+	29.08.2007	X				
Oy7-11-771-TO	IW	Chain saw+	29.08.2007	X				
Oy7-11-772-TO	IW	Chain saw+	29.08.2007	X				
Oy7-11-773-TO	IW	Chain saw+	29.08.2007	X				
Oy7-11-774-TO	IW	Chain saw+	29.08.2007	X				
Oy7-11-775-TO	IW	Chain saw+	29.08.2007	X				
Oy7-11-776-TO	IW	Chain saw+	29.08.2007	X				
Oy7-11-777-TO	IW	Chain saw+	29.08.2007	X				
Oy7-11-778-TO	IW	Chain saw+	29.08.2007	X				
Oy7-11-779-TO	IW	Chain saw+	29.08.2007	X				
Oy7-11-780-TO	IW	Chain saw+	29.08.2007	X				
Oy7-11-781-TO	IW	Chain saw+	29.08.2007	X				
Oy7-11-782-TO	IW	Chain saw+	29.08.2007	X				
Oy7-11-783-TO	IW	Chain saw+	29.08.2007	X				
Oy7-11-784-TO	IW	Chain saw+	29.08.2007	X				
Oy7-11-785-TO	IW	Chain saw+	29.08.2007	X				
Oy7-11-786-TO	IW	Chain saw+	29.08.2007	X				
Oy7-11-787-TO	IW	Chain saw+	29.08.2007	X				
Oy7-11-788-TO	IW	Chain saw+	29.08.2007	X				

Sample number	Sample type	Sampled By	Date	Sampled for measurement of				Corresponding sediment sample
				$\delta^{18}\text{O}/\delta\text{D}$	$^3\text{H}$	Anions/Cations	$^{36}\text{Cl}$	
Oy7-11-789-TO	IW	Chain saw+	29.08.2007	X				
Oy7-11-790-TO	IW	Chain saw+	29.08.2007	X				
Oy7-11-791-TO	IW	Chain saw+	29.08.2007	X				
Oy7-11-792-TO	IW	Chain saw+	29.08.2007	X				
Oy7-11-793-TO	IW	Chain saw+	29.08.2007	X				
Oy7-11-794-TO	IW	Chain saw+	29.08.2007	X				
Oy7-11-795-TO	IW	Chain saw+	29.08.2007	X				
Oy7-11-796-TO	IW	Chain saw+	29.08.2007	X				
Oy7-11-797-TO	IW	Chain saw+	29.08.2007	X				
Oy7-11-798-TO	IW	Chain saw+	29.08.2007	X				
Oy7-11-799-TO	IW	Chain saw+	29.08.2007	X				
Oy7-11-800-TO	IW	Chain saw+	29.08.2007	X				
Oy7-11-801-TO	IW	Chain saw+	29.08.2007	X				
Oy7-11-802-TO	IW	Chain saw+	29.08.2007	X				
Oy7-11-803-TO	IW	Chain saw+	29.08.2007	X				
Oy7-11-804-TO	IW	Chain saw+	29.08.2007	X				
Oy7-11-805-TO	IW	Chain saw+	29.08.2007	X				
Oy7-11-806-TO	IW	Chain saw+	29.08.2007	X				
Oy7-11-807-TO	IW	Chain saw+	29.08.2007	X				
Oy7-11-808-TO	IW	Chain saw+	29.08.2007	X				
Oy7-11-809-TO	IW	Chain saw+	29.08.2007	X				
Oy7-11-810-TO	IW	Chain saw+	29.08.2007	X				
Oy7-11-811-TO	IW	Chain saw+	29.08.2007	X				
Oy7-11-812-TO	IW	Chain saw+	29.08.2007	X				
Oy7-11-813-TO	IW	Chain saw+	29.08.2007	X				
Oy7-11-814-TO	IW	Chain saw+	29.08.2007	X				
Oy7-11-815-TO	IW	Chain saw+	29.08.2007	X				
Oy7-11-816-TO	IW	Chain saw+	29.08.2007	X				
Oy7-11-817-TO	IW	Chain saw+	29.08.2007	X				
Oy7-11-818-TO	IW	Chain saw+	29.08.2007	X				
Oy7-11-819-TO	IW	Chain saw+	29.08.2007	X				
Oy7-11-820-TO	IW	Chain saw+	29.08.2007	X				
Oy7-11-821-TO	IW	Chain saw+	29.08.2007	X				
Oy7-11-822-TO	IW	Chain saw+	29.08.2007	X				
Oy7-11-823-TO	IW	Chain saw+	29.08.2007	X				
Oy7-11-824-TO	IW	Chain saw+	29.08.2007	X				
Oy7-11-825-TO	IW	Chain saw+	29.08.2007	X				
Oy7-11-826-TO	IW	Chain saw+	29.08.2007	X				
Oy7-11-827-TO	IW	Chain saw+	29.08.2007	X				
Oy7-11-828-TO	IW	Chain saw+	29.08.2007	X				
Oy7-11-829-TO	IW	Chain saw+	29.08.2007	X				
Oy7-11-830-TO	IW	Chain saw+	29.08.2007	X				
Oy7-11-831-TO	IW	Chain saw+	29.08.2007	X				
Oy7-11-832-TO	IW	Chain saw+	29.08.2007	X				
Oy7-11-833-TO	IW	Chain saw+	29.08.2007	X				
Oy7-11-834-TO	IW	Chain saw+	29.08.2007	X				
Oy7-11-835-TO	IW	Chain saw+	29.08.2007	X				
Oy7-11-836-TO	IW	Chain saw+	29.08.2007	X				
Oy7-11-837-TO	IW	Chain saw+	29.08.2007	X				
Oy7-11-838-TO	IW	Chain saw+	29.08.2007	X				
Oy7-11-839-TO	IW	Chain saw+	29.08.2007	X				
Oy7-11-840-TO	IW	Chain saw+	29.08.2007	X				
Oy7-11-841-TO	IW	Chain saw+	29.08.2007	X				
Oy7-11-842-TO	IW	Chain saw+	29.08.2007	X				
Oy7-11-843-TO	IW	Chain saw+	29.08.2007	X				
Oy7-11-844-TO	IW	Chain saw+	29.08.2007	X				
Oy7-11-845-TO	IW	Chain saw+	29.08.2007	X				
Oy7-11-846-TO	IW	Chain saw+	29.08.2007	X				
Oy7-11-847-TO	IW	Chain saw+	29.08.2007	X				
Oy7-11-848-TO	IW	Chain saw+	29.08.2007	X				
Oy7-11-849-TO	IW	Chain saw+	29.08.2007	X				
Oy7-11-850-TO	IW	Chain saw+	29.08.2007	X				
Oy7-11-851-TO	IW	Chain saw+	29.08.2007	X				
Oy7-11-852-TO	IW	Chain saw+	29.08.2007	X				
Oy7-11-853-TO	IW	Chain saw+	29.08.2007	X				
Oy7-11-854-TO	IW	Chain saw+	29.08.2007	X				

Sample number	Sample type	Sampled By	Date	Sampled for measurement of				Corresponding sediment sample
				$\delta^{18}\text{O}/\delta\text{D}$	$^3\text{H}$	Anions/Cations	$^{36}\text{Cl}$	
Oy7-11-855-TO	IW	Chain saw+	29.08.2007	X				
Oy7-11-856-TO	IW	Chain saw+	29.08.2007	X				
Oy7-11-857-TO	IW	Chain saw+	29.08.2007	X				
Oy7-11-858-TO	IW	Chain saw+	29.08.2007	X				
Oy7-11-859-TO	IW	Chain saw+	29.08.2007	X				
Oy7-11-860-TO	IW	Chain saw+	29.08.2007	X				
Oy7-11-861-TO	IW	Chain saw+	29.08.2007	X				
Oy7-11-862-TO	IW	Chain saw+	29.08.2007	X				
Oy7-11-863-TO	IW	Chain saw+	29.08.2007	X				
Oy7-11-864-TO	IW	Chain saw+	29.08.2007	X				
Oy7-11-865-TO	IW	Chain saw+	29.08.2007	X				
Oy7-11-866-TO	IW	Chain saw+	29.08.2007	X				
Oy7-11-867-TO	IW	Chain saw+	29.08.2007	X				
Oy7-11-868-TO	IW	Chain saw+	29.08.2007	X				
Oy7-11-869-TO	IW	Chain saw+	29.08.2007	X				
Oy7-11-870-TO	IW	Chain saw+	29.08.2007	X				
Oy7-11-871-TO	IW	Chain saw+	29.08.2007	X				
Oy7-11-872-TO	IW	Chain saw+	29.08.2007	X				
Oy7-11-873-TO	IW	Chain saw+	29.08.2007	X				
Oy7-11-874-TO	IW	Chain saw+	29.08.2007	X				
Oy7-11-875-TO	IW	Chain saw+	29.08.2007	X				
Oy7-11-876-TO	IW	Chain saw+	29.08.2007	X				
Oy7-11-877-TO	IW	Chain saw+	29.08.2007	X				
Oy7-11-878-TO	IW	Chain saw+	29.08.2007	X				
Oy7-11-879-TO	IW	Chain saw+	29.08.2007	X				
Oy7-11-880-TO	IW	Chain saw+	29.08.2007	X				
Oy7-11-881-TO	IW	Chain saw+	29.08.2007	X				
Oy7-11-882-TO	IW	Chain saw+	29.08.2007	X				
Oy7-11-883-TO	IW	Chain saw+	29.08.2007	X				
Oy7-11-884-TO	IW	Chain saw+	29.08.2007	X				
Oy7-11-885-TO	IW	Chain saw+	29.08.2007	X				
Oy7-11-886-TO	IW	Chain saw+	29.08.2007	X				
Oy7-11-887-TO	IW	Chain saw+	29.08.2007	X				
Oy7-11-888-TO	IW	Chain saw+	29.08.2007	X				
Oy7-11-889-TO	IW	Chain saw+	29.08.2007	X				
Oy7-11-890-TO	IW	Chain saw+	29.08.2007	X				
Oy7-11-891-TO	IW	Chain saw+	29.08.2007	X				
Oy7-11-892-TO	IW	Chain saw+	29.08.2007	X				
Oy7-11-893-TO	IW	Chain saw+	29.08.2007	X				
Oy7-11-894-TO	IW	Chain saw+	29.08.2007	X				
Oy7-11-895-TO	IW	Chain saw+	29.08.2007	X				
Oy7-11-896-TO	IW	Chain saw+	29.08.2007	X				
Oy7-11-897-TO	IW	Chain saw+	29.08.2007	X				
Oy7-11-898-TO	IW	Chain saw+	29.08.2007	X				
Oy7-11-899-TO	IW	Chain saw+	29.08.2007	X				
Oy7-11-900-TO	IW	Chain saw+	29.08.2007	X				
Oy7-11-901-TO	IW	Chain saw+	29.08.2007	X				
Oy7-11-902-TO	IW	Chain saw+	29.08.2007	X				
Oy7-11-903-TO	IW	Chain saw+	29.08.2007	X				
Oy7-11-904-TO	IW	Chain saw+	29.08.2007	X				
Oy7-11-905-TO	IW	Chain saw+	29.08.2007	X				
Oy7-11-906-TO	IW	Chain saw+	29.08.2007	X				
Oy7-11-907-TO	IW	Chain saw+	29.08.2007	X				
Oy7-11-908-TO	IW	Chain saw+	29.08.2007	X				
Oy7-11-909-TO	TI	Chain saw+	29.08.2007	X				
Oy7-11-910-TO	TI	Chain saw+	29.08.2007	X				
Oy7-11-911-TO	TI	Chain saw+	29.08.2007	X				
Oy7-11-912-TO	TI	Chain saw+	29.08.2007	X				
Oy7-11-913-TO	TI	Chain saw+	29.08.2007	X				
Oy7-11-Hy-01-TO	TI	Chain saw+	29.08.2007	X		X		
Oy7-11-Hy-02-TO	IW	Chain saw+	29.08.2007	X		X		
Oy7-11-Hy-03-TO	IW	Chain saw+	29.08.2007	X		X		
Oy7-11-Hy-04-TO	IW	Chain saw+	29.08.2007	X		X		
Oy7-11-Hy-05-TO	IW	Chain saw+	29.08.2007	X		X		
Oy7-11-Hy-06-TO	IW	Chain saw+	29.08.2007	X		X		
Oy7-11-Hy-07-TO	IW	Chain saw+	29.08.2007	X		X		

Sample number	Sample type	Sampled By	Date	Sampled for measurement of				Corresponding sediment sample
				$\delta^{18}\text{O}/\delta\text{D}$	$^3\text{H}$	Anions/Cations	$^{36}\text{Cl}$	
Oy7-11-Hy-08-TO	IW	Chain saw+	29.08.2007	X		X		
Oy7-11-Hy-09-TO	IW	Chain saw+	29.08.2007	X		X		
Oy7-11-Hy-10-TO	IW	Chain saw+	29.08.2007	X		X		
Oy7-11-Hy-11-TO	IW	Chain saw+	29.08.2007	X		X		
Oy7-11-Hy-12-TO	IW	Chain saw+	29.08.2007	X		X		
Oy7-11-Hy-13-TO	IW	Chain saw+	29.08.2007	X		X		
Oy7-11-Hy-14-TO	IW	Chain saw+	29.08.2007	X		X		
Oy7-11-Hy-15-TO	IW	Chain saw+	29.08.2007	X		X		
Oy7-11-Hy-16-TO	IW	Chain saw+	29.08.2007	X		X		
Oy7-11-Hy-17-TO	IW	Chain saw+	29.08.2007	X		X		
Oy7-11-Hy-18-TO	IW	Chain saw+	29.08.2007	X		X		
Oy7-11-Hy-19-TO	IW	Chain saw+	29.08.2007	X		X		
Oy7-11-Hy-20-TO	IW	Chain saw+	29.08.2007	X		X		
Oy7-11-Hy-21-TO	IW	Chain saw+	29.08.2007	X		X		
Oy7-11-Hy-22-TO	IW	Chain saw+	29.08.2007	X		X		
Oy7-11-Hy-23-TO	IW	Chain saw+	29.08.2007	X		X		
Oy7-11-Hy-24-TO	IW	Chain saw+	29.08.2007	X		X		
Oy7-11-Hy-25-TO	IW	Chain saw+	29.08.2007	X		X		
Oy7-11-Hy-26-TO	IW	Chain saw+	29.08.2007	X		X		
Oy7-11-Hy-27-TO	IW	Chain saw+	29.08.2007	X		X		
Oy7-11-Hy-28-TO	IW	Chain saw+	29.08.2007	X		X		
Oy7-11-Hy-29-TO	IW	Chain saw+	29.08.2007	X		X		
Oy7-11-Hy-30-TO	IW	Chain saw+	29.08.2007	X		X		
Oy7-11-Hy-31-TO	IW	Chain saw+	29.08.2007	X		X		
Oy7-11-Hy-32-TO	IW	Chain saw+	29.08.2007	X		X		
Oy7-11-Hy-33-TO	IW	Chain saw+	29.08.2007	X		X		
Oy7-11-Hy-34-TO	IW	Chain saw+	29.08.2007	X		X		
Oy7-11-Hy-35-TO	IW	Chain saw+	29.08.2007	X		X		
Oy7-11-Hy-36-TO	IW	Chain saw+	29.08.2007	X		X		
Oy7-11-Hy-37-TO	IW	Chain saw+	29.08.2007	X		X		
Oy7-11-Hy-38-TO	IW	Chain saw+	29.08.2007	X		X		
Oy7-11-Hy-39-TO	IW	Chain saw+	29.08.2007	X		X		
Oy7-11-Hy-40-TO	IW	Chain saw+	29.08.2007	X		X		
Oy7-11-Hy-41-TO	IW	Chain saw+	29.08.2007	X		X		
Oy7-11-Hy-42-TO	IW	Chain saw+	29.08.2007	X		X		
Oy7-11-Hy-43-TO	IW	Chain saw+	29.08.2007	X		X		
Oy7-11-Hy-44-TO	IW	Chain saw+	29.08.2007	X		X		
Oy7-11-Hy-45-TO	IW	Chain saw+	29.08.2007	X		X		
Oy7-11-Hy-46-TO	IW	Chain saw+	29.08.2007	X		X		
Oy7-11-Hy-47-TO	IW	Chain saw+	29.08.2007	X		X		
Oy7-11-Hy-48-TO	TI	Chain saw+	29.08.2007	X		X		
Oy7-11 IW 6; 72.68257°N; 143.49466°E								
Oy7-11-602-TO	IW	Axe	27.08.2007	X				
Oy7-11-603-TO	IW	Axe	27.08.2007	X				
Oy7-11-604-TO	TI	Axe	27.08.2007	X				
Oy7-11 texture ice samples; 72.68347°N; 143.47526°E								
Oy7-11-01/02-S	TI		22.08.2007	X				X
Oy7-11-11-S	TI		22.08.2007	X				X
Oy7-11-12-S	TI		22.08.2007	X				X
Oy7-11-13-S	TI		22.08.2007	X				X
Oy7-11-14-S	TI		22.08.2007	X				X
Oy7-11-15-S	TI		22.08.2007	X				X

## Appendix precipitation samples

Sample number	Date	Time (UTC+9)	Remarks
Precipitation samples at Vankina mouth, Bol'shoy Lyakhovsky; 73.27995°N; 141.827710°E			
Lap-rain 01	20.07.2007	10:00	
Lap-rain 02	20.07.2007	12:00	
Lap-rain 03A	21.07.2007	09:00	two samples
Precipitation samples at Zimov'e mouth, Bol'shoy Lyakhovsky; 73.33223°N; 141.35473°E			
Lap-rain 04	31.07.2007	01:00	
Lap-rain 05	01.08.2007	11:00	
Precipitation samples at field camp, Oyogos Yar; 72.68131°N, 143.49247°E			
Lap-rain 06	03.08.2007	10:00	
Lap-rain 07	03.08.2007	23:30	
Lap-rain 08	04.08.2007	11:00	
Lap-rain 09	04.08.2007	18:00	
Lap-rain 10	05.08.2007	01:00	
Lap-rain 11	05.08.2007	09:30	
Lap-rain 12	05.08.2007	19:45	
Lap-rain 13	05.08.2007	23:00	
Lap-rain 14	06.08.2007	11:30	
Lap-rain 15	06.08.2007	18:30	
Lap-rain 16	06.08.2007	23:00	
Lap-rain 17	10.08.2007	01:30	fog, not rain
Lap-rain 18	11.08.2007	08:45	
Lap-rain 19	13.08.2007	18:30	
Lap-rain 20	13.08.2007	19:15	
Lap-rain 21	13.08.2007	22:00	
Lap-rain 22	13.08.2007	23:55	
Lap-rain 23	14.08.2007	06:00	
Lap-rain 24	16.08.2007	08:00	
Lap-rain 25	16.08.2007	23:00	
Lap-rain 26	19.08.2007	08:30	
Lap-rain 27	19.08.2007	17:00	
Lap-rain 28	20.08.2007	07:45	
Lap-rain 29	21.08.2007	06:30	
Lap-rain 30	21.08.2007	20:00	
Lap-rain 31	22.08.2007	08:00	
Lap-rain 32	22.08.2007	13:00	
Lap-rain 33	23.08.2007	18:00	sampled after 6 hours
Lap-rain 34	25.08.2007	07:00	
Lap-rain 35	26.08.2007	08:00	
Lap-rain 36	27.08.2007	07:30	fog, not rain
Lap-rain 37	28.08.2007	23:00	
Lap-rain 38	29.08.2007	08:00	

## Appendix surface water samples

Sample number	Sample type	Date	Sampled for measurements of		
			$\delta^{18}\text{O}/\delta\text{D}$	$^3\text{H}$	Anions/Cations
Oy7-97-1	Snow patch	04.08.2007	X	X	
Oy7-97-2	Snow patch	04.08.2007	X	X	
Oy7-90-1	Sea water	04.08.2007	X	X	
Oy7-90-2	Sea water	24.08.2007	X		
Oy7-96-1	Stream water	04.08.2007	X	X	
Oy7-96-2	Stream water	04.08.2007	X		X
Oy7-96-3	Stream water	07.08.2007	X		
Oy7-96-4	Pond water	08.08.2007	X		
Oy7-96-5	Stream water	14.08.2007	X		
Oy7-96-6	Stream water	24.08.2007	X		
Oy7-96-7	Stream water	28.08.2007	X		
Oy7-98-1	Ground water	04.08.2008	X	X	
Oy7-98-2	Ground water	28.08.2008	X		
Oy7-Pi-1	Palsa (?) ice	27.08.2007	X	X	X
Oy7-Pi-2	Palsa (?) ice	27.08.2007	X	X	X



### 6.3 List of bone samples from Oyogos Yar 2007

a – in situ, b – in front of the exposure, c – in thawed debris near the exposures, d – at sea shore, e – tundra surface

No.	N samples	Taxon	Skeleton element	Preservation	Loc. type	Notes
<b>West part of coast section, shore; point 07 US'T2Wood</b>						
1	Oyg-07-O1	Mammuthus primigenius	humerus	fragment	d	C14
2	Oyg-07-O2	Mammuthus primigenius	tusk	fragment	d	C14
3	Oyg-07-O3	Ovibos sp.	astrogalus		d	
4	Oyg-07-O4	Mammuthus primigenius	limb bone	fragment	d	C14
5	Oyg-07-O5	Mammuthus primigenius	mandibula	fragment	d	C14, with marrow
6	Oyg-07-O6	Mammuthus primigenius	tooth	fragment	d	
7	Oyg-07-O7	Rangifer tarandus	shed antler	fragment	d	
8	Oyg-07-O8	Bison priscus	scapula	fragment	d	
9	Oyg-07-O9	Rangifer tarandus	pelvis	fragment	d	
10	Oyg-07-O10	Mammuthus primigenius	tooth	fragment (2 pieces)	d	
11	Oyg-07-O11	Bison priscus	tibia	distal articulation	d	
12	Oyg-07-O12	Bison priscus	tibia	distal fragment	d	
13	Oyg-07-O13	Bison priscus	lower molar tooth	damaged	d	
14	Oyg-07-O14	Mammuthus primigenius	tooth	fragment	d	
15	Oyg-07-O15	Bison priscus	astrogalus		d	
16	Oyg-07-O16	Mammuthus primigenius	tooth	fragment	d	
17	Oyg-07-O17	Large herbivorous mammal	limb bone	proximal fragment	d	
18	Oyg-07-O18	Bison priscus	horn sheet	fragment	d	
<b>West part of coast section, shore; point 07W1</b>						
19	Oyg-07-O19	Equus sp.?	femur	fragment	d	
20	Oyg-07-O20	Mammuthus primigenius	tusk	fragment	d	C14
21	Oyg-07-O21	Mammuthus primigenius	tooth	fragment	d	
22	Oyg-07-O22	Rangifer tarandus	scapula	fragment	d	
23	Oyg-07-O23	Mammuthus primigenius	tooth	fragment	d	
24	Oyg-07-O24	Mammuthus primigenius	tusk	fragment	d	C14
25	Oyg-07-O25	Mammuthus primigenius	tusk	fragment	d	C14
26	Oyg-07-O26	Mammuthus primigenius	tusk	fragment	d	C14
27	Oyg-07-O27	Mammuthus primigenius	tooth	fragment	d	
28	Oyg-07-O28	Mammuthus primigenius	tusk	fragment	d	C14
29	Oyg-07-O29	Mammuthus primigenius	tooth	fragment	d	
30	Oyg-07-O30	Mammuthus primigenius	tooth	fragment	d	
31	Oyg-07-O31	Mammuthus primigenius	tooth	fragment	d	
32	Oyg-07-O32	Mammuthus primigenius	tusk	fragment	d	trashed
33	Oyg-07-O33	Mammuthus primigenius	tooth	fragment	d	trashed
34	Oyg-07-O34	Mammuthus primigenius	tooth	fragment	d	trashed
35	Oyg-07-O35	Mammuthus primigenius	tusk	fragment	d	trashed
36	Oyg-07-O36	Mammuthus primigenius	tooth	fragment	d	
37	Oyg-07-O37	Mammuthus primigenius	tooth	fragment	d	
38	Oyg-07-O38	Large herbivorous mammal	limb bone	proximal fragment	d	trashed
39	Oyg-07-O39	Mammuthus primigenius	tusk	fragment	d	C 14
40	Oyg-07-O40	Bison priscus	tooth	fragment	d	
41	Oyg-07-O41	Equus sp.	lower tooth	fragment	d	
42	Oyg-07-O42	Mammuthus primigenius	tooth	fragment	d	
43	Oyg-07-O43	Large herbivorous mammal	limb bone	fragment	d	
44	Oyg-07-O44	Bison priscus	Mc?	distal fragment	d	
45	Oyg-07-O45	Rangifer tarandus	shed antler	fragment	d	
46	Oyg-07-O46	Equus sp.	ph I		d	
47	Oyg-07-O47	Equus sp.	ph I		d	
48	Oyg-07-O48	Equus sp.	ph II		d	

No.	N samples	Taxon	Skeleton element	Preservation	Loc. type	Notes
49	Oyg-07-O49	Equus sp.	ph I		d	
50	Oyg-07-O50	Equus sp.	maxilla, right stem with P2-P3	fragment	d	
51	Oyg-07-O51	Rangifer tarandus	tibia	fragment	d	
52	Oyg-07-O52	Rangifer tarandus	antebrachium		d	probably recent?
53	Oyg-07-O53	Mammuthus primigenius	astrogalus	fragment	d	C 14
54	Oyg-07-O54	Equus sp.	os naviculare	damaged	d	
55	Oyg-07-O55	Alopex lagopus	molar tooth		d	recent?
56	Oyg-07-O56	Rangifer tarandus ?	upper tooth		d	
<b>East part of coast section; thermoterrace of the biggest and nearest thermo cirque; height 38,5 m - 8 m a.s.l.</b>						
57	Oyg-07-O57	Mammuthus primigenius	tooth	fragment	b	
58	Oyg-07-O58	Mammuthus primigenius	tooth	fragment	b	
59	Oyg-07-O59	Equus sp.	Mc III	witout proximal articulation	b	
60	Oyg-07-O60	Equus sp.	Mc III		b	
61	Oyg-07-O61	Equus sp.	pelvis, right part		b	
62	Oyg-07-O62	Equus sp.	ulna	damaged	b	
63	Oyg-07-O63	Equus sp.	femur	fragment	b	
64	Oyg-07-O64	Rangifer tarandus	femur	proximal fragment (2 pices)	b	probably recent?
65	Oyg-07-O65	Rangifer tarandus	pelvis	fragment	b	probably recent?
66	Oyg-07-O66	Equus sp.	calcaneus	damaged	b	
67	Oyg-07-O67	Mammuthus primigenius	tusk	fragment	b	C 14
68	Oyg-07-O68	Bison priscus	calcaneus		b	
69	Oyg-07-O69	Mammuthus primigenius	tusk	fragment	b	C 14
87	Oyg-07-O87	Mammuthus primigenius	rib	fragment	d	trashed
<b>East part of coast section, shore</b>						
70	Oyg-07-O70	Mammuthus primigenius	tooth heavily worn	fragment	d	rounded
71	Oyg-07-O71	Rangifer tarandus	upper tooth		d	probably recent?
72	Oyg-07-O72	Rangifer tarandus	ph I	distal fragment	d	
73	Oyg-07-O73	Equus sp.	lower milk tooth P2, heavily worn		d	
74	Oyg-07-O74	Equus sp.	os naviculare	fragment	d	
75	Oyg-07-O75	Equus sp.	lower tooth		d	
76	Oyg-07-O76	Rangifer tarandus	femur	proximal fragment	d	
77	Oyg-07-O77	Rangifer tarandus	metapodium	fragment	d	juv.
78	Oyg-07-O78	Bison priscus	large bone of tarsus		d	
79	Oyg-07-O79	Rangifer tarandus	antler	fragment	d	probably recent?; trashed
80	Oyg-07-O80	Rangifer tarandus	large bone of carpus		d	
81	Oyg-07-O81	Mammuthus primigenius	tusk	fragment	d	
82	Oyg-07-O82	Mammuthus primigenius	tooth	fragment	d	trashed
83	Oyg-07-O83	Lepus sp.	femur	distal fragment	d	
84	Oyg-07-O84	Mammuthus primigenius	tusk	fragment	d	trashed
85	Oyg-07-O85	Mammuthus primigenius	tusk	fragment	d	trashed
86	Oyg-07-O86	Mammuthus primigenius	tusk	fragment	d	trashed
88	Oyg-07-O88	Mammuthus primigenius	scapula	damaged	d	trashed, foto
<b>West part of coast section, shore; point 07W1</b>						
89	Oyg-07-O89	Mammuthus primigenius	tusk	fragment	d	C 14
<b>East part of coast section, shore near the stream mouth; (landing site in 2002); point 07RUCHEY</b>						
90	Oyg-07-O90	Mammuthus primigenius	tooth	fragment	d	
91	Oyg-07-O91	Equus sp.	ph I	fragment	d	
92	Oyg-07-O92	Equus sp.	lower tooth	damaged	d	
93	Oyg-07-O93	Mammuthus primigenius	tusk	fragment	d	C 14
94	Oyg-07-O94	Bison priscus	vertebra	fragment	d	
95	Oyg-07-O95	Mammuthus primigenius	tooth	fragment	d	

No.	N samples	Taxon	Skeleton element	Preservation	Loc. type	Notes
96	Oyg-07-O96	Bison priscus	metapodium	fragment of distal articulation	d	
97	Oyg-07-O97	Equus sp. ?	pelvis	fragment	d	
98	Oyg-07-O98	Equus sp.	ph I		d	
99	Oyg-07-O99	Bison priscus	maxilla, symphysis part	fragment	d	
100	Oyg-07-O100	Equus sp.	scapula	fragment	d	
101	Oyg-07-O101	Mammuthus primigenius	tooth	fragment	d	
102	Oyg-07-O102	Mammuthus primigenius	tooth	fragment	d	
103	Oyg-07-O103	Equus sp.	ph I	fragment	d	
104	Oyg-07-O104	Bison priscus	astrogalus	fragment	d	
105	Oyg-07-O105	Ovibos sp. ?	Mc	damaged	d	
106	Oyg-07-O106	Mammuthus primigenius	tooth	fragment	d	
107	Oyg-07-O107	Equus sp.	ph I		d	
108	Oyg-07-O108	Rangifer tarandus	shed antler	fragment	d	
109	Oyg-07-O109	Equus sp. ?	pelvis	fragment	d	juv.
110	Oyg-07-O110	Equus sp.	pelvis	fragment	d	
111	Oyg-07-O111	Ovibos sp.	astrogalus		d	
112	Oyg-07-O112	Rangifer tarandus	astrogalus		d	
113	Oyg-07-O113	Equus sp.	tibia	distal fragment	d	
114	Oyg-07-O114	Bison priscus	large bone of carpus		d	
115	Oyg-07-O115	Equus sp.	large bone of carpus		d	
116	Oyg-07-O116	Rangifer tarandus	sacrum		d	probably recent?
117	Oyg-07-O117	Bison priscus	horn sheet	fragment	d	
118	Oyg-07-O118	Bison priscus	large bone of tarsus		d	
119	Oyg-07-O119	Mammuthus primigenius	tibia	distal fragment	d	small, juv.
120	Oyg-07-O120	Mammuthus primigenius	tusk	fragment	d	C 14
121	Oyg-07-O121	Bison priscus ?	scapula	fragment	d	
122	Oyg-07-O122	Rangifer tarandus ?	scapula	fragment	d	
123	Oyg-07-O123	Rangifer tarandus	astrogalus	damaged	d	
124	Oyg-07-O124	Bison priscus ?	rib	fragment	d	trashed
125	Oyg-07-O125	Mammuthus primigenius	tooth	fragment	d	trashed
126	Oyg-07-O126	Bison priscus	astrogalus	fragment	d	trashed
127	Oyg-07-O127	Rangifer tarandus	shed antler	fragment	d	trashed
128	Oyg-07-O128	Rangifer tarandus	calcaneus	fragment	d	trashed
129	Oyg-07-O129	Rangifer tarandus	shed antler	fragment	d	trashed
130	Oyg-07-O130	Equus sp.	ph I	distal fragment	d	trashed
131	Oyg-07-O131	Equus sp.	ph I	proximal fragment	d	trashed
132	Oyg-07-O132	Equus sp.	tibia	distal fragment	d	trashed
133	Oyg-07-O133	Bison priscus	skull, os occipitale	fragment	d	
134	Oyg-07-O134	Equus sp.	astrogalus		d	rounded, rub ice marks
135	Oyg-07-O135	Equus sp.	tibia	distal fragment	d	
136	Oyg-07-O136	Bison priscus	small bone of tarsus	fragment	d	
137	Oyg-07-O137	Rangifer tarandus	astrogalus		d	
138	Oyg-07-O138	Bison priscus	large bone of carpus		d	
139	Oyg-07-O139	Mammuthus primigenius	tooth	fragment	d	
140	Oyg-07-O140	Mammuthus primigenius	tooth	fragment	d	
141	Oyg-07-O141	Equus sp.	ph I		d	
142	Oyg-07-O142	Equus sp.	cervical vertebra		d	
143	Oyg-07-O143	Rangifer tarandus	atlas	damaged	d	
144	Oyg-07-O144	Saiga tatarica ?	humerus	distal fragment	d	
145	Oyg-07-O145	Saiga tatarica ?	pelvis	fragment	d	
146	Oyg-07-O146	Rangifer tarandus	skull with antler	fragment	d	
147	Oyg-07-O147	Ovibos sp.	calcaneus		d	

No.	N samples	Taxon	Skeleton element	Preservation	Loc. type	Notes
148	Oyg-07-O148	Ovibos sp.	calcaneus	fragment	d	
149	Oyg-07-O149	Bison priscus ?	pelvis	fragment	d	
150	Oyg-07-O150	Large herbivorous mammal	limb bone	fragment	d	
151	Oyg-07-O151	Bison priscus	humerus	distal fragment	d	
152	Oyg-07-O152	Equus sp.	milk upper tooth (dP2)		d	
153	Oyg-07-O153	Mammuthus primigenius	limb bone	fragment	d	trashed
154	Oyg-07-O154	Bison priscus	humerus	distal fragment	d	
155	Oyg-07-O155	Equus sp.	humerus	distal fragment	d	
156	Oyg-07-O156	Large herbivorous mammal	limb bone	fragment	d	
157	Oyg-07-O157	Large herbivorous mammal	limb bone	fragment	d	
158	Oyg-07-O158	Equus sp.	ulna	fragment	d	
159	Oyg-07-O159	Mammuthus primigenius	skull	fragment, alveolar part	d	trashed
160	Oyg-07-O160	Rangifer tarandus	sacrum	fragment	d	
161	Oyg-07-O161	Bison priscus	metapodium	fragment	d	
162	Oyg-07-O162	Large herbivorous mammal	vertebra ?	fragment	d	
163	Oyg-07-O163	Equus sp.	humerus	distal fragment	d	with teeth traces of Carnivora
164	Oyg-07-O164	Rangifer tarandus	atlas	fragment	d	
165	Oyg-07-O165	Mammuthus primigenius	tooth	fragment	d	
166	Oyg-07-O166	Rangifer tarandus	caudal vertebra	damaged	d	
167	Oyg-07-O167	Bison priscus	upper tooth	fragment	d	
168	Oyg-07-O168	Bison priscus	small bone of tarsus		d	
169	Oyg-07-O169	Equus sp.	os naviculare	damaged	d	
170	Oyg-07-O170	Rangifer tarandus	large bone of carpus		d	
171	Oyg-07-O171	Bison priscus	small bone of carpus		d	
172	Oyg-07-O172	Rangifer tarandus	metapodium	distal fragment	d	
173	Oyg-07-O173	Rangifer tarandus ?	small bone of tarsus	fragment	d	
174	Oyg-07-O174	Mammuthus primigenius	tooth, heavily worn	fragment	d	
175	Oyg-07-O175	Rangifer tarandus	lower tooth		d	
176	Oyg-07-O176	Rangifer tarandus	ph I	distal fragment	d	
177	Oyg-07-O177	Mammuthus primigenius	scapula ?	fragment	d	C 14
178	Oyg-07-O178	Mammuthus primigenius	vertebra, process spinosus	fragment	d	trashed
179	Oyg-07-O179	Mammuthus primigenius	vertebra	fragment	d	trashed
180	Oyg-07-O180	Rangifer tarandus	antler	fragment	d	trashed
181	Oyg-07-O181	Rangifer tarandus	antler	fragment	d	trashed
182	Oyg-07-O182	Rangifer tarandus	scapula	fragment	d	trashed, recent?
183	Oyg-07-O183	Rangifer tarandus	ph I	distal fragment	d	rounded, trashed
184	Oyg-07-O184	Rangifer tarandus	pelvis	fragment	d	trashed
185	Oyg-07-O185	Mammuthus primigenius	tusk	fragment	d	trashed
186	Oyg-07-O186	Mammuthus primigenius	limb bone	fragment	d	C 14
187	Oyg-07-O187	Mammuthus primigenius	thorax vertebra	damaged	d	
188	Oyg-07-O188	Rangifer tarandus	skull	fragment	d	juv., recent?
189	Oyg-07-O189	Equus sp.	ulna		d	
190	Oyg-07-O190	Bison priscus ?	humerus ?	fragment	d	
191	Oyg-07-O191	Bison priscus	ph I		d	
192	Oyg-07-O192	Rangifer tarandus	tibia	fragment	d	
193	Oyg-07-O193	Rangifer tarandus	pelvis	fragment	d	
194	Oyg-07-O194	Rangifer tarandus	antler	fragment	d	
195	Oyg-07-O195	Equus sp. ?	tibia	fragment, without articulations	d	juv.
196	Oyg-07-O196	Bison priscus	scapula	fragment	d	

No.	N samples	Taxon	Skeleton element	Preservation	Loc. type	Notes
197	Oyg-07-O197	Mammuthus primigenius	tooth	fragment	d	
198	Oyg-07-O198	Ovibos sp.	cervical vertebra	damaged	d	
199	Oyg-07-O199	Ovibos sp. ?	ph I		d	
200	Oyg-07-O200	Bison priscus	ph I		d	
201	Oyg-07-O201	Bison priscus ?	scapula	fragment	d	
202	Oyg-07-O202	Mammuthus primigenius	tusk	fragment	d	C14
203	Oyg-07-O203	Mammuthus primigenius	tusk	fragment	d	
204	Oyg-07-O204	Rangifer tarandus	lumbar vertebra	damaged	d	
205	Oyg-07-O205	Bison priscus	vertebra	fragment	d	
206	Oyg-07-O206	Equus sp.	tibia	distal fragment, without articulation	d	juv.
207	Oyg-07-O207	Bison priscus	tibia	distal fragment	d	
208	Oyg-07-O208	Bison priscus	ulna	damaged	d	
209	Oyg-07-O209	Mammuthus primigenius	scapula	fragment	d	C 14
210	Oyg-07-O210	Mammuthus primigenius	mandible	fragment, symphysis part	d	C 14
211	Oyg-07-O211	Mammuthus primigenius	metapodium	proximal fragment	d	
212	Oyg-07-O212	Rangifer tarandus	radius	proximal fragment	d	
213	Oyg-07-O213	Mammuthus primigenius	metapodium ?	damaged	d	juv.
214	Oyg-07-O214	Rangifer tarandus	antler	fragment	d	
215	Oyg-07-O215	Equus sp.	radius	distal fragment	d	
216	Oyg-07-O216	Equus sp.	tibia	distal fragment	d	
217	Oyg-07-O217	Bison priscus	ph I	damaged	d	
218	Oyg-07-O218	Equus sp.	ph I		d	
219	Oyg-07-O219	Bison priscus	humerus	distal fragment	d	
220	Oyg-07-O220	Ovibos sp.	Mc		d	
221	Oyg-07-O221	Rangifer tarandus	vertebra	fragment	d	trashed
222	Oyg-07-O222	Equus sp.	astrogalus	fragment	d	trashed
223	Oyg-07-O223	Bison priscus	metapodium	distal fragment	d	trashed
224	Oyg-07-O224	Bison priscus	large bone of carpus		d	
225	Oyg-07-O225	Equus sp.	ph I	damaged	d	
226	Oyg-07-O226	Rangifer tarandus	humerus	distal fragment	d	
227	Oyg-07-O227	Bison priscus	metapodium	fragment	d	
228	Oyg-07-O228	Equus sp. ?	calcaneus	fragment	d	
229	Oyg-07-O229	Equus sp.	calcaneus	fragment	d	
230	Oyg-07-O230	Bison priscus	ph I	fragment	d	
231	Oyg-07-O231	Bison priscus	ph II		d	
232	Oyg-07-O232	Bison priscus	ph II	damaged	d	
233	Oyg-07-O233	Bison priscus	small bone of tarsus	small bone of tarsus	d	
234	Oyg-07-O234	Bison priscus			d	
235	Oyg-07-O235	Bison priscus	ph I		d	
236	Oyg-07-O236	Mammuthus primigenius ?	phalanx	without proximal articulation	d	juv.
237	Oyg-07-O237	Rangifer tarandus	shed antler	fragment	d	trashed
238	Oyg-07-O238	Bison priscus ?	small bone of tarsus	fragment	d	rounded
239	Oyg-07-O239	Bison priscus	ph III	damaged	d	
240	Oyg-07-O240	Rangifer tarandus	radius	proximal fragment	d	
241	Oyg-07-O241	Rangifer tarandus	tibia	distal fragment	d	
242	Oyg-07-O242	Rangifer tarandus ?	lumbar vertebra	fragment	d	
243	Oyg-07-O243	Rangifer tarandus	ph I	distal fragment	d	
244	Oyg-07-O244	Bison priscus ?	ph II		d	
245	Oyg-07-O245	Rangifer tarandus	astrogalus		d	rounded
246	Oyg-07-O246	Large herbivorous mammal	limb bone	fragment	d	
247	Oyg-07-O247	Large herbivorous mammal	limb bone	fragment	d	
248	Oyg-07-O248	Rangifer tarandus ?	calcaneus	fragment	d	
249	Oyg-07-O249	Large herbivorous	limb bone	fragment	d	

No.	N samples	Taxon	Skeleton element	Preservation	Loc. type	Notes
		mammal				
250	Oyg-07-O250	Mammuthus primigenius	small bone of tarsus	fragment	d	
251	Oyg-07-O251	Large herbivorous mammal	vertebra	fragment	d	
252	Oyg-07-O252	Rangifer tarandus	metapodium	distal fragment	d	
253	Oyg-07-O253	Pusa hispida	thorax vertebra	damaged	d	recent
254	Oyg-07-O254	Rangifer tarandus	tibia	distal articulation	d	juv.
255	Oyg-07-O255	Mammuthus primigenius	tusk	fragment	d	C 14, sample cut out
256	Oyg-07-O256	Mammuthus primigenius	vertebra	fragment	d	rounded, trashed
257	Oyg-07-O257	Mammuthus primigenius	humerus	distal articulation	d	juv., with teeth traces of Carnivora
258	Oyg-07-O258	Mammuthus primigenius	bone of tarsus		d	
259	Oyg-07-O259	Mammuthus primigenius	humerus	distal fragment	d	C 14
260	Oyg-07-O260	Mammuthus primigenius ?	pelvis	fragment	d	juv.
261	Oyg-07-O261	Bison priscus	horn sheet	fragment	d	
262	Oyg-07-O262	Bison priscus	vertebra	fragment	d	
263	Oyg-07-O263	Large herbivorous mammal	limb bone	fragment	d	
264	Oyg-07-O264	Large herbivorous mammal	limb bone	fragment	d	
265	Oyg-07-O265	Mammuthus primigenius	rib	fragment	d	trashed
266	Oyg-07-O266	Mammuthus primigenius	rib	fragment	d	trashed
<b>West part of coast section, shore; point 07 US'T2Wood</b>						
267	Oyg-07-O267	Mammuthus primigenius	small bone of tarsus	damaged	d	
268	Oyg-07-O268	Bison priscus	scapula	fragment	d	
269	Oyg-07-O269	Bison priscus	thorax vertebra	damaged	d	
270	Oyg-07-O270	Bison priscus	thorax vertebra	fragment	d	
271	Oyg-07-O271	Mammuthus primigenius	vertebra	fragment	d	
272	Oyg-07-O272	Equus sp.	radius	distal fragment	d	
273	Oyg-07-O273	Rangifer tarandus	radius	distal fragment	d	juv.
274	Oyg-07-O274	Rangifer tarandus	astrogalus	damaged	d	
<b>West part of coast section, shore; point 07W1</b>						
275	Oyg-07-O275	Mammuthus primigenius	tusk	fragment	d	trashed
276	Oyg-07-O276	Mammuthus primigenius	tusk	fragment	d	trashed
277	Oyg-07-O277	Mammuthus primigenius	tooth	fragment	d	trashed
278	Oyg-07-O278	Mammuthus primigenius	tooth	fragment	d	trashed
279	Oyg-07-O279	Mammuthus primigenius	tooth	fragment	d	trashed
280	Oyg-07-O280	Mammuthus primigenius	tooth	fragment	d	trashed
281	Oyg-07-O281	Bison priscus	scull	fragment	d	trashed
282	Oyg-07-O282	Mammuthus primigenius	mandible	fragment	d	juv.
<b>East part of coast section, shore near the stream mouth; (landing site in 2002); point 07RUCHEY</b>						
283	Oyg-07-O283	Bison priscus ?	cervical vertebra	damaged	d	
284	Oyg-07-O284	Large herbivorous mammal	limb bone	fragment	d	
<b>East part of coast section, shore; the most distant point; point 07EFAR</b>						
285	Oyg-07-O285	Mammuthus primigenius	scapula	fragment	d	C 14
286	Oyg-07-O286	Mammuthus primigenius	tusk	fragment	d	
287	Oyg-07-O287	Bison priscus	tibia	fragment	d	
288	Oyg-07-O288	Bison priscus	large bone of carpus	fragment	d	vivianate
289	Oyg-07-O289	Rangifer tarandus	tibia	distal fragment	d	
290	Oyg-07-O290	Rangifer tarandus	radius		d	probably recent?
<b>East part of coast section, shore; point 07EICTKICE</b>						
291	Oyg-07-O291	Rangifer tarandus	metapodium	distal fragment	d	
292	Oyg-07-O292	Mammuthus primigenius	scapula	fragment	d	

No.	N samples	Taxon	Skeleton element	Preservation	Loc. type	Notes
293	Oyg-07-O293	Mammuthus primigenius	pelvis ?	fragment	d	
294	Oyg-07-O294	Mammuthus primigenius	tusk	fragment	d	
295	Oyg-07-O295	Equus sp.	radius	distal fragment	d	large
296	Oyg-07-O296	Mammuthus primigenius	femur	distal fragment	d	C 14, vivianate
<b>East part of coast section, shore; point 07EICTKICE, thermoterrace</b>						
297	Oyg-07-O297	Mammuthus primigenius	tusk	fragment	d	C 14
<b>East part of coast section, shore; river mouth located west of the Rebrov River</b>						
298	Oyg-07-O298	Rangifer tarandus	radius	proximal fragment	d	
299	Oyg-07-O299	Rangifer tarandus	scapula	fragment	d	
300	Oyg-07-O300	Mammuthus primigenius	tooth	fragment	d	
301	Oyg-07-O301	Bison priscus	cervical vertebra	damaged	d	
<b>West part of coast section, shore; point 07W1</b>						
302	Oyg-07-O302	Rangifer tarandus ?	humerus	fragment	d	
<b>In situ, east part of coast section; Krest Yuryakh ice wedge casts under the big thermocirque (exposure Oy7-09)</b>						
303	Oyg-07-O303	Mammuthus primigenius	tusk	fragment	a	vivianate
<b>West part of coast section, shore near the mouth of r. Rebrova</b>						
304	Oyg-07-O304	Rangifer tarandus	shed antler	fragment	d	
305	Oyg-07-O305	Ovibos moschatus	cervical vertebra	damaged	d	
306	Oyg-07-O306	Bison priscus	cervical vertebra	damaged	d	
307	Oyg-07-O307	Large herbivorous mammal	limb bone	fragment	d	
308	Oyg-07-O308	Mammuthus primigenius	metapodium ?	proximal fragment	d	
309	Oyg-07-O309	Bison priscus	tibia	distal fragment	d	
310	Oyg-07-O310	Mammuthus primigenius	tusk	fragment	d	
311	Oyg-07-O311	Mammuthus primigenius	tooth	fragment	d	
312	Oyg-07-O312	Mammuthus primigenius	limb bone	fragment	d	C 14
313	Oyg-07-O313	Equus sp.	radius	proximal fragment	d	
314	Oyg-07-O314	Equus sp.	astrogalus		d	
315	Oyg-07-O315	Equus sp.	astrogalus		d	ice abrasion marks
316	Oyg-07-O316	Equus sp.	ph II		d	
317	Oyg-07-O317	Equus sp.	lower tooth	damaged	d	
318	Oyg-07-O318	Mammuthus primigenius	astrogalus	damaged	d	small
319	Oyg-07-O319	Mammuthus primigenius	tusk	fragment	d	C 14
320	Oyg-07-O320	Rangifer tarandus ?	thorax vertebra		d	
321	Oyg-07-O321	Rangifer tarandus	shed antler	fragment	d	
322	Oyg-07-O322	Bison priscus	cervical vertebra	damaged	d	
323	Oyg-07-O323	Mammuthus primigenius	bone of tarsus		d	
324	Oyg-07-O324	Mammuthus primigenius	tooth		d	by Dima
325	Oyg-07-O325	Mammuthus primigenius	tooth	fragment	d	
326	Oyg-07-O326	Mammuthus primigenius	tusk	fragment	d	
327	Oyg-07-O327	Mammuthus primigenius	tusk	fragment	d	
328	Oyg-07-O328	Mammuthus primigenius	tooth	fragment	d	
329	Oyg-07-O329	Bison priscus	calcaneus		d	
330	Oyg-07-O330	Bison priscus	sacrum	damaged	d	juv.
331	Oyg-07-O331	Bison priscus or Ovibos sp. ?	ph I		d	
332	Oyg-07-O332	Bison priscus	humerus	distal fragment	d	
333	Oyg-07-O333	Equus sp. ?	scapula	fragment	d	
334	Oyg-07-O334	Rangifer tarandus	mandible (left stem with P2 and P4)	fragment	d	
335	Oyg-07-O335	Equus sp.	ph I		d	
336	Oyg-07-O336	Equus sp.	tibia	distal fragment	d	
337	Oyg-07-O337	Mammuthus primigenius	tooth	fragment	d	
338	Oyg-07-O338	Mammuthus primigenius	skull (occipitale part)	fragment	d	juv.
339	Oyg-07-O339	Bison priscus	lumbar vertebra	fragment	d	
340	Oyg-07-O340	Bison priscus	antebrachium	distal fragment	d	

No.	N samples	Taxon	Skeleton element	Preservation	Loc. type	Notes
341	Oyg-07-O341	Bison priscus	Mc		d	
342	Oyg-07-O342	Ovibos moschatus	epistropheus	fragment	d	
343	Oyg-07-O343	Mammuthus primigenius	lumbar vertebra	damaged (without articulation surface)	d	small, juv.
344	Oyg-07-O344	Mammuthus primigenius	bone of tarsus		d	
345	Oyg-07-O345	Mammuthus primigenius	bone of tarsus	damaged	d	
346	Oyg-07-O346	Mammuthus primigenius	vertebra	fragment	d	trashed
347	Oyg-07-O347	Mammuthus primigenius	tooth	fragment	d	trashed
348	Oyg-07-O348	Mammuthus primigenius	tusk	fragment	d	trashed
349	Oyg-07-O349	Rangifer tarandus	antler	fragment	d	trashed
350	Oyg-07-O350	Rangifer tarandus	cervical vertebra	fragment	d	trashed
351	Oyg-07-O351	Rangifer tarandus	Mt	fragment	d	trashed
352	Oyg-07-O352	Equus sp.	radius	fragment (without articulation surface)	d	juv.
353	Oyg-07-O353	Equus sp.	ph I		d	
354	Oyg-07-O354	Rangifer tarandus	calcaneus	fragment	d	
355	Oyg-07-O355	Rangifer tarandus	humerus	distal fragment	d	
356	Oyg-07-O356	Rangifer tarandus	femur	fragment (distal articulation surface)	d	juv.
357	Oyg-07-O357	Rangifer tarandus	metapodium	distal fragment	d	
358	Oyg-07-O358	Bison priscus	ph II		d	
359	Oyg-07-O359	Mammuthus primigenius	tusk	fragment	d	
360	Oyg-07-O360	Mammuthus primigenius	tooth	fragment	d	
361	Oyg-07-O361	Equus sp.	lower tooth (M3)	fragment	d	
362	Oyg-07-O362	Ovibos moschatus	thorax vertebra	fragment	d	
363	Oyg-07-O363	Bison priscus	calcaneus	fragment	d	
364	Oyg-07-O364	Large herbivorous mammal	vertebra ?	fragment	d	
365	Oyg-07-O365	Bison priscus	metapodium	distal fragment	d	with teeth traces of Carnivora
366	Oyg-07-O366	Equus sp.	small bone of tarsus		d	
367	Oyg-07-O367	Equus sp.	small bone of tarsus		d	
368	Oyg-07-O368	Equus sp.	small bone of tarsus	fragment	d	
369	Oyg-07-O369	Bison priscus	small bone of tarsus		d	ice abrasion marks
370	Oyg-07-O370	Rangifer tarandus	atlas	damaged	d	ice abrasion marks
371	Oyg-07-O371	Equus sp.	pelvis	fragment	d	
372	Oyg-07-O372	Rangifer tarandus	lumbar vertebra	damaged	d	
373	Oyg-07-O373	Rangifer tarandus	thorax vertebra	damaged	d	
374	Oyg-07-O374	Equus sp.	astrogalus		d	
375	Oyg-07-O375	Equus sp.	astrogalus		d	
376	Oyg-07-O376	Rangifer tarandus	cervical vertebra	damaged	d	
377	Oyg-07-O377	Rangifer tarandus	cervical vertebra	fragment	d	
378	Oyg-07-O378	Rangifer tarandus	shed antler	fragment	d	
379	Oyg-07-O379	Rangifer tarandus	shed antler	fragment	d	
380	Oyg-07-O380	Rangifer tarandus	tibia	fragment (distal articulation surface)	d	juv.
381	Oyg-07-O381	Mammuthus primigenius	tusk	fragment	d	
382	Oyg-07-O382	Mammuthus primigenius	tusk	fragment	d	
383	Oyg-07-O383	Equus sp.	mandible (symphysis part)	fragment	d	
384	Oyg-07-O384	Equus sp.	skull (occipitale part)	fragment	d	
385	Oyg-07-O385	Bison priscus	small bone of tarsus	fragment	d	
386	Oyg-07-O386	Bison priscus	ph III	fragment	d	
387	Oyg-07-O387	Large herbivorous mammal	limb bone	fragment	d	
388	Oyg-07-O388	Bison priscus	tibia ?	distal fragment	d	
389	Oyg-07-O389	Large herbivorous	limb bone	proximal fragment	d	

No.	N samples	Taxon	Skeleton element	Preservation	Loc. type	Notes
		mammal				
390	Oyg-07-O390	Large herbivorous mammal	limb bone	proximal fragment	d	
391	Oyg-07-O391	Rangifer tarandus	small bone of tarsus		d	rounded
392	Oyg-07-O392	Rangifer tarandus	lower tooth		d	
<b>East part of coast section, shore from camp to stream (point 07RUCHEY)</b>						
393	Oyg-07-O393	Mammuthus primigenius	astrogalus		d	
394	Oyg-07-O394	Mammuthus primigenius	atlas		d	small
395	Oyg-07-O395	Equus sp.	skull with right and left C - M3	damaged	d	male
396	Oyg-07-O396	Equus sp.	maxilla with right I1 - I3	fragment	d	
397	Oyg-07-O397	Mammuthus primigenius	tooth	fragment	d	trashed
398	Oyg-07-O398	Mammuthus primigenius	tooth	fragment	d	trashed
399	Oyg-07-O399	Mammuthus primigenius	tooth	fragment	d	trashed
400	Oyg-07-O400	Rangifer tarandus	metapodium	distal fragment	d	trashed
401	Oyg-07-O401	Rangifer tarandus	pelvis	fragment	d	trashed, recent?
402	Oyg-07-O402	Mammuthus primigenius	tooth	fragment	d	
403	Oyg-07-O403	Mammuthus primigenius	tooth	fragment	d	
404	Oyg-07-O404	Mammuthus primigenius	tooth	fragment	d	
405	Oyg-07-O405	Mammuthus primigenius	tooth	fragment	d	
406	Oyg-07-O406	Mammuthus primigenius	tooth	fragment	d	
407	Oyg-07-O407	Mammuthus primigenius	tusk	fragment	d	
408	Oyg-07-O408	Mammuthus primigenius	tusk	fragment	d	C 14
409	Oyg-07-O409	Mammuthus primigenius	tusk	fragment	d	
410	Oyg-07-O410	Mammuthus primigenius	tusk	fragment	d	C 14
411	Oyg-07-O411	Mammuthus primigenius	tusk	fragment	d	
412	Oyg-07-O412	Mammuthus primigenius	tusk	fragment	d	
413	Oyg-07-O413	Mammuthus primigenius	tusk	fragment	d	
414	Oyg-07-O414	Mammuthus primigenius	tooth	fragment	d	
415	Oyg-07-O415	Mammuthus primigenius	limb bone	fragment	d	C 14
416	Oyg-07-O416	Bison priscus	humerus	distal fragment	d	
417	Oyg-07-O417	Mammuthus primigenius	humerus	fragment	d	iron crust
418	Oyg-07-O418	Equus sp.	tibia	distal fragment	d	
419	Oyg-07-O419	Equus sp.	ph II	proximal fragment	d	rounded
420	Oyg-07-O420	Bison priscus	small bone of tarsus	fragment	d	
421	Oyg-07-O421	Ovibos moschatus	small bone of carpus		d	
422	Oyg-07-O422	Bison priscus	upper tooth		d	
423	Oyg-07-O423	Equus sp.	os naviculare	damaged	d	
424	Oyg-07-O424	Equus sp.	lower tooth	damaged	d	
425	Oyg-07-O425	Equus sp.	astrogalus	damaged	d	
426	Oyg-07-O426	Mammuthus primigenius	tooth	fragment	d	
427	Oyg-07-O427	Mammuthus primigenius	tooth	fragment	d	
428	Oyg-07-O428	Equus sp.	upper tooth	fragment	d	
429	Oyg-07-O429	Equus sp.	upper tooth	fragment	d	
430	Oyg-07-O430	Large herbivorous mammal	bone	fragment	d	
431	Oyg-07-O431	Rangifer tarandus	thorax vertebra	damaged	d	
432	Oyg-07-O432	Rangifer tarandus	antler	fragment	d	trashed
433	Oyg-07-O433	Rangifer tarandus	shed antler	fragment	d	trashed
434	Oyg-07-O434	Rangifer tarandus	astrogalus	fragment	d	trashed
435	Oyg-07-O435	Equus sp.	metapodium	distal fragment	d	trashed
436	Oyg-07-O436	Mammuthus primigenius	tooth	fragment	d	trashed
437	Oyg-07-O437	Mammuthus primigenius	tooth	fragment	d	trashed
438	Oyg-07-O438	Mammuthus primigenius	tooth	fragment	d	trashed
439	Oyg-07-O439	Mammuthus primigenius	tooth	fragment	d	trashed
440	Oyg-07-O440	Mammuthus primigenius	tusk	fragment	d	trashed

No.	N samples	Taxon	Skeleton element	Preservation	Loc. type	Notes
441	Oyg-07-O441	Mammuthus primigenius	tusk	fragment	d	trashed
442	Oyg-07-O442	Mammuthus primigenius	tusk	fragment	d	trashed
443	Oyg-07-O443	Mammuthus primigenius	tusk	fragment	d	trashed
444	Oyg-07-O444	Mammuthus primigenius	tusk	fragment	d	trashed
445	Oyg-07-O445	Equus sp.	astrogalus	fragment	d	trashed
446	Oyg-07-O446	Equus sp.	Mc III	fragment	d	trashed
447	Oyg-07-O447	Rangifer tarandus	cervical vertebra	fragment	d	trashed
448	Oyg-07-O448	Mammuthus primigenius	tusk	fragment	d	C 14
449	Oyg-07-O449	Mammuthus primigenius	tusk	fragment	d	C 14
450	Oyg-07-O450	Mammuthus primigenius	tusk	fragment	d	
451	Oyg-07-O451	Mammuthus primigenius	tusk	fragment	d	C 14
452	Oyg-07-O452	Mammuthus primigenius	limb bone	fragment	d	C 14
453	Oyg-07-O453	Mammuthus primigenius	tusk	fragment	d	
454	Oyg-07-O454	Mammuthus primigenius	tusk	fragment	d	
455	Oyg-07-O455	Mammuthus primigenius	tusk	fragment	d	
456	Oyg-07-O456	Mammuthus primigenius	tooth	fragment	d	
457	Oyg-07-O457	Mammuthus primigenius	tooth	fragment	d	
458	Oyg-07-O458	Mammuthus primigenius	tusk	fragment	d	
459	Oyg-07-O459	Mammuthus primigenius	tooth	fragment	d	
460	Oyg-07-O460	Mammuthus primigenius	tusk	fragment	d	
461	Oyg-07-O461	Equus sp.	ph III	damaged	d	
462	Oyg-07-O462	Equus sp.	ph II		d	
463	Oyg-07-O463	Equus sp.	ph I		d	
464	Oyg-07-O464	Bison priscus	small bone of tarsus		d	
465	Oyg-07-O465	Bison priscus	ph I		d	
466	Oyg-07-O466	Bison priscus	ph II		d	
467	Oyg-07-O467	Bison priscus	ph II	damaged	d	
468	Oyg-07-O468	Large herbivorous mammal	pelvis	fragment	d	
469	Oyg-07-O469	Large herbivorous mammal	limb bone	fragment	d	
470	Oyg-07-O470	Large herbivorous mammal	atlas	fragment	d	
471	Oyg-07-O471	Rangifer tarandus	Mt		d	
472	Oyg-07-O472	Bison priscus	Mc		d	
473	Oyg-07-O473	Mammuthus primigenius	tusk	fragment	d	
474	Oyg-07-O474	Mammuthus primigenius	tusk	fragment	d	
475	Oyg-07-O475	Mammuthus primigenius	tooth	fragment	d	
476	Oyg-07-O476	Mammuthus primigenius	tooth	fragment	d	vivianate and iron crust
477	Oyg-07-O477	Mammuthus primigenius	tusk	fragment	d	
478	Oyg-07-O478	Mammuthus primigenius	tusk	fragment	d	C 14, vivianate
479	Oyg-07-O479	Mammuthus primigenius	tusk	fragment	d	
480	Oyg-07-O480	Mammuthus primigenius	tusk	fragment	d	
481	Oyg-07-O481	Mammuthus primigenius	tooth	fragment	d	
482	Oyg-07-O482	Mammuthus primigenius	tooth	fragment	d	
483	Oyg-07-O483	Mammuthus primigenius	tooth	fragment	d	
484	Oyg-07-O484	Equus sp.	mandible (symphysis part)	fragment	d	
485	Oyg-07-O485	Ovibos moschatus	thorax vertebra	fragment	d	
486	Oyg-07-O486	Rangifer tarandus	lumbar vertebra	damaged	d	
487	Oyg-07-O487	Rangifer tarandus	small bone of carpus		d	
488	Oyg-07-O488	Large herbivorous mammal	limb bone	fragment	d	rounded
489	Oyg-07-O489	Rangifer tarandus ?	large bone of carpus	damaged	d	
490	Oyg-07-O490	Large herbivorous mammal	phalanx	fragment	d	rounded
491	Oyg-07-O491	Pusa hispida	cervical vertebra		d	recent?
492	Oyg-07-O492	Equus sp.	canine	fragment	d	

No.	N samples	Taxon	Skeleton element	Preservation	Loc. type	Notes
493	Oyg-07-O493	Rangifer tarandus	metapodium	distal fragment	d	juv., trashed
494	Oyg-07-O494	Equus sp. ?	epistropheus	fragment	d	
<b>East part of coast section; thermoterrace of the biggest and nearest thermocirque; 38,5 m - 8 m a.s.l.</b>						
495	Oyg-07-O495	Bison priscus	atlas	damaged	b	
496	Oyg-07-O496	Bison priscus	lower tooth (M3)		b	
497	Oyg-07-O497	Equus sp.	humerus	fragment	b	
498	Oyg-07-O498	Rangifer tarandus	shed antler	fragment	b	
499	Oyg-07-O499	Rangifer tarandus	astrogalus		b	
500	Oyg-07-O500	Rangifer tarandus	shed antler	fragment	b	
501	Oyg-07-O501	Rangifer tarandus	shed antler	fragment	b	
502	Oyg-07-O502	Rangifer tarandus	antebrachium	damaged	b	recent?
503	Oyg-07-O503	Rangifer tarandus ?	rib	damaged	b	recent?
504	Oyg-07-O504	Mammuthus primigenius	scapula	fragment	b	C 14
505	Oyg-07-O505	Mammuthus primigenius	limb bone	fragment	b	C 14
506	Oyg-07-O506	Mammuthus primigenius	limb bone	fragment	b	C 14
507	Oyg-07-O507	Mammuthus primigenius	tooth	fragment	b	
508	Oyg-07-O508	Equus sp.	Mc III	distal fragment	b	
509	Oyg-07-O509	Equus sp.	femur	distal fragment	b	
<b>East part of coast section, shore from camp to stream (point 07RUCHEY)</b>						
510	Oyg-07-O510	Bison priscus	horn sheet	fragment	d	
511	Oyg-07-O511	Bison priscus	scapula	damaged	d	
512	Oyg-07-O512	Mammuthus primigenius	humerus	fragment (without articulation surface)	d	juv.
513	Oyg-07-O513	Mammuthus primigenius	tusk	fragment	d	C 14
514	Oyg-07-O514	Mammuthus primigenius	tusk	fragment	d	
515	Oyg-07-O515	Mammuthus primigenius	tusk	fragment	d	C 14
516	Oyg-07-O516	Mammuthus primigenius	pelvis ?	fragment	d	C 14
517	Oyg-07-O517	Rangifer tarandus	Mt		d	
518	Oyg-07-O518	Bison priscus	mandible (right stem with P1 - M3)	fragment	d	
519	Oyg-07-O519	Rangifer tarandus	shed antler	fragment	d	
520	Oyg-07-O520	Rangifer tarandus	shed antler	fragment	d	
521	Oyg-07-O521	Rangifer tarandus	shed antler	fragment	d	
522	Oyg-07-O522	Mammuthus primigenius	tusk	fragment	d	C 14
523	Oyg-07-O523	Mammuthus primigenius	tooth	fragment	d	
524	Oyg-07-O524	Bison priscus	Mt	fragment	d	
525	Oyg-07-O525	Rangifer tarandus	pelvis	fragment	d	trashed
526	Oyg-07-O526	Rangifer tarandus	tibia	distal fragment	d	juv., trashed
527	Oyg-07-O527	Rangifer tarandus	antler	fragment	d	trashed
528	Oyg-07-O528	Rangifer tarandus	shed antler	fragment	d	trashed
529	Oyg-07-O529	Mammuthus primigenius	tusk	fragment	d	trashed
530	Oyg-07-O530	Mammuthus primigenius	tusk	fragment	d	trashed
531	Oyg-07-O531	Mammuthus primigenius	tusk	fragment	d	trashed
532	Oyg-07-O532	Mammuthus primigenius	tusk	fragment	d	trashed
533	Oyg-07-O533	Mammuthus primigenius	tooth	fragment	d	trashed
534	Oyg-07-O534	Mammuthus primigenius	tooth	fragment	d	trashed
535	Oyg-07-O535	Mammuthus primigenius	tooth	fragment	d	trashed
536	Oyg-07-O536	Mammuthus primigenius	rib	fragment	d	trashed
537	Oyg-07-O537	Bison priscus	astrogalus	fragment	d	trashed
538	Oyg-07-O538	Mammuthus primigenius	tooth	fragment	d	trashed
539	Oyg-07-O539	Equus sp.	astrogalus	fragment	d	trashed
540	Oyg-07-O540	Rangifer tarandus	tooth	fragment	d	trashed
541	Oyg-07-O541	Bison priscus	pelvis	fragment	d	
542	Oyg-07-O542	Bison priscus	thorax vertebra	fragment	d	
543	Oyg-07-O543	Bison priscus	metapodium	distal fragment	d	
544	Oyg-07-O544	Mammuthus primigenius	mandible (symphysis part)	fragment	d	C 14

No.	N samples	Taxon	Skeleton element	Preservation	Loc. type	Notes
545	Oyg-07-O545	Mammuthus primigenius	tooth	fragment	d	
546	Oyg-07-O546	Mammuthus primigenius	tusk	fragment	d	
547	Oyg-07-O547	Equus sp.?	limb bone	fragment	d	
548	Oyg-07-O548	Equus sp.	limb bone	fragment	d	
549	Oyg-07-O549	Bison priscus	metapodium ?	fragment	d	
550	Oyg-07-O550	Rangifer tarandus	thorax vertebra	damaged	d	
551	Oyg-07-O551	Mammuthus primigenius	tooth	fragment	d	
552	Oyg-07-O552	Equus sp.	pelvis	fragment	d	
553	Oyg-07-O553	Bison priscus	metapodium	distal fragment	d	
554	Oyg-07-O554	Bison priscus	Mc		d	
555	Oyg-07-O555	Mammuthus primigenius	scull (maxilla?)	fragment	d	
556	Oyg-07-O556	Bison priscus	humerus	distal fragment	d	
557	Oyg-07-O557	Large herbivorous mammal	limb bone ?	fragment	d	
558	Oyg-07-O558	Bison priscus	calcaneus	damaged	d	
559	Oyg-07-O559	Bison priscus	pelvis	fragment	d	
560	Oyg-07-O560	Bison priscus	Mt		d	
561	Oyg-07-O561	Bison priscus	humerus	distal fragment	d	
562	Oyg-07-O562	Bison priscus	astrogalus	fragment	d	
563	Oyg-07-O563	Large herbivorous mammal	limb bone	fragment	d	
564	Oyg-07-O564	Mammuthus primigenius	tusk	fragment	d	
565	Oyg-07-O565	Equus sp.	radius	proximal fragment	d	
566	Oyg-07-O566	Mammuthus primigenius	metapodium	proximal fragment	d	
567	Oyg-07-O567	Mammuthus primigenius	tooth		d	by Sasha
568	Oyg-07-O568	Rangifer tarandus	shed antler	fragment	d	
569	Oyg-07-O569	Equus sp.	femur	fragment (without articulation surface)	d	juv.
570	Oyg-07-O570	Mammuthus primigenius	tusk	fragment	d	
571	Oyg-07-O571	Bison priscus	calcaneus		d	
572	Oyg-07-O572	Equus sp.	tibia	distal fragment	d	
573	Oyg-07-O573	Large herbivorous mammal	limb bone	fragment	d	
574	Oyg-07-O574	Bison priscus	tibia	distal fragment	d	
575	Oyg-07-O575	Mammuthus primigenius	tooth	fragment	d	
576	Oyg-07-O576	Mammuthus primigenius	tusk	fragment	d	
577	Oyg-07-O577	Mammuthus primigenius	tusk	fragment	d	
578	Oyg-07-O578	Rangifer tarandus	humerus	distal fragment	d	
579	Oyg-07-O579	Rangifer tarandus	scapula	fragment	d	
580	Oyg-07-O580	Rangifer tarandus	mandible (stem with P1 - M2)	fragment	d	
581	Oyg-07-O581	Mammuthus primigenius	tooth	fragment	d	
582	Oyg-07-O582	Equus sp.	mandible	fragment	d	
583	Oyg-07-O583	Equus sp.	ph II		d	
584	Oyg-07-O584	Equus sp.	Mc III	distal fragment	d	
585	Oyg-07-O585	Equus sp.	ph I	distal fragment	d	
586	Oyg-07-O586	Equus sp.	astrogalus		d	
587	Oyg-07-O587	Bison priscus	small bone of tarsus		d	
588	Oyg-07-O588	Equus sp.?	ph I	proximal fragment	d	
589	Oyg-07-O589	Bison priscus	ph II		d	
590	Oyg-07-O590	Bison priscus	metapodium	distal fragment	d	trashed
591	Oyg-07-O591	Large herbivorous mammal	limb bone	fragment	d	
592	Oyg-07-O592	Equus sp.	ph III	fragment	d	
593	Oyg-07-O593	Equus sp.	os naviculare	fragment	d	
594	Oyg-07-O594	Equus sp.	milk upper tooth (dP2)		d	
595	Oyg-07-O595	Bison priscus	sesamoideum		d	
596	Oyg-07-O596	Bison priscus	sesamoideum		d	rounded
597	Oyg-07-O597	Mammuthus primigenius	tusk	fragment	d	

No.	N samples	Taxon	Skeleton element	Preservation	Loc. type	Notes
598	Oyg-07-O598	Equus sp.?	limb bone	fragment	d	rounded
599	Oyg-07-O599	Bison priscus	small bone of tarsus		d	rounded
600	Oyg-07-O600	Rangifer tarandus	scapula	fragment	d	
601	Oyg-07-O601	Large herbivorous mammal	limb bone	fragment	d	
602	Oyg-07-O602	Large herbivorous mammal	limb bone	fragment	d	rounded
603	Oyg-07-O603	Bison priscus	tooth	fragment	d	
604	Oyg-07-O604	Mammuthus primigenius	tooth	fragment	d	
605	Oyg-07-O605	Mammuthus primigenius	spat tooth	fragment	d	heavily worn, trashed
606	Oyg-07-O606	Large herbivorous mammal	limb bone	fragment	d	
607	Oyg-07-O607	Large herbivorous mammal	bone	fragment	d	
608	Oyg-07-O608	Bison priscus	horn sheet	fragment	d	by Sasha
610	Oyg-07-O610	Mammuthus primigenius	first milk tooth		d	
613	Oyg-07-O613	Mammalia	skull	fragment	d	
<b>East part of coast section; ? thermoterrace of the biggest and nearest thermocirque; 38,5 - 8 m a.s.l.</b>						
609	Oyg-07-O609	Rangifer tarandus	skull with antler	fragment	b	
<b>East part of coast section, shore</b>						
611	Oyg-07-O611	Dicrostonyx sp.	skull		d	
612	Oyg-07-O612	Avis	limb bone	fragment (without articulation surface)	d	
<b>Shore</b>						
614	Oyg-07-O614	Mammuthus primigenius	tooth	fragment	d	trashed
615	Oyg-07-O615	Mammuthus primigenius	tooth	fragment	d	trashed
616	Oyg-07-O616	Mammuthus primigenius	tooth	fragment	d	trashed
617	Oyg-07-O617	Mammuthus primigenius	tooth	fragment	d	trashed
618	Oyg-07-O618	Mammuthus primigenius	tooth	fragment	d	trashed
619	Oyg-07-O619	Mammuthus primigenius	tooth	fragment	d	trashed
620	Oyg-07-O620	Mammuthus primigenius	tooth	fragment	d	trashed
621	Oyg-07-O621	Mammuthus primigenius	tooth	fragment	d	trashed
622	Oyg-07-O622	Mammuthus primigenius	tooth	fragment	d	trashed
623	Oyg-07-O623	Mammuthus primigenius	tooth	fragment	d	trashed
624	Oyg-07-O624	Mammuthus primigenius	tooth	fragment	d	trashed
625	Oyg-07-O625	Mammuthus primigenius	tooth	fragment	d	trashed
626	Oyg-07-O626	Mammuthus primigenius	tusk	fragment	d	trashed
627	Oyg-07-O627	Mammuthus primigenius	tusk	fragment	d	trashed
628	Oyg-07-O628	Mammuthus primigenius	tusk	fragment	d	trashed
629	Oyg-07-O629	Mammuthus primigenius	tusk	fragment	d	trashed
630	Oyg-07-O630	Mammuthus primigenius	tooth	fragment	d	
631	Oyg-07-O631	Mammuthus primigenius	tooth	fragment	d	
632	Oyg-07-O632	Mammuthus primigenius	tooth	fragment	d	
633	Oyg-07-O633	Bison priscus	small bone of tarsus	fragment	d	
634	Oyg-07-O634	Equus sp.	vertebra	fragment	d	
<b>East part of coast section; thermoterrace of the biggest and nearest thermocirque; west part of it ; 22,5 - 14 m a.s.l.</b>						
636	Oyg-07-O636	Rangifer tarandus	shed antler	fragment (2 pieces)	b	from Kunitsky V. V.
638	Oyg-07-O638	Large herbivorous mammal	tooth	fragment	b	from Kunitsky V. V.
<b>East part of coast section, shore from camp to stream (point 07RUCHEY)</b>						
637	Oyg-07-O637	Rangifer tarandus	unerupted tooth	fragment	d	from Kunitsky V. V.
635	Oyg-07-O635	Mammuthus primigenius	rib	damaged	d	from Kunitsky V. V., trashed
639	Oyg-07-O639	Rangifer tarandus	ph I		d	
640	Oyg-07-O640	Rangifer tarandus	ph I		d	
641	Oyg-07-O641	Rangifer tarandus	ph II		d	

No.	N samples	Taxon	Skeleton element	Preservation	Loc. type	Notes
642	Oyg-07-O642	Rangifer tarandus	metapodium	distal fragment	d	
643	Oyg-07-O643	Lepus sp.	pelvis	fragment	d	
<b>East part of coast section; thermoterrace of the biggest and nearest thermocirque; 38,5 - 8 m a.s.l</b>						
644	Oyg-07-O644	Mammuthus primigenius	femur	proximal fragment (головка)	b	juv., C 14
<b>East part of coast section; thermoterrace of the thermocirque locate more than 2 km east from the camp (lower part of Ice Complex); 8 m - 16 m a.s.l.</b>						
646	Oyg-07-O646	Mammuthus primigenius	tusk	fragment	b	C 14
<b>East part of coast section, shore near the stream mouth; (landing site in 2002); point 07RUCHEY</b>						
647	Oyg-07-O647	Mammuthus primigenius	mandible with tooth root	fragment	d	C 14
648	Oyg-07-O648	Mammuthus primigenius	scapula ?	fragment	d	C 14
649	Oyg-07-O649	Equus sp.	mandible (left stem with P3-M3)	fragment	d	
650	Oyg-07-O650	Equus sp.	ph II		d	
651	Oyg-07-O651	Bison priscus	horn sheet	fragment	d	
652	Oyg-07-O652	Bison priscus ?	pelvis	fragment	d	
653	Oyg-07-O653	Mammuthus primigenius	tooth	fragment	d	
654	Oyg-07-O654	Mammuthus primigenius	tooth	fragment	d	
655	Oyg-07-O655	Equus sp.	ph III		d	
656	Oyg-07-O656	Equus sp.	os naviculare		d	
657	Oyg-07-O657	Bison priscus	upper tooth	fragment	d	
658	Oyg-07-O658	Bison priscus	horn sheet	fragment	d	
659	Oyg-07-O659	Large herbivorous mammal	limb bone	fragment	d	
660	Oyg-07-O660	Rangifer tarandus	astrogalus	damaged	d	
661	Oyg-07-O661	Rangifer tarandus	large bone of carpus		d	
<b>East part of coast section; thermoterrace of the small, second thermocirque east of the camp</b>						
645	Oyg-07-O645	Mammuthus primigenius	tusk	fragment	b	C 14
662	Oyg-07-O662	Mammuthus primigenius	tibia	distal fragment	b	
663	Oyg-07-O663	Rangifer tarandus	femur	damaged	b	iron crust
664	Oyg-07-O664	Rangifer tarandus	humerus	distal fragment	b	recent?
665	Oyg-07-O665	Rangifer tarandus	thorax vertebra	damaged	b	recent?
<b>Shore</b>						
666	Oyg-07-O666	Bison priscus	scapula	fragment	d	
667	Oyg-07-O667	Equus sp.	1-st thorax vertebra		d	
668	Oyg-07-O668	Equus sp.	astrogalus	damaged	d	
669	Oyg-07-O669	Rangifer tarandus	ph I		d	
670	Oyg-07-O670	Rangifer tarandus	vertebra	damaged	d	
<b>East part of coast section; thermoterrace of the thermocirque located east of the stream in the middle of distance from the stream to the waterfall</b>						
671	Oyg-07-O671	Mammuthus primigenius	limb bone	fragment (without articulation surface)	b	C 14
672	Oyg-07-O672	Mammuthus primigenius	rib ?	fragment	b	
673	Oyg-07-O673	Mammuthus primigenius	ulna ?	fragment	b	C 14
674	Oyg-07-O674	Mammuthus primigenius	scapula	fragment	b	C 14
<b>east part of coast section, shore beyond the stream (point 07RUCHEY</b>						
675	Oyg-07-O675	Mammuthus primigenius	tusk	fragment	d	trashed
676	Oyg-07-O676	Mammuthus primigenius	tusk	fragment	d	trashed
677	Oyg-07-O677	Mammuthus primigenius	tusk	fragment	d	trashed
678	Oyg-07-O678	Mammuthus primigenius	tooth	fragment	d	trashed
679	Oyg-07-O679	Rangifer tarandus	pelvis	fragment	d	trashed
680	Oyg-07-O680	Bison priscus	large bone of carpus	fragment	d	
681	Oyg-07-O681	Bison priscus	large bone of carpus	fragment	d	

No.	N samples	Taxon	Skeleton element	Preservation	Loc. type	Notes
682	Oyg-07-O682	Mammuthus primigenius	tooth	fragment	d	
683	Oyg-07-O683	Bison priscus	lower tooth		d	
684	Oyg-07-O684	Equus sp.	astrogalus		d	
685	Oyg-07-O685	Equus sp.	ph I		d	
686	Oyg-07-O686	Rangifer tarandus	astrogalus		d	
687	Oyg-07-O687	Rangifer tarandus	lumbar vertebra	damaged	d	
688	Oyg-07-O688	Equus sp.	cervical vertebra	damaged	d	
689	Oyg-07-O689	Equus sp.	radius		d	
690	Oyg-07-O690	Bison priscus	thorax vertebra	fragment (without articulation surface)	d	juv.
691	Oyg-07-O691	Mammuthus primigenius	humerus	proximal fragment	d	C 14
692	Oyg-07-O692	Mammuthus primigenius	limb bone	fragment	d	
693	Oyg-07-O693	Mammuthus primigenius	limb bone	fragment	d	C 14
694	Oyg-07-O694	Rangifer tarandus	shed antler	fragment	d	
695	Oyg-07-O695	Panthera spelaea	molar tooth		d	
696	Oyg-07-O696	Mammuthus primigenius	astrogalus	fragment	d	C 14
697	Oyg-07-O697	Mammuthus primigenius	tooth	fragment	d	
698	Oyg-07-O698	Mammuthus primigenius	tooth	fragment	d	
699	Oyg-07-O699	Mammuthus primigenius	tusk	fragment	d	C 14
700	Oyg-07-O700	Rangifer tarandus	humerus	distal fragment	d	
701	Oyg-07-O701	Bison priscus	skull (occipitale part)	fragment	d	
702	Oyg-07-O702	Bison priscus	radius		d	
703	Oyg-07-O703	Bison priscus	scapula	fragment	d	
704	Oyg-07-O704	Bison priscus	horn sheet	fragment	d	
705	Oyg-07-O705	Bison priscus ?	cervical vertebra	fragment	d	
706	Oyg-07-O706	Ovibos moschatus	humerus	distal fragment	d	
707	Oyg-07-O707	Bison priscus	ph I		d	
708	Oyg-07-O708	Ovibos moschatus	atlas	fragment	d	
709	Oyg-07-O709	Rangifer tarandus ?	cervical vertebra	damaged	d	
710	Oyg-07-O710	Equus sp.	lumbar vertebra	fragment	d	
711	Oyg-07-O711	Equus sp.	ph II		d	
712	Oyg-07-O712	Bison priscus ?	small bone of tarsus	damaged	d	
713	Oyg-07-O713	Bison priscus ?	small bone of tarsus	fragment	d	
714	Oyg-07-O714	Bison priscus	lower tooth		d	
715	Oyg-07-O715	Rangifer tarandus	radius	distal fragment	d	
716	Oyg-07-O716	Rangifer tarandus	scapula	fragment	d	
717	Oyg-07-O717	Rangifer tarandus	ph I		d	
718	Oyg-07-O718	Rangifer tarandus	metapodium	distal fragment	d	
719	Oyg-07-O719	Rangifer tarandus	astrogalus	damaged	d	
720	Oyg-07-O720	Bison priscus ?	ph I	proximal fragment	d	
721	Oyg-07-O721	Bison priscus	bone of tarsus		d	
722	Oyg-07-O722	Bison priscus	astrogalus	fragment	d	trashed
723	Oyg-07-O723	Rangifer tarandus	antler	fragment	d	trashed
<b>West part of coast section, shore; ca 800 m west of the camp's stream; place where tusk in permafrost sediments was found</b>						
724	Oyg-07-O724	Mammuthus primigenius	tusk	fragment (3 pieces)	d	a lot of vivianate
725	Oyg-07-O725	Mammuthus primigenius	vertebra	fragment (articulation surface)	d	vivianate
<b>East part of coast section, shore; between 2 and 4 km from the camp</b>						
726	Oyg-07-O726	Equus sp.	mandible with right and left C - M3 teeth		d	from Tumskoy V. E.
<b>East part of coast section; shore</b>						
727	Oyg-07-O727	Rangifer tarandus	antler with skull part	fragment	d	trashed
728	Oyg-07-O728	Rangifer tarandus	shed antler	fragment	d	trashed
729	Oyg-07-O729	Rangifer tarandus	antler	fragment	d	trashed

No.	N samples	Taxon	Skeleton element	Preservation	Loc. type	Notes
730	Oyg-07-O730	Rangifer tarandus	Mc	fragment	d	trashed
731	Oyg-07-O731	Mammuthus primigenius	tooth	fragment	d	trashed
732	Oyg-07-O732	Mammuthus primigenius	tooth	fragment	d	trashed
733	Oyg-07-O733	Mammuthus primigenius	tooth	fragment	d	trashed
734	Oyg-07-O734	Mammuthus primigenius	tooth (root part)	fragment	d	trashed
735	Oyg-07-O735	Mammuthus primigenius	tusk	fragment	d	trashed
736	Oyg-07-O736	Mammuthus primigenius	tusk	fragment	d	trashed
737	Oyg-07-O737	Mammuthus primigenius	tusk	fragment	d	trashed
738	Oyg-07-O738	Mammuthus primigenius	tusk	fragment	d	trashed
739	Oyg-07-O739	Mammuthus primigenius	tusk	fragment	d	trashed
740	Oyg-07-O740	Mammuthus primigenius	tusk	fragment	d	trashed
741	Oyg-07-O741	Mammuthus primigenius	tusk	fragment	d	trashed
742	Oyg-07-O742	Mammuthus primigenius	tusk	fragment	d	trashed
743	Oyg-07-O743	Mammuthus primigenius	tusk	fragment	d	trashed
744	Oyg-07-O744	Mammuthus primigenius	tusk	fragment	d	trashed
745	Oyg-07-O745	Mammuthus primigenius	tusk	fragment	d	trashed
746	Oyg-07-O746	Mammuthus primigenius	tusk	fragment	d	trashed
747	Oyg-07-O747	Bison priscus	pelvis (left part)	fragment	d	
748	Oyg-07-O748	Bison priscus	humerus	distal fragment	d	
749	Oyg-07-O749	Bison priscus	mandible (stem with P4 - M2)	fragment	d	
750	Oyg-07-O750	Mammuthus primigenius	limb bone	fragment	d	
751	Oyg-07-O751	Mammuthus primigenius	tusk	fragment	d	
752	Oyg-07-O752	Mammuthus primigenius	tusk	fragment	d	
753	Oyg-07-O753	Mammuthus primigenius	tooth	fragment	d	
754	Oyg-07-O754	Mammuthus primigenius	tooth	fragment	d	
755	Oyg-07-O755	Mammuthus primigenius	tusk	fragment	d	
756	Oyg-07-O756	Mammuthus primigenius ?	rib	fragment	d	C 14
757	Oyg-07-O757	Mammuthus primigenius	tooth	fragment	d	
758	Oyg-07-O758	Rangifer tarandus	humerus	distal fragment	d	
759	Oyg-07-O759	Bison priscus	astrogalus		d	
760	Oyg-07-O760	Equus sp.	upper tooth (P)		d	
761	Oyg-07-O761	Equus sp.	os naviculare		d	
762	Oyg-07-O762	Equus sp.	astrogalus	damaged	d	
763	Oyg-07-O763	Equus sp.	metapodium	distal fragment	d	
764	Oyg-07-O764	Bison priscus	thorax vertebra	fragment	d	
765	Oyg-07-O765	Ovibos moschatus	thorax vertebra	damaged	d	
766	Oyg-07-O766	Bison priscus	ph I	proximal fragment	d	juv.
767	Oyg-07-O767	Rangifer tarandus	Mt	damaged (3 pieces)	d	recent?
768	Oyg-07-O768	Equus sp.	radius	fragment	d	
769	Oyg-07-O769	Equus sp.	radius		d	
770	Oyg-07-O770	Bison priscus	epistropheus	damaged	d	
771	Oyg-07-O771	Equus sp.	ph I		d	
772	Oyg-07-O772	Equus sp.	ph I		d	
773	Oyg-07-O773	Equus sp.	ph III	fragment	d	
774	Oyg-07-O774	Equus sp. ?	pelvis	fragment	d	
775	Oyg-07-O775	Bison priscus	large bone of carpus		d	
776	Oyg-07-O776	Mammuthus primigenius	tusk	fragment	d	
777	Oyg-07-O777	Bison priscus	limb bone	fragment	d	
778	Oyg-07-O778	Rangifer tarandus	epistropheus	damaged	d	
779	Oyg-07-O779	Rangifer tarandus	ph I	proximal fragment	d	
780	Oyg-07-O780	Mammuthus primigenius	tusk	fragment	d	trashed
781	Oyg-07-O781	Mammuthus primigenius	tusk	fragment	d	trashed
782	Oyg-07-O782	Mammuthus primigenius	tusk	fragment	d	trashed
783	Oyg-07-O783	Mammuthus primigenius	tusk	fragment	d	trashed
784	Oyg-07-O784	Mammuthus primigenius	tusk	fragment	d	trashed

No.	N samples	Taxon	Skeleton element	Preservation	Loc. type	Notes
785	Oyg-07-O785	Mammuthus primigenius	tusk	fragment	d	trashed
786	Oyg-07-O786	Mammuthus primigenius	tusk	fragment	d	trashed
787	Oyg-07-O787	Mammuthus primigenius	tusk	fragment	d	trashed
788	Oyg-07-O788	Mammuthus primigenius	tusk	fragment	d	trashed
789	Oyg-07-O789	Mammuthus primigenius	tusk	fragment	d	trashed
790	Oyg-07-O790	Mammuthus primigenius	tusk	fragment	d	trashed
791	Oyg-07-O791	Mammuthus primigenius	tusk	fragment	d	trashed
792	Oyg-07-O792	Mammuthus primigenius	tooth	fragment	d	trashed
793	Oyg-07-O793	Rangifer tarandus	antler	fragment	d	trashed
794	Oyg-07-O794	Rangifer tarandus	antler	fragment	d	trashed
795	Oyg-07-O795	Ovibos moschatus	scull	fragment	d	trashed
796	Oyg-07-O796	Mammuthus primigenius	scull	fragment	d	trashed
797	Oyg-07-O797	Bison priscus	astrogalus	fragment	d	trashed
798	Oyg-07-O798	Mammuthus primigenius	limb bone	fragment	d	C 14
799	Oyg-07-O799	Mammuthus primigenius	tusk	fragment	d	C 14
800	Oyg-07-O800	Mammuthus primigenius	tusk	fragment	d	
801	Oyg-07-O801	Mammuthus primigenius	tusk	fragment	d	
802	Oyg-07-O802	Rangifer tarandus	humerus	distal fragment	d	
803	Oyg-07-O803	Equus sp.	ph I	proximal fragment	d	
804	Oyg-07-O804	Bison priscus	ph I	fragment	d	
805	Oyg-07-O805	Large herbivorous mammal	limb bone	fragment	d	
806	Oyg-07-O806	Large herbivorous mammal	limb bone	fragment	d	
807	Oyg-07-O807	Mammuthus primigenius	tusk	fragment	d	C 14
808	Oyg-07-O808	Rangifer tarandus	mandible (right stem with P2 - M3)	fragment	d	
809	Oyg-07-O809	Rangifer tarandus	shed antler	fragment	d	
810	Oyg-07-O810	Rangifer tarandus	humerus	distal fragment	d	
811	Oyg-07-O811	Bison priscus	femur	proximal fragment	d	
812	Oyg-07-O812	Equus sp.	humerus	distal fragment	d	
813	Oyg-07-O813	Equus sp.	radius	proximal fragment	d	
814	Oyg-07-O814	Bison priscus	ph I	fragment	d	
815	Oyg-07-O815	Equus sp.	ph II		d	
816	Oyg-07-O816	Equus sp.	small bone of tarsus		d	rounded
817	Oyg-07-O817	Rangifer tarandus	metapodium	distal fragment	d	
818	Oyg-07-O818	Mammuthus primigenius	antebrachium	proximal fragment	d	C 14
819	Oyg-07-O819	Mammuthus primigenius	tooth	fragment	d	
820	Oyg-07-O820	Large herbivorous mammal	metapodium ?	fragment	d	
821	Oyg-07-O821	Mammuthus primigenius	tooth	fragment	d	
822	Oyg-07-O822	Mammuthus primigenius	sesamoideum	damaged	d	
823	Oyg-07-O823	Bison priscus	ph I	proximal fragment	d	juv.
824	Oyg-07-O824	Large herbivorous mammal	limb bone	fragment	d	
825	Oyg-07-O825	Bison priscus	small bone of tarsus	fragment	d	
826	Oyg-07-O826	Bison priscus ?	small bone of tarsus	fragment	d	
827	Oyg-07-O827	Bison priscus ?	upper tooth	fragment	d	
828	Oyg-07-O828	Equus sp.	upper tooth	fragment	d	
829	Oyg-07-O829	Equus sp.	upper tooth	fragment	d	
830	Oyg-07-O830	Bison priscus	upper tooth (P2)	fragment	d	
<b>East part of coast section, shore from camp to stream (point 07RUCHEY)</b>						
831	Oyg-07-O831	Mammuthus primigenius	femur	fragment (without articulation surface)	d	juv.
832	Oyg-07-O832	Mammuthus primigenius	limb bone	fragment	d	C 14
833	Oyg-07-O833	Mammuthus primigenius	limb bone	fragment	d	C 14
834	Oyg-07-O834	Mammuthus primigenius	tusk	fragment	d	C 14

No.	N samples	Taxon	Skeleton element	Preservation	Loc. type	Notes
835	Oyg-07-O835	Mammuthus primigenius	tooth	fragment	d	
836	Oyg-07-O836	Mammuthus primigenius	astrogalus		d	small
837	Oyg-07-O837	Mammuthus primigenius	limb bone	fragment (articulation surface)	d	juv.
838	Oyg-07-O838	Mammuthus primigenius	bone of tarsus	fragment	d	
839	Oyg-07-O839	Mammuthus primigenius	patella	damaged	d	
840	Oyg-07-O840	Mammuthus primigenius	tusk	fragment	d	
841	Oyg-07-O841	Mammuthus primigenius	thorax vertebra	damaged	d	C 14
842	Oyg-07-O842	Ovibos moschatus	scull (occipitale part)	fragment	d	
843	Oyg-07-O843	Bison priscus	ph II		d	
844	Oyg-07-O844	Ovibos moschatus	astrogalus		d	
845	Oyg-07-O845	Bison priscus	tibia	2 pieces	d	
846	Oyg-07-O846	Rangifer tarandus	lumbar vertebra	damaged	d	
847	Oyg-07-O847	Mammuthus primigenius	humerus	proximal fragment (2 pices)	d	C 14
848	Oyg-07-O848	Equus sp. ?	femur	fragment	d	juv.
<b>East part of coast section; thermoterrace of the biggest and nearest thermocirque; 38,5 - 8 m a.s.l.</b>						
849	Oyg-07-O849	Mammuthus primigenius	tusk	fragment	b	C 14; sample cut out
<b>Tundra surface to the east from the camp; near the stream (landing site in 2002); bazhdjerakhs of the Ice Complex; ca 12 m a.s.l.</b>						
850	Oyg-07-O850-a	Mammuthus primigenius	scull	a lot fragments	e	left
851	Oyg-07-O850-b	Mammuthus primigenius	thorax vertebra	fragment	e	left
852	Oyg-07-O850-c	Mammuthus primigenius	thorax vertebra	fragment	e	left
853	Oyg-07-O850-d	Mammuthus primigenius	thorax vertebra	fragment	e	left
854	Oyg-07-O850-e	Mammuthus primigenius	thorax vertebra	fragment	e	left
855	Oyg-07-O850-f	Mammuthus primigenius	thorax vertebra	fragment	e	left
856	Oyg-07-O850-g	Mammuthus primigenius	thorax vertebra	fragment	e	left
857	Oyg-07-O850-h	Mammuthus primigenius	rib	fragment	e	left
858	Oyg-07-O850-i	Mammuthus primigenius	rib	fragment	e	left
859	Oyg-07-O850-j	Mammuthus primigenius	rib	fragment	e	left
860	Oyg-07-O850-k	Mammuthus primigenius	rib	fragment	e	left
861	Oyg-07-O850-l	Mammuthus primigenius	rib	fragment	e	left
862	Oyg-07-O850-m	Mammuthus primigenius	rib	fragment	e	left
863	Oyg-07-O850-n	Mammuthus primigenius	rib	fragment	e	left
864	Oyg-07-O850-o	Mammuthus primigenius	rib	fragment	e	left
865	Oyg-07-O850-p	Mammuthus primigenius	rib	fragment	e	left
866	Oyg-07-O850-q	Mammuthus primigenius	lumbar vertebra	fragment	e	left
867	Oyg-07-O850-r	Mammuthus primigenius	lumbar vertebra	fragment	e	left
868	Oyg-07-O850-s	Mammuthus primigenius	lumbar vertebra	fragment	e	left
869	Oyg-07-O850-t	Mammuthus primigenius	pelvis	fragment	e	left
870	Oyg-07-O850-1	Mammuthus primigenius	tooth	fragment	e	
871	Oyg-07-O850-2	Mammuthus primigenius	мелкая кость заплюсны		e	
872	Oyg-07-O850-3	Mammuthus primigenius	rib	fragment	e	
873	Oyg-07-O850-4	Mammuthus primigenius	rib	fragment	e	
874	Oyg-07-O850-5	Mammuthus primigenius	thorax vertebra	fragment	e	
875	Oyg-07-O850-6	Mammuthus primigenius	thorax vertebra	fragment	e	
876	Oyg-07-O850-7	Mammuthus primigenius	thorax vertebra	fragment	e	
877	Oyg-07-O850-8	Mammuthus primigenius	lumbar vertebra	damaged	e	
878	Oyg-07-O850-9	Mammuthus primigenius	lumbar vertebra	damaged	e	
879	Oyg-07-O850-10	Mammuthus primigenius	metapodium		e	
880	Oyg-07-O850-11	Mammuthus primigenius	scapula		e	sample cut out
881	Oyg-07-O850-12	Mammuthus primigenius	thorax vertebra	fragment	e	
<b>West part of coast section, shore from camp's stream to 1 km to the west</b>						
882	Oyg-07-O851	Mammuthus primigenius	mandible (right stem with tooth)		d	

No.	N samples	Taxon	Skeleton element	Preservation	Loc. type	Notes
<b>East part of coast section, shore from camp to stream (point 07RUCHEY)</b>						
883	Oyg-07-O852	Mammuthus primigenius	tusk	fragment	d	C 14, sample cut out
884	Oyg-07-O853	Mammuthus primigenius	tusk	fragment	d	C 14, sample cut out
885	Oyg-07-O854	Mammuthus primigenius	tusk	fragment	d	C 14, sample cut out
<b>In situ, east part of coast section; wall under the second small thermocirque; Krest Yuryakh deposits</b>						
886	Oyg-07-O855	Mammuthus primigenius	tusk	fragment	a	C 14, sample cut out
<b>In situ, west part of coast section; ca 800 m west of the camp's stream; in taberal Ice Complex deposits</b>						
887	Oyg-07-O856	Mammuthus primigenius	tusk	fragment	a	C 14, sample cut out
<b>In situ, east part of coast section; permafrost deposits</b>						
888	Oyg-07-O857	Mammuthus primigenius	tusk	fragment	a	C 14, sample cut out
889	Oyg-07-O858	Bison priscus	radius	damaged	a	
<b>Shore</b>						
890	Oyg-07-O859	Mammuthus primigenius	tusk	fragment	d	C 14, sample cut out
892	Oyg-07-O861	Mammuthus primigenius	humerus	fragment (without upper articulation surface)		juv., C 14, sample cut out
<b>east part of coast section, shore beyond the stream (point 07RUCHEY)</b>						
891	Oyg-07-O860	Mammuthus primigenius	tusk	fragment	d	C 14, sample cut out
893	Oyg-07-O862	Mammuthus primigenius	humerus	fragment	d	C 14, sample cut out
894	Oyg-07-O863	Mammuthus primigenius	radius	fragment (without lower articulation surface)	d	C 14, sample cut out
895	Oyg-07-O864	Mammuthus primigenius	pelvis	fragment	d	C 14
896	Oyg-07-O865	Mammuthus primigenius	pelvis	fragment	d	C 14
<b>East part of coast section, shore</b>						
897	Oyg-07-O866	Mammuthus primigenius	pelvis	fragment	d	C 14; with teeth traces of Carnivora
<b>Shore</b>						
898	Oyg-07-O867	Mammuthus primigenius	tibia	fragment (without lower articulation surface)	d	juv., C 14, sample cut out
899	Oyg-07-O868	Mammuthus primigenius	antebrachium	fragment	d	C 14
900	Oyg-07-O869	Mammuthus primigenius	scapula	fragment	d	C 14
901	Oyg-07-O870	Mammuthus primigenius	limb bone	fragment	d	C 14
<b>West part of coast section, shore</b>						
902	Oyg-07-O871	Mammuthus primigenius	limb bone	fragment	d	C 14, with marrow
<b>East part of coast section, shore from camp to stream (point 07RUCHEY)</b>						
903	Oyg-07-O872	Odobenus rosmarus	canine	fragment	d	
904	Oyg-07-O873	Mammuthus primigenius	tusk	fragment	d	
<b>East part of coast section; east part of the thermoterrace in the biggest and nearest thermocirque</b>						
905	Oyg-07-O874	Mammuthus primigenius	rib	fragment	b	C 14
906	Oyg-07-O875	Mammuthus primigenius	femur	distal fragment	b	juv., C 14, sample cut out
907	Oyg-07-O876	Mammuthus primigenius	epistropheus	damaged	b	juv.
908	Oyg-07-O877	Bison priscus	radius		b	
909	Oyg-07-O878	Bison priscus	epistropheus	damaged	b	
910	Oyg-07-O879	Bison priscus	humerus	distal fragment	b	
911	Oyg-07-O880	Equus sp.	ulna	damaged	b	
912	Oyg-07-O881	Mammuthus primigenius	tusk	fragment	b	
913	Oyg-07-O882	Rangifer tarandus ?	caudal vertebra	fragment	b	
914	Oyg-07-O883	Equus sp.	mandible	fragment	b	

No.	N samples	Taxon	Skeleton element	Preservation	Loc. type	Notes
<b>West part of coast section, shore</b>						
915	Oyg-07-O884	Mammuthus primigenius	radius	proximal fragment	d	C 14, sample cut out; + 1 piece for fossilisation
916	Oyg-07-O885	Mammuthus primigenius	pelvis	fragment	d	juv., C 14, sample cut out
917	Oyg-07-O886	Mammuthus primigenius	femur	fragment	d	juv., C 14, sample cut out
<b>East part of coast section, shore between 2 km and the mouth stream (point 07RUCHEY)</b>						
918	Oyg-07-O887	Mammuthus primigenius	radius	proximal fragment	d	C 14, sample cut out; + 1 piece for fossilisation
919	Oyg-07-O888	Mammuthus primigenius	humerus	distal fragment	d	C 14, sample cut out
920	Oyg-07-O889	Mammuthus primigenius	humerus	fragment	d	C 14, sample cut out; + 1 piece for fossilisation
921	Oyg-07-O890	Mammuthus primigenius	tibia	proximal fragment	d	juv., C 14, with teeth traces of Carnivora
922	Oyg-07-O891	Mammuthus primigenius	femur	fragment	d	C 14
923	Oyg-07-O892	Mammuthus primigenius	tibia	damaged	d	C 14
926	Oyg-07-O895	Mammuthus primigenius	tusk	fragment	a	C 14
<b>West part of coast section, shore</b>						
924	Oyg-07-O893	Mammuthus primigenius	radius	fragment (2 pieces)	d	C 14, sample cut out
<b>East part of coast section; est part of the thermoterrace in the biggest and nearest thermocirquet</b>						
925	Oyg-07-O894	Mammuthus primigenius	tusk	fragment	b	C 14, sample cut out
927	Oyg-07-O896	Mammuthus primigenius	tusk	fragment	b	
<b>East part of coast section, shore between 2 km and 4 km from the camp</b>						
928	Oyg-07-O897	Mammuthus primigenius	tusk	fragment	d	
<b>West part of coast section, shore</b>						
929	Oyg-07-O898	Ovibos moschatus	scull with horns	fragment (2 pieces)	d	samples O898, O899, O900, O903 from one animal probably; from Dima and Volodya
930	Oyg-07-O899	Ovibos moschatus	mandible (two stems with I and P2-M3)	damaged	a	
931	Oyg-07-O900	Ovibos moschatus	humerus	distal fragment	a	
934	Oyg-07-O903	Ovibos moschatus	ulna	damaged	a	
935	Oyg-07-O904	Ovibos moschatus	cervical vertebra	damaged	d	
936	Oyg-07-O905	Bison priscus	humerus	distal fragment	d	
937	Oyg-07-O906	Bison priscus	Mc		d	
938	Oyg-07-O907	Ovibos moschatus	humerus	distal fragment	d	
939	Oyg-07-O908	Ovibos moschatus ?	calcaneus	damaged	d	
940	Oyg-07-O909	Rangifer tarandus	calcaneus	damaged	d	
941	Oyg-07-O910	Bison priscus	radius		d	from Volodva and Dima
949	Oyg-07-O918	Bison priscus	horn sheet		d	
961	Oyg-07-O930	Mammuthus primigenius	rib	damaged	b	
<b>region of r. Kondrat'eva</b>						
932	Oyg-07-O901	Mammuthus primigenius	tooth			museum of LDR
933	Oyg-07-O902	Mammuthus primigenius	tusk	fragment		museum of LDR
<b>East part of coast section; thermoterrace of the thermocirquees locate from 2 km to 4 km from the camp (Ice Complex)</b>						
942	Oyg-07-O911	Large herbivorous mammal	limb bone	fragment	b	
943	Oyg-07-O912	Bison priscus	astrogalus		b	
944	Oyg-07-O913	Bison priscus	horn sheet	fragment	b	
945	Oyg-07-O914	Bison priscus	femur	distal fragment	b	
946	Oyg-07-O915	Bison priscus	tibia	distal fragment	b	
947	Oyg-07-O916	Rangifer tarandus	Mt		b	
948	Oyg-07-O917	Mammuthus primigenius	tooth	fragment	b	
950	Oyg-07-O919	Mammuthus primigenius	tusk	fragment (2 pieces)	b	
951	Oyg-07-O920	Mammuthus primigenius	rib	fragment	b	
952	Oyg-07-O921	Mammuthus primigenius	limb bone	fragment	b	

No.	N samples	Taxon	Skeleton element	Preservation	Loc. type	Notes
953	Oyg-07-O922	Bison priscus	pelvis	fragment	b	
954	Oyg-07-O923	Bison priscus	skull	fragment	b	
955	Oyg-07-O924	Rangifer tarandus	lumbar vertebra	damaged	b	
956	Oyg-07-O925	Rangifer tarandus	shed antler	fragment	b	
957	Oyg-07-O926	Rangifer tarandus	shed antler	fragment	b	
958	Oyg-07-O927	Rangifer tarandus	shed antler	fragment	b	
959	Oyg-07-O928	Large herbivorous mammal	limb bone	fragment	b	
960	Oyg-07-O929	Large herbivorous mammal	skull	fragment	b	
962	Oyg-07-O931	Mammuthus primigenius	tooth		b	
<b>East part of coast section; est part of the thermoterrace in the biggest and nearest thermocirquet</b>						
963	Oyg-07-O932	Rangifer tarandus	shed antler	fragment	b	trashed
<b>East part of coast section shore</b>						
964	Oyg-07-O933	Mammuthus primigenius	tooth	fragment	d	trashed
965	Oyg-07-O934	Mammuthus primigenius	tooth	fragment	d	trashed
966	Oyg-07-O935	Mammuthus primigenius	tusk	fragment	d	trashed
967	Oyg-07-O936	Mammuthus primigenius	tusk	fragment	d	trashed
968	Oyg-07-O937	Mammuthus primigenius	1-st rib		d	
969	Oyg-07-O938	Mammuthus primigenius	rib	damaged	d	near the mammoth's skull
<b>West part of coast section, shore</b>						
970	Oyg-07-O939	Mammuthus primigenius	tusk	fragment	d	C 14, sample cut out
971	Oyg-07-O940	Mammuthus primigenius	tusk	fragment	d	C 14, vivianate
972	Oyg-07-O941	Mammuthus primigenius	tusk	fragment	d	
<b>West part of coast section, shore</b>						
973	Oyg-07-O942	Mammuthus primigenius	tusk	fragment	d	C 14
974	Oyg-07-O943	Mammuthus primigenius	tusk	fragment	d	
975	Oyg-07-O944	Mammuthus primigenius	tusk	fragment	d	C 14
976	Oyg-07-O945	Bison priscus ?	pelvis	fragment	d	
977	Oyg-07-O946	Mammuthus primigenius	mandible	fragment	d	C 14
978	Oyg-07-O947	Mammuthus primigenius	thorax vertebra	fragment	d	juv., C 14
979	Oyg-07-O948	Mammuthus primigenius	limb bone	fragment	d	C 14
980	Oyg-07-O949	Mammuthus primigenius	tusk	fragment	d	
981	Oyg-07-O950	Bison priscus	radius		d	
982	Oyg-07-O951	Bison priscus	skull	fragment	d	
983	Oyg-07-O952	Mammuthus primigenius	tusk	fragment	d	
984	Oyg-07-O953	Mammuthus primigenius	tooth	fragment	d	
985	Oyg-07-O954	Bison priscus	metapodium	fragment	d	
986	Oyg-07-O955	Bison priscus ?	lower tooth		d	
987	Oyg-07-O956	Bison priscus	ph III		d	
988	Oyg-07-O957	Bison priscus	small bone of tarsus		d	
989	Oyg-07-O958	Bison priscus	small bone of tarsus		d	
990	Oyg-07-O959	Bison priscus ?	pelvis	fragment	d	
991	Oyg-07-O960	Bison priscus	femur	distal fragment	d	
992	Oyg-07-O961	Bison priscus	tooth	fragment	d	
993	Oyg-07-O962	Large herbivorous mammal	limb bone	fragment	d	
994	Oyg-07-O963	Rangifer tarandus	small bone of tarsus	fragment	d	
995	Oyg-07-O964	Bison priscus	pelvis	fragment	d	
996	Oyg-07-O965	Equus sp.	metapodium ?	proximal fragment	d	
997	Oyg-07-O966	Mammuthus primigenius	tooth	damaged	d	
998	Oyg-07-O967	Mammuthus primigenius	tooth	damaged	d	vivianate
999	Oyg-07-O968	Bison priscus	skull (occipitale part)	fragment	d	
1000	Oyg-07-O969	Bison priscus	tibia	distal fragment	d	

No.	N samples	Taxon	Skeleton element	Preservation	Loc. type	Notes
1001	Oyg-07-O970	Bison priscus	ph I		d	
1002	Oyg-07-O971	Bison priscus	Mc		d	
1003	Oyg-07-O972	Equus sp. ?	femur	fragment	d	
1004	Oyg-07-O973	Bison priscus	astrogalus		d	juv.
1005	Oyg-07-O974	Equus sp.	ph I		d	
1006	Oyg-07-O975	Mammuthus primigenius	tusk	fragment	d	
1007	Oyg-07-O976	Mammuthus primigenius	tooth	fragment	d	
1008	Oyg-07-O977	Mammuthus primigenius	tusk	fragment	d	
1009	Oyg-07-O978	Mammuthus primigenius	tusk	fragment	d	
1010	Oyg-07-O979	Mammuthus primigenius	tusk	fragment	d	
1011	Oyg-07-O980	Mammuthus primigenius	tusk	fragment	d	
1012	Oyg-07-O981	Rangifer tarandus	scapula	fragment	d	
1013	Oyg-07-O982	Bison priscus	lumbar vertebra	damaged	d	
1014	Oyg-07-O983	Equus sp.	lower tooth (M3)	damaged	d	
1015	Oyg-07-O984	Equus sp.	ph III		d	
1016	Oyg-07-O985	Equus sp. ?	femur	fragment	d	
1017	Oyg-07-O986	Bison priscus	humerus	fragment	d	
1018	Oyg-07-O987	Equus sp. ?	femur	fragment	d	vivianate
1019	Oyg-07-O988	Equus sp.	metapodium	distal fragment	d	
1020	Oyg-07-O989	Equus sp.	os naviculare		d	
1021	Oyg-07-O990	Equus sp. ?	lumbar vertebra	damaged	d	
1022	Oyg-07-O991	Bison priscus	femur	distal fragment (articulation surface)	d	
1023	Oyg-07-O992	Mammuthus primigenius	bone of tarsus	damaged	d	
1024	Oyg-07-O993	Mammuthus primigenius	limb bone	fragment	d	C 14
1025	Oyg-07-O994	Bison priscus ?	sacrum	fragment	d	
1026	Oyg-07-O995	Rangifer tarandus	shed antler	fragment	d	
1027	Oyg-07-O996	Rangifer tarandus	shed antler	fragment	d	
1028	Oyg-07-O997	Equus sp.	astrogalus	fragment	d	
1029	Oyg-07-O998	Bison priscus	ph I		d	
1030	Oyg-07-O999	Bison priscus	ph I		d	
1031	Oyg-07-O1000	Bison priscus	ulna		d	
1032	Oyg-07-O1001	Mammuthus primigenius	tusk	fragment	d	
1033	Oyg-07-O1002	Mammuthus primigenius	tusk	fragment	d	
1034	Oyg-07-O1003	Mammuthus primigenius	tusk	fragment	d	
1035	Oyg-07-O1004	Mammuthus primigenius	tusk	fragment	d	
1036	Oyg-07-O1005	Mammuthus primigenius	tusk	fragment	d	trashed
1037	Oyg-07-O1006	Mammuthus primigenius	tusk	fragment	d	trashed
<b>East part of coast section; thermoterrace of the small and the westernmost thermocirque under the biggest thermocirque</b>						
1038	Oyg-07-O1007	Large herbivorous mammal	limb bone	fragment	b	from Volodya
<b>East part of coast section, shore near the stream mouth; (landing site in 2002); point 07RUCHEY</b>						
1039	Oyg-07-O1008	Rangifer tarandus	shed antler	fragment	d	
1040	Oyg-07-O1009	Bison priscus ?	metapodium	fragment	d	
1041	Oyg-07-O1010	Bison priscus	ph I		d	
1042	Oyg-07-O1011	Ovibos moschatus	thorax vertebra	damaged	d	
1043	Oyg-07-O1012	Bison priscus ?	humerus	fragment	d	
1044	Oyg-07-O1013	Equus sp.	pelvis	fragment	d	
1045	Oyg-07-O1014	Equus sp.	ph II		d	
1046	Oyg-07-O1015	Mammuthus primigenius	tooth	fragment	d	
1047	Oyg-07-O1016	Mammuthus primigenius	mandible (symphysis part)	fragment	d	
1048	Oyg-07-O1017	Mammuthus primigenius	fibula ?	distal fragment ?	d	
1049	Oyg-07-O1018	Mammuthus primigenius	metapodium		d	
1050	Oyg-07-O1019	Bison priscus	atlas	fragment	d	
1051	Oyg-07-O1020	Rangifer tarandus	sacrum	fragment	d	

No.	N samples	Taxon	Skeleton element	Preservation	Loc. type	Notes
1052	Oyg-07-O1021	Equus sp.	ph II		d	
1053	Oyg-07-O1022	Bison priscus	ph I		d	
1054	Oyg-07-O1023	Rangifer tarandus	astrogalus	damaged	d	
1055	Oyg-07-O1024	Mammuthus primigenius	tooth	fragment	d	
1056	Oyg-07-O1025	Equus sp.	femur	proximal fragment (articulation)	d	
1057	Oyg-07-O1026	Bison priscus	metapodium	distal fragment	d	
1058	Oyg-07-O1027	Rangifer tarandus	humerus	distal fragment	d	
1059	Oyg-07-O1028	Mammuthus primigenius	vertebra	fragment (process spinosus)	d	
1060	Oyg-07-O1029	Mammuthus primigenius	tusk	fragment	d	C 14
1061	Oyg-07-O1030	Mammuthus primigenius	tooth	fragment	d	
1062	Oyg-07-O1031	Large herbivorous mammal	limb bone	fragment	d	
1063	Oyg-07-O1032	Rangifer tarandus	tibia	proximal fragment	d	rounded, with marrow
1064	Oyg-07-O1033	Rangifer tarandus	radius	distal fragment	d	
1065	Oyg-07-O1034	Mammuthus primigenius	tooth	fragment	d	
1066	Oyg-07-O1035	Mammuthus primigenius	bone of tarsus		d	
1067	Oyg-07-O1036	Equus sp.	small bone of tarsus	fragment	d	rounded
1068	Oyg-07-O1037	Mammuthus primigenius	tooth	fragment	d	trashed
1069	Oyg-07-O1038	Mammuthus primigenius	tooth	fragment	d	trashed
1070	Oyg-07-O1039	Mammuthus primigenius	tusk	fragment	d	trashed
1073	Oyg-07-O1042	Mammuthus primigenius	tusk	fragment	d	vivianate, left
1074	Oyg-07-O1043	Mammuthus primigenius	tusk	fragment	d	vivianate, left
<b>East part of coast section; thermoterrace under the Ice Complex thermocirque</b>						
1071	Oyg-07-O1040	Bison priscus	small bone of carpus	fragment	c	
1072	Oyg-07-O1041	Rangifer tarandus	ph I		c	
<b>West part of coast section, shore</b>						
1075	Oyg-07-O1044	Bison priscus	thorax vertebra	fragment	d	
1076	Oyg-07-O1045	Mammuthus primigenius	vertebra	fragment (without articulation surface)	d	C 14
1078	Oyg-07-O1047	Mammuthus primigenius	pelvis	fragment	d	C 14
1079	Oyg-07-O1048	Mammuthus primigenius	pelvis	fragment	d	C 14
1080	Oyg-07-O1049	Mammuthus primigenius	astrogalus		d	
1083	Oyg-07-O1052	Bison priscus	Mt		d	
<b>West part of coast section, shore from camp to firewood's stream</b>						
1077	Oyg-07-O1046	Mammuthus primigenius	cervical vertebra	damaged	d	vivianate, probably samples O1046, O1050, O1053 from the one animal left
1081	Oyg-07-O1050	Mammuthus primigenius	skull (occipitale part)	fragment	d	
1084	Oyg-07-O1053	Mammuthus primigenius	skull	fragment	d	
1082	Oyg-07-O1051	Mammuthus primigenius	mandible	fragment	d	it was in situ and fell down from the permafrost deposits
1085	Oyg-07-O1054	Mammuthus primigenius	tusk	fragment	d	left
1086	Oyg-07-O1055	Mammuthus primigenius	tusk	fragment	d	vivianate, left
<b>East part of coast section, shore</b>						
1087	Oyg-07-O1056	Mammuthus primigenius	tusk	fragment	d	trashed
1088	Oyg-07-O1057	Mammuthus primigenius	tooth	fragment	d	trashed
1089	Oyg-07-O1058	Mammuthus primigenius	tooth	fragment	d	trashed
1090	Oyg-07-O1059	Mammuthus primigenius	rib	fragment	d	
1091	Oyg-07-O1060	Bison priscus	ph I		d	
1092	Oyg-07-O1061	Equus sp.	scapula	fragment	d	
1093	Oyg-07-O1062	Rangifer tarandus	tibia	distal fragment	d	
1094	Oyg-07-O1063	Mammuthus primigenius	tooth	fragment	d	
1095	Oyg-07-O1064	Equus sp.	ph I		d	
1096	Oyg-07-O1065	Rangifer tarandus	atlas	fragment	d	

No.	N samples	Taxon	Skeleton element	Preservation	Loc. type	Notes
1097	Oyg-07-O1066	Large herbivorous mammal	thorax vertebra	fragment	d	
1098	Oyg-07-O1067	Bison priscus	phalax ?	proximal fragment	d	
1099	Oyg-07-O1068	Mammuthus primigenius	tooth	fragment	d	
1100	Oyg-07-O1069	Equus sp.	tibia	distal fragment	d	
1101	Oyg-07-O1070	Equus sp.	calcaneus	damaged	d	
1102	Oyg-07-O1071	Bison priscus ?	mandible (with 2 tooth fragments)	fragment	d	very old
1103	Oyg-07-O1072	Equus sp.	ph I		d	
1104	Oyg-07-O1073	Equus sp.	ph II	fragment	d	
1105	Oyg-07-O1074	Equus sp.	ph II		d	
1106	Oyg-07-O1075	Equus sp.	ph II		d	
1107	Oyg-07-O1076	Rangifer tarandus	astrogalus	damaged	d	rounded (ice abrasion marks?)
1108	Oyg-07-O1077	Bison priscus	astrogalus		d	
1109	Oyg-07-O1078	Bison priscus	femur	distal fragment	d	
1110	Oyg-07-O1079	Bison priscus	large bone of carpus		d	
1111	Oyg-07-O1080	Rangifer tarandus	shed antler	fragment	d	
1112	Oyg-07-O1081	Ovibos moschatus	thorax vertebra	damaged	d	
1113	Oyg-07-O1082	Equus sp. ?	tibia	proximal fragment	d	
1114	Oyg-07-O1083	Equus sp.	ph II		d	
1115	Oyg-07-O1084	Mammuthus primigenius	thorax vertebra	fragment	d	
1116	Oyg-07-O1085	Equus sp.	pelvis	fragment	d	
1117	Oyg-07-O1086	Large herbivorous mammal	vertebra	fragment	d	
1118	Oyg-07-O1087	Rangifer tarandus	metapodium	distal fragment	d	
1119	Oyg-07-O1088	Rangifer tarandus	tibia	distal fragment (articulation surface)	d	
1120	Oyg-07-O1089	Equus sp.	os naviculare		d	
1121	Oyg-07-O1090	Bison priscus	small bone of carpus		d	
<b>West part of coast section, shore near the mouth of firewood's stream</b>						
1122	Oyg-07-O1093	Equus sp.	thorax vertebra	damaged	d	
1123	Oyg-07-O1094	Ovibos moschatus	thorax vertebra	fragment	d	
1124	Oyg-07-O1095	Rangifer tarandus	cervical vertebra	fragment	d	
1125	Oyg-07-O1096	Ovibos moschatus ?	cervical vertebra	fragment	d	
1126	Oyg-07-O1097	Equus sp.	lumbar vertebra	damaged	d	
1127	Oyg-07-O1098	Equus sp.	cervical vertebra	fragment	d	
1128	Oyg-07-O1099	Rangifer tarandus	atlas	damaged	d	
1129	Oyg-07-O1100	Rangifer tarandus	shed antler	fragment	d	
1130	Oyg-07-O1101	Mammuthus primigenius	tooth	fragment	d	
1131	Oyg-07-O1102	Mammuthus primigenius	tusk	fragment	d	
1132	Oyg-07-O1103	Equus sp.	ph II		d	
1133	Oyg-07-O1104	Equus sp.	ph I	damaged	d	
1134	Oyg-07-O1105	Equus sp.	humerus	distal fragment	d	
1135	Oyg-07-O1106	Rangifer tarandus	astrogalus	damaged	d	
1136	Oyg-07-O1107	Rangifer tarandus	astrogalus	fragment	d	
1137	Oyg-07-O1108	Bison priscus	pelvis	fragment	d	
1138	Oyg-07-O1109	Bison priscus	small bone of tarsus		d	
1139	Oyg-07-O1110	Bison priscus	small bone of tarsus		d	
1140	Oyg-07-O1111	Bison priscus	femur	distal fragment	d	
1141	Oyg-07-O1112	Mammuthus primigenius	tusk	fragment	d	
1142	Oyg-07-O1113	Mammuthus primigenius	tibia	fragment (without articulation surface)	d	juv.
1143	Oyg-07-O1114	Bison priscus	tibia	distal fragment	d	
1144	Oyg-07-O1115	Bison priscus	metapodium	distal fragment	d	
1145	Oyg-07-O1116	Lepus sp.	femur	distal fragment	d	

No.	N samples	Taxon	Skeleton element	Preservation	Loc. type	Notes
1146	Oyg-07-O1117	Mammuthus primigenius	tusk	fragment	d	trashed
1147	Oyg-07-O1118	Mammuthus primigenius	tusk	fragment	d	trashed
<b>West part of coast section, shore beyond the firewood's stream</b>						
1148	Oyg-07-O1119	Mammuthus primigenius	tooth	fragment	d	trashed
1149	Oyg-07-O1120	Mammuthus primigenius	tooth	fragment	d	trashed
1150	Oyg-07-O1121	Mammuthus primigenius	tooth	fragment	d	trashed
1151	Oyg-07-O1122	Equus sp.	astrogalus	fragment	d	trashed
1152	Oyg-07-O1123	Mammuthus primigenius	thorax vertebra	fragment	d	C 14
1153	Oyg-07-O1124	Bison priscus	lumbar vertebra	damaged	d	
1154	Oyg-07-O1125	Bison priscus	limb bone	fragment	d	vivianate, with marrow
1155	Oyg-07-O1126	Mammuthus primigenius	tusk	fragment	d	C 14
1156	Oyg-07-O1127	Mammuthus primigenius	tusk	fragment	d	
1157	Oyg-07-O1128	Mammuthus primigenius	tusk	fragment	d	
1158	Oyg-07-O1129	Mammuthus primigenius	tooth	fragment	d	
1159	Oyg-07-O1130	Mammuthus primigenius	tooth	fragment	d	
1160	Oyg-07-O1131	Bison priscus	metapodium	distal fragment	d	
1161	Oyg-07-O1132	Rangifer tarandus	thorax vertebra	damaged	d	
1162	Oyg-07-O1133	Bison priscus	astrogalus		d	
1163	Oyg-07-O1134	Alces alces	calcaneus	fragment	d	
1164	Oyg-07-O1135	Mammuthus primigenius	tooth	fragment	d	
1165	Oyg-07-O1136	Bison priscus	ph I		d	vivianate
1166	Oyg-07-O1137	Mammuthus primigenius	мелкая кость заплюстных	damaged	d	
1167	Oyg-07-O1138	Large herbivorous mammal	limb bone	fragment	d	
1168	Oyg-07-O1139	Bison priscus ?	metapodium	fragment	d	
1169	Oyg-07-O1140	Equus sp. ?	tibia	distal fragment	d	
1170	Oyg-07-O1141	Equus sp.	ph III	fragment	d	
1171	Oyg-07-O1142	Large herbivorous mammal	limb bone	fragment	d	
1172	Oyg-07-O1143	Large herbivorous mammal	limb bone	fragment	d	
1173	Oyg-07-O1144	Bison priscus	astrogalus	fragment	d	
1174	Oyg-07-O1145	Bison priscus	astrogalus		d	
1175	Oyg-07-O1146	Bison priscus	astrogalus		d	
1176	Oyg-07-O1147	Rangifer tarandus	large bone of carpus		d	
1177	Oyg-07-O1148	Equus sp.	small bone of tarsus	fragment	d	
1178	Oyg-07-O1149	Bison priscus	metapodium	fragment	d	rounded
1179	Oyg-07-O1150	Bison priscus	small bone of tarsus		d	
1180	Oyg-07-O1151	Rangifer tarandus	small bone of tarsus	fragment	d	
<b>West part of coast section, shore from camp to firewood's stream</b>						
1181	Oyg-07-O1152	Mammuthus primigenius	tooth	fragment	d	trashed
1182	Oyg-07-O1153	Mammuthus primigenius	tooth	fragment	d	trashed
1183	Oyg-07-O1154	Mammuthus primigenius	tooth	fragment	d	trashed
1184	Oyg-07-O1155	Mammuthus primigenius	tooth	fragment	d	trashed
1185	Oyg-07-O1156	Mammuthus primigenius	tooth	fragment	d	trashed
1186	Oyg-07-O1157	Mammuthus primigenius	tusk	fragment	d	trashed
1187	Oyg-07-O1158	Mammuthus primigenius	tusk	fragment	d	trashed
1188	Oyg-07-O1159	Mammuthus primigenius	tusk	fragment	d	trashed
1189	Oyg-07-O1160	Mammuthus primigenius	tusk	fragment	d	trashed
1190	Oyg-07-O1161	Mammuthus primigenius	tusk	fragment	d	trashed
1191	Oyg-07-O1162	Mammuthus primigenius	tusk	fragment	d	trashed
1192	Oyg-07-O1163	Mammuthus primigenius	tusk	fragment	d	trashed
1193	Oyg-07-O1164	Mammuthus primigenius	tusk	fragment	d	trashed
1194	Oyg-07-O1165	Mammuthus primigenius	tusk	fragment	d	trashed
1195	Oyg-07-O1166	Mammuthus primigenius	tusk	fragment	d	trashed

No.	N samples	Taxon	Skeleton element	Preservation	Loc. type	Notes
1196	Oyg-07-O1167	Rangifer tarandus	shed antler	fragment	d	trashed
1197	Oyg-07-O1168	Rangifer tarandus	shed antler	fragment	d	trashed
1198	Oyg-07-O1169	Rangifer tarandus	antler	fragment	d	trashed
1199	Oyg-07-O1170	Rangifer tarandus	astrogalus	fragment	d	trashed
1200	Oyg-07-O1171	Equus sp.	Mc III	fragment	d	trashed
1201	Oyg-07-O1172	Mammuthus primigenius	tusk	fragment	d	trashed
1202	Oyg-07-O1173	Mammuthus primigenius	tusk	fragment	d	trashed
1203	Oyg-07-O1174	Mammuthus primigenius	tooth	fragment	d	
1204	Oyg-07-O1175	Mammuthus primigenius	tooth	fragment	d	
1205	Oyg-07-O1176	Mammuthus primigenius	fibula	distal fragment	d	
1206	Oyg-07-O1177	Mammuthus primigenius	tusk	fragment	d	C 14
1207	Oyg-07-O1178	Mammuthus primigenius	humerus	fragment	d	juv.
1208	Oyg-07-O1179	Mammuthus primigenius	small bone of tarsus		d	
1209	Oyg-07-O1180	Mammuthus primigenius	tusk	fragment	d	
1210	Oyg-07-O1181	Rangifer tarandus	lumbar vertebra	damaged	d	
1211	Oyg-07-O1182	Bison priscus	cervical vertebra	damaged	d	
1212	Oyg-07-O1183	Equus sp.	radius		d	
1213	Oyg-07-O1184	Bison priscus	calcaneus	damaged	d	
1214	Oyg-07-O1185	Bison priscus	tibia	distal fragment	d	
1215	Oyg-07-O1186	Equus sp.	ph I		d	
1216	Oyg-07-O1187	Equus sp.	ph II		d	
1217	Oyg-07-O1188	Equus sp.	astrogalus		d	
1218	Oyg-07-O1189	Equus sp.	astrogalus		d	
1219	Oyg-07-O1190	Equus sp.	astrogalus		d	
1220	Oyg-07-O1191	Equus sp.	ph I		d	
1221	Oyg-07-O1192	Equus sp.	femur	distal fragment	d	
1222	Oyg-07-O1193	Large herbivorous mammal	epistropheus	damaged	d	
<b>West part of coast section, shore of small bones</b>						
1223	Oyg-07-O1194	Rangifer tarandus	shed antler	fragment	d	trashed
1224	Oyg-07-O1195	Rangifer tarandus	shed antler	fragment	d	trashed
1225	Oyg-07-O1196	Rangifer tarandus	shed antler	fragment	d	trashed
1226	Oyg-07-O1197	Equus sp.	astrogalus	fragment	d	trashed
1227	Oyg-07-O1198	Equus sp.	astrogalus	fragment	d	trashed
1228	Oyg-07-O1199	Equus sp.	astrogalus	fragment	d	trashed
1229	Oyg-07-O1200	Equus sp.	astrogalus	fragment	d	trashed
1230	Oyg-07-O1201	Equus sp.	ph I ?	fragment	d	trashed
1231	Oyg-07-O1202	Rangifer tarandus	astrogalus	fragment	d	trashed
1232	Oyg-07-O1203	Rangifer tarandus	astrogalus	fragment	d	trashed
1233	Oyg-07-O1204	Rangifer tarandus	metapodium	fragment	d	trashed
1234	Oyg-07-O1205	Rangifer tarandus	metapodium	fragment	d	trashed
1235	Oyg-07-O1206	Mammuthus primigenius	tooth	fragment	d	trashed
1236	Oyg-07-O1207	Mammuthus primigenius	tooth	fragment	d	trashed
1237	Oyg-07-O1208	Mammuthus primigenius	tooth	fragment	d	trashed
1238	Oyg-07-O1209	Mammuthus primigenius	tooth	fragment	d	trashed
1239	Oyg-07-O1210	Mammuthus primigenius	tooth	fragment	d	trashed
1240	Oyg-07-O1211	Mammuthus primigenius	tooth	fragment	d	trashed
1241	Oyg-07-O1212	Mammuthus primigenius	tooth	fragment	d	trashed
1242	Oyg-07-O1213	Mammuthus primigenius	tooth	fragment	d	trashed
1243	Oyg-07-O1214	Mammuthus primigenius	tooth	fragment	d	trashed
1244	Oyg-07-O1215	Mammuthus primigenius	tooth	fragment	d	trashed
1245	Oyg-07-O1216	Mammuthus primigenius	tooth	fragment	d	trashed
1246	Oyg-07-O1217	Mammuthus primigenius	tooth	fragment	d	trashed
1247	Oyg-07-O1218	Mammuthus primigenius	tooth	fragment	d	trashed
1248	Oyg-07-O1219	Mammuthus primigenius	tooth	fragment	d	trashed
1249	Oyg-07-O1220	Mammuthus primigenius	tooth	fragment	d	trashed
1250	Oyg-07-O1221	Mammuthus primigenius	tooth	fragment	d	trashed

No.	N samples	Taxon	Skeleton element	Preservation	Loc. type	Notes
1251	Oyg-07-O1222	Mammuthus primigenius	tooth	fragment	d	trashed
1252	Oyg-07-O1223	Mammuthus primigenius	tooth	fragment	d	trashed
1253	Oyg-07-O1224	Mammuthus primigenius	tooth	fragment	d	trashed
1254	Oyg-07-O1225	Mammuthus primigenius	tooth	fragment	d	trashed
1255	Oyg-07-O1226	Mammuthus primigenius	tooth	fragment	d	trashed
1256	Oyg-07-O1227	Mammuthus primigenius	tooth	fragment	d	trashed
1257	Oyg-07-O1228	Mammuthus primigenius	tooth	fragment	d	trashed
1258	Oyg-07-O1229	Mammuthus primigenius	tooth	fragment	d	trashed
1259	Oyg-07-O1230	Mammuthus primigenius	tooth	fragment	d	trashed
1260	Oyg-07-O1231	Mammuthus primigenius	tooth	fragment	d	trashed
1261	Oyg-07-O1232	Mammuthus primigenius	tooth	fragment	d	trashed
1262	Oyg-07-O1233	Mammuthus primigenius	tooth	fragment	d	trashed
1263	Oyg-07-O1234	Mammuthus primigenius	tooth	fragment	d	trashed
1264	Oyg-07-O1235	Mammuthus primigenius	tusk	fragment	d	trashed
1265	Oyg-07-O1236	Mammuthus primigenius	tusk	fragment	d	trashed
1266	Oyg-07-O1237	Mammuthus primigenius	tusk	fragment	d	trashed
1267	Oyg-07-O1238	Mammuthus primigenius	tusk	fragment	d	trashed
1268	Oyg-07-O1239	Mammuthus primigenius	tusk	fragment	d	trashed
1269	Oyg-07-O1240	Mammuthus primigenius	tusk	fragment	d	trashed
1270	Oyg-07-O1241	Mammuthus primigenius	tusk	fragment	d	trashed
1271	Oyg-07-O1242	Mammuthus primigenius	tusk	fragment	d	trashed
1272	Oyg-07-O1243	Mammuthus primigenius	tusk	fragment	d	trashed
1273	Oyg-07-O1244	Mammuthus primigenius	tusk	fragment	d	trashed
1274	Oyg-07-O1245	Mammuthus primigenius	tusk	fragment	d	trashed
1275	Oyg-07-O1246	Mammuthus primigenius	tusk	fragment	d	trashed
1276	Oyg-07-O1247	Mammuthus primigenius	tusk	fragment	d	trashed
<b>west part of coast section, shore from camp to firewood's stream</b>						
1277	Oyg-07-O1248	Bison priscus	ph I		d	
1278	Oyg-07-O1249	Bison priscus	astrogalus	damaged	d	
1279	Oyg-07-O1250	Bison priscus	astrogalus	damaged	d	
1280	Oyg-07-O1251	Bison priscus	ph I	fragment	d	
1281	Oyg-07-O1252	Bison priscus	metapodium	distal fragment	d	
1282	Oyg-07-O1253	Equus sp.	astrogalus	fragment	d	
1283	Oyg-07-O1254	Bison priscus	ph II	fragment	d	
1284	Oyg-07-O1255	Mammuthus primigenius	small bone of tarsus		d	rounded
1285	Oyg-07-O1256	Large herbivorous mammal	atlas	fragment	d	
1286	Oyg-07-O1257	Rangifer tarandus	atlas	damaged	d	
1287	Oyg-07-O1258	Equus sp.	atlas	fragment	d	
1288	Oyg-07-O1259	Bison priscus	astrogalus		d	
1289	Oyg-07-O1260	Mammuthus primigenius	tusk	fragment	d	
1290	Oyg-07-O1261	Mammuthus primigenius	tusk	fragment	d	
1291	Oyg-07-O1262	Bison priscus	upper tooth		d	
1292	Oyg-07-O1263	Equus sp.	lower tooth		d	
1293	Oyg-07-O1264	Bison priscus	lower tooth (M3)		d	
1294	Oyg-07-O1265	Mammuthus primigenius	ph III		d	
1295	Oyg-07-O1266	Mammuthus primigenius	tusk	fragment	d	
1296	Oyg-07-O1267	Rangifer tarandus	lumbar vertebra	damaged	d	
1297	Oyg-07-O1268	Rangifer tarandus	lumbar vertebra	damaged	d	juv.
1298	Oyg-07-O1269	Mammuthus primigenius	tusk	fragment	d	
1299	Oyg-07-O1270	Mammuthus primigenius	tusk	fragment	d	
1300	Oyg-07-O1271	Mammuthus primigenius	tusk	fragment	d	
1301	Oyg-07-O1272	Mammuthus primigenius	tusk	fragment	d	
1302	Oyg-07-O1273	Mammuthus primigenius	tusk	fragment	d	
1303	Oyg-07-O1274	Mammuthus primigenius	tusk	fragment	d	
1304	Oyg-07-O1275	Mammuthus primigenius	tusk	fragment	d	
1305	Oyg-07-O1276	Mammuthus primigenius	tusk	fragment	d	

No.	N samples	Taxon	Skeleton element	Preservation	Loc. type	Notes
1306	Oyg-07-O1277	Mammuthus primigenius	tusk	fragment	d	
1307	Oyg-07-O1278	Mammuthus primigenius	tusk	fragment	d	
1308	Oyg-07-O1279	Mammuthus primigenius	tusk	fragment	d	
1309	Oyg-07-O1280	Mammuthus primigenius	tusk	fragment	d	
1310	Oyg-07-O1281	Mammuthus primigenius	tooth	fragment	d	
1311	Oyg-07-O1282	Mammuthus primigenius	atlas	damaged	d	
1312	Oyg-07-O1283	Mammuthus primigenius	metapodium	fragment	d	
1313	Oyg-07-O1284	Mammuthus primigenius	scapula	fragment	d	C 14
1314	Oyg-07-O1285	Mammuthus primigenius	large bone of carpus	fragment	d	C 14
1315	Oyg-07-O1286	Mammuthus primigenius	vertebra (process spinosus)	fragment	d	C 14
1316	Oyg-07-O1287	Mammuthus primigenius	tusk	fragment	d	
1317	Oyg-07-O1288	Mammuthus primigenius	tusk	fragment	d	
1318	Oyg-07-O1289	Mammuthus primigenius	tusk	fragment	d	
1319	Oyg-07-O1290	Mammuthus primigenius	tooth	fragment	d	
1320	Oyg-07-O1291	Mammuthus primigenius	tooth	fragment	d	
1321	Oyg-07-O1292	Mammuthus primigenius	tooth	fragment	d	heavily worn
1322	Oyg-07-O1293	Mammuthus primigenius	tooth	fragment	d	
1323	Oyg-07-O1294	Mammuthus primigenius	tooth	fragment	d	heavily worn
1324	Oyg-07-O1295	Mammuthus primigenius	tooth	fragment	d	
1325	Oyg-07-O1296	Mammuthus primigenius	tooth	fragment	d	
1326	Oyg-07-O1297	Mammuthus primigenius	tusk	fragment	d	
1327	Oyg-07-O1298	Mammuthus primigenius	tusk	fragment	d	
1328	Oyg-07-O1299	Mammuthus primigenius	tusk	fragment	d	
1329	Oyg-07-O1300	Mammuthus primigenius	tusk	fragment	d	
1330	Oyg-07-O1301	Mammuthus primigenius	tusk	fragment	d	
1331	Oyg-07-O1302	Mammuthus primigenius	tusk	fragment	d	
1332	Oyg-07-O1303	Mammuthus primigenius	milk? tooth	fragment	d	heavily worn
1333	Oyg-07-O1304	Rangifer tarandus	shed antler	fragment	d	
1334	Oyg-07-O1305	Bison priscus	small bone of tarsus		d	
1335	Oyg-07-O1306	Equus sp.	scapula	fragment	d	
1336	Oyg-07-O1307	Bison priscus	ph I	fragment	d	
1337	Oyg-07-O1308	Bison priscus	ph I	damaged	d	
1338	Oyg-07-O1309	Bison priscus	astrogalus		d	
1339	Oyg-07-O1310	Equus sp.	pelvis	fragment	d	
1340	Oyg-07-O1311	Bison priscus	calcaneus	damaged	d	with teeth traces of Carnivora
1341	Oyg-07-O1312	Bison priscus	calcaneus	damaged	d	
1342	Oyg-07-O1313	Bison priscus	metapodium	damaged	d	
1343	Oyg-07-O1314	Equus sp.	ph I	fragment	d	
1344	Oyg-07-O1315	Equus sp.	ph II		d	
1345	Oyg-07-O1316	Equus sp.	ph II		d	
1346	Oyg-07-O1317	Equus sp.	tibia	distal fragment	d	
1347	Oyg-07-O1318	Equus sp.	astrogalus		d	
1348	Oyg-07-O1319	Equus sp.	upper tooth	fragment	d	
1349	Oyg-07-O1320	Equus sp.	ph II		d	
1350	Oyg-07-O1321	Rangifer tarandus	radius	proximal fragment	d	
1351	Oyg-07-O1322	Rangifer tarandus	Mt; without lower articulation	fragment	d	juv.
1352	Oyg-07-O1323	Rangifer tarandus	Mt	proximal fragment	d	
1353	Oyg-07-O1324	Rangifer tarandus	Mt	distal fragment	d	
1354	Oyg-07-O1325	Bison priscus	upper tooth		d	
1355	Oyg-07-O1326	Bison priscus	astrogalus	fragment	d	
1356	Oyg-07-O1327	Bison priscus	metapodium	distal fragment	d	
1357	Oyg-07-O1328	Bison priscus	ph I	fragment	d	
1358	Oyg-07-O1329	Bison priscus	ph	fragment	d	
1359	Oyg-07-O1330	Bison priscus	small bone of		d	

No.	N samples	Taxon	Skeleton element	Preservation	Loc. type	Notes
			tarsus			
1360	Oyg-07-O1331	Bison priscus	calcaneus ?	fragment	d	
1361	Oyg-07-O1332	Bison priscus	ph II	fragment	d	
1362	Oyg-07-O1333	Bison priscus	tibia	distal fragment	d	
1363	Oyg-07-O1334	Bison priscus	radius ?	fragment	d	
1364	Oyg-07-O1335	Bison priscus	radius ?	fragment	d	
1365	Oyg-07-O1336	Bison priscus ?	vertebra	fragment	d	
1366	Oyg-07-O1337	Bison priscus	astrogalus	fragment	d	
1367	Oyg-07-O1338	Bison priscus	small bone of tarsus	fragment	d	
1368	Oyg-07-O1339	Bison priscus	tibia ?	fragment	d	
1369	Oyg-07-O1340	Bison priscus	metapodium	fragment	d	
1370	Oyg-07-O1341	Bison priscus	small bone of tarsus		d	
1371	Oyg-07-O1342	Bison priscus ?	upper tooth (P)		d	
1372	Oyg-07-O1343	Bison priscus	upper tooth	fragment	d	
1373	Oyg-07-O1344	Bison priscus	upper tooth	fragment	d	
1374	Oyg-07-O1345	Bison priscus	upper tooth	fragment	d	
1375	Oyg-07-O1346	Mammuthus primigenius	tusk	fragment	d	
1376	Oyg-07-O1347	Mammuthus primigenius	tusk	fragment	d	
1377	Oyg-07-O1348	Mammuthus primigenius	tooth	fragment	d	
1378	Oyg-07-O1349	Mammuthus primigenius	tooth	fragment	d	
1379	Oyg-07-O1350	Mammuthus primigenius	tooth	fragment	d	
1380	Oyg-07-O1351	Mammuthus primigenius	tusk	fragment	d	
1381	Oyg-07-O1352	Mammuthus primigenius	tusk	fragment	d	
1382	Oyg-07-O1353	Mammuthus primigenius	tooth	fragment	d	
1383	Oyg-07-O1354	Rangifer tarandus	shed antler	fragment	d	
1384	Oyg-07-O1355	Rangifer tarandus	astrogalus	damaged	d	
1385	Oyg-07-O1356	Rangifer tarandus	astrogalus	damaged	d	
1386	Oyg-07-O1357	Rangifer tarandus	astrogalus	damaged	d	
1387	Oyg-07-O1358	Rangifer tarandus	astrogalus		d	
1388	Oyg-07-O1359	Rangifer tarandus	astrogalus		d	
1389	Oyg-07-O1360	Rangifer tarandus	pelvis	fragment	d	
1390	Oyg-07-O1361	Mammuthus primigenius	small bone of tarsus	damaged	d	juv.
1391	Oyg-07-O1362	Equus sp.	canine		d	heavily worn
1392	Oyg-07-O1363	Equus sp.	ph II	fragment	d	
1393	Oyg-07-O1364	Equus sp.	ph I	fragment	d	
1394	Oyg-07-O1365	Equus sp.	ph I	fragment	d	
1395	Oyg-07-O1366	Equus sp.	ph I	distal fragment	d	
1396	Oyg-07-O1367	Equus sp.	ph I	distal fragment	d	
1397	Oyg-07-O1368	Equus sp.	Mc III	fragment	d	
1398	Oyg-07-O1369	Equus sp.	astrogalus	fragment	d	
1399	Oyg-07-O1370	Bison priscus	metapodium	fragment	d	
1400	Oyg-07-O1371	Equus sp.	metapodium	fragment	d	
1401	Oyg-07-O1372	Equus sp.	lateral metapodium	fragment	d	
1402	Oyg-07-O1373	Equus sp.	ph I		d	
1403	Oyg-07-O1374	Equus sp.	ph I	fragment	d	
1404	Oyg-07-O1375	Equus sp.	ph I	fragment	d	
1405	Oyg-07-O1376	Equus sp.	astrogalus	fragment	d	
1406	Oyg-07-O1377	Equus sp.	astrogalus		d	
1407	Oyg-07-O1378	Bison priscus	small bone of tarsus		d	
1408	Oyg-07-O1379	Bison priscus	small bone of tarsus		d	
1409	Oyg-07-O1380	Equus sp.	small bone of tarsus		d	
1410	Oyg-07-O1381	Equus sp.	small bone of tarsus		d	
1411	Oyg-07-O1382	Equus sp.	astrogalus	fragment	d	trashed

No.	N samples	Taxon	Skeleton element	Preservation	Loc. type	Notes
1412	Oyg-07-O1383	Mammuthus primigenius	tooth	fragment	d	trashed
1413	Oyg-07-O1384	Mammuthus primigenius	tooth	fragment	d	
1414	Oyg-07-O1385	Mammuthus primigenius	tooth	fragment (корень)	d	
1415	Oyg-07-O1386	Equus sp.	ph I	fragment	d	
1416	Oyg-07-O1387	Equus sp.	ph II	fragment	d	
1417	Oyg-07-O1388	Equus sp.	ph I		d	
1418	Oyg-07-O1389	Equus sp. ?	pelvis	fragment	d	
1419	Oyg-07-O1390	Equus sp.	ph II	fragment	d	
1420	Oyg-07-O1391	Equus sp.	ph I	fragment	d	
1421	Oyg-07-O1392	Equus sp.	ph I	fragment	d	
1422	Oyg-07-O1393	Equus sp.	small bone of tarsus		d	
1423	Oyg-07-O1394	Equus sp.	ph II		d	
1424	Oyg-07-O1395	Equus sp.	small bone of tarsus		d	
1425	Oyg-07-O1396	Equus sp.	astrogalus	fragment	d	
1426	Oyg-07-O1397	Equus sp.	calcaneus	damaged	d	
1427	Oyg-07-O1398	Equus sp.	ph I	fragment	d	
1428	Oyg-07-O1399	Equus sp.	small bone of tarsus		d	
1429	Oyg-07-O1400	Equus sp.	small bone of tarsus		d	
1430	Oyg-07-O1401	Equus sp.	ph I	fragment	d	
1431	Oyg-07-O1402	Equus sp.	ph II	fragment	d	rounded
1432	Oyg-07-O1403	Equus sp.	sesamoideum		d	
1433	Oyg-07-O1404	Equus sp.	sesamoideum		d	
1434	Oyg-07-O1405	Equus sp.	incisor	damaged	d	
1435	Oyg-07-O1406	Equus sp.	small bone of tarsus	fragment	d	
1436	Oyg-07-O1407	Equus sp.	small bone of tarsus	fragment	d	
1437	Oyg-07-O1408	Equus sp.	small bone of tarsus	damaged	d	
1438	Oyg-07-O1409	Equus sp.	small bone of tarsus		d	
1439	Oyg-07-O1410	Mammuthus primigenius	tooth	fragment	d	
1440	Oyg-07-O1411	Rangifer tarandus	humerus	distal fragment	d	
1441	Oyg-07-O1412	Rangifer tarandus	metapodium	distal fragment	d	
1442	Oyg-07-O1413	Rangifer tarandus	humerus	distal fragment	d	
1443	Oyg-07-O1414	Rangifer tarandus	metapodium	distal fragment	d	
1444	Oyg-07-O1415	Bison priscus	small bone of tarsus		d	
1445	Oyg-07-O1416	Rangifer tarandus	large bone of carpus		d	
1446	Oyg-07-O1417	Rangifer tarandus	astrogalus		d	
1447	Oyg-07-O1418	Rangifer tarandus	astrogalus		d	light rounded
1448	Oyg-07-O1419	Rangifer tarandus	astrogalus		d	light rounded
1449	Oyg-07-O1420	Rangifer tarandus	astrogalus	damaged	d	
1450	Oyg-07-O1421	Rangifer tarandus	astrogalus	damaged	d	
1451	Oyg-07-O1422	Rangifer tarandus	astrogalus		d	
1452	Oyg-07-O1423	Rangifer tarandus	metapodium	distal fragment	d	
1453	Oyg-07-O1424	Rangifer tarandus	large bone of carpus		d	
1454	Oyg-07-O1425	Rangifer tarandus	lower tooth ?	fragment	d	
1455	Oyg-07-O1426	Rangifer tarandus	lower tooth ?	fragment	d	
1456	Oyg-07-O1427	Rangifer tarandus	upper tooth	fragment	d	
1457	Oyg-07-O1428	Mammuthus primigenius	tooth	fragment	d	
1458	Oyg-07-O1429	Large herbivorous mammal	tibia	distal fragment	d	
1459	Oyg-07-O1430	Equus sp.	metapodium	distal fragment	d	
1460	Oyg-07-O1431	Equus sp.	small bone of tarsus	fragment	d	
1461	Oyg-07-O1432	Large herbivorous	bone	fragment	d	

No.	N samples	Taxon	Skeleton element	Preservation	Loc. type	Notes
		mammal				
1462	Oyg-07-O1433	Bison priscus	astrogalus	fragment	d	
1463	Oyg-07-O1434	Ovibos moschatus	astrogalus		d	
1464	Oyg-07-O1435	Bison priscus	ph I	fragment	d	
1465	Oyg-07-O1436	Bison priscus	ph I		d	
1466	Oyg-07-O1437	Bison priscus	ph II	fragment	d	easy rounded
1467	Oyg-07-O1438	Bison priscus	ph I	fragment	d	easy rounded
1468	Oyg-07-O1439	Bison priscus	ph II	fragment	d	
1469	Oyg-07-O1440	Bison priscus	ph II	fragment	d	easy rounded
1470	Oyg-07-O1441	Bison priscus	ph I	fragment	d	
1471	Oyg-07-O1442	Bison priscus	small bone of tarsus	fragment	d	
1472	Oyg-07-O1443	Bison priscus	small bone of tarsus		d	easy rounded
1473	Oyg-07-O1444	Bison priscus	small bone of tarsus	fragment	d	
1474	Oyg-07-O1445	Bison priscus	small bone of tarsus		d	
1475	Oyg-07-O1446	Bison priscus	small bone of tarsus	fragment	d	
1476	Oyg-07-O1447	Bison priscus	small bone of tarsus	fragment	d	
1477	Oyg-07-O1448	Bison priscus	small bone of tarsus	fragment	d	
1478	Oyg-07-O1449	Bison priscus	small bone of tarsus		d	
1479	Oyg-07-O1450	Bison priscus	small bone of tarsus	fragment	d	easy rounded
1480	Oyg-07-O1451	Bison priscus	small bone of tarsus		d	
1481	Oyg-07-O1452	Bison priscus	small bone of tarsus		d	
1482	Oyg-07-O1453	Bison priscus	tooth	fragment	d	
1483	Oyg-07-O1454	Bison priscus	upper tooth (P1)		d	
1484	Oyg-07-O1455	Equus sp.	metapodium ?	distal fragment	d	
1485	Oyg-07-O1456	Mammuthus primigenius	tooth	fragment	d	
1486	Oyg-07-O1457	Large herbivorous mammal	bone	fragment	d	
1487	Oyg-07-O1458	Large herbivorous mammal	limb bone	fragment	d	
1488	Oyg-07-O1459	Rangifer tarandus ?	vertebra	fragment	d	
1489	Oyg-07-O1460	Large herbivorous mammal	limb bone	fragment	d	
1490	Oyg-07-O1461	Large herbivorous mammal	limb bone	fragment	d	rounded
1491	Oyg-07-O1462	Large herbivorous mammal	scapula ?	fragment	d	
1492	Oyg-07-O1463	Large herbivorous mammal	scull	fragment	d	
1493	Oyg-07-O1464	Rangifer tarandus ?	atlas ?	fragment	d	
1494	Oyg-07-O1465	Large herbivorous mammal	limb bone	fragment	d	rounded
1495	Oyg-07-O1466	Mammuthus primigenius	tusk	fragment	d	
1496	Oyg-07-O1467	Mammuthus primigenius	metapodium	proximal fragment	d	
1497	Oyg-07-O1468	Equus sp.	metapodium	distal fragment	d	
1498	Oyg-07-O1469	Equus sp.	metapodium	distal fragment	d	
1499	Oyg-07-O1470	Equus sp.	metapodium	distal fragment	d	
1500	Oyg-07-O1471	Equus sp.	phalanx	proximal fragment	d	
1501	Oyg-07-O1472	Equus sp.	os pisiform		d	
1502	Oyg-07-O1473	Equus sp.	os pisiform	fragment	d	
1503	Oyg-07-O1474	Equus sp.	ph III	fragment	d	
1504	Oyg-07-O1475	Equus sp.	small bone of tarsus	fragment	d	
1505	Oyg-07-O1476	Equus sp.	small bone of tarsus	fragment	d	
1506	Oyg-07-O1477	Equus sp.	small bone of tarsus	fragment	d	

No.	N samples	Taxon	Skeleton element	Preservation	Loc. type	Notes
1507	Oyg-07-O1478	Equus sp.	small bone of tarsus	fragment	d	rounded
1508	Oyg-07-O1479	Equus sp.	metapodium	proximal fragment	d	
1509	Oyg-07-O1480	Equus sp.	small bone of tarsus	fragment	d	
1510	Oyg-07-O1481	Equus sp.	small bone of tarsus	fragment	d	
1511	Oyg-07-O1482	Equus sp.	small bone of tarsus	fragment	d	rounded
1512	Oyg-07-O1483	Equus sp.	small bone of tarsus	fragment	d	rounded
1513	Oyg-07-O1484	Equus sp.	small bone of tarsus	fragment	d	
1514	Oyg-07-O1485	Bison priscus	large bone of carpus	fragment	d	
1515	Oyg-07-O1486	Bison priscus	small bone of tarsus	fragment	d	rounded
1516	Oyg-07-O1487	Bison priscus	phalanx	fragment	d	rounded
1517	Oyg-07-O1488	Bison priscus	small bone of tarsus	fragment	d	rounded
1518	Oyg-07-O1489	Bison priscus	small bone of tarsus	fragment	d	
1519	Oyg-07-O1490	Bison priscus	small bone of tarsus	fragment	d	rounded
1520	Oyg-07-O1491	Bison priscus	small bone of tarsus	fragment	d	rounded
1521	Oyg-07-O1492	Bison priscus	small bone of tarsus	fragment	d	
1522	Oyg-07-O1493	Bison priscus	metapodium	fragment	d	rounded
1523	Oyg-07-O1494	Bison priscus	small bone of tarsus		d	easy rounded
1524	Oyg-07-O1495	Rangifer tarandus	small bone of tarsus	damaged	d	
1525	Oyg-07-O1496	Bison priscus	sesamoideum		d	rounded
1526	Oyg-07-O1497	Bison priscus	sesamoideum	fragment	d	
1527	Oyg-07-O1498	Bison priscus	sesamoideum		d	
1528	Oyg-07-O1499	Bison priscus	sesamoideum		d	rounded
1529	Oyg-07-O1500	Bison priscus	small bone of tarsus	fragment	d	
1530	Oyg-07-O1501	Bison priscus	sesamoideum		d	rounded
1531	Oyg-07-O1502	Bison priscus	small bone of tarsus	fragment	d	rounded
1532	Oyg-07-O1503	Bison priscus	small bone of tarsus		d	
1533	Oyg-07-O1504	Bison priscus	small bone of tarsus		d	
1534	Oyg-07-O1505	Bison priscus	small bone of tarsus	fragment	d	rounded
1535	Oyg-07-O1506	Bison priscus	small bone of tarsus	fragment	d	rounded
1536	Oyg-07-O1507	Bison priscus	sesamoideum	fragment	d	rounded
1537	Oyg-07-O1508	Bison priscus	astrogalus	fragment	d	
1538	Oyg-07-O1509	Bison priscus	small bone of tarsus	fragment	d	
1539	Oyg-07-O1510	Bison priscus	small bone of tarsus		d	rounded
1540	Oyg-07-O1511	Rangifer tarandus	ph I	fragment	d	
1541	Oyg-07-O1512	Rangifer tarandus	large bone of carpus	fragment	d	
1542	Oyg-07-O1513	Rangifer tarandus	tibia	proximal fragment	d	rounded
1543	Oyg-07-O1514	Rangifer tarandus	ph I	proximal fragment	d	
1544	Oyg-07-O1515	Rangifer tarandus	small bone of tarsus	damaged	d	rounded
1545	Oyg-07-O1516	Rangifer tarandus	small bone of tarsus		d	rounded
1546	Oyg-07-O1517	Rangifer tarandus	small bone of tarsus		d	rounded
1547	Oyg-07-O1518	Rangifer tarandus	small bone of tarsus	fragment	d	rounded
1548	Oyg-07-O1519	Rangifer tarandus	small bone of		d	rounded

No.	N samples	Taxon	Skeleton element	Preservation	Loc. type	Notes
			tarsus			
1549	Oyg-07-O1520	Rangifer tarandus	small bone of tarsus		d	easy rounded
1550	Oyg-07-O1521	Rangifer tarandus	small bone of tarsus		d	rounded
1551	Oyg-07-O1522	Rangifer tarandus	phalanx	proximal fragment	d	rounded
1552	Oyg-07-O1523	Rangifer tarandus	small bone of tarsus	damaged	d	rounded
1553	Oyg-07-O1524	Rangifer tarandus	small bone of tarsus	damaged	d	rounded
1554	Oyg-07-O1525	Rangifer tarandus	small bone of tarsus	damaged	d	rounded
1555	Oyg-07-O1526	Rangifer tarandus	small bone of tarsus	fragment	d	rounded
1556	Oyg-07-O1527	Rangifer tarandus	small bone of tarsus	fragment	d	heavily rounded
1557	Oyg-07-O1528	Rangifer tarandus	small bone of tarsus	fragment	d	rounded
1558	Oyg-07-O1529	Rangifer tarandus	ph III	proximal fragment	d	
1559	Oyg-07-O1530	Rangifer tarandus	tibia	distal fragment	d	
1560	Oyg-07-O1531	Rangifer tarandus	small bone of tarsus	fragment	d	rounded
1561	Oyg-07-O1532	Rangifer tarandus	small bone of tarsus	fragment	d	rounded
1562	Oyg-07-O1533	Rangifer tarandus	tibia	distal fragment	d	rounded
1563	Oyg-07-O1534	Rangifer tarandus	small bone of tarsus	fragment	d	rounded
1564	Oyg-07-O1535	Rangifer tarandus	large bone of carpus	fragment	d	rounded
1565	Oyg-07-O1536	Rangifer tarandus	large bone of carpus	fragment	d	
1566	Oyg-07-O1537	Rangifer tarandus	large bone of carpus	damaged	d	rounded
1567	Oyg-07-O1538	Rangifer tarandus	tibia	distal fragment	d	
1568	Oyg-07-O1539	Bison priscus	sesamoideum	fragment	d	
1569	Oyg-07-O1540	Bison priscus	small bone of tarsus		d	
1570	Oyg-07-O1541	Panthera spelaea	canine		d	
1571	Oyg-07-O1542	Canis lupus	canine		d	
1572	Oyg-07-O1543	Panthera spelaea	molar tooth (M2)		d	
1573	Oyg-07-O1544	Canis lupus	molar toth		d	
1574	Oyg-07-O1545	Equus sp.	upper tooth	fragment	d	
1575	Oyg-07-O1546	Large herbivorous mammal	tooth	fragment	d	
1576	Oyg-07-O1547	Mammuthus primigenius	premolar tooth (dP2)		d	
1577	Oyg-07-O1548	Lepus sp. ?	humerus	distal fragment	d	
1578	Oyg-07-O1549	Canis lupus ?	femur	distal fragment	d	rounded
1579	Oyg-07-O1550	Lepus sp.	calcaneus		d	
1580	Oyg-07-O1551	Pisces	vertebra		d	
1581	Oyg-07-O1552	Dicrostonyx sp.	mandible with 2 tooth; right stem	fragment	d	
1582	Oyg-07-O1553	Dicrostonyx sp.	pelvis	fragment	d	
<b>List of bone samples from the Bol'shoy Lyakhovsky Island, south coast. 2007 year</b>						
<b>in situ, Ice Complex deposits; L7-07, height 1,5 m a.s.l.</b>						
1	L7-07-O3	Equus sp.	Mc III		a	15.07.2007; from Lutz
<b>in situ, Ice Complex deposits; L7-07, height 5 m a.s.l.;</b>						
2	L7-04	Rangifer tarandus	shed antler	fragment	a	from Lutz fall down from the baidjerakh
<b>in situ, Ice Complex deposits; L7-07, height 2,5 m a.s.l.</b>						
3	L7-07-O5	Mammuthus primigenius	fibula	distal fragment	a	25.07.2007; from Lutz
<b>in situ, Ice Complex deposits; L7-07, height 3,5 m a.s.l.</b>						
4	L7-07-O6	Rangifer tarandus	hair		a	25.07.2007; from Lutz; found
5	L7-07-O7a	Rangifer tarandus	ph I		a	

No.	N samples	Taxon	Skeleton element	Preservation	Loc. type	Notes
6	L7-07-O7b	Rangifer tarandus	ph III		a	together with samples L7-07-O7a and L7-07-O7b; probably from one animal, very fresh
<b>Ice Complex deposits; scree under the loc. L7-07</b>						
7	L7-07-O8	Rangifer tarandus	Mt	proximal fragment (2 pices)	c	25.07.2007; from Lutz
8	L7-07-O9a	Large herbivorous mammal	limb bone	fragment	c	26.07.2007; from Lutz; sample L7-07-O9a, O9b, O9c probably from one animal?
9	L7-07-O9b	Large herbivorous mammal	limb bone	fragment	c	
10	L7-07-O9c	Large herbivorous mammal	limb bone	fragment	c	
13	L7-07-O13	Equus sp.	Mt III		c	30.07.2007; from Lutz
11	L7-07-O11	Rangifer tarandus	hoof	fragment	c	26.07.2007; from Lutz
<b>Debris fan under the Ice Complex and above the Krest-yuryakh ice wedge cast of the exposure L7-16; height 10-12 m a.s.l.</b>						
12	L7-07-O12	Mammuthus primigenius	limb bone	fragment	c	from Lutz; C14
<b>List of bone samples from the Lena Delta Region, Kurungnakh Island in 2007</b>						
<b>Buor-Khaya loc., shore</b>						
1	Oyg-07-O1091	Equus sp.	tibia			from Valdemar
2	Oyg-07-O1092	Equus sp.	ph I			

## 6.4 Features of the studied waters

### 6.4.1 Geographical features of the studied waters

Sample LAP-	Date	Time	Region*	Locality	Coordinates	
					°N	°E
1a	08.07.07	21:15	Lya	Yedomia top	73,34138	141,33472
2	10.07.07	22:00	Lya	Yedomia top	73,33941	141,33532
1b	12.07.07	22:30	Lya	Yedomia top	73,34138	141,33472
3	14.07.07	19:30	Lya	Yedomia top	73,33654	141,32316
4	14.07.07	20:30	Lya	Yedomia top	73,33654	141,32316
1c	16.07.07	09:00	Lya	Yedomia top	73,34138	141,33472
5	20.07.07	18:00	Lya	Floodplain (Vankina River)	73,28358	141,82969
6	20.07.07	19:00	Lya	Floodplain (Vankina River)	73,28397	141,83026
7	21.07.07	22:30	Lya	Alas	73,28005	141,83369
8	22.07.07	21:45	Lya	Alas	73,28161	141,83794
1d	24.07.07	16:00	Lya	Yedomia top	73,34138	141,33472
9	25.07.07	17:00	Lya	Yedomia top	73,34331	141,33281
10	26.07.07	19:30	Lya	Yedomia slope	73,33929	141,31746
1e	28.07.07	09:30	Lya	Yedomia top	73,34138	141,33472
11	29.07.07	17:30	Lya	Yedomia slope (mid part)	73,35067	141,43241
12	29.07.07	18:50	Lya	Yedomia slope (lower part)	73,35002	141,43619
13	29.07.07	19:30	Lya	Yedomia slope (upper part)	73,35089	141,42957
14	31.07.07	12:30	Lya	Floodplain (Zimov'e River)	73,33419	141,36087
15	31.07.07	13:30	Lya	Floodplain (Zimov'e River)	73,33395	141,35875
1f	31.07.07	15:20	Lya	Yedomia top	73,34138	141,33472
16a	03.08.07	18:45	Oy	Alas	72,67847	143,51226
16b	07.08.07	14:00	Oy	Alas	72,67847	143,51226
17	07.08.07	16:00	Oy	Yedomia top	72,67618	143,57487
18	07.08.07	17:00	Oy	Yedomia slope (lower part)	72,67929	143,52379
19	11.08.07	15:00	Oy	Yedomia slope (lower part)	72,67628	143,55814
20	11.08.07	15:30	Oy	Yedomia slope (lower part)	72,67567	143,55878
16c	11.08.07	17:30	Oy	Alas	72,67847	143,51226
16d	15.08.07	14:15	Oy	Alas	72,67847	143,51226
21	15.08.07	15:00	Oy	Yedomia slope (mid part)	72,67663	143,51715
22	15.08.07	16:00	Oy	Yedomia slope (lower part)	72,67512	143,52354
23	15.08.07	17:00	Oy	Alas	72,67852	143,51609
16e	19.08.07	12:00	Oy	Alas	72,67847	143,51226
24	21.08.07	13:00	Oy	Alas	72,6833	143,44108
25	21.08.07	14:00	Oy	Alas	72,6825	143,42822
16f	23.08.07	21:00	Oy	Alas	72,67847	143,51226
26	24.08.07	15:00	Oy	Alas	72,67223	143,3429
27	24.08.07	15:45	Oy	Yedomia slope (mid part)	72,67281	143,34018
28	24.08.07	19:00	Oy	Alas	72,68007	143,43851
29	26.08.07	13:45	Oy	Yedomia top	72,6742	143,5371
30	26.08.07	14:30	Oy	Yedomia top	72,67318	143,5376
31	26.08.07	16:00	Oy	Yedomia top	72,66842	143,53186
32	26.08.07	17:30	Oy	Alas	72,67358	143,50972
16g	27.08.07	14:30	Oy	Alas	72,67847	143,51226
35	01.09.07	11:00	Tiksi	Valley	71,59701	128,80182
36	01.09.07	12:00	Tiksi	Valley	71,59725	128,80026
37	01.09.07	14:00	Tiksi	Valley	71,61335	128,79614

\* Lya – on Bol'shoy Lyakhovsly Island; Oy – on Oyogos Yar; Tiksi – near Tiksi

**6.4.2 Morphological and sedimentological features of the studied waters**

Sample	Water type	Substrate	Size	Total depth	Sample depth
LAP-			[m x m]	[m]	[m]
1a	Interpolygon	Grey silt below moss	15 x 20	0.6	0.2
2	Interpolygon	Grey silt below moss	10 x 15	0.2	0.2
1b	Interpolygon	Grey silt below moss	15 x 20	0.6	0.3
3	Interpolygon	Grey silt below moss	10 x 20	0.4	0.4
4	Interpolygon	Grey silt below moss	5 x 7	0.2	0.2
1c	Interpolygon	Grey silt below moss	15 x 20	0.6	0.3
5	Intrapolygon	Fine sand, organic rich	7 x 11	0.2	0.2
6	Intrapolygon	Fine sand, organic rich	5 x 7	0.15	0.15
7	Interpolygon	Detritus, decomposed, mud	10 x 10	0.2	0.2
8	Interpolygon	Detritus, decomposed, mud	20 x 100	0.3	0.2
1d	Interpolygon	Grey silt below moss	15 x 20	0.6	0.3
9	Interpolygon	Grey silt below moss	7 x 10	0.3	0.3
10	Interpolygon	Grey silt below moss	8 x 10	0.3	0.3
1e	Interpolygon	Grey silt below moss	15 x 20	0.6	0.3
11	Interpolygon	Grey silt below moss	5 x 15	0.4	0.4
12	Interpolygon	Grey silt below decomposed mud	7 x 20	0.5	0.5
13	Interpolygon	Grey silt below decomposed mud	7 x 12	0.4	0.4
14	Intrapolygon	Mud	19 x 19	0.1	0.1
15	Intrapolygon	Mud	7 x 10	0.1	0.1
1f	Interpolygon	Grey silt below water moss	15 x 20	0.6	0.3
16a	Interpolygon	Plants, detritus, low decomposed	4 x 7	0.65	0.3
16b	Interpolygon	Plants, detritus, low decomposed	4 x 7	0.65	0.3
17	Interpolygon	Grey silt below water moss	7 x 15	0.4	0.4
18	Interpolygon	Detritus, decomposed, mud	7 x 11	0.4	0.4
19	Interpolygon	Plants, mud	7 x 25	0.5	0.4
20	Interpolygon	Grey silt water moss, mud,	10 x 25	0.5	0.4
16c	Interpolygon	Plants, detritus, low decomposed	4 x 7	0.65	0.4
16d	Interpolygon	Plants, detritus, low decomposed	4 x 7	0.65	0.4
21	Interpolygon	Plants, detritus, low decomposed	2 x 5	0.6	0.5
22	Interpolygon	Detritus, low decomposed	7 x 12	0.4	0.4
23	Log	Plants	7 x 300	0.15	0.15
16e	Interpolygon	Plants, detritus, low decomposed	4 x 7	0.65	0.4
24	Interpolygon	Flooded tundra soil	10 x 10	0.2	0.1
25	Interpolygon	Flooded tundra soil		0.1	0.1
16f	Interpolygon	Plants, detritus, low decomposed	4 x 7	0.65	0.4
26	Alas lake	Flooded tundra soil at the alas margin	1000 x 1000		0.5
27	Interpolygon	Plants, detritus, decomposed, mud	4 x 7	0.45	0.4
28	Interpolygon	Plants, detritus, decomposed, mud	4 x 12	0.4	0.4
29	Interpolygon	Detritus, decomposed, mud	2 x 4	0.2	0.2
30	Interpolygon	Plants, detritus, decomposed, mud	15 x 30	0.5	0.5
31	Interpolygon	Moss	5 x 15	0.35	0.3
32	Interpolygon	Detritus, decomposed, mud	4 x 4	0.45	0.4
16g	Interpolygon	Plants, detritus, low decomposed	4 x 7	0.65	0.4
35	Pond	Mud	20 x 30	> 1	0.5
36	Pond	Mud	7 x 7	1	0.5
37	Lake	Coarse sand and gravel		> 1	0.4

## 6.4.3 Physico-chemical features of the studied waters

Sample LAP-	T <sub>Air</sub> [°C]	T <sub>water</sub> [°C]	EC* [μS/cm]	pH Viscolor	pH WTW	O <sub>2</sub> [mg/l]	Alk* [mmol/l]	Aci* [mmol/l]	TH* [°dH]	TH* [mmol/l]
1a	1.7	5.1	143		7.8	>10	1.4	1.4	6.5	1.15
2	4.1	7.7	121		7.8	>10	1	0.2	7.5	1.6
1b	9	9.8	149	7.5	8	>10	1.8	0.6	3.5	0.6
3	4.2	7.8	245		8.7	>10	1.8	0.4	5.5	0.9
4	3.6	7.4	100		8.3	>10	1	0.4	4	0.7
1c	5.3	5.1	154		7.9	>10	1.6	0.2	5	0.9
5	4.7	5.3	80	7		> 10	0.8	0.4	4	0.7
6	4	5.2	48	7		> 10	0.6	0.4	3	0.5
7	5.7	6.5	80	6.5		> 10	0.4	0.3	2.2	0.8
8	5	8.6	90	7		> 10	0.6	0.2	1.5	0.3
1d	13.1	9.5	192	7.5	8	> 10	1.7	0.2	5.5	0.9
9	14	13	138	7.5	8.7	> 10	0.9	0.2	4	0.7
10	12.8	12.5	190	7.5	8.6	> 10	1.6	0.2	6	1
1e	14.5	12.5	219	7	8.4	> 11	2	0.2	5.5	0.9
11	16.5	18.2	168	7	7.8	> 10	1.6	0.2	4.2	0.6
12	13.8	18.7	97	6.5	7	> 10	0.8	0.4	2.2	0.5
13	13.5	17.4	200	6.5	7	> 10	1.8	0.2	7.2	1.3
14	14.5	9.4	163	7	7.6	> 10	1.2	0.4	4	0.7
15	9.1	14.5	148	7	7.6	> 10	1.4	0.4	4.2	0.8
1f	13.4	12.5	234	7	8.1	> 10	2.3	0.2	6	1
16a	5.5	7.7	48	5.5	6	> 10	0.4	0.4	2.5	0.4
16b	7.3	7.6	47	5.5	6.2	> 10	1	0.2	3.5	0.6
17	7.1	5.2	127	6	6.3	> 10	1	0.3	3.5	0.6
18	5.9	6.2	54	6	6.4	> 10	0.2	0.2	2.2	0.4
19	6.6	7.7	123	7	6.9	> 10	1.4	0.2	3	0.5
20	6.8	7.4	112	7	6.9	> 10	1.4	0.2	3.5	0.6
16c	6.3	6.5	51	6.5	6	> 10	0.8	0.4	2	0.3
16d	18.3	10	50	6	6.2	> 10	0.4	0.2	4	0.7
21	19.6	9.1	59	6.5	6.5	> 10	0.4	0.4	3	0.5
22	18.6	9.1	70	6.5	6.7	> 10	0.6	0.2	3	0.5
23	19.4	15.1	58	6.5	6.7	> 10	0.6	0.4	3	0.5
16e	8	6.5	59	6.5	6	> 10	0.4	0.4	3.5	0.6
24	13.4	6.8	63	6.5	6.3	9	0.4	0.2	3	0.5
25	13.6	8.1	86	6.5	6	> 10	1	1.2	2	0.3
16f	6.3	6.2	58	6.5	6.5	7	0.8	0.6	3	0.45
26	8.6	8.4	96	7	7.5	> 10	0.8	0.4	4	0.6
27	8.7	7	175	6.5	6.9	4	2	0.4	6	1
28	7.5	7.6	48	6.5	6.2	> 10	1	0.6	2	0.35
29	10.5	4.6	49	6	6.2	> 10	1	0.4	4	0.7
30	11	9.6	114	7	7.1	9	1	0.4	6	1
31	11.5	6.9	72	6	6.1	3.2	1	0.4	5	0.8
32	11	8.8	98	7	6.7	> 10	0.6	0.4	2.5	0.4
16g	16.5	7.5	61	6	6.2	7.5	0.6	0.2	3	0.5
35	7.6	9.5	14	6.5	6.3	8.8	1	0.4	2.5	0.4
36	7.8	8.4	17	6.5	5.9	6.5	1.2	0.6	3.5	0.6
37	8.4	10	59	7	7	> 10	0.6	0.4	4.5	0.8

\* EC – electrical conductivity; Alk – Alkalinity; Aci – Acidity; TH – Total hardness



### 6.3 List of vegetation records from Oyogos Yar 2007

Cardinality (artmaechtigkeit, explanation in the text): + – sporadic, 1– <5%,  
2 – 5-15%, 3 – 15-50%, 4– 50-80%, 5– >80%

Record №	07.08./1	07.08./2	07.08./3	07.08./4	09.08./1
<b>Date/ Time</b>	07.08.07 14.00	07.08.07 14.20	07.08.07 14.40	07.08.07 15.00	09.08.07 17.00
<b>Location</b>	Thermokarst pond on degrading Yedoma east of the camp				Degrading Yedoma east of the camp
<b>Habitat</b>	Shallow, open water	riparian	Wet depression	hump	Thermokarst mound
<b>Decline/ exposition</b>	No decline	Very slight decline	Very slight decline	Very slight decline	Steep, SW
<b>Vegetation type</b>	Aquatic, emerged	wetland	wetland	Moist upland	upland
<b>Hydrology</b>	Water body	Water logged	Water logged	moist	Well drained, quite dry
<b>Taxon</b>	<i>Pleuropogon sabinei</i> 3	<i>Dupontia fisheri</i> 3	<i>Arctophila fulva</i> 2	<i>Alopecurus alpinus</i> 3	<i>Dryas punctata</i> 3
	<i>Arctophila fulva</i> 2	<i>Eriophorum scheuchzeri</i> 2	<i>Deschampsia borealis</i> 2	<i>Salix polaris</i> 2	<i>Salix polaris</i> 3
	<i>Ranunculus hyperboreus</i> 2	<i>Ranunculus hyperboreus</i> 2	<i>Dupontia fisheri</i> 2	<i>Deschampsia borealis</i> 2	<i>Alopecurus alpinus</i> 3
		<i>Pleuropogon sabinei</i> 2	<i>Ranunculus hyperboreus</i> 2	<i>Luzula confusa</i> 2	<i>Valeriana capitata</i> +
		<i>Arctophila fulva</i> 2	<i>Poa alpigena</i> +	<i>Tephrosaris atropurpurea</i> 1	<i>Deschampsia borealis</i> +
		<i>Saxifraga nelsoniana</i> 1	<i>Saxifraga cernua</i> 1	<i>Potentilla hyarctica</i> 1	<i>Papaver polare</i> +
		<i>Saxifraga cernua</i> 1	<i>Pleuropogon sabinei</i> 1	<i>Oxyria digyna</i> 1	<i>Ranunculus sp.</i> +
		<i>Alopecurus alpinus</i> 1	<i>Alopecurus alpinus</i> +	<i>Saxifraga nelsoniana</i> 1	<i>Oxyria digyna</i> +
				<i>Cardamine bellidifolia</i> +	<i>Potentilla hyarctica</i> +

Record №	09.08./2	09.08./3	09.08./4	09.08./5	09.08./6
<b>Date/ Time</b>	09.08.07 17.20	09.08.07 17.30	09.08.07 17.40	09.08.07 18.00	09.08.07 18.15
<b>Location</b>	degrading Yedoma east of the camp				
<b>Habitat</b>	thermocarst mound, between humps	foot of thermocarst mound	depression at foot of thermocarst mound	shore of thermocarst pond	thermocarst pond
<b>Decline/ exposition</b>	irregular	irregular	very slight decline	very slight decline	flat
<b>Vegetation type</b>	moist site pioneers	upland	wetland	wetland	aquatic, emerged
<b>Hydrology</b>	moist	moist	wet	wet	water body
<b>Taxon</b>	<i>Draba sp.</i> +		<i>Alopecurus alpinus</i> 2	<i>Eriophorum scheuchzeri</i> 4	<i>Pleuropogon sabinei</i> 4
	<i>Cochlearia arctica</i> 1	<i>Alopecurus alpinus</i> 2	<i>Eriophorum scheuchzeri</i> 2	<i>Dupontia fisheri</i> 2	<i>Eriophorum scheuchzeri</i> 2
	<i>Ranunculus cf nivalis</i> 1	<i>Ranunculus sp.</i> 2	<i>Cochlearia arctica</i> 2	<i>Arctagrostis latifolia</i> 1	<i>Cochlearia arctica</i> 1
	<i>Saxifraga cernua</i> +	<i>Luzula confusa</i> 1	<i>Salix polaris</i> 1	<i>Saxifraga cernua</i> +	<i>Saxifraga cernua</i> +
		<i>Saxifraga hieracifolia</i> 1	<i>Saxifraga cernua</i> 1	<i>Ranunculus sp.</i> 1	<i>Papaver polare</i> +
		<i>Saxifraga nelsoniana</i> 1	<i>Arctagrostis latifolia</i> 1	<i>Cochlearia arctica</i> +	
		<i>Valeriana capitata</i> +	<i>Saxifraga hieracifolia</i> +		
		<i>Papaver polare</i> +	<i>Ranunculus sp.</i> +		
		<i>Saxifraga cernua</i> +	<i>Draba sp.</i> +		
		<i>Tephrosieris atropurpurea</i> +	<i>Calamagrostis holmii</i> +		
			<i>Dupontia fisheri</i> +		

10.08.2007: transect from the top of the degrading Yedoma down to the adjacent thermo-erosional valley

Record №	10.08./1	10.08./2	10.08./3	10.08./4	10.08./5
Date/ Time	10.08.07 15.20	10.08.07 15.40	10.08.07 16.00	10.08.07 16.20	10.08.07 16.40
Location	degrading Yedoma east of the camp				
Habitat	thermokarst mound	foot of thermokarst mound	thermokarst mound	thermokarst mound	slope below 10.08./4
Decline/ exposition	steep, WSW	steep, WSW	steep, WSW	steep, WSW	irregular
Vegetation type	upland	upland	upland	upland	upland
Hydrology	well drained, quite dry	drained	well drained, quite dry	well drained, quite dry	well drained
Taxon	<i>Salix polaris</i>	3 <i>Salix polaris</i>	3 <i>Poa arctica</i>	<i>Alopecurus alpinus</i> 2 <i>Poa arctica</i>	3 <i>Salix polaris</i> 2 <i>Alopecurus alpinus</i> 2 <i>Pedicularis sp.</i> 1 <i>Saxifraga hieracifolia</i> 1 <i>Tephroseris atropurpurea</i> + <i>Saxifraga nelsoniana</i> 1 <i>Ranunculus sp.</i> + <i>Papaver polare</i> 1 <i>Saxifraga nelsoniana</i> 1 <i>Poa arctica</i> + <i>Potentilla hyparctica</i> + <i>Saxifraga cernua</i> 1 <i>Saxifraga nelsoniana</i> + <i>Gastrolychnis apetala</i> + <i>Cardamine bellidifolia</i> + <i>Festuca brachyphylla</i> + <i>Potentilla hyparctica</i> + <i>Draba sp.</i> + <i>Festuca brachyphylla</i> + <i>Cardamine bellidifolia</i> + <i>Saxifraga cespitosa</i> + <i>Ranunculus cf sabinii</i> 1 <i>Oxyria digyna</i> + <i>Cochlearia arctica</i> + <i>Stellaria sp.</i> + <i>Luzula confusa</i> + <i>Gastrolychnis apetala</i>

Record №	10.08./6	10.08./7	10.08./8	10.08./9	11.08./1
Date/ Time	10.08.07 17.15	10.08.07 17.45	10.08.07 18.00	10.08.07 18.30	11.08.07 17.00
Location	Yedoma slope east of the camp				
Habitat	flat thermokarst mound	slope below 10.08./6	slope below 10.08./7	slope below 10.08./7	slope below 10.08./9
Decline/exposition	irregular	almost flat	sSlightly declined	moderately declined	irregularly declined
Vegetation type	upland	wetland	wetland	moist tundra	moist tundra
Hydrology	well drained	wet, standing water	wet	moist	moist
Taxon	<i>Salix polaris</i> 2	<i>Alopecurus alpinus</i> 2	<i>Arctagrostis latifolia</i> 3	<i>Arctagrostis latifolia</i> 3	<i>Arctagrostis latifolia</i> 2
	<i>Alopecurus alpinus</i> 2	<i>Gastrolychnis apetala</i> 1	<i>Alopecurus alpinus</i> 2	<i>Alopecurus alpinus</i> 1	<i>Alopecurus alpinus</i> 3
	<i>Potentilla hyparctica</i> 1	<i>Ranunculus sp</i> +	<i>Gastrolychnis apetala</i> 1	<i>Dupontia fisheri</i> 1	<i>Salix polaris</i> 3
	<i>Saxifraga hieracifolia</i> +	<i>Salix polaris</i> +	<i>Saxifraga nelsoniana</i> 1	<i>Salix polaris</i> 2	<i>Luzula confusa</i> 2
	<i>Saxifraga cespitosa</i> +	<i>Saxifraga nelsoniana</i> +	<i>Saxifraga cernua</i> 1	<i>Saxifraga nelsoniana</i> 1	<i>Saxifraga nelsoniana</i> 2
	<i>Tephroseris atropurpurea</i> +	<i>Saxifraga cernua</i> +	<i>Salix polaris</i> 1	<i>Tephroseris atropurpurea</i> 1	<i>Potentilla hyparctica</i> 1
	<i>Ranunculus sp</i> +	<i>Cerastium beeringianum</i> +	<i>Tephroseris atropurpurea</i> +	<i>Potentilla hyparctica</i> +	<i>Tephroseris atropurpurea</i> 1
	<i>Cerastium beeringianum</i> +	<i>Eriophorum scheuchzeri</i> 2	<i>Luzula confusa</i> +	<i>Saxifraga cernua</i> +	<i>Saxifraga cernua</i> +
	<i>Luzula confusa</i> +	<i>Polygonum viviparum</i> +	<i>Saxifraga hieracifolia</i> +	<i>Saxifraga hieracifolia</i> +	<i>Festuca brachyphylla</i> +
	<i>Poa arctica</i> 1	<i>Arctagrostis latifolia</i> 1	<i>Ranunculus sp.</i> +	<i>Luzula confusa</i> +	<i>Oxyria digyna</i> +
	<i>Oxyria digyna</i> +	<i>Saxifraga hieracifolia</i> +	<i>Eriophorum scheuchzeri</i> 1	<i>Juncus biglumis</i> (on muddy ground)	<i>Papaver polare</i> +
	<i>Papaver polare</i> +	<i>Tephroseris atropurpurea</i> +			<i>Draba sp.</i> +
	<i>Gastrolychnis apetala</i> +	<i>Juncus biglumis</i> 1		<i>Draba sp.</i> +	<i>Stallaria sp.</i> +
	<i>Saxifraga cernua</i> 1				<i>Cardamine bellidifolia</i> +
	<i>Draba sp.</i> +				<i>Gastrolychnis apetala</i> +
	<i>Cochlearia arctica</i> +				<i>Saxifraga cernua</i> +

Record №	11.08./2	11.08./3	11.08./4	11.08./4	13.08./1
Date/ Time	11.08.07 17.20	11.08.07 17.40	11.08.07 18.00	11.08.07 18.30	13.08.07 17.00
Location	11.08.2007: continuation of the transect from 10.08.2007				degrading Yedoma
Habitat	decayed thermokarst mound	reddish, raw slope below 11.08./2	reddish slope below 11.08./3	green log ground	mud boil
Decline/ exposition	irregularly declined	irregularly declined	moderately declined	moderately declined	flat
Vegetation type	moist tundra	moist tundra	wetland	wetland	upland pioneers
Hydrology	moist	moist	wet	wet	drained
Taxon	<i>Arctagrostis latifolia</i> 4	<i>Arctagrostis latifolia</i> 3	<i>Eriophorum polystachion</i> 5	<i>Dupontia fisheri</i> 2	<i>Festuca brachyphylla</i> 1
	<i>Alopecurus alpinus</i> 2	<i>Alopecurus alpinus</i> 1	<i>Salix polaris</i> 2	<i>Eriophorum polystachion</i> 4	<i>Deschampsia borealis</i> 2
	<i>Salix polaris</i> 2	<i>Salix polaris</i> 2	<i>Petasites frigidus</i> 2	<i>Ranunculus sp.</i> 2	<i>Potentilla hyarctica</i> 2
	<i>Saxifraga nelsoniana</i> 1	<i>Saxifraga nelsoniana</i> 1	<i>Valeriana capitata</i> 1	<i>Petasites frigidus</i> 2	<i>Tephroseris atropurpurea</i> 1
	<i>Ranunculus sp.</i> 1	<i>Ranunculus sp.</i> 1	<i>Arctagrostis latifolia</i> 1	+ <i>Calamagrostis holmii</i> 1	<i>Salix polaris</i> 2
	<i>Saxifraga cernua</i> +	<i>Petasites frigidus</i> 2	<i>Saxifraga cernua</i> 2	+ <i>Eriophorum medium</i> 1	<i>Luzula confusa</i> 1
	<i>Potentilla hyarctica</i> +	<i>Papaver polare</i> +	+ <i>Luzula confusa</i> +	+ <i>Saxifraga cernua</i> +	
	<i>Papaver polare</i> +	<i>Stellaria sp.</i> +	+ <i>Saxifraga nelsoniana</i> +	+ <i>Chrysospleniu m alternifolium</i> +	
	<i>Tephroseris atropurpurea</i> +	<i>Potentilla hyarctica</i> +	+ <i>Ranunculus sp.</i> +	+ <i>Pedicularis sp.</i> +	
	<i>Polygonum viviparum</i> +	<i>Valeriana capitata</i> +	+ <i>Alopecurus alpinus</i> +		
	<i>Saxifraga hieracifolia</i> +	<i>Saxifraga cernua</i> +	+ <i>Calamagrostis holmii</i> +		
		<i>Tephroseris atropurpurea</i> +			
		<i>Ranunculus sp.</i> +			

Record №	13.08./2	13.08./3	15.08./1	15.08./2	15.08./3
Date/ Time	13.08.07 17.30	13.08.07 18.00	15.08.07 15.00	15.08.07 15.10	15.08.07 15.20
Location	Yedomas slope east of the camp				
Habitat	slope below mud boil	shore of thermokarst pond	on tussocks on hump in thermokarst pond	between tussocks on hump in thermokarst pond	flat part of hump in thermokarst pond
Decline/exposition	slightly declined	flat	irregular	irregular	flat
Vegetation type	upland pioneers, later succession (higher coverage)	aquatic emerged	upland	moist tundra	wetland
Hydrology	drained	water body	drained	moist	wet
Taxon	<i>Festuca brachyphylla</i> 1	<i>Pleuropogon sabinei</i> 3	<i>Alopecurus alpinus</i> 3	<i>Ranunculus sp.</i> 1	<i>Eriophorum angustifolium</i> 4
	<i>Deschampsia borealis</i> 2	<i>Eriophorum scheuchzeri</i> 2	<i>Saxifraga cernua</i> 2	<i>Poa sp.</i> 1	<i>Saxifraga hieracifolia</i> +
	<i>Potentilla hyperarctica</i> 2	<i>Ranunculus hyperboreus</i> 1	<i>Potentilla hyperarctica</i> 2	<i>Tephroseris atropurpurea</i> +	<i>Potentilla hyperarctica</i> +
	<i>Tephroseris atropurpurea</i> 1	<i>Alopecurus alpinus</i> 1	<i>Oxyria digyna</i> 1	<i>Luzula confusa</i> 1	<i>Eriophorum medium</i> 1
	<i>Salix polaris</i> 2	<i>Luzula confusa</i> 1	<i>Salix polaris</i> 2	<i>Alopecurus alpinus</i> 1	
	<i>Luzula confusa</i> 1	<i>Poa arctica</i> 1	<i>Cetraria</i> 2	<i>Saxifraga hieracifolia</i> +	
	<i>Alopecurus alpinus</i> +			<i>Saxifraga cernua</i> 1	
	<i>Lloydia serotina</i> +				
	<i>Salix glauca</i> +				
	<i>Cardamine bellidifolia</i> +				
	<i>Gastrolychnis apetala</i> +				
	<i>Ranunculus cf. sabinii</i> +				
	<i>Oxyria digyna</i> 1				
	<i>Saxifraga nelsoniana</i> 1				
	<i>Draba sp.</i> +				
	<i>Ranunculus sp.</i> +				
	<i>Cerastium sp.</i> +				
	<i>Saxifraga hieracifolia</i> +				
	<i>Papaver polare</i> +				
	<i>Saxifraga cernua</i> +				

Record №	15.08./4	15.08./5	15.08./6	15.08./7	15.08./8
<b>Date/ Time</b>	15.08.07 15.30	15.08.07 15.40	15.08.07 15.50	15.08.07 16.00	15.08.07 16.10
<b>Location</b>	Yedoma slope east of the camp				
<b>Habitat</b>	flat part of hump in thermokarst pond, <i>Dupontia</i> zone	flat part of hump in thermokarst pond, <i>Arctophila</i> zone	flat part of hump in thermokarst pond, <i>Eriophorum scheuchzeri</i> zone	thermokarst pond, <i>Pleuropogon</i> zone	mud boil behind thermokarst pond
<b>Decline/ exposition</b>	flat	flat	flat	flat	flat
<b>Vegetation type</b>	wetland	wetland	wetland	aquatic emerged	upland pioneers
<b>Hydrology</b>	wet, standing water	wet, standing water	wet, standing water	water body	drained
<b>Taxon</b>	<i>Dupontia fisheri</i> 5	<i>Arctophila fulva</i> 5	<i>Eriophorum scheuchzeri</i> 4	<i>Pleuropogon sabinei</i> 5	<i>Alopecurus alpinus</i> 2
	<i>Poa alpigena</i> +	<i>Dupontia fisheri</i> 1	<i>Dupontia fisheri</i> 1		<i>Festuca brachyphylla</i> 1
	<i>Eriophorum scheuchzeri</i> 2				<i>Salix polaris</i> 2
	<i>Saxifraga cernua</i> +				<i>Cetraria</i> 2
	<i>Arctophila fulva</i> +				<i>Saxifraga hieracifolia</i> +
					<i>Tephrosieris atropurpurea</i> +
					<i>Luzula confusa</i> 1
					<i>Lloydia serotina</i> +
					<i>Poa sp.</i> 2
					<i>Potentilla hyperctica</i> 1
					<i>Ranunculus sp.</i> +
					<i>Stellaria sp.</i> +

Record №	15.08./9	15.08./10	15.08./11	15.08./12	15.08./13
<b>Date/ Time</b>	15.08.07 16.30	15.08.07 17.00	15.08.07 17.30	15.08.07 17.45	15.08.07 18.00
<b>Location</b>	Yedoma slope east of the camp				
<b>Habitat</b>	slope below 15.08./8	tussock tundra below 15.08./9	on humps of thermokarst mound	between humps of thermokarst mound	shore of thermokarst pond
<b>Decline/ exposition</b>	slightly declined	W declined	irregular	irregular	flat
<b>Vegetation type</b>	upland	upland	upland	moist pioneers	wetland
<b>Hydrology</b>	drained	drained	well drained	moist	wet
<b>Taxon</b>	<i>Salix polaris</i> 3	<i>Alopecurus alpinus</i> 2	<i>Salix polaris</i> 3	<i>Papaver polare</i> 1	<i>Eriophorum polystachion</i> 3
	<i>Alopecurus alpinus</i> 1	<i>Festuca brachyphylla</i> 1	<i>Potentilla hyperctica</i> 2	<i>Ranunculus sp.</i> +	<i>Salix polaris</i> 3
	<i>Poa sp.</i> 1	<i>Salix polaris</i> 3	<i>Alopecurus alpinus</i> 2	<i>Draba sp.</i> 1	<i>Salix sp.</i> 1
	<i>Tephroseris atropurpurea</i> +	<i>Papaver polare</i> +	<i>Poa sp.</i> 1	<i>Saxifraga cernua</i> +	<i>Tephroseris atropurpurea</i> +
	<i>Valeriana capitata</i> +	<i>Luzula confusa</i> 1	<i>Oxyria digyna</i> 2	<i>Saxifraga cespitosa</i> +	<i>Saxifraga nelsoniana</i> +
	<i>Luzula confusa</i> 1	<i>Saxifraga hieracifolia</i> +	<i>Festuca brachyphylla</i> +	<i>Ranunculus nivalis</i> +	<i>Saxifraga hieracifolia</i> +
	<i>Potentilla hyperctica</i> +	<i>Saxifraga nelsoniana</i> 1	<i>Valeriana capitata</i> +	<i>Cochlearia arctica</i> +	<i>Potentilla hyperctica</i> +
	<i>Polygonum viviparum</i> +	<i>Poa sp.</i> 1		<i>Tephroseris atropurpurea</i> +	<i>Ranunculus sp.</i> 1
	<i>Saxifraga cespitosa</i> +	<i>Tephroseris atropurpurea</i> +		<i>Gastrolychnis apetala</i> +	<i>Luzula confusa</i> 1
	<i>Cardamine bellidifolia</i> +	<i>Draba sp.</i> +			
		<i>Potentilla hyperctica</i> +			
		<i>Gastrolychnis apetala</i> +			

Record №	15.08./14	16.08./1	16.08./2	16.08./3	16.08./4
<b>Date/ Time</b>	15.08.07 18.20	16.08.07 17.00	16.08.07 17.10	16.08.07 17.15	16.08.07 17.20
<b>Location</b>		floodplain of the "bone" river	floodplain of the "bone" river	floodplain of the "bone" river	floodplain of the "bone" river
<b>Habitat</b>	shore of thermocarst pond, <i>Poa</i> <i>alpigena</i> zone	muddy river bank	muddy river bank, <i>Phippsia</i> zone	muddy river bank, transition zone	muddy river bank, <i>Arctophila</i> zone
<b>Decline/ exposition</b>	flat	flat	flat	flat	Slightly declined
<b>Vegetation type</b>	wetland	riparian pioneers	riparian pioneers	riparian pioneers	riparian pioneers
<b>Hydrology</b>	wet	wet	wet	wet	wet
<b>Taxon</b>	<i>Poa alpigena</i> 4	<i>Phippsia algida</i> 1	<i>Phippsia algida</i> 4	<i>Phippsia algida</i> 2	<i>Arctophila fulva</i> 3
	<i>Saxifraga cernua</i> 1	<i>Cochlearia arctica</i> +		<i>Cochlearia arctica</i> 1	<i>Phippsia algida</i> 2
	<i>Eriophorum polystachion</i> 1			<i>Stellaria sp.</i> 1	<i>Cochlearia arctica</i> +
	<i>Ranunculus sp.</i> 1				<i>Stellaria sp.</i> 1
	<i>Gastrolychnis apetala</i> +				
	<i>Cochlearia arctica</i> +				
	<i>Tephroseris atropurpurea</i> +				
	<i>Alopecurus alpinus</i> 1				
	<i>Saxifraga hieracifolia</i> +				

Record №	16.08./5	16.08./6	18.08./1	18.08./2	18.08./3
Date/ Time	15.08.07 17.30	15.08.07 18.00	18.08.07 15.00	18.08.07 15.30	18.08.07 16.00
Location	floodplain of the "bone" river	floodplain of the "bone" river	18.08.2007: transect from the Yedoma ridge east of the camp down to the adjacent slope		
Habitat	slope above river bank, Alopecurus zone	in level river bank, from 16.08./3 into the log	Mud boil, 25-30% coverage	downslope 18.8./1, 50% coverage	downslope 18.8./1, 60% coverage less windy
Decline/exposition	quite steep	Slightly declined	SSW slightly declined	SSW slightly declined	SSW slightly declined
Vegetation type	moist to upland	riparian pioneers	Upland pioneers	Upland pioneers	Upland pioneers
Hydrology	moist	wet	drained	drained	drained
Taxon	<i>Alopecurus alpinus</i> 3	<i>Dupontia fisheri</i> 3	<i>Poa cf arctica</i> 2	<i>Alopecurus alpinus</i> 2	<i>Arctagrostis latifolia</i> 2
	<i>Arctophila fulva</i> 2	<i>Stellaria sp.</i> 2	<i>Festuca brachyphylla</i> 1	<i>Luzula confusa</i> 2	<i>Alopecurus alpinus</i> 2
	<i>Cochlearia arctica</i> 1	<i>Alopecurus alpinus</i> 1	<i>Luzula confusa</i> 2	<i>Salix polaris</i> 3	<i>Salix polaris</i> 2
	<i>Ranunculus nivalis</i> 1	<i>Saxifraga cernua</i> +	<i>Salix polaris</i> 1	<i>Potentilla hyparctica</i> 2	<i>Lloydia serotina</i> +
	<i>Tephroseris atropurpurea</i> +		<i>Potentilla hyparctica</i> 2	<i>Tephroseris atropurpurea</i> +	<i>Luzula confusa</i> 2
	<i>Ranunculus sp.</i> 1	<i>Ranunculus sp.</i> +	<i>Tephroseris atropurpurea</i> +	<i>Androsace triflora</i> +	<i>Tephroseris atropurpurea</i> +
	<i>Saxifraga hieracifolia</i> +	<i>Eriophorum scheuchzeri</i> +	<i>Oxyria digyna</i> 1	<i>Lloydia serotina</i> +	<i>Poa sp.</i> 1
	<i>Saxifraga cernua</i> +	<i>Cochlearia arctica</i> +	<i>Draba sp.</i> +	<i>Poa cf arctica</i> +	<i>Festuca brachyphylla</i> 1
	<i>Gastrolychnis apetala</i> +	<i>Gastrolychnis apetala</i> +	<i>Androsace triflora</i> +	<i>Dryas punctata</i> 2	<i>Saxifraga nelsoniana</i> +
	<i>Papaver polare</i> +	<i>Saxifraga hieracifolia</i> +	<i>Lloydia serotina</i> +	<i>Papaver polare</i> 1	<i>Potentilla hyparctica</i> +
	<i>Phippsia algida</i> +		<i>Papaver polare</i> +	<i>Oxyria digyna</i> 1	<i>Oxyria digyna</i> +
	<i>Poa alpigena</i> 1			<i>Festuca brachyphylla</i> +	<i>Valeriana capitata</i> +
	<i>Oxyria digyna</i> 1				<i>Gastrolychnis apetala</i> +
	<i>Potentilla hyparctica</i> +				<i>Ranunculus sp.</i> +
further above additionally	<i>Saxifraga foliolosa</i> +				<i>Saxifraga cernua</i> +
	<i>Saxifraga hyperborea</i> +				
	<i>Saxifraga nelsoniana</i> +				
	<i>Saxifraga cernua</i> +				

Record №	18.08./4	21.08./1	21.08./2	23.08./1	23.08./2
Date/ Time	18.08.07 16.30	21.08.07 16.30	21.08.07 16.30	23.08.07 17.30	23.08.07 17.50
Location		thermokarst depression W of the camp		23.08.2007: continuation of the transect from the Yedoma ridge down to the camp depression Yedoma slope east of the camp	
Habitat	downslope 18.8./3, 80% coverage typical upland tundra	center of a high center polygon, 100 % coverage	margin of a high center polygon, standing water	Tussock tundra near the sampled thermocirque	beside 23.08./1 in wet depressions
Decline/ exposition	SSW slightly declined	flat	flat	W declined	W declined
Vegetation type	Upland pioneers	wetland	wetland	Upland	moist pioneers
Hydrology	drained	wet	wet	drained	moist
Taxon	<i>Dryas punctata</i> 2	<i>Dupontia fisheri</i> 2	<i>Eriophorum polystachion</i> 3	<i>Alopecurus alpinus</i> 3	<i>Ranunculus nivalis</i> +
	<i>Arctagrostis latifolia</i> 2	<i>Luzula nivalis</i> 2	<i>Carex aquatilis</i> s.l. 3	<i>Luzula confusa</i> 3	<i>Cardamine bellidifolia</i> +
	<i>Alopecurus alpinus</i> 2	<i>Saxifraga foliolosa</i> +	<i>Arctophila fulva</i> 1	<i>Oxyria digyna</i> +	
	<i>Gastrolychnis apetala</i> +	<i>Saxifraga cernua</i> 1	<i>Saxifraga cernua</i> +	<i>Saxifraga nelsoniana</i> 1	
	<i>Saxifraga nelsoniana</i> +	<i>Luzula confusa</i> 2	<i>Dupontia fisheri</i> +	<i>Ranunculus</i> sp. 1	
	<i>Valeriana capitata</i> +	<i>Tephroseris atropurpurea</i> +	<i>Alopecurus alpinus</i> +	<i>Gastrolychnis apetala</i> 1	
	<i>Poa</i> sp. +	<i>Sphagnum</i> sp. 1	<i>Poa alpigena</i> +	<i>Salix polaris</i> 2	
	<i>Potentilla hyparctica</i> +	<i>Salix cf glauca</i> +	<i>Calamagrostis holmii</i> +	<i>Valeriana capitata</i> 1	
	<i>Ranunculus</i> sp. +		<i>Carex</i> sp. 1	<i>Saxifraga hieracifolia</i> +	
	<i>Tephroseris atropurpurea</i> +			<i>Saxifraga foliolosa</i> +	
	<i>Festuca brachyphylla</i> +			<i>Tephroseris atropurpurea</i> +	
	<i>Luzula confusa</i> 1			<i>Cerastium</i> sp. 1	
	<i>Pedicularis</i> sp. +			<i>Arctagrostis latifolia</i> 1	
	<i>Salix polaris</i> 1			<i>Saxifraga cernua</i> +	
	<i>Saxifraga cernua</i> +			<i>Papaver polare</i> +	
	<i>Lloydia serotina</i> +			<i>Poa</i> sp. 1	
	<i>Papaver polare</i> +			<i>Potentilla hyparctica</i> +	

Record №	23.08./3	26.08./1	26.08./2	26.08./3	26.08./4
<b>Date/ Time</b>	23.08.07 18.00	26.08.07 15.00	26.08.07 15.30	26.08.07 16.00	26.08.07 16.20
<b>Location</b>	down slope the degrading Yedoma,	small thermokarst depression E of the camp			
<b>Habitat</b>	spotty tundra with mud boils, 40% coverage	center of small shallow pond with lots of Sphagnum	small shallow pond, Arctophila zone	shore of small shallow pond,	shore of small shallow pond, Eriophorum zone
<b>Decline/ exposition</b>	W declined	flat	flat	flat	flat
<b>Vegetation type</b>	upland	Aquatic emerged	Aquatic emerged	wetland	wetland
<b>Hydrology</b>	drained	aquatic	aquatic	wet	wet
<b>Taxon</b>	<i>Festuca brachyphylla</i> 3	<i>Ranunculus pallasii</i> 3	<i>Arctophila fulva</i> 3	<i>Carex aquatilis s.l.</i> 3	<i>Eriophorum medium</i> 4
	<i>Alopecurus alpinus</i> 1	<i>Arctophila fulva</i> 3	<i>Sphagnum sp.</i> 4	<i>Eriophorum medium</i> 1	<i>Carex aquatilis s.l.</i> 1
	<i>Poa sp.</i> 1	<i>Sphagnum sp.</i> 4	<i>Ranunculus pallasii</i> +	<i>Ranunculus pallasii</i> +	<i>Dupontia fisheri</i> +
	<i>Lloydia serotina</i> +			<i>Sphagnum sp.</i> 2	<i>Saxifraga foliolosa</i> +
	<i>Luzula confusa</i> 1				<i>Sphagnum sp.</i> 4
	<i>Valeriana capitata</i> +				
	<i>Salix polaris</i> 2				
	<i>Oxyria digyna</i> 1				
	<i>Potentilla hyarctica</i> +				
	<i>Papaver polare</i> +				
	<i>Saxifraga hieracifolia</i> +				
	<i>Saxifraga nelsoniana</i> 1				
	<i>Arctagrostis latifolia</i> 1				
	<i>Dryas punctata</i> 3				

<b>Record №</b>	26.08./5	26.08./6	26.08./7
<b>Date/ Time</b>	26.08.07 16.30	26.08.07 16.40	26.08.07 16.50
<b>Location</b>	small thermokarst depression E of the camp		
<b>Habitat</b>	rim of low center polygon	standing water between polygonal rims	reddish signature in thermokarst depression
<b>Decline/ exposition</b>	irregular	flat	flat
<b>Vegetation type</b>		wetland	wetland
<b>Hydrology</b>	moist	wet	wet
<b>Taxon</b>	<i>Luzula confusa</i> 5	<i>Carex aquatilis s.l.</i> 2	<i>Eriophorum polystachion</i> 5
	<i>Saxifraga cernua</i> +	<i>Eriophorum medium</i> 2	<i>Saxifraga cernua</i> +
		<i>Eriophorum polystachion</i> 1	<i>Alopecurus alpinus</i> +

### **Die "Berichte zur Polar- und Meeresforschung"**

(ISSN 1866-3192) werden beginnend mit dem Heft Nr. 569 (2008) ausschließlich elektronisch als Open-Access-Publikation herausgegeben. Ein Verzeichnis aller Hefte einschließlich der Druckausgaben (Heft 377-568) sowie der früheren "**Berichte zur Polarforschung** (Heft 1-376, von 1982 bis 2000) befindet sich im Internet in der Ablage des electronic Information Center des AWI (**ePIC**) unter der URL <http://epic.awi.de>. Durch Auswahl "Reports on Polar- and Marine Research" auf der rechten Seite des Fensters wird eine Liste der Publikationen in alphabetischer Reihenfolge (nach Autoren) innerhalb der absteigenden chronologischen Reihenfolge der Jahrgänge erzeugt.

*To generate a list of all 'Reports' past issues, use the following URL: <http://epic.awi.de> and select the right frame: Browse. Click on "Reports on Polar and Marine Research". A chronological list in declining order, author names alphabetical, will be produced. If available, pdf files will be shown for open access download.*

### **Verzeichnis der zuletzt erschienenen Hefte:**

**Heft-Nr. 572/2008** — "Climatic and hydrographic variability in the late Holocene Skagerrak as deduced from benthic foraminiferal proxies", by Sylvia Brückner

**Heft-Nr. 573/2008** — "Reactions on surfaces of frozen water: Importance of surface reactions for the distribution of reactive compounds in the atmosphere", by Hans-Werner Jacobi

**Heft-Nr. 574/2008** — "The South Atlantic Expedition ANT-XXIII/5 of the Research Vessel 'Polarstern' in 2006", edited by Wilfried Jokat

**Heft-Nr. 575/2008** — "The Expedition ANTARKTIS-XXIII/10 of the Research Vessel 'Polarstern' in 2007", edited by Andreas Macke

**Heft-Nr. 576/2008** — "The 6<sup>th</sup> Annual Arctic Coastal Dynamics (ACD) Workshop, October 22-26, 2006, Groningen, Netherlands", edited by Pier Paul Overduin and Nicole Couture

**Heft-Nr. 577/2008** — "Korrelation von Gravimetrie und Bathymetrie zur geologischen Interpretation der Eltanin-Impaktstruktur im Südpazifik", von Ralf Krockner

**Heft-Nr. 578/2008** — "Benthic organic carbon fluxes in the Southern Ocean: regional differences and links to surface primary production and carbon export", by Oliver Sachs

**Heft-Nr. 579/2008** — "The Expedition ARKTIS-XXII/2 of the Research Vessel 'Polarstern' in 2007", edited by Ursula Schauer.

**Heft-Nr. 580/2008** — "The Expedition ANTARKTIS-XXIII/6 of the Research Vessel 'Polarstern' in 2006", edited by Ulrich Bathmann

**Heft-Nr. 581/2008** — "The Expedition of the Research Vessel 'Polarstern' to the Antarctic in 2003 (ANT-XX/3)", edited by Otto Schrems

**Heft-Nr. 582/2008** — "Automated passive acoustic detection, localization and identification of leopard seals: from hydro-acoustic technology to leopard seal ecology", by Holger Klinck

**Heft-Nr. 583/2008** — "The Expedition ANT-XXIII/9 of the Research Vessel 'Polarstern' in 2007", edited by Hans-Wolfgang Hubberten

**Heft-Nr. 584/2008** — "Russian-German Cooperation SYSTEM LAPTEV SEA: The Expedition Lena - New Siberian Islands 2007 during the International Polar Year 2007/2008", edited by Julia Boike, Dmitry Yu. Bolshiyarov, Lutz Schirrmeyer and Sebastian Wetterich